NT21: International Conference on the Science and Application of Nanotubes and Low-Dimensional Materials

June 6–11, 2021

Virtually hosted from
Rice University
Houston, USA

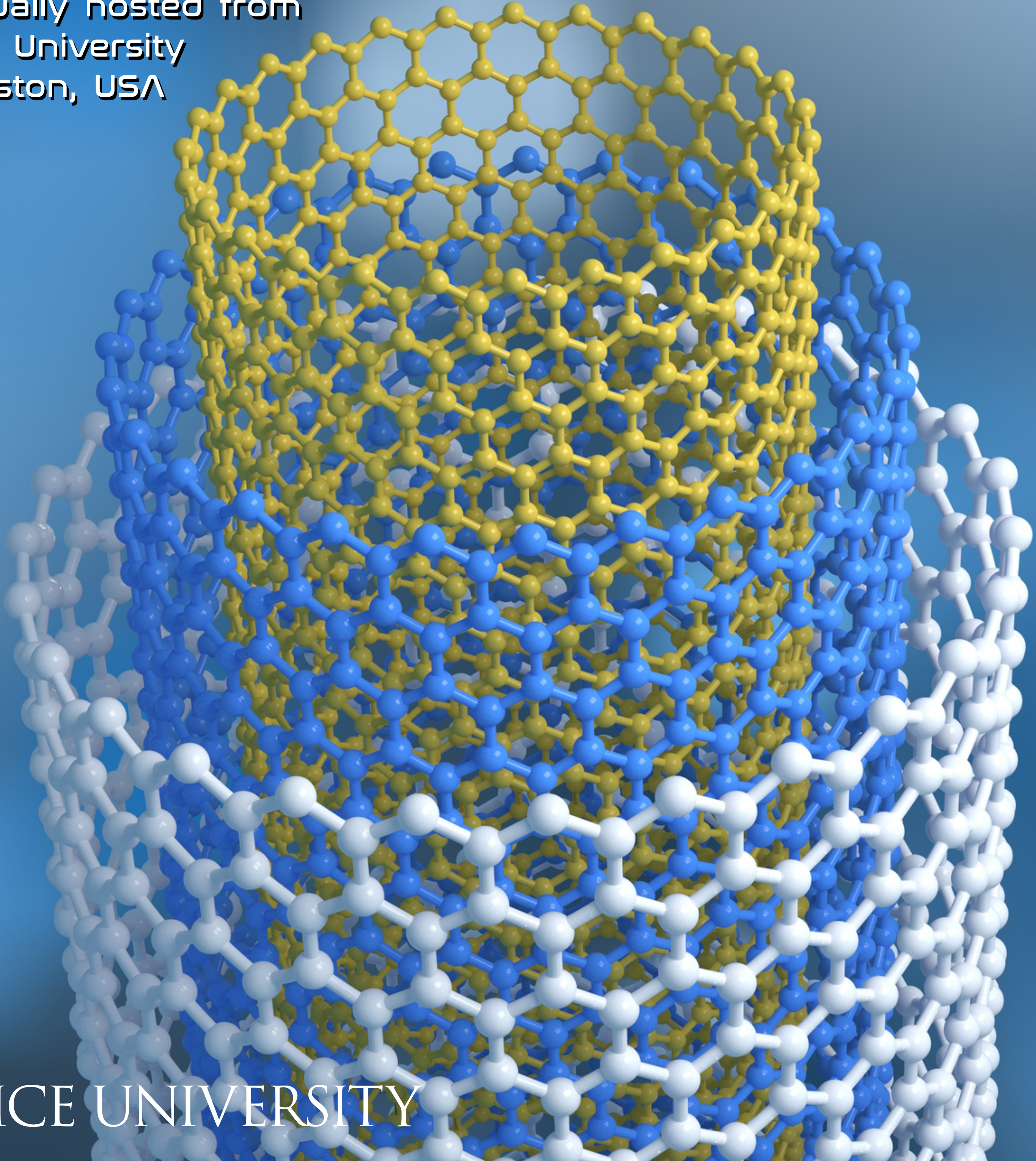

RICE UNIVERSITY

Contents

Organizers

Chair	**Junichiro Kono,** Rice University, USA
Co-chair	**Matteo Pasquali,** Rice University, USA
Co-chair	**R. Bruce Weisman,** Rice University, USA
Program Chair	**Erik Einarsson,** University at Buffalo, USA

Local Organizing Committee

Weilu Gao, University of Utah, USA
James Hayward, Rice University, USA
Daniel Heller, Memorial Sloan Kettering Cancer Center, USA
Glen Irvin, Rice University, USA
Angel Martí, Rice University, USA
Nicole McAdoo, Rice University, USA
Anton Naumov, Texas Christian University, USA
Thomas A. Searles, Howard University, USA
Aki Shimada, Rice University, USA
Emmanuel Tunley, Rice University, USA
Ginny Whitaker, Rice University, USA
Anna Ziegler, Rice University, USA

Technical Team

Chloe Corbitt, Rice University, USA
Jacques Doumani, Rice University, USA
Natsumi Komatsu, Rice University, USA
Nicolas Marquez Peraca, Rice University, USA
Ali Mojibpour, Rice University, USA
Fuyang Tay, Rice University, USA
Raiyan Zannat, Rice University, USA

NT Steering Committee

Co-chair	**Annick Loiseau,** ONERA–CNRS, France
Co-chair	**Shigeo Maruyama,** University of Tokyo, Japan
Members	**Tobias Hertel,** University of Würzburg, Germany
	Ado Jorio, University of Minas Gerais, Brazil
	Esko Kauppinen, Aalto University, Finland

	Jing Kong, MIT, USA
	Yan Li, Peking University, Peking, China
	Masako Yudasaka, AIST, Japan
	Ming Zheng, NIST, USA
Honorary Member	**David Tománek,** Michigan State University, USA

NT Advisory Board

Members	**Michael S. Arnold,** University of Wisconsin–Madison, USA
	Seunghyun Baik, Sungkyunkwan University, Korea
	Christophe Bichara, CINAM, CNRS, France
	Laurent Cognet, LP2N, CNRS, France
	James Elliott, University of Cambridge, UK
	Tobias Hertel, University of Würzburg, Germany
	Hiromichi Kataura, AIST, Japan
	Junichiro Kono, Rice University, USA
	Qingwen Li, SINANO, CAS, China
	Chang Liu, IMR, CAS, China
	Kazunari Matsuda, Kyoto University, Japan
	Janina Maultzsch, FAU Erlangen-Nürnberg, Germany
	Albert Nasibulin, Skoltech, Russia
	Suguru Noda, Waseda University, Japan
	Matteo Pasquali, Rice University, USA
	Lianmao Peng, Peking University, China
	Stephanie Reich, Freie Universität Berlin, Germany
	Lara Kühl Teles, Aeronautics Institute of Technology, Brazil
	Yuhuang Wang, University of Maryland, USA

Symposium Organization

Co-chair	**Tobias Hertel,** University of Würzburg, Germany
Co-chair	**Yoshiyuki Miyamoto,** AIST, Japan

2nd Symposium on Synthesis, Purification, Functionalization, and Manufacturing of Carbon Nanotubes and Low-Dimensional Materials

Chair	**Yan Li,** Peking University, China
Organizers	**Adam Boies,** University of Cambridge, UK
	Benji Maruyama, Air Force Research Lab, USA

3rd Symposium on Nanocarbon Materials for Energy and Sustainability

Chair	**James Elliott,** University of Cambridge, UK
Organizers	**Leonardo Spanu,** Shell Corporation
	Mauricio Terrones, Penn State University, USA

8th Symposium on Carbon Nanotube Macromaterials and Their Electronic, Thermal, and Structural Properties

Chair	**Elena Obraztsova,** Prokhorov General Physics Institute, Russia
Organizers	**Glen Irvin,** Rice University, USA
	Juan Vilatela, IMDEA Materials, Spain

11th Symposium on Carbon Nanomaterials Biology, Medicine, and Toxicology

Chair	**Dan Heller,** Memorial Sloan Kettering Cancer Center, USA
Organizers	**Ardemis Boghossian,** EPFL, Switzerland
	Delphine Bouilly, Université de Montréal, Canada
	Masako Yusadaka, AIST, Japan

11th Graphene and 2D Materials Symposium

Chair	**Alexander Sinitskii,** University of Nebraska–Lincoln, USA
Organizers	**Micah Green,** Texas A&M University, USA
	Alexander Högele, LMU München, Germany

14th Symposium on Nanotube Spectroscopy, Photonics, and Applications in Metrology

Chair	**Angela Hight Walker,** NIST, USA
Organizers	**Sofie Cambré,** University of Antwerp, Belgium
	Jeff Fagan, NIST, USA

15th Symposium on Computational Challenges in Nanotubes, 2D Materials, and Their Macroscopic Assemblies

Chair	**Christophe Bichara,** CNRS and Aix-Marseille Université
Organizers	**Traian Dumitricã,** University of Minnesota
	Vasili Perebeinos, University at Buffalo

Sponsors

RICE UNIVERSITY

Applied
NanoFluorescence

Carbon
Hub

MilliporeSigma

Nobo
NANOTECHNOLOGIES

RICE ENGINEERING
Electrical and
Computer Engineering

ROYAL SOCIETY
OF CHEMISTRY

Keynote Talks

Carbon Nanotechnology: A Timeline

Pulickel Ajayan*†

Rice University

The last two decades in materials science have been dominated by spectacular discoveries in nanotechnology, specifically by the high impact provided by materials such as carbon nanotubes and graphene. This talk will focus on the time line of carbon nanotechnology. The discovery of fullerenes laid the foundation of this phenomenal journey leading up to unexplored terrains in the landscape of carbon based nanostructures, their properties and applications. Carbon nanotubes and graphene lit up this landscape with their amazing properties and potential. This talk will take a realistic look at the last two decades of developments and a perspective on the state of the art in the field and some speculations on what could be there in store for the future.

Optical properties of carbon nanotube and two-dimensional material

Riichiro Saito*†

Tohoku University

Optical properties of single-wall carbon nanotube (SWNT) and two-dimensional (2D) materials are overviewed. Optical absorption for chiral SWNT depends on the helicity of the circularly polarized light (CPL), which is known as circular dichroism (CD). Conventional theory for CD gives a zero value because of the time-reversal symmetry in the hexagonal Brillouin zone. When we introduce phase of CPL at a carbon atom [1], the calculated CD reproduces experimental observation [2]. When we doped SWNT, the optical absorption is suppressed by occupied electrons in the conduction sub-bands and new absorption peak appears. The origin of the new peak is surface plasmon (SP) [3]. The diameter or Fermi energy dependence of SP is observed which is explained by the theoretical results [4]. The CD for doped SWNT shows a large value of CD compared with non-doped CD [5]. In a doped SWNT or doped graphene, there are several kinds of SP which are coupled with the light and optical absorption by SP is understood by the Joule heat induced by the induced electric current [6]. Edge plasmon is excited by linear-polarized light in the graphene nanoribbon, in which the induced electric field is localized and show in-plane rotation near the surface of nanoribbon [7]. The rotating electric field generates CPL or orbital magnetic moment. Raman spectroscopy by using the CPL shows the helicity-changing Raman spectra [8]. CPL emission in the p-n junction of 2D material is enhanced by applying strain [9]. Finally, we discuss CD and Kerr rotation in 2D material with intrinsic Hall conductivity [10]. References [1] N. Sato, Y. Tatsumi, R. Saito, Phys. Rev. B. 95, 155436, (2017). [2] X. Wei, et al., Nat. Comm. 7, 12899, (2016). [3] D. Satco, et al., Phys. Rev. B, 99, 075403, (2019). [4] D. Satco, et al., ACS Appl. Electron. Mater., 2, 195, (2020). [5] R. Saito, et al., J. Appl. Phys., 128, 164301, (2020). [6] M. S. Ukhtary, R. Saito, Carbon, 167, 455, (2020). [7] M. S. Ukhtary, M. Maruoka, R. Saito, Phys. Rev. B, 100, 155432, (2019). [8] Y. Tatsumi, T. Kaneko, R. Saito, Phys. Rev. B, 97, 195444, (2018). [9] S. Wang, M. S. Ukhtary, R. Saito, Phys. Rev. Res., 2, 033340, (2020). [10] F. R. Pratama, M. S. Ukhtary, R. Saito, Phys. Rev. B, 101, 045426, (2020). *Acknowledgements:* RS acknowledges JSPS KAKENHI (No. JP18H01810).

Purified and Functionalized Carbon Nanotubes for Optical and Electronic Applications

Jana Zaumseil*†

Heidelberg University

Polymer-wrapping has enabled the sorting and purification of large amounts of semi-conducting and monochiral single-walled carbon nanotubes (SWNTs) that can be applied in a wide range of (opto-)electronic devices with outstanding charge transport properties. Their near-infrared emission properties are tunable either by strong-light matter coupling, i.e., formation of exciton-polaritons in Fabry-Pérot cavities (ACS Photonics 2021, 8, 182), by intentional doping (Adv. Electron. Mater. 2020, 6, 2000717, ACS Appl. Mater. Interfaces 2020, 12, 28392) or by controlled introduction of different luminescent sp3-defects. These quantum defects with characteristically red-shifted emission and long photoluminescence (PL) lifetimes enable higher PL quantum yields and single-photon emission at room temperature. They can be created in a controlled manner in polymer-wrapped semiconducting nanotubes in organic solvents using diazonium chemistry with a phase-transfer agent (ACS Nano 2019, 13, 9259).

---

* denotes primary author, † denotes presenting author.

Various substituents are possible including the stable and neutral perchlorotriphenylmethyl (PTM) radical, which directly interacts with the sp3-defects (ACS Nano 2021, 10.1021/acsnano.0c10341). Furthermore, the type of defect emission (E11* or E11*-) is governed by the precise binding configuration for chiral (6,5) SWNTs. A simple synthetic protocol relying on nucleophilic addition instead of radical-based reactions facilitates the introduction of only the more red-shifted E11*- defects with even longer PL lifetime and high single-photon purity. Here, I will give an overview of our recent progress on the targeted functionalization of polymer-wrapped (6,5) SWNTs, their emission and charge transport properties with and without defects and their application in devices. *Acknowledgements:* ERC Consolidator Grant TRIFECTs (Grant# 817494)

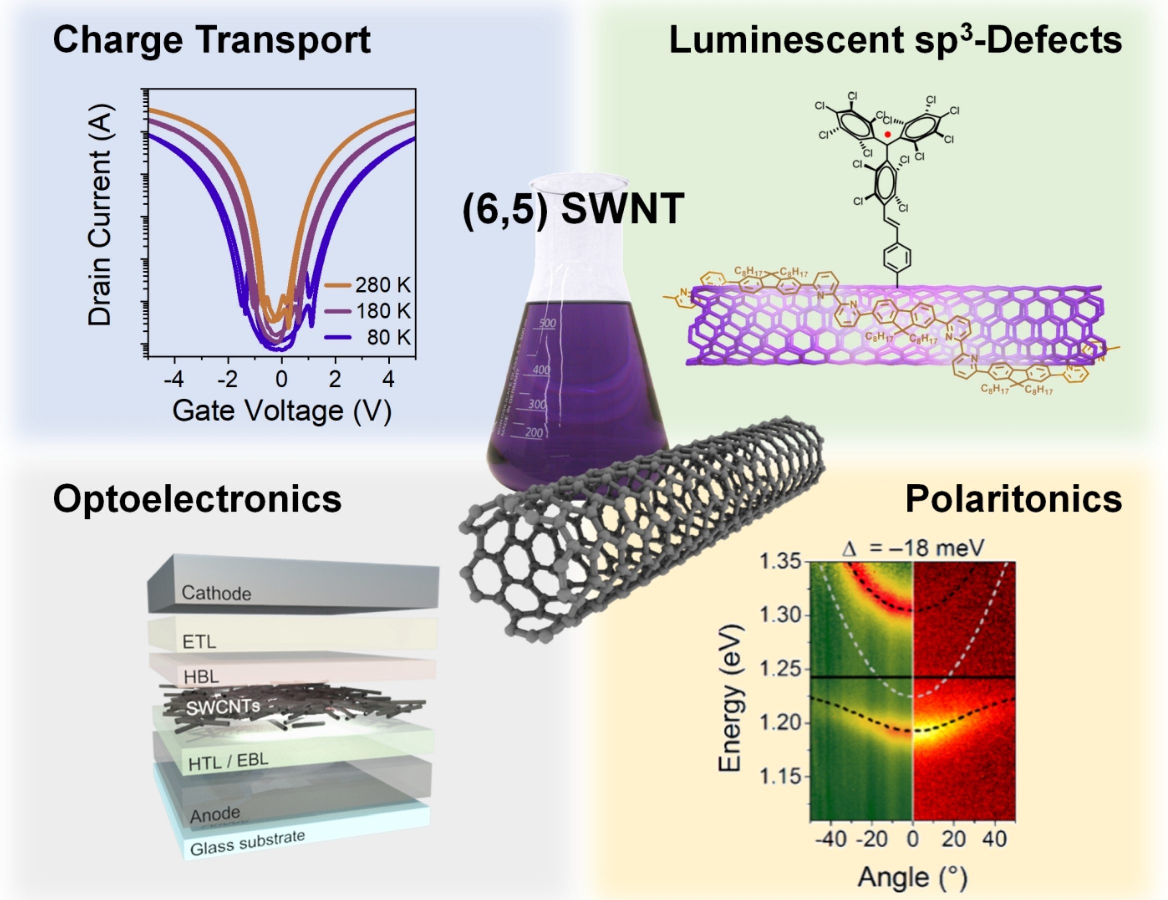

Fig. 1: Applications of polymer-sorted (6,5) SWNTs: field-effect transistors, luminescent defects, exciton-polaritons, light-emitting diodes.

Synthesis and Applications of Carbon Nanotubes

KaiLi Jiang*†

**Tsinghua University*

Carbon nanotubes (CNTs) are on their way to industrial applications, among which the killer application is believed to be the successor to silicon in next generation integrated circuits. In this talk, I will show our recent progress on the controlled synthesis of high purity semiconducting carbon nanotubes, and the device applications of carbon nanotube at extreme conditions such as superconducting quantum interference devices (SQUID), nanomechanical oscillators (NEMS), as well as torsion balances. [1] J. Wang, X. Jin, Z. Liu, et al. Nature Catalysis 1, 326-331 (2018). [2] X. Wang, L. Cong, D. Zhu, et al. Nano Res. 14(4), 1156–1161 (2021). [3] L. Cong, Z. Yuan, Z. Bai, et al. Science Advances 7: eabd2358 (2021).

Understanding electron-beam-stimulated reactions in functional low-dimensional material

Ute Kaiser*†

**Central Facility for Electron Microscopy, Electron Microscopy Group of Materials Science, Ulm University, Ulm 89081, Germany*

Two-dimensional (2D) materials exhibit properties, which often differ strongly from those of their bulk counterparts and may alter even by changing the positions of a single atom. Graphene liquid cells as well as single-walled carbon nanotubes can act as container to realize controlled reactions or translations of molecules confined in the narrow space of the container.In this study we demonstrate that the electron beam in the transmission electron microscope (TEM) can act as stimulus and initiator for reactions while imaging the result of the interactions. Thus, detailed understanding of the electron beam – specimen interactions is a crucial task. We present recent results on atomically-resolved, time-dependent in-situ TEM imaging using the chromatic- and spherical-aberration-corrected low-voltage SALVE instrument operating in the voltage range between 80kV and 20kV [1-5]. First, we elucidate the accelerating-voltage-dependent formation of defects in the case of single-layer MoS_2. The results suggest that knock-on damage and electronic excitations are combined in the TMD materials and lower drastically the knock-on damage threshold. Density functional theory molecular dynamics shows that excitations in the electronic system can form vacancies through ballistic energy transfer at electron energies, which are much lower than the knock-on threshold for the ground state [6]. We further identify the structure of electron-beam-induced defects and their electronic properties and follow the migration paths and associated property changes in a variety of 2D TMD and TMPT crystals [6-8]. We show that also 2D polymers and their defects can be resolved at near-atomic level when selecting the appropriate accelerating voltage [9]. On the more fundamental base, we show that differentiating between the bond nature by measuring the distance between two metal atoms is possible, when confined in the narrow space of a SWNT [10]. Although rotational motions have been observed in carbon-nanotube-based mass transfer systems [11,12], we show here the interaction between the moving matter and the carbon nanotube and its application for carrying metal atoms to a nucleation seed, realizing in situ observation of metal nucleation. We identify three main processes prior to heterogeneous nucleation and demonstrate the roles of the amorphous precursors and the existence of an energy barrier before nuclei formation. In all three cases we find that crystal nucleus formation occurrs through a two-step nucleation mechanism [13]. Finally, we intercalate bilayer graphene in-situ by lithium, study in-situ the lithiation and delithiation processes, as well as the formation process of the new high-density crystalline Li- phase [14]. [1] U. Kaiser et al., (2011) Ultramicroscopy, 111, 8, 1239[2] M. Linck, et al. (2016), PRL 117, 076101. [3] www.salve-project.de[4] F. Börrnert and U. Kaiser (2018) Physical Review A 98 (2) 023861-1[5] M. Mohn, et al. (2020), Ultramicroscopy 219, 113119. [6] S. Kretschmer, et al (2020), Nano Lett. 20, 2865. [7] T. Lehnert et al. ACS Appl. Nano Mater. 2 (2019) 3262. [8] J. Köster et al. (2021). Nanotechnology 32, 075704. [9] H. Qi et al. (2020), Science Advances 6, eabb5976. [10] K. Cao, (2020), Science Advances 6, eaay5849. [11] M. Koshino et. al. (2007), Science, 316, 853. [12] J. H. Warner et. al. (2008), Nano Lett., 8, 2328[13] K. Cao et. al. (2020), Nat. Chem. 12, 921–928. [14] M. Kühne et al. (2018), Nature 564, 234.We thank the DFG and the state Baden-Württemberg in the frame of the SALVE project as well as the European Union's Horizon 2020 programme Grant agreement No. 881603. *Acknowledgements:* We thank the DFG and the state Baden-Württemberg in the frame of the SALVE project as well as the European Union's Horizon 2020 programme Grant agreement No. 881603.

Invited Talks

1D-nanomaterial confinement: Red-phosphorus encapsulated within single-walled carbon nanotubes

Chris Ewels*†, Victor Koroteev, Dmitry Rybkovskiy, Anthony Impellizeri, Anna Vorfolomeeva, Alexandr Okotrub, Andrey Chuvilin, Lyuba Bulusheva, Alain Penicaud, Emmanuel Picheau, Marc Monthioux, Abraao Cefas Torres Dias

**Institute of Materials, Université de Nantes - CNRS*

Carbon nanotube cavities present excellent tools for exploration of low-dimensional allotropes. In this talk I will explore recent work looking at new phases, emergent materials properties, and effective routes to couple predictive DFT modelling to experimental characterisation data. We will take as our principal example phosphorus, a material with a complex variety of 3D-allotropes which has recently seen extensive structural exploration in the literature. We identify the ”missing” 1D-phosphorus allotrope, red phosphorus chains, formed in the interior of single-walled carbon nanotubes (SWCNTs). Via comprehensive experimental and theoretical study we show that in intermediate diameter cavities (1.5-2.5 nm), Phosphorus forms a combination of linear [P2P8] chains and red-phosphorus type cross-linked double-chains. Phosphorus interacts with highly purified and tip-opened Tuball SWCNTs at 800°C in sealed vacuum ampoules. Thermogravimetric and X-ray photoelectron spectroscopy (XPS) analysis shows ~8 at.% of phosphorus, predominantly in the elementary form. High-resolution transmission electron microscopy (HRTEM) shows long chains inside the nanotubes with varying arrangement and packing density. A detailed match is obtained between Density Functional Theory simulations and both HRTEM and low frequency Raman spectroscopy. Notably a signature spectroscopic signal for Phosphorus chain cross-linking is identified. When coupled with reinterpretation of literature data, these new results allow construction of a complete phase diagram for confined one dimensional phosphorus allotropes. We also propose a new defect model linking the two structures to account for the observed behaviour. If time allows, I will also briefly cover other available encapsulation cavity types including collapsed nanotube cavities and non-circularity in multi-walled tube walls. *Acknowledgements:* Many calculations performed at the CCIPL. A.I. and C.P. Ewels acknowledge ANR Projects “EdgeFiller” and OPIFCat for funding.

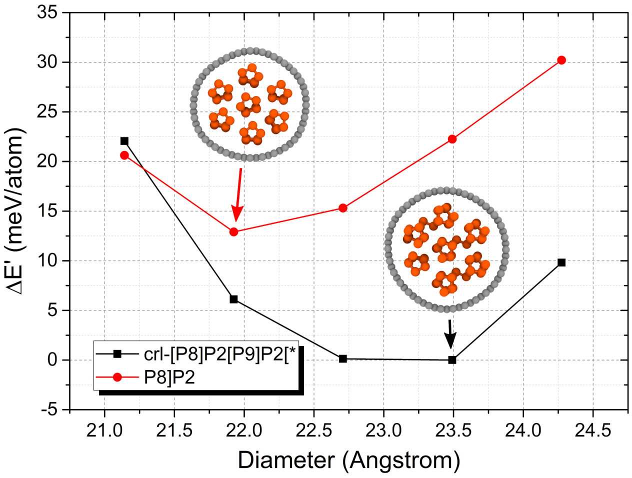

Fig. 1: Relative energies (meV/atom) of 7-chain Phosphorus structures encapsulated in carbon nanotubes, relative to the lowest energy value, plotted as a function of the encapsulating nanotube diameter.

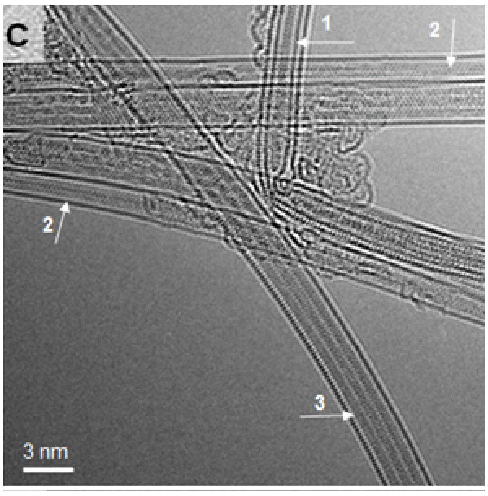

Fig. 2: Typical HRTEM image of individual P-filled SWCNTs

2D materials plasmons: physics and applications

Tony Low*†

**University of Minnesota*

Recent years have observed a plethora of strong dipole type polaritonic excitations in 2D materials owing to the reduced screening [1,2]. These polaritons can be sustained as electromagnetic modes at the interface between a positive and negative permittivity material [3]. In this talk, I will discuss our recent efforts in understanding

---

* denotes primary author, † denotes presenting author.

plasmons behavior in various 2D materials, such as graphene [4,5,6], black phosphorus [7,8], and transition metal dichalcogenides [9], and how these systems can also exhibit rich transport behavior, such as hyperbolic rays [10,12], non-reciprocal chiral propagation [13,14], and time reversal of waves [11]. Lastly, I will discuss key applications where graphene plasmonic are uniquely suited; graphene for the manipulation of mid-infrared beam [17], gas and biosensing [15,16]. References:Low, T., Chaves, A., Caldwell, J.D., Kumar, A., Fang, N.X., Avouris, P., Heinz, T.F., Guinea, F., Martin-Moreno, L. and Koppens, F., 2017. Polaritons in layered two-dimensional materials. Nature materials, 16(2), pp.182-194.Basov, D.N., Fogler, M.M. and De Abajo, F.G., 2016. Polaritons in van der Waals materials. Science, 354(6309).Low, T. and Avouris, P., 2014. Graphene plasmonics for terahertz to mid-infrared applications. ACS nano, 8(2), pp.1086-1101.Yan, H., Low, T., Zhu, W., Wu, Y., Freitag, M., Li, X., Guinea, F., Avouris, P. and Xia, F., 2013. Damping pathways of mid-infrared plasmons in graphene nanostructures. Nature Photonics, 7(5), pp.394-399.Freitag, M., Low, T., Zhu, W., Yan, H., Xia, F. and Avouris, P., 2013. Photocurrent in graphene harnessed by tunable intrinsic plasmons. Nature communications, 4(1), pp.1-8.Lee, I.H., Yoo, D., Avouris, P., Low, T. and Oh, S.H., 2019. Graphene acoustic plasmon resonator for ultrasensitive infrared spectroscopy. Nature nanotechnology, 14(4), pp.313-319.Low, T., Roldán, R., Wang, H., Xia, F., Avouris, P., Moreno, L.M. and Guinea, F., 2014. Plasmons and screening in monolayer and multilayer black phosphorus. Physical review letters, 113(10), p.106802.Nemilentsau, A., Low, T. and Hanson, G., 2016. Anisotropic 2D materials for tunable hyperbolic plasmonics. Physical review letters, 116(6), p.066804.Kumar, A., Nemilentsau, A., Fung, K.H., Hanson, G., Fang, N.X. and Low, T., 2016. Chiral plasmon in gapped Dirac systems. Physical Review B, 93(4), p.041413.Nemilentsau, A., Stauber, T., Gómez-Santos, G., Luskin, M. and Low, T., 2019. Switchable and unidirectional plasmonic beacons in hyperbolic two-dimensional materials. Physical Review B, 99(20), p.201405.Wilson, J., Santosa, F., Min, M. and Low, T., 2018. Temporal control of graphene plasmons. Physical Review B, 98(8), p.081411.Wang, H. and Low, T., 2020. Hyperbolicity in two-dimensional transition metal ditellurides induced by electronic bands nesting. Physical Review B, 102(24), p.241104.Lin, X., Liu, Z., Stauber, T., Gómez-Santos, G., Gao, F., Chen, H., Zhang, B. and Low, T., 2020. Chiral plasmons with twisted atomic bilayers. Physical review letters, 125(7), p.077401.Stauber, T., Low, T. and Gómez-Santos, G., 2018. Chiral response of twisted bilayer graphene. Physical review letters, 120(4), p.046801.Hu, H., Yang, X., Guo, X., Khaliji, K., Biswas, S.R., de Abajo, F.J.G., Low, T., Sun, Z. and Dai, Q., 2019. Gas identification with graphene plasmons. Nature communications, 10(1), pp.1-7.Khaliji, K., Biswas, S.R., Hu, H., Yang, X., Dai, Q., Oh, S.H., Avouris, P. and Low, T., 2020. Plasmonic Gas Sensing with Graphene Nanoribbons. Physical Review Applied, 13(1), p.011002.Biswas, S.R., Gutiérrez, C.E., Nemilentsau, A., Lee, I.H., Oh, S.H., Avouris, P. and Low, T., 2018. Tunable graphene metasurface reflectarray for cloaking, illusion, and focusing. Physical Review Applied, 9(3), p.034021.

3D Carbon Nanotube Current Collectors for Li-Ion Batteries

Michael De Volder*†

**University of Cambridge*

Vertically aligned CNT forests offer a unique template for fabricating hierarchical structures with a controlled morphology at different length-scales. In particular for energy storage applications, patterned CNT forest offer opportunities for creating highly conductive networks with aligned pores to create electrodes with improved ion transport. This allows for creating thick battery electrodes with good electron and ion transport, which are interesting to increase the energy density of Li-Ion batteries.To use CNTs as advanced current collectors in Li-Ion batteries as suggested above, they need to be coated with active materials for storing Li-Ions. However, because CNT forests are fragile, their surface chemistry or surface decoration is typically limited to gas phase processes. In this presentation, methods will be discussed to create 3D CNT collector electrodes using a combination of micro and nano lithographic patterning methods as well as transfer printing. The resulting 3D CNT structures can be coated using a wet microwave-assisted hydrothermal synthesis method. Overall, this is attractive because of the high electrical conductivity and good tortuosity of the CNTs as well as the good interface which is formed between the CNTs and the active battery material as a result of this 'in situ' synthesis process. In addition, manufacturing challenges such as the phase segregation of conductive additives that occur in thick electrodes are addressed using this process. We have fabricated 350 μm thick electrodes showing specific capacities of over 900 mAh g−1 along with a fourfold improvement in cyclability compared to CNT forests decorated by drop-casting. Finally, post-mortem analysis suggests that the developed 3D CNT electrode structures do not deteriorate during battery cycling.The experiments described in the presentation were carried out by Dr Sarah Jessl, Tommy Zhao, Dr Simon Engelke, Dr Davor Copic and Prof Shahab Ahmad. The work was funded by an ERC Consolidator Grant – MIGHTY 866005.

Accelerating the Energy Transition with Carbon Nanotubes Requires Closing Critical Policy Gaps and an Understanding of Nano-related Environment, Health and Safety Information

Rachel Meidl*†

**Baker Institute for Public Policy*

Global energy and environmental challenges have spurred increased focus on regenerative and sustainable sources of energy. Nanotechnology is an emerging, rapidly growing, and promising field with advanced applications in industrial, commercial, and medical sectors and the ability to convey solutions that help the world meet global climate targets and sustainability goals. Carbon nanotubes (CNTs), a family of carbon-based hollow cylindrical structures with unique physicochemical properties, hold great promise for new materials with far fewer environmental and energy requirements. They have many potential use applications, including structural reinforcements that could displace or supplement steel, aluminum, and other metals, concrete, and plastics, decreasing the need for energy-intensive primary minerals and materials with high CO2 footprints. CNTs are critical components for future decarbonization strategies. As society progresses toward a clean energy revolution, it will be imperative that the field of advanced nanomaterials have a clear and consistent path to commercialization shepherded by industry best practices, guided by informed life-cycle-based policies, and underpinned by a comprehensive, interdisciplinary research strategy. The distinctive electrical, thermal, and mechanical properties of CNTs will advance U.S. leadership in innovation, energy, and environment, but there is a need to standardize, define, and communicate policy-driving information on their safe manufacturing, handling, use, and disposal, in particular, developing and implementing environmental, health, and safety (EHS) research-based protocols for addressing nano-safety issues. Closing this gap will help expedite commercialization and full market integration of nanotechnology-enabled applications and ensure responsible development from lab to market and reuse. Prior to full market integration and to attain public acceptance of CNTs, it will be imperative to consider these critical components in order to achieve sustainability-the interaction of social, environmental, and economic elements. A clear set of guidelines, best practices, and standard operating procedures, formulated with input from academia, industry, and regulatory bodies, will greatly improve the public understanding and acceptance of CNTs and thus increase their commercial viability and sustainability.

Application of Cryo-EM to DNA-CNTs

Leti Beltran*, Ming Zheng, Edward Egelman†

**University of Virginia*

Since the introduction of direct electron detectors around 2012, cryo-EM has emerged as the main technique in structural biology for determining the atomic structure of macromolecular complexes. A near-atomic level of resolution is now routinely reached for many biological specimens, and cryo-EM has supplanted x-ray crystallography as the method of choice for understanding the structure of molecular assemblies. However, in materials science, chemistry and nanotechnology the applications of cryo-EM have been quite sparse. We have used cryo-EM to study the structure of carbon nanotubes wrapped with a 12 base single stranded oligonucleotide. We can show that the phosphate backbone of the DNA forms a nearly continuous 16.8 Å pitch helix around the CNT, and that the bases are stacked against the CNT surface and paired across the helical grooves. Our results not only illuminate how particular DNA sequences can select particular CNT lattices, but open the door for the more widespread use of cryo-EM to directly visualize such structures.

Bioengineering DNA-based Optical Nanotube Sensors Using Directed Evolution and Xenonucleic Acids (XNAs)

Ardemis Boghossian*†

**Ecole Polytechnique Federale de Lausanne*

Single-walled carbon nanotubes (SWCNTs) demonstrate distinctive fluorescence properties that have motivated their use as optical sensors in biology, medicine, and toxicology. Their fluorescence properties, such as quantum yield and optical responsivity and specificity towards analytes, are controlled by the non-covalent wrapping that is used to solubilize the SWCNTs in aqueous media. Single-stranded DNA are among the most common SWCNT wrappings, whereby sensor properties such as specificity can be modulated by altering the DNA sequence. However, the relationship between the DNA sequence and its effects on the sensors are unknown, limiting the ability to engineer these sensors in a predictive and rational manner. Inspired by strategies in protein engineering, we have developed bioengineering approaches that allow us to modulate the DNA-SWCNT optoelectronic behavior in a more controlled and directed manner. Through directed evolution, we demonstrate a guided approach to orthogonally tuning optical sensor properties, including specificity, sensitivity, brightness, and even chirality-dependent responsivity. We further enhance the responsivity and resilience of these sensors against fluctuating salt concentrations through artificial nucleotides, XNAs, which allow us to achieve sensors that can be used in biofluids with performances that reach beyond the limits of natural nucleotides. Finally, we apply these techniques to illustrate the application of these bioengineered sensors in neurochemical and toxin measurements. The disruptive synthetic biology approaches presented herein therefore offers a pragmatic means of engineering nanotube optoelectronic behavior, unlocking previously unexplored possibilities for developing nano-bioengineered sensors with augmented capabilities.

Calibrating Raman cross-sections of sorted SWCNT samples

Salome Forel*†, Alice Castan, Dmitry Levshov, Frédéric Fossard, Joeri Defillet, Han Li, Benjamin S. Flavel, Jeff Fagan, Annick Loiseau, Valentin Popov, Wim Wenseleers, Sofie Cambré

**Nanostructured and Organic Optical and Electronic Materials, Department of Physics, University of Antwerp, Antwerp, Belgium*

Single-wall carbon nanotubes (SWCNTs) possess unique electronic and optical properties, strongly depending on their chiral structures. In particular, macroscopic samples containing just a single chirality, with, e.g., a specific electronic bandgap or a specific emission wavelength, are highly desired for applications in opto-electronics. The recent progress in the sorting and the selective synthesis of specific SWCNT chiralities1 enabled to approach this objective, but also demands an optimized characterization methodology to assess this chiral purity. In a previous work2, we reported a comparison between high-resolution transmission electron microscopy (HRTEM) and "Raman mapping", the latter statistically counting Raman peaks from individual SWCNTs at a few discrete wavelengths, for characterizing the diameter or chirality distribution of a macroscopic SWCNT sample. Large discrepancies between both methodologies highlighted the various biases involved, and demonstrated that, without taking these biases into account, the diameter distribution and, thus, the chiral distribution can be severely altered. One of the main biases in Raman counting are the very different Raman cross-sections observed for different SWCNT chiralities. Following that work, we now investigate these chirality-dependent Raman cross-sections, by comparing wavelength-dependent Raman spectroscopy (RRS) over a very broad range (from UV to NIR) with optical absorption spectroscopy (OAS) and IR fluorescence-excitation spectroscopy (PLE). By detailed simultaneous and multi-dimensional fitting of the OAS spectra, PLE and RRS maps, intensity distributions obtained from these techniques are compared to statistical chirality-distributions in HRTEM. Moreover, by calibrating the obtained intensity distributions with e.g., theoretical Raman cross-sections3, a very good correspondence is obtained for most chiral structures, with only a few exceptions. Even though it is well known that absorption cross-sections, PL quantum efficiencies and Raman cross-sections are strongly dependent on the chiral structure of the SWCNTs, corrections for these cross-sections/efficiencies have rarely been applied for sample characterization and quantification. Here we provide a method to perform such corrections, thereby paving the way towards future routine calibration of Raman spectra. References :1 F. Yang, M. Wang, D. Zhang, J. Yang, M. Zheng and Y. Li,, DOI:10.1021/acs.chemrev.9b00835.2 A. Castan, S. Forel, F. Fossard, J. Defillet, A. Ghedjatti, D. Levshov, W. Wenseleers, S. Cambré and A. Loiseau, Carbon N. Y., 2021, 171, 968–979.3 V. N. Popov, L. Henrard and P. Lambin, Phys. Rev. B - Condens. Matter Mater. Phys., 2005, 72, 1–10. *Acknowledgements:* The research leading to these results has received funding from the European Research Council Starting Grant No. 679841 (ORDERin1D).

Carbon Nanomaterial Enabled Oxygen Electrocatalysts

Yuan Chen*†

**The University of Sydney*

The electrochemical redox reactions of oxygen (i.e., oxygen reduction reaction (ORR) to water and oxygen evolution reaction (OER) from water) govern the overall reaction rate in many electrochemical systems, including fuel cells, metal-air batteries, and water electrolyzers. Carbon materials, e.g., carbon black, have long been exclusively used as catalyst support for platinum-based electrocatalysts for ORR in low-temperature fuel cells. The emergence of carbon nanomaterials, such as carbon nanotubes (CNTs) and graphene, with well-defined structures and unique electronic, electrical, and chemical properties, offers opportunities to create new oxygen electrocatalysts. In this talk, two of our works in this area will be introduced. First, graphene oxide (GO) was used as a substrate to produce a family of amorphous bimetallic oxide nanoparticles anchored on N-doped reduced GO, achieving simultaneous control of nanoparticle elemental composition, size, and crystallinity. [1] Prussian blue analogues (PBAs) with controllable ratios and types of metal cations and cyanometallate anions were used as metal precursors, leading to nanoparticles with precisely controlled elemental composition. The size of PBA nanocrystals was controlled on GO surfaces using a polyethylenimine binder. Further, the crystallinity of metal oxide nanoparticles was controlled via oxidative decomposition. The optimal $Fe_{0.5}CO_{0.5}O_x$ anchored on N-doped reduced GO serves as an efficient bifunctional oxygen electrocatalyst to enable high-performance rechargeable zinc-air batteries. Second, coaxial one-dimensional van der Waals heterostructures (1D vdWHs) comprised of a CNT core and a thickness tunable thienothiophene-pyrene covalent organic framework (COF) shell using a solution-based in situ wrapping method. [2] Carbon–sulfur regions in thienothiophene groups in the COF serve as active catalytic sites. The coaxial structure enables n-doping from the CNT core to the COF shell, which is controllable by varying COF shell thickness. The charge transfer from CNTs lowers COF's bandgap and work function, which reduces the charge transfer barrier between the active catalytic sites and adsorbed oxygen intermediates, resulting in dramatically enhanced catalytic activity. The 1D vdWHs based on the coaxial structure of 2D COF wrapped around CNT cores may be further used as versatile building units to create multidimensional vdWHs for exploring fundamental physics and chemistry as well as practical applications in electrochemistry, electronics, photonics, and beyond. [1] L. Wei, Y. Chen et al., Advanced Materials 29, 1701410 (2017). [2] C. Liu, Y. Chen, et al., ACS Nano 15, 3309-3319 (2021). *Acknowledgements:* This work is supported Australian Research Council.

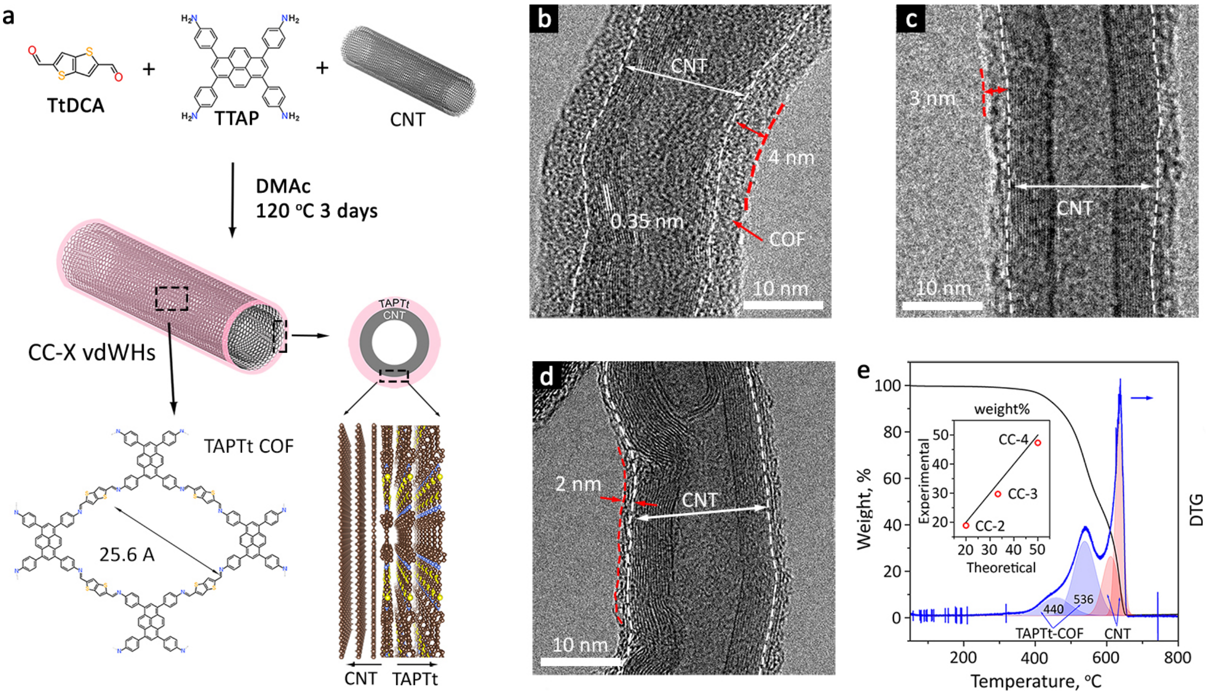

Fig. 1: (a) Schematic illustration of the synthesis of 1D vdWHs. (b–d) TEM images of 1D vdWHs. (e) TGA and DTG profiles (inset: weight fraction of COF).

Carbon Nanotubes Enable Delivery of Biomolecules to Plants Without Transgene Integration

Markita Landry*†

**University of California Berkeley*

Genetic engineering of plants is at the core of sustainability efforts, natural product synthesis, and agricultural crop engineering. The plant cell wall is a barrier that limits the ease and throughput with which exogenous biomolecules can be delivered to plants. Current delivery methods either suffer from host range limitations, low transformation efficiencies, tissue regenerability, tissue damage, or unavoidable DNA integration into the host genome. Here, we demonstrate efficient diffusion-based biomolecule delivery into tissues and organs of intact plants of several species with a suite of pristine and chemically-functionalized carbon nanotubes [1]. Efficient DNA delivery and strong protein expression without transgene integration is accomplished in mature Nicotiana benthamiana, Eruca sativa (arugula), Triticum aestivum (wheat) and Gossypium hirsutum (cotton) leaves and arugula protoplasts [2]. Notably, we demonstrate that transgene expression is transient and devoid of transgene integration into the plant host genome, of potential utility for easing regulatory oversight of transformed crops as genetically modified organisms (GMOs) [3]. We demonstrate that our platform can be applied for CRISPR-based genome editing for transient expression of Cas9 and gRNAs [4]. We also demonstrate a second nanoparticle-based strategy in which small interfering RNA (siRNA) is delivered to mature Nicotiana benthamiana leaves and effectively silence a gene with 95% efficiency. We find that nanomaterials both facilitate biomolecule transport into plant cells, while also protecting polynucleotides such as RNA from nuclease degradation. DNA origami and nanostructures further enable siRNA delivery to plants at programmable nanostructure loci [5], which we use to elucidate force-independent transport phenomena of nanoparticles across the plant cell wall [6]. Our work provides a tool for species-independent, targeted, and passive delivery of genetic material, without transgene integration, into plant cells for diverse plant biotechnology applications.1. Demirer, G.S., et al. Carbon nanotube-mediated DNA delivery without transgene integration in intact plants. Nature Protocols (2019). 2. Demirer, G.S., et al. High Aspect Ratio Nanomaterials Enable Delivery of Functional Genetic Material Without DNA Integration in Mature Plants. Nature Nanotechnology (2019). 3. Landry, M.P. et al. How nanocarriers delivering cargoes in plants can change the GMO landscape. Nature Nanotechnology 2019.4. Demirer, G.S. et al. Nanotechnology to advance CRISPR/Cas genetic engineering of plants. Nature Nanotechnology (2021). 5. Zhang, H., et al. Engineering DNA nanostructures for siRNA delivery in plants. Nature Protocols (2020).6. Zhang, H. et al. Low-dimensional DNA Nanostructures Coordinate Gene Silencing in Mature Plants. PNAS (2019).

Chemistry in the World's Tiniest Test Tube

Andrei Khlobystov*[†]

University of Nottingham

How do we know that molecules react in one way rather than another? Conventional analytical techniques, such as spectroscopy or diffraction, can only support rather than confirm a chemical reaction mechanism. Ultimate knowledge of the reactions can be provided only by studying them at the single-molecule level. Carbon nanotubes, 80,000 times thinner than a single strand of human hair, allow us to entrap molecules and film chemical reactions triggered by heat, electric potential or electron beam with atomic resolution [1] (Figure 1). Reactions in nanotubes often deliver unusual products, such as graphene nanoribbons [2,3], or enable improvements of important physical and chemical processes. For example, loaded with metal nanoparticles the nanotubes exhibit remarkable catalytic properties that can be exploited in many applications, including electrocatalysis in fuel cells [4], outperforming traditional materials (Figure 2). All this becomes possible due to the world's tiniest test tubes. References[1] S. T. Skowron et al., Acc. Chem. Res., 2017, 50, 1797-1807. [2] A. Chuvilin et al., Nature Mater., 2011, 10, 687-692. [3] T. W. Chamberlain et al., ACS Nano, 2017, 11, 2509-2520. [4] M. D. Gimenez-Lopez et al., Adv. Mater., 2016, 28, 9103-9105 *Acknowledgements:* Engineering and Physical Sciences Research Council (EPSRC), Royal Society, and Nanoscale & Microscale Research Centre (nmRC).

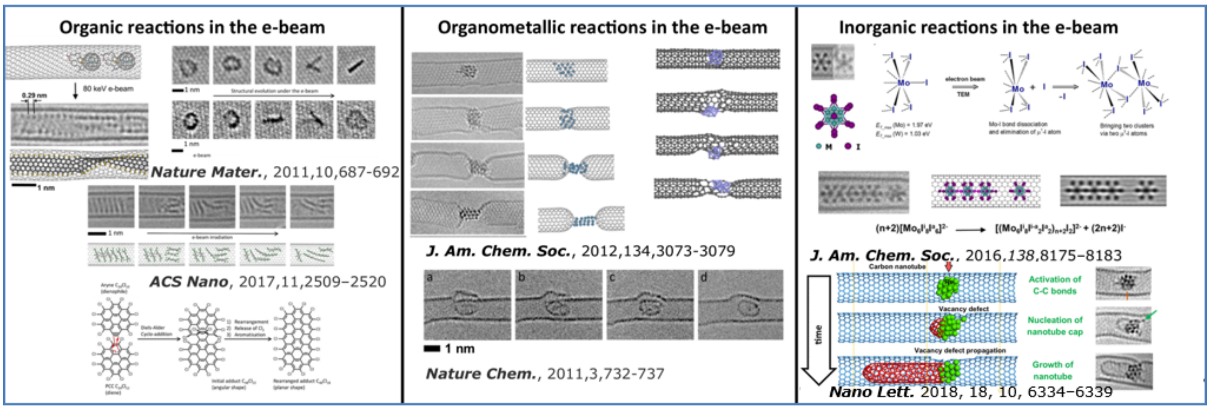

Fig. 1: Single-walled carbon nanotubes act as excellent nano-containers for molecules, chemical reactions of which can be explored with atomic resolution using transmission electron microscopy (TEM).

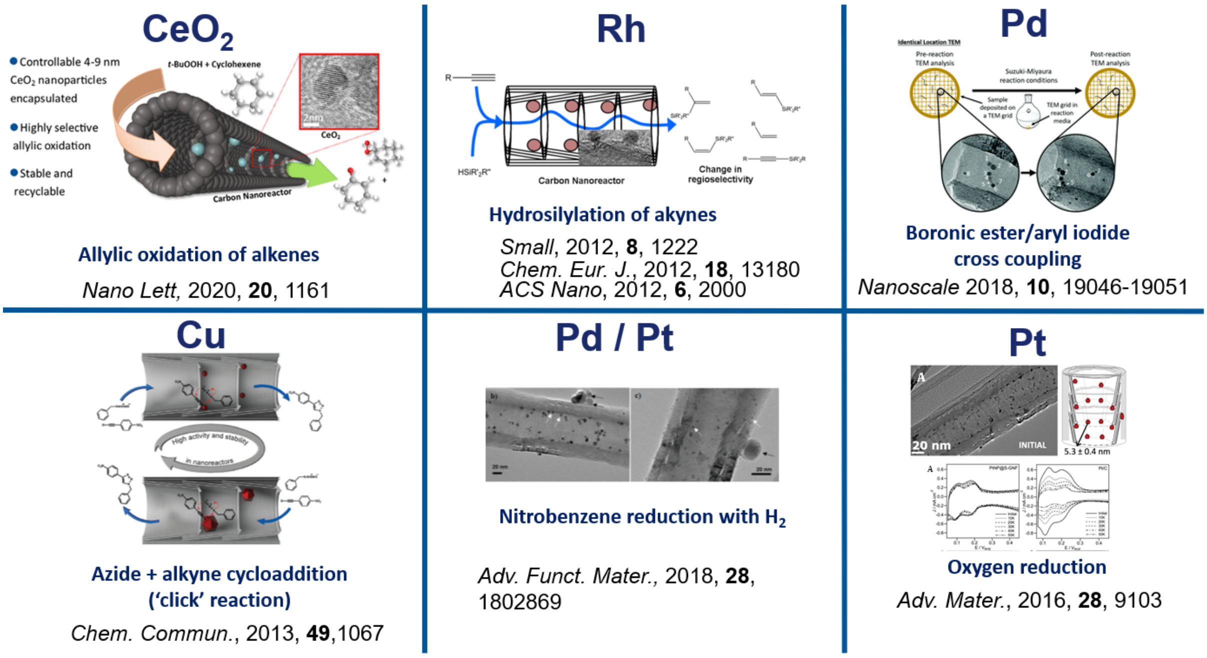

CeO_2

Allylic oxidation of alkenes

Nano Lett, 2020, **20**, 1161

Rh

Hydrosilylation of akynes

Small, 2012, **8**, 1222
Chem. Eur. J., 2012, **18**, 13180
ACS Nano, 2012, **6**, 2000

Pd

Boronic ester/aryl iodide cross coupling

Nanoscale 2018, **10**, 19046-19051

Cu

Azide + alkyne cycloaddition ('click' reaction)

Chem. Commun., 2013, **49**,1067

Pd / Pt

Nitrobenzene reduction with H_2

Adv. Funct. Mater., 2018, **28**, 1802869

Pt

Oxygen reduction

Adv. Mater., 2016, **28**, 9103

Fig. 2: Catalysis inside nanotubes can be performed on the preparative scale, with the nanotube protecting the catalytic centres and controlling selectivity of reactions.

Competing phases of correlated Chern insulators in Superconducting Twisted Bilayer Graphene

Dmitri K. Efetov*†

ICFO

Flat-bands in magic angle twisted bilayer graphene (MATBG) have recently emerged as a rich platform to explore strong correlations, superconductivity and magnetism. Here we use magneto-transport and Hall measurements to reveal a rich sequence of wedge-like regions of quantized Hall conductance with Chern numbers C = ±1, ±2, ±3, ±4 which nucleate from integer fillings of the moiré unit cell ???? = ±3, ±2, ±1, 0 correspondingly. We interpret these phases as spin and valley polarized many-body Chern insulators. The exact sequence and correspondence of Chern numbers and filling factors suggest that these states are driven directly by electronic interactions, which specifically break time-reversal symmetry in the system. In addition we observe correlated Chern insulator in zero magnetic field in hBN non-aligned MATBG, which manifests itself in an anomalous Hall effect around a filling of one electron per moiré unit cell n = +1 with a Chern number of C = 1 and has a relatively high Curie temperature of Tc ≈ 4.5 K. Slight gate tuning away from this state exposes strong superconducting phases with critical temperatures of up to Tc ≈ 3.5 K. In a perpendicular magnetic field above B > 0.5 T we observe a transition of the n = +1 Chern insulator from a Chern number C = -1 to a higher C = 3, which is characterized by a quantized Hall plateau with Ryx = h/3e2. These observations show that interaction-induced time-reversal symmetry breaking in MATBG leads to a zero-field ground state which consists of almost degenerate and closely competing Chern insulators, where the B-field always couples strongest to states with higher Chern numbers. Our study is also the first demonstration of a system which allows gate-induced transitions between magnetic and superconducting phases, and hence marks a major milestone in the creation of a new generation of quantum electronics.

Computational exfoliation of all inorganic materials, and what one can find there

Nicola Marzari*†

EPFL

We have performed an extensive high-throughput screening of all known inorganic materials, in order to identify those that could be exfoliated into novel two-dimensional monolayers and multilayers. The screening protocol first identifies bulk materials that appear layered according to a simple and robust chemical definition of bonding, determining then for all of these the binding energies of the respective monolayers, and their electronic state, magnetic configuration, and phonon dispersions. Such protocol identified a portfolio of close to 2,000 inorganic materials that appear either easily or potentially exfoliable, to be investigated further for promising properties - further enhancements have brought these to more than 3,500 candidates. I'll discuss some of the first notable case studies, involving 2D quantum spin Hall insulators and superconductors. *Acknowledgements:* Swiss National Center for Computational Design and Discovery of Novel Materials (NCCR MARVEL) and EU MaX Centre of Excellence

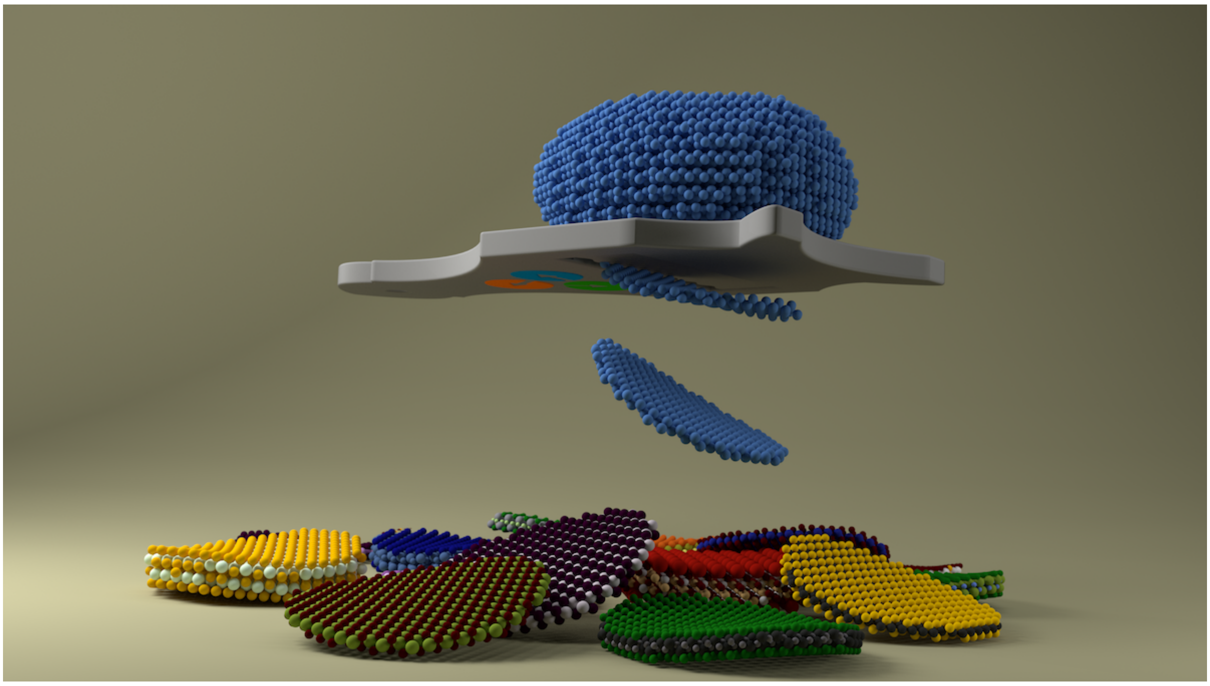

Fig. 1: A graphical illustration of the computational exfoliation.

Contact-Induced Phase Separation of Alloy Catalyst to Promote Carbon Nanotube Growth

Feng Ding*[†]

**Rice University/Ulsan National Institute of Science and Technology*

High yield of the alloy catalyst for carbon nanotube (CNT) growth has been a long-term mystery, and deep understanding on the mechanism is urgently needed. Using density functional theory molecular dynamic simulation, we observed that the alloy particle generally will undergoes a phase separation during the CNT growth due to the carbon affinity difference between the metal components. This CNT-catalyst contact induced phase separation led to the accumulation of the relatively more active metal at the CNT growth front, and the inert metal atoms then were pushed to the other side of the alloy particle. Further investigation shows that the phase separated alloy benefits for the CNT growth by attracting the dissolved carbon atoms to quickly diffuse to the CNT-catalyst interface and, therefore, facilitating the CNT growth; preventing the dissolved carbon atoms to aggregate on the catalyst particle surface to avoid the poisoning of the catalyst during tube growth. The work reveals the mechanism of the high efficiency of alloy catalysts and paves the way of rational catalyst design for CNT growth.

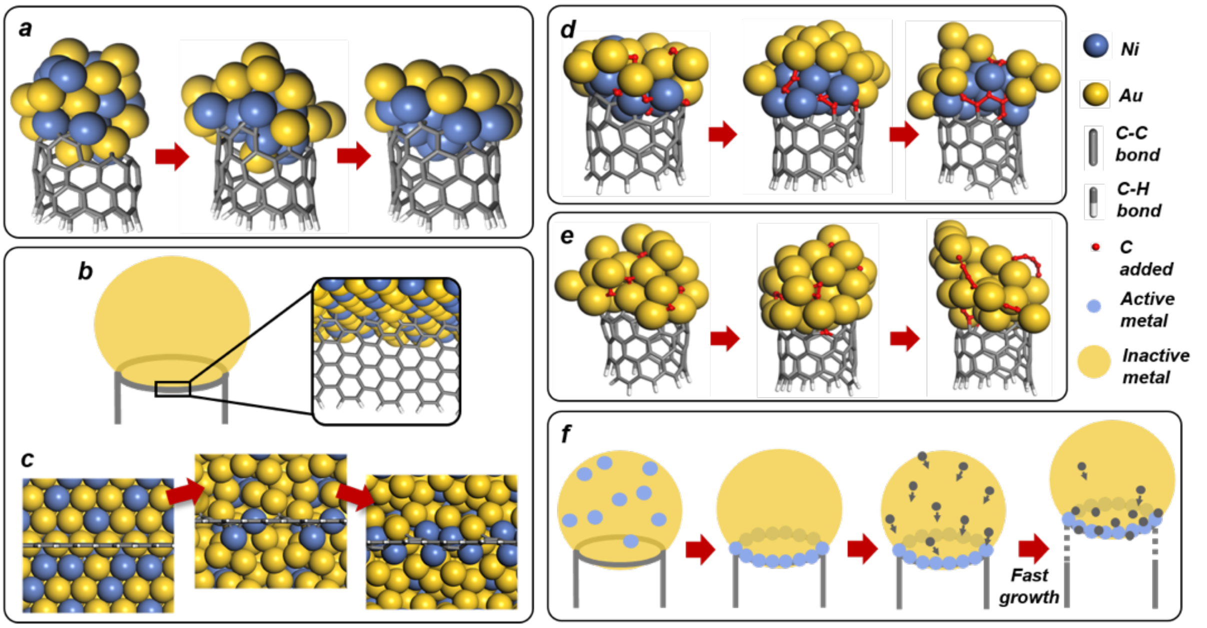

Fig. 1: Separation of the two metal components in alloy catalysts during CNT growth (a) in a small particle and (b-c) at the interface of a large particle. (d) Phase separated alloy catalyst leads to the fast diffusion of carbon source to the growth front, resulting in efficient CNT growth. (e) Random diffusion of carbon source in mono-metallic catalyst. (f) Illustration of the alloy catalyst promoted CNT growth.

Deep-ultraviolet spectroscopy in hexagonal boron nitride: from bulk to monolayer

Guillaume Cassabois*[†]

**Montpellier University*

Hexagonal boron nitride (hBN) is an ultrawide bandgap semiconductor with a large range of basic applications relying on its low dielectric constant, high thermal conductivity, and chemical inertness. The growth of high-quality crystals in 2004 has revealed that hBN is also a promising material for light-emitting devices in the deep ultraviolet domain, as illustrated by the demonstration of lasing at 215 nm by accelerated electron excitation [1], and also the operation of field emitter display-type devices in the deep ultraviolet [2]. With a honeycomb structure similar to graphene, bulk hBN has gained tremendous attention as an exceptional substrate for graphene with an atomically smooth surface, and more generally, as a fundamental building block of Van der Waals heterostructures [3].I will discuss here our recent results shining a new light on the efficient light-matter interaction in hBN. I will first present experiments in monolayer hBN epitaxially grown on graphite. Compared to the reflectivity spectrum of the bare graphite substrate, a huge contrast is observed in the reflectivity of atomically-thin hBN deposited on graphite, demonstrating a radiative efficiency close to unity in monolayer hBN. I will then address the optoelectronic properties of bulk hBN where high-resolution measurements in high-quality samples allow to resolve the respective contributions of indirect and direct optical transitions and quantify the strength of the light-matter interaction in bulk hBN.References[1] K. Watanabe, T. Taniguchi, and H. Kanda, Nature Mater. 3, 404 (2004). [2] K. Watanabe, T. Taniguchi, T. Niiyama, K. Miya, and M. Taniguchi, Nature Photon. 3, 591 (2009). [3] A. K. Geim and I. V. Grigorieva, Nature 499, 419 (2013).

Developing twisted stacked 2D heterostructures with atomic resolution in situ imaging and vice-versa

Sarah Haigh*[†]

**University of Manchester*

2D materials and their heterostructures provide an exciting playground for pioneering science. In this talk I will demonstrate how atomic resolution scanning transmission electron microscopy (STEM) imaging and analysis is being used to support advancement of these systems and how 2D heterostructures provide possibilities for new in-situ imaging experiments.As an exemplar of STEM applied to develop new understanding of 2D heterostructures, I will discuss structural relaxation when two transition metal dichalcogenide (TMDC) monolayers are misoriented by a small twist (rotation angle). Many high profile experimental measurements of the exciting physics present in twisted TMDCs have necessarily neglected the potential for local structural relaxation. We have used atomic resolution STEM to reveal the local reconstructions that occur when TMDCs bilayers twisted to a small angle (Fig1a) [1]. Complementary tunneling spectroscopy measurements (Fig1b) reveal that reconstruction creates strong piezoelectric textures and pseudo-magnetic fields, opening new avenues for engineering of 2D material properties on the nanometre scale [1]. Measurement of strain, stacking and creases in 2D stacks can also be achieved by convergent beam elemental mapping [2]. Our STEM imaging of the most challenging 2D heterostructures has been enabled via a new design of TEM support grid [3]. Other examples where these support grids have facilitated new STEM characterization are revealing oxidation induce improvement of superconductivity in few layer TaS2 [4], defects and edges in CrBr3 [3] and GaSe/InSe [5].As an exemplar of heterostructures for new in-situ imaging, we have demonstrated nanopatterning of hBN/graphene encapsulated black phosphorus in the STEM, optimizing etching parameters that were then successfully applied to electron beam lithography, patterning with improved resolution compared to traditional photoresists [6]. More recently we have demonstrated the use of a complex 2D heterostructure platform for performing liquid mixing experiments. This provides the advantage that imaging of the mixing products can be achieved at atomic resolution and the mixing occurs directly in the field of view to the earliest stages of growth can be observed. [1] A. Weston et. al, Nature Nanotechnology, 15, 592–597, (2020) https://www.nature.com/articles/s41565-020-0682-9[2] T. Latychevskaia, et al PNAS, 115 (29) 7473-7478 (2018) https://doi.org/10.1073/pnas.1722523115[3] M.J. Hamer et al., Nano Lett. 20, 9, 6582–6589, (2020) https://pubs.acs.org/doi/abs/10.1021/acs.nanolett.0c02346[4] J Bekaert, et al, Nano Letters, 20 (5), 3808-3818, (2020) https://pubs.acs.org/doi/abs/10.1021/acs.nanolett.0c00871[5] D G Hopkinson et al, ACS Nano, 13 (5), 5112-5123, (2019) https://pubs.acs.org/doi/abs/10.1021/acsnano.8b08253[6] N. Clark et al, Nano Letters, 18 (9), 5373-5381, (2018) https://pubs.acs.org/doi/abs/10.1021/acs.nanolett.8b00946 *Acknowledgements:* EPSRC, ERC Starter Grant H2020 715502

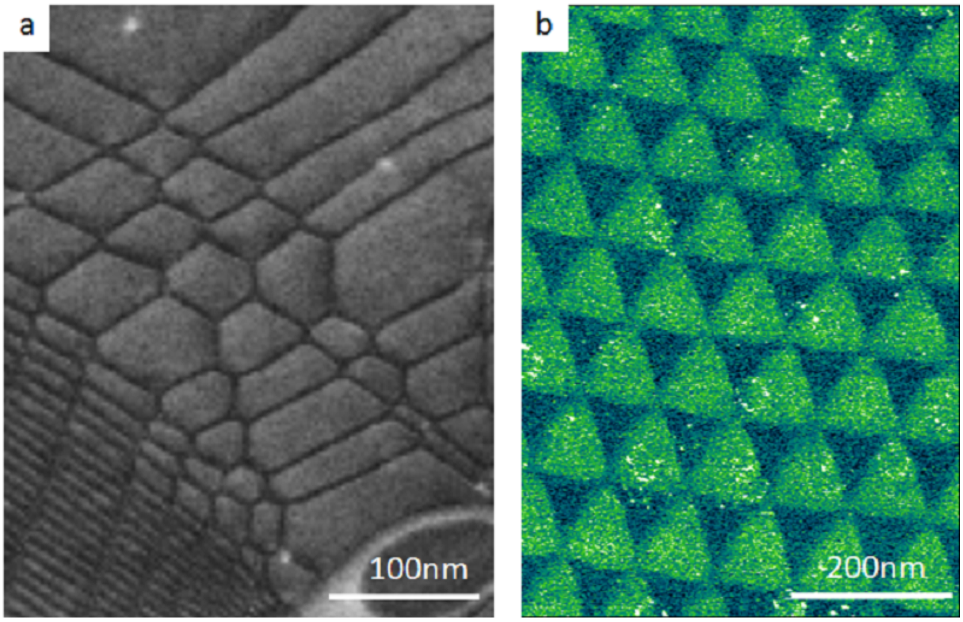

Fig. 1: Images of lattice reconstruction in twisted TMDC lattices. (a) annular dark field STEM and (b) conductive atomic force microscopy data.

Directed evolution of carbon nanotube growth and its unique properties

Fei Wei*†

**Tsinghua University*

Extraordinary properties and great application potentials of carbon nanotubes (CNTs) fundamentally rely on their large-scale perfect sp2 structure. Particularly for high-end applications, ultralow defect density and ultrahigh selectivity are prerequisites. CNTs can themselves provide growth templates and nonlocal dual conductance, serving as template autocatalysts with tunable bandgap during the CVD. We will show that the CNT growth is a clear single-atom-level evolvable system only composed of carbon atom replicators. Based on the template autocatalytic kinetics, defective, metallic and semiconducting CNTs sequentially die out during the 650-mm-long evolution. Rate analysis verified the Schulz-Flory (SF) distribution for both metallic (m-) and s-CNTs, indicating their different decay rates as length increased. Quantitatively, a nearly ten-fold faster decay rate of m-CNTs, led to a spontaneous purification of the predicted 99.9999% s-CNTs at a length of 154 mm through an optimization of the reactor. We show that defect-free CNTs have superior comprehensive mechanical properties, by using an in-situ gas flow focusing synthesis method and a synchronous tightening and relaxing strategy to minimize the "defects", we successfully fabricated CNT bundles with tensile strength close to that of single CNTs. Future trends and prospects in the development of CNTs used as energy storage and conversion materials are presented.

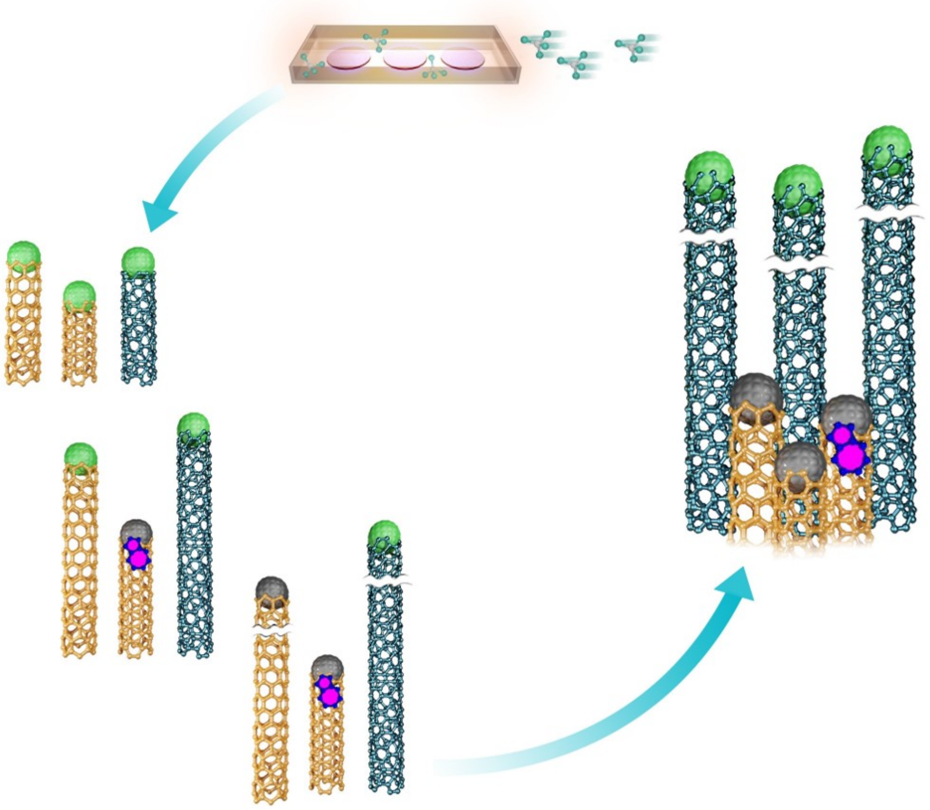

Fig. 1: Schematic of the directed evolution method for selected carbon nanotube growth

DNA-directed precise pitch-scaling for high-performance CNT FETs

Wei Sun*[†]

**Department of Electronics, Peking University*

Precise scaling the channel pitch of CNTs is one prerequisite towards future ultra-scaled field-effect transistors (FETs). Although bio-fabrication is promising for patterning CNTs at a resolution beyond the existing lithographic limit, current bio-templated electronics still suffer from both poor transport performance and array uniformity smaller than 1 micron. To overcome these technical obstacles, we report precise scaling of inter-CNT pitch using a supramolecular assembly method called Spatially Hindered Integration of Nanowire Electronics (SHINE). Specifically, by using nano-trenches to align CNTs and DNA hybridization to stabilize them in place, we constructed parallel CNT arrays with uniform pitch as small as 10.4 nm, at an assembly yield over 95%. The pitch precision improves on that prepared from conventional thin-film approaches by more than two orders of magnitude. Compared to the lithography-patterned Si channels at 10 nm technology node, SHINE simultaneously provides both 70% smaller averaged pitch value and molecular-scale pitch precision in the channel area. By engineering the interfacial compositions, metal ions and surface charges that are destructive to FET performance have been excluded from the channel area without degrading CNT alignment. Transconductance reaches up to 0.6 mS/μm at a subthreshold swing of 160 mV/dec when channel length scales down to 100 nm. DNA-directed nanofabrication thus balances both high transconductance and fast on/off switching, which is still difficult from other approaches. And the key FET performance metrics are improved by more than one order of magnitude than previous bio-templated FETs. Furthermore, using spatially confined placement within PMMA cavities, we demonstrate centimeter-scale alignment of fixed-width CNT arrays with prescribed orientations, periodicity, and inter-CNT pitch. The minimal orientation distribution could reach ±3.4° standard deviation depending on the DNA lengths. At the interface of high-performance electronics and bio-molecular self-assembly, DNA-directed nano-fabrication could provide ultra-scaled devices or circuits compatible with or sensitive to local biological environments.

Electroluminescence from graphene-contacted (7,5) carbon nanotubes with defects

Ralph Krupke*†, Min-Ken Li, Frank Hennrich, Simone Dehm

Institute of Nanotechnology, Karlsruhe Institute of Technology, Karlsruhe 76021, Germany

We have recorded low-temperature electroluminescence spectra from (7,5) carbon nanotubes with side-wall defects. The defected nanotubes, which have been wired tographene electrodes, show emission peaks that are sensitive to gate voltage and overall doping. We will discuss the results in view of complementary electrical transport andphotoluminescence measurements.

Enhancing Carbon Nanotube Production via Careful Control over Catalyst

Suguru Noda*†

Waseda University

Extensive research has been made for carbon nanotube (CNT) synthesis, but continuing progress is important to meet the industrial demands.Catalyst underlayer should be carefully designed to enhance the densities of catalyst particles and resulting CNTs on substrates. By controlling the formation process of Fe catalyst particles on TiN/Ta layer, we realized ~50 µm-tall, ~0.30 g/cm3-dense CNT arrays on both faces of Cu foils, which showed promising performance for thermal interface materials [1]. By applying the Fe on Fe-Al-O bilayer structure to the catalyst deposition from nitrate mists, we realized submillimeter-long few-wall CNTs on ceramic beads by fluidized bed [2]. Enhancing the catalyst lifetime is also important. Using CO2 as additive, we realized > 1 mm tall CNT arrays on Al, which will be used for thermal management and electrochemical energy storage [3]. CO2 is milder than H2O in oxidation thus can be used at high concentration. By CO2-assited CVD, we realized uniform millimeter-tall array of single-wall CNTs (SWCNTs) over large number of substrates (Figure) [4].Quick heating is effective in making small catalyst particles at high densities. By applying resistive heating to the flame-synthesized Co-Al-O nanopowder, we synthesized highly crystalline SWCNTs at ten-second time scale [5]. Using a premixed flame for instantaneous gas heating and catalyst source decomposition, we realized continuous production of 1-nm-diameter SWCNTs (Figure) [6]. [1] N. Na, et al., Jpn. J. Appl. Phys. 54, 095102 (2015). [2] M. Li, et al., Carbon 167, 256 (2020). [3] S. Miura, et al., Carbon 130, 834 (2018). [4] T. Sato, et al., Carbon 136, 143 (2018). [5] H. Shirae, et al., Carbon 114, 31 (2017). [6] S. Okada, et al., Carbon 138, 1 (2018).

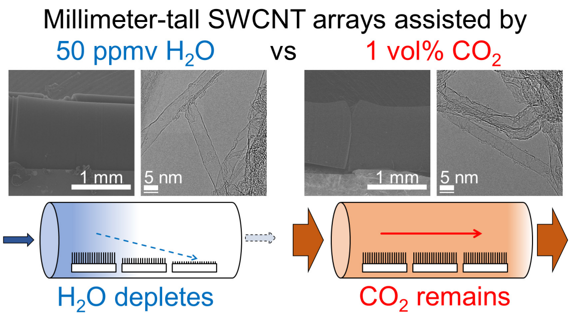

Fig. 1: Millimeter-tall SWCNT array over multiple substrates via CO2-assisted CVD [4].

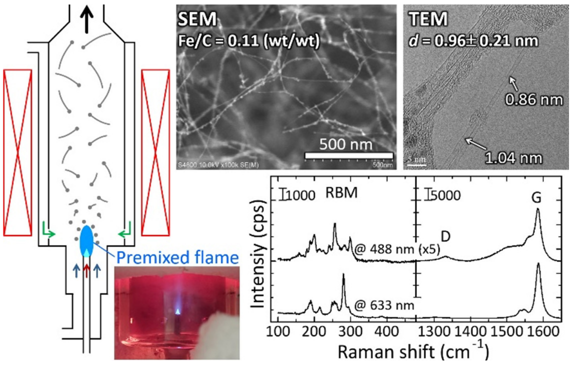

Fig. 2: Continuous production of 1-nm-diameter SWCNTs by flame-assisted CVD [6].

Flash Graphene. Trash to Treasure

James Tour*†

Rice University

A route to graphene from any carbon source using flash Joule heating will be discussed. The process is scalable. And it can be used for other 2D materials syntheses as well. *Acknowledgements:* AFOSR and DOE

Full spectrum Raman excitation mapping of carbon nanotubes and making Raman spectroscopy more metrological

Paul Finnie*†

**National Research Council Canada*

An important effort in the early days of single walled carbon nanotube (SWNCTs) was to determine the relationship between the optical resonances and physical structure which is summarized by the Kataura plot. Knowing this relationship, in Raman spectroscopy (RS) the presence and abundance of (n,m) species can be determined for example by exciting with fixed wavelength, resonant lasers and evaluating the intensities of Raman bands . A practical application is estimating semiconducting purity (or ”metallicity”). But, SWCNTs have many optical excitation resonances, and also many (vibrational) Raman bands. Also, it is understood that the Kataura plot is not fixed, but rather shifts. Furthermore, the required data can be experimentally challenging to obtain. The ideal would be to get the entire optical excitation spectra and the entire vibrational spectrum quickly, together, making a map of the vibrational modes as a function of excitation wavelength - the Raman excitation map (REM). While this has been possible to capture, until recently it has been experimentally difficult, rather time consuming, and costly. Motivated by this, I will describe our work on the ”full spectrum” REM technique which can obtain such data quickly and in a relatively straightforward way. I will explain how this can enable detection and quantification with great sensitivity and great specificity.More than just REM mapping alone, in general, RS is critical for characterization of SWCNTs and other carbons, and its use is becoming more and more widespread in advanced materials and many other fields. Given growth of RS, there is a need to update standards and references to make the technique more fully metrological. I will discuss work underway to improve the metrology of RS, particularly through the Versailles Project on Advanced Materials and Standards (VAMAS). I will describe how anyone involved in RS can contribute and outline some related opportunities for the metrology of SWCNTs and nanocarbons.

High-performance materials based on nanoscopic building blocks: from composites to electrodes

Juan Vilatela*†

**IMDEA Materials*

This talk is focused on methods to assemble one-dimensional nanomaterials into macroscopic ensembles with bulk properties in the high-performance range, i.e. on par or above reference engineering materials. First, it provides a brief review of the different assembly methods and the resulting volume fractions attained: i) by dispersing nanomaterials as fillers, ii) from thermodynamic solutions of nanocarbons analogous to rigid-rod polymers iii) by direct assembly from the gas phase. Next, progress on the development of the fibres of aligned carbon nanotubes (CNT) is presented (1). The tensile properties of CNT fibres and fabrics are shown to be dominated by the degree of alignment of their constituents and fail by CNT pull-out, with no evidence of CNT fracture, analogous to a macromolecular network of crystallites. The micromechanics of these systems can be described through the uniform stress transfer model using 2D X-ray diffraction methods to obtain structural descriptors of the orientation of CNTs (2). Finally, the talk presents examples of fabrics of other 1D nanomaterials also produced by assembly from the gas phase, supporting the view that spinning of yarns from aerogels produced by floating catalyst chemical vapour deposition is a universal route for 1D inorganic materials (3), with particular promise as a method for solvent-free fabrication of nanostructured electrodes for energy storage and conversion. ReferencesAnastasiia Mikhalchan and Juan José Vilatela - A Perspective on High-performance CNT fibres for Structural Composites. Carbon 150, 191-215, 2019. DOI: 10.1016/j.carbon.2019.04.113J. C. Fernández-Toribio, B. Alemán, A. Ridruejo and J. J. Vilatela - Tensile properties of carbon nanotube fibres described by the fibrillar crystallite model. Carbon 133, 44-52, 2018. DOI: 10.1016/j.carbon.2018.03.006Richard S. Schäufele, Miguel Vazquez-Pufleau, Juan J. Vilatela - Tough sheets of nanowires produced floating in the gas phase. Materials Horizons 7, 2978-2984, 2020. DOI: 10.1039/D0MH00777C

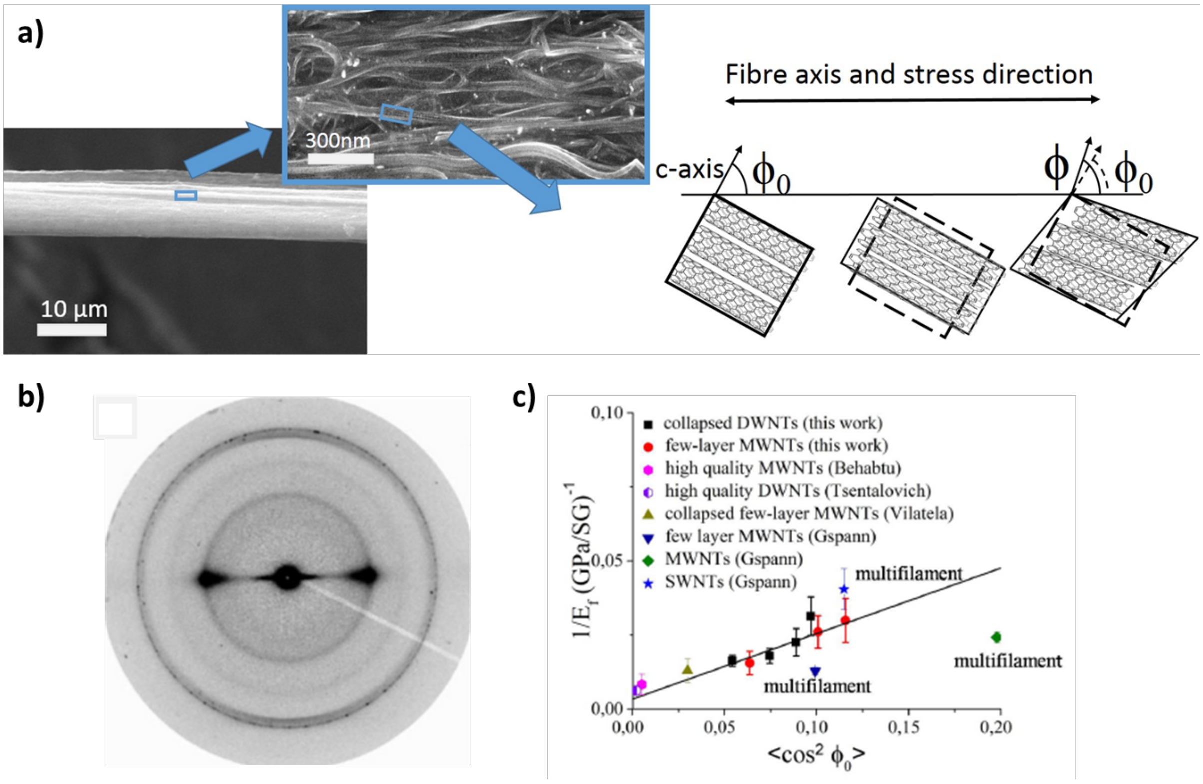

Fig. 1: Tensile properties of CNT fibres. A) micrographs of am aligned CNT fibre and schematic representation of the predominant deformation mechanisms. B) 2D WAXS/SAXS patterns. C) Relation between fibre compliance and orientation parameter.

Imaging of Brown Adipose Tissues by Using Carbon Nanotubes as NIR Fluorescent Probes

Masako Yudasaka*†, Yuko Okamatsu-Ogura, Takeshi Tanaka, Kumiko Saeki, Hiromichi Kataura

**National Institute of Advanced Industrial Science and Technology (AIST)*

Near-infrared (NIR) photoluminescent single-walled carbon nanotubes (CNTs) are effective bio-imaging agents, providing clear images of mice vasculature. This is because the biological auto fluorescence is weak, light transmittance through the tissue is high, and light scattering by the biological system is low in NIR wavelength region. We have shown that CNTs coated with poly(2-methacryloyloxyethyl phosphoryl choline-co-n-butyl methacrylate) (PMB) with high bio-affinity did not image vasculature but imaged brown adipose tissues (BAT) of mice clearly as certain apolipoproteins in blood transferred to PMB-CNT [1]. Since BAT has an exceedingly high heat-productive capacity, BAT is considered as a new target for therapeutic researches of obesity-associated metabolic disorders, where non-invasive imaging of BAT will be crucial. Interestingly, CNTs coated with phospholipid polyethylene glycol (PLPEG-CNTs) did not image BAT in normal mice, but clearly imaged BAT in the fasted mice [2]. NIR-fluorescent microscopy revealed that the PLPEG-CNT accumulation in BAT under fasting was due to the extravasation of PLPEG-CNTs from capillaries and arterioles, suggesting that fasting induced the disorders in vascular basal membranes. In response to this, extracellular matrix (ECM) in BAT were remarkably damaged under the fasting. However, these disorders were quickly recovered with high integrity by re-feeding, and, therefore, the ECM disorders induced by fasting in BAT can be regarded as physiological change but not pathological one [2]. Analogous phenomena were observed in BAT of mice against the cold stimulation. In summary, this study has shown that the CNTs are NIR fluorescence agent useful to find the physiological ECM-remodeling occurring in BAT under the life crisis such as starving and low body temperature, which had been unknown phenomenon until this study has revealed. Details are discussed in the presentation. Acknowledgement: Authors acknowledge the collaborators, Dr. M. Zhang and Dr. Y. Yomogida in AIST, Dr. M. Nakahara and Dr. N. Kobayashi in NCGM, and Prof. K. Ishihara in the Univ. of Tokyo. This work was supported by JSPS KAKENHI, grants no. 16H02085 and 25220602[1] Yudasaka et al. Sci. Rep. 2017; 7: 44760. [2] Yudasaka et al. Sci. Rep. 2018; 8: 14446.

Interacting Excitons in van der Waals Heterostructures of TMDs

Ajit Srivastava*†

Emory University

Atomically thin materials, such as graphene and transitional metal dichalcogenides (TMDs), have recently come to the forefront of research in materials physics. This is largely due to the ease with which they can be combined into artificially engineered heterostructures that exhibit emergent electronic and optical properties. Enhanced Coulomb interactions in the truly 2D limit and flat bands in TMD moiré heterostructures, such as $MoSe_2/WSe_2$, provide a rich platform to explore correlated quantum phases of matter.In this talk, I will begin by highlighting some unique properties of optical excitations in TMDs which result from the chiral nature of constituent single-particle electronic states. Unlike their monolayer counterparts, excitons in heterobilayers feature a permanent electric dipole which can be used to tune their emission energy electrically. I will present our results showing few-body interactions between dipolar excitons which result can be exploited for quantum nonlinearity1. I will also present our recent results wherein many-exciton dipolar interactions result in exchange fields of ~6 Tesla2. Finally, I will conclude by discussing the outlook for realizing strongly interacting phases of optical excitations in 2D materials.1. W. Li, X. Lu et al., Nature Materials. 19, 624-629 (2020).2. W. Li, X. Lu et al., Nature Nanotechnology 16, 148-152 (2021).

Is Nanocarbon Black, Green, or Both? Towards Sustainable Energy with Carbon Nanotubes

Dawid Janas*†

Silesian University of Technology, Poland

Methane, carbon dioxide, and coal brought ill fame to carbon-based materials. For a long time, avoiding solutions based on this element was a somewhat accurate rule of thumb on how to make technology appear more eco-friendly. The discovery of carbon nanomaterials such as fullerenes, carbon nanotubes, and graphene at the turn of the 21st century revolutionized the way we perceive this building block. Exceptional electrical, thermal, optical, and mechanical properties convinced the R&D environment that, under the right circumstances, carbon could be the solution, not the problem. Ever since these structures were first synthesized, more and more evidence comes to light that they can outperform many classical materials used for hundreds of years. In this talk, the key merits of carbon nanostructures for sustainable development will be presented. First, a selection of methods for synthesizing and tuning the properties of nanocarbon by modifying its properties will be illustrated. Then, straightforward techniques of transforming these powder materials into macroscopic networks will be shown. Finally, an outline of the most mature applications in the field of energy management will be described. *Acknowledgements:* National Center for Research and Development (LIDER/0001/L-8/16/NCBR/2017) and the National Science Center (2019/33/B/ST5/00631)

Machine learning enabled nanosensor array platform for cancer diagnosis

Mijin Kim*, Peng Wang, Chen Chen, Yoona Yang, Hongbin Luo, Merav Antman-Passig, Christopher Wun, Anand Jagota, Ming Zheng, YuHuang Wang, Daniel Heller, Zvi Yaari†

Memorial Sloan Kettering Cancer Center

Organic color centers (OCCs) are synthetic quantum defects incorporated into semiconducting single-walled carbon nanotubes by the covalent attachment of functional groups to the nanotube sidewalls. OCCs feature extraordinary traits that make these synthetic materials an ideal platform for biochemical sensing applications. First, the OCC-induced fluorescence peak confers new sensitivities determined by the chemical nature of the defect, making OCCs the molecular focal points for chemical detection. Second, the OCC fluorescence is extremely sensitive to the local microenvironment and can be systematically controlled by tailoring the functional defects. Such structural diversity and chemical sensitivity of OCCs can be translated into a rich family of biochemical probes that sensitively and selectively respond to diverse classes of analytes. Herein, we present an array of OCC-based nanosensors that enables multiplexed sensing of biomarkers in serum. The diverse spectral responses of the sensor array, processed by data analytics, collectively determine the disease state.

Morphogenesis of Assembled Carbon Nanostructures towards High-Performance Materials

Zhiping Xu*†

**Tsinghua University*

Low-dimensional carbon nanostructures such as carbon nanotubes and graphene are unconventional macromolecules. Their macroscopic assemblies in the forms of fibers and films hold great potential as high-performance and multifunctional materials for applications in, for example, aerospace engineering.The cooperative van der Waals adhesion between sp2 graphitic lattices in these nanostructures make the closely-packed bundles of nanotubes or laminates of graphene sheets ground states in the potential energy landscape. However, the non-equilibrium conditions of the fabrication processes (dry or wet spinning, filtration or evaporation) accommodate entropic effects that modulate morphology and arrangement of the nanostructures, as well as symmetry-breaking processes where phases are separated.In this presentation, I will introduce our recent theoretical and experimental exploration of the 'morphogenesis' of assembled carbon nanostructures, including (1) morphological phase diagram of graphene as two-dimensional macromolecules, (2) alignment of low-dimensional nanostructures with entropy effects, (3) microstructural heterogeneity in fibers and films made of carbon nanostructures. Load transfer and energy transport in these assemblies will also be discussed to understand the processing-microstructures-performance relationship.

New theory insights in 1D-nanotubes and 2D-layers growth and properties

Boris Yakobson*†, Ksenia V. Bets

**Rice University*

There is no unified, synthetic theory of nanotube or 2D-materials growth, no "ToE". Perhaps never will be, yet useful progress can be achieved. By embracing old ideas of Burton–Cabrera–Frank, we introduced a dislocation-growth model for nanotubes [PNAS 106, 2506, 2009], a seed for the later general nanoreactor approach [PNAS 109, 15136, 2012], allowing to use DFT computations for 2D-material growth kinetics or emerging shapes. It works well in many cases but not all, leaving room for creativity. We will discuss things new since NT19: from the complementarity in lateral epitaxy [Nano Lett. 19, 2027, 2019 || Nature 579, 219, 2020], to chemically induced grapheneàdiamond transformation ("no pressure - good science", as AVS T-shirts once claimed) [Small 16, 2004782, 2020], to possibly—if time permits—new physics achievable in hetero-bilayers [Nat. Comm. 11, 2989, 2020 || Nano Lett. 20, 3240, 2020 || Science, 367, 506, 2020 || Nano Lett. 21, 785, 2020 || JACS 143, 350, 2021], and even the machine learning (ML) about the CNT [A. Kutana, P. O'Driscoll, K. Bets, BIY, in progress].

Pushing the Bounds of CNT Floating Catalyst Synthesis Quality Versus Quantity

Adam Boies*†, Liron Issman, Michael Glerum, Jeronimo Torrones Portas, Mabel Rulan Qiao, Fiona Smail, James Elliott

**University of Cambridge*

Increased production of CNTs requires high density reactors that produce sufficient quality CNTs for industrial applications. The complexity of the FC-CVD synthesis process in reactors at increasing product density has historically limited efforts for increased volumetric reactor yields. Our work targets the trade-offs associated with different rates within the reactor to bound the synthesis windows for precursor concentrations. We will discuss how the competing collision and reaction rates provide fundamental limits for FC-CVD production that are bounded by catalyst coarsening and unwanted pyrolytic reactions. Thus, targeting CNT growth requires finding operation windows whereby carbon radical – catalyst collisions leads to the predominant reaction pathway. Our findings indicate that under typical synthesis conditions common in literature the carbon radical – catalyst collision rate is 106 and 102 times higher than catalyst-catalyst or radical-radical collisions, respectively. Typical CNT carpet growth rates, without sulphur, found in literature span 0.2-17 microns per second and rates are typically enhanced by sulphur addition. The growth rate of CNTs in an FC-CVD process is approximated to ~100 µm/s. The aerogelation reaction produces long CNTs (minimum tens of microns) in only a few seconds growth time. Improved reactor control based on understanding how to increase the temporal growth window while preventing catalyst encapsulation will be key in increasing overall production.Collectively, studies from the CNT FC-CVD community show that increased reactor yields often leads to decreases in product quality. Therefore, additional strategies for processing or controlling the macroscopic structure of CNTs are needed. Improved quality of individual CNTs may be brought about by more precise control of catalysts, but methods for single chirality control by means of catalyst engineering are still problematic for large-scale synthesis methods. Our recent work has used in-situ electrical fields to control the formation of the aerogel allowing for a greater degree of alignment. Our studies show that alignment of bulk aerogel increases from nearly isotropic random alignment of CNTs in a 2-D plane to bulk 1-D alignment when aerogel synthesis occurs in the presence increasing electric field strengths. The work shows promise to enable high throughput material production that can achieve aligned CNT bundles prior to post processing. Further work may allow post-processing techniques that may ultimately allow for further advancement of these aligned CNT materials.

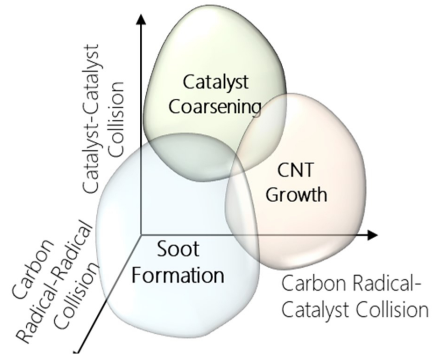

Fig. 1: Conceptual schematic of operational window for FC-CVD CNT synthesis.

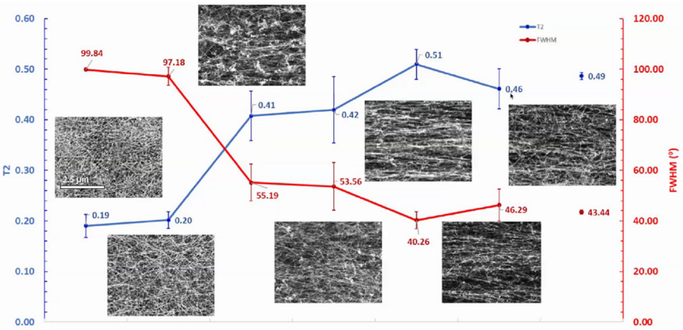

Fig. 2: Alignment of FC-CVD CNTs with increasing electric field (x-axis). The alignment was quantified from SEM by the Chebyshev polynomial T2 (left) and full-width-at-half-maximum (right).

Raman D bands appears upon folding: the case of flattened carbon nanotubes

Alain Penicaud†, Emmanuel Picheau*, Anthony Impellizeri, Dmitry Rybkovskiy, Maxime Bayle, Chris Ewels, Pascal Puech, Abraao Cefas Torres Dias, Jean Yves Mevellec, Marc Monthioux, Bernard Humbert

**Centre de Recherche Paul Pascal UMR CNRS Bordeaux*

Above a critical diameter, single or few-walled carbon nanotubes spontaneously collapse as flattened carbon nanotubes. Raman spectra of isolated flattened and cylindrical carbon nanotubes have been recorded. The collapsing provokes an intense and narrow D band, despite the absence of any lattice disorder. The curvature change near the edge cavities activates a D band, despite framework continuity. Theoretical calculations fully corroborate this experimental finding. Usually used as a tool to quantify defect density in graphenic structures, the D band cannot be used as such in the presence of graphene fold. This conclusion should serve as a basis to revisit materials comprising structural distortion where poor carbon organization was concluded on Raman basis. This finding also emphasizes the different visions of a defect between chemists and physicists, a possible source of confusion for researchers working in nanotechnologies.

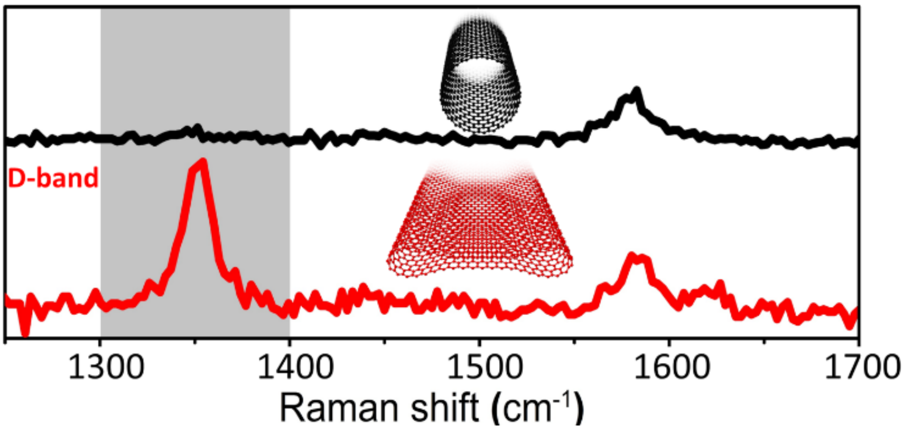

Fig. 1: Experimental spectra of a flattened carbon nanotube (bottom, red) and a circular carbon nanotube (top, black).

Revealing the nucleation, growth mechanisms and role of catalyst of single walled carbon nanotube growth

Renu Sharma*†

**National Institute of Standards and Technology*

Direct observation of chemical processes, at an atomic scale, provide unprecedented information about the structural mechanisms involved. For example, the vapor-liquid-solid (VLS) model for the nucleation and growth of carbon nanotubes (CNTs), proposed by Baker[1] and confirmed by theory, was universally accepted for long time. However, in-situ environmental transmission electron microscope (ETEM) offered a platform to directly image the chemical vapor deposition process for the CNT growth and showed that the nanotubes grow via vapor solid-solid (VSS) mechanism instead. [2, 3] These observations were confirmed for various catalyst and by other groups [4, 5], opening the door to investigate the possibility to control the chirality of single walled nanotubes (SWCNTs) by keeping the catalyst in solid state at growth temperatures. [6] Over last 20 years, my group, in collaboration with a number of research groups around the world, have made direct observations of SWCNT nucleation and growth mechanisms at an atomic scale. We have used various catalyst/support systems with acetylene as carbon source. With the help of our theory collaborators, we have been able to decipher the role of catalyst structure and surface facet in controlling the lift-off and deactivation. We also find that the growth dynamics are also associated with the catalyst structure fluctuations. Critical contributions towards the synthesis SWCNTs will be highlighted. Reference: 1. Baker, R.T.K., Barber, M.A., Harris, P.S., Feates, F.S., Waite, R.J., Nucleation and growth of carbon deposits from the Ni catalyzed decomposition of acetylene. Journal of Catalysis, 1972. 26: p. 51-62.2. Helveg, S., Lopez-Cartes, C., Sehested, J., Hansen, P.L.,Clausen, B.S., Rostrup-Nielsen, J.R., Abild-Pedersen, F., and Norskov J., Atomic-scale imaging of carbon nanofibre growth. Nature, 2004. 427: p. 426-4293. Hofmann, S., et al., In situ Observations of Catalyst Dynamics during Surface-Bound Carbon Nanotube Nucleation. Nano Letters, 2007. 7(3): p. 602-608.4. He, M., et al., Chiral-selective growth of single-walled carbon nanotubes on lattice-mismatched epitaxial cobalt nanoparticles. Sci Rep, 2013. 3: p. 1460.5. Yoshida, H., et al., Atomic-Scale In-situ Observation of Carbon Nanotube Growth from Solid State Iron Carbide Nanoparticles. Nano Letters, 2008. 8(7): p. 2082-2086.6. Yang, F., et al., Chirality-specific growth of single-walled carbon nanotubes on solid alloy catalysts. Nature, 2014. 510(7506): p. 522-524. *Acknowledgements:* Contributions from collaborators (Perla Balbuena, Hua Jiang, Pin Ann Lin, Matthieu Picher, Ying Wang, Zahra Hussaini, Hsin-min (Joy) Chao)

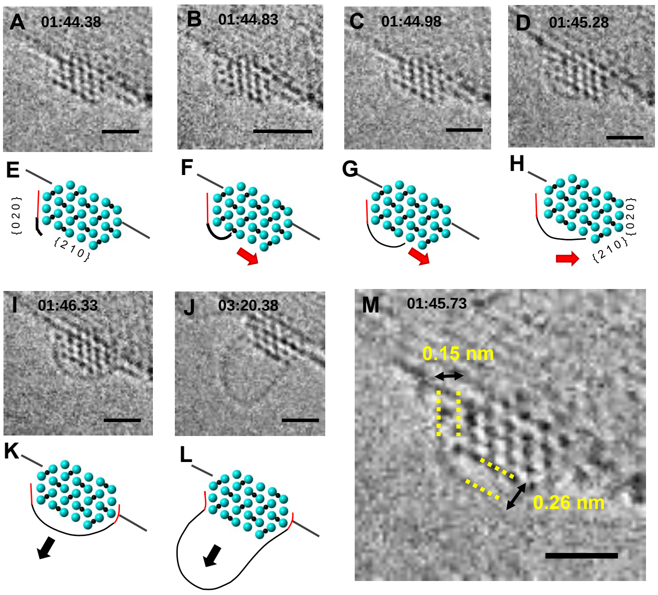

Fig. 1: In situ time-resolved ESTEM observation of SWNT:A series of images extracted from a video recording of a Co2C showing SWCNT nucleation and growth. (a, b, c, d, i, j)

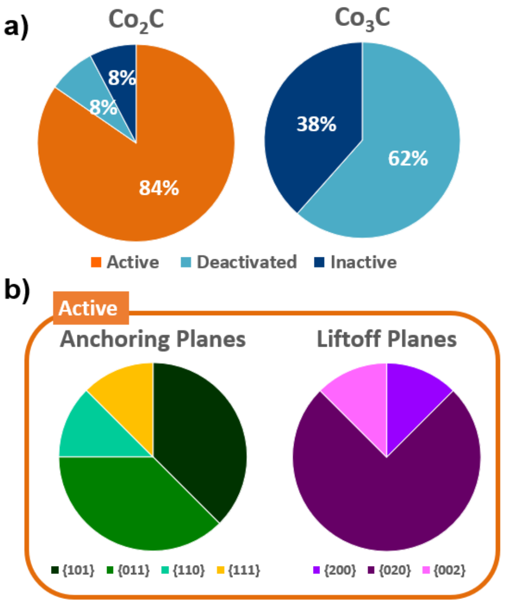

Fig. 2: Statistical analysis of nanoparticles. a) shows the percentages of phases that are active, deactivated, and inactive, b) shows the planes for anchoring and liftoff for the active catalysts

Semiconductor physics of 2D organic-inorganic perovskites

Aditya Mohite*†

Rice University

Organic-inorganic two-dimensional halide perovskites (2DPKs) are soft semiconductors formed by combining organic and inorganic moieties, which self-assemble in solution to form highly ordered periodic stacks. They exhibit a large compositional and structural phase space, which has led to novel and emergent physical properties. In this talk today, I will describe two exciting results.First we overcome a long-standing challenge in 2D perovskites of realizing phase pure thin-films. Briefly, we demonstrate a scalable approach involving dissolution of single-phase crystalline powders with homogeneous perovskite layer thickness in desired solvents, to fabricate 2D perovskite thin-films with high phase purity. In-situ characterizations reveal the presence of sub-micron-sized seeds in solution that preserve the memory of the dissolved single-crystals, and dictates nucleation and growth of grains with identical layer thickness of the perovskite layers in thin-films. Photovoltaic devices fabricated with such films, yields an efficiency of 17.1% and 1.20V open-circuit voltage, while preserving 97.5% of their peak-performance after 800 hours under illumination without any external thermal management.Second, we report sunlight-activated anisotropic lattice contraction in 2D perovskites, which is reversible and strongly dependent of both the nature of the interlayer organics and the details of the structure. Our theory suggests that light-generated charge accumulation results in the build-up of a bulk compressive strain, which induces a continuous lattice contraction over minutes. In-situ structural measurements on photovoltaic devices directly correlate the light-induced lattice contraction to an increase in the photovoltaic efficiency of Dion-Jacobson 2D perovskite solar cells from 13.8% to 16.4%.

Skin-attachable sensor based on graphene

Jong-Hyun Ahn*†

Yonsei University

Skin attachable sensors, that can directly measure various bio-signals and external stimuli, have been actively studied owing to the increasing demand for wearable electronics and healthcare monitoring systems. The sensors need special materials and mechanical design aspects that satisfy the device fabrication requirements on unusual substrates like skin and also for achieving good sensing capabilities and stable device operation in high-strain conditions. Graphene, that is atomically thin and possesses unique electrical and optical properties, offers several important features that can address the challenging needs in skin attachable sensors. In this talk, I present skin attachable devices based on graphene that exhibits a variety of device functions including information input and output and in vitro and in vivo healthcare and diagnosis.

SW, DW and FW CNTs and graphene-CNT hybrids for flexible electronics applications

Esko Kauppinen*†

Aalto University

We discuss the recent developments on floating catalyst chemical vapour deposition (FC-CVD) synthesis of single, double and few walled carbon nanotube synthesis from CO and hydrocarbons carbon precursors, followed by the direct, dry deposition of thin films for transparent electronics applications. When using hydrocarbons as the carbon precursors, graphene flakes can be produced together with SWNTs. When tuning the SWNT atomic structure i.e. (n,m) distributions via CO2 with CO as the carbon source, coloured thin films are produced directly. We explore computationally what would be colours of single chirality SWNT films. Finally we discuss the effect of production yield on the conductivity of SWNT films. We find that in order to produce highly conductive SWNT thin films with sheet resistance below 40 ohms/sq at 90 % transmittance after doping, the synthesis yield must be very low, orders of magnitude below the yield level required for SWNT film production to be at the cost level comparable to that of ITO. Interestingly, DWNT films produced from CH4 with FC-CVD using elemental sulphur as the growth promoter showed the sheet resistance below 40 ohms/sq at 90 % transmittance, with the production yield being more than two orders of magnitude higher than the yield of SWNT films with comparable conductivity.

SWCNT Heterojunctions with Low-Dimensional Perovskites for Novel Optoelectronic Functionality and Devices

Jeff Blackburn*†, Ji Hao, Haipeng Lu, Young-Hoon Kim, Joey Luther, Matt Beard

**The National Renewable Energy Laboratory*

Low-dimensional semiconductors provide a rich tapestry of tunable optical and electrical properties for a wide variety of applications. Semiconducting single-walled carbon nanotubes (s-SWCNTs) have shown tremendous potential in applications ranging from digital logic, biological imaging, quantum information processing, photovoltaics, and thermoelectric energy harvesting. Many of these applications rely critically upon the creation of tailored interfaces that enable the movement of energetic species (excitons, electrons, holes, and other quasiparticles) in specified directions over wide ranges of temporal scales. We have demonstrated previously that high-quality interfaces between SWCNTs and metal halide perovskites can be used to improve the efficiency and stability of perovskite solar cells, in particular by facilitating fast charge extraction, slow charge recombination, and low open-circuit voltage losses.In this talk, I will discuss our recent efforts at exploring new opto-electronic functionalities for SWCNT/perovskite interfaces beyond this traditional PV focus. In particular, we are interested in exploring novel materials and strategies for energy-efficient computing and information processing, since transmitting, storing, and processing data already account for ~10% of global energy use. For our recent studies, we pair highly enriched s-SWCNTs with low-dimensional quantum-confined metal halide semiconductors to produce versatile mixed-dimensionality thin-film heterojunctions. These hybrid interfaces capitalize upon the attractive properties of each individual material to enable efficient photoinduced conductance switching with properties and performance metrics that exceed either material alone. Thin-film device studies demonstrate novel functionalities with implications for optically initiated information processing, while complimentary static and time-resolved optical spectroscopy and electrical transport techniques provide insights into the mechanisms underlying these unique functionalities.

Symmetry Engineering in Nanotubes and Heterostructures of Transition Metal Dichalcogenides

Yoshihiro Iwasa*†

**The University of Tokyo*

Symmetry frequently plays central roles in the properties and functions of materials. In bulk materials, symmetry is basically determined by the space group of single crystals. In sharp contrast, in nanomaterials, symmetry can be controlled as designed. For instance, graphene and bilayer graphene have totally different symmetry, and needless to say, rolling them into tublar structures makes their symmetry reduced to chiral. In this presentation, we discuss one of the symmetry sensitive properties, bulk photovoltaic effect, in nanotubes of transition metal dicalcogenides (TMD) [1] and its van der Waals (vdW) heterostructures [2]. Bulk photovoltaic effect is the photovoltaic effect of uniform materials without p-n junctions, which have been known as a characteristic property of ferroelectric or polar bulk materials. Monolayer TMD has a trigonal structure, which is a noncentrosymmetric but nonpolar structure. Therefore no bulk photovoltaic effect for random light polarization is expected. However, TMD can be changed to polar structures by making tubular structures or vdW heterostructures, and thus bulk photovoltaic effect becomes allowed. Importantly, the observed photocurrent density is rather large comparing to those in bulk polar materials. The present result may indicate a novel route to create new functionalities based on nanostructures through symmetry engineering. [1] Y. J. Zhang et al., Nature 570, 349 (2019). [2] T. Akamatsu et al., Science in press.

Synthesis and Electrical Contact to Two-dimensional Materials

Jing Kong*†

**Massachusetts Institute of Technology*

In recent years tremendous efforts have been devoted to the research on two dimensional (2D) materials. They have attracted significant attention owing to their unique structures, remarkable properties, and great potential for a wide range of applications in electronics, optoeletronics, valleytronics, catalysis, etc. Chemical vapor deposition(CVD) method has been widely investigated to synthesis these materials in large area (wafer scale) and good quality. In this talk I will present our recent work on understanding the CVD synthesis of MoS_2, a representative transition metal dichalcogenides(TMD), and our findings via modifying the CVD to achieve novel 2D structures that do not have a bulk counter part. As monolayer semiconductors are promising for future electronics, I will also present our recent progress to achieve reliable low contact resistance for n-type semiconductors.

Synthesis of single-walled carbon nanotube @ boron nitride nanotubes and their optical properties

Shohei Chiashi*†

The University of Tokyo

Various novel materials have been produced by stacking single-layer materials (2D materials) and the hetero-structure has attracted much attention. Since the layers are bonded with van der Waals interactions, their intrinsic properties are preserved and the interfaces between them provide useful and interesting functions. On the other hand, the hetero-structure in one-dimension was also realized by using single-walled carbon nanotubes (SWCNTs) as a template and directly-synthesizing the outer layer [1]. It is more difficult to synthesize the hetero-structure of one-dimension than two-dimension because the mechanical exfoliation and transfer techniques which are widely used are not possible in a one-dimensional system. Therefore, it is important to establish the synthesis and analysis techniques of the one-dimensional heterostructure. Here, we synthesized SWCNT wrapped with boron-nitride (BN) nanotubes (SWCNT@BNNT) and investigated their properties by using spectroscopy. Suspended SWCNTs were grown by the alcohol catalytic CVD method between a pair of pillars or slit substrates, and then BNNTs were synthesized as the outer layer of the SWCNT layer by supplying ammonia borane. In Fig. 1(a), SEM image showed the suspended SWCNT which was partially BN-coated. SWCNT at both edge parts were covered with BNNT, while it was not covered at the center part. SWCNT@BNNT part exhibited the downshift of the G-band of SWCNT as shown in Fig. 1(b), probably due to the thermal distortion between SWCNT and BNNT. Rayleigh scattering spectroscopy was performed for suspended SWCNT@BNNT between trenches, and the scattering peaks showed the environment dependence (Fig. 2). The peak was red-shifted in water vapor in comparison with that in air, and the red-shift might be caused by the formation of the water adsorption layer. The water layer increased the effective dielectric constant around SWCNT, which suggested that even SWCNTs coated with BNNTs were sensitive to the surrounding states. [1] R. Xiang, et al., Science, 367 (2020) 537.

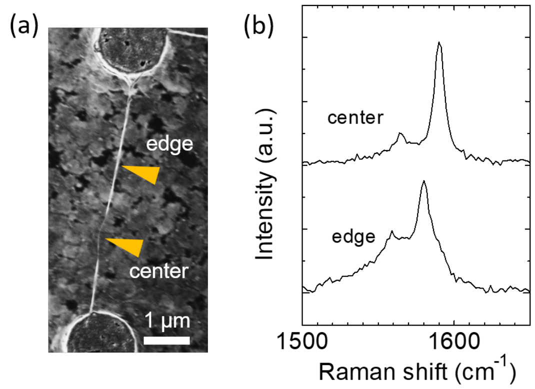

Fig. 1: (a) SEM image of suspended SWCNT@BNNT between pillars and (b) Raman scattering spectra measured at the center and edge parts.

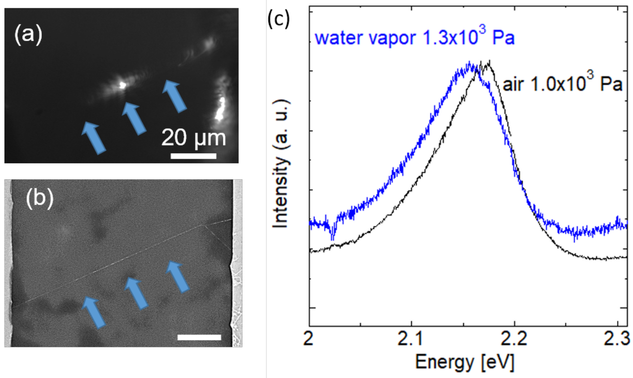

Fig. 2: (a) Rayleigh scattering and (b) SEM images of SWCNT@BNNT, and (c) Rayleigh spectra measured in vapor and air.

Tailoring carbon nanotubes to propel super-resolution microscopy applications at near-infrared wavelengths

Laurent Cognet*†

Institut d'Optique, CNRS - University of Bordeaux

Single-molecule localization super-resolution microscopy has set a new paradigm in the field of optical imaging, by delivering super-resolution images i.e. with resolution much better than the diffraction limit. Yet, super-resolution microscopy remains difficult at NIR wavelengths above 800 nm due to lack of suitable emitters and the use of long wavelength does not represent an asset in terms of optical resolution. It would however be highly advantageous for many applications such as for in vivo studies because of low light extinction by biological constituents at these wavelengths. Designing new solutions to allow super-resolution microscopy in the NIR is thus urgently needed.Because single wall carbon nanotubes display bright photoluminescence in the near-infrared, our aim is to engineer carbon nanotube photophysics in order to propel them as novel nano-emitters in super-resolution imaging. In his quest I will present our efforts to control (e.g. by chemical environment, or by photocontrol) carbon nanotube exciton localization and luminescence blinking properties in pristine and sp3-defect functionalized carbon nanotube hybrids. Applications of concepts developed in super-resolution imaging to carbon nanotube imaging will then be presented.References Cognet et al Nanoletters, 8 (2008) 749 - 753.Godin et al Nat. Nanotechnol. 12 (2017) 238-243 Danné et al. ACS Nano, 12 (2018) 6059Godin et al Science Advances, 5, (2019) eaax1166 Mandal et al Sci. Rep 10 (2020) 5286

The Effect of Endohedral Filling on Separation

Benjamin S. Flavel*†

Institute of Nanotechnology, Karlsruhe Institute of Technology, Karlsruhe 76021, Germany

Aqueous two-phase extraction (ATPE) is a fast, facile and scalable technique to purify carbon nanotubes. A recipe driven approach to separate small and large diameter single chiral nanotubes will be presented and the impact endohedral functionalization has on sensitivity discussed. Likewise, the effect of filling on the polymer extraction method is examined. Empty, water and perfluorooctane filled large and single chirality small diameter SWCNTs are dispersed with poly[(9,9-dioctylfluorenyl-2,7-diyl)-alt-co-(6,6'-(2,2'-bipyridine))] (PFO-BPy) and the extent of filling followed spectroscopically. These findings are then used to interpret separation results obtained for raw soot (without intentional filling) and with a view to the low yield of polymer based SWCNT extraction. [1] ACS Nano, 2019, 13 (2), pp 2567 – 2578. [2] ACS Nano, 2020, 14 (1), pp 948 – 963.

The effects of gas flow patterns and configurations of injection part of reactor on the synthesis of carbon nanotube/carbon nanotube fiber

Seung Min Kim*†, Sung-Hyun Lee, Junbeom Park, Ji Hong Park, Dong-Myeong Lee, Hyeon Su Jeong, Sei Young Lee

Korea Institute of Science and Technology (KIST)

Floating catalyst chemical vapor deposition (FCCVD) can be a method to synthesize carbon nanotubes (CNTs) with high crystallinity or to directly synthesize CNT fibers (CNTFs) with high strength. In both cases, the synthesis of CNTs or CNTFs occurs in a vapor phase, so the gas flow patterns inside the reactor critically affect the synthesis of CNTs or CNTFs. In the first part of the presentation, the synthesis of CNTs with high crystallinity and aspect ratio using a horizontal reactor will be dealt with [1]. For successful synthesis, a deep-injection FCCVD (DI-FCCVD) technique is introduced. In this technique, all reactants are injected directly and rapidly into high-temperature reaction zone through thin alumina tube; this process leads to simultaneous thermal decomposition of well-mixed catalyst precursors and formation of uniformly-sized catalyst particles, and thus synthesis of CNTs with high aspect ratio (AR > 17000) and high crystallinity (IG/ID > 60) at relatively high production rate (> 6 mg/min). In the last part of the presentation, the direct synthesis of CNTFs with high specific strength and specific conductivity using a vertical reactor will be dealt with [2]. To achieve this goal, the correlation between synthesis conditions and the properties of CNTFs according to the configuration of the injection tube during the direct spinning process is investigated. Adjusting the configuration of the injection tube is highly effective in improving the synthesis of CNTFs because the gas flow pattern critically affects the synthesis. CNTFs synthesized from reactants injected into the high-temperature region of the reactor are composed of CNTs with uniform diameter and have denser internal structure than CNTFs synthesized from reactants injected into the low-temperature region. As-spun CNTF that has specific strength up to 2.29 N/tex (average: 2.03 N/tex) is synthesized by directly injecting the reactants into the high-temperature region using a deep injection method. Both works demonstrate how important the gas flow patterns inside the reactor and thus the adjustment of reactor configurations are to the synthesis of CNTs and CNTFs. [1] S. Lee, et al., Carbon, 173, 901 (2021)[2] S. Lee, et al., ACS Appl. Nano Mater., accepted (2021) *Acknowledgements:* This work was supported by Samsung Research Funding & Incubation Center of Samsung Electronics under Project Number SRFC-MA1801-06.

Unravelling the properties of carbyne confined inside carbon nanotubes

Thomas Pichler*†

**University of Vienna, Faculty of Physics, 1090 Wien, Austria*

Controlling the function on an atomistic scale for bulk scale synthesis and functionalization processes of emerging low dimensional materials is the key for their application. Among all these emerging materials, low-D carbon allotropes exhibit outstanding properties and a leading applicability in fields ranging from materials science, solid state physics, physical chemistry to biochemistry and medicine. Especially, 1D allotropes, either as cylindrical 1D quantum wires (nanotubes (CNT)), or as ultra-long 1D chains (carbyne) offer unique possibilities. Whereas for CNTs the control of the inner and outer surfaces and charge transfer and hybridization are crucial for designing materials towards applications, carbyne -the material itself- remained elusive for more than 130 years hindering the determination of its properties. In this presentation I will present an overview on the recent progress regarding synthesis and functionalization of bulk samples of carbyne confined inside CNTs starting from our breakthrough of a bulk synthesis of carbyne confined inside CNT with a record length of more than 6000 carbon atoms (Nature Mat. 15, 634 (2016)) up to the recent synthesis of isotope engineered carbyne@SWCNT hybrids (Angew. Chem. Int. Ed. 2021, DOI: 10.1002/anie.202017356). In addition, I ll report on our recent progress in understanding of the physical properties in order to access the application potential of confined carbyne@CNT hybrids.Finally I want to highlight that our additional studies on confined carbyne will be presented at the NT21. For more detailed information please also visit the presentations NT2159 by Cla Duri Tschannen, NT2185 by Weili Cui and NT21120 by Lei Shi.

Contributed Talks

Aligned carbon nanotubes and twisted bilayer graphene as linear nanoactuators

Zhao Wang*†

Guangxi University

We propose a linear actuation mechanism for aligned carbon nanotubes and twisted bilayer graphene [1-2]. Using molecular dynamics simulations, we show that the translational motion of a tube/layer can cause another tube/layer to move in an orthogonal direction. Such an effect depends strongly on the crystallographic orientation with respect to the direction of displacement. We predict the existence of a linear and a nonlinear actuation regimes separated by a critical bilayer twisting angle. This critical angle is determined by the overlap between the van der Waals interaction ranges of the moire superlattice. Based on this mechanism, a linear nanoactuator with desired transmission efficiency can be designed by adjusting the nanotube chirality or the interlayer twisting angle of bilayer graphene. [1] Z. Meng, Z. Wu, J. Carrete and Z. Wang, Twisted bilayer graphene as a linear nanoactuator. Phys. Rev. B 102, 155424 (2020). [2] Z. Wang, Chirality-dependent motion transmission between aligned carbon nanotubes. Carbon 151, 130-135 (2019)

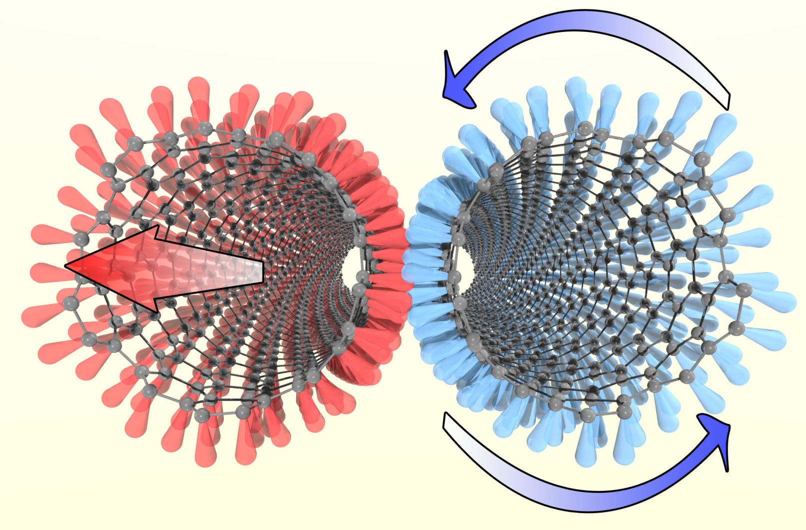

Carrier-exciton dynamics in aligned and random semiconducting carbon nanotubes probed by terahertz emission and photocurrent spectroscopy

Filchito Renee Bagsican*†, Michael Wais, Natsumi Komatsu, Weilu Gao, Kazunori Serita, Hironaru Murakami, Karsten Held, Iwao Kawayama, Junichiro Kono, Masayoshi Tonouchi, Marco Battiato

Institute of Laser Engineering, Osaka University

The discovery of carbon nanotubes (CNTs) has opened up exciting possibilities for developing next-generation optoelectronic devices. The optical properties of CNTs are dominated by highly-bound excitons as a consequence of their one-dimensionality. Their 1D nature also ensures a highly-restricted phase space for scattering that results in a fundamentally different quasiparticle dynamics compared to bulk materials. Fully understanding such dynamics is critical to realize their potential applications.In this work, we show that excitons also dominate the terahertz (THz) dynamics in CNTs (Nano Lett. 2020, 20 (5), 3098–3105). We fabricated photoconductive antenna devices on (6,5) CNTs films and simultaneously measured the THz emission and photocurrent generated after optical excitation at E22 exciton resonance (Fig. 1). Our first measurements with aligned CNT films showed that the photocurrent increases superlinearly with bias while the THz emission amplitude is linear (Fig. 2a). These results were reproduced by our numerical simulations based on far-from-equilibrium Boltzmann transport equations. Specifically, the simulations were able to clarify the role of exciton autoionization (in THz emission) and impact generation (resulting to the superlinear photocurrent) in aligned CNTs.We also show that the dynamics becomes drastically different for a random CNT network. Both the THz amplitude and PC show saturation-like behavior with bias (Fig. 2b). Our numerical simulations show that this effect possibly arises from an increased impurity-like scattering of electrons due to multiple tube distortions coming from the intersecting tubes. This prevents the electrons from

---

* denotes primary author, † denotes presenting author.

gaining enough kinetic energy to undergo exciton impact generation, and thus the absence of a bias-driven component to the photocurrent that leads to the superlinearity observed in aligned CNTs. The results obtained in our work provide fundamental understanding of the carrier-exciton dynamics in CNTs and in optimizing performance for future device applications. *Acknowledgements:* US DOE BES & NSF, Robert A Welch & Iketani Fndn, NTU & Austrian Sci Funds, JSPS Kakenhi, Core-to-Core & Intl Joint Research Promotion Prgm

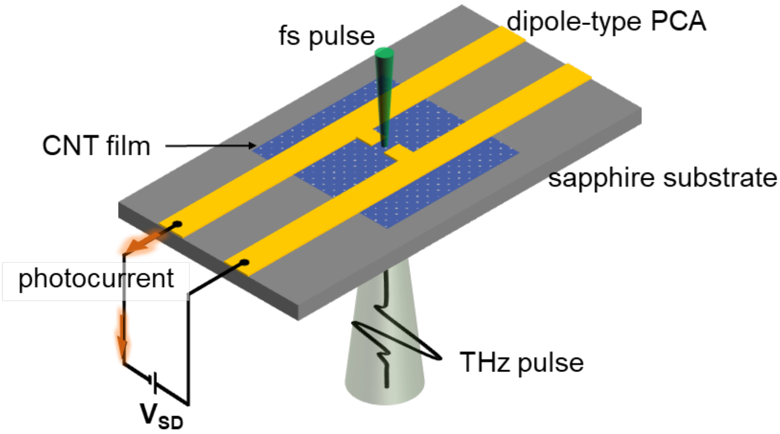

Fig. 1: Device and experimental schematic diagram.

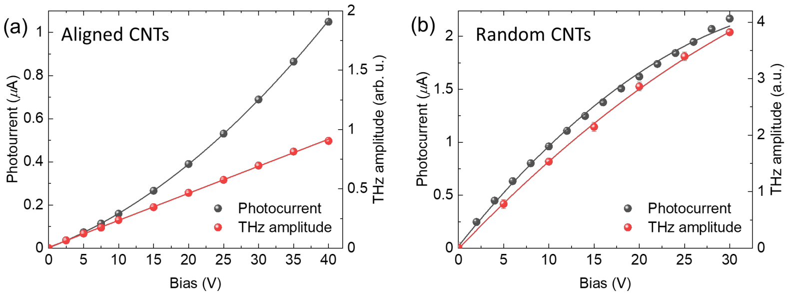

Fig. 2: Bias-dependence of THz emission amplitude and photocurrent for (a) aligned and (b) random CNTs.

Catalyst-feedstock tandem in the structure synthesis inside a carbon nanotube

Umedjon Khalilov*†, Dilfuza Husanova, Sirojiddin Mirzaev, Erik Neyts

**University of Antwerp, Belgium, and Institute of Ion-Plasma and Laser Technologies, Uzbekistan*

The possibility of confinement effects inside a carbon nanotube provides new application opportunities, e.g., growth of novel carbon nanostructures. A comprehensive understanding of the synthesis mechanisms motivates controlled formation of nanomaterials with controllable dimensions.In our simulation-based study, we investigate the Ni-catalyzed growth mechanism of encapsulated carbon nanostructures from different carbon and hydrocarbon precursors using reactive molecular dynamics simulations and first-principles calculations.In particular, we find that the nanotube, carbyne and nanoribbon growth is determined by a catalyst-vs-feedstock competition effect [1]. Also, our calculations indicate that all encapsulated nanostructures contain metal (catalyst) atoms and such structures are less stable than their pure counterparts [1]. Therefore, we study the oxidation-based purification mechanism of these structures as well [1]. We also find that both hydrogenation and fluorination of grown carbyne result in structural changes and semiconducting to metallic transition [2, 3].In general, this study opens a possible route to the controllable synthesis of chain, tubular and planar carbon structures with tunable electronic transport properties.1. Khalilov, U., Neyts, E.C., Mechanisms of selective nanocarbon synthesis inside carbon nanotubes. Carbon 171 (2021) 72-782. Khalilov, U., Vets, C., H., Neyts, E.C., Catalyzed growth of encapsulated carbyne. Carbon 153 (2019) 1-53. Berdiyorov, G.R., Khalilov, U., Hamoudi, H., Neyts, E.C., Effect of chemical modification on electronic transport properties of carbyne. J Comput Electron (2021). https://doi.org/10.1007/s10825-020-01639-7 *Acknowledgements:* The authors gratefully acknowledge the financial support from the Fund of Scientific Research Flanders (FWO), Belgium, Grant number 12M1318N

Collective Excitations and Optical Response of Ultrathin Carbon Nanotube Films

Igor Bondarev*†, Chandra Adhikari

**North Carolina Central University*

Self-assembled quasiperiodic finite-thickness single-wall carbon nanotube (SWCN) films have been recently shown experimentally to exhibit extraordinary optoplasmonic properties [1-4]. Thin and ultrathin aligned arrays and films of SWCNs are currently in the process of rapid experimental development [5,6]. Here we study theoretically the intrinsic collective quasiparticle excitations responsible for the in-plane electromagnetic (EM) response of the ultrathin plane-parallel homogeneous periodic SWCN arrays (Fig.1) and weakly inhomogeneous SWCN films [7,8]. The key features that make this system interesting are the periodic CN alignment and the spatially periodic anisotropy associated with it. Additionally, the vertical confinement in dense ultrathin planar systems of finite thickness leads to the effective dimensionality reduction from 3D to 2D while still retaining the thickness as a parameter to represent the vertical size [7-9]. This is the transdimensional regime — neither 3D nor 2D but something in-between — turning into 2D as thickness tends to zero, challenging to study what the 3D-to-2D continuous transition has to offer to improve material functionalities [10]. We show that in addition to varying the film composition, the collective EM response can be controlled by varying the film thickness. For single-type nanotube arrays, the real part of the dielectric response exhibits a broad negative refraction band near a quantum interband transition of the constituent nanotube (Fig.2), whereby the system behaves as a hyperbolic metamaterial at higher frequencies than those classical plasma oscillations have to offer. By decreasing nanotube diameters it is possible to push this negative refraction into the visible region, and using weakly inhomogeneous multi-type nanotube films broadens its bandwidth. [1] J.A. Roberts, et al., Phys. Rev. Applied 14, 044006 (2020). [2] W.Gao, et al., ACS Photonics 6, 1602 (2019). [3] J.A. Roberts, et al., Nano Lett. 19, 3131 (2019). [4] P.-H. Ho, et al., PNAS 115, 12662 (2018). [5] S. Schöche, et al., J. Vac. Sci. Technol. B 38, 014015 (2020). [6] N. Komatsu, et al., Nano Lett. 20, 2332 (2020). [7] I.V. Bondarev and C.M. Adhikari, Phys. Rev. Applied 15, 034001 (2021). [8] C.M. Adhikari and I.V. Bondarev, J. Appl. Phys. 129, 015301 (2021). [9] I.V. Bondarev, H. Mousavi, and V.M. Shalaev, Phys. Rev. Research 2, 013070 (2020). [10] A. Boltasseva and V.M. Shalaev, ACS Photonics 6, 1 (2019). *Acknowledgements:* This research is supported by the U.S. National Science Foundation under Condensed Matter Theory Program Award No. DMR-1830874 (I.V.B.)

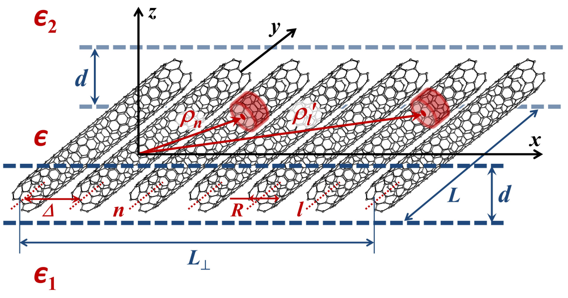

Fig. 1: Schematic of a plane-parallel, closely packed, periodically aligned array of SWCNs of radius R and length L embedded in a dielectric of thickness d.

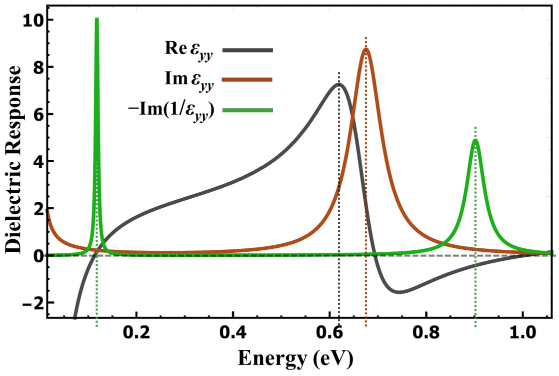

Fig. 2: The room-temperature in-plane dielectric response functions along the CN alignment direction calculated for a 10 nm-thick weakly-inhomogeneous film of (16,0), (17,0), (18,0), (19,0) and (20,0) SWCNs.

Comparison of Infrared and Raman Spectra of Doped (6,5) Single-Wall Carbon Nanotubes

Klaus Eckstein*†, Daniel Müller, Florian Martens, Florian Hirsch, Richard Martel, Tobias Hertel

**Julius-Maximilians-Universität Würzburg*

Electron-phonon coupling is at the heart of many physical phenomena like superconductivity, charge transport, and the Raman effect [Ferrari2007]. In single-wall carbon nanotubes (SWNTs), this coupling depends on the doping level [Tsang2007] and has mostly been studied using resonance Raman spectroscopy [Das2007, Grimm2017] and less frequently using far- and mid-infrared (FIR/MIR) spectroscopy [Lapointe2012]. However, such studies were often performed on mixed-chirality samples with poorly characterized doping levels. Moreover, a direct comparison of Raman and IR spectra is still missing.Here, we present a systematic study of the IR absorption and Raman scattering of purely semiconducting, (6,5)-SWNT thin-films over a large range of doping levels. In contrast to the nearly featureless FIR/MIR spectrum of intrinsic CNTs, doped samples reveal IR-forbidden phonon bands as Fano resonances [Fano1961] due to the coupling to the bright Drude-like intraband continuum. Both the spectrum of the continuum absorption and the amplitude of the Fano resonances were found to depend on the doping level. These observations show that carrier localization and delocalization as well as disorder induced by defects play a critical role for both charge transport and electron-phonon coupling as evidenced by the Fano resonances [Eckstein2021].In contrast, visible resonance Raman experiments show how doping affects the coupling between phonons and electronic interband excitations. Upon doping, we observe an overall reduction of Raman intensity. This can partly be attributed to the loss of an excitonic resonance at the excitation wavelength as determined by absorption spectroscopy. However, the nonuniformity of this intensity reduction for distinct phonon bands additionally points to different doping level dependences of the exciton-phonon matrix elements. Moreover, we find that some phonon bands become broadened and blue shifted, with the strongest effects observed for degenerately doped SWNTs.A. C. Ferrari, Solid State Commun. 2007, 143, 47-57.Tsang et al., Nat. Nanotechnol. 2007, 2, 725-730.Das et al., Phys. Rev. Lett. 2007, 99, 136803.Grimm et al., Carbon 2017, 118, 261-267.Lapointe et al., Phys. Rev. Lett. 2012, 109, 097402.U. Fano, Phys. Rev. 1961, 124, 1866-1878.Eckstein et al., J. Phys. Chem. C 2021, accepted.

Densification of Single-Walled Carbon Nanotube Films: Mesoscopic Distinct Element Method (mDEM) Simulations and Experimental Validation

Grigorii Drozdov*†, Igor Ostanin, Hao Xu, Yuezhou Wang, Artem Grebenko, Yuriy Gladush, Georgy Ermolaev, Sebastian Eibl, Ulrich Rude, Albert Nasibulin, Traian Dumitrica

**University of Minnesota*

Nanometer-thin single-walled carbon nanotube (CNT) films collected from the aerosol chemical deposition reactors have gathered attention for their promising applications. Densification of these pristine films provides an important way to manipulate mechanical, electronic, and optical properties. To elucidate the underlying microstructural level restructuring, we performed large scale vector-based mesoscopic distinct element method1 (mDEM) simulations in conjunction with electron microscopy and spectroscopic ellipsometry characterization of pristine and densified films by drop-cast volatile liquid processing. Matching with the microscopy observations (Figure 1), pristine CNT films with a finite thickness are modeled as self-assembled CNT networks comprising entangled dendritic bundles with branches extending down to individual CNTs (Figure 2). The mDEM simulations reveal significant structural changes occurring at the 100nm scale and indicated that the simulated samples undergo homogeneous densification in a two-stage regime comprising a sub-GPa plastic compression followed, at above ~75% strain, by a sharp rise of stress. In the first regime, the film is lowering irreversibly its van der Waals cohesive energy by zipping, while increasing the bending energy of those CNTs joining into new bundles and of other entangled CNTs, which develop nm-scale waviness. In the second deformation regime, the application of few GPa stress values is required. These large values reflect the resistance to interpenetration of the mDEM-represented CNTs.When removing the loads, the pre-compressed samples evolve into homogeneously densified films with thickness values depending on both the pre-compression level and the sample microstructure. The significant reduction in thickness is attributed to the underlying structural changes occurring at the 100 nm scale, including the zipping of the thinnest dendritic branches.The ”dendritic” microstructure of the pristine films proposed by our mDEM model (Figure 2), differs qualitatively from the usual adhesion dominated ”cellular” structure obtained by the simpler bead and spring (B&S) mesoscopic model. Our simulations indicate that accounting for the thinnest branches and individual CNTs is important for describing the densification process. Unfortunately, these microstructural features are not captured by the popular B&S model for CNTs. Since the realistic description of the microstructure ties directly to the mesoscale interactions, our work points to the need for accuracy in the coarse-grained modeling of CNT and of semiflexible polymer self-assembled networks in general. *Acknowledgements:* NASA NNX16AE03G, UMN MnDrive, Grant-in-Aid programs, RFBR grants 18-18-29-19198, 18-29-20032, 19-32-90143, Fulbright U.S. Scholars program

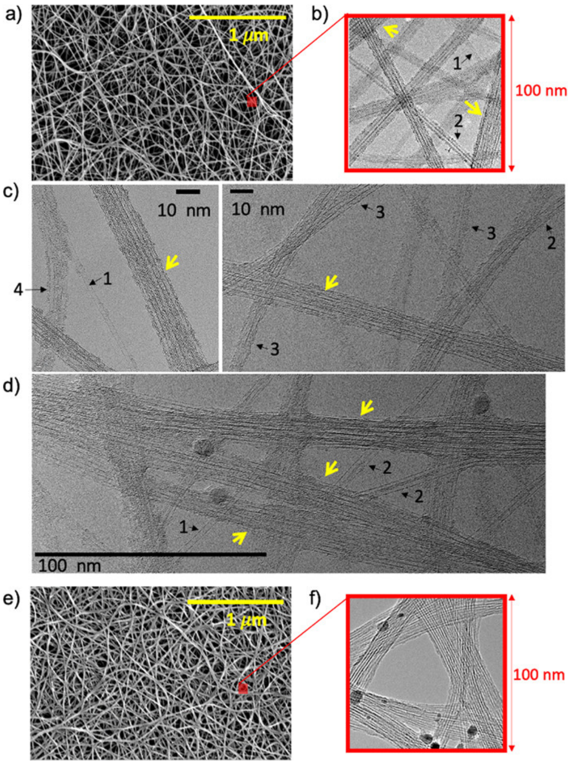

Fig. 1: Pristine CNT film multiscale structure: a) SEM showing ????m-long bundles. TEM b) of individual, 2-CNT and ”medium” ~10nm diameter bundles, detailing c) ”medium” bundles and d) their merging.

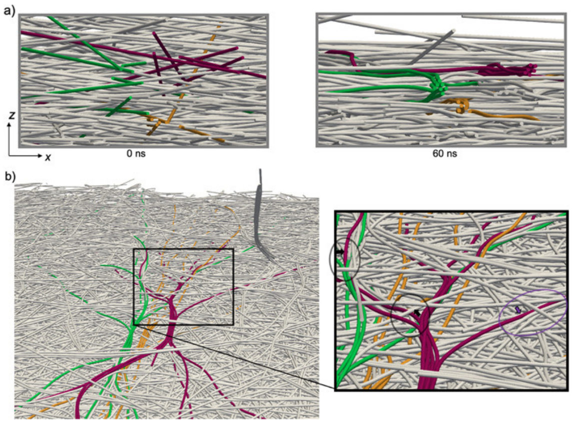

Fig. 2: mDEM simulations: a) A region near the top surface of a simulated sample before (left) and after relaxation (right). b) Birds’ eye view showing the branching structure of the

Detection of plant polyphenols via near infrared fluorescent SWCNT nanosensors

Robert Nißler*†, Andrea Müller, Frederike Dohrmann, Larissa Kurth, Axel Mithöfer, Sebastian Kruss

**Georg-August University Göttingen*

Plants use secondary metabolites such as polyphenols for chemical defense against pathogens and herbivores. Tools that visualize this defense response promise novel insights into plant biology and can improve agriculture. Here, we used near-infrared (NIR) fluorescent single wall carbon nanotubes (SWCNTs) as sensors for plant polyphenol detection and imaging. We identified surface modifications making SWCNTs sensitive to different polyphenols. Polyphenol binding cause both a red-shift (up to 20 nm) and quenching the emission of (6,5)-SWCNTs (~1000 nm) in a concentration dependent matter. These SWCNTs are therefore probes for the total polyphenol content. First, we used these sensors to analyze in vitro different model plant systems (Glycine max cell cultures and seedlings; Tococa spp. leaf tissue extracts) and show how polyphenol levels change after herbivore or pathogen challenge. Inside agar medium, these nanosensors enabled in vivo remote chemical imaging of pathogen induced polyphenol release from soybean seedlings. Those sensors visualize in situ polyphenol-based plant defense and can improve our understanding of rhizosphere chemical communication. Furthermore, it could enable precision-agriculture by phenotyping cultivars with optimized polyphenol secretion. *Acknowledgements:* VW foundation

Determining SWCNT chiralities from high resolution electron microscopy images using deep learning

Alice Castan†, Georg Daniel Förster*, Annick Loiseau, Jaysen Nelayah, Damien Alloyeau, Frédéric Fossard, Christophe Bichara, Hakim Amara

**Aix Marseille University*

Since the properties of single-walled carbon nanotubes (SWCNT) depend on their atomic structure, having access to fast and reliable methods to determine the chirality distributions of SWCNT samples is highly desired. Aberration-corrected transmission electron microscopy (AC-TEM) enables atomic resolution imaging of SWCNTs, providing an accurate direct access to the chirality of any observed nanotube. Unfortunately, the time required for data analysis with this technique makes the process of obtaining a chirality distribution from a significant number of nanotubes very tedious and time-consuming. To facilitate and make this process faster, we have developed an image recognition procedure to automatically determine the chirality of a SWCNT from a high resolution TEM (HRTEM) image based on a convolutional neural network (CNN).The large and realistic training data set of SWCNT images was generated by atomistic computer simulations [1] coupled with the multi-slide approach for HRTEM image simulation. 1000 independent atomistic simulations were run for each of the 261 chiralities of SWCNTs with diameters between 0.48 and 2.30 nm. For each obtained SWCNT configuration, 5 HRTEM images were simulated with varying aberration coefficients and orientations [2]. After training [3], the deep learning algorithm can accurately and rapidly determine the chiralities of SWCNTs from simulated HRTEM images with an accuracy of more than 90%. Comparing the results obtained manually and using the deep learning algorithm on 91 experimental HRTEM images of varying quality, we find a 71% agreement between the two methods.This work paves the way to fast and robust TEM-based chirality distribution assessment [4]. 1. J. Tersoff, Phys Rev B, 1989, 39, 5566.2. J. Barthel, Ultramicroscopy, 2018, 193, 1.3. F. Chollet et al., https://keras.io, 2015.4. D. Förster et al., Carbon, 2020, 169, 456.

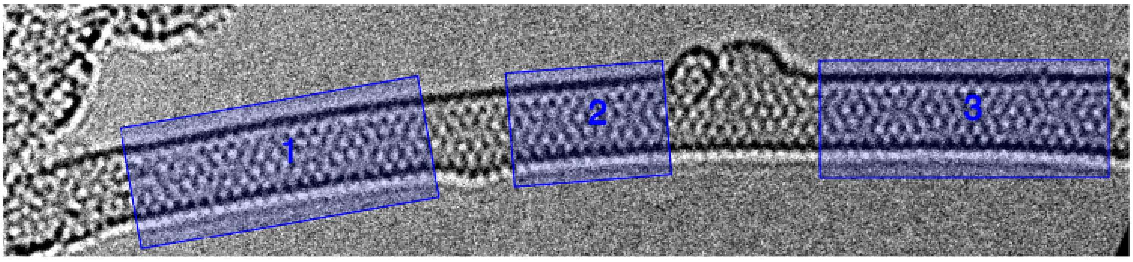

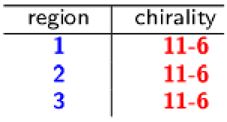

region	chirality
1	11-6
2	11-6
3	11-6

Fig. 1: HRTEM image of a SWCNT analyzed using the developed deep learning algorithm

Determining SWCNT Extraction Conditions in Aqueous Two-Polymer Phase Extraction with Near-Infrared Fluorescence

Christopher Sims*†, Jeffrey Fagan

**NIST*

Aqueous two-polymer phase extraction (ATPE) is an effective, yet still developing, separation method for enriching or isolating single species of single-wall carbon nanotubes (SWCNTs). However, methods for rapidly determining the aqueous surfactant concentration conditions that yield upper or lower polymer phase extraction for specific (n,m) species SWCNTs in ATPE separations are a missing component limiting quicker development and optimization of the ATPE technique. Here, we demonstrate the use of near-infrared fluorescence emission from single-phase dispersions of multiple SWCNT specie mixtures to determine these partition coefficient conditions without performing ATPE separations. This new methodology enables rapid quantitative determination of partitioning conditions for individual (n,m) species and their handed enantiomers, while using dramatically less material and without ambiguity of mass transfer limitations or interfacial adsorption present when conducting the ATPE separation itself. Investigation of complicating factors such as temperature effects or polymer concentration are likewise enabled by this methodology and will also be described. *Acknowledgements:* This effort was funded through internal National Institute of Standards and Technology funds.

Dynamic instability of individual carbon nanotube growth revealed by in situ optical imaging

Vladimir Pimonov*†, Huy-Nam Tran, Léonard Monniello, Saïd Tahir, Thierry Michel, Renaud Podor, Michael Odorico, Christophe Bichara, Vincent Jourdain

**Université de Montpellier*

Current models of carbon nanotube growth assume that the nanotube growth rate is unambiguously fixed by its chirality and the growth conditions, an assumption which is at the heart of all current strategies of chirality selection based on kinetics. Here, we report on in situ optical imaging of hundreds of long individual carbon nanotubes under real growth conditions (at ambient pressure, on a substrate) using the method of homodyne polarization microscopy [1,2]. Our observations reveal that, despite overall constant growth conditions, most CNTs display dynamic instability during their growth (Fig. 1) [3]. This instability is characterized by stochastic fluctuations between different growth rates, and between growth, pause and etching (i.e. shrinkage of tube length), a behavior reminiscent of that observed for microtubule growth. Statistical analysis shows that the growth rate of a CNT varies essentially between two values whose ratio is similar for all CNTs. Structural fluctuations of the catalyst nanoparticles or of the nanotube-catalyst interface might be the cause of the dynamic instability revealed by our in situ observations. [1] Liu et al, Nature Nanotechnology (2013), 8, 917. [2] Comprehensive model of the optical spectra of carbon nanotubes on a substrate by polarized microscopy, L. Monniello, H.-N. Tran, R. Vialla, G. Prévot, S. Tahir, T. Michel, V. Jourdain, Physical Review B (2019), 99, 115431. [3] Submitted. *Acknowledgements:* Agence Nationale de la Recherche: grant ANR-20-CE09-0007-01. Air Force Office of Scientific Research: award number FA9550-17-1-0027.

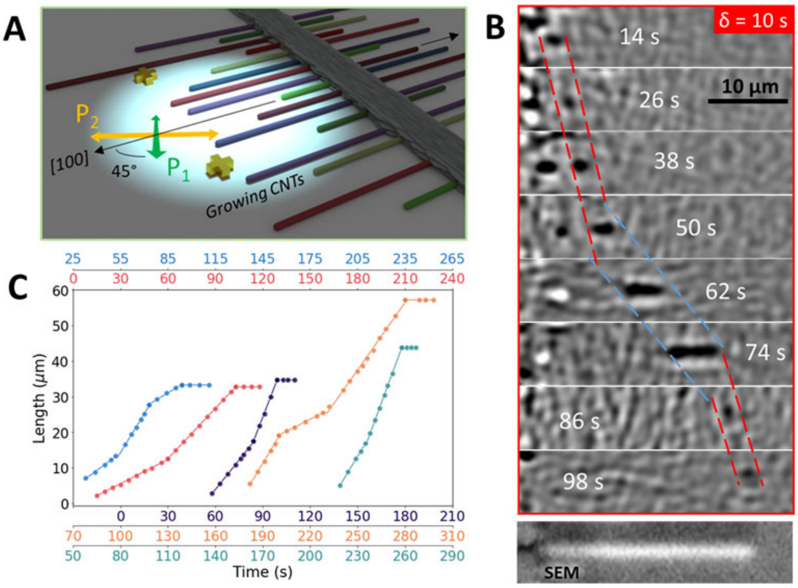

Fig. 1: A) Experimental schema. B) Growth rate changes with no change of CNT structure: video snapshots in differential mode (delay =10 s). C) Kinetic curves displaying abrupt changes of growth rate.

Electrical Conductance Mechanisms in Carbon Nanotube Films

Vasili Perebeinos*†, Weilu Gao, Davoud Adinehloo, Ali Mojibpour, Junichiro Kono

University at Buffalo

In recent years, much progress has been achieved in controlling the quality of carbon nanotube films in terms of chirality separation, orientation, and doping levels. Many theoretical models can be tested to explore chirality-dependent electrical properties of single-wall carbon nanotubes (SWCNTs) on a single-tube level. However, macroscopic manifestations of chirality dependence have been limited, despite the fact that such distinct behaviors are needed for any applications of SWCNTbased devices. Here, we report the observation of pronounced chirality-dependent electronic localization in temperature conductivity measurements on single-chirality SWCNT films. The samples included semiconducting (6,5) and (10,3) films, chiral metallic (7,4) and (8,5) films, and armchair (6,6) films. Experimental data and theoretical calculations revealed variable-range-hopping dominated transport in all samples except the armchair SWCNT film. We obtained localization lengths that fall into three distinct categories depending on their band gaps. The clear deviation of the armchair films from the other films suggests their robustness toward defects and possible additional transport mechanisms. To explain conductance temperature dependence in (6,6) tube, we employ a full-band model within the perturbation theory to account for the phonon-assisted tunneling conductance across the CNTs. The phonon-assistant tunneling accounts for the observed temperature dependence in (6,6) CNTNs sample. Our detailed analyses on electronic transport properties of single-chirality SWCNT films provide significant new insight into electronic transport in ensembles of nanoobjects, offering foundations for designing and deploying macroscopic SWCNT solid-state devices [1]. [1] Weilu Gao, Davoud Adinehloo, Ali Mojibpour, Yohei Yomogida, Atsushi Hirano, Takeshi Tanaka, Hiromichi Kataura, Ming Zheng, Vasili Perebeinos, Junichiro Kono, "Band structure-dependent electronic localization in macroscopic films of single-chirality single-wall carbon nanotubes", arXiv:2101.07503

Extremely Efficient Photocurrent Generation in Individual Carbon Nanotube Photodiodes

Ethan Minot*†, Mitchell Senger, Andrea Bertoni, Vasili Perebeinos, Daniel McCulley

**Oregon State University*

Carbon nanotubes (CNTs) offer unique relaxation pathways for energetic charge carriers. Of particular interest are carrier multiplication pathways that can boost the quantum efficiency of CNT photodiodes. We have studied, both experimentally and theoretically, the photocurrent generation process in individual suspended CNT pn junctions [1]. In our experiments we control the axial electric field inside the pn junction, and also control the Coulomb interaction strength between charge carriers. We determined the photocurrent quantum yield (PCQY) by accounting for the length of the intrinsic region, optical cavity effects, and the integrated absorption cross-section of the exciton resonance. At low electric fields (a few volts per micron), we confirmed previous experimental measurements of modest PCQY in CNT photodiodes. At higher electric fields, however, (~10 volts per micron) we found evidence for PCQY > 100%. Our experiments show that the highest PCQY is achieved by increasing CNT diameter, and increasing the relative dielectric constant of the environment. Our work elucidates the role of Coulomb interaction in nanotube-based optoelectronic devices, and will guide future efforts to build high-efficiency photodiodes. [1] D. R. McCulley et al., "Extremely Efficient Photocurrent Generation in Carbon Nanotube Photodiodes Enabled by a Strong Axial Electric Field" Nano Letters 20, 433-440 (2020).

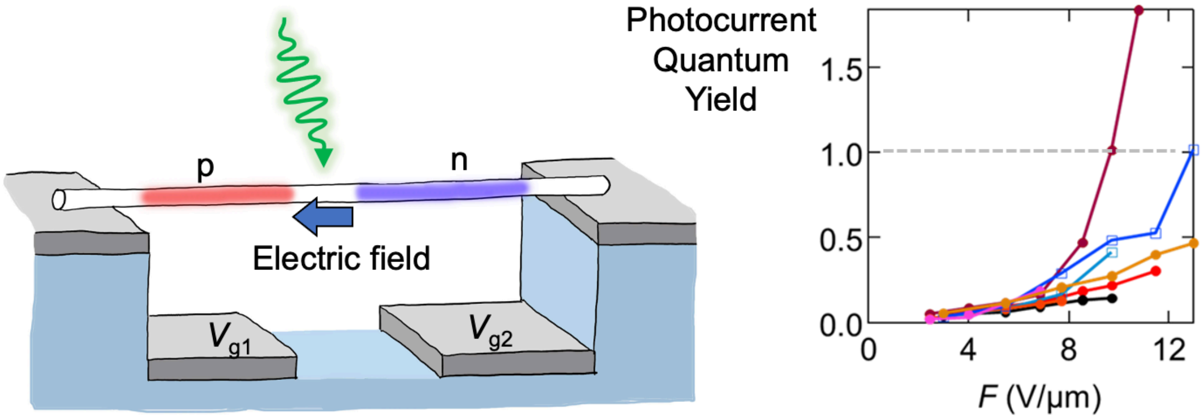

Fig. 1: Schematic of the device geometry and a graph of photocurrent quantum yield as a function of axial electric field for various CNT diameters. Larger diameter CNTs show higher quantum yield.

Foldable Perovskite Solar Cells Using Carbon Nanotube-Embedded Ultrathin Polyimide Conductor

IL Jeon*†, Shigeo Maruyama, Esko Kauppinen

**Pusan National University*

Recently, foldable electronics technology has become the focus of both academic and industrial research. The foldable device technology is distinct from flexible technology, as foldable devices have to withstand severe mechanical stresses such as those caused by an extremely small bending radius of 0.5 mm. To realize foldable devices, transparent conductors must exhibit outstanding mechanical resilience, for which they must be micrometer-thin, and the conducting material must be embedded into a substrate. Here, a single-walled carbon nanotubes–polyimide (SWNT-PI) composite film with a thickness of 7 µm is synthesized and used as a foldable transparent conductor in perovskite solar cells. During the high-temperature curing of the carbon nanotubes-embedded polyimide conductor, the carbon nanotubes are stably and strongly p-doped using MoOx, resulting in enhanced conductivity and hole transportability. The ultrathin foldable transparent conductor exhibits a sheet resistance of 82 Ω sq.-1 and transmittance of 80% at 700 nm, with a maximum-power-point-tracking-output of 15.2% when made into a foldable solar cell. The foldable solar cells can withstand more than 10,000 folding cycles with a folding radius of 0.5 mm. Such mechanically resilient perovskite solar cells are unprecedented; further they exhibit the best performance among the carbon-nanotube-transparent-electrode-based flexible solar cells.

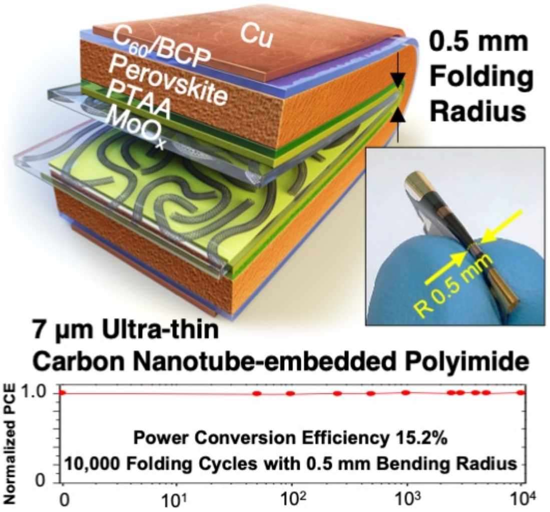

Fig. 1: 3D illustration, picture and mechanical data of the single-walled carbon nanotube-based foldable perovskite solar cells

Gold-vapor-assisted chemical vapor deposition of aligned monolayer WSe$_2$ with large domain size and fast growth rate

Chongwu Zhou*†

**University of Southern California*

Orientation-controlled growth of two-dimensional (2D) transition metal dichalcogenides (TMDCs) may enable many new electronic and optical applications. However, previous studies reporting aligned growth of WSe$_2$ usually yielded very small domain sizes. Herein, we introduced gold vapor into the chemical vapor deposition (CVD) process as a catalyst to assist the growth of WSe$_2$ and successfully achieved highly aligned monolayer WSe$_2$ triangular flakes grown on c-plane sapphire with large domain sizes (130 µm) and fast growth rate (4.3 µm/s). When the aligned WSe$_2$ domains merged together, a continuous monolayer WSe$_2$ was formed with good uniformity. After transferring to Si/SiO2 substrates, field effect transistors were fabricated on the continuous monolayer WSe$_2$, and an average mobility of 12 cm2/Vs was achieved, demonstrating the good quality of the material. This report paves the way to study the effect of catalytic metal vapor in the CVD process of TMDCs and contributes a novel approach to realize the growth of aligned TMDC flakes. [1] "Gold-vapor-assisted chemical vapor deposition of aligned monolayer WSe$_2$ with large domain size and fast growth rate", M. Chen, A. Zhang, Y. Liu, D. Cui, Z. Li, Y. Chung, S. P. Mutyala, M. Mecklenburg, X. Nie, C. Xu, F. Wu, Q. Liu, and C. Zhou, Nano Res. 13, 2625–2631 (2020).

Harnessing the Photovoltaic Properties of Carbon Nanotube Networks

Gideon Oyibo*†, Prathamesh Dhakras, Jeff Blackburn, Ji Ung Lee

**SUNY Polytechnic Institute*

Single-walled carbon nanotubes (SWNTs) have properties that make them attractive for photovoltaic applications. The large variation of SWNT chiralities makes it possible to absorb a broader range of the solar spectrum compared to other semiconductors. Previous works have studied the optical properties of SWNT-based heterojunction devices. In general, such architectures with different chiralities make it hard to study the light-harvesting potential of a SWNT network because every chirality with its unique bandgap forms a distinct heterojunction.Here, we fabricate a network consisting of only SWNTs and form P-N diodes using buried split gates. This configuration allows us to study the intrinsic optical properties of the SWNT network without requiring a separate electron or hole acceptor material. Split gates are used to create P- and N-doped regions in the SWNT network and electric fields to dissociate the photogenerated excitons into electron-hole pairs. We study the diode properties of both monochiral and polychiral networks, including those fashioned into tandem cells to explore the potential of SWNTs in photovoltaic applications.We examine the current-voltage characteristics of these diodes in the dark and find correlations between the key figure of merits, including the diode leakage current and the ideality factor, to different SWNT networks. We also examine their optical properties by measuring wavelength-dependent photocurrent spectroscopy to gain insights into the dynamics of excitons in a network of SWNTs. *Acknowledgements:* Dr Ji Ung Lee, Dr Jeffrey Blackburn, Prathamesh Dhakras, Sharadh Jois, Nargess Arabchigavkani

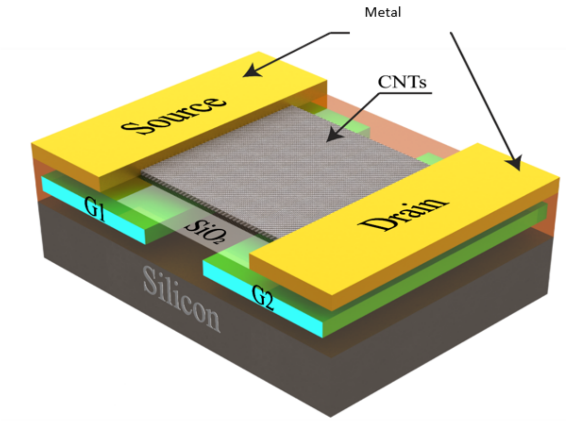

Fig. 1: Schematic of our gated P-N diode formed using a network of SWNTs

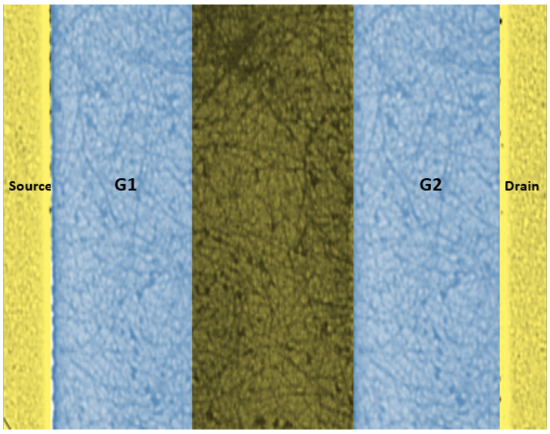

Fig. 2: SEM image of SWNTs over the split gates

Harvesting Radio-frequency Signals with Carbon Nanotube Electronic Ratchets

Andrew Ferguson*†, Ji Hao, Sanjini Nanayakkara, Jeff Blackburn

**National Renewable Energy Laboratory*

Portable sensing and electronic devices often require lightweight and flexible power solutions that cannot be easily provided by traditional battery technologies. In the last decade, organic electronic ratchets, thin-film transistor devices based on organic semiconductors, have been proposed as a potential power source, since they can harvest energy from radio-frequency radiation ubiquitous to our modern lifestyles. Initial implementations, employing molecular and polymeric semiconductors were limited by somewhat complex device architectures and poor charge-carrier transport, respectively. Here we show that these limitations can be overcome in simple transistors of enriched semiconducting single-walled carbon nanotubes (s-SWCNTs) networks doped via charge-transfer from redox-active molecules. We demonstrate that the spatial asymmetry required to afford a rectifying device can be generated through either post-doping voltage bias (poling) or patterning of the dopant profile during the doping process. The carbon nanotube electronic ratchets can transform radio-frequency AC signals to a stable DC current with higher output power ($>$ 1 mW) and can even generate power when driven by simulated electronic noise. The performance of these s-SWCNTs electronic ratchets exceeds that of their polymer counterparts by an order of magnitude, providing motivation for further exploration of these materials and devices for portable power generation.

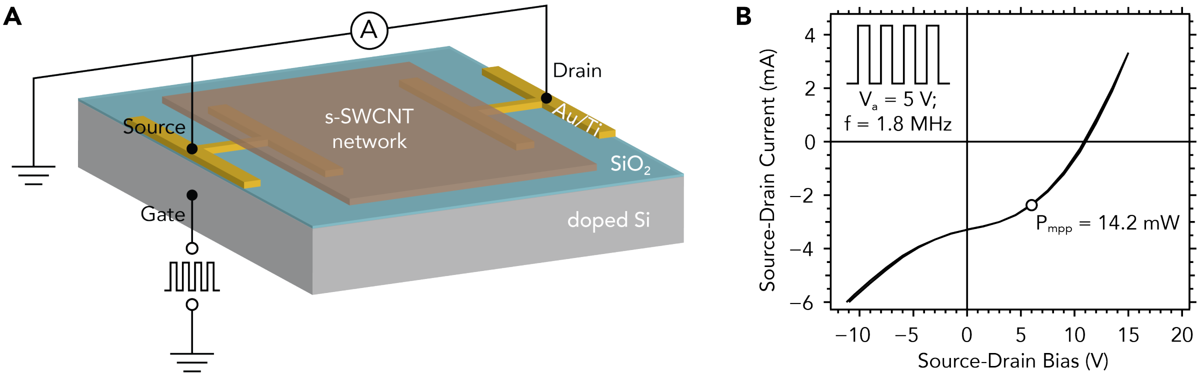

Fig. 1: (A) Carbon nanotube electronic ratchet device. (B) Rectification behavior of the electronic ratchet under application of an unbiased square wave signal with a zero time-average amplitude.

High-Performance Radio-Frequency and Nano Electronics Based on Assembled High-Density and High-semiconducting-Purity Carbon Nanotube Films

Chongwu Zhou*†

University of Southern California

Carbon nanotubes hold great promise for high-performance electronics but also face significant challenges in terms of assembly and integration. On one hand, aligned carbon nanotubes are proposed as an alternative to III-V semiconductor technologies in radio frequency (RF) applications because of their high linearity as amplifiers and compatibility with CMOS electronics. We will first report high-performance RF transistors with operation frequencies beyond 100 GHz. These devices are built upon high-density (~50 nanotubes / micron) and high semiconducting-purity (> 99.99%) aligned single-wall carbon nanotube films assembled at wafer scale. With gate length ~110 nm and T-shaped gate to reduce the gate charging resistance, the devices showed an extrinsic cutoff frequency and maximum oscillation frequency of over 100 GHz. The performance surpasses the 90 GHz cutoff frequency of radio-frequency CMOS transistors with gate length of 100 nm and is close to the performance of GaAs technology. [1] On the other hand, Carbon nanotubes are ideal candidates for beyond-silicon nanoelectronics because of their high mobility and low-cost processing; however, n-type transistors based on assembled aligned nanotubes has not been reported yet. Fabrication of n-type behavior field effect transistors (FETs) based on assembled aligned CNT arrays is needed for advanced CNT electronics. We will report a scalable process to make n-type transistors based on assembled aligned CNT arrays. Air-stable and high-performance n-type CNT FETs are achieved with high yield by combining atomic layer deposition dielectric and Ti contacts with gold overcoating, which are stable in air and widely used for III-V semiconductors. We also systematically studied the contribution of metal contacts and atomic layer deposition passivation in determining the transistor polarity. [2] Based on these experimental results, we report the successful demonstration of complementary metal-oxide-semiconductor inverters with good performance, which paves the way to realizing the promising future of carbon nanotube nanoelectronics. [1] ”Wafer-scalable, aligned carbon nanotube transistors operating at frequencies of over 100 GHz”, C. Rutherglen, A. A. Kane, P. F. Marsh, T. A. Cain, B. I. Hassan, M. R. AlShareef, C. Zhou and K. Galatsis, Nature Electronics, volume 2, pages 530–539, 2019. [2] ”Air-Stable n-Type Transistors based on Assembled Aligned Carbon Nanotube Arrays and Their Application in CMOS Electronics”, Z. Li, K. R. Jinkins, D. Cui, M. Chen, Z. Zhao, M. S. Arnold and C. Zhou, under review.

In Vivo Detection and Tissue Extraction of Single Walled Carbon Nanotube Sensors from a Large Animal Model

Nicole Iverson*†, Eric Hofferber, Jakob Meier, Nicolas Herrera, Joseph Stapleton, Chris Calkins

University of Nebraska-Lincoln

During this unprecedented health situation, the need for fast and accurate sensors is more important than ever. Single walled carbon nanotubes (SWNT) have been shown to have many desirable characteristics for in vivo sensing, including fluorescence in the tissue transparency window, a lack of photobleaching, and biocompatibility. The use of SWNT sensors in a large animal model has remained an elusive target until now. We used a relatively inexpensive and easy to set up system to detect our SWNT sensors within 9 sheep (approximately 100 pounds at sacrifice). The SWNT were packaged within hydrogels to allow for easy removal after the conclusion of the 21-day test period. We developed methods to extract the SWNT from both tissue and the hydrogels post-sacrifice, determining that at least 89% of the SWNT remained within the hydrogels and that there was no accumulation of SWNT within the animals’ tissue. This is the first demonstration of SWNT sensor detection within a large animal model. This is also a demonstration of the ability of hydrogels to retain SWNT during in vivo implantation, removing concerns about possible long-term SWNT accumulation and toxicity.

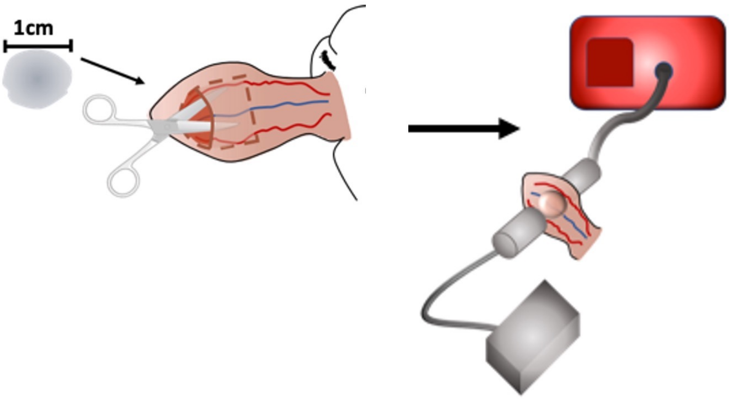

Fig. 1: SWNT sensor loaded hydrogels are placed in the ear of a sheep and the signal is detected with an inexpensive, easily transported device.

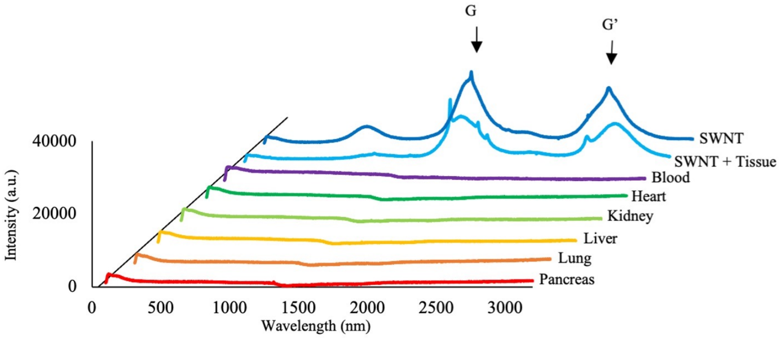

Fig. 2: SWNT remains within the hydrogel, they do not accumulate within the tissues of the sheep.

In vivo nanosensors using organic color centers for pharmacodynamic monitoring

Mijin Kim*†, Chen Chen, Zvi Yaari, Xiaojian Wu, Rachel Langenbacher, Rune Frederiksen, YuHuang Wang, Daniel Heller

**Memorial Sloan Kettering Cancer Center*

Organic color centers (OCCs) are covalent sp3 defects intentionally introduced to semiconducting carbon nanotubes to modify their electronic and optical properties. Small numbers of OCCs create localized potential wells that effectively harvest the mobile excitons through the nanotube, which acts as an optical antenna, turning these color centers into bright emitters. The OCC-induced fluorescence in the second near-infrared window significantly boosts the quantum yield (up to 28 fold compared to those of unfunctionalized nanotubes) and confers new chemical sensitivities to the local dielectric environments. To benefit from the unique chemical sensitivity and specificity of OCC fluorescence, we discuss a new method that controls the biological interactions and biocompatibility of OCC-based nanosensors. The resulting nanosensors can real-time monitor local intracellular events in live cells and in vivo.

Laser Direct Writing of 2D Transition Metal Chalcogenides/Oxides Heterostructures

Kai Liu*†

**Tsinghua University*

In recent years, two-dimensional (2D) transition metal chalcogenides (TMDs) have attracted growing attention due to their ultra-thin structure and novel optical and electrical properties. However, their facilitation of oxidization and weak van der Waals interlayer coupling have limited the improvement of their functions. In contrast, transition metal oxide (TMOs) materials have advantages in greater chemical stability, stronger correlation coupling, and unique phase transition properties. Construction of TMDs/TMOs heterojunctions can synergistically improve the functions of both materials. However, they are not easy to be in-situ grown because their growing atmospheres are mutually exclusive. Van der Waals stacking is a possible way to build TMDs/TMOs heterojunctions but this method is quite limited because TMOs are typically not of layered structures. In this report, I will introduce the recent work in my group on the construction of TMDs TMOS heterostructures, including the preparation of NbS2-Nb2O5, NbS2-NbOx, and VS2/VO2 heterostructures by laser direct writing technology. We also explored their applications in photoelectric detection, gas sensing, and neuromorphic devices. This series of work is expected to open up a new application direction of TMDs/TMOs heterostructures.References1. B. L. Wang, K. Liu, et al. ACS Nano, in revision.2. B. L. Wang, H. Luo, X. W. Wang, E. Z. Wang, Y. F. Sun, Y.-C. Tsai, H. Zhu, P. Liu, K. L. Jiang, K. Liu. ACS Nano, 14, 175 (2020). 3. B. L. Wang, H. Luo, X. W. Wang, E. Z. Wang, Y. F. Sun, Y.-C. Tsai, J. X. Dong, P. Liu, H. L. Li, Y. Xu, S. Tongay, K. L. Jiang, S. S. Fan, K. Liu. Nano Res., 13, 2035 (2020).4. H. Luo, B. L. Wang, E. Z. Wang, X. W. Wang, Y. F. Sun, Q. Q. Li, S. S. Fan, C. Cheng, K. Liu. Appl. Phys. Rev. 6, 041407 (2019).

Lateral epitaxy: the entropic source of ordered monocrystalline growth of 2D materials

Ksenia V. Bets*†, Boris Yakobson

**Rice University*

Scalable monocrystalline growth of 2D materials remains an obstacle for the industrial applications of many novel materials. A common approach to monocrystalline growth requires a careful selection of the substrate material and surface to ensure good structural matching with the target 2D material. This structural matching, in turn, promotes the co-orientation of independently nucleated islands allowing them to merge seamlessly during growth. In essence, the perfectly ordered substrate surface is expected to result in the well-ordered growing material. However, the non-covalent nature of the interaction between 2D materials and the surface results in minimal energy variation associated with the nucleus's relative rotation, eventually leading to low selectivity in islands' orientation. Furthermore, at growth temperatures, substrate surfaces are rarely flat, containing many meandering steps caused by thermal entropic processes (Fig.1). Counterintuitively, this surface disorder ensures perfect monocrystalline growth of 2D materials through stronger lateral epitaxy. We would demonstrate this phenomenon on the example of the epitaxial growth of hexagonal boron nitride on the Cu (111) surface that is further complicated by the absence of inversion crystal symmetry. The importance of the lateral epitaxy over the van der Waals epitaxy for the growth of 2D materials is also discussed and offers a better understanding of the general principles necessary for the monocrystalline growth processes.

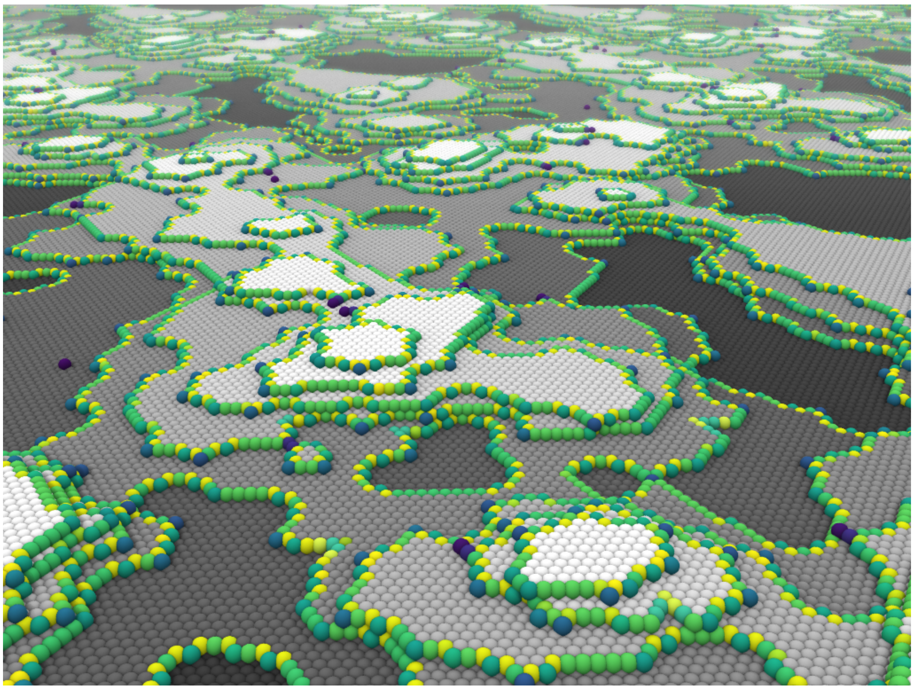

Fig. 1: Illustration of the roughness level of Cu(111) surface at 1500 K.

Liquid Crystals of Neat Boron Nitride Nanotubes and their Assembly into Ordered Macroscopic Materials

Cedric Ginestra*†

**Rice University*

Boron nitride nanotubes (BNNTs) have attracted much attention for their extraordinary properties, since their first synthesis in 1995. With tensile strengths on the order of 100 GPa, a wide electrical band gap, high thermal conductivity, and excellent thermal oxidative resistance, BNNTs are poised to become the electrically insulating analog to carbon nanotubes (CNTs) for applications involving extreme temperatures. Thus far, synthesis and purification challenges have hindered the widespread manufacturing of neat BNNT objects with macroscopic properties that reflect those observed on the microscopic scale. Here we report liquid crystalline solutions of neat BNNTs in chlorosulfonic acid (CSA). The BNNTs used for this work have been processed through a high temperature steam treatment to remove hexagonal boron nitride (h-BN), a two-dimensional allotrope of BNNTs that is considered a synthesis impurity. Polarized optical microscopy (POM) of solutions of these highly purified BNNTs (HP-BNNTs) reveals a Schlieren birefringence texture, which is a hallmark of nematic liquid crystals. Cryogenic scanning electron microscopy of solutions of HP-BNNTs in CSA directly shows aligned BNNT domains. In contrast, POM of lightly purified BNNTs (LP-BNNTs) shows no birefringence, indicating that LP-BNNTs form isotropic solutions likely because intercalated h-BN impedes BNNT alignment. Higher magnification images of HP-BNNT solutions reveals discrete ellipsoid domains with the birefringence pattern of bipolar tactoids, nematic BNNT droplets in equilibrium with an isotropic phase. To our knowledge, this is the first direct evidence of liquid crystalline phases of BNNTs. The intrinsic ordered structure of BNNT liquid crystals in CSA enables their assembly into aligned thin-films and fibers through scalable solution processing methods. The BNNT films produced in this work show mild alignment by scanning electron microscopy and a periodic birefringence intensity that is agrees with theory. Neat BNNT fibers extruded into acetone have a tensile strength of 10.4 MPa ± 4.3 MPa and Young's modulus of 400 MPa ± 160 MPa, values comparable to early CNT fiber properties. Wide angle X-ray scattering and polarized Raman show axial BNNT alignment. Further mapping of the BNNT liquid crystalline phase diagram and optimization of film and fiber production will improve their macroscopic properties, putting BNNTs in competition with their carbon analogs. *Acknowledgements:* Funding from AFOSR. Material provided by BNNT, LLC.

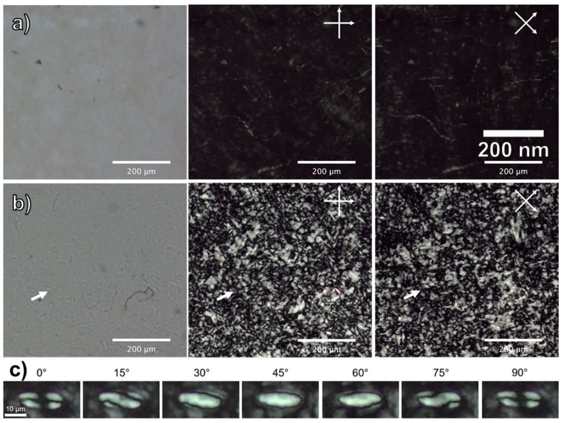

Fig. 1: (a) Isotropic solution of LP-BNNTs at 7000 ppmw. (b) Nematic solution of HP-BNNTs at 7260 ppmw. (c) Tactoid of HP-BNNTs at 3000 ppmw.

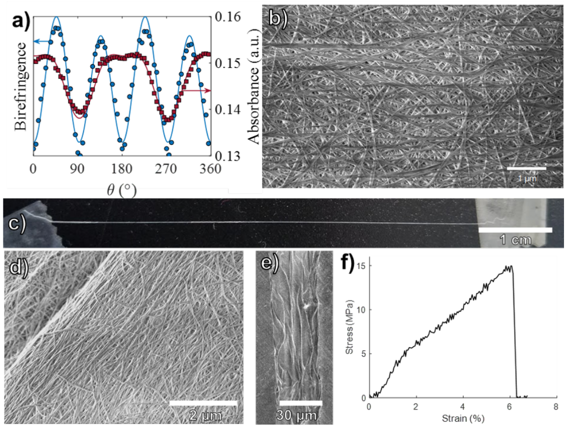

Fig. 2: (a) Birefringence intensity and absorbance and (b) SEM of shear-aligned BNNT film. (c) Photograph, (e) high and (e) low magnification SEM, and (f) tensile test of a BNNT fiber.

Molecular n-Doping of Large- and Small-Bandgap Carbon Nanotube Field-Effect Transistors with ttmgb

Jan Gotthardt*†, Severin Schneider, Simone Leingang, Hans-Jörg Himmel, Jana Zaumseil

**Applied Physical Chemistry, Heidelberg University*

Purely p- and n-type field-effect transistors (FETs) are desirable for complementary circuits to minimize power dissipation. One way to achieve these properties with intrinsically ambipolar semiconducting single-walled carbon nanotube (SWCNT) networks is molecular doping. However, creating n-type SWCNT-FETs is particularly challenging due to the air-sensitivity and instability of many n-dopants. Guanidino-functionalized aromatic compounds such as 1,2,4,5-tetrakis(tetramethylguanidino)benzene (ttmgb) have been shown to efficiently and reliably n-dope (6,5) SWCNT network FETs with gold electrodes (ACS Nano 2018, 12, 5895). Here, we investigate the broader applicability of ttmgb as a molecular n-dopant in bottom-contact/top-gate FETs with different electrode metals and large- and small-bandgap polymer-sorted semiconducting SWCNTs (ACS Appl. Electron. Mater. 2021, 3, 804). Contact doping with ttmgb significantly reduces the work function of gold, palladium and platinum, lowers the contact resistance for electron injection by orders of magnitude and blocks hole injection. The application of optimized ttmgb concentrations can thus transform FETs based on networks of large-bandgap SWCNTs as well as mixed-chirality plasma torch SWCNTs with small bandgaps from ambipolar to purely n-type. Carrier concentration- and temperature-dependent current-voltage characteristics of pristine and doped FETs corroborate that ttmgb treatment does not change the maximum electron mobilities at high carrier densities. However, ttmgb doping improves the subthreshold slope by removing shallow electron trap states. This positive effect on the switching behavior of the FETs is greatest for large-bandgap SWCNTs.

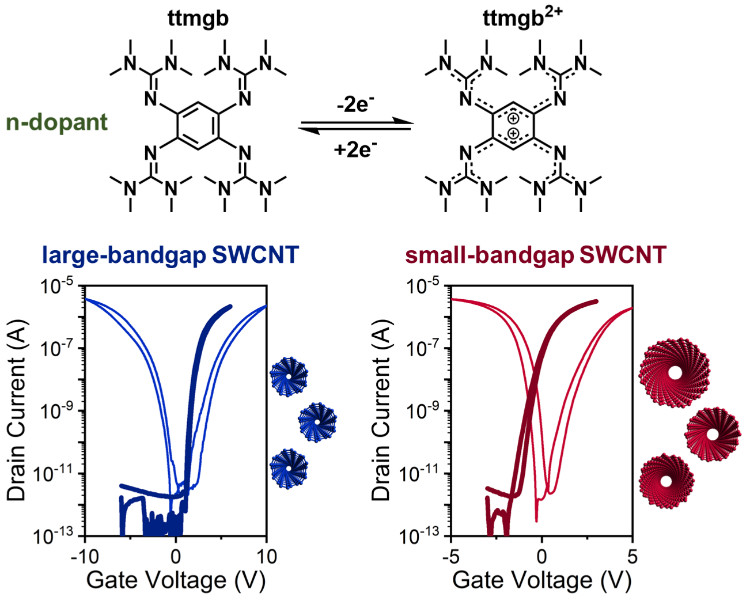

Fig. 1: Reversible oxidation of molecular n-dopant ttmgb and transfer characteristics of pristine (ambipolar) and ttmgb-treated (n-type) large-bandgap (6,5) SWCNT and small-bandgap plasma torch SWCNT network FETs.

Multispectral Fingerprinting Resolves Dynamics of Nanomaterial Trafficking in Primary Endothelial Cells

Daniel Roxbury*†, Mitchell Gravely

University of Rhode Island

Intracellular vesicle trafficking involves a complex series of biological pathways used to sort, recycle, and degrade extracellular components, including engineered nanomaterials which gain cellular entry via active endocytic processes. A recent emphasis on routes of nanomaterial uptake has established key physicochemical properties which direct certain mechanisms, yet relatively few studies have identified their effect on intracellular trafficking processes past entry and initial subcellular localization. Here, we developed and applied an approach where single-walled carbon nanotubes (SWCNTs) play a dual role - that of an engineered nanomaterial (ENM) undergoing intracellular processing, in addition to functioning as the signal transduction element reporting these events in individual cells with single organelle resolution. We used the unique optical properties exhibited by non-covalent hybrids of single-stranded DNA and SWCNTs (DNA-SWCNTs) to report the progression of intracellular processing events via two orthogonal hyperspectral imaging approaches of near-infrared (NIR) fluorescence and resonance Raman scattering. A positive correlation between fluorescence and G-band intensities was uncovered within single cells, while exciton energy transfer and eventual aggregation of DNA-SWCNTs were observed to scale with increasing time after internalization. These were confirmed to be consequences of intracellular processes using pharmacological inhibitors of endosomal maturation, which suppressed spectral changes through two distinct mechanisms. An analysis pipeline was developed to colocalize and deconvolute the fluorescence and Raman spectra of subcellular regions of interest (ROIs), allowing for single-chirality component spectra to be obtained with sub-micron spatial resolution. This approach uncovered a complex relationship between DNA-SWCNT concentration, fluorescence intensity, environmental transformations, and irreversible aggregation resulting from the temporal evolution of trafficking events. Finally, a spectral clustering analysis was applied to delineate the dynamic sequence of processes into four distinct populations, allowing stages of the intracellular trafficking process to be identified by the multi-spectral fingerprint of encapsulated DNA-SWCNTs.

Near-unity radiative quantum efficiency of excitons in carbon nanotubes

Hidenori Machiya, Daiki Yamashita, Akihiro Ishii, Yuichiro Kato*†

**RIKEN*

The efficiencies of photonic devices are primarily governed by radiative quantum efficiency, which is a property given by the light emitting material. Quantitative characterization for carbon nanotubes, however, has been difficult despite being a prominent material for nanoscale photonics. Here we determine the radiative quantum efficiency of bright excitons in carbon nanotubes by modifying the exciton dynamics through cavity quantum electrodynamical effects [1]. Silicon photonic crystal nanobeam cavities [2] are used to induce the Purcell effect on individual carbon nanotubes. Spectral and temporal behavior of the cavity enhancement is characterized by photoluminescence microscopy, and the fraction of the radiative decay process is evaluated. We find that the radiative quantum efficiency is near unity for bright excitons in carbon nanotubes at room temperature. [1] H. Machiya, D. Yamashita, A. Ishii, Y. K. Kato, arXiv:2102.10718 (2021). [2] R. Miura, S. Imamura, R. Ohta, A. Ishii, X. Liu, T. Shimada, S. Iwamoto, Y. Arakawa, Y. K. Kato, Nat. Commun. 5, 5580 (2014).This work is supported by MIC (SCOPE 191503001), JSPS (KAKENHI JP20H02558, JP20J00817, JP20K15199, JP19J10319), MEXT (Nanotechnology Platform JPMXP09F19UT0072), and RIKEN (Incentive Research Project). H.M. and D.Y. are supported by JSPS (Research Fellowship for Young Scientists). H.M. acknowledges support from RIKEN (Junior Research Associate Program). FDTD calculations are performed using HOKUSAI BigWaterfall supercomputer at RIKEN. We acknowledge the Advanced Manufacturing Support Team at RIKEN for technical assistance.

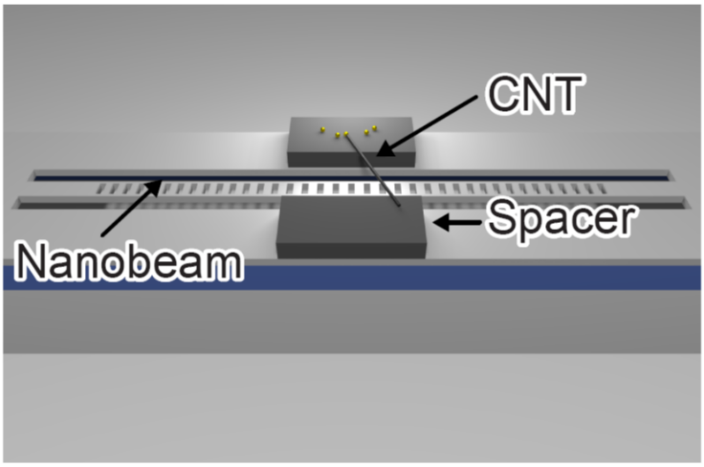

Fig. 1: Schematic of the device.

Protein site-specific coupling to carbon nanotubes : from single-molecule nanohybrids to nanoscale biosensors with tuned electrostatic gating

Matteo Palma*†

**Queen Mary University of London*

A central challenge in nanobiotechnology is the bottom-up assembly of platforms capable of monitoring and exploiting biomolecular interactions with nanoscale or single-molecule control; this in turn can allow the investigation of ligand-receptor functions, the fabrication of next generation ultrasensitive and nanoscale biosensing devices, as well as the development of novel bioelectronics interfaces.In this regard, we developed different platforms based on single-walled carbon nanotubes (SWCNTs) as building blocks that allow for single-molecule and nanoscale studies to be performed in a variety of research fields. Here, I will discuss the assembly and fabrication of bioelectronic systems and devices with engineered protein interfacing. In particular, I will demonstrate site-specific assembly of single proteins on individual SWCNTs. As a proof of concept, we investigated different CNT-protein configurations and obtained evidence of site-specific coupling between SWCNTs and specific proteins of interest. Notably, only the right bioengineered system exhibited the expected direct protein-nanotube communication, paving the way to selective electrical addressability of proteins via the use of carbon nanoelectrodes.I will then present the fabrication of bioelectronic devices for the development of real-time biosensors with engineered protein interfacing. In particular, we assembled b-lactamase (BL) inhibitory proteins (BLIPs) onto SWCNT sidewalls in electronic device configurations, with controlled protein orientation. This allowed us to control the local electrostatic surface presented within the Debye length (see Figure 1), and thus modulate the conductance gating effect upon sensing protein targets. We recorded the current responses in real-time for the detection of a range of concentrations of a class BL enzymes, that degrade antibiotics, in the context of investigating antimicrobial resistance (AMR). The strategy presented here is of general applicability for the control and detection of protein-protein interactions in nanoscale device configurations, through electrostatic surface profiling; moreover, it may open up new opportunities for the development of AMR-related diagnostic devices.

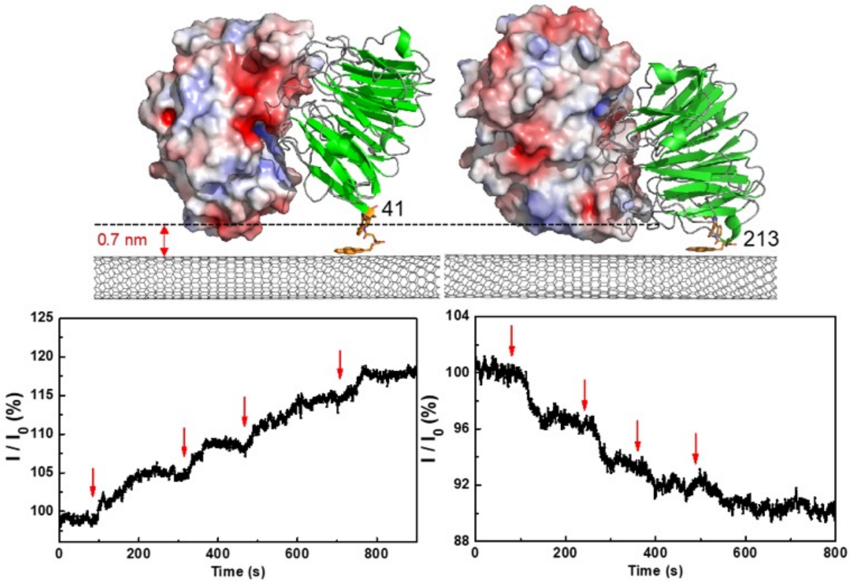

Fig. 1: TEM - an important -lactamase involved in antimicrobial resistance - electrostatic surface presentation on binding BLIP proteins engineered at different designed positions and corresponding conductance traces measured across SWCNT-FETs

Rapid Feedback experimentation for continuous carbon nanotube growth

Arthur Sloan*†, Matteo Pasquali, Glen Irvin, Rahul Rao, Benji Maruyama, John Bulmer

**Rice University*

Carbon nanotubes (CNTs) are among the most promising candidates for the creation of next generation materials, as well as applications across diverse fields such as medicine and communications. Moreover, they provide a pathway to fix fossil or biological carbon into useful solid materials. Adoption into large scale applications is still stifled by the limited scale of synthesis of the long, highly crystalline CNTs needed to attain strength and conductivity at the macroscale. Despite major cost-reductions continuous production techniques such as floating catalyst chemical vapor deposition (FCCVD) have not yet attained the efficiencies to allow economic process scale-up. This is partially due to the large parameter space of the FCCVD process, which includes diverse carbon sources, catalyst chemistries, and process configurations, making systematic optimization challenging due to the large number of experimental combinations possible and extremely labor-intensive nature of such work.To address these issues, the autonomous research system (ARES) was developed at the Air Force Research Laboratory and has proved invaluable by providing rapid feedback experimentation coupled with autonomous or semi-autonomous operation. ARES dramatically decreases the research effort required for each experiment, allowing for rapid exploration of the CNT growth parameter space as well as the collection of statistics on process variability.Thus far, ARES has been used to optimize surface-bound CTN growth. Here, we apply the ARES to FCCVD growth (FC-ARES) with the goal to develop an autonomous, closed loop research system for FCCVD reactors. Our custom built FCCVD reactor has an inline Raman spectrometer enabling rapid iterations through the FCCVD parameter space with near instantaneous feedback on the crystallinity and composition of the produced CNTs. We present two test cases to demonstrate the utility of this system. The first is a set of 179 experiments exploring how differing molecular structures of related carbon sources (ethanol, n-propanol, and i-propanol) impact the morphology of produced CNTs while controlling for flow rates as well as various interatomic ratios. The second is a set of 360 experiments which examines the effect of sulfur to iron ratios on the produced CNTs. It also examines the effect of the oxidative or reducing nature of the system, by the addition of CO2 and H2 respectively. We expect FC-ARES to interrogate the large parameter space and identify impactful parameters that increase process efficiency, yield, and control over morphology and crystallinity, thereby defining pathways to geometric scaling of FCCVD reactors. *Acknowledgements:* Funding for this work was provided by the NASA NSTRF program, Shell, ARPA-E, and AFOSR

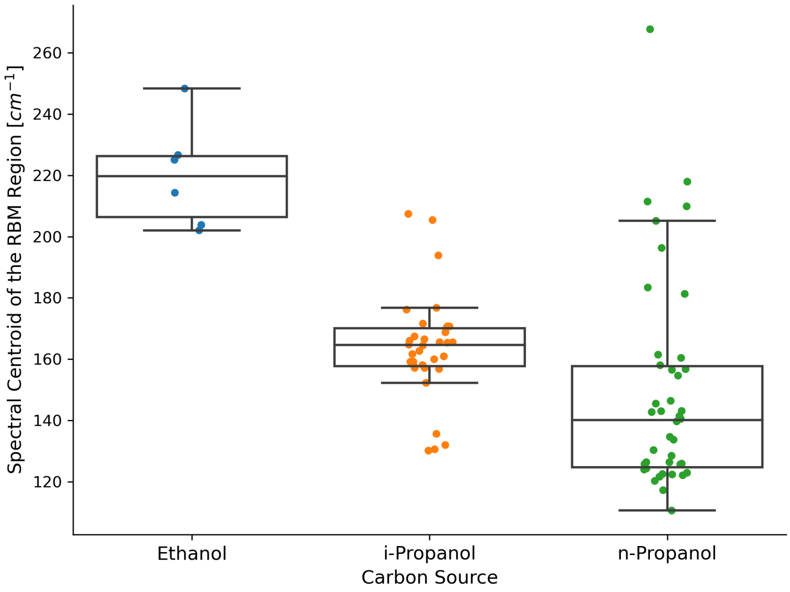

Fig. 1: CNTs grown on the FC-ARES show diameter differences depending on the carbon source, as determined from the RBM region's spectral centroid.

Selectively twisting carbon nanotubes into semiconducting chiralities by low-work-function contact

Jiangtao Wang*†, Gregory Pitner, Xiang Ji, Jiadi Zhu, Jinchi Han, Han Wang, Lain-Jong Li, Jing Kong

**Massachusetts Institute of Technology*

With the development of carbon nanotube (CNT) based electronics, efficient growth of both high-quality and high-purity semiconducting carbon nanotube (s-CNT) array becomes one of the most important challenge in the carbon nanotube community. Most of selective synthesis methods are utilizing either the native free energy or native stability difference between the growth of semiconducting and metallic tubes. However, such native energy separation is not enough large to sufficiently suppress the random thermal fluctuation in high growth temperature and efficiently delivery semiconducting carbon nanotubes with required high purity. Here we reported an approach to opening a significant gap in the free energy plot of both epitaxial growth and chirality change by keeping the growing CNTs in contact with low-work-function electrodes. As a result, selectively twisting horizontally aligned CNTs with initially random chiralities into high-purity semiconducting chiralities is achieved by applying a weak perturbation (10V/mm-alternating electric field). When connect with low-work-function electrodes, CNTs as well as tipped catalysts will be negatively charged since the difference in work function. Due to the large aspect ratio of CNTs, the strong local electric field generated by the charge stored at the CNTs tip contributes a prominent electrostatic work that greatly affects the total free energy change. Because of the remarkable difference of quantum capacitance between metallic CNT (m-CNT) and s-CNT, the free energy plot of CNTs growth is separated into two branches. As the CNTs are highly n-doped, a large free energy gap is opened between m-CNTs and s-CNTs and the twisting barrier of metallic to semiconducting is dramatically lowered. By applying a weak perturbation, vast majority of

CNTs are twisted into semiconducting chiralities during the growth. Our observation also opens a possibility of controlling the catalytic pathway through the contact engineering and will pave the way for practical applications of CNT electronics. *Acknowledgements:* TSMC

Separation of metallic single-chirality carbon nanotubes using gel-column chromatography

Hiromichi Kataura*†, Mayumi Tsuzuki, Takeshi Tanaka

**National Institute of Advanced Industrial Science and Technology*

Single-chirality separation of single-wall carbon nanotubes (SWCNTs) is critical to understanding their physical properties and developing suitable applications. Many reports on the structural sorting of SWCNTs have been reported so far. However, most reports focus on semiconducting SWCNTs rather than metallic SWCNTs probably because of their high importance in electronic device applications. Furthermore, single-chirality separation of metallic SWCNTs is not easy. DNA wrapping is always powerful even for metallic SWCNTs, but number of reports using other methods such as aqueous two-phase extraction method is limited [1]. This report shows a single-chirality separation of metallic SWCNTs using gel-column chromatography. Previously, it was thought that only semiconducting SWCNTs would be adsorbed on the polysaccharide gels when sodium dodecyl sulfate was used as a surfactant. This selectivity resulted in metal/semiconductor separation. However, adsorption mechanism was not well understood. Today, we have a better understanding of the adsorption mechanism and have more precise control over the adsorption process. In this study, we succeeded in adsorbing metallic SWCNTs on the gel column. When the metallic SWCNTs were adsorbed on the column, interestingly, the elution behaved very much like the semiconducting SWCNTs. Diameter selective elution can be achieved by stepwise increasing concentration of the surfactant. As a result, high-purity (5,5) and (6,6) SWCNTs could be sorted from SG65, CoMoCAT. This method can be applied to other SWCNT sources. We will show the latest results in the presentation. [1] Han Li et al., ACS Nano 2019, 13, 2567–2578 *Acknowledgements:* This works was supported by JSPS KAKENHI, grant No. 20H05668, Japan and JST CREST, grant No. JPMJCR18I5, Japan.

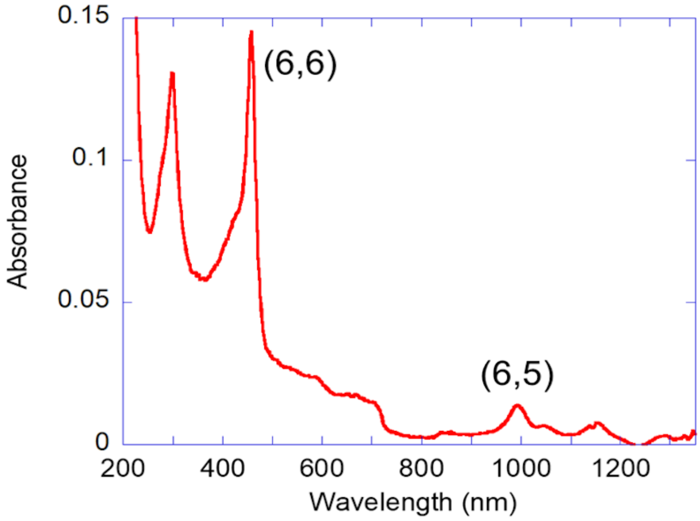

Fig. 1: Optical absorption spectrum of (6,6) SWCNTs obtained from SG65.

Synthesis and Applications of Ultralong Carbon Nanotubes

Rufan Zhang*†

**Tsinghua University*

Ultralong carbon nanotubes (CNTs) exhibit unique mechanical, electrical and optical properties. In this presentation, I will talk about three aspects of ultralong CNTs. First, the controlled synthesis of centimeters-long CNTs with perfect structures and their excellent mechanical and electrical properties. Second, the fabrication of unique CNT networks with sensitive response to light and their applications. Third, the structural coloration of ultralong CNTs and CNT fibers.

The CNT biocorona: a challenge in nanobiotechnology

Lorena García-Hevia*†, Mahsa Saramiforoshani, Jesús González, Jorge Monge-Ruiz, Mónica L Fanarraga

**Nanomedicine Group, Valdecilla Health Research Institute, Santander, Spain*

Carbon nanotubes (CNTs) represent a highly versatile heterogeneous family of two-dimensional nanomaterials that display many extraordinary properties in the field of nanobiotechnology. Their physico-chemical uniqueness in addition to their morphology have a huge added value in many new ground-breaking advances in nanomedicine. However, their use in medicine strongly depends on how we understand and control their interactions with the surrounding biomolecules.The large variety of proteins that nonspecifically bind to CNTs endow these filaments with a biological identity that dictates their in vivo behavior. Therefore, knowledge and predesign of the composition of the biocorona is crucial to endows these nanomaterials unique ability to interact with specific cell receptors, penetrate through membranes, or even intermingle with the cell polymers, interfering with cellular biomechanics.Here we study the spontaneous interaction of different CNTs with serum components and show how, upon spontaneous functionalization, these nanomaterials capture different amounts of proteins on their surfaces. In addition, we show how protein coating is affected by several condition during functionalization, how a single type on CNTs can capture a different protein assortment when exposed to different human sera, and how a single serum interacts differently with a variety of CNTs. In the view of the many different bio-identities that CNTs can adopt, we conclude that there is an urgent need to develop a predictable functionalization method to control the cellular responses the functionalized CNT trigger.

The Light, the Dark, and the Role of Charges and Defects in Carbon Nanotubes

Todd Krauss*†, Trevor Tumiel, Erin Christensen

**University of Rochester*

A long-standing challenge in the field of single-walled carbon nanotube (SWCNT) optics is to determine the influence of local topological and electrostatic perturbations on the photophysical properties of the nanotube. In this presentation we will directly address this issue through reporting on experiments combining single nanotube photoluminescence (PL) spectroscopy with electrostatic force microscopy (EFM), the latter of which are designed to measure the number, location and magnitude of localized (and unavoidable) charge states near the NT. EFM is a variation of atomic force microscopy that allows for a quantitative imaging with sub-25 nanometer resolution of localized charges and dielectric constants. Using EFM, we found that for SWCNTs there exists a significant heterogeneity in static charge along the NT (Figure 1), even for NTs that in topographic images show a homogeneous NT height. EFM data for dozens of long NTs (length greater than 1.5 microns) solubilized in aqueous suspension using standard ionic surfactants (e.g. sodium deoxycholate) revealed that NTs possess charge variations all along their length with magnitudes on the order of 1 e to a few e, with both positive and negative signs. In terms of their origin, the charges seem to be correlated with the presence of surfactant coating the NT, as when the surfactant was diligently rinsed away the NTs imaged as charge neutral and do not show significant charge variation. The surface potential measured with EFM is similar to potentials reported from EFM images of NTs with localized sp3 defects arising from covalent functionalization of the SWCNT sidewall. This finding led to a working hypothesis that the presence of the charges along the NT is a significant source of the potential barriers that localize the exciton at low temperatures, and further, can potentially be exploited to localize the exciton at 300 K. Indeed, EFM measurements of the same SWCNT before and after photoexcitation show distinct localized regions of the NT with pronounced changes in the charge signal, rather than a uniformly charged NT as would be expected for a freely diffusing free charge (Figure 1). Comparison of individual SWCNT PL images with AFM topographic and EFM charge images allow for an unambiguous determination of localized excitons along the NT (Figure 1). Note that simple optical spectroscopy can often be significantly misleading in this regard, and thus having AFM and PL images from the same NT is critical.

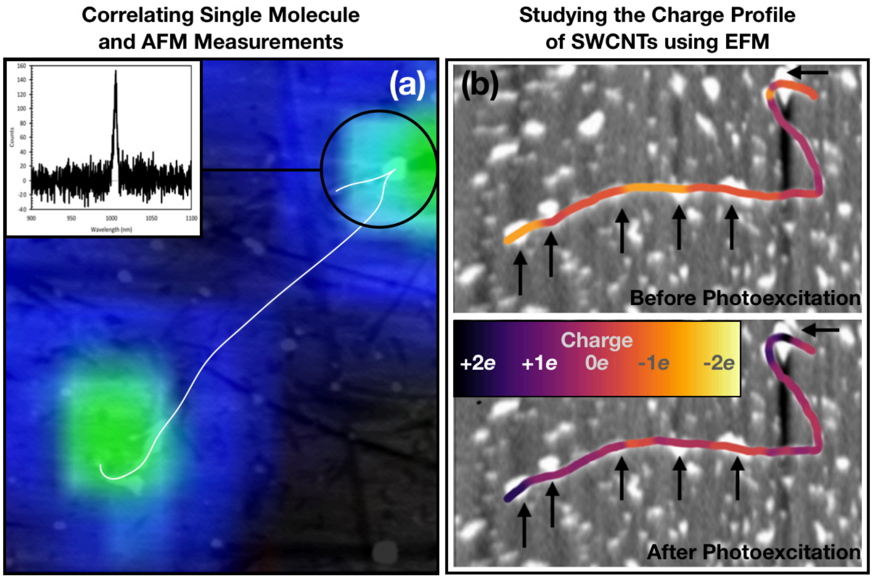

Fig. 1: (a) PL overlaying an AFM image (SWCNT outlined). Inset: PL spectrum of circled region. (b) Charge profile before and after photoexcitation. Arrows indicate surfactant aggregates. Scale bars are 500 nm.

Time-resolved Optical Microscopy of Single Semiconducting Carbon Nanotubes

Konrad Birkmeier, Friedrich Schöppler, Ivonne Vollert, Tobias Hertel, Achim Hartschuh*†

**LMU Munuch*

We study the excited dynamics in thin semiconducting single-walled carbon nanotubes (SWCNTs) on glass using transient scattering microscopy with sub-ps temporal resolution. In the experiment, the intensity of the elastically scattered light from a tightly focused spot is detected for variable time delay between excitation and probe pulse. We find that the transient scattering response of single semiconducting SWCNTs can be recorded with high signal to noise ratio. Transients detected for different probe energies reflect an interplay of positive and negative signal contributions, as observed in transmission experiments in solution [1]. For individual (6,5) SWCNTs we typically find bi-exponential decays with time constants of around 1 – 3 ps and 20 – 30 ps varying from nanotube to nanotube (Figure 1). We correlate the observed excited state dynamics with the photoluminescence decay recorded from the same SWCNTs using time-correlated single photon counting to illuminate the role of non-emitting transient states [2] and to bridge the existing gap between the two techniques. References:[1] Zhu et al. J. Phys. Chem. C 111, 3831 (2007)[2] Soavi et al. Adv. Optical Mater. 4, 1670 (2016)

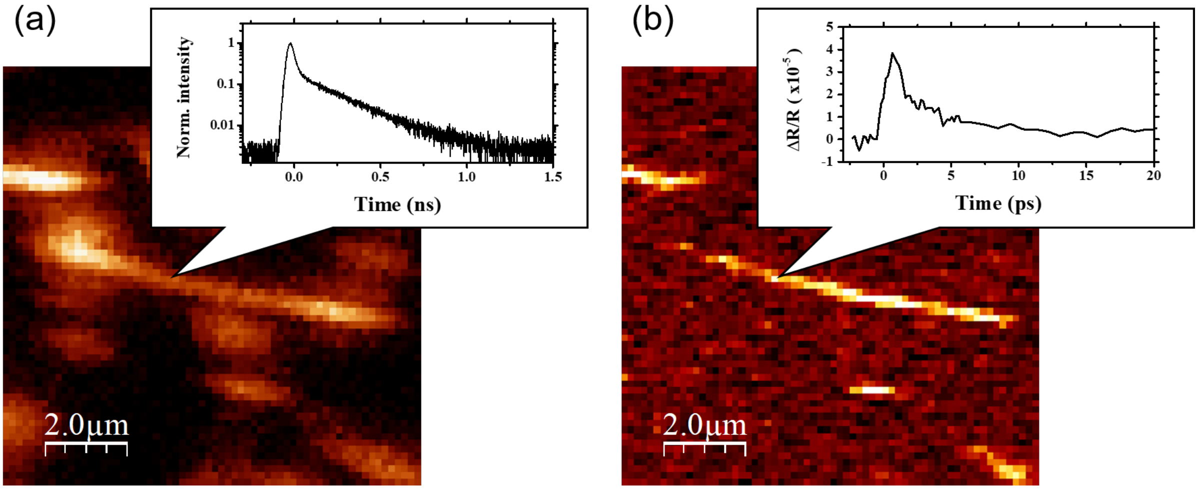

Fig. 1: Confocal PL (a) and transient scattering (b) image of (6,5) SWCNTs on glass together with the corresponding signal transients detected for the same SWCNT.

Transparent and Freestanding Single-Walled Carbon Nanotube Films Synthesised Continuously via Floating Catalyst Chemical Vapor Deposition

Qiang Zhang*†

NanoMaterials Group, Department of Applied Physics, Aalto University School of Science,

Single-walled carbon nanotube (SWCNT) films are promising materials as flexible transparent conductive films (TCFs). Here, we present a new floating catalyst chemical vapor deposition (FCCVD) method of producing freestanding, continuous SWCNT TCFs at a rate of several hundred meters per hour [1]. The synthesis mechanism, involving blowing a stable aerosol bubble and transforming the bubble into an aerogel, is investigated and a general phase diagram is established for this method. For the fabrication of SWCNT TCFs here, both carbon conversion efficiency and SWCNT TCF yield can reach three orders of magnitude of those with the conventional FCCVD. The film manifests a sheet resistance of 40 ohm/sq at 90% transmittance after being doped, representing the record performance based on large-scale SWCNT films. The transparent, flexible, and stretchable electrodes based on BACVD films are demonstrated. Moreover, this high throughput method of producing SWCNT TCFs can be compatible with the roll-to-roll process for the mass production of flexible displays, touch screens, solar cells, and solid-state lighting, and is expected to have a broad and long-term impact on many fields from consumer electronics to energy conversion and generation. [1] Q. Zhang et al., Advanced Materials 32 (39), 2004277

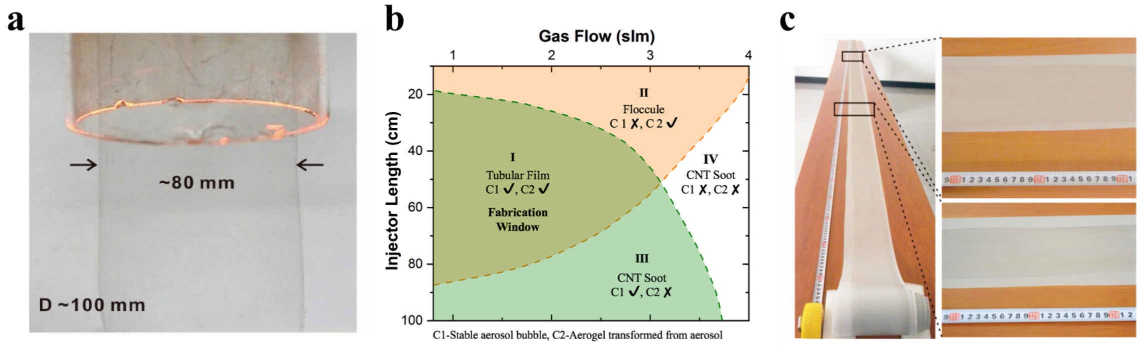

Fig. 1: Transparent SWCNT films fabricated via FCCVD with an ultra-high yield and the corresponding synthesis phase diagram.

Tunable Doping and Characterization of Single-Wall Carbon Nanotube Macrosystems in air

Alexander Tonkikh*†, Valentina Eremina, Ekaterina Obraztsova, Alexander Pereyaslavtsev, Esko Kauppinen, Elena Obraztsova

A.M. Prokhorov General Physics Institute, Russian Academy of Science, 119991 Moscow, Russia

In this study, we consider two important issues devoted to CNT doping. First, we demonstrate a way, allowing the formation of a material with adjusted Fermi level, WF, and electrophysical characteristics within one approach. We have developed a methodology for adjusting the electrophysical properties based on tuning of concentration and type of dopant in the channels of carbon nanotubes. Second, we have developed a simple empirical method for prediction and achievement of the required values of the transport and optical characteristics. We propose a simple approach for the macro-objects composed of carbon nanotubes doping characterization. This approach is an empirical representation of the thermoelectric coefficient on the electrical resistance (specific resistance, sheet resistance (Rsq), or conductivity) dependence. In our work, we use the S – Rsq/Rsq-max dependence and propose a general approach, which we call the ”doping map”, applicable to all types of macroscopic objects composed of CNTs. This ”doping map” gives us complete information about the initial and the doped states of the conducting system. Moreover, the method allows the prediction of the maximum achievable values of transport characteristics at the adjusted doping level (tuned Fermi level). Finally, based on the thermoelectric properties, we demonstrate the achievement of optimal values for parameters required for a specific application task.A. A. Tonkikh, V. A. Eremina, E. A. Obraztsova, D. A. Musatov, A. Yu. Pereyaslavtsev, E. I. Kauppinen, and E. D. Obraztsova, Tunable Doping and Characterization of Single-Wall Carbon Nanotube Macrosystems for Electrode Material Applications, ACS Applied Nano Materials, Article ASAP, DOI: 10.1021/acsanm.1c00411 *Acknowledgements:* The Raman studies were funded

by RSF project 20-42-08004. The reported study was funded by RFBR, project 20-32-70013.

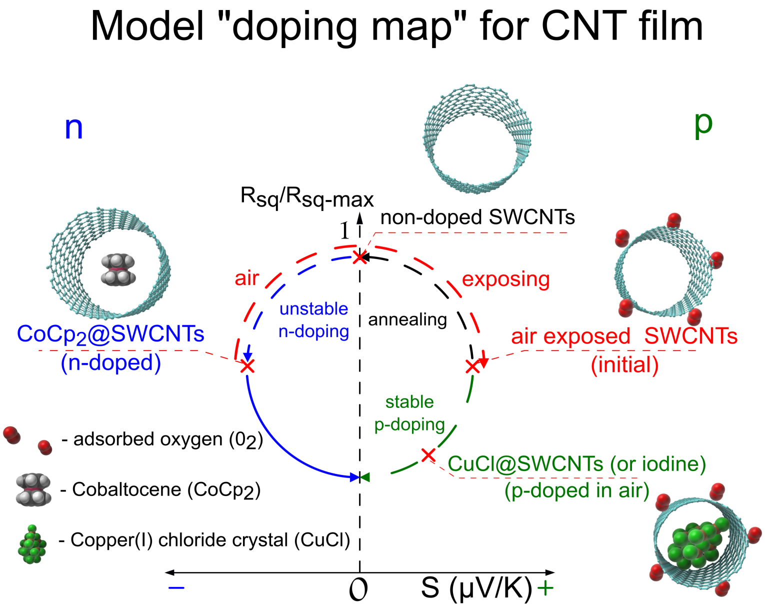

Fig. 1: Model "doping map" based on experimental cycle for characterization of SWCNT macro-objects. The dashed lines on the graph show the experimental stages carried out to plot the dependence.

Wafer-scale Alignment of 2D Carbon Nanotube Liquid Crystals for Electronics

Katherine Jinkins*†, Sean Foradori, Vivek Saraswat, Robert Jacobberger, Jonathan Dwyer, Padma Gopalan, Arganthaël Berson, Michael Arnold

**Northwestern University*

Floating evaporative self-assembly (FESA) is a solution-based technique for fabricating aligned nanotube arrays.1 The excellent alignment, individualization, and nanotube packing in FESA films have enabled field-effect transistors (FETs) with on-state current densities exceeding that of Si and GaAs devices.2 However, FESA relies on the dropping and spreading of organic nanotube ink at a substrate/water interface. This drop-by-drop nature is inherently difficult to scale and additionally results in films of alternating stripes of aligned and randomly oriented carbon nanotubes. In the work here, we discover that carbon nanotubes confined at a liquid/liquid interface form two-dimensional (2D) lyotropic liquid crystal assemblies. We exploit this phenomenon to develop a new solution-based nanotube alignment technique, termed tangential flow interfacial self-assembly (TaFISA), yielding wafer-scale arrays of uniformly aligned semiconducting carbon nanotubes with state-of-the-art electrical performance and exceptional spatial uniformity.32D nanotube liquid crystal assemblies spontaneously form at a liquid/liquid interface and are comprised of domains of highly-ordered nanotubes. When the liquids are static, the domains lack a global orientation. However, by flowing one liquid tangentially across the surface of the other, the 2D liquid crystalline domains globally orient with the direction of flow to form uniform arrays of carbon nanotubes with exceptional alignment (within ± 6°). Nanotube ordering improves with increasing concentration and decreasing temperature due to the underlying liquid crystal phenomena. The excellent alignment and wafer-scale uniformity (demonstrated alignment across a 10 cm wafer) of the transferred nanotube assemblies enable FETs with high on-state current density averaging 520 μA μm-1 at –0.6 V, with FET to FET variation of only 19%. Subthreshold swing as low as 60 mV decade-1 is reported, when using a strong gate (comprised of an ionic gel), demonstrating that the intrinsic properties of TaFISA arrays meet both high on current and efficient switching requirements needed for next-generation microelectronic devices. 1. Jinkins, K. R. et al. Langmuir 33, 13407–13414 (2017).2. Brady, G. J. et al. Sci Adv 2, (2016).3. Jinkins, K. R. et al. Under Review (2021).

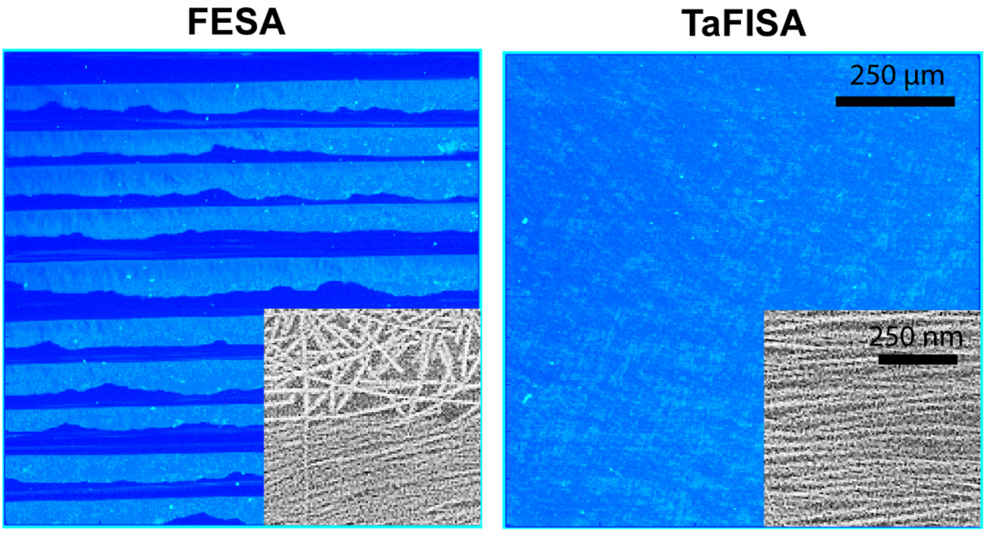

Fig. 1: Comparison of nanotube film morphology from FESA and TaFISA techniques using Raman spectroscopy mapping (showing nanotube density variation) and scanning electron microscopy (insets).

Well-Defined Armchair Graphene Nanoribbons Synthesized inside Carbon Nanotubes

Wim Wenseleers*†, Miles Martinati, Sofie Cambré, Hans Kuzmany, Lei Shi, Thomas Pichler, Kecheng Cao, Ute Kaiser, Jenő Kürti, János Koltai, Gergő Kukucska, Takeshi Saito

**University of Antwerp*

The hollow core and well-defined diameters of carbon nanotubes (CNTs) make them the ideal template for ordering one-dimensional (1D) arrays of molecules and for the controlled synthesis of 1D carbon nanostructures from suitable precursor molecules. For instance, we previously demonstrated that in this way dipolar dye molecules can be naturally aligned in an ideal head-to-tail arrangement to create assemblies with a giant total nonlinear optical response,[1] and that the optical properties of dye molecules encapsulated in SWCNTs can be strongly modulated by the SWCNT diameter, indicating very specific diameter-dependent stacking and interactions of the molecules. [2] By thermal conversion also well-defined carbon structures can be synthesized inside the hollow core of CNTs, such as long 1D carbon chains (carbyne), for which the band-gap was determined for the first time using wavelength-dependent Raman spectroscopy,[3] or graphene nanoribbons (GNRs). Here we show by means of extensive wavelength dependent resonance Raman (excitation) spectroscopy, that GNRs synthesised inside CNTs display remarkably clean electronic and vibrational spectra, in good agreement with theoretical calculations, allowing them to be identified with very well-defined armchair GNR (AGNR) structures with sub-nanometer width (in particular the 6- and 7-atom wide structures 6-AGNR and 7-AGNR). [4] These remarkably well-defined structures are obtained despite the use of rather non-specific precursors (ferrocene) indicating that the final structure obtained is governed completely by the diameter of the CNT template. [1] S. Cambré, J. Campo et al., Nature Nanotechnol. 10, 248 (2015). [2] S. van Bezouw, D. H. Arias et al., ACS Nano 12, 6881 (2018). [3] L. Shi et al., Phys. Rev. Mater. 1, 075601 (2017). [4] H. Kuzmany et al., Carbon 171, 221 (2021).

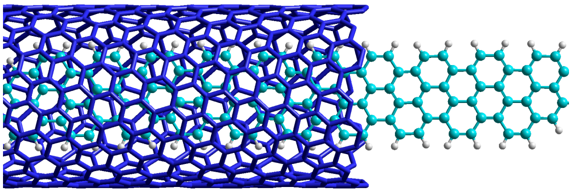

Fig. 1: Molecular model of a 6-AGNR inside a (14,6) SWCNT.

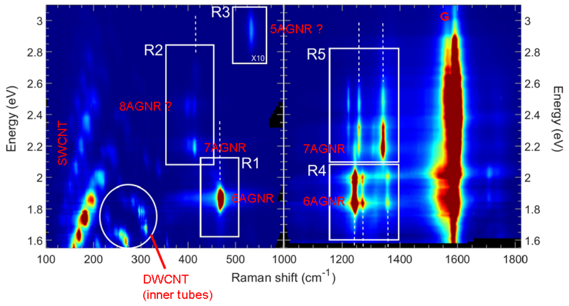

Fig. 2: 2D (i.e. laser-wavelength-dependent) resonant Raman spectroscopy of carbon nanotubes in which armchair graphene nanoribbons have been synthesized.

What Dictates Rashba Splitting in 2D van der Waals Heterobilayers

Sunny Gupta*†, Boris Yakobson

**Rice University*

Spintronics, where the spin degree of freedom of the electrons is manipulated to process information in devices, is a rapidly growing field and has immense potential in next-generation electronics. Electron spins are usually manipulated by bulky magnets, which is difficult to control in small length scales and is a bottleneck in devising spin-based devices. Rashba spin-orbit coupling, on the other hand, enables electric control of spin states, promising enormous advances from conventional charge-based computing. Until now, a general scheme or a descriptor to find an optimal system with isolated spin states with large tunable splitting is still lacking. Here based on first-principles calculations, we explore the microscopic physicochemical mechanism responsible for the Rashba effect in 2D van der Waals heterobilayers. We find that the difference in Born effective charge of atoms at the interface can be used as a single-layer descriptor to predict hetero-pairs with large Rashba splitting, thus reducing the scaling factor in materials search. Moreover, we discover that for most 2D materials, the routinely used Rashba parameter αR is not a good gauge of the effect's strength. From our general scheme, MoTe2|Tl2O, and MoTe2|PtS2, with spin splitting above 120 meV, Rashba energy ER = 94 meV, and wavenumber difference 2k0 = 0.36 Å-1 ("effective" αR > 1 eVÅ), emerge as the best candidates for spin transistors at room temperature.

Poster Presentations

A1: Free Space Resonant Electromagnetic Sensing Techniques to Detect Airborne Viral and Environmental Particles Using Atomic Layer Graphene

Massood Tabib-Azar*†, Shaun McKellar, Cynthia Furse

**ECE Dept. University of Utah*

The main objective of this work is to develop sensors that can detect and identify airborne particles and viruses. Measurements with microwaves operating at 5-20 GHz offer a good balance between covering relatively large volumes (proportional to the wavelength cubed~ l3 where 2< l <3.75 cm) and providing high sensitivity. Sensitivity can be further enhanced using free-space Fabry-Perot (F-P) resonators, as shown in Fig. 1a. A paper filter material or a permeable mesh structure is located at the center of the F-P resonator where the standing wave electric field is maximum. It is used to capture the particles in the air passing through the device (Fig. 1a). The mesh/paper filter can also be replaced with an atomic layer of graphene or other suitable 2-D layered materials with specific sensitivity to the particles of interest. In most cases, the conductivity of the atomic layer materials changes when charged particles deposit on them, increasing the F-P sensor's sensitivity. Fig. 1.b shows the transmission coefficient, S21, of a plain CVD graphene layer and with 5 μL of COVID-infected and uninfected saliva. The inset shows the resonator frequency shift with respect to the plain graphene. Interestingly, uninfected saliva increased the resonant frequency, while the infected saliva reduced it. Assuming that the graphene layer exchanges electrons with the saliva through hybrid p bonds, the change in the resonant frequency indicates that the graphene layer donated electrons to the infected saliva, while it accepted electrons from the uninfected saliva. Fig.2a shows the resonant frequency as a function of the saliva volume deposited on the paper filter in the 16.4 GHz F-P resonator with the paper filter sensor. The frequency shift as a function of the saliva volume is negative in both infected and uninfected saliva cases when the paper filter was used. Fig. 2b shows the S21 spectrum of the graphene layer between 0.75 GHz and 0.83 GHz. These spectra were normalized to the S21 spectrum of the plain graphene. The spectrum of the infected saliva (5 μL) is different than that of the uninfected saliva between 0.81-0.815 THz. The paper filter F-P sensor sensitivity using 16.4 GHz F-B sensor, defined as Df0/dm was around 200 kHz/ng for high contrast conducting particles such as gold nanoparticles. It was 500 kHz/mg for dielectric (polyester) micro-particles, and it was around 800 kHz/1000 COVID-19 viruses in saliva. The sensitivity using single atomic layer graphene at 16.4 GHz was 508 kHz/1000 COVID-19. Acknowledgement: This work was partially supported by The National Science Foundation and Examin Corporation. SCM is supported by the University of Utah Undergraduate Research Opportunity program. *Acknowledgements:* Acknowledgement: This work was partially supported by The National Science Foundation and Examin Corporation.

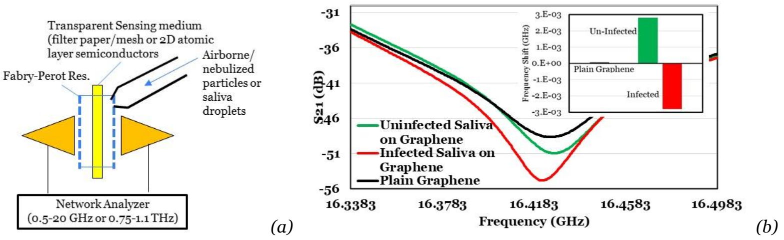

Fig. 1: a) The experimental set up used to perform X-band and terahertz studies. b) S21 spectra of the Fabry-Perot resonator and its frequency shift with 5 μL of saliva.

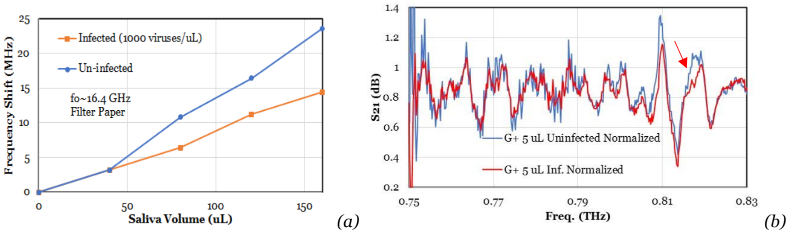

Fig. 2: a) Frequency shift of the Fabry-Perot paper filter resonator as a function of saliva volume. b) The plain graphene normalized S21 spectra of 5 μL saliva.

---

* denotes primary author, † denotes presenting author.

A2: A Hydrogen free approach for activating an Fe catalyst nanoparticle using trace amounts of noble metals to synthesize tall vertically-aligned carbon nanotubes

Shunsuke Sakurai*†, Maho Yamada, Jinping He, Kenji Hata, Don Futaba

**National Institute of Advanced Industrial Science and Technology (AIST)*

Although metallic iron (Fe) is a remarkably active catalyst exemplified by its ability to dissociate nitrogen gas molecules as in Haber-Bosch process, the ease of corrosion by oxidation represents a significant obstacle. In fact, the most applications of metallic Fe catalyst are limited to the reactions where hydrogen was supplied as one of the reactants. Also, in the case of CNT synthesis, the importance of hydrogen has been frequently recognized to prepare the active nanoparticle catalyst of Fe, especially for the synthesis of vertically-aligned assembly of small-diameter CNT (forest) via chemical vapor deposition (CVD) process [1-3].Here, a novel approach to fabricate reduced, highly active, and corrosion-resistive Fe-based catalysts without reduction by hydrogen is presented [4]. Central to our approach is the incorporation of trace levels (< 1 at%) of noble metals (NM = Ir, Rh, Pt) to Fe oxide nanoparticle on alumina support layer. X-ray photoelectron spectroscopy (XPS) analysis revealed that reduction of Fe by annealing in a non-reducing ambient (nitrogen, argon, or helium) could be achieved with as little as 0.3 at% NM, suggesting only a few NM atoms per one Fe oxide NP was required to reduce hundreds of Fe atoms. The efficient synthesis of tall (>500 µm) and vertically aligned CNT forests within 10 minutes by a completely hydrogen-free CVD process demonstrated the high catalytic activity of Fe-NM system fabricated without hydrogen. The mechanism of trace amounts of NM is presented based on further XPS analysis suggesting the metallic NM appeared by the self-reduction, and then reduced catalytically the surrounding Fe atoms. The possibility to apply our novel catalyst into the widespread chemical reactions under oxidative ambient, such as the reforming of hydrocarbons for hydrogen production, by Fe-based catalysts will be also presented. [1] S. Sakurai, H. Nishino, D. Futaba, S. Yasuda, T. Yamada, A. Maigne, Y. Matsuo, E. Nakamura, M. Yumura, K. Hata, J. Am. Chem. Soc., 134, 2148 (2012). [2] S. Sakurai, M. Inaguma, D. Futaba, M. Yumura, K. Hata, Small, 9, 3584 (2013). [3] T. Tsuji, J. Kim, H. Sakakita, Y. Shimizu, G. Chen, K. Hata, D. Futaba, S. Sakurai, submitted. [4] S. Sakurai, M. Yamada, J. He, K. hata, D. Futaba, submitted. *Acknowledgements:* This work was supported by JSPS KAKENHI Grant Number JP17K14090.

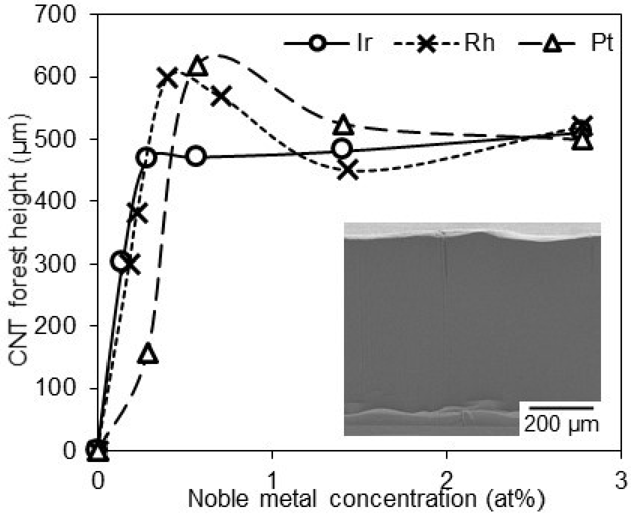

Fig. 1: CNT forest heights as a function of NM (Ir, Rh, and Pt) concentration. Inset shows the SEM image of CNT forest synthesized from Fe-Rh (0.4 at%) without hydrogen.

A3: Multifaceted approaches to quantitative surface characterization of as-grown and acid treated single-walled carbon nanotubes

Kazufumi Kobashi*†, Yoko Iizumi, Kazutoshi Hirota, Naoki Shinomori, Kazuhiro Shimamoto, Yasumasa Koga, Takahiro Morimoto, Toshiya Okazaki

**National Institute of Advanced Industrial Science and Technology (AIST)*

The surfaces of an individual carbon nanotube (CNT) and its bundle have been characterized over a few decades. Understanding the macroscale surfaces created by large number of CNTs is recently getting essential to utilize CNTs in the academic and industrial fields. The averaged or localized surface data have so far been collected by various analytical methods, however the quantitative characterization remains challenging.Here, we propose multifaceted approaches to quantitatively characterize the macroscale surfaces of CNTs by 11 different analytical methods (Raman, far and mid IR, TEM, Boehm titration, TGA, weight change, TPD/MS, EGA/MS, XPS, SEM/EDS). Our characterization is composed of the averaged, localized, mapped data of surface functional groups, revealing the kind, amount, distribution of both as-grown and acid treated, single-walled CNTs. Through the analyses, interestingly the adsorbed water on the surfaces was quantified, which we believe important to understand CNTs surfaces and quantitatively estimate the surface functional groups.A comparison between as-grown and functionalized CNTs can act as a good guide to understand the surfaces. Loosely bundled, single-walled CNTs with high carbon purity (>99 wt%) and modest crystallinity (Zeonano SG101) were chosen to achieve a homogeneous functionalization. The CNT powder was first exfoliated in viscous liquid of glycerol at rt by stir bar, then the acid treatment was conducted with 22 wt% H2SO4 aqueous solution and KMnO4 at 80oC for 2h. The acid treated CNTs mainly had carboxylic acid (13 wt%) and hydroxy (6 wt%) groups in the total functional groups (41 wt%). The amount of adsorbed water increased by the acid treatment and came up to ~20 wt%. Furthermore, taking the obtained quantitative results fully into account, the plausible chemical structural model of the acid treated CNTs can be drawn (Figure). Taken together, our findings showed an importance to characterize the macroscale CNTs surfaces in a multiple manner, and would be useful to understand surfaces of nanocarbon materials.

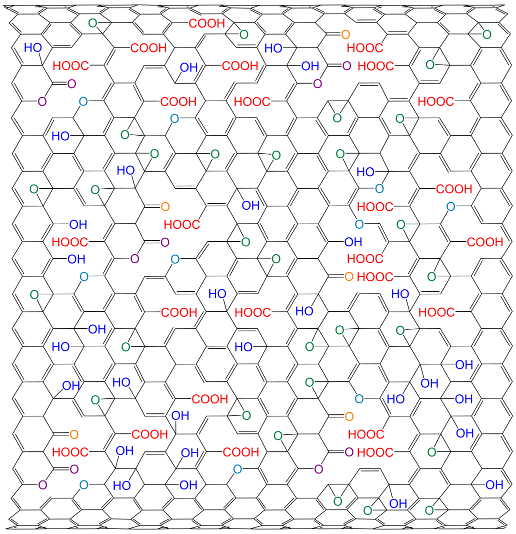

Fig. 1: Chemical structural model for the sidewalls of acid treated single-walled CNTs.

A4: Investigating Carbon doping in 2-D Hexagonal Boron Nitride (hBN) Films

Eoin O'Sullivan*†, Dillon McGurty, John Ballentine, Ian Griffiths, Philip Holdway, Nicole Grobert

**University of Oxford*

The optical and electronic properties of hBN – wide band gap, electrically insulating and great thermal transport properties – make it a fascinating 2-D material for future electronics and opto-electronics. Introduction of carbon into the lattice has been shown to modulate some of these properties. Recently, carbon doping has been identified as the source of visible quantum emitters in hBN [1]. However, experimental investigation into hBN-C formation has been limited, including comprehensive studies of its structural and electronic properties. Carbon incorporation into hBN can be achieved through various routes and is dependent on the mode of growth. As such, hBN-C films can exhibit differing properties depending on the synthesis method used. Thus, research into the synthesis methods and their relationship with resulting material properties requires further examination and understanding. In this work, Atmospheric Pressure Chemical Vapor Deposition (APCVD) is used to synthesize carbon doped hBN (hBN-C), building on synthesis methods developed in our group [2]. Characterization of the resultant film is carried out in comparison to its intrinsic form. Results show carbon is incorporated though graphitic regions in the material, resulting in Stranski-Krastanov growth. Spectroscopic analysis show distinct modulations in the vibrational and optical properties of hBN with carbon inclusion. This work contributes to the development of 2D hBN-C towards application in advanced, next-gen materials. [1] 'Identifying carbon as the source of visible single-photon emission from hexagonal boron nitride', Noah Mendelson, Dipankar Chugh, Jeffrey R. Reimers, Tin S. Cheng, Andreas

Gottscholl, Hu Long, Christopher J. Mellor, Alex Zettl, Vladimir Dyakonov, Peter H. Beton, Sergei V. Novikov, Chennupati Jagadish, Hark Hoe Tan, Michael J. Ford, Milos Toth, Carlo Bradac & Igor Aharonovich, Nature Materials volume 20, pages 321–328 (2021). [2] 'Time dependent decomposition of ammonia borane for the controlled production of 2D hexagonal boron nitride', Vitaliy Babenko, George Lane, Antal A. Koos, Adrian T. Murdock, Karwei So, Jude Britton, Seyyed Shayan Meysami, Jonathan Moffat & Nicole Grobert, Scientific Reports volume 7, Article number: 14297 (2017) *Acknowledgements:* EPSRC, Royal Society, David Cockayne Center for Electron Microscopy (DCCEM), Oxford Material Characterisation Service (OMCS)

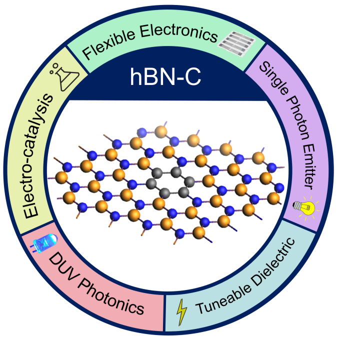

Fig. 1: Introducing carbon into the lattice alters the physical properties of hBN, tuning electronic parameters, increasing photo-responsivity, creating reactive sites for electrocatalysis, and even creating single photon emitters.

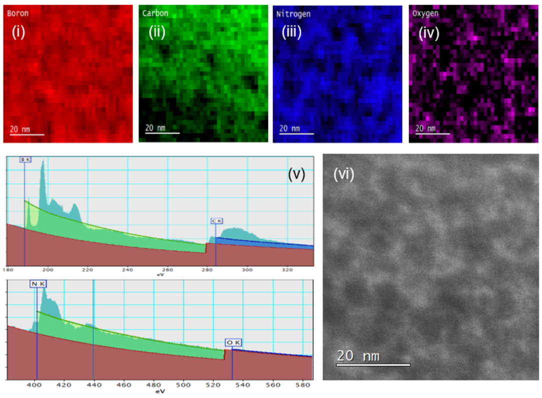

Fig. 2: Structure and composition of hBN-C film: (i-iv) EELS maps showing elemental composition and corresponding (v) spectra and (vi) DF TEM image for the region of interest

A5: A real-time, quantitative approach to evaluate the dispersion state of carbon nanotube aggregates using particle image analysis

Kazufumi Kobashi*[†], Don Futaba, Shun Muroga, Takeo Yamada, Toshiya Okazaki, Kenji Hata

**National Institute of Advanced Industrial Science and Technology (AIST)*

Carbon nanotube (CNT) aggregates in dispersions are widely applied to fabricate the neat and composite materials as macroscale assemblies such as fibers, films, and bulks. However, the relationship between the CNT aggregate structures and the intrinsic CNT properties has been unclear. To clarify this point, the size and shape of thousands of CNT aggregates were investigated using particle image analysis from which we generated the map to describe the aggregate structures.Central to this study is the use of ISO area diameter and anisotropy (Feret length/ISO area diameter) of CNT aggregates (Figure (a,b)). In the map Figure (b) from mildly agitated Zeonano/propylene glycol dispersion, moving vertically upward corresponds to an increase in the anisotropy of the dispersed, exfoliated aggregate. The shapes of the individual CNT aggregate change from perfectly circular (ratio: 1) to long and thin for a fixed size (ISO area diameter). In contrast, moving along a horizontal cross-section, the size of the aggregate increases for a fixed isotropy (i.e. shape). Based on the map we categorized the CNT aggregate structures into 4 groups (Figure (c)). By this quantitative approach, we demonstrated robust CNT films having high electrical conductivity and high specific surface area, revealing correlations between the CNT aggregate structures in dispersions and the film properties. Furthermore, a precise tracking of CNT aggregate structures at different stages of dispersion was made, which has been elusive issues for CNT applications. The structural changes from as-grown aligned CNTs to mesh-like, round aggregate structures were traced to analyze the dispersion states. These findings would be an asset for CNT users to identify tailored CNT aggregate structures for their applications.

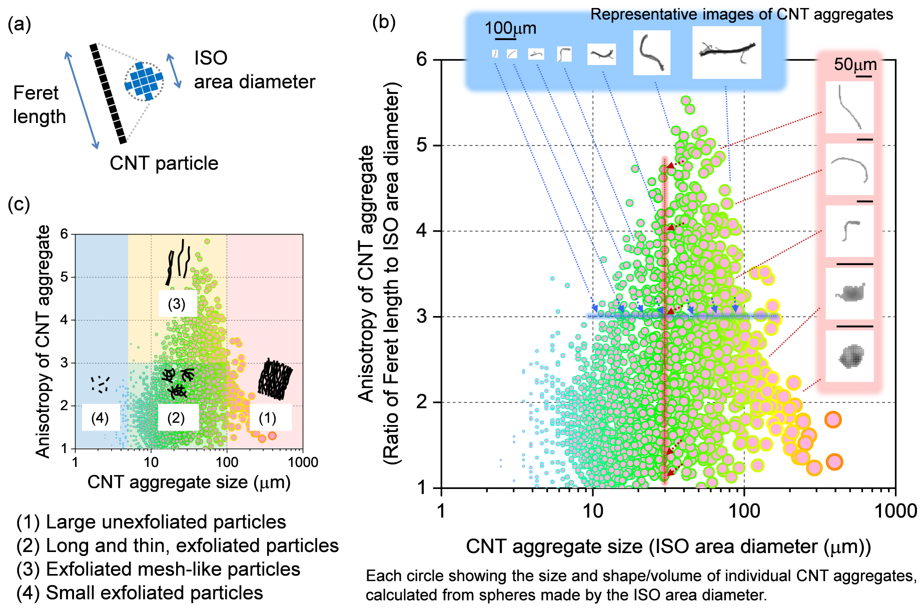

Fig. 1: (a) Drawing for CNT particle size, (b) map of CNT aggregate size and shape distributions by particle image analysis, (c) category of CNT aggregates with different size and shape.

A6: The origin of quantum effects in low-dimensional thermoelectric materials

Nguyen Tuan Hung*†, Riichiro Saito

Tohoku University

Thermoelectric material, which directly converts waste heat to electricity, provides an ideal supply for the Internet of things (IoT) sensors. New attempts had started for thermoelectricity of low-dimensional materials since 1993 when Hicks and Dresselhaus presented the confinement theory [1]. This theory is based on the fact that the density of states (DOS) has sharp peaks at the energy edges of one-dimensional carbon nanotubes (CNT), as shown in figure 1 (a). The confinement theory has inspired experimental works to use low-dimensional materials for improving thermoelectric efficiency for more than two decades, as shown in figure 1 (b). However, experimentalists cannot answer the following question: what kind of materials would give effective performance by the confinement effect? In 2016, we showed a new parameter of the low-dimensional materials, so-called the thermal de Broglie wavelength, that could answer this question [2]. The new concept of the thermal de Broglie length for enhancement thermoelectricity is verified experimentally by many groups [3-4]. Although the relationship between the thermal de Broglie length and the enhancement thermoelectricity was given analytically, first-principle calculations [5] and experiments, the physical picture of thermal de Broglie length in confinement were not given clearly. In this work, we show how recent theories and experiments have made progress on the quantum confinement effects of the 1D CNTs and 2D related materials. In particular, we would like to discuss why the thermal de Broglie wavelength becomes a key parameter to enhance the power factor [6]. [1] L. D. Hicks, M. S. Dresselhaus, Phys. Rev. B 47, 12727 (1993); Phys. Rev. B 47, 16631 (1993). [2] N. T. Hung, E. H. Hasdeo, A. R. T. Nugraha, M. S. Dresselhaus, R. Saito, Phys. Rev. Lett. 117, 036602 (2016). [3] J. Zeng, X. He, S. J. Liang, E. Liu, Y. Sun, C. Pan, et al., Nano Lett. 18, 7538 (2018). [4] H. Ohta, S. W. Kim, S. Kaneki, A. Yamamoto, T. Hashizume, Adv. Sci. 5, 1700696 (2018). [5] N. T. Hung, A. R. T. Nugraha, R. Saito, Nano Energy 58, 743 (2019). [6] N. T. Hung, R. Saito, Adv. Quantum Technol. 4, 2000115 (2021). *Acknowledgements:* N.T.H. acknowledges JSPS KAKENHI (Grant No. JP20K15178) and R.S. acknowledges JSPS KAKENHI (Grant No. JP18H01810).

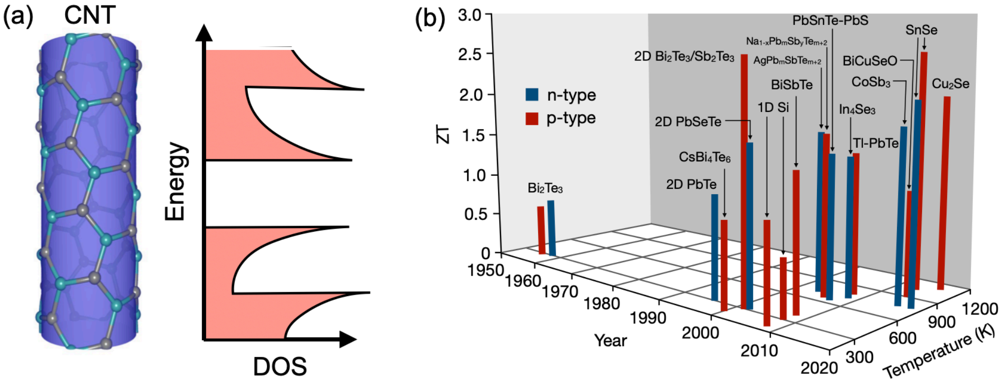

Fig. 1: (a) The density of states of the semiconducting CNT. (b) Thermoelectric figure of merit, ZT, as a function of temperature and year [6].

A7: Understanding the important System Design Elements to Build an Efficient Synthesis of High Quality CNTs at Scale by FC-CVD Method

Muxiao Li*†, Daniele Micale, Arthur Sloan, Emily Yedinak, Jacob Arredondo, Glen Irvin, Matteo Pasquali

**Rice University*

Carbon nanotubes (CNTs) have been promising nanomaterials with their great optical, thermal, electrical and mechanical properties but have not achieved any commercial success to date. Since the 1990s, a number of CNT synthesis methods have been utilized but with an array of unresolved challenges to efficiently produce CNTs. Among those methods to produce CNTs, floating catalyst chemical vapor deposition (FCCVD) is commonly used due to its expected low cost, high production yield and potential high CNT selectivity. However, using FCCVD has not resulted in widespread capability to efficiently produce CNTs. In this presentation, I will outline the thought process and critical parameters to address efficiency issues and my experimental results thus far, utilizing methane as a carbon source, a catalyst precursor, ferrocene, and a growth promoter, thiophene in an Ar/H2 growth environment. This study covers in-progress investigations of parameters including carrier gas type, catalyst solvent composition, feedstock preheating and CH4 thermochemistry as determined by the H2:CH4 feed ratio/temperature setpoint/residence time. My approach is to use a systematic process exploration informed by extensive characterization of the reaction environment (GC-MS, in-situ thermocouples, microkinetic modeling) and as-produced CNT materials analyses (multi-spectral Raman, TGA, purifications, extensional rheology for CNT aspect ratio) in order to identify the most important control factors to determine a reaction design to increase the FCCVD CNT production efficiency. The optimal goal is to efficiently grow high quality CNTs (high crystallinity, high aspect ratio with longer average length) with a high production rate and low cost which will enable more rapid commercial adoption. *Acknowledgements:* Many thanks to the team members, my advisors, Jacob Arredondo for helping with GC-MS work and funding sources, Shell and ARPA-E.

A9: Diameter-based separation of SWNTs through their mechanical interlocking with nanorectangle

Guoqing Cheng*†, Naoki Komatsu

**Graduate School of Human and Environmental Studies, Kyoto University*

Although mechanical interlocking of SWNTs has attracted considerable attention, it has not been used for separating SWNTs. In this work, a new host molecule named ”nanorectangle” connecting two nanocalipers by metal was designed, synthesized, and employed for separating SWNTs. After HiPCO SWNTs were sonicated in 2-propanol followed by centrifugation, the resulting extract showed the red shift in the absorption of nanorectangle, indicating its complexation with SWNTs. The mechanical interlocking of nanorectangle was observed in TEM, where two anthracenes attached on the both faces of SWNT (Fig. 1a). After removal of host molecule through demetalation, the resulting SWNTs were analyzed by Raman and absorption spectroscopies, revealing the diameter enrichment around 0.9 nm (Fig. 1b). Such high selectivity was also confirmed with (6,5) and (7,6)-CoMoCAT SWNTs. As compared with nanocalipers, the better selectivity was observed toward the smaller diameters (Fig. 1b).

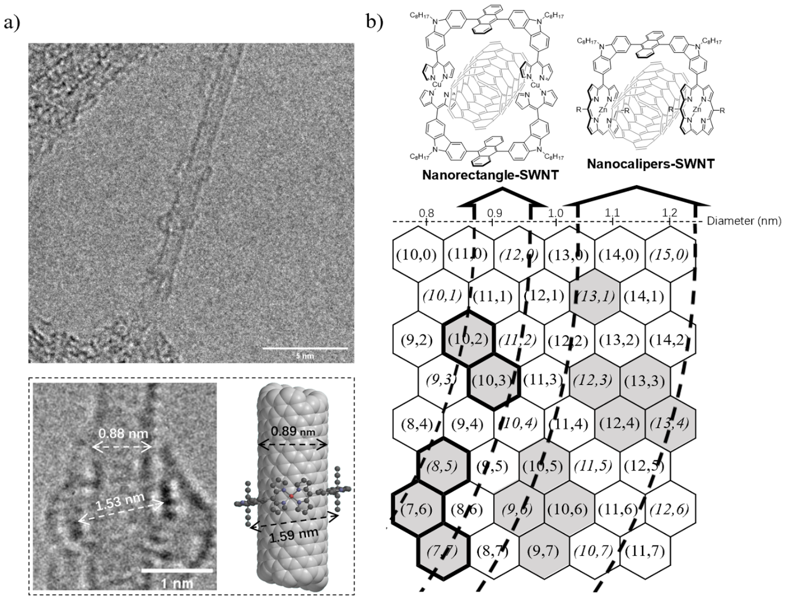

Fig. 1: a) TEM image and model structure (alkyl chains omitted) of SWNT wrapped with nanorectangle. b) Schematic structures of nanorectangle and nanocalipers complexing SWNTs and their (n,m) selectivity in the map.

A10: Moiré-induced vibrational coupling in double walled carbon nanotubes

Georgy Gordeev*†, Sören Wasserroth, Han Li, Benjamin S. Flavel, Stephanie Reich

**Department of Physics, Freie Universität Berlin, 14195 Berlin, Germany*

The moiré induced interactions between twisted atomic lattices in low-dimensional structures attracted tremendous attention recently. We study the one-dimensional moiré coupling of vibrational and electronic states in double walled carbon nanotubes. The electronic states get perturbed by the moiré potential changing the frequencies of radially oriented phonons. We find that the frequency shift is proportional to the changes in transition energies and construct a Kataura plot for double walled carbon nanotubes [1]. This is the first manifestation of strong moire effects onto the vibrational states. In addition to moiré coupling dielectric screening affects the optical transition energies of the inner tube in double walled nanotubes. The dielectric effect depends on the electronic type of the outer wall. Metallic outer walls provide higher screening, than semiconducting tubes. Higher screening results in a stronger red-shift of the inner tubes transition energies. We discuss that dielectric screening reduces the Raman intensities. In the metallic@metallic nanotubes the RBM mode intensity of the inner tubes is up to five times smaller than of the outer tube. This contrast RBMs in single walled nanotubes, where smaller tubes show higher Raman intensities. [1] Gordeev et al., arXiv:2103.07337

A11: Zeolite-Templated Carbon: a Promising Material for Supercapacitors

Sara Amar*†

**Centre de Recherche Paul Pascal UMR CNRS Bordeaux*

Chemical vapor infiltration (CVI) of a hydrocarbon in a molecular sieve is a synthesis technique used to generate a crystalline structure of carbon that remains up to now purely theoretical: Schwarzite [1-2]. This structure has indeed been foreseen as a promising material to manufacture electrodes for supercapacitors. Nonetheless, many technological challenges still have to be overcome in order to make this synthesis technique more accessible [1]. The molecular sieve that was selected for this study is zeolite, for its extraordinary adsoption properties. Zeolite is used as a template: the aim is to replicate its structure by infiltrating carbon atoms inside the nanopores [3]. The idea is to obtain, after zeolite dissolution by means of hydrofluoric acid treatment, a material that is exclusively composed of carbon, with a 3D porosity network consisting of nano-sized pores and thus displaying a high specific surface (see figure1). SEM observation shows that the obtained material has a very similar structure to that of the initial zeolite (see figure 2) which augurs well for the successful replication of the zeolite structure. Therefore, the presentation will focus on the synthesis and characterization of these materials, using thermogravimetric analysis, X-Ray diffraction, Raman, etc. References[1] : E. Braun, Y. Leeb, S. M. Moosavib, S. Barthelb, R. Mercadod, I. A. Baburine, D. M. Proserpiof,g, and B. Smit, Generating carbon schwarzites via zeolite-templating, E8116–E8124 | PNAS | vol. 115 | no. 35[2] : M. Tagami, Y. Liang, H. Naito, Y. Kawazoe, M. Kotani, Negatively curved cubic carbon crystals with octahedral symmetry, Carbon 76, 2014, 266-27[3]: H. Nishihara and T. Kyotani, Zeolite-templated carbons – three-dimensional microporous graphene frameworks, Chem. Commun., 2018, 54, 5648

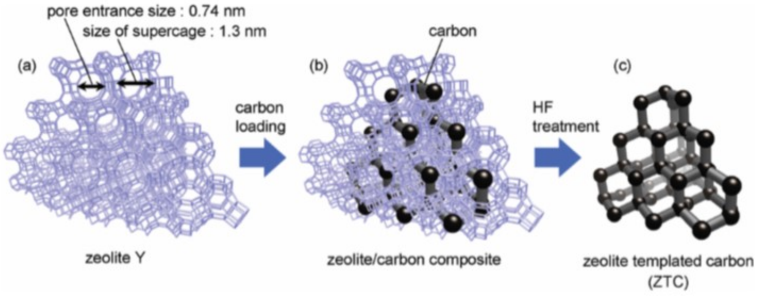

Fig. 1: Schematic Zeolite-Templated Carbon (ZTC) Synthesis, Chem. Commun., 2018, 54, 5648

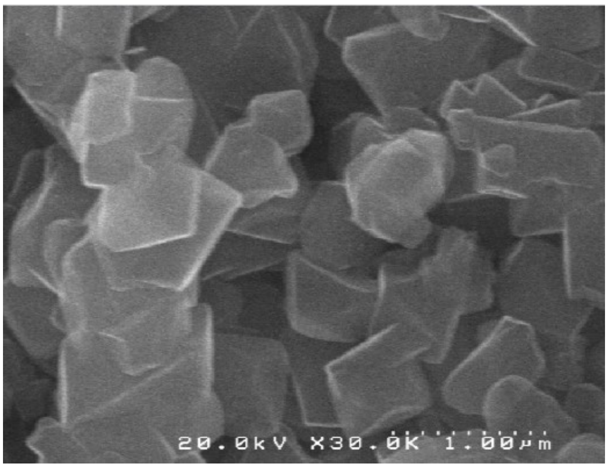

Fig. 2: SEM image of carbon material obtained after zeolite dissolution with hydrofluoric acid

A12: Wet etching with hypochlorite for patterning of graphene

Minfang Zhang*†, Mei Yang, Yuki Okigawa, Takatoshi Yamada, Toshiya Okazaki

**National Institute of Advanced Industrial Science and Technology*

Graphene has attracted tremendous attention, as its unusual electronic, thermal and mechanical properties promise its applications in electric and photoelectric fields such as a transparent conductive film to thin-film solar cells, organic EL lighting, touch panels, and to electronic and photoelectric devices. In order to create a device that requires various complicated circuits, it is necessary to use lithography technology and pattern it with processing technology such as dry etching and wet etching. Currently, there have been several research reports on reactive ion etching using a microscope, such as oxygen plasma, and dry etching of graphene using hydrogen ions and helium ions [1-2]. However, the wet etching technology that has advantages in easy operation and mass production has not yet been developed. Recently, we have found that hypochlorite solution assisted with light irradiation can rapidly degrade graphene completely, which is similar to that for carbon nanotubes as we reported previously [3]. This methodology is then applied as wet-etching technique for patterning graphene at subtracts. The technique consists of three steps, that are, the preparation of protect cover or mask on graphene sheet using gold or photoresists, the wet etching with a hypochlorite solution and light irradiation for about 5 min, and then the removal of covers. By using this process, we have successfully obtained well patterned graphene for devices uses as shown in Figure 1. The detail will be introduced in the symposium. [1] C. X. Cong et al. J. Phys. Chem. C 113, 6529–6532 (2009)[2] M. C. Lemme, et al. ACS Nano 3, 2674 (2009). [3] M. Zhang, et al. Sci Rep 9, 1284 (2019).

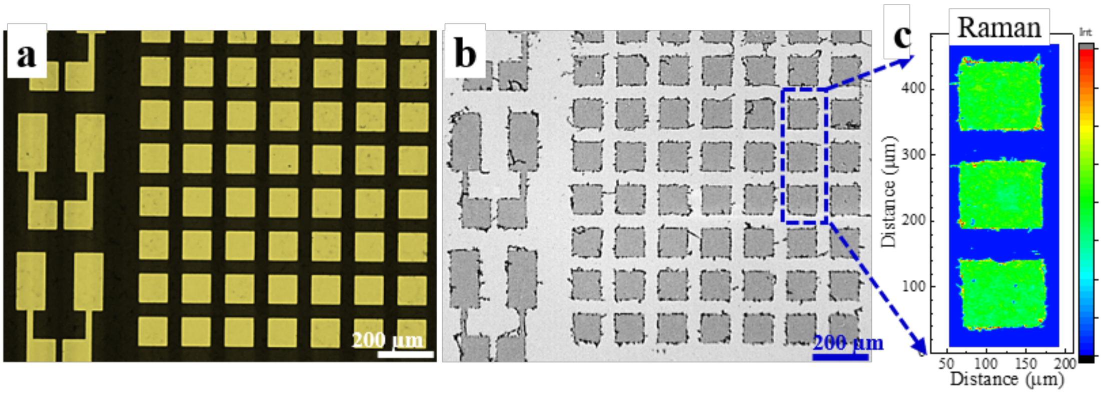

Fig. 1: Figure 1. Optical images of patterned gold mask on a graphene sheet (a), patterned graphene by using NaClO treatment (b) and that Raman mapping for the peak at 2680 cm-1

A13: Robust supercurrent and phase slip centers in a ballistic carbon nanotube embedded into a van der Waals heterostructure

Nicola Paradiso*†, Christian Bäuml, Lorenz Bauriedl, Magdalena Marganska, Milena Grifoni, Christoph Strunk

**Univ*ersity of Regensburg*

We demonstrate a robust supercurrent in a macroscopically long carbon nanotube (CNT) embedded into a van der Waals stack between hBN and NbSe2, see Fig.1. We show that a finite supercurrent also flows through the 2 µm-long section not in contact with it NbSe2, thus demonstrating a long-range lateral proximity in our hybrid 1D-2D van der Waals heterostructure. As expected for 1D superconductors, the current-induced breakdown of superconductivity is characterized by resistance steps due to the nucleation of phase slip centers (peaks B, D in Figure 2). These resistive features are observed together with phase slip lines features nucleating at the NbSe2-CNT interface. The location of phase slip features is determined by comparing the 2-terminal measurements in our 3-terminal device. The observation of phase-slip-induced resistance peaks, together with that of a robust supercurrent, constitute an unambiguous proof of the proximitization of a nominally normal CNT region. Measurements in finite in-plane and out-of-plane magnetic field corroborate the identification of the resistive peaks as due to phase slip centers in CNT and phase slip lines in NbSe2, owing to their different behavior for large magnetic fields. In particular, measurements in in-plane field clearly demonstrate that superconductivity induced in the CNT is inherited from the NbSe2 crystal, since it shows the dramatic critical field enhancement typical of Ising superconductors. All elements of our hybrid device are active building blocks of a recently proposed setup for realization of Majorana fermions in carbon nanotubes. *Acknowledgements:* Deutsche Forschungsgemeinschaft – Project-ID 314695032 – SFB 1277, Subproject B04. Horizon 2020 Grant No 862660 QUANTUM E-LEAPS.

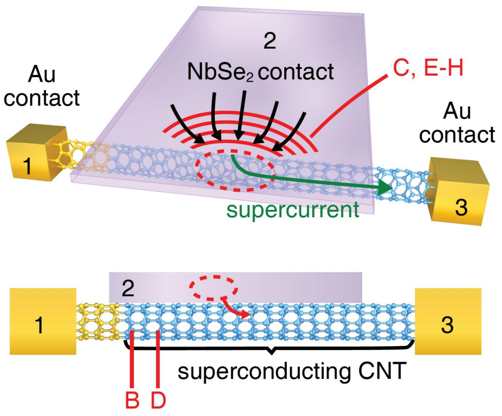

Fig. 1: Scheme of our hybrid carbon nanotube-NbSe2 van der Waals heterostructure.

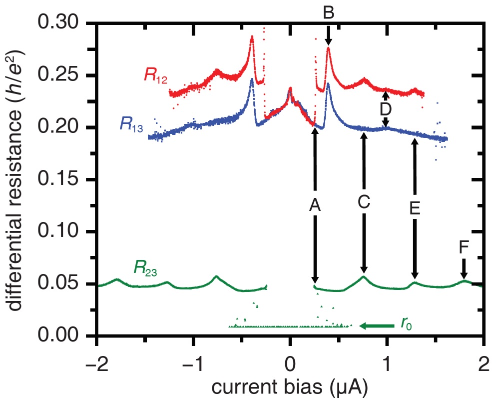

Fig. 2: Differential resistance as a function of current bias for the three 2-terminal configurations of our device.

A15: Stereoselective Photoluminescent Properties of DNA-SWCNTs: a Primer for Molecular Perceptron

Zeus De Los Santos*†, Ming Zheng

National Institute of Standards and Technology

Single-wall carbon nanotubes (SWCNTs) have emerged to be useful tools in molecular recognition in recent years. Due to their well-defined optical properties, SWCNTs offer unique properties that most small-molecule sensors lack, such as a near-IR (NIR) photoluminescence that makes them great candidates for sensing biomolecules. Typically, the synthesis of SWCNTs yields over 30 distinct tube chiralities, with two-thirds of the mixture comprising semiconducting and the remaining third consisting of quasi-metallic or true-metallic tubes. To add to the mixture's structural complexity, each chirality with the same helicity could also have different handedness – species that are enantiomeric in nature. In our lab at NIST, we have recently developed techniques based on aqueous two-phase extraction (ATPE) to separate enantiomers of SWCNTs wrapped with specific DNA sequences. Most of the sensors that developed thus far in this field, whether they are coated and dispersed by surfactants or DNA, take advantage of the mixture of various SWCNT helicities to elicit an optical response from interactions of small molecules. However, the responses obtained from each enantiomeric species of SWCNT are largely ignored, or at best, assumed to be similar. This presentation discusses the differences in photoluminescence response observed when SWCNTs wrapped with various DNA sequences interact with enantiopure small molecules. With this study, we give proof that specific DNA sequences allow for specific optical responses between the mixtures of diastereomeric DNA-SWCNT nanohybrids and single-chirality enriched DNA-SWCNTs, and enantiomeric amino acids. This study is the first proof-of-concept that small chiral molecules interact with chirality enriched DNA-SWCNTs to different extents and give rise to specific optical signatures that could be exploited for future developments of sensing arrays for complex biological mixtures. *Acknowledgements:* NRC Postdoctoral Research Associateship, Jeff Fagan, Christopher Sims, Zhiwei Lin, Matthew Noor

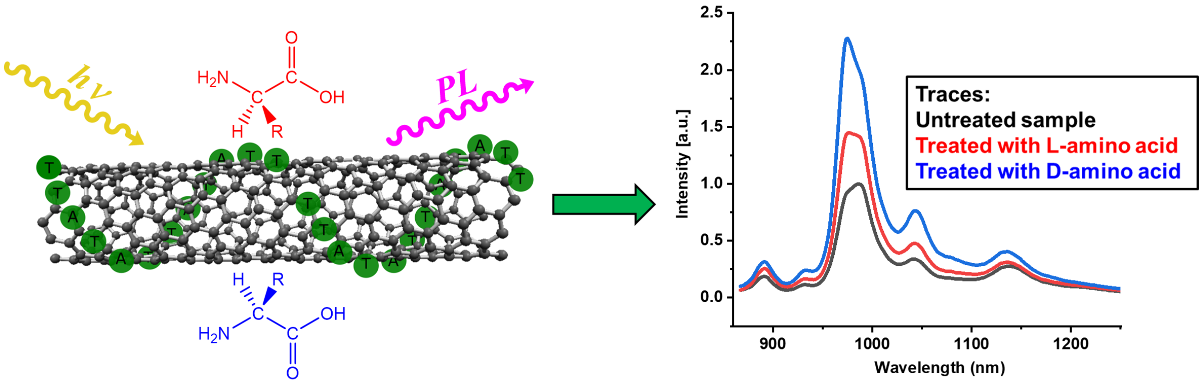

Fig. 1: Stereoselective PL responses arising from the interaction of L- and D-amino acids with DNA-wrapped SWCNTs.

A16: Progress in Using Carbon Nanotube Spectra for Mechanical Strain Sensing

R. Bruce Weisman*†, Wei Meng, Sergei Bachilo, Satish Nagarajaiah

Rice University

A characteristic property of semiconducting single-wall carbon nanotubes (SWCNTs) is distinct near-infrared photoluminescence following excitation by visible light. Theory and experiment show that these optical emission peaks shift predictably in wavelength as nanotubes are compressed or stretched along their axis. We are exploiting this effect in a powerful new method intended for measuring mechanical strain in critical infrastructure components such as airframes, pressurized vessels, pipelines, support beams, etc. The method involves applying a dilute dispersion of nanotubes in a polymeric host onto the surface of the specimen to form a sub-micron thick film in which SWCNTs act as strain sensors. This layer is overcoated with a transparent protective top coat such as a polyurethane varnish. Subsequent strains in the substrate are transmitted to the nanotubes by load transfer. The substrate strain magnitude and direction are then measured by illuminating the surface at any point of interest with a small visible laser beam and spectrally analyzing the resulting near-IR nanotube emission. Single-point measurements currently provide strain magnitude resolution of ca. 30 microstrain, strain angle resolution of ca. 5 degrees, and spatial resolution of ca. 50 mm. Each reading takes less than one second, allowing compilation of strain maps from scanned data. Unlike digital image correlation, which is currently the leading commercial non-contact strain technology, the new method can measure strains accumulated when the specimen is not under observation. It thus has the potential for routine use in industrial structural health monitoring as well as in testing and development laboratories. Results will be presented showing strain measurements in metallic, plastic, and concrete specimens. We will also describe recent progress in adapting the technology to camera-based measurements using spectrally resolved fluorescence imaging.

A17: Activation of Catalyst Particles for Single-walled Carbon Nanotube Synthesis

Dmitry Krasnikov†, Eldar Khabushev*, Julia Kolodiazhnaia, Albert Nasibulin

**Skolkovo Institute of Science and Technology*

In this work, we evaluate the effect of ferrocene delivery in the reactor on the growth of single-walled carbon nanotubes (SWCNTs) in an aerosol CVD utilizing carbon monoxide as a feedstock. For this purpose, we assess the reactor output parameters varying a gas flow rate through a ferrocene vapor injector in the hot zone with other conditions (temperature, total flow rate, and reactant concentration) being fixed. Our experimental results reveal the adjustment of the ferrocene injection strategy (injector flow rate) to cause a 9-fold improvement in the synthesis yield while preserving the SWCNT properties. Moreover, we consider carbon source supply to be rate-limiting step during the SWCNT nucleation as the diameter distribution is insensitive to catalyst precursor delivery. We show the catalyst injection optimization to enhance catalyst activation degree as a result of a streamline catalyst delivery, preventing particle over-growth; the experimental data are supported by the computational fluid dynamics. We believe our work to highlight the importance of appropriate aerosol CVD reactor engineering and to facilitate the optimization of reactor productivity, which is one of the fundamental milestones towards SWCNT-based technology. *Acknowledgements:* This work was supported by Russian Foundation for Basic Research grant 18-29-20032.

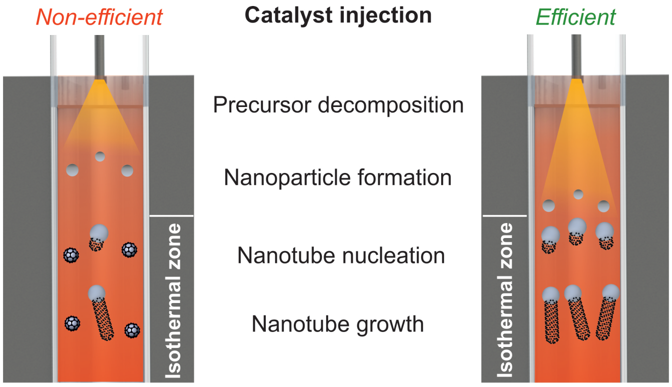

Fig. 1: Strategies efficient and non-efficient catalyst activation.

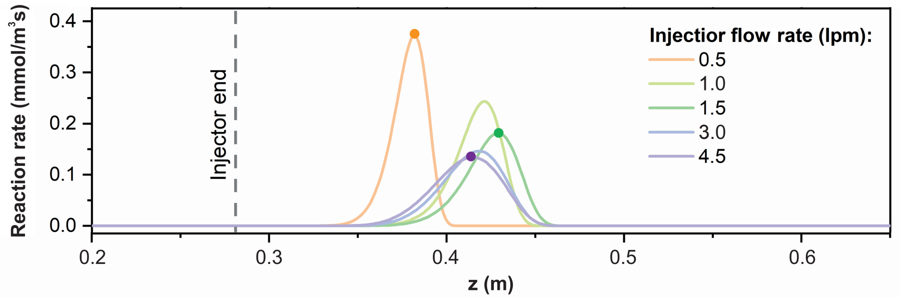

Fig. 2: Calculated ferrocene decomposition rate at different precursor catalyst injection rates showing the optimal strategy to provide the biggest delay in ferocene decomposition.

A18: Residence time effect on single-walled carbon nanotube synthesis in an aerosol CVD reactor

Dmitry Krasnikov†, Ilya Novikov*, Eldar Khabushev, Anton Bubis, Anastasia Goldt, Sergey Shandakov, Albert Nasibulin

**Skolkovo Institute of Science and Technology*

We examine an effect of residence time on the growth of single-walled carbon nanotubes (SWCNTs) in an aerosol (floating catalyst) chemical vapor deposition (CVD) process using CO as a carbon source and ferrocene as a catalyst precursor. The key feature of aerosol CVD reactors, namely stabilization of fine nanoparticles by an extreme dilution, limits the method for catalyst evolution studies. We show an approach to maintain all the processes preceding the nanotube growth (catalyst formation, nanotube nucleation) while varying the residence time. Using the SWCNT diameter distribution as a fingerprint of the nanotube nucleation stage, we have proven the latter to be unaffected by changes in the residence time. Using SEM observations, we have revealed a quite intuitive but inspiring correlation between the carbon nanotube length and residence time. We have also found a decrease in the SWCNT yield caused by the drop in the aerosol concentration, which could be attributed to the gas-phase losses as well as the shift in the catalyst activation degree. Nevertheless, the trends observed allowed us to reach a tenfold decrease in an equivalent sheet resistance (sheet resistance of a film with 90% transmittance at 550 nm) by a threefold increase in the residence time at optimal CO2 concentration. SWCNT films with the equivalent sheet resistance as low as 245 Ω/☐ and 51 Ω/☐ (for pristine and doped carbon nanotubes, correspondingly) ensure the promising future of the proposed strategy for optimization of both aerosol CVD reactors and SWCNT-based films for optoelectronic applications. *Acknowledgements:* This work was supported by Russian Science Foundation grant No. 20-73-10256.

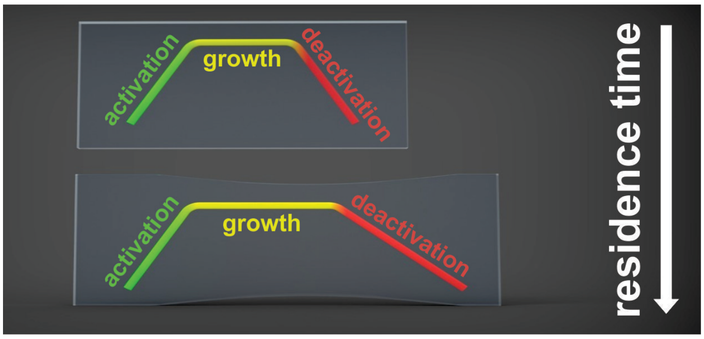

Fig. 1: ideology of the residence time changes

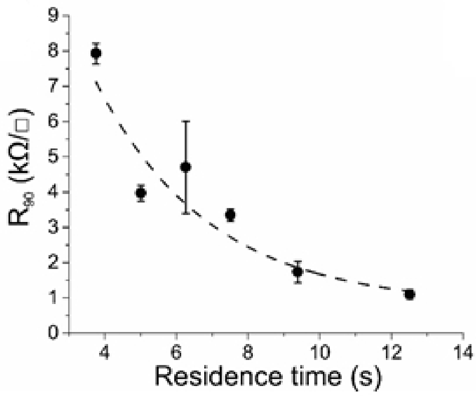

Fig. 2: Equivalent sheet resistance (R90) dependence on the residence time

A19: Endohedral and Exohedral Atomic Nanostructures on Boron Nitride Nanotubes

Yoke Khin Yap*†

**Michigan Technological University*

The nanotubular structure of carbon nanotubes (CNTs) has enabled the formation of unique endohedral and exohedral materials on their interior and exterior surfaces, respectively. However, property measurement of these endohedral and exohedral structures has interfered with the metallic or semiconducting nature of CNTs. In contrast, the electrically insulating and optically transparent boron nitride nanotubes (BNNTs) have enabled direct probing of these endohedral and exohedral materials. Such an emerging opportunity is enabled by the controlled synthesis of high-purity, and high-quality BNNTs by simple chemical vapor deposition techniques. 1-3 For example, we have reported that BNNTs can be used to form one-dimensional array of gold nanoparticles for the fabrication of room-temperature single-electron transistors (SETs)4. Here, we demonstrated that two-dimensional, monatomic gold quantum dots (2D Au QDs) can be formed on the exterior surfaces of BNNTs. Our theoretical simulation suggests that 2D Au QDs can be stabilized on h-BN surfaces5. Our experimental result showed that these atomic structures exhibit tunable optical bandgaps, well co-related with our simulation. On the other hand, we also demonstrated the formation of van der Waals Tellurium atomic chains inside BNNTs 6. The electronic transport properties of field-effect transistors (FETs) based on these atomic nanostructures have been revealed. The detailed data of these endohedral and exohedral atomic nanostructures will be discussed in the meeting.References C. H. Lee, M. Xie, V. Kayastha, J. Wang, Y. K. Yap, Chem. Mater. 22 (2010) 1782-1787.(Review) J. Wang, C. H. Lee, Y. K. Yap, Nanoscale2 (2010) 2028-2034.(Review) C. H. Lee, S. Bhandari, B. Tiwari, N. Yapici, D. Zhang, Y. K. Yap, Molecules 21 (2016) 922.C. H, Lee, S. Qin, M. A. Savaikar, J. Wang, B. Hao, D. Zhang, D. Banyai, J. A. Jaszczak, K. W. Clark, J-C Idrobo, A-P. Li, and Y. K. Yap, Adv. Mater. 25 (2013) 4544-4548.S. Bhandari, B. Hao, K. Waters, C. H. Lee, J-C Idrobo, D. Zhang, R. Pandey, Y. K. Yap, ACS Nano 13 (2019) 4347-4353.J-K. Qin, P-Y. Liao, M. Si, S. Gao, G. Qiu, J. Jian, Q. Wang, S-Q. Zhang, S. Huang, A. Charnas, Y. Wang, M. J. Kim, W. Wu, X. Xu, H-Y. Wang, L. Yang, Y. K. Yap, P. D. Ye, Nature Electronics3, (2020) 141-147.

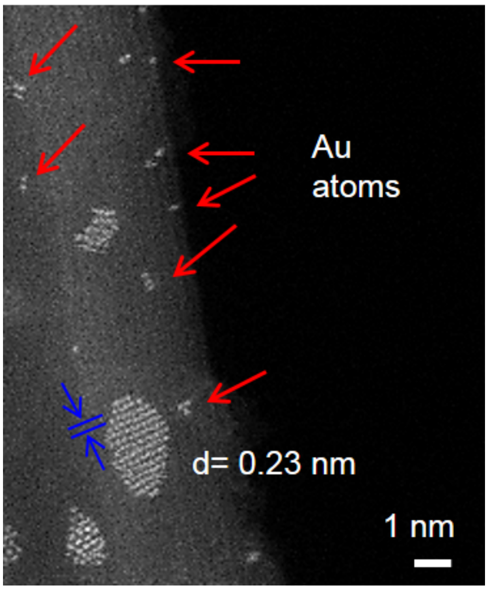

Fig. 1: 2D Monatomic gold quantum dots and gold atoms on BNNTs.

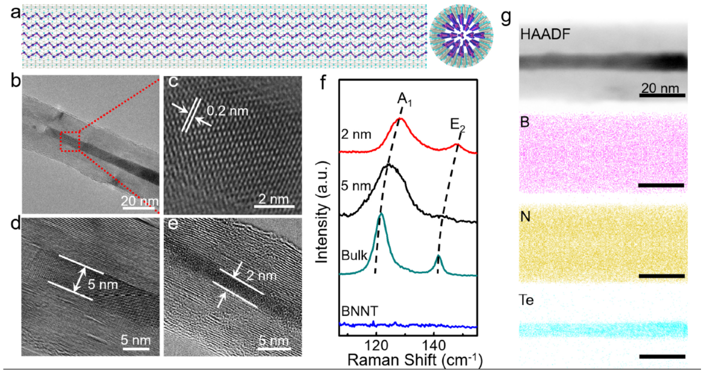

Fig. 2: (a) Graphical model, (b to e) TEM images, (f) Raman spectra, and (g) energy-filtered images of Tellurium atomic chains inside BNNTs.

A20: Growth mechanism and handedness relation of one-dimensional van der Waals heterostructures

Yongjia Zheng*†, Akihito Kumamoto, Rong Xiang, Kaoru Hisama, Keigo Otsuka, Yuta Sato, Taiki Inoue, Shohei Chiashi, Daiming Tang, Qiang Zhang, Anton Anisimov, Esko Kauppinen, Kazu Suenaga, Shigeo Maruyama, Yuichi Ikuhara

**The University of Tokyo*

Recently, we presented one-dimensional (1D) van der Waals (vdW) heterostructure that includes single-walled carbon nanotubes (SWCNTs), boron nitride nanotubes (BNNTs) and molybdenum disulfide (MoS_2). The shell-by-shell growth of this heteronanotube is different from conventional growth of 1D homo-material nanotubes where multiple walls are formed simultaneously from a nanoparticle. Therefore, nucleation and crystal growth behaviors on these highly curved surfaces are of fundamental research interest. Here we present a comprehensive and thorough characterization on the formation process of BN layer on SWCNT surface. This is achieved by combining transmission electron microscopy (TEM) approach with the direct growth of 1D vdW heterostructures on TEM grid. This combination allows heterostructures to keep in the most intrinsic morphology, and many structure details can be clearly visualized. Furthermore, their crystal relationship and handedness correlation are also investigated.

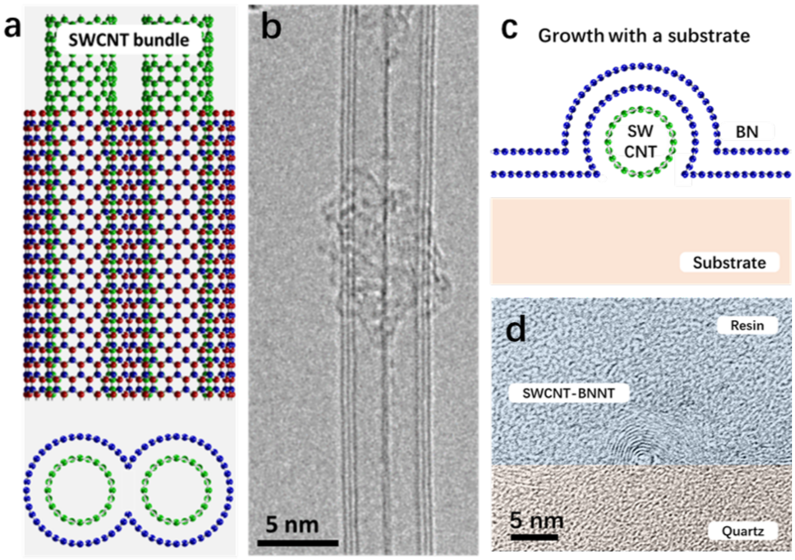

Fig. 1: (a) Atomic model and (b) TEM image of a BN coated bundle. (c) Atomic model and (d) TEM characterization of a BN coated coated SWCNT on a flat substrate.

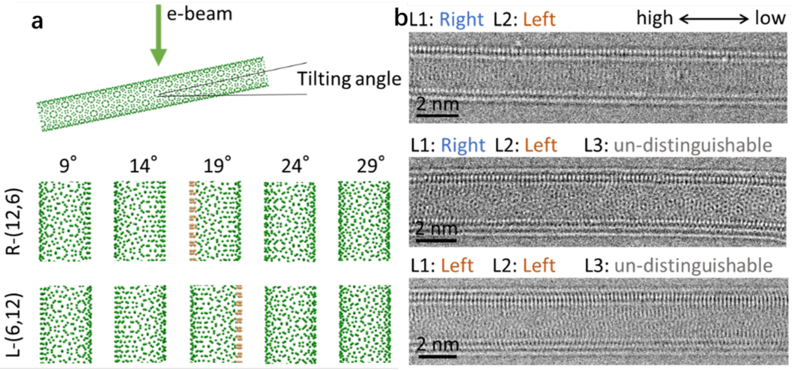

Fig. 2: (a) Schematic illustration of identifying the handedness of inner SWCNT or outer BNNT under TEM measurement. (b) Representative TEM images of three SWCNT-BNNT heterostructures having different handedness combinations.

A22: Machine learning for optimization of single-walled carbon nanotube synthesis by aerosol CVD reactor

Dmitry Krasnikov[†], Eldar Khabushev*, Vsevolod Iakovlev, Anastasia Goldt, Orisia Zaremba, Albert Nasibulin
**Skolkovo Institute of Science and Technology*

Unique properties of single-walled carbon nanotubes (SWCNTs) make them prospective material to be implemented in different areas from biomedicine to nanoelectronics. A key step in the successful promotion of this outstanding material in the industry is the development of cost-effective and robust technology for the controllable production of the material with tunable characteristics.Despite all the advantages and advances already achieved in the field, of SWCNT production the production of nanotubes with precisely tuned and even defined properties on an industrial scale is still challenging. The main factor inhibiting the progress is usually attributed to the complexity of mechanisms for the nanotube nucleation, growth, and termination burdened by the lack of the general model, providing a quantitative relationship between the synthesis conditions and SWCNT parameters. Though the main aspects of the SWCNT growth are deduced, the multiparametric nature of the chemical processes associated with the inconsistency of the results among reactors worldwide inhibits the progress towards the precise control over nanotube properties and actualizes the development of novel approaches to govern synthesis process .In this work, we combine the problem with another vastly developing field which shows its best with multiparametric complex tasks – Machine Learning (ML). We report the utilization of ML numerical models for processing of experimental data, obtained using a single aerosol CVD reactor, based on thermal decomposition of ferrocene and the Boudouard reaction on the surface of iron catalyst. We demonstrate the prediction of the reactor output (yield, diameter, and quality of producing carbon nanotubes) with an accuracy of as low as 4%, using temperature and gas mixture compound as input parameters. We developed a predictive model based on an artificial neural network (ANN) and trained it on a pre-processed experimental data adjusting hyperparameters for the best performance [10.1016/j.carbon.2019.07.013]. For optimization of reactor operation and further development of approach employed, we also solve regression tasks and refine synthesis conditions to enhance the performance of SWCNT films as a transparent and conductive material. The strategy employed allowed us to fabricate films with equivalent sheet resistance (at 90 % transmittance) of 39 Ω/☐ — one of the lowest values achieved so far [10.1021/acs.jpclett.9b02777]. Collected dataset accompanied by proof-of-the-concept experiments formed a basis for fine optimization of reactor performance, governed by ML algorithm. *Acknowledgements:* This work was supported by the Russian Science Foundation, grant 20-73-10256

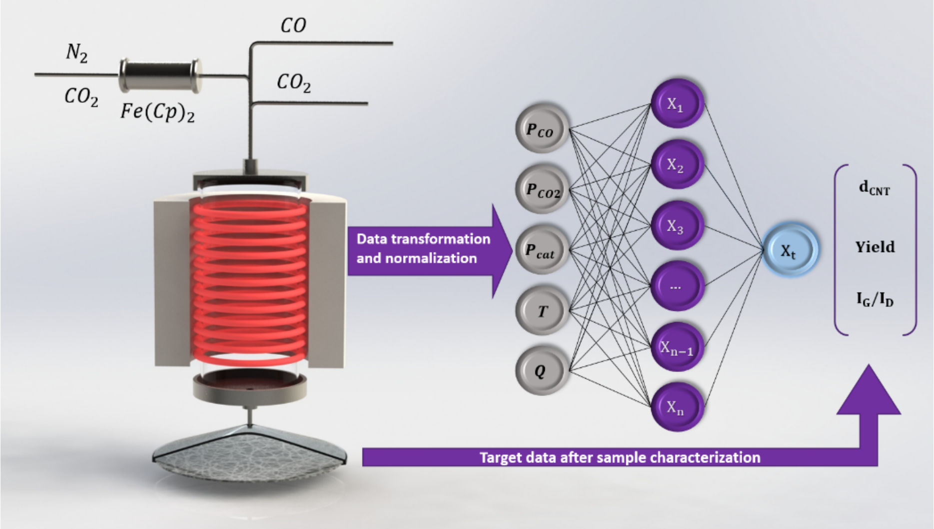

Fig. 1: Strategy for SWCNT optimization.

A23: Structure-dependent performance of single-walled carbon nanotube films in transparent and conductive applications

Dmitry Krasnikov[†], Eldar Khabushev[*], Julia Kolodiazhnaia, Albert Nasibulin
**Skolkovo Institute of Science and Technology*

Despite the abundance of realized approaches, current advances in SWCNT-based transparent conductive films still have not met the industrial requirements, being inferior to metal-oxide counterparts (e.g. indium-tin oxide) We investigate a complex relationship between structural parameters of single-walled carbon nanotubes (namely, mean length, diameter, and defectiveness) and optoelectrical properties (equivalent sheet resistance) of thin films composed of the nanotubes. As a rule, numerous studies related to the fabrication of highly transparent and conductive SWCNT films using the aerosol CVD technique consider the influence of the growth parameters on the optoelectronic performance. Though the most of publications in the field refer optoelectronic performance to the structural aspects of the SWCNTs, the complex relation between reaction parameters and SWCNT structure results in controversial or incomparable trends and conclusions. Such a lack of a proven and direct connection inhibits the targeted optimization of the SWCNT-based transparent conductive film performance and, thereby, the implementation of SWCNT-based devices.We obtained a systematic dataset describing the influence of CO2 concentration and growth temperature. We link the highest performance of the SWCNT-based transparent conductive films (equivalent sheet resistance of 430 Ω/☐ for pristine films) with the carbon nanotubes of the lowest defectiveness (ratio of G and D modes of a Raman spectrum) and large diameter. The SWCNT growth splits into two temperature regions (according to the yield): length-dependent (T< 925 oC) and activation degree controlled (T>925 oC). The yield is shown to correlate with nanotube length, and as follows, to decrease equivalent sheet resistance at temperatures below 925 oC; while at high temperatures (above 925 oC) no visible trend is observed. The change in the yield-determining factor (900 – 925 oC) can be accounted for the phase transition of Fe catalyst (≈912 oC; fig.1). The obtained results could contribute to the targeted tuning of the SWCNT thin film properties for the advanced optoelectronic devices. We believe this work to be of high interest for researchers working not only in the field of transparent and conductive films based on nanocarbons, but also for those who reveals the fundamentals of the nanotube growth mechanism. *Acknowledgements:* This work was supported by Russian Science Foundation No. 17-19-01787

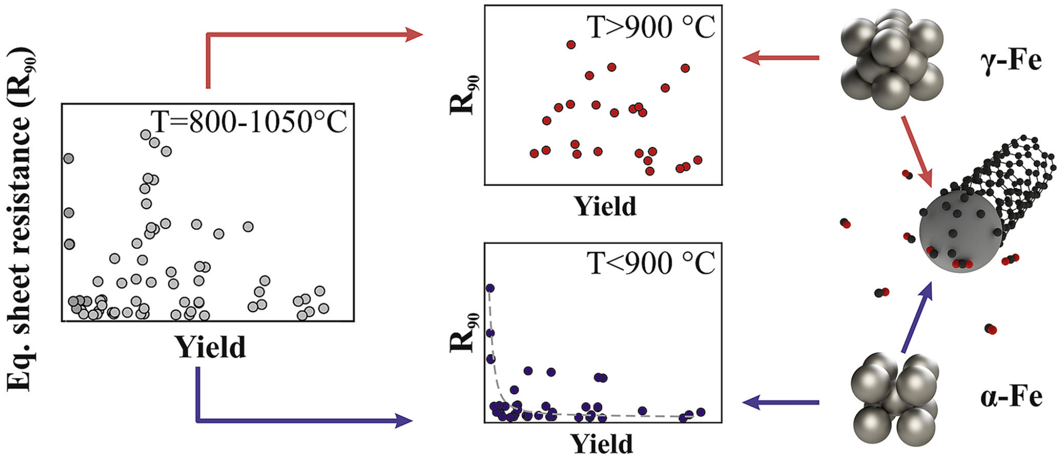

Fig. 1: Influence of iron catalyst phase on the yield/equivalent sheet resistance relation

A24: Spin-current generation by edge-plasmon in graphene ribbon

Muhammad Shoufie Ukhtary*†, Yuan Tian, Riichiro Saito

**Tohoku University & Indonesian Institute of Sciences*

Spin-current is defined as the difference between charge-currents of the spin up and down [1]. Generating and tuning the spin-current are the main topic of spintronics. Conventionally, spin-current is generated by applying voltage on a stack of a ferromagnetic material and normal metal, or by using spin-Hall effect on a two-dimensional (2D) material. However, the spin-current generated by those methods is tunable only by the external magnetic field, which is not convenient for a nano device. Recently, Oue and Matsuo theoretically proposed an optically generated spin-current in a non-magnetic metal that is tunable not by magnetic field, but frequency of light [2]. They showed that surface plasmon (SP) on a surface of three-dimensional (3D) metal generates spin-current due to the rotating of the electric field of the SP [3]. They found a resonant condition that enhances the generated spin-current. However, the spin-current flows in the perpendicular direction to the surface and the spins are polarized in the planar direction.In this work, we discuss the generation of spin-current by edge-plasmon on a graphene ribbon. Edge-plasmon is an electromagnetic wave that is localized near the edges of the ribbon. In contrast with the SP on 3D metal, the electric field of edge-plasmon rotates on the plane of graphene, which means that the spin-angular momentum of edge-plasmon is out-of-plane [4]. We found that the spin-current flows between the edges of graphene with spin-polarization in the out-of-plane direction as illustrated in Fig. 1 [5]. Moreover, the spin-current induced by edge-plasmon is tunable not only by the frequency, but also by the Fermi energy of graphene. [1] Shi et al. PRL 96, 076604 (2006)[2] Oue and Matsuo. PRB 101, 161404R (2020)[3] Bliokh et al. PRL 119, 073901 (2017)[4] Ukhtary et al. PRB 100, 155432 (2019)[5] Ukhtary et al. unpublished

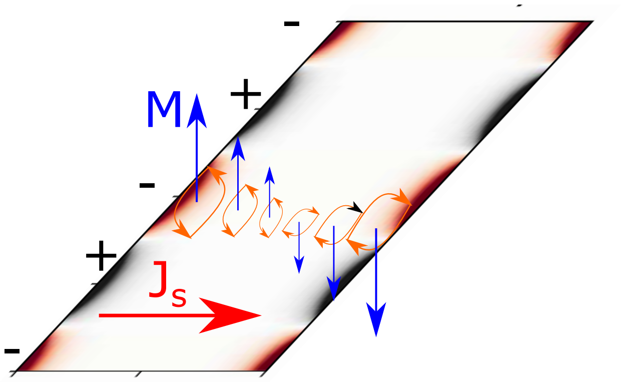

Fig. 1: Edge-plasmon (red and black showing oscillation of induced charges) and the induced magnetization (M). The spin current Js flows on the surface due to the inhomogenously distributed M

A25: Double-walled carbon nanotube transparent conductor overcoming performance-yield tradeoff

Qiang Zhang*†, Jeong-Seok Nam, IL Jeon, Esko Kauppinen

**NanoMaterials Group, Department of Applied Physics, Aalto University School of Science,*

The floating catalyst chemical vapor deposition (FCCVD) method for producing single-walled carbon nanotubes (SWNTs) has demonstrated great potential in transparent conductive film (TCF) application. In FCCVD, reducing the concentration of carbon nanotubes (CNTs), is the most well-known method of improving the conductivity of SWNT TCF, achieved by producing thinner and longer CNT bundles. However, this method dramatically reduces the yield by orders of magnitude, which has persisted throughout the development of SWNT TCF. Here, we report a new FCCVD method of producing large-diameter double-walled CNT (DWNT) TCFs that overcomes the performance-yield tradeoff. These DWNT TCFs have a low sheet resistance of 35 Ω/sq at 90% transmittance. The conductivity here aligns with the best-performing SWNT TCFs reported to date, with a production yield greater than two orders of magnitude. The device application of DWNT TCFs is tested in perovskite solar cells, which exhibit a power conversion efficiency of 17.4%, currently the highest efficiency reported from indium-free CNT-based solar cells.

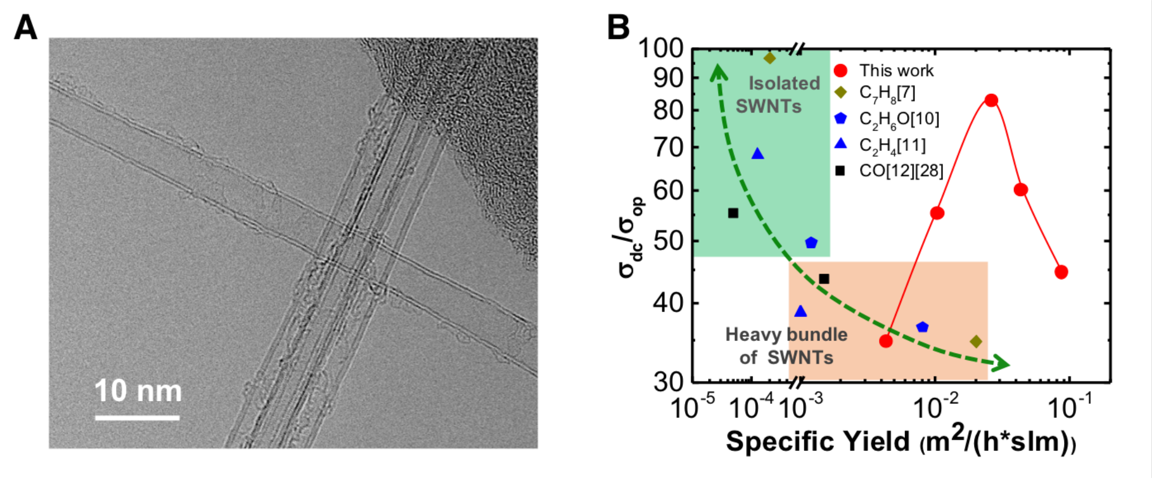

Fig. 1: Highly-conductive transparent films of large-diameter DWCNTs are produced with an unparalleled high yield.

A26: Sp3 Defects Implanted Ultrashort Carbon Nanotubes as NIR-II Biomarkers

Somen Nandi*†, Laurent Cognet

**INSTITUT D OPTIQUE D AQUITAINE, LP2N, University of Bordeaux, France*

Due to deep tissue penetration of light, near-infrared (NIR) fluorescence imaging have been emerged as an important technique for a variety of fundamental processes viz biomedical research, sensing and clinical applications.1 The principal aim of this work is to create sp3 defects implanted and immuno-labelled bright fluorescent ultrashort (~20 nm) carbon nanotubes (usCNTs) to use them for cancer diagnostic. Unfortunately, their intrinsic NIR PL is known to be quenched in usCNTs because of their small size compared to the excitation diffusion length (< 100 nm). Sp3-defects implantation of SWCNTs has opened the route toward enhancement of PL properties, which occurs in the NIR-II region (~900-1700 nm), a biologically transparent region for in vivo bio-imaging owing to less photo-absorption, reduced scattering and negligible autofluorescence by tissue. Although the demonstration of usCNTs has been performed recently,2,3 the process experienced limitations like long processing time including a very low yield (< 10%). In order to augment the production yield of fluorescent usCNTs required for bio-application, herein we now present a synthesis route, where the functionalization is first done followed by chemical oxidation.4 We first introduced aryl defects into the sidewall of CNTs by diazonium chemistry. The defect implantation has been confirmed by the appearance of strong red shifted peak at ~1150 nm in PL experiments, compared to the pristine one (~980 nm) (Fig. 1). After that these have been subjected to chemical oxidation at the defect sites by hydrogen peroxide to produce ultrashort ones with a relatively high yield (>50%) with its intact fluorescent properties. We characterized them by various spectroscopy (UV-Vis-NIR, PL, IR, Raman etc.) and microscopy techniques. The length of usCNTs have been estimated by AFM imaging and nanotubes diffusion analysis. Subsequently, we introduce surface bio-functionalization to couple them with antibody (IgG) to be used as diagnostic biomarkers in cancer. [1] J. Zhao, D. Zhong, S. Zhou, J. Mater. Chem. B, 6, 349-365 (2018). [2] Z. Gao, L. Oudjedi, R. Faes, F. Moroté, C. Jaillet, P. Poulin, B. Lounis, L. Cognet, Sci. Rep, 2015, 5, 17093-17103. [3] N. Danne, M. Kim, A. G. Godin, H. Kwon, Z. Gao, X. Wu, N. F. Hartmann, S. K. Doorn, B. Lounis, Y. Wang, L. Cognet, ACS Nano, 2018, 12, 6059–6065. [4] Y. Li, X. Wu, M. Kim, J. Fortner, H. Qu, Y. Wang, Chem. Mater., 2019, 31, 4536-4544.

Acknowledgements: This work was supported by grants from Agence Nationale de la Recherche (ANR) project (n°18CP121-00 INSERM – PhysCancer)

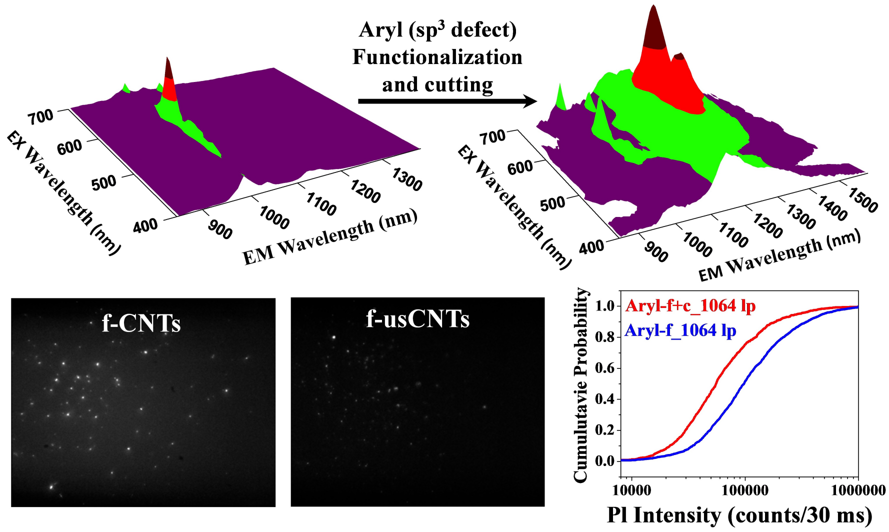

Fig. 1: 2D PL of CNTs showing evolution of E11* peak after functionalization which remains intact even after oxidation. PL Images of individual f-CNTs and f-usCNTs with their cumulative distribution.

A27: Modulation of oxygen molecule adsorption doping by Fermi energy control of MoS_2

Takumi Yoshida*†, Kazuyuki Takai

**Hosei University*

2D-materials are susceptible to adsorbents in the environment because all constituent atoms are present on the surface. For example, it is known that when oxygen molecules are adsorbed on MoS_2, which is one of the 2D-materials, it causes hole doping [1]. There are two types of adsorption of molecules: physical adsorption and chemisorption. In the case of chemisorption involving charge transfer, the adsorption rate differs depending on the charge state of the host substance. Previous studies have shown that upshifting the fermi energy (EF) of graphene increases the characteristic rate of charge transfer in oxygen molecule adsorption [2]. Therefore, in this study, the EF of MoS_2 was modulated by applying gate voltage (VG) during gas exposure, and the adsorption characteristics in that state were investigated.MoS_2-FET was fabricated after mechanical exfoliation on a 285 nm SiO2 / Si substrate. The conductivity was measured after exposure oxygen gas. This study was also performed applying VG during gas exposure.Fig. 1 shows the VG dependence of the source-drain current ISD when exposed to oxygen (VG = 0 V). It can be seen that hole doping by oxygen molecule adsorption is progressing as the exposure time increases. Fig. 2 shows the dependence of the threshold voltage difference ΔVTH from before oxygen exposure (0 s) when exposed to oxygen gas (VG = -60, 0, +60 V) to oxygen gas exposure time. It can be seen that the appearance of holes being doped with oxygen gas progresses with increasing time, but gradually shows a tendency to saturate. In addition, the relaxation time when VG = +60 V was applied and exposed to oxygen gas was shorter than that of VG = -60 V. These results indicate that the adsorption of oxygen molecules on MoS_2 is similar to the chemisorption with charge transfer to graphene. [1] Y. Minakawa, T. Umehara, and K. Takai, The 58th FNTG (2020),[2] Y. Sato, K. Takai, and T. Enoki, Nano Lett., 11, 8 (2011),

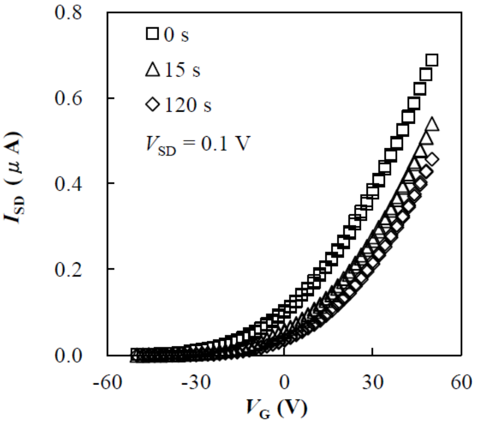

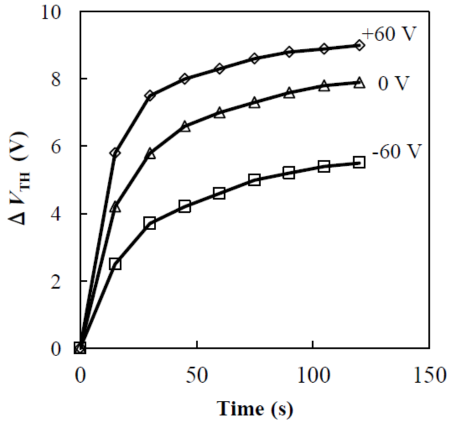

Fig. 1: VG dependence of ISD for 100Pa O2 adsorption

Fig. 2: ΔVTH time dependence

A28: Ni3S2 nanowires filled carbon nanotubes: Synthesis, characterization, and electrical properties

Yuba Poudel*†, Wenzhi Li

**Florida International University*

Filled carbon nanotubes (CNTs) possess unique physical properties which emerge because of the synergy of the qualities of CNTs and those of the filling material. Until now, a heterogeneity of foreign materials has been successfully encapsulated inside the CNT cores using ex situ filling method, however, there exists a serious lack of in situ filling approaches which can guarantee a continuous and complete filling of the CNT core. We have developed for the first time, a simple and reliable in situ method to synthesize the CNTs filled with Ni3S2 nanowires (Ni3S2@CNTs) directly on different substrates using a chemical vapor deposition technique. Ni3S2@CNTs have been characterized using several techniques such as SEM, TEM, EDX, Raman spectroscopy, XRD, UV-Vis, TGA, and FTIR. Ni3S2@CNTs possess a linear and a tapering structure with highly graphitized carbon walls (ID/IG= 0.26) encapsulating a continuous and single crystalline Ni3S2 nanowire up to several micrometers in length. The intrinsic I-V characteristics of individual Ni3S2@CNTs were studied using both two probe and four-point probe methods which reveal the metallic properties of Ni3S2@CNTs. A size dependent electrical breakdown of the Ni3S2@CNTs was observed at higher currents which make the thin Ni3S2@CNTs (diameter below 150 nm) as potential candidates for nano circuit breakers in the future electronic devices. *Acknowledgements:* This work is supported by the National Science Foundation under Grant DMR- 1506640.

A29: Effect of iron ion beam irradiation on MoS_2 fluorescence

Takumi Hidaka*†, Tomoaki Nishimura, Kazuyuki Takai

**Hosei University*

In 2D material, defects and impurities significantly affect the electronic properties compared to 3D materials due to its low-dimensional structure. Meanwhile, ion beam implantation is one of the methods that can quantitatively and reproducibly introduce defects and impurities into materials. We can maintain the maximum implantation ion distribution on 2D materials by using a sacrificial layer [1]. The effect of the chemical properties of the implanted ion is not widely known yet in spite of many reports on the ion-dose dependence on 2D materials. In this study, Fe+ which is a magnetic impurity that can cause spin scattering were introduced by ion beam irradiation into MoS_2 as a 2D material in which fluorescence strongly correlates with the degree of freedom of spin. The irradiation effects on structural and electronic properties were investigated using Raman spectroscopy and Photoluminescence (PL). Cr / NaCl of 10 nm / 250 nm was deposited as a sacrificial layer on the single-layer MoS_2 obtained by the cleavage method on a SiO2 / Si substrate. The film thickness of the sacrificial layer was optimized using Monte Carlo simulation for Fe+ distribution by SRIM2013. Fe+ irradiation to the sample was performed at an acceleration voltage of 200 keV with a dose of 1012 cm-2. Raman spectroscopy and PL were measured using a spectrometer (LabRAMHR, Horiba). With Fe+ irradiation, no significant change in shape was observed on the E12g and A1g peaks characteristic of the Raman spectrum of MoS_2 (Fig. 1). This confirms that MoS_2 maintains its fundamental crystal structure even after Fe+ irradiation. The PL spectra of MoS_2 consisting A and B peaks, corresponds to the transitions to two spin-subbands, showed a low energy shift of the A peak after Fe+ irradiation (Fig. 2). The low energy shift of the A peak indicates n-doping of MoS_2 by Fe+ irradiation [2], which was not observed in previous studies on Ar+ irradiation [3]. Moreover, long tail was observed in low A peak energy side. This indicates that the introduction of defects in MoS_2 caused new defect levels with various energy eigenvalues in the gap. In addition, the increasing of B peak intensity suggests that the introduced Fe+ caused spin-dependent relaxation in MoS_2.Reference[1] Y.Nakamura et al, FNTG Symposium (2019)[2] S. Mouri et al, Nano Lett (2013)[3] Y. Zhao et al, RPGR (2019)

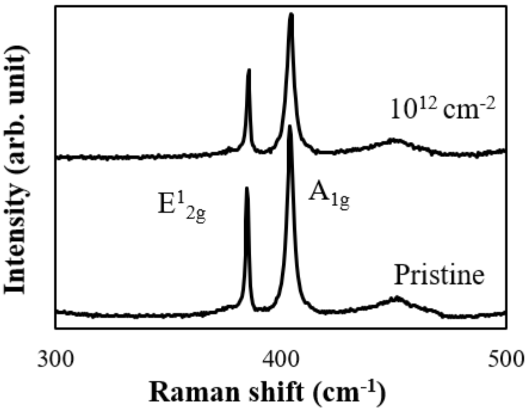

Fig. 1: Raman spectra for Fe+ irradiated MoS_2 before and after irradiation

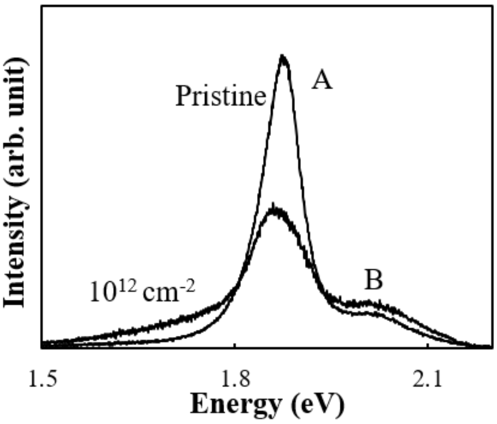

Fig. 2: PL spectra for Fe+ irradiated MoS_2 before and after irradiation

A30: Majorana bound states in proximitized carbon nanotubes

Magdalena Marganska*[†], Lars Milz, Wataru Izumida, Christoph Strunk, Milena Grifoni

**University of Regensburg*

Using both numerical and analytical approaches, we study the emergence and properties of Majorana bound states forming in carbon nanotubes (CNTs) in proximity of a superconducting material. For this purpose we account for the intrinsic CNT spin-orbit coupling of carbon nanotubes (CNTs) combined with the action of a perpendicular magnetic field, gate potential, and both symmetry breaking and superconducting pairing induced by the substrate.Due to the tiny size of CNTs, we have been able to trace the transition into the topological phase with tight-binding numerical simulations on the atomic lattice, which served as a benchmark for our analytical effective models [1]. The transition to the topological regime is characterized by the formation of zero-energy excitations localized at the ends of the system - the Majorana bound states. We demonstrate their intricate helical wave functions and spin structures, due to the contributions of the two valleys [2].Our calculations of the topological invariant, based on the effective model, predict the topological phase to be reachable at experimentally accessible magnetic fields. Even though these fields are high, the use of an Ising superconductor as the source of the proximity effect provides us with superconducting correlations which are stable even above 10 T. The recent experiment [3] proves that the proximity effect in CNTs can extend at long distance beyond the area contacted by the superconductor. By gating this laterally proximitized part of the CNT, we may be able to control its chemical potential as well, finally driving it into the topological phase. Once it is achieved, carbon nanotubes may be confirmed as viable Majorana platforms in solid state physics. [1] Marganska et al., PRB 97, 075141 (2018)[2] Milz et al., PRB 100, 155417 (2019)[3] Bäuml et al., arXiv:2010.07755

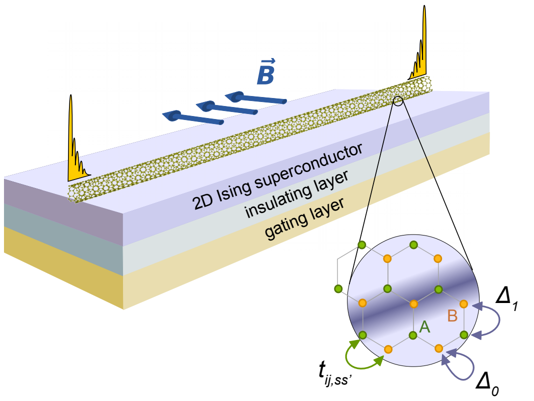

Fig. 1: Majorana device based on a carbon nanotube in proximity of an Ising superconductor. Theoretical modelling includes spin-orbit coupling, superconducting pairing, magnetic field, gate and symmetry breaking by the substrate.

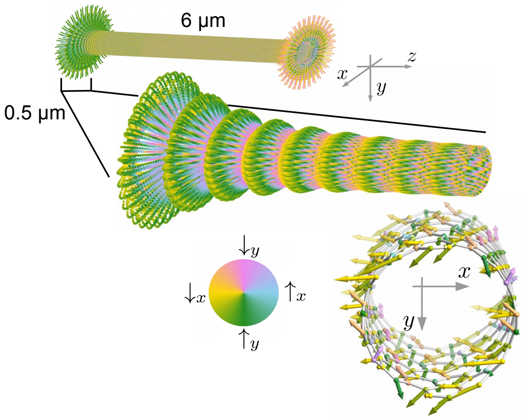

Fig. 2: Majorana wave function in a CNT, color indicating local spin canting angle. Variations in the transverse profile and the spin structure are due to the contribution of two valleys.

A32: Bilateral Doping of Single-Walled Carbon Nanotubes for Tranpsarent Conducting Applications

Albert Nasibulin*[†], Anastasia Goldt, Orysia Zaremba, Mikhail O. Bulavskiy, Fedor Fedorov, Kimmo Mustonen, Jani Kotakoski, Konstantin Larionov, Zakhar Popov, Pavel Sorokin

**Skolkovo Institute of Science and Technology*

Transparent conductive films (TCFs) have a wide range of applications in various electronic devices, such as flat panel displays, touch sensors, solar cells, etc. Nowadays the most commonly used transparent conductor in the electronic industry is indium tin oxide (ITO) due to its excellent optoelectrical performance and stability under ambient conditions. However, it has several drawbacks such as limited flexibility, high refractive index, high vacuum and deposition temperatures, haze, spectrally non-uniform optical transmission, restricted chemical robustness, depleted raw material supply and therefore relatively high cost. Therefore, new transparent conductive materials have been an urge topic and intensively examined to replace ITO. Among a large number of materials single-walled carbon nanotubes have been widely investigated as the transparent conductors due to their excellent electrical properties, chemical stability, abundant amount of carbon, and excellent adhesion to various substrates. SWCNT networks have been demonstrated potential advantages in performance and cost reduction in comparison with ITO. Furthermore, high flexibility and stretchability of the SWCNT films open avenues beyond the ITO, i.e. allow to create completely new components in flexible and stretchable transparent electronics. However, to replace ITO, the optoelectronic properties of the SWCNT films must be still improved. Adsorption doping approach is one of the most efficient ways to obtain high conductivity SWCNT films. We propose an easy and efficient method to modulate the SWCNT optoelectronic properties, comprising the thermal treatment at environmental atmosphere and subsequent doping by HAuCl4 ethanol solution to deliver the dopant to the outer surface and inner cavity of SWCNTs. Such a strategy has allowed us to significantly enhance the optoelectronic properties of the SWCNT networks and achieve a record value of the equivalent sheet resistance of 31 Ω/sq, which stems from the double-side doping of SWCNT by HAuCl4 as confirmed by DFT and electrochemical studies. *Acknowledgements:* This work was supported by the Russian Science Foundation (Project identifier: 17-19-01787) and RFBR (project number: 20-03-00804).

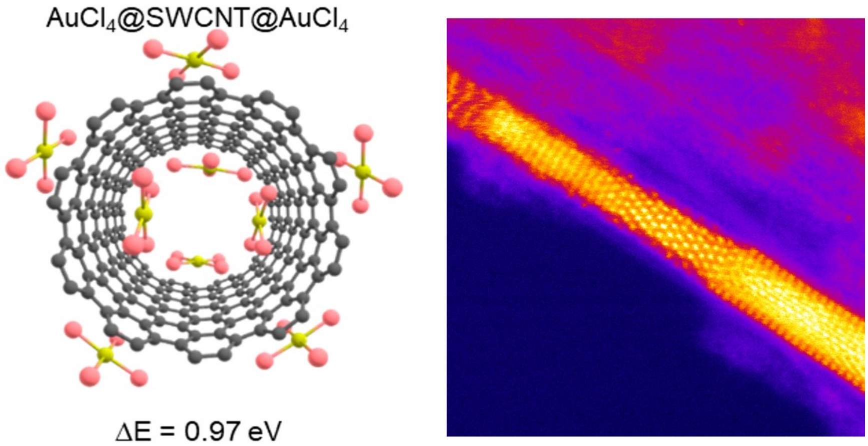

Fig. 1: Atomic structures of pristine SWCNT(10,10) doped both inside and outside with HAuCl4 and STEM image of 15 mM HAuCl4-doped opened SWCNTs with encapsulated gold nanowire.

A33: Understanding the Process Variables to Achieve Global Alignment of Single-Wall Carbon Nanotubes

Christian Rust*†, Han Li, Georgy Gordeev, Manuel Spari, Markus Guttmann, Benjamin S. Flavel

**Karlsruhe Institute of Technology (KIT)*

Carbon nanotubes (CNTs) are a 1D dimensional material with anisotropy in their thermal, electronic and optical properties. It is therefore a grand challenge to control their orientation in an ensemble and prepare large scale aligned thin-films. In this direction, slow flow dead-end filtration using polyvinylpyrrolidone-coated polycarbonate membranes has recently been shown to achieve global alignment of CNTs across an entire membrane. This route is highly attractive because it allows for purified dispersions to be used but it has proven to be difficult to reproduce. In this work, we present a custom dead-end filtration setup capable of precise in-situ measurement of flow, trans-membrane pressure and effective retention. This setup allows us to identify the important variables to achieve global alignment and explain why others have found it hard to reproduce in their own laboratory.

A34: Effect of supercritical nitrogen treatment on formation of dispersions of individual SWCNTs

Albert Nasibulin*†, Polina Kalachikova, Anastasia Goldt, Eldar Khabushev, Timofei Eremin, Elena Obraztsova, Konstantin Ustinovich, Artem Grebenko, Olga Parenago, Timofei Zatsepin, Oleg Pokrovskiy

**Skolkovo Institute of Science and Technology*

High quality single-walled carbon nanotubes (SWCNT) dispersions containing individual nanotubes are of a great potential for many technological applications, including biosensors, optical devices and conductive films. However, strong van der Waals interaction between tubes together with their large surface area and high aspect ratio force SWCNTs to form bundles to minimize their free surface energy. Several techniques are used to prepare homogeneous dispersions of SWCNTs in aqueous solutions. They are based on covalent and noncovalent modification of SWCNTs, respectively including partial oxidation by strong inorganic acids and surface coverage with surfactants or polymers. Besides, to preserve intact SWCNT structures various surfactants can be used to cover the tube surface and thereby to protect the tubes from agglomeration. However, to get high quality SWCNT dispersions by separating bundles into individual tubes, detrimental ultrasonication process is required. We propose a novel technique to improve dispersion of SWCNTs in aqueous media by direct injection of SWCNTs treated in supercritical nitrogen into aqueous surfactant solution (2% SDS). Exfoliation of SWCNT bundles is caused by rapid expansion of supercritical nitrogen intercalated inside the bundles. The tubes after the supercritical conditions immediately enter the solution are covered by the surfactant before they form bundles (Figure 1). This technique significantly decreases the time necessary for dispersion of SWCNTs from powder, increases the yield of individual nanotubes in aqueous dispersions and decreases their damage in comparison to prolonged ultrasonication. *Acknowledgements:* This work is supported by the by Russian Foundation for Basic Research, project No. 18-29-06071

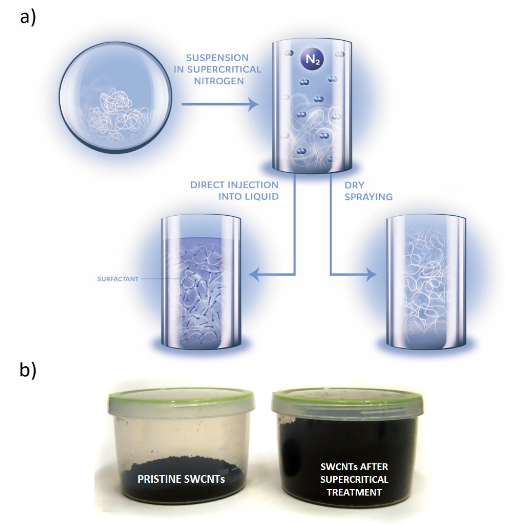

Fig. 1: a) Schematic diagram of direct injection into liquid and dry spraying method; b) a photograph of 2 g SWCNT powders before and after supercritical nitrogen treatment.

A35: Detection of bacteria using near infrared fluorescent nanosensors

Robert Nißler*†, Oliver Bader, Maria Dohmen, Sebastian Walter, Christine Noll, Gabriele Selvaggio, Uwe Groß, Sebastian Kruss

**Georg-August University Göttingen*

Infectious diseases are worldwide a major cause of morbidity and mortality. Fast and specific detection of pathogens such as bacteria is needed to combat these diseases. Optimal methods would be non-invasive and without extensive sample-taking/processing. Here, we developed a set of near infrared (NIR) fluorescent nanosensors and used them for remote fingerprinting of clinically important bacteria. The nanosensors are based on single-walled carbon nanotubes (SWCNTs) that fluoresce in the NIR optical tissue transparency window, which offers ultra-low background and high tissue penetration. They are chemically tailored to detect released metabolites as well as specific virulence factors (lipopolysaccharides, siderophores, DNases, proteases) and integrated into functional hydrogel arrays with 9 different sensors. These hydrogels are exposed to clinical isolates of 6 important bacteria (Staphylococcus aureus, Escherichia coli, …) and remote (≥25 cm) NIR imaging allows to identify and distinguish bacteria. Sensors are also spectrally encoded (900 nm, 1000 nm, 1250 nm) to differentiate the two major pathogens P. aeruginosa as well as S. aureus and penetrate tissue (>5 mm). This type of multiplexing with NIR fluorescent nanosensors enables remote detection and differentiation of important pathogens and the potential for smart surfaces. *Acknowledgements:* VW foundation

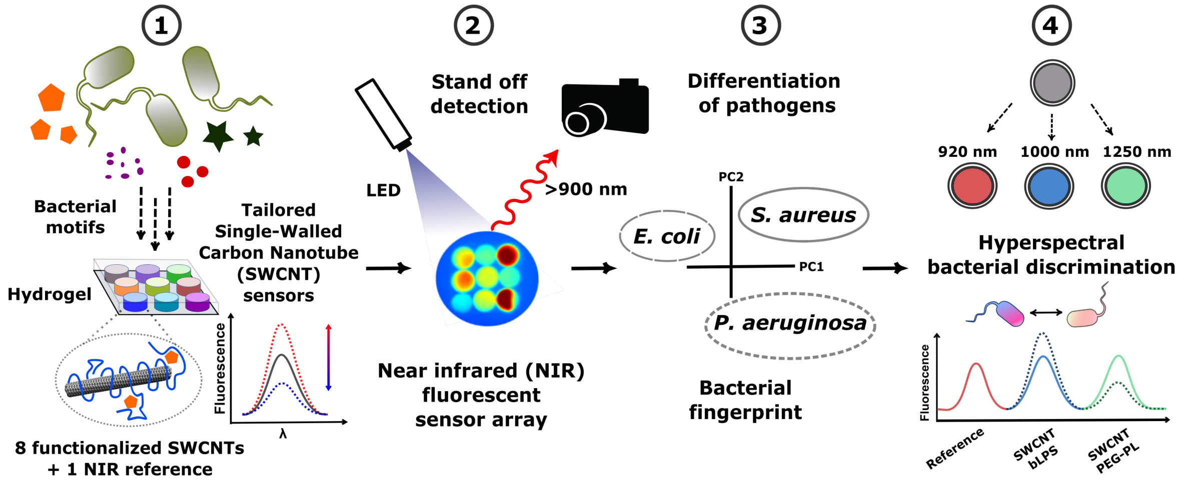

Fig. 1: Remote detection of pathogens: Multiple nanosensors based on NIR fluorescent single-walled carbon nanotubes (SWCNTs) monitor bacterial metabolites and virulence factors, which enables pathogen fingerprinting and differentiation.

A36: Proposal for tunable THz detection realized in CNT quantum dots with broken symmetries

Dario Bercioux[†], Magdalena Marganska, Gilles Buchs*, Jhon Gonzalez, Kristjan Eimre, Carlo Pignedoli, Daniele Passerone, Andres Ayuela Fernandez, Oliver Gröning

**Silicon Quantum Computing, Sydney, NSW 2052, Australia*

Quantum dots (QD) in metallic single-walled carbon nanotubes (SWNT) have shown great potential to build sensitive terahertz (THz) detection devices usually based on photon-assisted tunnelling. A recently reported mechanism based on a combination of resonant QD transitions and asymmetries in the tunnelling barriers results in a narrow linewidth photocurrent response with a large signal-to-noise ratio under weak THz radiation. However, in such devices, due to the linear dispersion relation of metallic SWNTs, the detection range is intrinsically limited to allowed energy transitions between equidistant quantized states set by the QD length. Here, we show that simultaneously breaking translational, rotational, and mirror symmetries in metallic SWNT QDs leads to a quantized spectrum with non-equidistant energy levels. This result stems from tight-binding and first-principle simulations of a defect-induced metallic zigzag SWNT QD and is validated experimentally by scanning tunnelling spectroscopy studies. Importantly, our calculations show that breaking symmetries in metallic SWNT QDs of arbitrary chirality strongly relaxes the selection rules in the electric dipole approximation, leading to a richer set of allowed optical transitions spanning frequencies from as low as 1~THz up to several tens of THz for a ~10 nm QD. Based on these findings, we propose a device design for a THz detector based on a metallic SWNT QD engineered with artificial defects. Depending on the QD length and contact transparency, we can establish the device's operating regime to be anywhere between a high-resolution gate-tunable THz sensor and a broadband THz detector. Our calculations also indicate that the device is mainly unaffected by temperatures up to 100 K. Buchs et al., arXiv:2006.10837

A37: Development of Single-Walled Carbon Nanotube/Defect-Based Sensors via Machine Learning

Daniel Heller*, Zvi Yaari[†], Mijin Kim, Yoona Yang, Chen Chen, Merav Antman-Passig, Peng Wang, YuHuang Wang, Anand Jagota, Ming Zheng

**Memorial Sloan Kettering Cancer Center*

The photoluminescence of single-walled carbon nanotubes (SWCNTs) and organic color center (OCC) defects offer unique advantages for the development of biological sensors, including the potential to sensitize emission to many classes of analytes. Methods to selectively transduce the local concentration of an analyte via an optical signal often involves the attachment of existing molecular recognition elements to the nanotube surface, or the development of selectivities by high-throughput screening or selection techniques. Due to the existence of several mechanisms of optical modulation of OCCs and SWCNTs, as well as multiple carbon nanotube species with differing bandgaps, and the increasing number of excipients and polymers that can be used for colloidal suspension and non-covalent functionalization, new methods in data analytics can be used to facilitate selective recognition of bioanalytes to detect and process multi-parametric spectroscopic fingerprints. These methods will be discussed for the detection of analytes and identification of disease indications.

A38: 2D-band resonance behavior in Raman excitation maps of chirality-sorted SWCNTs

Dmitry Levshov*[†], Salome Forel, Valentin Popov, Joeri Defillet, Han Li, Benjamin S. Flavel, Jeff Fagan, Wim Wenseleers, Sofie Cambré

**Nanostructured and Organical Optical and Electronic Materials, Department of Physics, University of Antwerp, Antwerp, Belgium*

An intense second-order line near 2700 cm-1 in the Raman spectra of carbon nanotubes (CNT), the so-called 2D band, arises from the electron (or hole) scattering by two transverse optical phonons with opposite momenta [1]. It depends critically on the nanotube's electronic band structure and phonon dispersion and is used in practice for quantifying single-/double-wall relative concentration in CNT mixtures, monitoring the level of doping, isotope-enrichment and estimating CNT diameters. Recently, it has been the focus of extensive experimental and theoretical research [1-3]. However, the high complexity of the theoretical description of second-order Raman scattering in CNTs due to the quantum confinement and curvature effects, and, on the other hand, the lack of detailed and extensive experimental data leads to controversies in the interpretation of the resonance behavior and dispersive character of the 2D bands [1,2]. In this work, we aim to resolve the existing problems by performing systematic experimental and theoretical studies of the 2D-bands for a large number of chirality-defined SWCNTs. The sorted SWCNT samples are structurally characterized by a combination of wavelength-dependent Raman spectroscopy, fluorescence-excitation spectroscopy and optical absorption techniques. By continuously changing the excitation wavelength from UV to NIR (375 - 710 nm, 5 nm step) and simultaneously monitoring the radial breathing mode and 2D band resonances, we can unambiguously resolve the second-order features corresponding to particular (n,m) chiralities with high resolution. These experimental data are complemented with a full calculation of the 2D-band Raman intensity within a symmetry-adapted ab-initio-based non-orthogonal tight-binding model [1]. The obtained results reveal the importance of the explicit account of the interactions of electrons, photons, and phonons in the description of the resonance behavior of the 2D bands and unlock the full characterization power of second-order Raman scattering in CNTs.References:[1] V.N. Popov, Phys. Rev. B. 98 (2018) 085413. [2] L.G. Moura et al., Carbon 117 (2017) 41–45. [3] J. Laudenbach et al., Carbon 112 (2017) 1–7. *Acknowledgements:* D.L. acknowledges FWO Postdoc Fellowship No. 12ZP720N. S.F., J.D., S.C. acknowledge funding from ERC Starting Grant No. 679841 (ORDERin1D)

A40: Synthesis of small-diameter SWCNTs by ACCVD using the period 6 platinum-group elements as catalysts

Takahiro Maruyama*†, Kamal Prasad Sharma, Takuya Okada, Daiki Yamamoto, Takahiro Saida, Shigeya Naritsuka
**Meijo University*

A single-walled carbon nanotubes (SWCNTs) have many potential applications because of their unique structural and physical properties. For applications to transistors, synthesis of small-diameter SWCNTs, i.e., diameters below ~1 nm is important, since the band gap of an SWCNT increases with the decrease of its diameter. Also, aligned small-diameter SWCNTs are applicable as a membrane filter for purifying water. Here, we performed SWCNT growth by alcohol catalytic chemical vapor (ACCVD) with the platinum-group elements in the period 6 of the periodic table, that is, Ir and Pt. Using Ir as a catalyst, vertically aligned (VA)-SWCNTs were grown on SiO2/Si substrates at 800°C under the optimal growth condition. The SWCNT length increased with increasing growth time, and the VA-SWCNT thickness reached almost 5 mm after SWCNT growth for 180 min. Raman and photoluminescence spectroscopies showed that the diameters of the grown SWCNTs were mainly between 0.8 and 1.1 nm; this is much smaller than those of VA-SWCNTs grown with Fe and Co catalysts in previous studies. X-ray photoelectron spectroscopy and X-ray absorption near-edge structure spectroscopy showed that the Ir catalyst retained the metallic state during SWCNT growth. We also performed SWCNT growth by ACCVD using a Pt catalyst, and obtained web-like SWCNTs whose diameters were mainly distributed between 0.6 and 1.1 nm at 700 °C. We demonstrated that the 6 group platinum-group elements act as catalysts to grow small-diameter SWCNTs. Highly efficient suppression of aggregation, an appropriate carbon–metal bond strength and dissociation of ethanol molecules would lead to the growth of small-diameter SWCNTs with the 6 group platinum-group elements as catalysts. *Acknowledgements:* We thank Meijo University Research Branding Project for Cultivation and Invention of New Nanomaterials under the MEXT

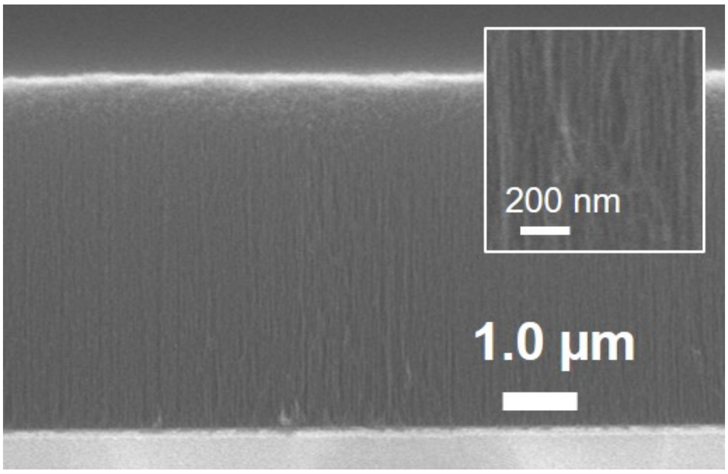

Fig. 1: Cross-sectional SEM image of SWCNTs grown with Ir catalyst (Inset shows magnified SEM image of SWCNTs).

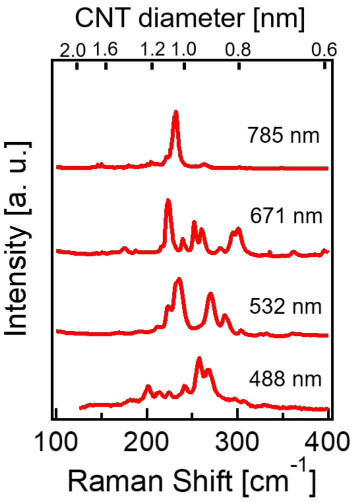

Fig. 2: Raman spectra in RBM region of SWCNTs grown with Ir catalyst.

A41: Molecular Dynamics Simulation of Graphene Sinking during Chemical Vapor Deposition Growth on Semi-molten Cu Substrate

Ziwei Xu*†

Jiangsu University

Copper foil is the most promising catalyst for the synthesis of large-area, high-quality monolayer graphene. Experimentally, it has been found that the Cu substrate is semi-molten at graphene growth temperatures. In this study, based on a self-developed C-Cu empirical potential and density functional theory (DFT) methods, we performed systematic molecular dynamics simulations to explore the stability of graphene nanostructures, i.e., carbon nanoclusters and graphene nanoribbons, on semi-molten Cu substrates. Many atomic details observed in the classical MD simulations agree well with those seen in DFT-MD simulations, confirming the high accuracy of the C-Cu potential. Depending on the size of the graphene island, two different sunken-modes are observed: (i) graphene island sinks into the first layer of the metal substrate and (ii) many metal atoms surround the graphene island. Further study reveals that the sinking graphene leads to the unidirectional alignment and seamless stitching of the graphene islands, which explains the growth of large single-crystal graphene on Cu foil. This study deepens our physical insights into the CVD growth of graphene on semi-molten Cu substrate with multiple experimental mysteries well explained and provides theoretic references for the controlled synthesis of large-area single-crystalline monolayer graphene. *Acknowledgements:* This work is supported by the National Natural Science Foundation of China (11774136, 11404144, 11574262).

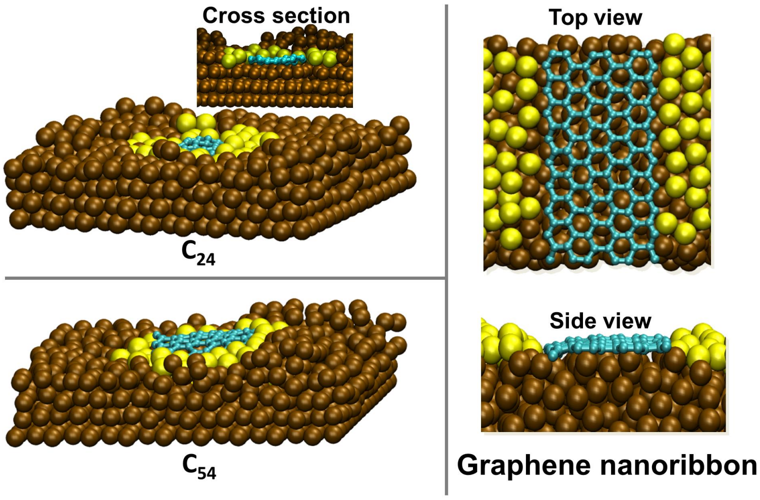

Fig. 1: Molecular dynamics simulations of graphene nanostructures on semi-molten Cu substrate. Small graphene island (C24) sinks into the first layer of the metal substrate directly; larger graphene island (C54) and

A42: Catalyst Particle Size Dependent Carbon Nanotube Cloning

Ziwei Xu*†

**Jiangsu University*

The single walled carbon nanotube (SWCNT) cloning or its seeded growth with a catalyst particle docked on one of its ends was proposed as the ultimate solution for chirality-specific SWCNT synthesis and, therefore, revealing the effect of catalyst particle size on the robustness of the SWCNT cloning is crucial for experimental designs. Through systematic atomic simulations, we have clearly demonstrated that the robustness of SWCNT cloning depends on both the chiral angle of the SWCNT and the ratio of the diameters between the SWCNT and the docked catalyst particle. The zigzag (ZZ) or near ZZ SWCNTs are highly sensitive to the size of the docked catalyst particle. A small change of the catalyst particle size could lead to a variation of the SWCNT's chirality. In contrast, armchair (AC) or near-AC SWCNTs are less sensitive to the size of the docked catalyst particle and able to maintain their original chiralities within ~30% variation of the catalyst particle size. This study greatly deepens our understanding of SWCNT's growth mechanism and provides a quantitative guidance for SWCNT cloning. *Acknowledgements:* National Natural Science Foundation of China (11774136), Research Foundation in Institute for Basic Science (IBS-R019-D1)

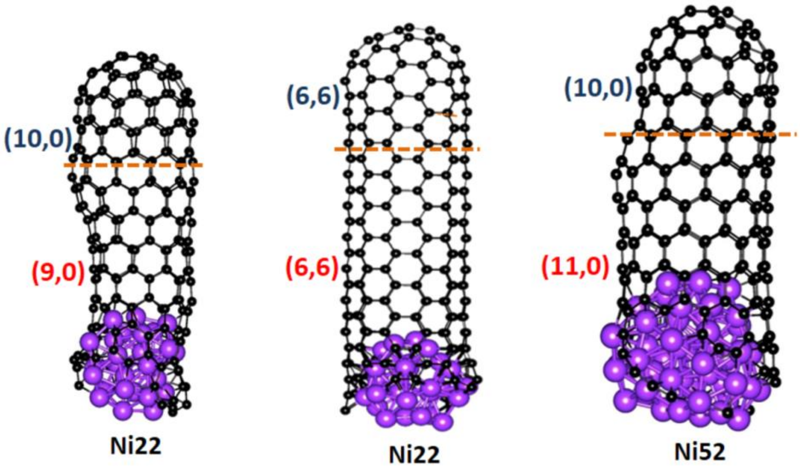

Fig. 1: In the cloning of single-walled carbon nanotube (SWCNT), seeding SWCNTs with different chiralities present different robustness to the size variation of the catalyst during the seeded growth.

A43: In-situ formed non-oxidized copper nanoparticle-carbon nanotube nanocomposites with enhanced electrical and thermal properties

Muhammed Ajmal Chathanchira†, Aby Paul Benny, Wonjae Jeon, Seongkyun Kim, Sung Wng Kim, Seunghyun Baik*

**Sungkyunkwan University*

We have employed silver (Ag)-based fillers to enhance electrical and thermal conductivities of polymer-matrix nanocomposites [1, 2]. However, the high cost of Ag has limited the scale-up application and industrialization. Copper (Cu) is an attractive economic alternative while providing comparable electrical and thermal conductivities. However, the practical application of Cu nanoparticles has been hindered by its susceptibility to oxidation in air. Here we report a novel scalable synthesis method of non-oxidized copper nanoparticles (InSituCuNPs) via premixing Cu precursors in matrix polymer and subsequent in-situ thermal reduction [3]. Since the InSituCuNPs were surrounded by the thick matrix polymer as soon as they were formed, the particles were well protected from oxidation. The thermal and electrical properties of the nanocomposites were further enhanced by introducing a novel multi-dimensional filler, 1-dimensional multiwalled carbon nanotubes (MWNTs) decorated with 0-dimensional CuNPs (< 4 nm) (nCuMWNTs) [3]. The nCuMWNTs constructed electron and phonon transport bridges between the larger 3-dimensional InSituCuNP islands. Air-stable and record-high electrical (31,974 Scm-1) and thermal (74.1 Wm-1K-1) conductivities were achieved, compared with isotropic Cu-based nanocomposites in literature [3]. A recent progress in the laboratory and heat dissipation demonstration will also be introduced. References [1] Suh, D. et al. Nature Communications 2020, 11, 2252. [2] Ajmal, C. M. et al Small 2019, 15, 1803255. [3] Ajmal, C. M. et al. Materials Today 2021, In Press.

A44: Transmissible plasma evolved graphene: a facile technique for 0D, 1D and 2D heterostructure production

Kamal Prasad Sharma*†, Aliza Khaniya Sharma, Daiki Yamamoto, Toru Asaka, Takahiro Maruyama

**Meijo University*

The chemical vapour deposition (CVD) of carbon feedstock onto a catalyst surface, carbon species that are excited by a plasma, and high-energy laser irradiation of carbon surfaces are important methods for graphene production [1-3]. Among them, plasma enhanced CVD (PECVD) utilizing microwave, surface wave, or radio frequency (rf) plasma has been realized as promising techniques for graphene synthesis at low temperature and with short processing time [4]. However, for most CVD and PECVD techniques, time-consuming transfer and chemical treatment processes are essential to produce graphene for subsequent applications. Here, we propose a simple technique to produce suspended graphene, [5] which address these issues and is relevant for 0D to 2D heterostructure production in a single set of experiment.For transmissible plasma evolved graphene (TPEG) production, commercially available TEM microgrids with amorphous carbon (a-C) membranes were utilized, onto which Co plasma produced from Co target in a pulsed arc plasma deposition system (APD-2S, Advance Riko) was exposed (Figure 1(a)). Each arc pulse is triggered by a surface flashover from a trigger electrode to the cathode surface (trigger duration ~10 mS) and the discharge voltage between cathode and anode was varied, which affects mainly the density of metal plasma. As produced TPEG was analyzed by OM, Raman spectroscopy, XPS, AFM, and TEM. Figure 1(b) shows the Co plasma utilized with biased voltage of 140V (3 pulses) or more produced the TPEG and high quality TPEG was produced at 170V (Figure 1(c)). As produced TPEG was comprised of 3 to 12 layers with interlayer distance of 0.34 nm (Figure 1(f)), and is of uniform quality throughout the suspended part of a-C as seen in G-band map (Figure 1(e)). Besides graphene production in both time and energy efficient ways, this technique was employed to produce heterostructures (Figure 2(a-f)), and would serve as graphene grids for TEM characterization.Li, X. et al., Science 324, 1312 (2009).Jacov, M. V. et al., Nano Lett. 15, 5702 (2015).Lin, J. et al. Nat. Commun. 5, 5714 (2014).Pharm, V. P. et al., Chem. Soc. Rev. 46, 6276 (2017).Sharma, K.P. et al., ACS Appl. Nano Mater 4, 1485 (2021). *Acknowledgements:* This work was supported in part by Private University Research Branding Project from the Ministry of Education, Culture, Sports, Science and

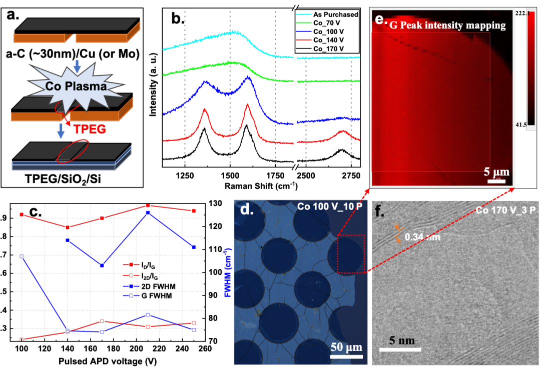

Fig. 1: (a) Schematic of a TPEG process. Qualitative Raman analysis (c) of spectra (b) for biased voltages. (e) G-peak map of TPEG/SiO2/Si indicated in OM image (d). (f) HRTEM image.

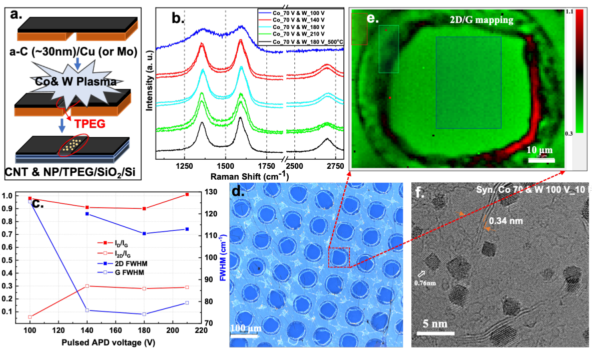

Fig. 2: (a) Schematic representation of 0D-2D onto TPEG. Qualitative Raman analysis(c) of spectra(b) at different biased voltages. (e)G-peak map of TPEG/SiO2/Si as indicated in OM image(d). (f) HRTEM image.

A45: Mechanism of indirect-to-direct band gap crossover of single walled MoS$_2$ nanotubes

Kaoru Hisama†, Mina Maruyama, Susumu Okada, Shohei Chiashi, Shigeo Maruyama*

The University of Tokyo

Molybdenum disulfide (MoS$_2$) is known to form tubular structure, owing to its honeycomb covalent network with three-atom thickness. Semiconducting electronic structure of monolayer sheet of MoS$_2$ also makes MoS$_2$ nanotubes (MoS$_2$ NTs) semiconductors irrespective of their diameter and helicity. Several theoretical works predicted that MoS$_2$ NTs have indirect band gaps except with zigzag chiral indices [1-3]. This indirect band gap should be direct in a large diameter, because the band edge alignment of MoS$_2$ NTs asymptotically corresponds to the direct band gap at the K point of monolayer MoS$_2$ sheet, with increasing their diameter. Thus, we aim to reveal this indirect-to-direct band gap crossover of armchair MoS$_2$ NTs in a wide diameter range using the density functional theory. Although a small diameter (9,9) NT is a semiconductor with an indirect band gap between Γ and approximately $k = 2\pi/3$ where K point in 2D BZ is folded [Fig. 1(a)], a large diameter (39,39) NT is a semiconductor with a direct band gap at approximately $k = 2\pi/3$ [Fig. 1(b)]. To study the critical diameter at which the band gap crossover occurs, we investigated the energy difference between the highest occupied states at near the Γ point, and at $k = 2\pi/3$, of MoS$_2$ NTs. Figure 1(c) showed that the crossover occurred at the diameter about 5.2 nm. This indirect band gap structure in small NTs is ascribed to strain effect due to curvature, which gradually decreases with increasing the diameter of the NTs. [1] G. Seifert, et al., Phys. Rev. Lett. 85, 146 (2000). [2] D. B. Zhang, et al., Phys. Rev. Lett. 104, 065502 (2010). [3] N. Zibouche et al., Euro. Phys. J. B, 85, 49 (2012).

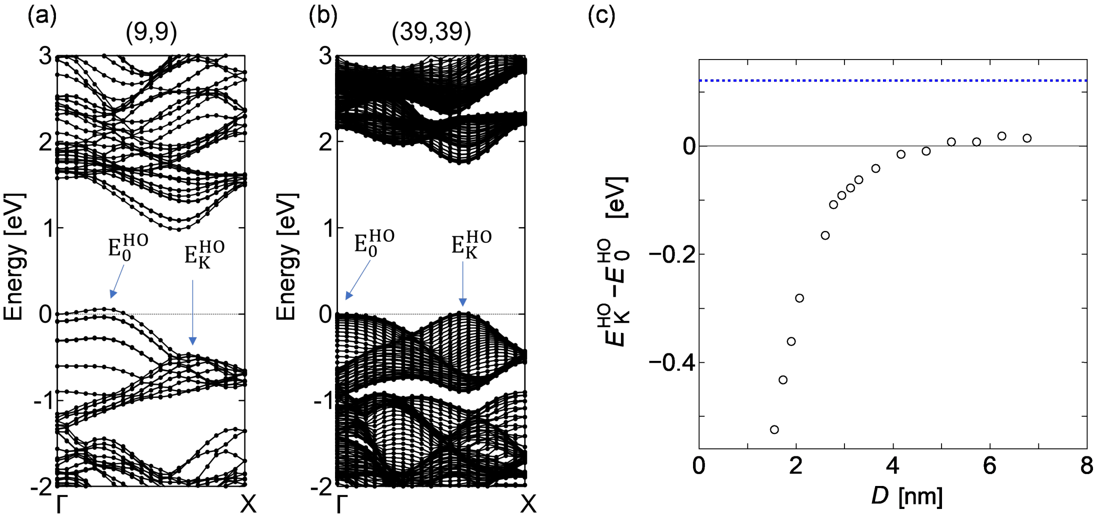

Fig. 1: Electronic structure of (a) (9,9) and (b) (39,39) MoS$_2$ NT. (c) $E_K^{HO} - E_0^{HO}$ as a function of diameter. Dotted line in (c) shows the value of 2D monolayer MoS$_2$.

B46: Characterization of Single-Walled Carbon Nanotubes functionalized with 11-Bromoundecyltrichlorosilane

Laura Meingast*†, Gririraj Manoharan, Carola Meyer, Janina Maultzsch

**Friedrich-Alexander University Erlangen-Nuremberg*

Research on carbon nanotubes in the last years has shown their high potential for a wide range of applications. To meet different demands, the customization of nanotube properties via chemical functionalization is a widely used approach. Especially click chemistry offers the possibility to attach a large variety of molecules in a simple and efficient way [1]. Here, we present the investigation of single-walled carbon nanotubes functionalized with 11-Bromoundecyltrichlorosilane. The silanization is the base reaction of a three-step click chemistry approach, consisting of silanization, azidization, and final molecule clicking. To obtain insight into the base reaction, the silanized carbon nanotubes were investigated with Raman spectroscopy. A first characterization and determination of the (n,m)-branches is presented. The influence of the silane attachment on the defect amount of the nanotubes is studied via the D/G Raman intensity ratio at different laser wavelengths. Additionally, reference spectra of 11-Bromoundecyltrichlorosilane are shown and compared with the Raman spectra of silanized nanotubes. [1] G.Clavé, S.Campidelli, Chem. Sci., 2, 1887 (2011).

B47: Photo-induced volume phase transition in SWNT/PNIPAM smart hybrid microgels

Rosa D'Ambrosio*†, Eric Anglaret, Ty Phou, Christophe Blanc

**Université de Montpellier*

The development of smart nanomaterials has attracted great attention in several fields like nanoscience, materials science, engineering and nanotechnology due to their unique response to external stimuli. Many of them are based on polymers that can exhibit great shape-changes when submitted to environmental modifications. Poly(N-isopropylacrylamide), PNIPAM, is such a thermo-responsive polymer. It is water soluble at room temperature, forming gels by cross-linking but undergoes a reversible coil-to-globule volume phase transition (VPT) at a lower critical solution temperature (LCST) close to 32 °C due to the dehydration and subsequent collapse of its chains into compact globules. Hybrid nanocomposite microgels associating PNIPAM and gold nanoparticles (GNP) have been designed in order to take advantage of the outstanding plasmonic and photo-thermal properties of GNP to promote the volume phase transition of the microgels through an efficient photo-thermal conversion. With their strong diameter-dependent optical absorption in the near infrared (NIR) and their large surface area favoring photo-thermal transfer, semiconducting SWNT (s-SWNT) are good candidates for photo-thermal conversion in the NIR and may therefore be used to prepare multi-responsive hybrid microgels (Figure 1). However, to the best of our knowledge, no thorough studies of such nanomaterials have been reported so far.Here we report the preparation of smart SWNT/PNIPAM nanocomposites through non-covalent functionalization techniques. These SWNT/PNIPAM hybrid microgels are stable in water and show a VPT, which can be promoted either by direct heating or by excitation of the resonant absorption of s-SWNT in the near infrared. Furthermore, the photoluminescence (PL) signal of s-SWNT is modulated at the phase transition and therefore, the PL signal can be used to monitor the VPT. This is illustrated in Figure 2, showing coupled Raman/PL measurements below and above the LCST, where a redshift of the PL bands is observed when crossing the LCST while the Raman signatures remain essentially the same.

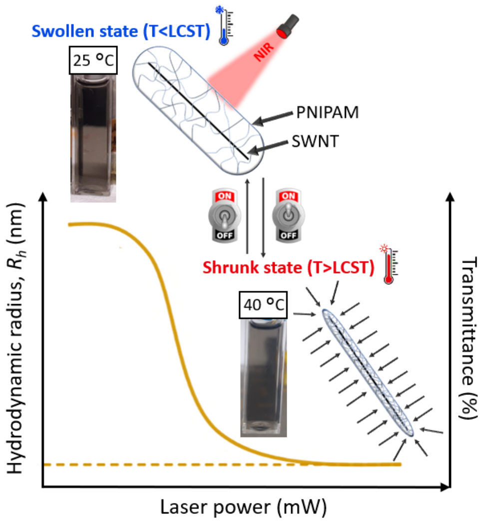

Fig. 1: Schematic illustration of photo-induced coil-to-globule transition in smart SWNT/PNIPAM hybrid microgels.

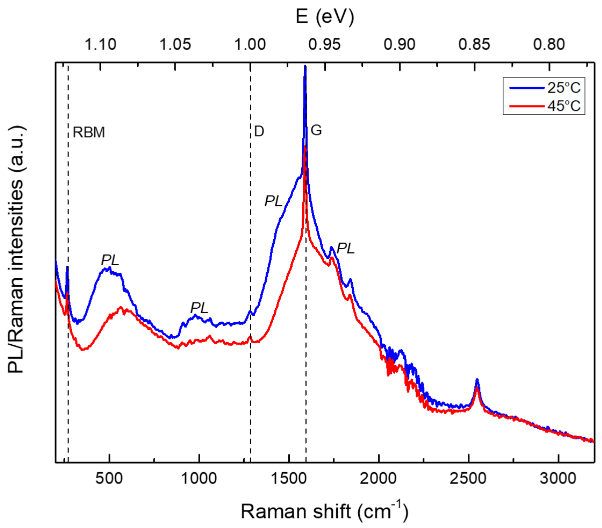

Fig. 2: Coupled PL/Raman spectra (λexc = 1064nm) of the hybrid microgels below and above the LCST of PNIPAM. Raman signatures, labelled RBM, D and G, are superimposed to broader PL bands.

B49: Defined Nondestrcutive Functionalization of Single Walled Carbon Nanotubes

Alphonse Fiebor*†, Antonio Setero, Mohsen Adeli, Rainer Haag, Stephanie Reich

**Department of Physics, Freie Universität Berlin, Arnimallee 14, 14195 Berlin, Germany*

In spite of their unique physicochemical and optoelectronic properties, two main drawbacks including poor functionality and dispersibility limit the application of single walled carbon nanotubes (SWNTs)1. Exohedral functionalization of SWNTs by covalent and noncovalent approaches are two main strategies to add functionality to nanotubes and to improve their low dispersibility1,2. Noncovalent interaction between SWNTs and (macro) molecules is limited in terms of stability and covalent attachment of molecular species to SWNTs, on the other hand, disturbs the π system of the tubes.In 2017, we developed a new approach for the nondestructive covalent functionalization of SWNTs based on nitrene [2+1] cycloaddition reaction at room temperature that preserved the delocalized π electrons and their photoluminescence3. However, post-functionalization and attachment of additional (macro) molecules through their functional groups by ”grafting from” approach was challenging in terms of controlling the number of the attached species and their homogeneity.This work is a step ahead to solve this problem by changing the functionalization paradigm using ”grafting to” method; we first create ex-novo multifunctional probes with desired advanced functions and then attach them onto the SWNTs as shown below. We herein report a new class of nondestructive covalent attachment of different molecular probes onto SWNTs with defined functionalities. References Shadpour Mallakpour and Samaneh Soltanian, RSC Adv. 2016, 6, 109916.Hirsch, A. Functionalization of single-walled carbon nanotubes. Angew. Chem. Int. Ed. 2002, 41, 1853–1859.Setaro et al. Nat Commun. 2017, 8, 14281. *Acknowledgements:* DFG, European Research Council (ERC), FU Berlin

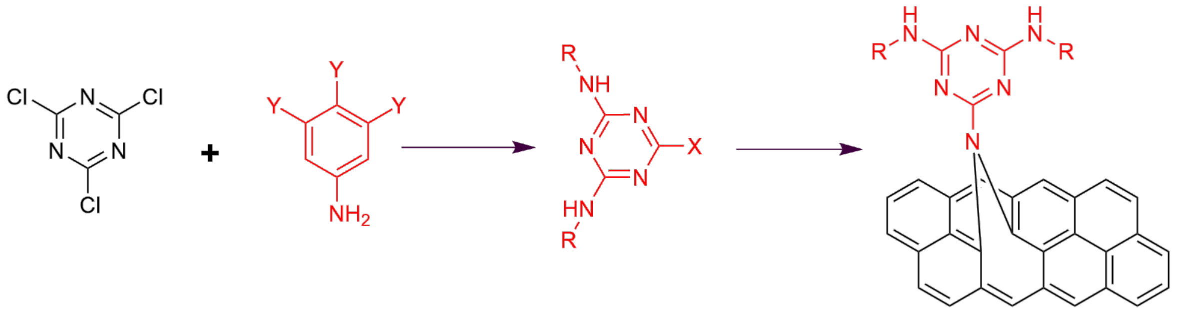

Fig. 1: Schematic representation of nondestructive functionalization of SWNTs and production of nanotubes with preserved π conjugated system and defined functionality.

B51: General Matrix Multiplication Hardware Acceleration Based on Graphene Optoelectronics

Ruiyang Chen†, Cunxi Yu, Weilu Gao*

**University of Utah*

Optical and optoelectronic hardware of executing general matrix multiplication (GEMM) operations outperforms electronic counterparts, because of the reduced power consumption of devices, ultrafast speed-of-light processing, and high parallelism and throughput. In addition, the incorporation of nanomaterials can further enhance the device and system performance. However, the non-uniformity and variation of nanostructure severely limit the deployment of large-scale hardware. Here, we present a new high-performance optoelectronic architecture consisting of two-dimensional (2D) array of spatial light modulators (SLMs) and 2D array of photodetectors with electrically tunable photoresponse. In this architecture, the multiplication part in GEMM is done by the modulation of optical transmission in SLMs and photoresponsivity of photodetectors; the summation is done by electronically adding up all the photocurrents generated by photodetectors in the same row. The SLMs and photodetectors are both constructed by large-scale graphene monolayers as well as optical metamaterials. Our architecture relaxes the requirement of large-scale uniformity in high-quality devices, making tolerance of device variations larger, which also removes the need of beam splitter and simplifies optical alignment. To correct the non-uniformity and variation of the devices, the tuning curve of each unit in SLMs and photodetectors is obtained from the readout with sweeping gate bias of SLMs and photodetectors. The minimum tuning range in a row of units is set as the normalization unit of tuning so that all the units in the row can reach the full tuning range. To benchmark our architecture after the calibration, an 8X8 multiplier based on our architecture is compared with a general-purpose processor (GPP) on image reconstruction, support vector machine (SVM) algorithms and multi-layer perceptron (MLP) neural networks. The reconstructed image has equal quality from multiplier and GPP. In the clustering of Blobs dataset using SVM, the results obtained on multiplier match the GPPs' result with loss differs < 0.2%. In MLP neural networks, a two-layer MLP network is built and trained on MNIST10 and Fshion-MNIST10. The MLPs achieved comparable results with GPPs. *Acknowledgements:* We thank the support from the University of Utah start-up fund. Y. C. thanks the support from grants NSF-2019336 and NSF-2008144.

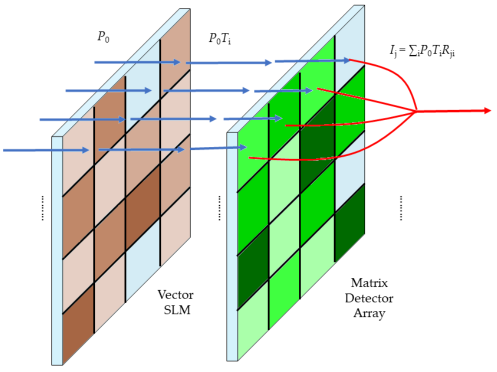

Fig. 1: Schematic of graphene-based optoelectronic matrix-vector multiplier. The input is modulated by SLMs then received by photodetectors. The generated photocurrents from photodetectors in a row are added together electronically

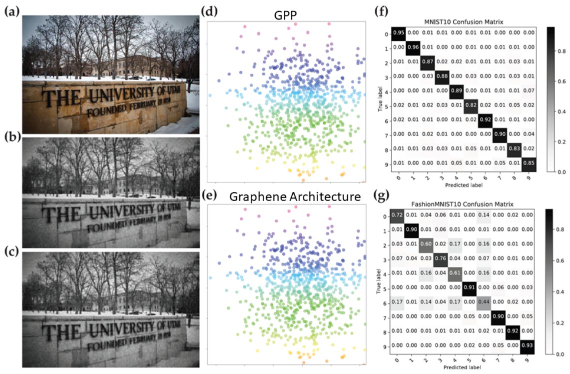

Fig. 2: Comparison in algorithms: Original picture in image reconstruction (a), results from GPP (b) and graphene architecture (c); SVM results (d)(e) and neural network classification results from graphene architecture

B52: Efficient Catalytic Growth of Carbon Nanotube Carpets Enabled by on-site Generation of Water

Placidus Amama*†

**Kansas State University*

Catalytic chemical vapor deposition (CVD) utilizing the gaseous product mixture of Fischer-Tropsch synthesis (FTS-GP) offers the potential for scale-up and controlled growth of carbon nanotube (CNT) carpets. In comparison to conventional feedstocks, FTS-GP exhibits the ability to support an exceptionally long catalyst lifetime with Fe catalysts. The role of the feedstock in growth enhancement is still poorly understood. In this study, a combination of experimental and thermodynamic analyses reveal on-site generation of water to be the secret for observed growth enhancement in FTS-GP CVD. The concentration of water generated in situ decreases with increasing reactor temperature (Figure 1). Further investigations using an Autonomous Research System (ARES) - an automated, high-throughput, laser-induced CVD system with in-situ Raman spectral feedback - reveal FTS-GP not only exhibits exceptionally long catalyst lifetimes compared to a standard feedstock (C2H4), but also shows a high tolerance for relatively high levels of water. *Acknowledgements:* National Science Foundation

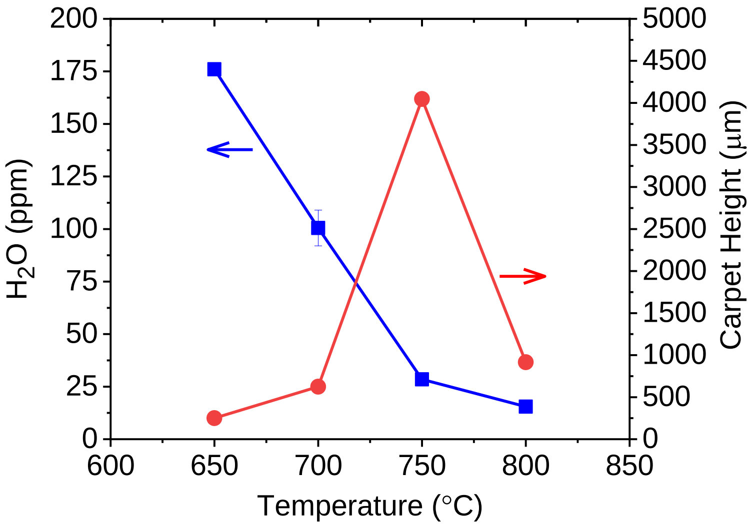

Fig. 1: Figure 1. Concentration of water produced via gas-phase reaction of FTS-GP in a batch reactor as a function of temperature. Plot of carpet height after 90 min of growth versus

B53: Exploring the Effects of Counterion Chemistry in Doped Thermoelectric Carbon Nanotube Networks

Andrew Ferguson*†, Jeff Blackburn, Taylor Aubry, Tucker Murrey, Omar Leon, Julia Stauber, Alexander Spokoyny, Benjamin Schwartz

**National Renewable Energy Laboratory*

We have previously demonstrated that the careful control of the charge carrier density required to optimize the thermoelectric performance of carbon nanotube networks can be afforded by charge injection from chemical dopants. This process results in counterions to the injected charge carrier density that reside within the porous, doped network. Here we demonstrate effective p-type doping by a series of novel charge-transfer dopants based on dodecaborane (DDB) clusters appended with various organic moieties that control both the structure and redox properties of the dopant. We find that the extent of p-type doping is determined by the oxidation potential of the functionalized DDB cluster, but that their increased size and steric bulk result in weaker doping than for oxidants like triethyloxonium hexachloroantimonate (OA) and 2,3,5,6-tetrafluoro-7,7,8,8-tetracyanoquinodimethane (F4-TCNQ). In contrast, the unique chemical and electronic structure of these functionalized DDB dopants allow the electron extracted from the carbon nanotube to be localized on the center of the dodecaborane cluster. This results in spatial separation of the negative counter-charge from the hole density injected into the carbon nanotube, which reduces their coulombic attraction. As a consequence, the mobility of the injected charge carriers is improved, yielding an increase in the thermopower (Seebeck coefficient) for a given electrical conductivity. This enhanced transport ultimately results in an increase in the thermoelectric power factor that surpasses the previous best-in-class for enriched semiconductor single-walled nanotube thin film networks.

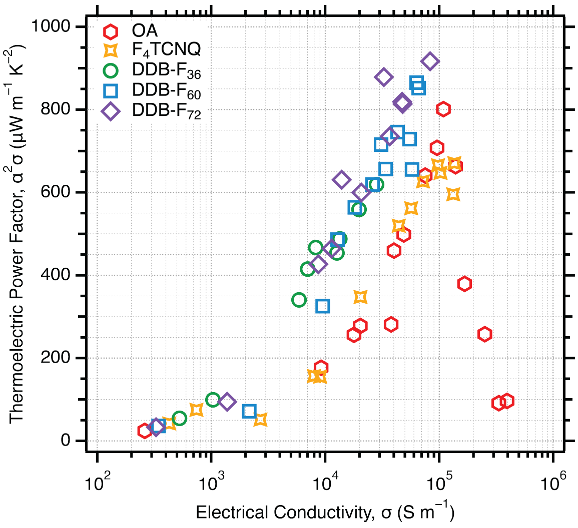

Fig. 1: Thermoelectric power factor (α2σ) versus electrical conductivity (σ) for the doped PT s-SWCNT networks, illustrating the enhanced power factor for the dodecaborane-doped samples.

B54: Origin and reduction of BN impurities in boron nitride nanotube synthesis by high temperature plasma

Keun Su Kim*†

National Research Council Canada

Since their first synthesis in 1995, the applications of boron nitride nanotubes (BNNTs) have been widely expanded in various research fields such as composite materials, nanoelectronics, radiation shielding materials, and biomedical. Broader availability of high-quality BNNTs becomes crucial for full realization of their potential. Recent notable progress in BNNT synthesis has been achieved by high temperature plasmas1-3. Our group demonstrated high-yield growth of high-quality BNNTs for the first time by introducing hydrogen-mediated plasma chemsity1,3, which led to a successful commercialization4. However, the commercial plasma process still suffers from production of BN impurities whose properties are very close to those of BNNTs. This makes their purification even more challenging. Reduction of such BN impurities during BNNT synthesis is highly demanded for their targeted applications, which requires a better understanding of impurity formation. In this study5, we have employed both experimental and numerical approaches for a mechanistic understanding of BN impurity formation in the high temperature plasma process. First, a parametric study on a variety of plasma operating conditions has been performed to identify the key parameter which dictates BN impurity formation. To understand our experimental finding, a numerical study via computational fluid dynamics (CFD) simulation was also performed using an in-house plasma code. Based on both experimental and numerical results, our study suggests that the flow structure of the plasma jet such as turbulence plays a key role in the formation of BN impurities by governing the transport phenomena of BNNT seeds such as boron droplets. We discussed that the turbulence enhances radial diffusion of B droplets as well as their inter-particle coagulation, which leads to a significant reduction in the population of effective BNNT seeds in the BNNT growth zone, and thus promotes formation of BN impurities. We believe this finding offers new insight into a process design capable of suppressing the BN impurity formation, and will have broad and significant impacts by rendering high purity BNNT material more accessible.References1. Kim, K. S. et al. ACS Nano, 8, 6211-6220 (2014).2. Fathalizadeh, A., Pham, T., Mickelson, W., & Zettl, A. Nano Lett., 14, 4881-4886 (2014).3. Kim, K. S. et al. ACS Nano, 12, 884-893 (2018).4. http://www.tekna.com/boron-nitride-nanotubes5. Kim, K. S. et al., Submitted.

B55: Atmospheric Pressure Radio-Frequency Plasma Nanoparticle Generator for Scalable CNT Production in a FCCVD Process

Clayton Kacica*†, Arthur Sloan, Oliver Dewey, Glen Irvin, Matteo Pasquali

Rice University

Carbon nanotubes (CNTs) are one of the most promising candidates for next-generation materials for applications ranging from high-strength, low-weight construction materials to field emission transistors. Unfortunately, wide-scale adoption of CNTs is impeded by the high production cost of crystalline, high aspect ratio CNTs needed for high performance in applications. Floating catalyst chemical vapor deposition (FCCVD) is the most promising synthesis method for scale-up due to its continuous nature and ability to directly produce powders, fibers, films, or foams. However, the FCCVD process currently exhibits low process efficiency and poor reactant utilization leading to production costs that are prohibitively high for most applications.One major source of process inefficiency is from the catalyst nanoparticles used to grow CNTs. CNT diameter and number of walls is known to be proportional the catalyst nanoparticle diameter. To grow high-quality CNTs with few walls, catalyst nanoparticles need to be below 2 nm in diameter. Larger catalyst nanoparticles (diameters greater than 5-10 nm) will not be able to efficiently grow the desired CNTs. Catalyst utilization, defined as the proportion of catalyst material that successfully grows a CNT, is below 1% in current reactors. This leads to low productivity, low feedstock conversion, and additional post-processing steps to remove residual catalyst. Introducing the catalyst is generally done by the injection of metal precursors, such as ferrocene or iron pentacrabonyl, which decompose in-flight. This process introduces a high degree of complexity to the reaction system as the catalyst formation and CNT growth are occurring simultaneously and are poorly controlled since process parameters are optimized for CNT growth, not catalyst formation. Additionally, the metal precursors contain carbon that is released during thermal decomposition leading to a second carbon source, introducing potential competitive reaction pathways.In this work, we describe an atmospheric pressure, radio-frequency plasma catalyst nanoparticle generator used to produce a scalable, consistent, and controllable stream of catalyst nanoparticles in the sub-2 nm diameter range with mass flowrates that can enable higher CNT productivity. Designing a preformed catalyst generator decouples the catalyst formation and CNT growth, allowing for process parameters to be optimized for both separately. Additionally, this process utilizes an elemental iron source for the catalyst particles, thus removing extraneous carbon from reaction management. We present our results in optimizing this process to improve CNT productivity, catalyst utilization, and reactant conversion. *Acknowledgements:* This work was supported by the US Department of Energy award DE-AR0001015 (Advanced Research Projects Agency - Energy)

B56: Finite (6,6) Single-Walled Carbon Nanotubes with Organic Surface Defects as Candidate Single Photon Emitters

Benjamin Eller*†, Jacek Klos, YuHuang Wang, Charles Clark

**University of Maryland*

We used density functional theory (DFT) calculations to investigate the possibility of using finite (6,6) ”armchair” single-walled carbon nanotubes (SWCNT), which are metallic in the limit of infinite tube length, as hosts for organic color centers (OCC) made by sidewall functionalization of the nanotubes, as has been done recently with chiral semi-conducting SWCNTs. Our ground-state calculations show that appreciable HOMO-LUMO gaps exist in finite segments with lengths of several nanometers. This suggests a possibility of creating in finite (6,6) SWCNTs the localized exciton states responsible for enhanced photoluminescence in chiral SWCNTs via the introduction of organic defects to the nanotube wall, changing the local bonding configuration from the native sp2 to sp3. The problem then becomes a question of which defects are likely to produce optically allowed ”bright” exciton states with lower energy than the ”dark” states prevalent in the native SWCNTs. To this end, we employ TDDFT calculations to compare the nature of low-lying excited states of defect-free segments to segments with various organic defects. Preliminary results suggest identifying appropriate defect molecules for finite (6,6) SWCNTs is not a straightforward mapping of what works for the chiral semi-conducting SWCNTs. *Acknowledgements:* We would like to thank the NSF for funding (award # 1839165)

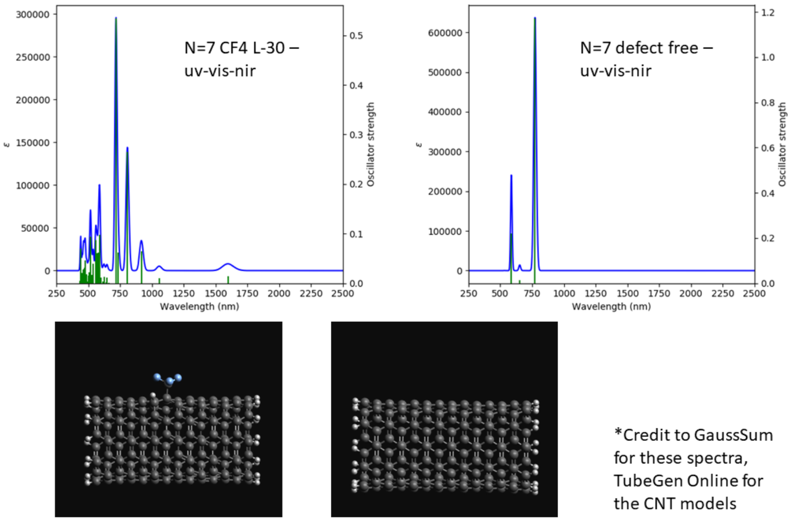

*Credit to GaussSum for these spectra, TubeGen Online for the CNT models

Fig. 1: Oscillator strengths for low-lying excited states of finite (6,6) SWCNTs with and without an organic surface defect.

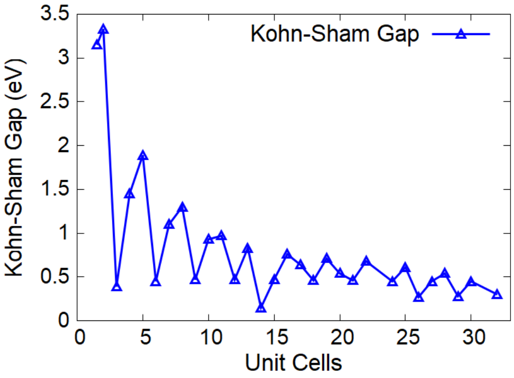

Fig. 2: Plot of the calculated Kohn-Sham HOMO-LUMO gap for defect-free finite (6,6) SWCNTs.

B57: New insights to LPE of graphene using eco-friendly solvents - replacing NMP

Barbara Maciejewska*[†], Kai Ling Ng, Ling Qin, Zhicheng Xu, Dmitry Eskin, Iakovos Tzanakis, Kyriakos Porfyrakis, Jiawei Mi, Nicole Grobert

**Department of Materials, University of Oxford, Oxford OX1 3PH, UK*

Liquid Phase Exfoliation (LPE) has been studied widely and often is aimed at the upscaling of low-cost production of high-quality graphene and other layered materials. Whilst N-Methyl-2-pyrrolidone (NMP) is popular within the nanomaterials research community and recognised as the most efficient solvent used for both, the exfoliation and dispersion of graphene, it is neither sustainable nor suitable for up-scaling for environmental reasons. To tackle this challenge we have applied shear mixing to different types of graphite in a range of 'green' solvents and have used the Hansen Solubility Parameters (HSP) of NMP as a property descriptor in order to evaluate the exfoliation efficiency and dispersion capability of environmentally friendly solvents both experimentally and theoretically. Here we propose new insights into the role of the solvent in the LPE of graphite evidenced through detailed qualitative and quantitative studies. In particular, our experimental findings show that despite the low HSP of isopropanol when compared to NMP it is as efficient as NMP, but its limited ability to form stable dispersions of graphene hinders further evaluation of the same. By modelling the shear force distribution within a typical rotor-stator system for rotor speeds of < 5K RPM, we show that generated shear forces during processing are largely unaffected by the solvent. Therefore, the exfoliation efficiency of the 'green' solvent such as IPA and NMP are comparable and both are equally suitable for the process of exfoliating graphite. Therefore, our findings very strongly suggest that the study of the precipitates should be revisited and new ways of approaching the LPE processing of graphite are required to unlock scalable and sustainable graphene production. *Acknowledgements:* We thank the Physical

Sciences Research Council (Grant No. EP/L019965/1, EP/L019884/1, EP/L019825/1 and EP/R031975/1) and the Royal Society.

B58: Fundamental Process Parameters in Wet-Spinning of Carbon Nanotube Fibers

Oliver Dewey*†, Lauren Taylor, Cedric Ginestra, Samantha Fowler, Glen Irvin, Matteo Pasquali

**Rice University*

The mechanical and electrical properties of neat carbon nanotube fiber (CNTF) produced from solutions of pristine CNTs in chlorosulfonic acid are rapidly improving. CNTF is on track to be the strongest synthetic fiber by the end of the decade, and it already surpasses high performance carbon fibers and polymeric fibers in flexibility and electrical/thermal conductivities. As properties begin to exceed those of widely adopted materials (polyaramids, polypropylene, polyethylene, etc.), process cost and environmental efficiency need to be competitive to bring the technology to market. While some research efforts have focused on the impact of the CNT material on CNTF properties, many details of the processing conditions that lead to optimal CNTF properties have not been reported. It is understood that CNT solution concentration and spin-line throughput are two primary efficiency determining variables, but the impact of these variables on the spinning window (the range of parameters over which certain grades of CNTF are able to be produced) for the wet spinning process have not yet been thoroughly studied. Here, we seek to define and understand the experimental spinnings windows to identify which process parameters govern optimal CNTF properties. We studied the impact of extrusion and take-up parameters, CNT solution concentration, and coagulation conditions on the CNTF properties to determine viable spinning windows. To gain insight and understanding to correlate rheological properties with spinning windows, we measured the viscosity and shear rate behavior of CNT solutions using capillary rheometry. Additionally, we used in-line microscopy on the spinning system to visualize the phenomena occurring at the exit of the spinneret, including die swell, coagulation rate, and filament formation and stability. Finally, we identify the most important factors for CNTF properties and spinning efficiency, and we propose a path forward for efficient production of high-quality CNTF.

B59: In situ monitoring of CNT deposition on filter in FCCVD

Hisayoshi Oshima*†, Katsunori Iwase, Yutaka Ohno

**Institute of Material and Systems for Sustainability, Nagoya University*

A CNT film thickness obtained by a filter collection in floating catalyst chemical vapor deposition (FCCVD) is usually controlled by a collection time, though FCCVD synthesis conditions including deposition rate change with time, depending on the surface condition of inner wall of the reactor tube. [1] Here, we propose a novel method for in-situ monitoring of CNT deposition on a filter, using impedance measurement. An interdigitated electrode was set on the backside of a filter for the impedance measurement. (Fig. 1) The impedance between two electrodes changes, depending on the conductance of a CNT thin film deposited on the filter. CO and ferrocene were used as carbon source and catalyst precursor, respectively. Fig. 2 shows a change in impedance with collection time. From the comparison with an equivalent circuit model, it was found that the reciprocal of the real part of the impedance was related to CNT volume (as indicated arrow #1 in Fig.2). Furthermore, a formation of percolating CNT network was clearly observed in the phase angle curve (as indicated arrow #2 in Fig. 2). This method is applicable not only for a CNT film manufacturing process easily, but also for in situ analysis of alignment of CNTs. [1] A. Moisala et al., Chem. Eng. Sci. 61, 4393 (2006). *Acknowledgements:* This study was partially supported by DENSO CORPORETION.

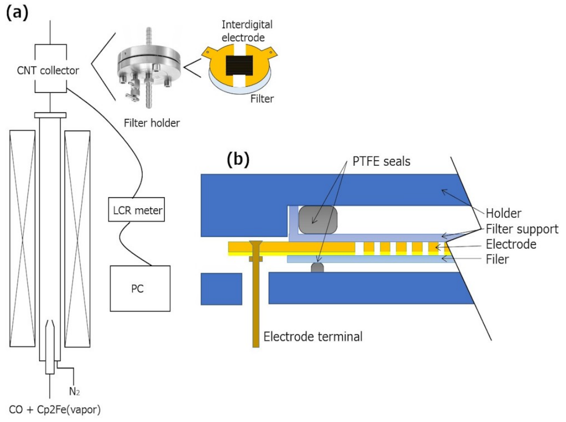

Fig. 1: Schematic diagram of impedance measurement (a) setup and (b) a part of cross section of the filter folder.

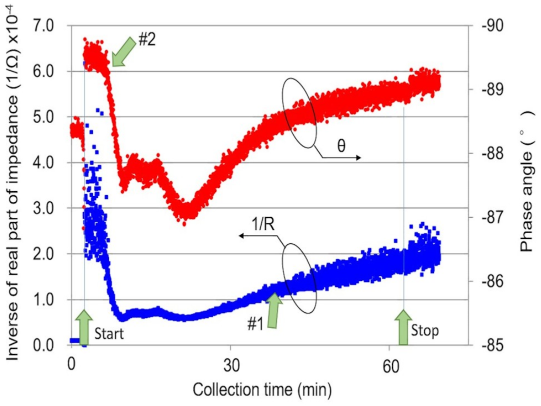

Fig. 2: A typical progress of impedance with collection time. Blue and red dots show the reciprocal of real part and phase angle of the impedance, respectively.

B60: Electroluminescence from Electrolyte-gated (6,5) SWCNT Networks at Cryogenic Temperatures

Abdurrahman Ali El Yumin*†, Nicolas Frederic Zorn, Felix Berger, Daniel Heimfarth, Jana Zaumseil
**Heidelberg University*

Single-walled carbon nanotubes (SWCNTs) are promising candidates for quantum emitters in the near infrared. To achieve electrically driven light emission, i.e., electroluminescence, ambipolar light-emitting field-transistors (LEFETs) are ideal due to the high and balanced hole and electron mobilities in SWCNTs. Here, we investigate electroluminescence and photoluminescence from electrolyte-gated monochiral (6,5) SWCNT networks at variable cryogenic temperatures down to 4.2 K. Electrolyte-gating with an ionic liquid enables extremely high charge carrier densities (~1014 cm-2) and the formation of a stable (frozen) p-n-junction by cooling samples below the melting point of the ionic liquid while in the ambipolar regime. The resulting electroluminescence spectra reveal large contributions of trion emission (charged excitons) that depend sensitively on the applied source-drain (VSD) and gate voltage (VG) combinations and thus the concentration of excess charges. The intensity ratios of trions to excitons show no temperature dependences, implying that the generated trions originate from mobile excitons. *Acknowledgements:* ERC-2018-COG, TRIFECTs: Trions and sp3 Defects in Single-Walled Carbon Nanotubes for Optoelectronics GrantNo.: 817494

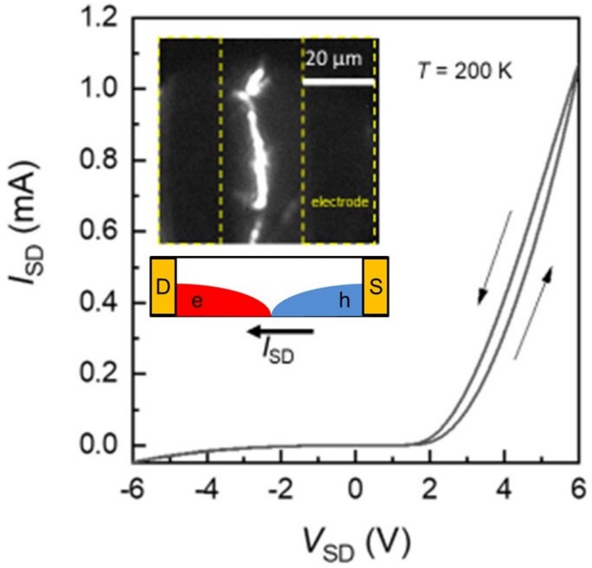

Fig. 1: Typical I-V characteristics of network of (6,5) SWCNTs with frozen p-n junction and image of static emission zone within the channel.

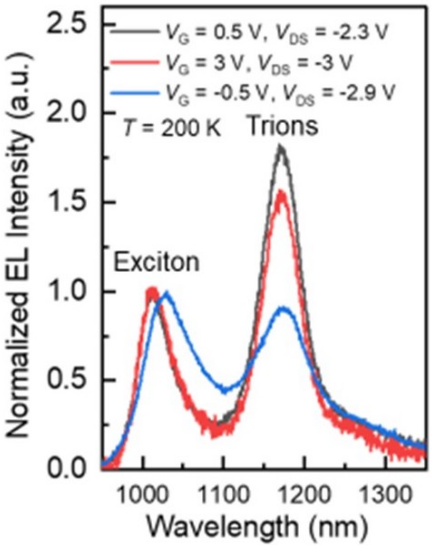

Fig. 2: Normalized EL spectra of (6,5) SWCNT network for different VSD-VG combinations.

B61: Transport in Carbon Nanotubes Network: Theory and Experiment

Davoud Adinehloo†, Weilu Gao, Ali Mojibpour, Junichiro Kono, Vasili Perebeinos*

**University at Buffalo*

We report a comprehensive experimental and theoretical study on the temperature-dependence of conductance in single-wall carbon nanotubes (SWCNTs) network. Our experimental results demonstrate up to four orders of magnitude change with temperature in electrical conductance. Some of the data can be accounted by the variable range hopping (VRH) mechanism. In particular, we report an analytical formula for the localization length as a function of the Fermi energy and SWCNT bandstructure, which explains the different families of the observed behavior. In the zero-gap armchair (6,6) SWCNT, the localization length is much longer than in other single chirality SWCNTs. To explain conductance temperature dependence in (6,6) tube, we employ a full-band model within the perturbation theory to account for the phonon-assisted tunneling conductance across the SWCNTs. The theoretical study shows that while corresponding purely electronic conductance is not-negligible, it does not depend on temperature. On the other hand, phonon-assistant tunneling accounts for the observed temperature dependence in (6,6) SWCNTs sample.

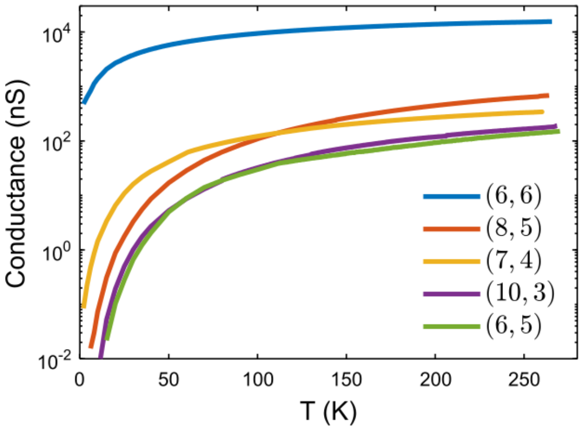

Fig. 1: Film conductivity of 5 different single-chirality single-wall carbon nanotubes.

B62: Growth of Double-Walled Carbon Nanotube Films

Guodong Jia*†, Yan Li

**College of Chemistry and Molecular Engineering, Peking University*

Double-walled carbon nanotube (DWCNT) films were prepared by floating catalyst chemical vapor deposition with methane as carbon source. The diameter distribution is 3-5 nm. By optimizing the synthesis conditions, the films can be free-standing after densification. The main factors affecting the yield and wall number are the amount of catalyst, the ratio of catalyst and the cocatalyst of H2S, and the carbon supply. Due to the excellent electrical conductivity and mechanical properties, the DWCNT films will have many potential applications in energy storage and conversion.

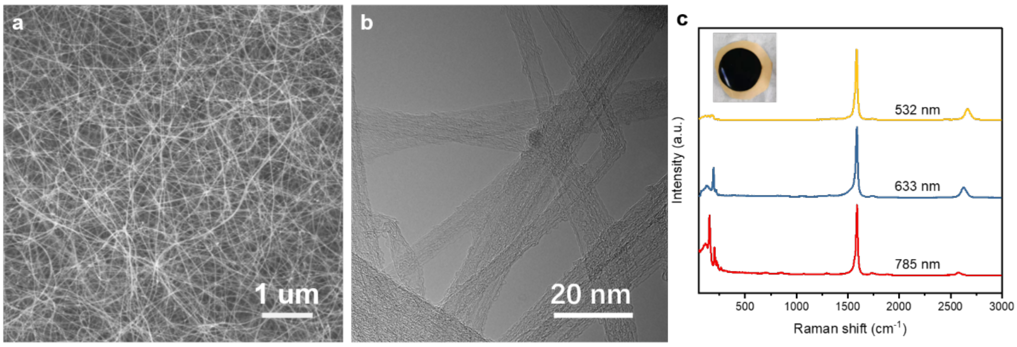

Fig. 1: SEM (a), TEM (b) and Raman spectra (c) of the DWCNT films. Inset of (c) is the photograph of DWCNT film on copper mesh.

B63: Raman fingerprint of low-pressure chemical vapor deposited bilayer graphene film: The temperature variation studies

Girija Shankar Papanai[*†], Bipin Kumar Gupta

**CSIR-NPL*

The Raman spectroscopy at different temperature in graphene plays a vital role to understand the thermal properties and become useful to set up the metrology at the nano scale [1]. The study of graphene stability with temperature variation is a prerequisite for graphene-based device fabrication. In this view, here we present the temperature-dependent Raman spectroscopy of twisted bilayer graphene film on the Si substrate having SiO2 thickness 300 nm [2]. The two samples have been grown using a home-built low-pressure chemical vapor deposition (LPCVD) setup on copper foil substrate with varying annealing times of copper for 30 and 50 min, which are named as G1 and G2. The twisting properties of synthesized film have been confirmed on the basis of different peaks such as R, G, and 2D peaks that are obtained in Raman spectra. The peak frequency of G and 2D peak has been examined in the temperature range from 80 to 450 K. The Raman images have been captured with respect to different peak parameters, namely intensity, width, and position of G and 2D peak to probe the uniformity of the synthesized film. The temperature coefficient of G peak in samples G1 and G2 has been obtained - (0.97 ± 0.34)× 10-2 cm-1/K, and - (1.08 ± 0.15)×10-2 cm-1/K, respectively [2]. In addition, the temperature coefficient of the 2D peak is obtained - (2.92 ± 0.80) ×10-2 cm-1/K, and - (3.01 ± 0.29) ×10-2 cm-1/K in samples G1 and G2 respectively. Moreover, the twist angle has been estimated in both the samples and found that it lies within the scope of a small angle regime at high temperature and belongs to a large angle regime at low temperature. The Raman spectra of sample G1 in the temperature range of 80-450 K have been shown in Fig.1 [2]. *Acknowledgements:* The authors acknowledge the Director, CSIR-NPL, for providing the research facility for the FTT mission mode project on graphene growth.

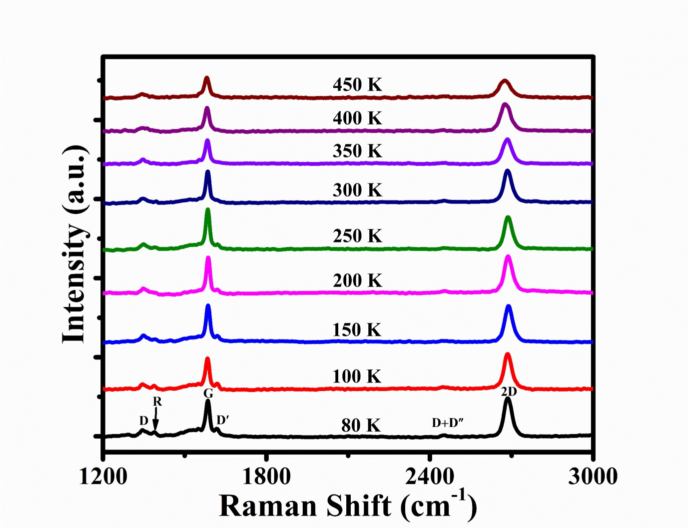

Fig. 1: Raman spectra of sample G1 over Si/SiO2 substrate having SiO2 thickness of 300 nm in the temperature range of 80-450 K.

B64: Optical Nanosensors for Real-time Feedback on Insulin Secretion by Beta-Cells

Roni Ehrlich[*†], Adi Hendler-Neumark, Verena Wulf, Dean Amir, Gili Bisker

**Tel Aviv University*

Quantification of insulin is essential for diabetes research in general, and for the study of pancreatic β-cell function in particular. Herein, fluorescent single-walled carbon nanotubes (SWCNT) are used for the recognition and real-time quantification of insulin. Two approaches for rendering the SWCNT sensors for insulin are compared, using surface functionalization with either a natural insulin aptamer with known affinity to insulin, or a synthetic PEGylated-lipid (C16-PEG(2000Da)-Ceramide), both of which show a modulation of the emitted fluorescence in response to insulin. Although the PEGylated-lipid has no prior affinity to insulin, the response of C16-PEG(2000Da)-Ceramide-SWCNTs to insulin is more stable and reproducible compared to the insulin aptamer-SWCNTs. The C16-PEG(2000Da)-Ceramide-SWCNTs optical response is excitation-wavelength dependent, where resonant excitation leads to a larger fluorescence decrease in response to insulin. The SWCNT sensors successfully detect insulin secreted by β-cells within the complex environment of the conditioned media. The insulin is quantified by comparing the SWCNTs fluorescence response to a standard calibration curve, and the results are found to be in agreement with an enzyme-linked immunosorbent assay (ELISA). This novel analytical tool for real time quantification of insulin secreted by β-cells provides new opportunities for rapid assessment of β-cell function, with the ability to push forward many aspects of diabetes research. *Acknowledgements:* Israel Science Foundation, The Ministry of Science, Technology, and Space, Israel, Zuckerman STEM Leadership Program

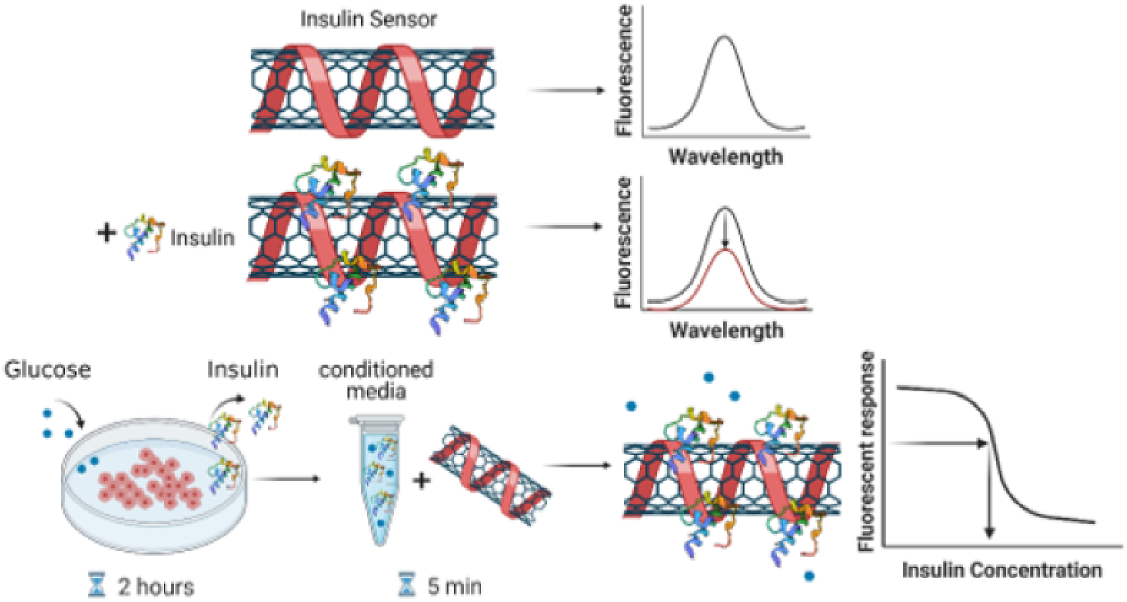

Fig. 1: Illustration of fluorescent single-walled carbon nanotubes (SWCNT) as insulin nanosensors. The concentration of insulin secreted by beta-cells is calculated based on the SWCNT fluorescence response.

B65: Click-functionalization of Single-Walled Carbon Nanotubes

Gririraj Manoharan*†, Jannis Thien, Mercedes Runge, Laura Meingast, Suresh Maniyarasu, Janina Maultzsch, Martin Steinhart, Joachim Wollschläger, Carola Meyer

**University of Osnabrueck*

Single-walled carbon nanotubes (SWNTs) are extremely promising for applications in molecular electronics, materials science and bio applications because of their unique structural, chemical and physical properties. Grafting molecules to a CNT allows for the promotion of specific functionality for targeted applications. Click chemistry defines highly efficient, versatile, and clean reactions with simple procedures [1]. One remaining challenge is to integrate this functionalization technique with electronic devices, i.e. to carry it out on SWNTs after device fabrication.Here, we present the covalent functionalization of SWNTs yielding a platform for Strain Promoted Alkyne-Azide Cycloaddition (SPAAC). SPAAC is a copper-free click chemistry approach that has a broad range of applications including bio-functionalization since it is non-toxic [2]. Gold nanoparticles functionalized with Dibenzocyclooctyne (DBCO) are used to demonstrate the feasibility of our approach. The DBCO is grafted to the Azide group at the end of a Silane, which is covalently attached to a SWNT (Fig. 1). We present a chemical characterization of each functionalization step using IR Spectroscopy, X-Ray Photoelectron Spectroscopy (XPS), and Raman spectroscopy. The results are correlated with structural information gained from Transmission Electron Microscopy (TEM). We achieve clean and densely functionalized SWNTs as shown in the TEM image of Fig. 2. Our platform of functionalized SWNTs is capable of clicking versatile molecules such as metal nanoparticles and fluorescent dyes with high efficiency. We demonstrate that this chemical route can also be used for click-chemistry on SWNTs done on the substrate. This work lays thus the foundation for tailoring SWNTs not only with a wide range of molecules and to study their functional characteristics, but also to carry out functionalization directly on the substrate after device fabrication.References[1] S. Campideilli et al., Current Organic Chemistry, 15, 1151-1159 (2011). [2] J.C. Jewett et al., Chemical Society Reviews, 39, 1272-1279 (2010). *Acknowledgements:* We thank Mrs. Petra Bösel and Mr. Henning Eickmeier for the assistance during the experiments and TEM measurements respectively.

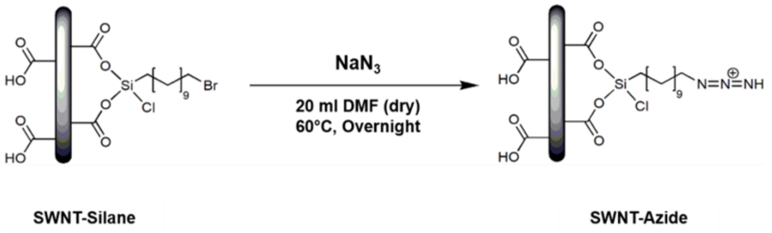

Fig. 1: Schematic representation of Azide functionalization with Silanized SWNTs.

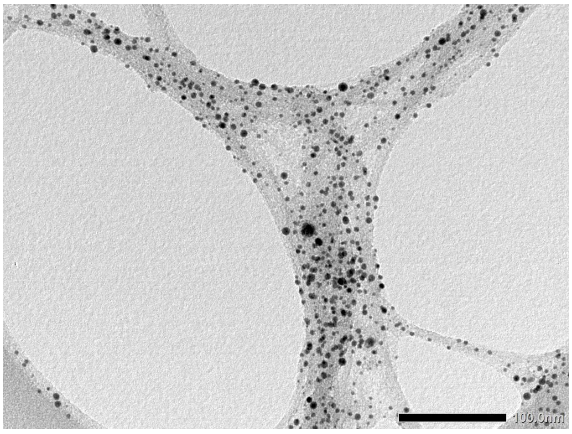

Fig. 2: TEM image of gold nanoparticle-DBCO functionalized SWNTs after the click reaction.

B66: High Resolution Maskless Photolithography: Fabrication of Single Carbon Nanotube Field Effect Transistor

Mykola Fomin*†, Michael Phillippi, Martin Steinhart, Carola Meyer

**University Osnabrück, Department of Physics*

It has been already more than two decades since the first carbon nanotube-based field-effect transistor (CNTFET) has been presented [1]. Nowadays CNTFETs are a promising candidate for electronics and bio-sensing applications due to their outstanding on/off current ratio, high selectivity, reactivity, and many other marvelous properties. Nevertheless, it is still a pressing issue that for the single nanotube devices fabrication e-beam lithography has no credible alternative yet. This means that despite rapid progress and numerous improvements such structures are mostly being fabricated in academic or research laboratories due to the low resource efficiency. On the other hand, direct laser writers (DLW) are more cost-efficient machines and have a perspective to gain interest in single nanotube studies. The PicoMaster 100 system used in this work (4PICO Litho, Netherlands) has a maximum resolution of 300 nm employing the 405 nm UV-laser line.A CNTFET fabricated with this system from drop casted nanotubes is illustrated in Fig. 1. The CNT was located using an AFM marker grid-patterned by DLW on the first metallization procedure, while feedline contacts were added on the next step. This is possible due to the complex marker alignment system that enables to overlay of several fabrication steps. Here, we present and discuss the resolution, repeatability, and optimization of the process we developed. In addition, we show the first steps toward catalyst patterning. It is not an option to copy the common e-beam lithography approach to pattern holes for the catalyst particles, because photoresists quickly dissolve in the organic solvents used to disperse catalyst particles (Ethanol, Isopropanol, Methanol, etc.). Instead, we employ spongy mesoporous silica stamps for microcontact stamping [2]. We explore the perspectives of this method in the nanofabrication of CNT devices. References[1] S. J. Tans, A. R. M. Verschueren, and C. Dekker, "Room-temperature transistor based on a single carbon nanotube," Nature, 1998. [2] M. Runge et al., "Capillary Stamping of Functional Materials: Parallel Additive Substrate Patterning without Ink Depletion," Adv. Mater. Interfaces, vol. 8, no. 5, p. 2001911, 2021.

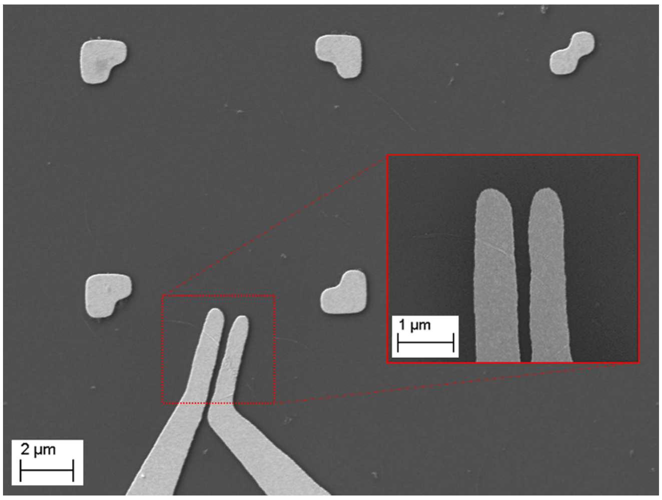

Fig. 1: SEM image of fabricated CNT FET with AFM markers. Inset: zoomed-in view on the device.

B67: First-principles study on effect of doping on electronic properties of pentagraphene carbon nanotubes

Khurshed Shah*†, Muhammad Shunaid Parvaiz, Ghulam Nabi Dar

*Department of Nanotechnology, University of Kashmir/ Department of Physics, S. P. College Srinagar

In this report we investigate the effect of doping on electronic properties of a (4, 4) pentagraphene carbon nanotube (PGCNT) by using substitutional doping in the configuration. We choose atoms of elements Boron (B) and Nitrogen (N) because of their similar atomic radii to that of carbon. The model is simulated using Atomistic Tool Kit software (ATK) and its graphical interface Virtual Nanolab (VNL) in device mode. The calculations were carried out by using Density Functional Theory (DFT) in combination with Non-Equilibrium Greens Function (NEGF) formalism and the study of current-voltage characteristics, conductance and transmission spectrum of the proposed models were done under low bias conditions. The results show that BN doping brings significant changes in the electronic properties of the device. It is found that electronic bandgap change occurs depending on the concentration of BN dopants. Boron doped model shows better performance than nitrogen doped model. Hence the study is very beneficial for designing various futuristic PGCNT devices for commercial applications including amplifiers and oscillators.

B68: Complex industrial waste solutions as an alternative source of metal ions for copper-nickel nanocomposites

Tomasz Wasiak*†, Pyry-Mikko Hannula, Mari Lundström, Dawid Janas

*Silesian University of Technology

Industrial process and waste solutions are a growing issue. High toxicity for the environment enlarges the need for advanced treatment of wastes and by-products. Particularly, appropriate handling of acidic wastes is mandatory. The development of modern methods for utilizing these complex mixtures should be a priority. However, selective removal of desired elements is often challenging and expensive [1]. Mixtures enriched with heavy metals such as nickel and copper are especially interesting due to the global demand for resources in the electronic field. In this work, we present a convenient solution for transforming industrial process wastes into nanomaterials of high added value [2]. Based on aqueous chemical reduction involved during copper nanowires synthesis [3] we developed a method for obtaining bimetallic anisotropic nanostructures from a complex mixture containing 14 different metallic elements. Appropriate dilution followed by in-depth optimization allowed obtaining copper-nickel composite nanowires. Modulation of different parameters allowed convenient tuning of both nanostructure morphology and properties. Furthermore, applying an external magnetic field improved anisotropic morphology even more due to the nickel self-assembly mechanism during nanowires' growth. EDX measurements revealed a homogeneous distribution of both elements and confirmed high purity of the product due to the lack of other element signals in the spectrum. Such bimetallic nanomaterials can be tailored to specific applications, mainly for electronic nanodevices due to their unique electrical and mechanical properties. Multimetallic materials may possess wider tuning possibilities than monometallic counterparts. Additionally, they can act as a valuable component in composites based on carbon nanomaterials. Based on synergistic effects commonly observed between nanomaterials, combined materials may exhibit even more beneficial properties. Virtually endless configurations of metals and their concentration can be exploited to discover state-of-the-art materials. A new source of building blocks for nanomaterial synthesis and promising results encourages further study of this subject. References:[1] F. Fu, Q. Wang, Removal of heavy metal ions from wastewaters: A review, Journal of Environmental Management, 3, 2011, 407-418[2] T. Wasiak, P-M. Hannula, M. Lundström, D. Janas, Transformation of industrial wastewater into copper-nickel nanowire composite: straightforward recycling of heavy metals to obtain products of high added value, Scientific Reports, 10, 2020, 1-10[3] Y. Chang, M. L. Lye, H. Ch. Zeng, Large-Scale Synthesis of High-Quality Ultralong Copper Nanowires, Langmuir, 9, 2005, 3746-3748 *Acknowledgements:* Authors thanks NCBR, Poland (LIDER/0001/L-8/16/NCBR/2017), NAWA (PPI/APM/2018/1/00004), Academy of Finland ("No WASTE" Grant 297962)

B69: Creation of Organic Color Centers in Air-Suspended Carbon Nanotubes Using Vapor-Phase Reaction

Daichi Kozawa*†, Xiaojian Wu, Akihiro Ishii, Jacob Fortner, Keigo Otsuka, Rong Xiang, Taiki Inoue, Shigeo Maruyama, YuHuang Wang, Yuichiro Kato

**RIKEN*

Organic color centers in single-walled carbon nanotubes have demonstrated exceptional ability to generate single photons at room temperature in the telecom range. Combining the color centers with pristine air-suspended tubes would be desirable for improved performance, but all current synthetic methods occur in solution which makes them incompatible. Here we demonstrate formation of color centers in air-suspended nanotubes using vapor-phase reaction [1]. Functionalization is directly verified on the same nanotubes by photoluminescence spectroscopy, with unambiguous statistics from more than a few thousand individual nanotubes. The color centers show a strong diameter-dependent emission intensity, which can be explained with a theoretical model for chemical reactivity taking into account strain along the tube curvature. We are also able to estimate the defect density by comparing the experiments with simulations based on a one-dimensional diffusion equation, whereas the analysis of diameter dependent peak energies gives insight to the nature of the dopant states. Time-resolved measurements show a longer lifetime for color center emission compared to E11 exciton states. Our results highlight the influence of the tube structure on vapor-phase reactivity and emission properties, providing guidelines for development of high-performance near-infrared quantum light sources.This work is supported in part by MIC (SCOPE 191503001), JSPS (JP18H05329, JP20H00220, JP20H02558, JP20K15112, JP20K15137), MEXT (Nanotechnology Platform JPMXP09F19UT0077), NSF (RAISE-TAQS PHY-1839165), and JST (CREST JPMJCR20B5). D.K. acknowledges support from RIKEN Special Postdoctoral Researcher Program. K.O. is supported by JSPS Research Fellowship. We thank the Advanced Manufacturing Support Team at RIKEN for technical assistance. [1] D. Kozawa, X. Wu, A. Ishii, J. Fortner, K. Otsuka, R. Xiang, T. Inoue, S. Maruyama, Y. Wang, and Y. K. Kato, arXiv:2103.10665 [Cond-Mat.Mes-Hall] (2021).

B70: Experimental and Theoretical Studies of Hydrogen Generation by Binary Metal (Oxide)-Graphene Oxide Composite Materials

Omar Faye*†

**University of Saskatchewan*

Theoretical and experimental studies focused on hydrogen generation through the hydrolysis of graphene oxide (GO) functionalized with magnesium (GOMg), titanium (GOTi), and niobium (GONb) were performed. Thermogravimetric (TGA) results reveal variable thermal decomposition profiles for the composites, in agreement with the decomposition of the labile oxygenated groups of GO. X-ray photoelectron spectroscopy (XPS)results show variable oxygen content (%) for the composites and the formation of MgO, TiO2, and NbO2 layers on the GO surface. The hydrogen generation studies suggest that the formation of aMg(OH)2 layer on the GO surface is a critical limiting factor for the hydrolysis of GOMg, whereasTiO2 and NbO2 catalyze the hydrolysis of GONb and GOTi.The hydrogen generation results reveal that GONb produced the highest H2 yield of 2L in 2h compared to1.5L for GOTi and 1.3L for GOMg. The results support the claim that the hydrolysis of GO functionalized with niobium and titanium are promising candidates for on-board H2generation applications. *Acknowledgements:* We acknowledge access to high-performance supercomputers, Compute Canada, and Plato at the University of Saskatchewan. This work was support

B71: Preparation of Three-dimensional Aramid Nanofiber Nanostructures using Covalent Bonding with Citric Acid

Guk-Hwan Lee†, Wonoh Lee*

**Chonanm National University*

Inheriting excellent properties of aramid fibers, aramid nanofibers (ANFs) also promise high strength, excellent chemical and heat resistance as nano-scaled forms; therefore, they have gathered great interests in various structural and functional applications. The ANFs are generally synthesized by the decomposition of macro-sized aramid fibers through the deprotonation. In addition, three-dimensional nanostructures (3D NSs) have been received with great attention due to their superior stress-transfer capability and large surface area. Even though there have been several attempts to manufacture the 3D NS of ANFs, most approaches have used water in order to produce the gelation of ANFs. However, the use of water occurs re-protonation to amide bonds resulting in the agglomeration of ANFs. Consequently, the water-based method limits to manufacture the individually separated ANF NS. In this study, we tried to establish the structurally strong 3D ANF NS by constructing covalent bonds between individual ANFs instead of using water. Since citric acid has abundant carboxylic acids, imide bonds can be readily constructed with amide groups in ANFs with preventing the re-agglomeration. Figure 1 demonstrates a successfully manufactured 3D ANF NS as an aerogel form and a highly porous micro-morphology. The covalent bond in 3D ANF NS can be also confirmed by observing a new peak at 1724 cm−1 in Fourier transform-infrared (FT-IR) spectra, representing a symmetric amide bond as shown in Figure 2. Furthermore, the 3D ANF NS by covalent bonding exhibited 10 times higher compressive strength than that of the water-based one. Therefore, it can be concluded that the covalently constructed 3D ANF NS becomes stronger than the gelated ANF NS owing to chemical crosslinking. *Acknowledgements:* This work was supported by National Research Foundation (NRF) of Korea grant (2021R1A2C2005751).

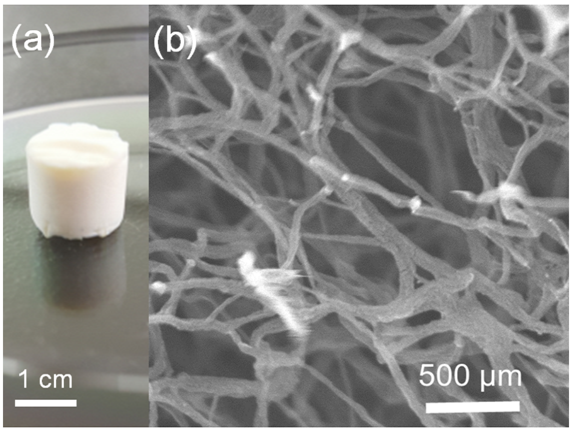

Fig. 1: (a) A photograph and (b) a scanning electron microscopic image of the 3D ANF NS by covalent bonding.

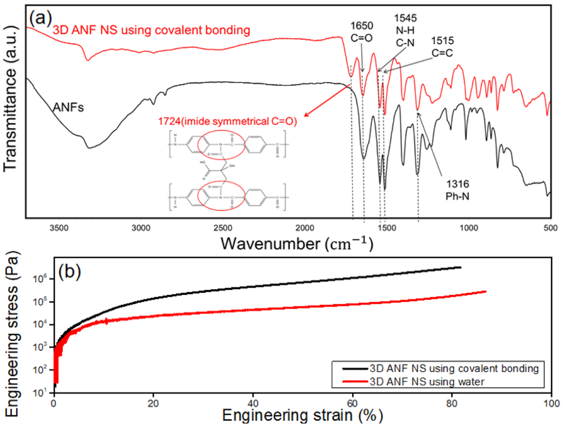

Fig. 2: (a) FT-IR spectra of a 3D ANF NS and ANFs, and (b) compressive stress-strain curves of the 3D ANF NSs by covalent bonding and water treatment.

B72: Adsorption of block-copolymers on the surface of multi-walled carbon nanotubes in organic solvent

Yachin Cohen*†, Irena Levin

**Technion-Israel Institute of Technology*

Carbon nanotubes (CNTs), find attractive applications due to their unique properties. In some cases, such as polymer nanocomposites, the processing method requires their dispersion in an organic solvent. The dispersion quality strongly impacts the properties of the final nanocomposite. This research characterizes the adsorption of block copolymers of the styrene-block-4-vinylpyridine family (S4VP) onto multi-walled CNTs (MWCNT) in N,N-dimethyl-formamide (DMF), using cryogenic transmission electron microscopy (cryo-TEM) and small angle neutron scattering (SANS) measurements with contrast variation. The results show that the block copolymer adsorbs onto the MWCNT surface as a continuous coverage of low polymer concentration. PS blocks adsorb more tightly (forming a 20 Å layer containing of about 6 wt.% PS), whereas P4VP blocks emanate into the solvent, forming a thicker shell (totaling 110 Å in radius) but dilute (< 1%) layer, indicating chain extension. Increasing the PS molecular weight increases the thickness of the adsorbed layer, but decreases the overall polymer concentration within it. These results are relevant for the ability of dispersed CNTs to form a strong interface with matrix polymers in composites, and to the ability to form CNT-CNT contacts that are important for electrical or thermal conductivity. Finally, some comparison will be made with adsorption of PS4VP from DMF onto the surface of dispersed single-walled CNTs and graphene nanoplatelets, indicating the effect of surface curvature. *Acknowledgements:* The Israel Science Foundation

B73: CNT/copper composite yarn made from copper nanoparticles decorated spin capable CNT forest

Kosuke Tanaka†, Takayuki Nakano, Yoku Inoue*

**Shizuoka University*

CNT yarns are expected to replace the widely used metallic wires as the lightweight wires of the future. CNT yarns have a high current capacity, but their conductivity is much lower than that of metallic wires. Therefore, a composite of CNTs and copper, which has high conductivity, is an effective way to solve this problem. To develop lightweight wires with high conductivity and high current capacity, homogeneous composites of CNTs and copper are required. In this study, we fabricated CNT/Cu composite yarns with homogeneously electroplating copper inside the CNT yarns. The dry-spin capable CNT forests were synthesized by chloride-mediated CVD using FeCl2 as a catalyst. Copper nanoparticles were loaded on the entire CNT forest by thermal decomposition of copper (II) acetylacetonate (Cu(acac)2) on the CNT surfaces by thermal CVD method. CNT web was drawn out from the CNT forest coated with copper nanoparticles, and CNT twisted yarns were fabricated. The CNT twisted yarns were immersed in copper sulfate solution for copper plating to make CNT/Cu composite yarns. The CNT/Cu composite yarn was homogeneous, which was attributed to the homogeneous deposition of copper nanoparticles into the interior of the CNT yarn. Detailed electrical properties will be presented.

B74: Kinetic Study of Tetracycline Asorption Using Magnetic Carbon Nanotubes With Different Iron Proportions

Theodoro Da Rosa Salles*†, Franciele Da Silva Bruckmann, Cristiano Bohn Rhoden

**UFN - Universidade Franciscana*

The use of medicines grows exponentially worldwide. Many of them are not completely metabolized by the human organism and, consequently, are excreted in the active form. Along with this, the effluent treatment techniques currently employed, often prove to be inefficient in removing microcontaminants, enabling them to pass directly through water treatment and get re-ingested. Tetracycline is one of the most widely used antibiotics in the world. Its low biodegradability and high aqueous solubility hinder its removal by conventional methods, making it necessary the development of more efficient methods. The adsorption using carbon nanomaterials, such as carbon nanotubes (CNT), and the easy incorporation of magnetic nanoparticles in their structures, aiming to eliminate centrifugation and filtration steps, relays as great alternative to remove aquatic micropollutants. In this context, the present work aimed to carry out a kinetic study of remotion of tetracycline using carbon nanotubes (CNT.Fe3O4) in adsorption protocols with different proportions of CNT/magnetite as an adsorbent. The adsorption experiments were carried out in batch mode, with room temperature and initial tetracycline concentration equal to 50 mg L-1 and 50 mg of the CNT adsorbents, and CNT with different amounts of magnetite incorporated in the mass:mass ratio (CNT.Fe3O4 1:1, CNT. Fe3O4 1: 5 and CNT. Fe3O4 1:10) and volume of 100 mL of the solution. During the tests, aliquots were collected at predetermined times (0, 5, 15, 30, 45, 60, 75, 90, 120, 150 and 180 minutes) and sequentially quantified via spectroscopy in the ultraviolet region (λ = 380 nm). To evaluate the adsorption kinetics of the experiments, the pseudo-first order and pseudo-second order models were used. From the obtained kinetic models, it was possible to observe that the pseudo-second order model presented a better adjustment of the experimental data, considering higher correlation coefficients. Based on this, it is possible to observe that the CNT is characterized by a more accurate kinetics in relation to the magnetic samples. However, it is observed that magnetic compounds have greater adsorption capacity when compared to non-magnetic CNTs. Along with this, through the PSO model, it is possible to ascertain that the adsorption process of tetracycline occurs by predominantly chemical mechanisms. Based on the kinetic study it can be assumed that the PSO model was better adjusted to the experimental data obtained. It is also observed that the amount of iron incorporated in CNT structure directly influences the kinetic parameters.

B75: Biofunctionalization of conductive carbon nano-materials for reversible site-specific protein immobilization

Lara Jorde[*†], Zehao Li, Adrian Pöppelwerth, Jacob Piehler, Changjiang You, Carola Meyer

*Universität Osnabrück

Carbon nanotubes (CNTs) and graphene have emerged as highly sensitive biosensors due to their extraordinary electrical transport properties. By interfacing proteins with CNTs in controlled orientation while maintaining their structural integrity, these one-dimensional sp2-carbon nanomaterial sensors provide versatile opportunities for sensitive detection of protein interactions and conformational dynamics. In this work, we devised a novel surface architecture for reversible protein immobilization on CNTs or graphene via a short peptide tag for multiple protein analysis. Pyrene-poly(ethylene glycol) was conjugated with tris-nitrilotriacetic acid (Py-PEG-tris-NTA) for site-specific immobilization of oligohistidine(His)-tagged proteins (Fig. 1). Self-assembly of Py-PEG-tris-NTA on CNTs and graphene were demonstrated which allows specific capturing of His-tagged green fluorescent protein after loading the NTA chelators with Ni(II) ions. The protein binding capacity of tris-NTA-functionalized CNTs and graphene could be restored by an imidazole wash, resulting to repeated immobilization cycles. Reflectance interference spectroscopy and fluorescence lifetime analysis quantified the characteristic biofunctionalization features on CNT and graphene via π-π-stacking and van der Waals interaction. These results confirmed specific and reversible binding of His-tagged proteins on graphene- or CNT-coated silica substrates as well as close interfacing to the carbon nanomaterial surface1. The obtained surface architectures thus pave the way for electronic transport measurements by single CNT-field effect transistor (FET) for biomolecular interaction analysis with reversibly immobilized proteins.1 L. Jorde, Z. Li, A. Pöppelwerth, J. Piehler, C. You and C. Meyer, "Biofunctionalization of carbon nanotubes for reversible site-specific protein immobilization", Journal of Applied Physics 129, (2021) *Acknowledgements:* Fluorescence microscopy was performed with technical support from the DFG microscopy facility iBiOs.

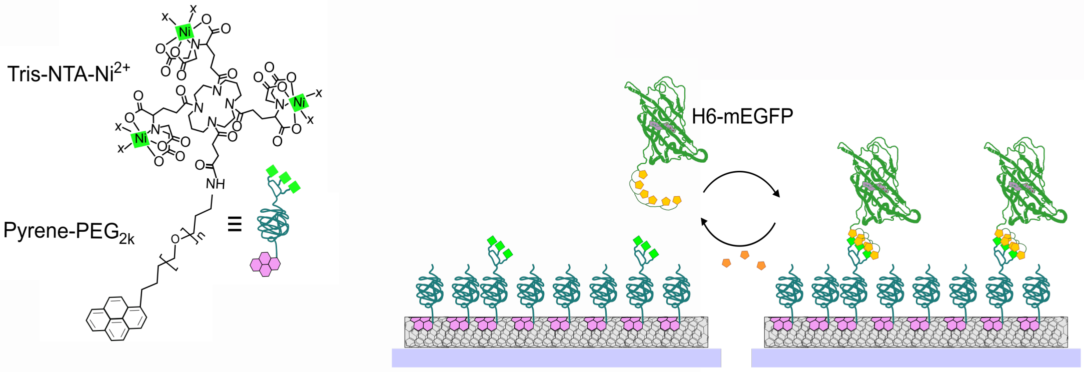

Fig. 1: Pyrene-PEG-tris-NTA modification of CNTs or graphene for specific and biocompatible protein immobilization of histidine tagged proteins using NTA-Ni2+-complexes. Competing ligand imidazole can reverse protein immobilization.

B76: Controlling density of the self assembled carbon nanotube wool in floating catalyst chemical vapor deposition

Rajath Alexander[*†], Amit Amit Kaushal, P. T. Rao, Kinshuk Dasgupta

*Bhabha Atomic Research Centre

Carbon nanotubes (CNTs) have been made into the self assembled form of wool by floating catalyst chemical vapor deposition (FCCVD). The density of the CNT-wool could be controlled by adjustment of catalyst to promoter concentration during FCCVD. The specific surface areas of CNT wool were very high and also were found to be varying with processing conditions. Scanning electron microscopy (SEM) revealed highly porous structure with very long carbon nanotubes with size in the range of 100 µm. Phase analysis by Raman spectroscopy indicated that the carbon nanotubes formed were multiwall in nature. Cyclic voltametry studies revealed the possibility of using these structures as electric double layer capacitors having high value of capacitance. The capacitance can be tuned based on processing conditions. *Acknowledgements:* Authors would like to thank Mr. S.A. Thakur for assisting in CVD furnace operation.

B77: Appropriate properties of carbon nanotube for 3D current collector of lithium-ion battery

Kentaro Kaneko[*†], Suguru Noda

[*] *Waseda University*

High-energy-density secondary battery is necessary to satisfy the increasing demand for electric energy storage. Conventional positive and negative electrodes of lithium-ion battery have heavy foils of metals as current collectors. To achieve high energy density by eliminating non-capacitive components, we developed electrodes based on 1 mass% 3D current collector of submillimeter-long few-wall carbon nanotube (CNT) that held 99 mass% active materials [1]. The CNT played the roles of the binder, conductive filler, and current collector. The metal-foil free CNT-based electrodes were demonstrated, however, only one type of CNT was used. We here report the effects of the structural properties of CNT on the battery performance.The graphite-CNT negative electrode and the lithium cobalt oxide (LCO)-CNT positive electrodes with an areal capacity of 1 mA h cm−2 were prepared by adding the powders of the active materials and CNT at 97:3 mass ratio to 2-propeanol, co-dispersion by ultrasonication, and filtration. 9 types of CNT prepared by fluidized bed CVD method [2] were used. All the CNTs (SSA of 187–960 m2 g−1, lengths of ~30-200 µm yielded self-supporting films without using polymeric binder except one type with small SSA (of 498 m2 g−1) and short length (53.4 µm). 2032-coin cells were assembled using polypropylene separator and electrolyte (1M LiPF6, EC:DEC=1:1, v:v).The first charge/discharge was performed with a low current density of 0.1 mA cm−2 (Figure (a)).At the first charge, solid electrolyte interphase (SEI) formed on negative electrode, causing irreversible capacity (difference between charge and discharge capacities). The irreversible capacity increased with increasing SSA, causing depletion of active lithium by side reaction and decreasing reversible capacity. Then the rate and cycle performances were evaluated with increasing current density from 0.1 to 10 mA cm−2 with increasing cycles (Figure (b)). The capacity was higher with CNTs of smaller SSA (187, 240 m2 g−1) at current densities £ 2 mA cm−2 while the capacity was higher with CNTs of moderate SSA (287, 501 m2 g−1) at a high current density of 10 mA cm−2. CNTs of lower SSA is beneficial to suppress the side reaction on negative electrodes while those of moderate SSA is beneficial to achieve high rate performance. [1] K. Hasegawa, S. Noda, J. Power Sources 321 (2016) 155. [2] M. Li, M. Risa, T. Osawa, H. Sugime, and S. Noda, Carbon 167 (2020) 256. *Acknowledgements:* This work is financially supported by Grand-in-Aid for Scientific Research (S) (JP16H06368) from JSPS and by Zeon Corporation.

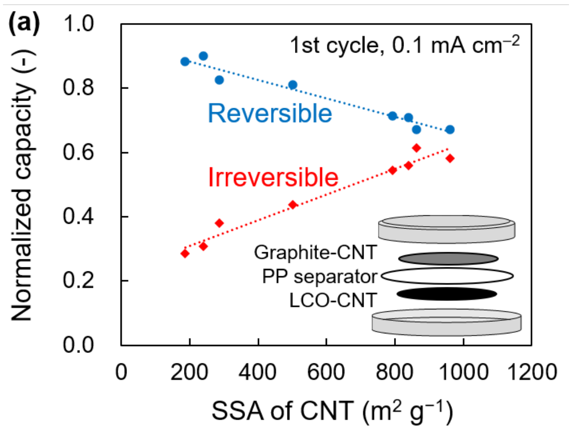

Fig. 1: (a) Reversible and irreversible capacities of the LCO-CNT||Graphite-CNT full cell. Capacity is normalized to the theoretical capacity (1 mA h cm−2).

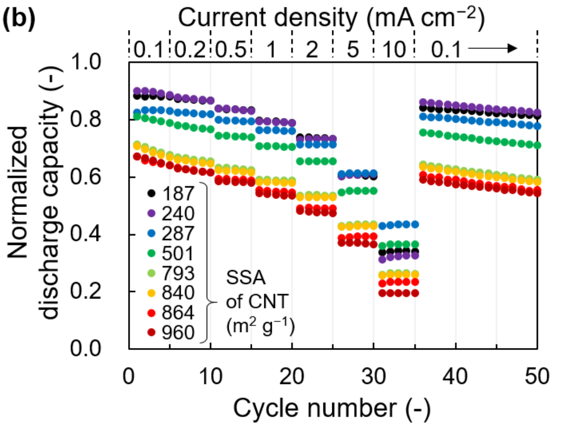

Fig. 2: (b) Rate and cycle performances of the LCO-CNT||Graphite-CNT full cell taken at current density increasing with cycles. Capacity is normalized to the theoretical capacity (1 mA h cm−2).

B78: Fabrication and hierarchical structure control of carbon nanotube electron field emitter for X-ray tube

Kotaro Yasui*†, Sae Kitagawa, Hisashi Sugime, Hayato Ochi, Yuichi Nishikiori, Suguru Noda

**Waseda University*

Compared with thermal emitters, electron field emitters are effective for miniaturization and low energy consumption of X-ray tube which is expected for various use such as medical and industrial uses. Carbon nanotube (CNT) which has high electric conductivity and high aspect ratio is one of the most promising material for electron field emitters and has been researched intensively [1]. In this research, field electron emitters were fabricated by controlling morphology of vertically aligned (VA) CNT variously by a simple process for X-ray tubes. As shown in Fig. 1, the morphology of the VACNT was controlled, and the emitter performance was evaluated by applying electrical field with 2.5 kV/mm under 10-4 – 10-5 Pa over 1001 cycles. As shown in the cycle performance over 1001 cycles (Fig. 2a) and the current density at 1001th cycle (Fig. 2b), the micrometer-order morphology control of VACNT was found to have little effect on performance improvement (sample B). On the other hand, sub-millimeter-order morphology control such as sample C and D were effective for performance improvement.References[1] Y. Cheng & O. Zhou, C.R. Physique, 4, 1021 (2003). *Acknowledgements:* This work is supported by Meidensha Corporation.

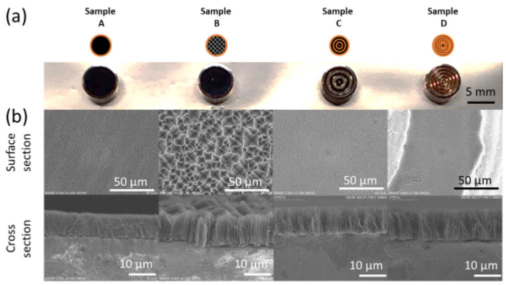

Fig. 1: Fig. 1. (a) Fabricated emitters (Sample A, B, C, and D) (b) SEM Images of surface VACNTs morphology on emitters.

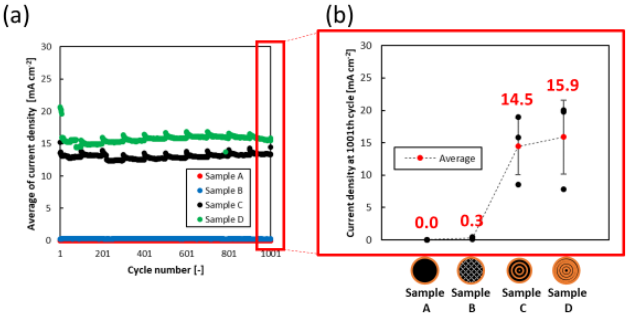

Fig. 2: Fig. 2. (a) Cycle performance of fabricated emitters (Sample A, B, C, and D) (b) Current density at 1001th cycle of fabricated emitters (Sample A, B, C, and D)

B79: Time-domain thermoreflectance study on the figure of merit for aligned semiconducting single walled carbon nanotube film with tuned Fermi-level

Kan Ueji*†, Yota Ichinose, Yuya Matsuoka, Yohei Yomogida, Takashi Yagi, Junichiro Kono, Kazuhiro Yanagi

**Tokyo Metropolitan University*

Thermoelectric devices made of flexible thin films have attracted significant attention because of the demand for batteries of ubiquitous sensors in the Internet-of-things society. The thermoelectric performance is determined by the dimensionless figure of merit (ZT) ZT = (S2σ)/κ, where S, σ, and κ denote the Seebeck coefficient, electrical conductivity, and thermal conductivity. In many studies, the relationships between S and σ has been well discussed, however, the relationships between κ and σ in flexible thin films with various electronic structures and morphologies have not been well understood because of the lack of an effective measurement technique to evaluate κ and σ simultaneously. In our group, a time-domain thermoreflectance (TDTR) method using gold as thermal transducer was developed in order to evaluate the κ of nanoscale materials in situ electrolyte gating. [1] In this study, we investigate the ZT values of semiconducting single-wall carbon nanotube (SWCNT) thin films with different doping levels using the electrolyte gating TDTR method.The SWCNT is a promising candidate for enhancing ZT owing to its low dimensionality. In this study, we used an aligned SWCNT thin film to discuss the charge carrier and heat transports along the transverse direction between a CNT–CNT junction. The macroscopically aligned semiconducting SWCNT films were prepared by filtration techniques [2], and electrolyte-gating devices were fabricated for TDTR and transport measurements.When the Fermi level of a semiconducting SWCNT thin film is modulated by electrolyte gating, we observed two peaks in the power factor as a function of σ, reflecting 1st and 2nd van Hove singularities (vHs). The maximal power factor is approximately 56 μW/mK2 when the Fermi level is located at the first vHs. However, κ is almost constant (approximately 0.15 W/mK), even when σ changes by approximately four orders of magnitude, indicating that a phonon is dominant through heat transport. Regarding the ZT value, the ZT of the aligned SWCNT thin film is assumed to be approximately 0.1 for charge and heat transport across the transverse direction to the tube axis, which is relatively high for flexible materials. The details of this study will be discussed in the presentation.References: [1] Ueji et al, Jpn. J. Appl. Phys. 58, 128006 (2019), id., Appl. Phys. Lett. 117, 133104 (2020) [2] He et al., Nat. Nanotech. 11, 633 (2016) *Acknowledgements:* JST-CREST

B80: Effect of Supported Substrate on van der Waals Epitaxy of Nitride Semiconductors on Graphene by MBE

Shinichiro Mouri*†, Kenta Matsushima, Yuta Kawase, Tsutomu Araki

**Ritsumeikan University*

Integration of graphene and conventional compound semiconductors is a promising solution towards future electronic device applications. Van der Waals epitaxy is an effective way to fabricate thin film or nanostructure of compound semiconductors on graphene [1][2]. However, the control of in-plane orientation of crystal grown on graphene is difficult due to the lack of epitaxial relation. Recently, it was pointed out that the substrate potential under graphene plays crucial role to align in-plane orientation of crystal on graphene [3][4]. However, detailed mechanism including the effect of ionicity of substrate is still under discussion [5]. Here, we studied how the substrate under graphene affects the crystal growth of the nitride semiconductor.We conducted crystal growth of Indium Nitride (InN) on graphene using radio-frequency plasma-assisted molecular beam epitaxy (RF-MBE). We prepared CVD graphene transferred on different two substrates, a home-made InN substrate and a GaN template (NTT-AT Co.). Note that ionicity of both substrates is almost same [6]. InN was grown by simultaneous supply of indium beam and nitrogen plasma (RF-plasma power was 100W). III/V ratio was set to satisfy indium rich condition. Two step sequence of temperature control, 30 minutes growth at 350 °C and following 30 minutes growth at 425 °C was adapted to control the number of nuclear center and migration of supplied stuff. Figures 1 (a) and (b) show images of the scanning electron microscopy (SEM: left) and Electron back scatter diffraction (EBSD: right) of obtained InN crystals on graphene/InN and graphene/GaN, respectively. Surface morphology of InN grown on graphene/InN is much better than that on graphene/GaN and the number of misoriented grains was reduced. EBSD image indicates that the inclusion ratio of cubic phase is suppressed below 20 % on graphene/InN substrate as contrast to 60 % cubic phase inclusion on graphene/GaN substrate. These results suggest that quasi epitaxial relationship is essential rather than the ionicity for the van der Waals epitaxy of wurtzite nitride thin film. In the poster presentation, the effect of layered number or quality of graphene will also be discussed. Reference[1] A. Koma et.al., Microlectron. Eng. 2, 129 (1984). [2] J. Kim et.al., Nat. Commun. 5, 4836 (2014). [3] Y. Kim et.al., Nature 544, 340 (2017). [4] U. Ooe, S. Mouri et.al., Jpn. J. Appl. Phys. 58 SC1053 (2019). [5] W. Kong et.al., Nat. Materials 17, 999 (2018). [6] D.Vanderbilt et.al., Phys. Rev. B 56, R10 024 (1997). *Acknowledgements:* This work was supported by JSPS KAKENHI Grant Numbers 16H0615, 18H04294, 21H01017, 21H01831.

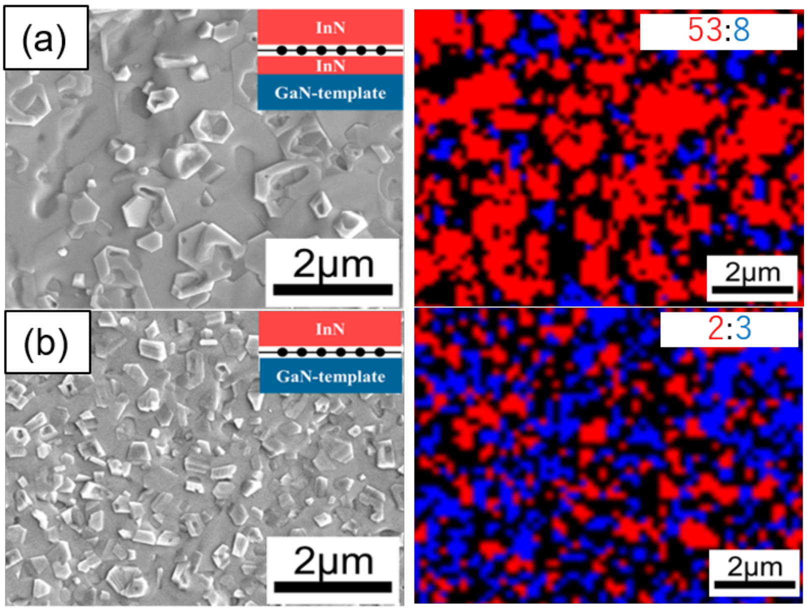

Fig. 1: (a) SEM (left) and EBSD (right) image of InN thin film grown on graphene/InN. (b) SEM (left) and EBSD (right) image of InN thin film grown on graphene/GaN.

B81: Electrodeposition of copper from wastewater onto nanocarbon networks

Grzegorz Stando*†, Pyry-Mikko Hannula, Bogumiła Kumanek, Mari Lundström, Dawid Janas
**Silesian University of Technology*

Combination of nanocarbon such as carbon nanotubes and graphene with other materials is often beneficial. As an example, copper-nanocarbon composites have improved electrical [1] and mechanical [2] properties due to the synergy effect between these two materials. Although the integration between copper and nanocarbon is not an easy task because of the "cuprophobic" nature of nanocarbon [3], many methods were developed to accomplish this challenge. One of them is electrodeposition, which might be used to deposit copper onto nanocarbon electrodes. In our research, we demonstrated the recovery of copper from industrial wastewater by thin films based on carbon nanotubes (CNTs), which was found as an ideal feed for electrodeposition of metallic particles. Single/multi-walled CNTs, and graphene were combined to obtain the electrodes [4], and then, they were characterized by Raman Spectroscopy and Scanning Electron Microscope (SEM) upon coating. In addition, a 4-probe method was used to gauge electrical conductivity of such nanocomposites. To establish parameters of the coating process, synthetic solution of CuSO4 was used first as a source of copper ions. Then, wastewater of complex composition was employed directly for the electrodeposition process. Besides the 40 ppm of Cu, the wastewater contained other elements like salts Fe, Mg, Al, Zn and As. The results showed that the composite materials based on nanocarbon materials may be an excellent substrate for electrochemical recovery of Cu also from such a problematic waste, while simultaneously giving a product of high added value. Interestingly, the product was free from other metals, and only copper was detected on the nanocarbon surface. After just 1-hour electrodeposition at -0.1V vs. SCE, a nanocarbon-based composite evenly coated with Cu was manufactured[5]. [1] C. Arnaud, F. Lecouturier, D. Mesguich, N. Ferreira, G. Chevallier, C. Estournès, A. Weibel and C. Laurent, Carbon, 2016, 96, 212–215. [2] R. Jiang, X. Zhou, Q. Fang, Z. Liu, Mater. Sci. Eng. A., 2016, 654, 124–130. [3] D. Janas and B. Liszka, Mater. Chem. Front., 2018, 2, 22–35. [4] D. Janas, M. Rdest, K.K.K. Koziol, Mater. Des., 2017, 121, 119–125. [5] G.Stando, P.-M. Hanulla, B. Kumanek, M. Lundström and D. Janas, Copper recovery from industrial wastewater - synergistic electrodeposition onto nanocarbon materials (under review) *Acknowledgements:* Authors thank MEiN, Poland (0036/DIA/201948), EU (Europ. Social Fund, POWR.03.05.00-00-Z305), NCBiR, Poland (LIDER/0001/L-8/16/NCBR/2017)

B82: STUDY OF THE ADSORPTION KINETIC OF HYDROCHLOROTHIAZIDE ONTO MAGNETIC GRAPHENE OXIDE

Franciele Da Silva Bruckmann*†, Theodoro Da Rosa Salles, Ivana Zanella Da Silva, Sergio Roberto Mortari, Cristiano Bohn Rhoden

**Universidade Franciscana*

The occurrence of drugs and their metabolites in wastewater has been widely reported in the literature. Inadequate disposal associated with methods that have low efficiency of decontamination, causes an imbalance of the ecological microbiota as well as putting human health in risk. Among the emerging micropollutants, hydrochlorothiazide (HCTZ), worldwide used for the treatment of hypertension, stands out for its high excretion rate, in which about 72% of the ingested dose is eliminated through the kidneys in the unchanged form. Studies have reported the presence of HCTZ in effluents and coastal waters. Considering such potential environmental harm, graphene oxide rises as an excellent candidate for removal of HCTZ with has unique properties such as hydrophilicity and high surface area. The incorporation of magnetic nanoparticles in the nanoadsorbent offers exceptional advantages, such as the exclusion of the filtration/centrifugation steps. This work aimed to evaluate the adsorption kinetic of the hydrochlorothiazide onto magnetic graphene oxide (GO.Fe3O4) with different amounts, (weight: weight proportion) of magnetite incorporated. The adsorption experiments were carried in batch, under the test conditions: initial concentration of HCTZ (50 mg L-1), pH = 7.0, 50 mg of adsorbent (GO, GO 1:1, GO 1:5 and GO 1:10) and volume of 100 mL of solution. During the tests, aliquots were collected at predetermined times, and later quantified on UV-Vis spectrophotometer at λ = 323 nm. Prior to the analyzes, the GO was filtered from the solution and sequentially carried out to centrifugation for 10 minutes at 10000 rpm. For the GO samples containing Fe3O4 no filtration was necessary, the adsorbent/adsorbed complex was removed from the solution by approaching a simple magnet at the flask surface. According to results, the pseudo-second-order (PSO) model represented the best adjust for the experimental data once higher values for the correlation coefficient were presented. Based on this, it can be inferred that, while GO and GO 1:1 sample are characterized by accurate adsorption kinetics, GO.Fe3O4 1:5 and 1:10 samples resulted in slower kinetics. However, as the amount of magnetite incorporated into the GO increased, linear growth in the adsorption capacity could be observed. In addition, using PSO model, it was possible to assume that the HCTZ adsorption process occurs by predominantly chemical mechanisms. Through the results presented in this study, it can be concluded that GO.Fe3O4 proved to be efficient in the removal of HCTZ, avoiding filtration/centrifugation steps, simplifying the process.

B83: Spectroscopic study of chemically functionalized MoS_2 and liquid-exfoliated CrTe3

Narine Moses Badlyan*†, Nina Pettinger, Xin Chen, Kevin Synnatschke, Claudia Backes, Kathrin Knirsch, Andreas Hirsch, Janina Maultzsch

**Department of Physics, Friedrich-Alexander University Erlangen-Nuremberg, D-91058 Erlangen, Germany*

2D materials, such as molybdenum disulfide (MoS_2), qualify as candidates for novel applications in various fields, including electronic and optical devices. The electronic and optical properties of chemically and mechanically exfoliated MoS_2 can be further tuned by covalent or non-covalent functionalization.Here, we present a Raman and photoluminescence (PL) study of functionalized MoS_2 flakes. They are prepared by mechanical exfoliation from MoS_2 crystals and are subsequently covalently functionalized with organic molecules. We discuss the impact of functionalization on the Raman modes of chemically functionalized MoS_2 multilayer samples. We show for multilayer MoS_2 flakes evidence for a transition to the 1T'- phase. Additionally, we observe PL quenching after functionalization for both the multilayer MoS_2 flakes and the free-standing MoS_2 monolayers. Moreover, we have studied the optical properties of liquid-exfoliated CrTe3 nanosheets of different sizes and of the bulk crystal. Here, we discuss the excitation-wavelength dependence of the Raman modes of the CrTe3 nanosheets and the polarization-angle dependence of the Raman modes of bulk CrTe3. *Acknowledgements:* This work was supported in part by the Deutsche Forschungsgemeinschaft (DFG) through the SFB 953 "Synthetic Carbon Allotropes"- B13.

B84: Dark and Bright Exciton-Photon Coupling in Semiconducting Carbon Nanotube Microcavity Polaritons

Abitha Dhavamani*†, Louis Haeberlé, Jialiang Wang, Stéphane Kéna-Cohen, Michael Arnold

**University of Wisconsin-Madison*

Polaritons are hybrid light-matter quasiparticles that form when elementary excitations such as excitons or phonons in a semiconductor material interact strongly with light or quantum vacuum electromagnetic field. This occurs when the interaction rate is sufficiently higher than the electronic or photonic decay rates resulting in new eigenstates that possess both excitonic and photonic characteristics. In the recent past, polaritons have gained significant attention that have led to the demonstration of several quantum electrodynamic, optical, and magnetic phenomena, the advent of innovative optoelectronic devices and modification/manipulation of chemical molecular systems. Semiconducting single-walled carbon nanotubes (SWCNTs) are an exquisite candidate for realizing stable exciton-polaritons at room temperature. SWCNTs have a combination of both bright and dark excitonic states and exciton-phonon coupling gives rise to additional emission and absorption channels, some of which may ”brighten” the sidebands of optically forbidden (dark) excitonic transitions. Here, we demonstrate the formation of exciton-polaritons in an optical microcavity containing high density (6,5) SWCNTs fabricated by a custom lamination approach. We show that light-matter hybridization in the cavity is not limited to the typical electronic transitions but also phonon-assisted vibronic transitions. This is evidenced by the coupling of the photonic cavity mode with the mixed bright exciton as well as dark exciton-phonon coupled state forming a middle polariton branch. The resulting polariton dispersions are measured and fit to a three-level Hopfield Hamiltonian model, evidencing high coupling strengths of g1 as large as 230 meV between bright excitons and cavity photons (which would correspond to a Rabi splitting $\Omega 1 = 2g1 = 460$ meV in the absence of the second oscillator) and g2 as large as 100 meV for phonon-brightened dark excitons and cavity photons. The high quality-factor of the cavity via the lamination technique and the high SWCNT density result in ultrastrong coupling between the bright excitons and cavity photons. Furthermore, photoluminescence is observed from the lower polariton branch with a full width at half maximum of only 30 meV. *Acknowledgements:* This work is supported by the Army Research Office (ARO) award number W911NF1810149

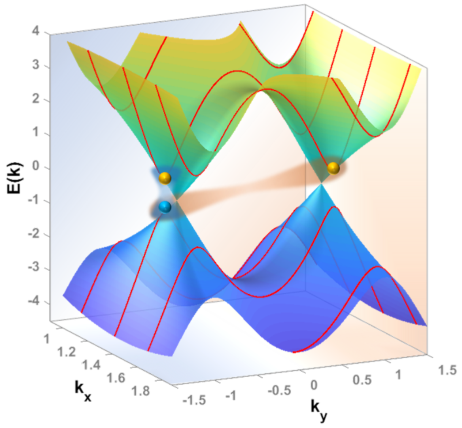

Fig. 1: Electronic structure of graphene in energy-momentum space with allowed quantized states in (6,5) SWCNTs, S11 bright exciton and S11-Kmomentum dark excitons shown in red, blue, and orange, respectively.

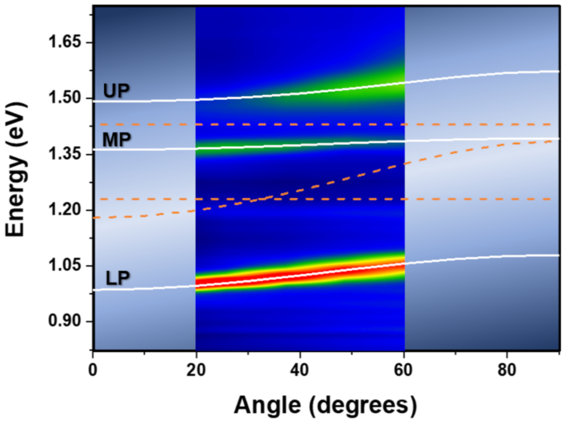

Fig. 2: Angle resolved TE-polarized reflectance contour plot showing three different features corresponding to the upper (UP), middle (MP) and lower (LP) polariton branches in single walled carbon nanotube microcavity.

B85: Optically induced Spin Current in Two-dimensional Metal

Yuan Tian*†, Muhammad Shoufie Ukhtary, Riichiro Saito

**Tohoku University*

Manipulation of spin current is a technique in the field of spintronics, which promises new designs for memory storage and logic circuit. It is expected that a device using spin current instead of electric current will have higher energy efficiency [1]. Although methods for generating spin currents that rely on either spin Hall effect or spin injection are well established, these conventional methods have problems such as either complicated structure or magnetic material, making the application harder. If we can establish a method to generate spin currents on a simple two-dimensional (2D) structure with a light, many applications of spin devices are easier. Recently Daigo Oue et.al. [2] theoretically show that by using the inverse Faraday effect, surface plasmon on the surface of the metal can induce a spin current in the direction perpendicular to the surface, due to the rotating electric field of the surface plasmon. Here we discuss that we can apply this photo-induced spin current on a 2D material by another geometry.In this presentation, we show the calculated result of the spin current generated by an edge plasmon on a 2D material. Edge plasmon is an electromagnetic (EM) wave that propagates at the edge of a 2D surface, as is shown in Fig. 1. We start by giving an expression of the EM field of the edge plasmon by solving the wave equation. We found that the electric field of the edge plasmon is rotating in the 2D surface as a function of time. According to the inverse Faraday effect, we propose that edge plasmon induces out-of-plane magnetization. As the edge plasmon is confined to the edge, the induced magnetization decays from the edge, which generates spin current due to the magnetization gradient [2] as shown in Fig. 2.We find a spin current is induced on the 2D surface by the edge plasmon. The spin polarization is perpendicular to the surface, while the in-plane spin current JS is perpendicular to the edge, as shown in Fig. 2. The magnitude of the spin current is tunable by the frequency of the light. Since the edge plasmon is excited by light, thus we can realize the optical generation of spin current on 2D material [3]. [1] S. Maekawa, et al., ”Spin current”. Oxford University Press, (2017). [2] D. Oue and M. Matsuo, Physical Review B 101, 161404, (2020). [3] Y. Tian, M. S. Ukhtary, R. Saito, In preparations. *Acknowledgements:* Yuan Tian acknowledges support from GP-Spin at Tohoku University

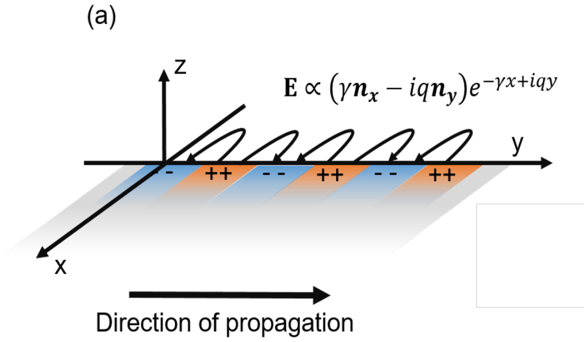

Fig. 1: Edge plasmon propagating along the edge of 2D material with wave vector q. The circular oscillating electric field of the plasmon decays in the x-direction with decaying parameter γ.

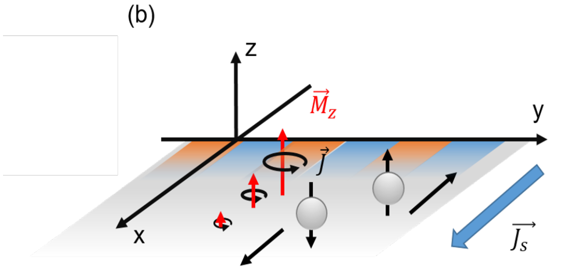

Fig. 2: Induced magnetization Mz that decays in the x-direction. The gradient of magnetization generates a spin current Js that flows in the x-direction.

B86: Hydrogenation of bilayer GaN: Plane orientation and new structures

Anh Khoa Augustin Lu*†, Tomoe Yayama, Tetsuya Morishita, Takeshi Nakanishi
**The National Institute of Advanced Industrial Science and Technology (AIST)*

In recent years, two-dimensional gallium nitride (GaN) has been theoretically studied and experimentally demonstrated [1]. Unlike other two-dimensional materials such as transition metal dichalcogenides (TMDs), GaN has dangling bonds. Previous studies have reported that bilayer GaN adopts buckled atomic configurations that differ from that of Xenes and TMDs [2, 3]. The presence of dangling bonds suggests that two-dimensional GaN is likely to interact its surroundings, such as a substrate or atoms from the environment.In the present work, the impact of hydrogenation on bilayer GaN is studied using first-principles calculations. Our results reveal that the plane orientation of the most stable structure depends on the hydrogen concentration (Figure 1) [4]. Unlike in the pristine case, hydrogenated bilayer GaN is not systematically oriented along the c-plane. This plane is the one typically considered in the case of two-dimensional materials. In particular, at high hydrogen concentration, it is shown that the most stable atomic structures are oriented along either the a-plane or the m-plane. First-principles molecular dynamics simulations show that these structures are stable at room temperature. By controlling the temperature and the hydrogen coverage of bilayer GaN, one can therefore control the type of structure obtained, its plane orientation and thus, modulate its properties including band gap. [1] Z. Y. Al Balushi, K. Wang, R. K. Ghosh, R. A. Vila, S. M. Eichfeld, J. D. Caldwell, X. Qin, Y.-C. Lin, P. A. DeSario, G. Stone, S. Subramanian, D. F. Paul, R. M. Wallace, S. Datta, J. M. Redwing, and J. A. Robinson, Nat. Mater., 15, 1166 (2016)[2] A. K. A. Lu, T. Yayama, T. Morishita, and T. Nakanishi, J. Phys. Chem. C, 123, 1939 (2019)[3] T. Yayama, A. K. A. Lu, T. Morishita, and T. Nakanishi,

Jpn. J. Appl. Phys., 58, SCCB35 (2019)[4] A. K. A Lu, T. Yayama, T. Morishita, T. Nakanishi, J. Phys. Chem. C, 124 (31), 16888-16894 (2020)

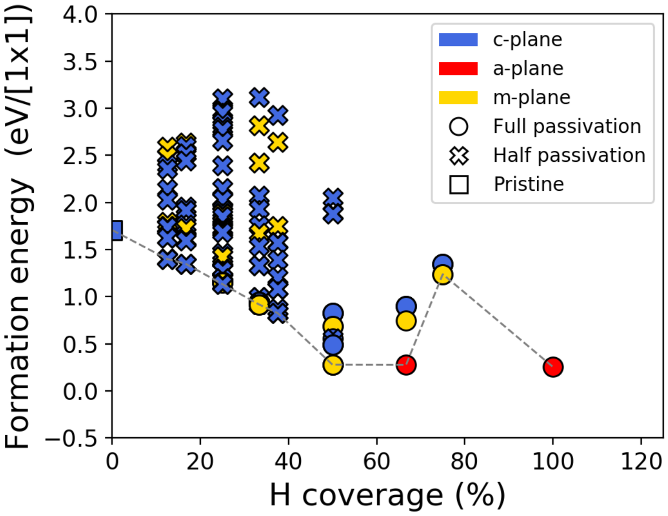

Fig. 1: Formation energy with respect to the hydrogen coverage

B87: Cumulene-Polyyne Transitions in Long Carbyne Chains Driven by Singlet-Triplet Excitations

Sándor Pekker*†, András Jánossy

**Wigner Research Centre for Physics*

Early studies of carbon chains were restricted to short oligomers of conjugated triple bonded polyynes and cumulated double bonded cumulenes. The recent synthesis of carbon chains inside carbon nanotubes drew attention to long carbon oligomers. To better understand the unusual optical and magnetic properties of carbyne, we present systematic quantum chemical calculation of the singlet and triplet states of HCnH polyynes and H2CnH2 cumulenes with n≤100 and compare to carbyne. Total energy calculations were performed at DFT B3LYP method with TZVP basis set. Molecular geometries, energies of formation, MO levels or energy bands, atomic charges and spin densities were determined. Like previously known for polyynes, alternating triple and single bonds are found. HCnH polyynes and carbyne have similar structures and physical properties. Normalized formation energies of HC10H and carbyne are close. In contrast, H2CnH2 cumulenes are different; the topology of double bonds excludes an asymptotic approach to the conjugated triple bonds of carbyne. The stability of the cumulene structure weakens with increasing length until the excess formation energy overrides the energy of triplet excitation i.e. the braking of a bond, accompanied with the formation of a biradical. Figures show results for D2d and D2h molecular symmetry singlet and triplet states respectively. Other configurations were also considered. For even carbon number chains the unpaired electrons split the chain into three regions. The terminal hydrogens maintain cumulene-like bonding near the ends. These higher energy regions are extended to a dozen of atoms. The central polyyne-like region has alternating triple and single bonds. The lower energy of this region decreases the total energy of the system. Unpaired electrons are localized in narrow regions, making possible a transition between the different topologies of cumulene and polyyne fragments. The length of the polyyne region increases with the number of carbon atoms, so the average structures and properties approach those of infinite carbyne. A similar singlet-triplet energy crossing is observed in cumulenes of odd number of carbons but with more complicated structures. The formation of polyyne regions in odd number cumulenes requires the brake of two bonds and four unpaired electrons in the molecules. Two of them are near the ends, as in the even systems, while the other two are localized around the center of the molecules. Long odd 2n+1 cumulenes have two polyyne regions, each half as long as the polyyne fragment in even 2n cumulene.

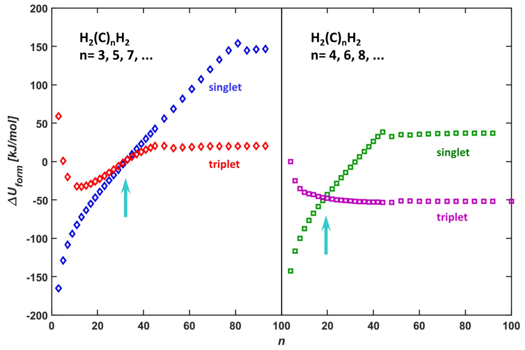

Fig. 1: Energies of formation of odd (left) and even C-atom cumulenes (right) versus chain length, n. Arrows show singlet-triplet transitions.

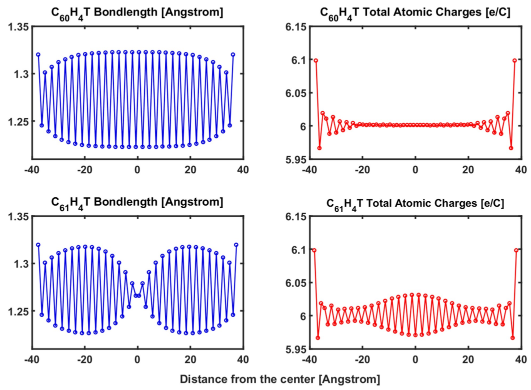

Fig. 2: Bondlength alternation and charge density of long cumulenes. C60H4 is predominantly polyyne-like; C61H4 consists of two polyyne-like segments divided and ended by cumulene-like segments.

B88: Boron Nitride Nanotubes and Their Impurities

Jingwen Guan*†, Keun Su Kim, Benoit Simard, Christopher Kingston

**National Research Council Canada*

Boron nitride nanotubes (BNNTs) are a counterpart of carbon nanotubes (CNTs), having a similarity in structure and mechanical properties. In addition, BNNTs are transparent in the visible region of the optical spectrum and are thermally stable in air, up to about 1000 oC. The additional properties of BNNTs have drawn much attention for different applications than CNTs in the past ten years since large scale and different sources of BNNT material has become available for research. The development of large scale production of BNNTs has inspired research directed at commercial applications in composite materials such as polymer, ceramics, glass, and metal composites and, bio-applications. Like the case with CNTs, the presence of non-nanotube impurities is an important factor affecting the ultimate properties of BNNT composites. This challenge can be even more complex for BNNTs than CNT materials because as-produced BNNT material contains non-tubular impurities that cannot be removed as easily as the amorphous carbon impurities of CNTs by methods such as thermal oxidation. This poster intends to present the identification and isolation of the non-tubular impurities present in BNNT material produced by thermal plasma, and the achievement of high purity BNNT materials through a multi-stage purification protocol. *Acknowledgements:* The authors express thanks to the financial support from NRC-SDTech-SMT program.

B89: Tailor-made two-dimensional nano-scale super-structures

Nanami Ichinose*†, Satoshi Iida, Zheng Liu, Ryo Kitaura

**Department of Chemistry, Nagoya University, Nagoya 464-8602, Japan*

Two-dimensional (2D) heterostructures have attracted plenty of attention. To fully explore the enormous potential of 2D heterostructures, developing a precise fabrication technique is crucial. Although 2D van der Waals stackings have been intensively studied, the research on the lateral heterostructures is still limited due to the difficulty in fabrication. In this work, we focus on superstructures, in which different 2D materials are repeated and laterally integrated with the periodicity of several nanometers. These are novel low-dimensional materials, whose electronic states can show crossover from 2D to 1D depending on the junction width.This study has focused on a metal-organic chemical vapor deposition (MOCVD) growth of transition-metal-dichalcogenide-based (TMD-based) superstructures. Since various TMDs, including metals, semiconductors, superconductors, and topological insulators, are available, novel 2D superstructures with various electronic structures can be realized based on TMDs. The MOCVD equipment used can rapidly switch the supply of source materials to achieve several nanometers junction width. Also, the MOCVD equipment is a cold-wall type, preventing the re-evaporation of source materials from the chamber wall.Figure 2 shows HAADF-STEM images of a lateral heterostructure (WS_2/MoS_2). In the HAADF-STEM images, W atoms are imaged as bright spots, whereas Mo and S atoms are images as much darker spots. As clearly seen, the MOCVD-grown multi-step lateral heterostructure possesses atomically steep interfaces with width down to 3 nm. Although a trace amount of W atoms is seen in the MoS_2 region, we can reduce the W atoms by increasing the interval time during consecutive MOCVD growth. In the presentation, further details of the MOCVD setup and structural characterizations will be shown.

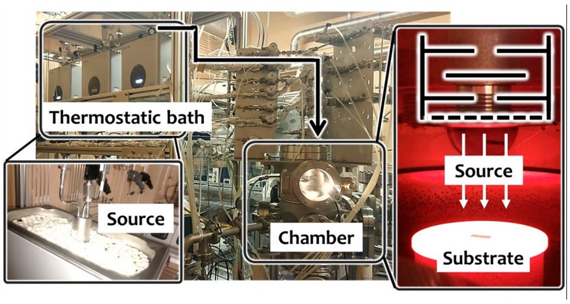

Fig. 1: Experimental setup of the MOCVD

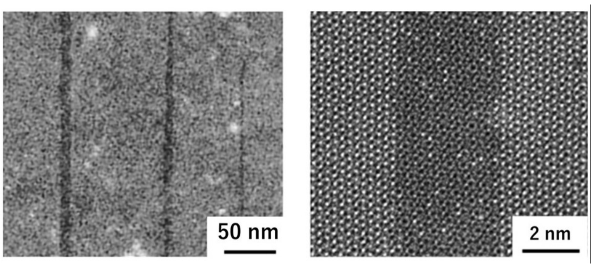

Fig. 2: The left (right) image is HAADF STEM image of low (high) magnification.

B90: Structural design of multifunctional nanocarbon materials for extreme-environmental applications

Ming Xu*†

Huazhong University of Science and Technology (HUST), China

Structural design has always been considered as one of the approaches to obtain and optimize material properties, realizing their value in applications. The same material will display different macro performances through the construction of different structures. One-dimensional and two-dimensional nanomaterials, such as carbon nanotubes, graphene, etc., have a series of excellent physical properties that other traditional materials cannot reach, and have become the preferred research materials in many application fields. Taking them as the "Building Blocks", the final performance of their assembly also depends on the structural design and construction. This time, we will show how to apply the concept of structural design to these nanostructured "building blocks" such as carbon nanotubes and graphene to achieve new breakthroughs in adhesion, sensing, energy storage in extreme environments [1-5].References[1] M. Xu et al. Science, 330, 6009 (2010)[2] M. Xu et al. Nat. Commun., 7, 13450 (2016)[3] X. Wan et al, Nat. Catalysis, 2, 259 (2019)[4] M. Zhang et al., Adv. Func. Mat., 30, 2004564 (2020)[5] X. Gao et al., Nat. Commun., 11, 6160 (2020)

B91: Magnetizations and De Haas-van Alphen oscillations in massive Dirac fermions

Fenda Rizky Pratama*†, Muhammad Shoufie Ukhtary, Riichiro Saito

Tohoku University

Graphene and related two-dimensional materials are known to possess intrinsic orbital diamagnetism (OD) [1], which is originated from the coalescence of states of the Dirac fermions at the valence bands to form the zeroth Landau levels (LLs) in the presence of an external magnetic field B. A method to calculate the orbital susceptibility χ is given by applying the Euler-Maclaurin formula for the thermodynamic potential Ω and by using the relation $\chi = -(\partial 2\Omega/\partial B2)B=0$, as employed by Landau [2] to show the OD in metals. In the context of the Dirac materials, the method was used to calculate the chemical potential dependence of χ in gapped graphene [3], MoS_2 [4], and the Weyl semimetals [5]. However, the magnetization M as a function of B and temperature T can not be calculated by using the Euler-Maclaurin formula, because $M = -(\partial\Omega/\partial B)$ diverges due to the infinite number of the occupied LLs at the valence bands which should be included in the calculation of Ω.In this study [6], we analytically calculate Ω(B,T) for strong-B/low-T and weak-B/high-T limits with the method of zeta function regularization, in order to avoid the divergence in the expression of M(B,T). Our formula reproduces the experimental observation of M(B,T) for graphene by Li et al. [7], which is fitted empirically into a Langevin function [7] (see Fig. 1). Moreover, we generalize the result by including the effect of band-gap and impurity scattering on M and χ. We found that in the presence of impurity, χ of graphene can be scaled by the chemical potential and relaxation time. In the case of gapped Dirac fermions, a large band-gap in MoS_2 gives a smaller but more robust magnetization with respect to T and impurity. In the doped system, we show that the opening of band-gap yields a decreasing frequency and amplitude of the De Haas-Van Alphen oscillation at T = 0 K. [1] J. W. McClure, Phys. Rev. 104, 666 (1956). [2]

L. Landau, Z. Phys. 64, 629 (1930). [3] M. Koshino, T. Ando, Phys. Rev. B 81, 195431 (2010). [4] T. Cai et al., Phys. Rev. B 88, 115140 (2013). [5] M. Koshino, I. F. Hizbullah, Phys. Rev. B 93, 045201 (2016). [6] F. R. Pratama, M. S. Ukhtary, R. Saito, arXiv:2101.01367 (submitted to Phys. Rev. B, under review) (2021). [7] Z. Li et al., Phys. Rev. B 91, 094429 (2015). *Acknowledgements:* FRP acknowledges MEXT scholarship. MSU acknowledges JSPS KAKENHI Grant No. JP18J10199. RS acknowledges JSPS KAKENHI Grant No. JP18H01810.

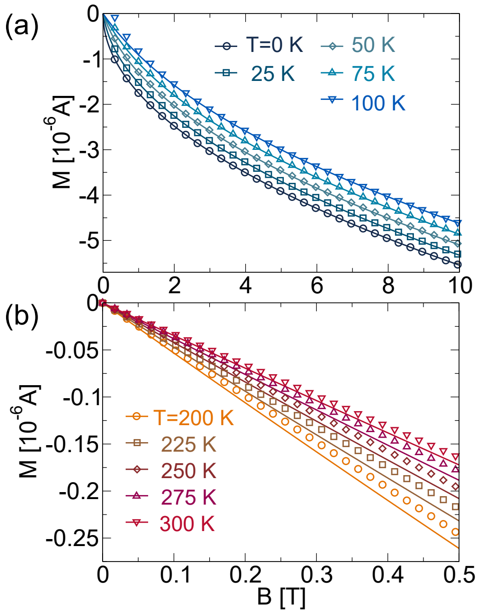

Fig. 1: M(B,T) of graphene for (a) strong-B/low-T and (b) weak-B/high-T limits. Symbols and lines denote the analytical calculation and the experimental Langevin fitting (from ref. [7]), respectively.

C94: Tracing acetylene-accelerated growth process of horizontally aligned carbon nanotubes by isotope labeling

Akari Kobayashi*, Ryoya Ishimaru, Keigo Otsuka, Taiki Inoue, Shohei Chiashi, Shigeo Maruyama†

**The University of Tokyo*

Horizontal arrays of single-walled carbon nanotubes (SWCNTs) are promising as transistor channels for logic applications. For simultaneous control over their chirality, length, and density, growth processes (e.g. nucleation, elongation, and termination) of individual SWCNTs remain to be studied. The alcohol CVD method has been widely adopted for controlled growth of SWCNTs including chirality-specific growth [1], but thermal decomposition of alcohol results in various uncontrolled compounds supplied to catalysts, which complicates the understanding of the mechanisms behind it. Here we study the effects of additional acetylene, one of the pyrolysis products of ethanol, on alcohol CVD growth of horizontally aligned SWCNTs by isotope labeling technique [2]. We synthesized SWCNTs by introducing 12C (natural abundance) and 13C-enriched ethanol alternatively and extracted the time evolution of SWCNT lengths from a Raman mapping (Fig. 1). In the middle of synthesis, we started adding 12C acetylene at a flow rate of 1/50 to ethanol. Such a small amount of acetylene resulted in the growth rate acceleration by a factor of >3 (Fig. 2(a)) but inhibited the nucleation of newly grown nanotubes. The acceleration by acetylene can also be quantified considering the G-mode frequency shift of nanotube segments grown from 13C ethanol and 12C acetylene (Fig. 2(b)). Combined with thermal decomposition analysis of ethanol by COMSOL, comparison of the acceleration behaviors in each nanotube captured by inter-label distances and intra-label Raman spectra provides further information on roles of acetylene and other gas species.References: [1] S. Zhang et al., Nature543, 234 (2017). [2] K. Otsuka et al., ACS Nano 12, 3994 (2018).

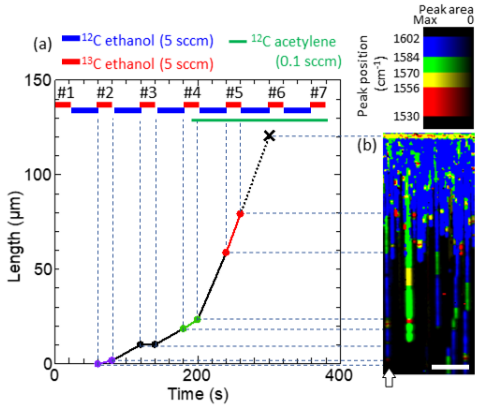

Fig. 1: (a) Length evolution of an SWCNT extracted from isotope labeling during alcohol CVD with acetylene. (b) Raman mapping of aligned SWCNTs. Scale bar is 20 μm.

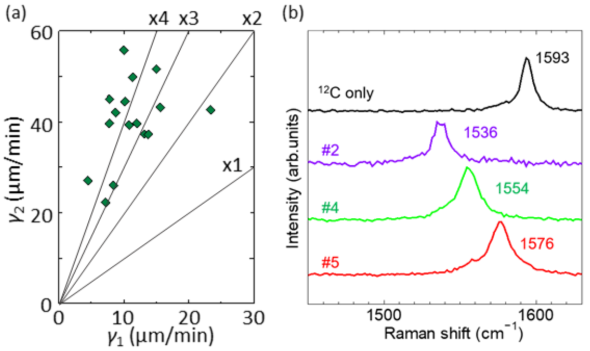

Fig. 2: (a) Growth rate of individual CNTs with ethanol feedstock only (γ1) and with addition of acetylene (γ2). (b) G-band spectra a nanotube at different positions shown in Fig. 1(a).

C95: Vertically aligned growth of small-diameter SWCNTs by ACCVD with Os catalyst

Daiki Yamamoto*†, Masaya Kobayashi, Kamal Prasad Sharma, Takahiro Saida, Shigeya Naritsuka, Takahiro Maruyama
**Meijo University*

A single-walled carbon nanotubes (SWCNTs) have many potential applications because of their unique structural and physical properties. For applications to transistors, synthesis of small-diameter SWCNTs, i.e., diameters below ~1 nm is important, since the band gap of an SWCNT increases with the decrease of its diameter. Here, we showed that single-walled carbon nanotubes (SWCNTs) can be grown on SiO2/Si substrates by alcohol catalytic chemical vapor deposition (CVD) with an Os catalyst in a cold-wall CVD system. At a growth temperature of 700 °C, web-like SWCNTs were grown with diameters distributed below 0.9 nm. At 800 °C, the SWCNT density increased and vertically aligned SWCNTs (VA-SWCNTs) were grown on the SiO2/Si substrates after growth for 30 min. Raman and transmission electron microscope results showed that the diameters of the grown SWCNTs were distributed between 0.7 and 1.1 nm, and were much smaller than those of VA-SWCNTs obtained from conventional catalysts such as Fe and Co. Additionally, neither an alumina buffer layer nor cocatalyst were necessary to grow VA-SWCNTs with the Os catalyst. We consider that highly efficient suppression of aggregation and the relatively strong carbon-Os bond strength contributed to growth of small-diameter SWCNTs from the Os catalyst. *Acknowledgements:* The Meijo University Research Branding Project for Cultivation and Invention of New Nanomaterials

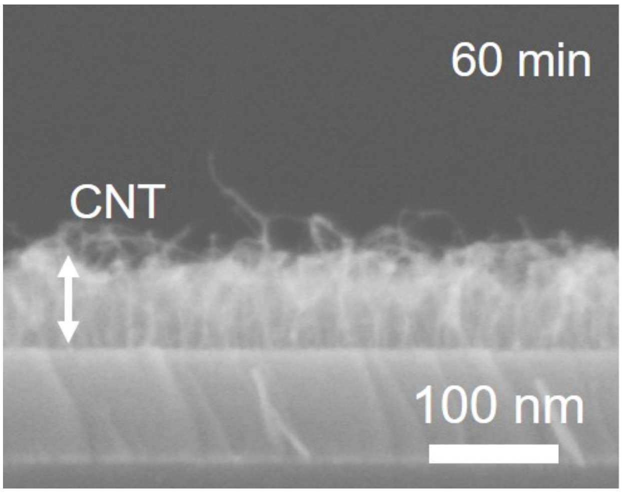

Fig. 1: Cross-sectional SEM images for SWCNTs grown on SiO2/Si substrates at 800°C.

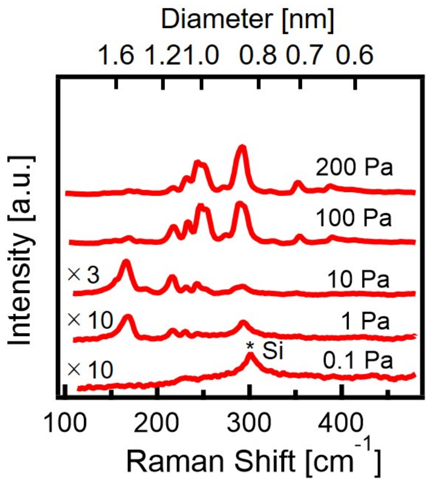

Fig. 2: Raman spectra in the RBM of SWCNTs grown from Os catalyst on SiO2/Si substrate at 800°C.

C96: Strain effect on circularly-polarized electroluminescence in transition metal dichalcogenides

Sake Wang*†, Muhammad Shoufie Ukhtary, Riichiro Saito

Tohoku University

In this presentation, we calculate electroluminescence (EL) spectra in the strained transition metal dichalcogenide (TMD) [1].Zhang et al. [2] have fabricated a light-emitting diode (LED) in a p–i–n junction of tungsten diselenide. The LED emits circularly-polarized EL by applying in-plane electric field E between the source and drain electrodes. Helicity of the circularly-polarized EL changes by changing the electric current direction. Since TMD possesses broken inversion symmetry, a left- (right-) handed circularly-polarized light (L, R) is emitted from the K (K') valley in the hexagonal Brillouin zone [3]. In particular, either L or R EL photon is emitted in the overlapping region of the occupied k-states by an electron (e) in the conduction band and a hole (h) in the valence band [Fig.1(a1)]. Therefore, the circularly-polarized EL occurs when the two overlapping regions in the K and K' valleys are unequal to each other. This situation occurs when we apply E [Fig.1(a2)], the overlapping regions for L and R change the area since the (e) and (h) states shift to left and right respectively for the both valleys. In order to get unequal area of the two overlapping regions, we need so-called trigonal warping (TW) effect [4] in the valence band which we exaggeratedly show as a triangle in Fig.1(a).However, the degree of circular polarization in the experiment which takes advantage of TW effect only reaches to 45% [2]. In order to improve the degree of circular polarization, we consider the strain effect on the energy dispersion in which the (e) and (h) circles are originally mutually shifted [Fig.1(b1)] with keeping time-reversal symmetry in K and K' [1, 5]. When we apply E, the overlapping regions [Fig.1(b2)] become more unequal between two valleys than the case of the TW effect [Fig. 1(a2)]. We get 100% circularly polarized EL without losing the EL intensity. We would like to discuss with experimentalist for realizing the phenomenon.References[1] S. Wang, M. S. Ukhtary, and R. Saito, Phys. Rev. Research 2, 033340 (2020). [2] Y. J. Zhang et al., Science 344, 725 (2014). [3] D. Xiao et al., Phys. Rev. Lett. 108, 196802 (2012). [4] A. Kormányos et al., Phys. Rev. B 88, 045416 (2013). [5] H. Rostami et al., Phys. Rev. B 92, 195402 (2015). *Acknowledgements:* SW acknowledges the NSFC (Grant No. 11704165) and CSC (Grant No. 201908320001). MSU and RS acknowledge JSPS KAKENHI (Grant No. JP18H01810).

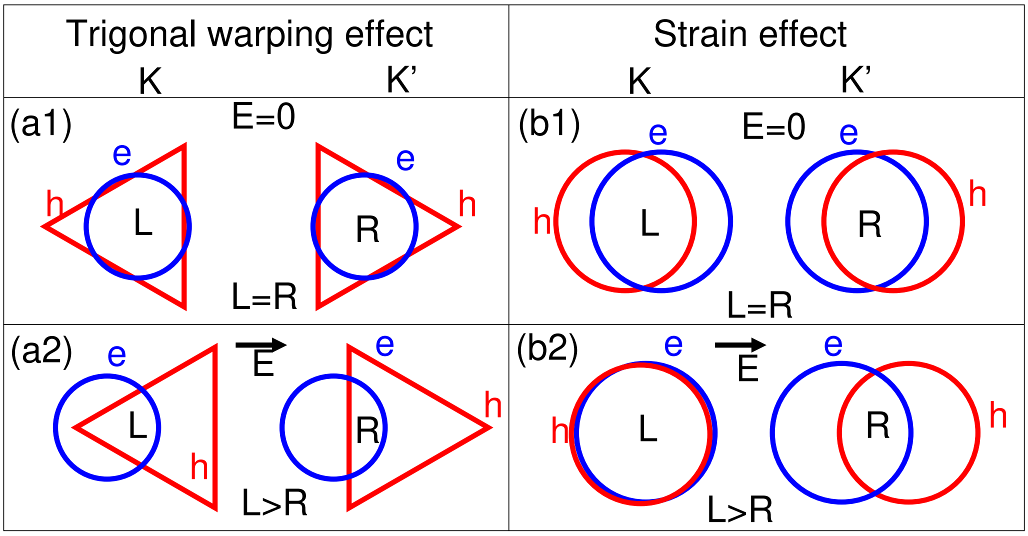

Fig. 1: Circularly-polarized EL by (a) TW, (b) strain effects. When we apply E, the overlapping regions by strain effect (b2) become more unequal between two valleys than TW effect (a2).

C97: Effects of defect formation by low energy Ar+ ion beam irradiation on monolayer MoS$_2$

Yangzhou Zhao*†, Kazuyuki Takai, Yasushi Ishiguro, Hiroki Yokota, Haruna Ichikawa

Hosei University

MoS$_2$ is a kind of promising material in the application of electronic devices using two-dimensional (2D) materials, but the structural defects of MoS$_2$ always exist in either of samples by CVD-grown or exfoliated from natural mineral. Due to its 2D nature, the presence of defects in monolayer MoS_2 has a great influence on the structure and electronic properties. In this study, in view of verifying the influence by defects on the structure and electronic properties, the monolayer MoS_2 is irradiated with low energy Ar+ ion beam in order to introduce defects under a well-controlled condition, and then evaluated by Raman spectroscopy, photoluminescence, and electrical conductivity.A field effect transistor using monolayer MoS_2 obtained by mechanical exfoliation is fabricated on the SiO2 / Si substrate. For defect-introduction, atomic vacancies are introduced into the surface of annealed MoS_2 by low energy Ar+ beam irradiation at 100 eV accelerating voltage. After Ar+ ion irradiation, both of the line widths for E2g and A1g peaks in Raman spectra increase and become broad with the increasing of irradiation time. The observed increase of the line width is considered mainly because of the increase of the contribution of satellite peaks caused by the introduction of defects. Interestingly, the effect of the irradiation is more significant for E2g in spite of its less sensitivity to charge transfer by molecular adsorption, where A1g peak is much more sensitive due to the larger electron-phonon coupling.As for photoluminescence (PL), after Ar+ ion irradiation, with the increasing of irradiation time, the intensity of the peak at 1.84 to 1.88 eV decreases significantly with the emerging of a tail at the lower energy side. Interestingly, the peak around 1.35 eV assigned to the emission related to impurity levels also rapidly decreases upon ion beam irradiation.The electrical conductivity measurements indicate that the shift of threshold voltage for MoS_2-FET ”Vg shift” increases upon the irradiation time, suggesting the hole doping formation during the Ar+ ion irradiation. This might be explained by charge transfer from terminating oxygen atoms of defects originating from the residue oxygen gas in the measurement vacuum chamber.

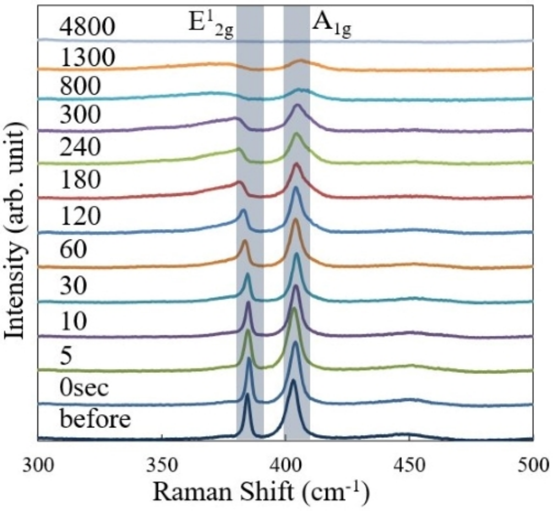

Fig. 1: Raman spectra for monolayer MoS_2 before annealing and irradiated Ar+ ion beam for 0 – 4800 sec

C98: Synthesis of single-walled carbon nanotubes with Ir catalyst prepared by solution process

Shu Kondo*†, Kamal Prasad Sharma, Takahiro Saida, Takahiro Maruyama, Shigeya Naritsuka

**Meijo University*

Single-walled carbon nanotubes (SWCNTs), which have cylindrical structures of rolled-up graphene sheets, have been anticipated for future applications in electronics. Our group has succeeded in growing vertically aligned SWCNTs (VA-SWCNTs) having diameters less than 1 nm by the alcohol catalytic CVD (ACCVD) method with an Ir catalyst prepared by a pulsed arc plasma deposition [1]. However, the deposition by the pulsed arc plasma gun is less productive because it is performed under high-vacuum. In this study, we attempted to grow SWCNTs from Ir catalysts prepared by a dip-coating process and succeeded in growing VA-SWCNTs.After immersing the SiO2/Si substrates into a 0.01 M iridium acetate-containing ethanol solution, an Ir catalyst was deposited by the dip-coating method. Then, the substrates were annealed for 15 min to remove the solvent and acetic acid. SWCNT growth was carried out in a hot-wall CVD apparatus. The substrate temperature was raised to 850 °C in an Ar/H2 atmosphere whose flow rate was 100 sccm. Then, ethanol vapor was supplied into the furnace for 10 min while the temperature was kept at 850 °C to grow SWCNTs. The samples were characterized by FE-SEM and Raman spectroscopy.Fig. 1 shows the RBM region and the high-frequency region of Raman spectra for SWCNTs, when the withdrawal speed was 0.05 mm/sec in the dip-coating. These show that SWCNTs of diameters between 0.8 and

1.0 nm were grown. Fig. 2 shows a cross-sectional FE-SEM image for the same sample. This image shows that the SWCNT forest was grown and its thickness was about 0.16 µm. We demonstrated that SWCNT can be grown with an Ir catalyst prepared by the dip-coating process. [1] T. Maruyama et al. Appl. Surf. Sci., 509 (2020) 145340.

Acknowledgements: JSPS Bilateral International Joint Research Projects

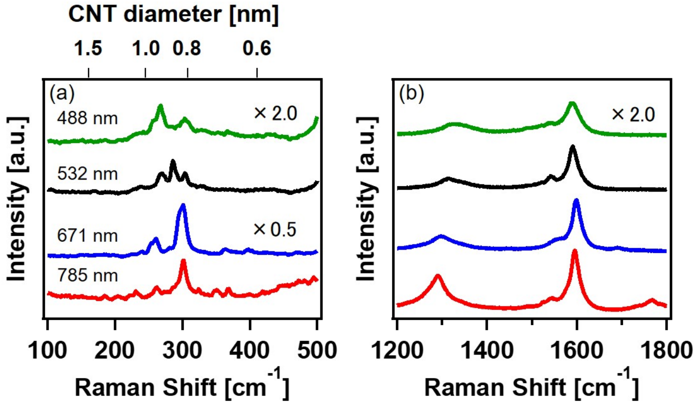

Fig. 1: Raman spectra in (a) the RBM region and (b) the high-frequency region of SWCNTs grown from an Ir catalyst.

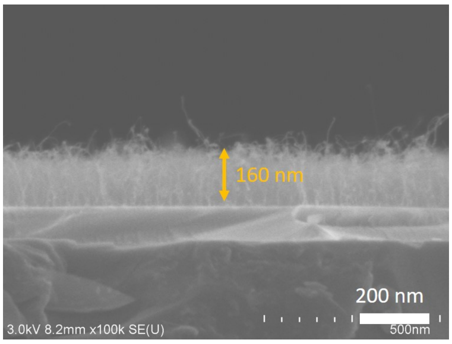

Fig. 2: Cross-sectional FE-SEM images of SWCNTs grown from an Ir catalyst.

C99: Thermoelectric properties of melt-mixed composites of CNTs with thermoplastic polymers

Petra Pötschke[†], Beate Krause*

**Leibniz-Institut für Polymerforschung Dresden e.V.*

CNTs can typically be used to make insulating polymers electrically conductive at low levels of addition, e.g. below 5 wt%. Such composites can be also used to harvest electrical energy from waste heat using the thermoelectric effect (Seebeck effect). Depending on the type of CNTs (SWCNTs, MWCNTs) and the chemical character of the polymer, as well p-type as n-type electrical behavior can be generated. In addition, n-type CNTs such as nitrogen doped CNTs and additives with dope the CNTs can be used to generate n-type materials. Using melt mixing such composites can easily fabricated in an environmentally friendly way and large quantities. The poster presents results concerning the Seebeck coefficient, electrical conductivity and power factor of different CNTs, different polymers with of the same CNTs, the effect of the CNT type and content in the same polymer. In addition, the effect of polyethylene glycol content on the switching from p-to n-type behavior. Furthermore, properties are shown for cellulose based composites with MWCNTs and SWCNTs. The maximum Seebeck coefficients achieved so far with such materials are 66.4 µV/K (PBT+5 wt% SWCNT), -59.8 µV/K (PA6+ 1 wt% SWCNTs) and the best power factors is 1.1 µW/mK2 (cellulose + 10 wt% SWCNTs). In addition, a thermoelectric module consisting of 49 pairs of p- and n-type polypropylene based composite strips is presented, which reached at a temperature difference of 70 K a thermovoltage of 110 mV. Despite the much lower values achieved compared to traditional thermoelectric materials, such as Bi2Te3, polymer based thermoelectric materials and modules are lightweight, cost effective and environmentally friendly materials and may find their applications e.g. in providing the needed energy for IoT sensor applications leading to energy autarkic systems. *Acknowledgements:* Support of the EU project InComEss Grant ID: 862597; 03/2020 - 08/2023 is acknowledged.

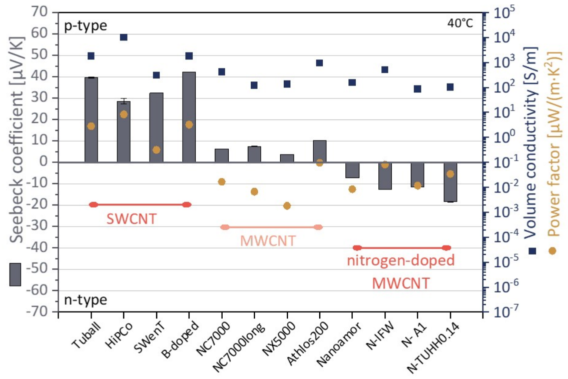

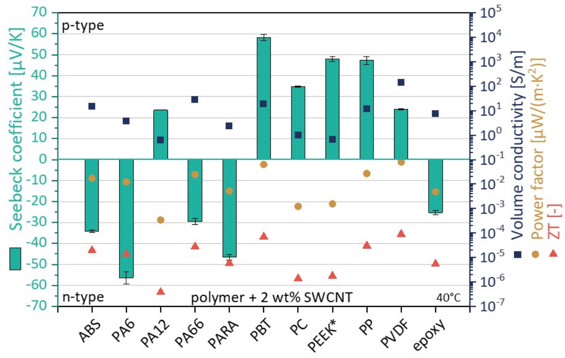

Fig. 1: Thermoelectric properties of different kinds of CNTs like singlewalled (SWCNT), multiwalled (MWCNT), boron-doped (B-SWCNT), nitrogen-doped (N-MWCNTs) at the measurement temperature of 40 °C

Fig. 2: Thermoelectric properties of different kinds of thermoplastic polymers and epoxy resin with 2 wt% SWCNT content at the measurement temperature of 40 °C

C100: Protected Catalyst Growth of Carbon Nanotubes

Muhammad Ahmad*†, S. Ravi P. Silva, Jose Anguita, David Carey, Caterina Ducati
**Advanced Technology Institute, University of Surrey, Guildford, UK*

Poor attachment of carbon nanotubes (CNTs) to the substrate and poisoning of the catalyst by environmental contamination prior to the growth are amongst the key challenges in many applications of carbon nanotubes. We present here a 'protected catalyst' method which overcomes above challenges and provides a novel CVD based production route for single wall and multiwall CNTs, as well as for graphene. The method involves capping the catalyst with a protective layer of a suitable material such as TiN, Cr, Ta etc. The protective layer protects the catalyst from environmental contaminants such as oxidation or etchant attack, whilst allows carbon supply to the catalyst for the CVD growth of carbon nanomaterials. We show that the CNTs grown using this technique exhibit significantly improved adhesion to the substrate in sonication bath test. A thin Fe catalyst layer remained protected due to the protective layer in the CF4 based reactive-ion-etching of SiO2, thus allowing us to demonstrate the fabrication of CNT based vias in a buried catalyst arrangement. The technique also allows better control over various CNT growth parameters such as growth rate, morphology, and structural quality.

C101: Maximization of thermoelectric power factor of nitrogen-substituted carbon nanotubes with various diameters

Manaho Matsubara*†, Kenji Sasaoka, Takahiro Yamamoto, Hidetoshi Fukuyama
**Tokyo University of Science*

One-dimensional semiconductors are expected to have high thermoelectric performance due to a van Hove singularity at band edges [1]. Semiconducting single-walled carbon nanotubes (SWCNTs) have been attracting attention as thermoelectric materials with high thermoelectric power factor (PF) as well as flexibility and lightweight. To develop SWCNT-based thermoelectric devices, n-type semiconducting SWCNTs are required in addition to p-type ones. In this study, we theoretically investigate the thermoelectric properties of nitrogen-substituted (N-doped) SWCNTs as typical n-type semiconducting SWCNTs using the Kubo-Luttinger formula combined with thermal Green's function technique. First, we showed the optimal N concentration per unit cell (copt) that gives the maximum PF of N-doped (20,0) SWCNTs with the diameter of 1.6 nm and the band gap of 0.497 eV, e.g., PF = 0.30 W/K2 m with copt = 3.1 × 10−5 at 300K [2]. Because copt depends on the tube diameter, we investigate copt of N-doped SWCNTs for various diameters. In addition, we found that the maximum PF at 300K increases exponentially as the SWCNT-diameter decreases; that is, the band gap increases. This is because the thermal excitation from the valence band to the conduction band is suppressed for small-diameter SWCNTs. [1] L. D. Hicks and M. S. Dresselhaus, Phys. Rev. B47, 16631 (1993). [2] M. Matsubara, K. Sasaoka, T. Yamamoto, and H. Fukuyama, J. Phys. Soc. Jpn. 90, 044702 (2021).

C102: Low-Temperature Growth of Large-Diameter Double Walled Carbon Nanotubes by Photo-thermal Chemical Vapour Deposition

Naigui Shang†, Jose Anguita, Pagona Papakonstantinou, S. Ravi P. Silva*

**Advanced Technology Institute, University of Surrey, Guildford, UK*

With a geometrical bridge between single-walled carbon nanotubes (SWCNTs) and multi-walled carbon nanotubes (MWCNTs), double walled carbon nanotubes (DWCNTs) not only are an ideal model for studying the coupling interaction between different shells in MWCNTs, but also present many unique properties, better than both SWCNTs and MWCNTs such as excellent thermal and electrical stability, as well as superior resistance to chemicals etc. Recently, theoretic calculation has revealed that DWCNTs with a diameter over 2.4 nm have staggered band alignment and could be a potential candidate material for charge separation in photovoltaic devices. However, the growth of DWCNTs, particular large-diameter ones, is a challenge. Here, we use a photo-thermal chemical vapour deposition method to successfully grow vertically aligned DWCNTs on Si substrates at around 500oC. The morphology and structure of DWCNTs are investigated by using transmission electron microscope, scanning electron microscope and Raman spectroscopy. The as-grown DWCNTS have an inner diameter up to 6.5nm. The study of relations between the growth parameter and the DWCNTs' structure shows that the growth of DWCNTs follows a base growth mechanism.

C104: Aqueous two-phase extraction of single-walled carbon nanotubes facilitated by basic salts

Błażej Podleśny*†, Tomohiro Shiraki, Dawid Janas

**Silesian University of Technology*

To take full advantage of the potential of single-walled carbon nanotubes (SWCNTs), it is often crucial to increase homogeneity of the material considerably by chirality, diameter, or electrical conductivity character. Unfortunately, so far, only a handful of selective methods of synthesizing were developed. They either give a subset of common SWCNT types or produce chirality-defined material at an unsatisfactorily small scale. Therefore, mixtures of SWCNTs have to be sorted post-synthetically to resolve them into fractions. A significant part of this purpose's methods is based on classical separation techniques like chromatography, electrophoresis, density gradient centrifugation, and extraction [1].Aqueous two-phase extraction (ATPE) has recently emerged as one of the most convenient purification methods of SWCNTs. The advantages of this method are simplicity of implementation, no need for advanced equipment or sophisticated chemicals, and - most importantly - tunability. The separation conditions can be easily adjusted by modifying the extraction system's composition consisting of water, phase-forming chemicals, and surfactants. Recently, several groups started to consider a different approach wherein additional compounds (so-called chemical modulators) are introduced to influence the differentiation course. Such modulators can be simple chemical compounds composed of several atoms (ammonia, hydrochloric acid) or macromolecules [2-3]. A large portion of them operates on redox principles or influences the pH, both of which can change the affinity of individual SWCNT types to either top or the bottom phase. Consequently, monochiral SWCNT fractions can be easily harvested.In this work, we present how inorganic salts of basic character can be employed as chemical modulators of the ATPE method [4]. By introducing appropriate amounts of alkaline salts into the system consisting of poly(ethylene glycol), dextran, sodium cholate, sodium dodecyl sulfate, and SWCNTs, we obtained an effective tool for the single-step extraction of high purity (6,5)-SWCNT fractions. References:[1] D. Janas, Mater. Chem. Front., 2018, 2, 36–63. [2] E. Turek, T. Shiraki, T. Shiraishi, T. Shiga, T. Fujigaya and D. Janas, Sci. Rep., 2019, 9, 535. [3] B. Podlesny, B. Kumanek, A. Borah, R. Yamaguchi, T. Shiraki, T. Fujigaya and D. Janas, Materials, 2020, 13, 13173808 [4] B. Podlesny, T. Shiraki and D. Janas, Sci. Rep., 2020, 10, 9250. *Acknowledgements:* Authors thank National Science Centre, Poland (2019/33/B/ST5/00631) and National Agency for Academic Exchange, Poland (PPI/APM/2018/1/00004)

C105: Fullerene growth with hydrogen -- new growth model in the interstellar medium

Yuri TANUMA*†, Toru MAEKAWA, Chris Ewels

**Institut des Matériaux Jean Rouxel Université de Nantes & Graduate School of Interdisciplinary New Science Toyo University*

In the interstellar medium, formation and dissociation of carbon molecules are cycled by energy absorption such caused by electron irradiation and UV exposure in the extreme environmental conditions. According to the diffuse interstellar bands (DIBs), there are a tremendous number of molecules causing the complicated absorption and most of the candidates are considered to be carbonaceous molecules such as PAHs, carbon chains, and fullerenes. Up to now, C60+ has been experimentally assigned as one of the DIB carriers. In laboratory experiments, hydrogen-deficient conditions encourage the synthesis of C60. Top-down dissociation and bottom-up growth models of fullerenes have been proposed so far and in that case the formation follows the isolated pentagon rule (IPR). Interestingly, however, astrochemists found that fullerenes are abundant in hydrogen-containing stars and not in hydrogen-deficient stars. In this study, we focused on non-IPR fullerenes stabilisation by adding hydrogen and theoretically investigated a new rule for the growth of fullerenes with hydrogen by the density functional theory (DFT) using the AIMPRO codes.There are exactly 12 pentagons in all of the fullerenes (Euler's theorem on polyhedron). According to the IPR, the structures with fused-pentagons are not stable due to the local strain, however, we anticipate that fused-pentagons can be stabilised by hydrogenation. Since there are a huge number of isomers for each cage size of fullerenes, we introduced the following three local properties as test conditions; hybridisation, pyramidalisation angle, and sum of the neighbouring three bond length, in order to build molecular structures for input in systematic ways. Hydrogenation (+1H to +5H) of small fullerene isomers (C20, C24, C26, C28, C30, …, C52, C60) was performed by the local properties and the structures were optimised sequentially. As a result, as for one C40 isomer for example, hybridisation and pyramidalisation which have hydrogenated 4 triple-fused pentagons showed almost the same hydrogenation route due to their mathematical meaning. The stability of the structures was more influenced by the hybridisation and pyramidalisation than the bond length sum. We suppose there are still other properties which determine the stability of the structures. This study may construct a novel growth model from C20 to C60 with hydrogen for the progress of astrochemistry. *Acknowledgements:* T.Y. acknowledges French government scholarships and Inoue Enryo Memorial Grant for funding.

C106: Top Down Synthesis of Graphene Quantum Dots from Reduced Graphene Oxide for NIR in vitro/in vivo/ex vivo Bioimaging Applications

Bong Han Lee*†, Md Tanvir Hasan, Ching-Wei Lin, Ainsley McDonald-Boyer, Roberto Gonzalez-Rodriguez, Satvik Vasireddy, Uyanga Tsedev, Jeffery Coffer, Angela Belcher, Anton Naumov

**Texas Christian University*

Near-infrared (NIR) emissive nanomaterials are desired for bioimaging and drug delivery applications due to the high tissue penetration depth of NIR light, enabling in vitro/ex vivo/in vivo fluorescence tracking. Considering the scarcity of NIR-fluorescing biocompatible nanostructures, we have for the first-time synthesized nanometer-sized reduced graphene oxide-derived graphene quantum dots (RGQDs) with NIR (950 nm) emission highly biocompatible in vitro with no preliminary toxic response in vivo. RGQDs are obtained in a high-yield (~90%) top-down sodium hypochlorite/UV-driven synthetic process from non-emissive micron-sized reduced graphene oxide (RGO) flakes. This oxidation of RGO yields quantum dots with an average size of 3.54 ± 0.05 nm and a highly crystalline graphitic lattice structure with distinguishable lattice fringes. RGQDs exhibit excitation-independent emission in the visible and NIR-I region with a maximum NIR quantum yield of ~7%, where in situ fluorescence measurements of the synthesis also showed an interdependence of evolution for the visible and NIR-I emissions. Unlike their parent material, RGQDs show substantial biocompatibility with ~75-80% cell viability up to high (1 mg/mL) concentrations verified via both MTT and luminescence-based cytotoxicity assays. Tracked in vitro via their NIR fluorescence, RGQDs exhibit efficient internalization in HeLa cells maximized at 12 h with further anticipated excretion. In vivo, RGQDs introduced intravenously to NCr nude mice allow for fluorescence imaging in live sedated animals without the need in sacrificing those at imaging time points. Their distribution in spleen, kidneys, liver, and intestine assessed from NIR fluorescence in live mice, is further confirmed by excised organ analysis and microscopy of organ tissue slices. This outlines the potential of novel RGQDs as NIR imaging probes suitable for tracking therapeutic delivery in live animal models. A combination of smaller size, water-solubility, bright NIR emission, simple/scalable synthesis, and high biocompatibility gives RGQDs a critical advantage over a number of existing nanomaterials-based imaging platforms. *Acknowledgements:* TCU RCAF; Marble Center for Cancer Nanomedicine; Koch Institute Support Grant P30-CA14051 NCI; Robert A. Welch Foundation Grant P-1212 to JL

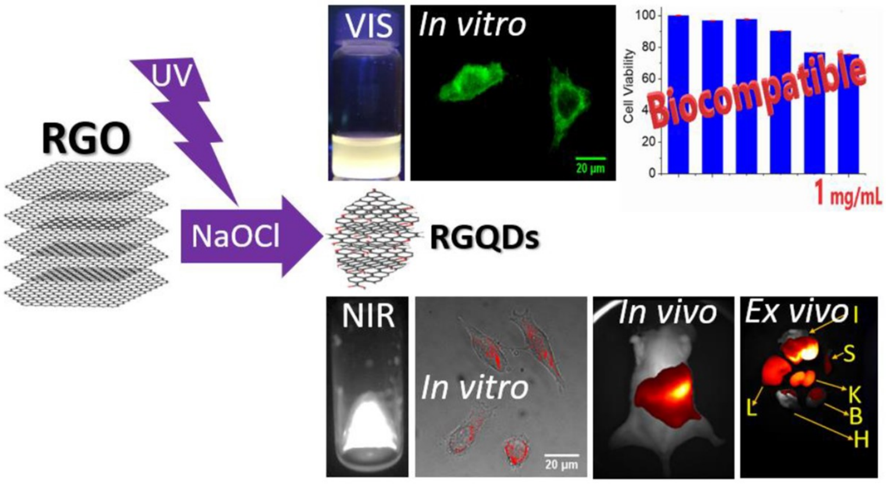

Fig. 1: RGO treated with NaOCl and UV source to yield biocompatible RGQDs for visible and NIR bioimaging in vitro/in vivo/ex vivo.

C107: Bio-engineered carbon nanotube optical sensor for detecting amyloid beta

Merav Antman-Passig*†, Daniel Heller, Eitan Wong, Georgia Frost, Christian Cupo, Albert Agustinus, Ziyu Chen, Chiara Mancinelli, Maikel Kamel

**Memorial Sloan Kettering Cancer CTR*

With no treatment and largely unfruitful therapeutic breakthroughs Alzheimer's disease (AD) and other dementias pose an increasing global health challenge as the proportions of elderly population increase demographically. Current hypotheses connect dyshomeostasis of amyloid-ß (Aβ) protein as a key event in AD, in which the accumulation of self-aggregated Aβ triggers a cascade of toxic molecular events that lead to memory decline and ultimately advanced AD. However, there is a remining gap of knowledge in understanding Aβ relationship to AD initiation and progression, which can be directly linked to the failure of several Aβ-targeting drug trials. Quantitative measurements and high-resolution imaging of Aβ help elucidate the role of Aβ in AD, and provide information required for optimal therapeutic targeting and timing. We developed a new optical probe that is capable of monitoring Aβ accumulation in live cells. Optical probes derived from dispersed single-walled carbon nanotubes (SWCNT) offer unique properties for biomedical purposes, from their intrinsic near-infrared photoluminescence within the optical transparency window of biological tissue and high photo-stability, to their high optical sensitivity towards the vicinity of nanotube surface. Engineered SWCNT probes are non-covalently or chemically modified to establish molecular affinity toward specific analytes. Specifically, modified SWCNT sensors are ideally suited for long-term sensors in live samples. We have engineered a non-covalent protein-modification of SWCNTs, to generate affinity toward AD biomarkers. We found the modified SWCNTs specifically detects Aβ via shifting of their intrinsic near-infrared emission wavelength. We investigated the sensor's ability to monitor Aβ aggregation and to detect Aβ aggregated species. We studied the interaction between Aβ and the modified SWCNTs via atomic force microscopy. We investigated the capability of the sensor to respond in living cells in neuronal and phagocytic cell models, and found the sensor responded to Aβ . Finally, we show proof-of-concept in-vivo application within extracellular brain environment. We examined the response of the sensor after intracranial injection in AD mice model and found the sensor differentiated between AD and wild type mice.

C108: Graphene Oxide Photoluminescence Quenching by Electric Field

Alina Valimukhametova†, Bong Han Lee*, Conor Ryan, Thomas Paz, Fabian Grote, Anton Naumov

**Texas Christian University*

With the advent of graphene, there has been an interest in utilizing this material and its derivative, graphene oxide

(GO) for novel applications in nanodevices such as bio and gas sensors, solid-state supercapacitors and solar cells. Although GO exhibits lower conductivity and structural stability, it possesses an energy band gap that enables fluorescence emission in the visible/near infrared leading to a plethora of optoelectronic applications. In order to allow fine-tuning of its optical properties in the device geometry, new physical techniques are required that, unlike existing chemical approaches, yield substantial alteration of GO structure. Such a desired new technique is one that is electronically controlled and leads to reversible changes in GO optoelectronic properties. In this work, we for the first time investigate the methods to controllably alter the optical response of GO with the electric field and provide theoretical modeling of the electric field-induced changes. Field-dependent GO emission is studied in bulk GO/polyvinylpyrrolidone films with up to 6% reversible decrease under 1.6 V μm−1 electric fields. On an individual flake level, a more substantial over 50% quenching is achieved for select GO flakes in a polymeric matrix between interdigitated microelectrodes subject to two orders of magnitude higher fields. This effect is modeled on a single exciton level by utilizing Wentzel, Kremer, and Brillouin approximation for electron escape from the exciton potential well. In an aqueous suspension at low fields, GO flakes exhibit electrophoretic migration, indicating a degree of charge separation and a possibility of manipulating GO materials on a single-flake level to assemble electric field-controlled microelectronics. As a result of this work, we suggest the potential of varying the optical and electronic properties of GO via the electric field for the advancement and control over its optoelectronic device applications.

C109: Enhancement of graphene oxide antibacterial activity in solution

Grecia Guadalupe Montes-Duarte*†, Guillermo Tostado-Blázquez, Carlos Achete, Jose Luis Sánchez-Salas, Jessica Campos-Delgado

**Universidad de las Américas Puebla*

Graphene oxide (GO) has been one of the most studied carbon nanomaterials in recent years thanks to its novel qualities; which has allowed its application in different areas, the health area being one of the least exploited and perhaps the most promising of all. In this work the effect of some parameters to improve the antimicrobial activity of GO has been studied: morphology, concentration, decoration of the material with silver/ceria nanoparticles, methodology and exposure time to two pathogenic bacteria. The inhibition effect of GO, silver nanoparticles, ceria nanoparticles and aqueous solutions of GO/silver and GO/ceria was evaluated against Escherichia coli and Salmonella Typhimurium suspended in saline solutions (without growth medium) for 6 different exposure times and 3 different concentrations. Additionally, our materials have been characterized by SEM, EDX, DLS, FTIR and Raman spectroscopy. The experiments show concentration-dependent results and confirm that as exposure time increases, the inactivation rate also increases; demonstrating that 30 minutes of exposure is sufficient to display the antimicrobial effects of these materials. GO has the lowest inactivation rate; however, the presence of silver and ceria nanoparticles on its surface increases its antimicrobial effect. *Acknowledgements:* G. G. Montes-Duarte thanks UDLAP for funding.

C110: A carbon nanotube film photo-thermoelectric imager for terahertz computed tomography systems

Tomoya Furukawa*†, Takeru Suyama, Kou Li, Imari Sato, Yukio Kawano

**Tokyo Institute of Technology*

I. INTRODUCTIONCarbon nanotube (CNT) film-based flexible uncooled broadband photo-detectors have been exhibiting their potential for various imaging applications[1]. To enrich the above systems, effective combination with image processing techniques needs to be tackled. To this end, this paper demonstrates fundamental CT measurement employing the CNT film device.II. RESULTFigure 1a depicts the photo-detection mechanism of the CNT film device based on the photo-thermoelectric (PTE) effect. This phenomenon governs the uncooled and broadband photo-detection operations. The proposed device works under chemical carrier doping as shown in Fig. 1b. The graph demonstrates a change of the originally P-type Seebeck coefficient of CNT films into N-type, enabling PN-junction formation. Here, this process allows the photo-detection with the maximum intensity as presented in a PTE response mapping across the device channel (Fig. 1c). Figure 2a depicts the measurement setup of this study. Here, the CT measurement was performed by horizontal and rotational scan where the target object is located between an emitter and a photo-detector device. Figure 2b shows the structure of the target object in this measurement. This measurement used the cylinder model as the target object. The target object, consisting of poly-lactic acid, was fabricated via three-dimensional printing. Figure 2c demonstrates the CT image reconstruction of the used target. Figs. 2b-c represents that the shape of the target was successfully visualized in a non-destructive manner. The presented image reconstruction was performed in accordance with the conventional data processing of the X-ray CT measurement[2]. These results potentially facilitate non-contact inner structure monitoring schemes of multi-layered components in diverse social sectors including security and quality screening fields of industrial, agricultural, and healthcare. REFERENCE[1]. D. Suzuki, Y. Kawano, Flexible terahertz imaging systems with single-walled carbon nanotube films, Carbon 162, 13-24, 2020. [2]. J.P. Mathews, Q.P. Campbell, H. Xu, P. Halleck, A review of the application of X-ray computed tomography to the study of coal, Fuel 209, 10-24, 2017.

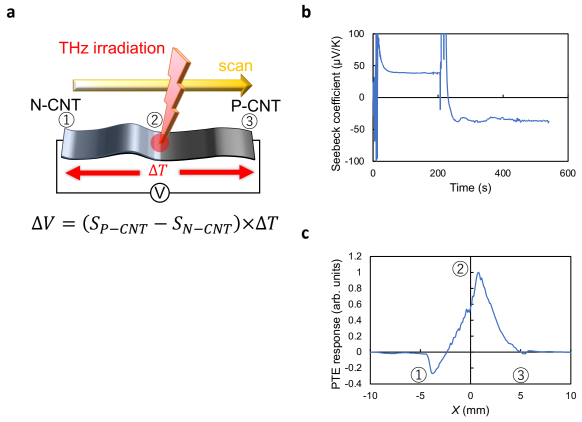

Fig. 1: a. The photo-thermoelectric (PTE) effect. b. Seebeck coefficient change of the CNT film. c. The PTE response mapping by scanning the THz irradiation across the channel length direction.

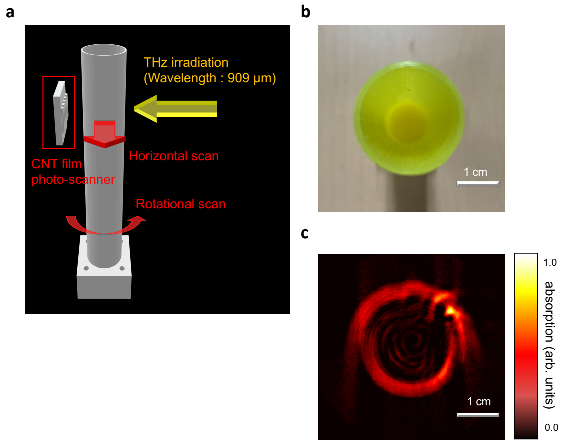

Fig. 2: a. The measurement setup of this study. b. The structure of the used target object. c. Non-destructive THz CT image reconstruction of the target (b).

C111: Transport behaviors of excitonic carriers in monolayer transition metal dichalcogenides

Mengsong Xue*†, Takato Hotta, Ruben Canton Vitoria, Ryo Kitaura

Nagoya University

An exciton is a hydrogen-like quasi-particle, where the electrons in the conduction band and holes in the valence band bind together due to the Coulomb interaction. The exciton binding energies in two-dimensional (2D) systems, such as monolayer transition metal dichalcogenides (TMDs), can reach hundreds of millielectronvolts due to reduced dielectric screening; two orders of magnitude larger than in conventional semiconductors such as silicon or GaAs [1]. Due to the strong Coulomb interaction, various excitonic states, including neutral excitons, trions (charged excitons), and biexcitons (exciton molecules), can exist in 2D TMD, and these excitonic states can carry the information of valley degree of freedom. 2D TMDs, therefore, provide an excellent platform to explore exciton and valley-related physics.Understanding and controlling the spatial motion of excitons and trions is of central importance for both fundamental research and optoelectrical applications. However, the surface roughness and charged impurities of TMDs-based van der Waals heterostructures and high contact resistance between metal and TMDs prohibit the exploration of intrinsic excitonic transport properties of monolayer TMDs. In this work, we fabricated hexagonal boron nitride (hBN) encapsulated monolayer TMDs with super clean and flat surfaces realized by a graphene-capping-assisted AFM nanosqueezing (GCAN) method [2] and corresponding field-effect transistors (FETs) with low contact resistance to explore the transport behaviors of excitonic carriers. Using these FETs, trions can basically be driven by the bias voltage, which allows us to actively control the motion of excited states in 2D TMDs. The details will be discussed at the presentation. [1] Chernikov. A et al. Phys. Rev. Lett. 113, 076802 (2014). [2] Takato. H et al. ACS Nano. 15, 1, 1370–1377 (2021).

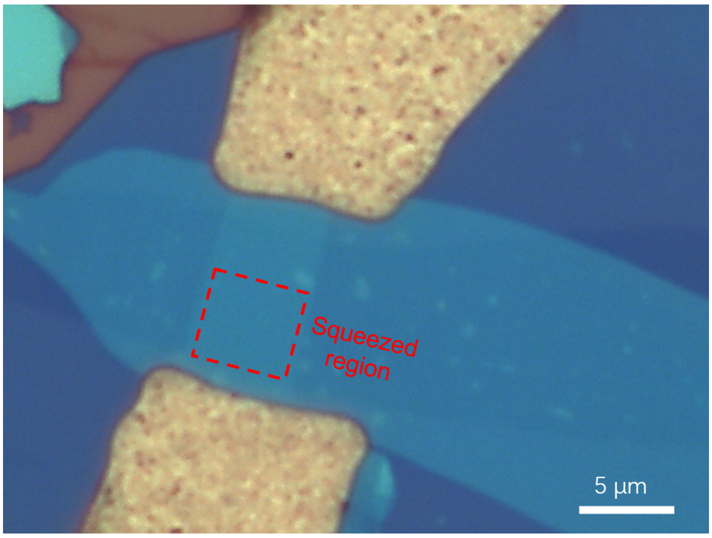

Fig. 1: An optical image of a FET based on a Van der Waals heterostructure cleaned by GCAN method.

C112: One-dimensionality of Thermoelectric Properties of Semiconducting Single-Walled Carbon Nanotubes

Yota Ichinose*†, Manaho Matsubara, Yohei Yomogida, Akari Yoshida, Kan Ueji, Kaito Kanahashi, Jiang Pu, Taishi Takenobu, Takahiro Yamamoto, Kazuhiro Yanagi

**Tokyo Metropolitan University*

Thermoelectrics is an important technology for the efficient conversion of waste heat to electrical power. Theoretical studies suggested that lowering the dimensionalities can enhance thermoelectric (TE) performance due to the following two factors, (1) the quantum confinement effect and (2) the reduction of thermal conductivity [1]. The reduction of thermal conductivity by fabrication of nano-structures has been well confirmed, however, experimental verification of how low-dimensional electronic structures enhance TE performance remains elusive. Single-walled carbon nanotube (SWCNT) is a very good model for studying relationships between one-dimensional (1D) electronic structure and TE properties. Our recent study revealed the unique 1D characteristic in their TE properties [2,3]. For example, in conventional metallic materials, the increase of their electrical conductivity (σ) induces the decrease of their Seebeck coefficient (S), which is known as TE trade-off. By contrast, metallic SWCNTs violate the trade-off. We can observe the enhancement of both S and σ because of the presence of van-Hove singularity (vHs), reflecting 1D metallic electronic structures [2]. Regarding semiconducting SWCNTs, however, it is difficult to discuss 1D characteristics in the behaviors of S and power factor (P). The line-shapes of S and P as a function of chemical potential (μ) in one-, two, three dimensional semiconductors exhibit almost the same [3]. For example, Fig. 1 shows the relationships between S and μ for 3D, 2D, and 1D semiconductors, which are calculated based on Boltzmann transport theory. As shown in the figure, any trances reflecting dimensionalities cannot be observed in S vs μ.However, a recent theoretical study pointed out the importance of ”thermoelectrical conductivity,” L12 [4]. Only in the case of 1D materials, a sharp peak structure can be observed around first vHs in L12. Thus, in this study, we investigated L12 of high-purity semiconducting (6,5) SWCNTs with the purity more than 99%. As a result, L12 as a function of σ shows a peak structure at σ ~1.6×104 (Fig. 2). According to the comparison with the Kubo-Lüttinger theory, we found that this peak structure is caused by the vHs of 1D semiconductor [3]. In this poster presentation, we will discuss the background.References: [1] Hicks & Dresselhaus, Phys. Rev. B 47, 16631 (1993), [2] Ichinose et al., Nano Lett. 19, 7370 (2019), [3] Ichinose et al., Phys. Rev. Mater. 5, 025404 (2021) [4] Yamamoto & Fukuyama, J. Phys. Soc. Jpn. 87, 114710 (2018) *Acknowledgements:* We acknowledge support by JSPS KAKENHI and JST CREST.

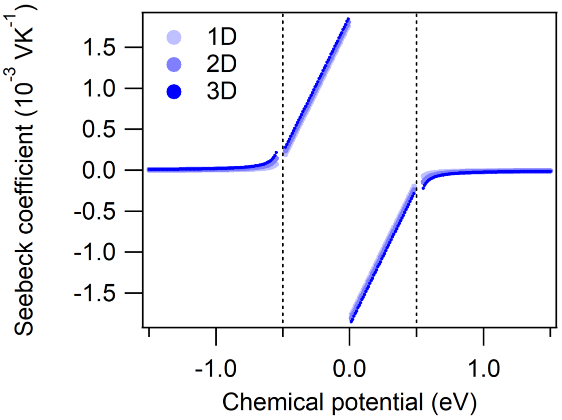

Fig. 1: Chemical potential dependence of the Seebeck coefficient in 3D, 2D, and 1D semiconductor model. The dashed lines show band edges of semiconductors (±0.5 eV).

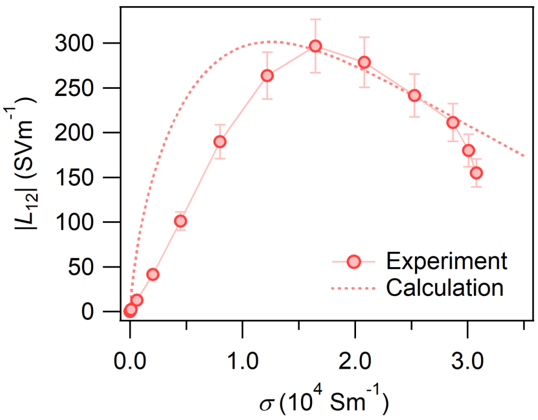

Fig. 2: Thermoelectrical conductivity (L12) of high-purity semiconducting (6,5) SWCNTs as a function of electrical conductivity. The dashed plot is calculated by the Kubo-Lüttinger theory.

C113: Effect of annealing treatment on mechanical properties of aerographite particles

Yuexuan Li*†, Hiromu Hamasaki, Kaori Hirahara

**Osaka University*

Aerographite is an ultralight carbon material with a unique hollow structure [1]. The hollow structure morphology is derived from the zinc oxide (ZnO) during fabrication. A micrometer-sized sea-urchin-like cage structure of aerographite can be fabricated by choosing a ZnO nanorod-microsphere [2] as the template [3]. Previous studies showed that these particles have extremely flexible behavior based on single-particle-level compression tests conducted using a manipulator in a scanning electron microscope (SEM). The observed flexible behavior originated in a unique cage structure of the aerographite [3]. However, graphitic layers of the pristine aerographite particles were still defective. This observation demonstrated that the mechanical property could be improved by the annealing treatment. This study investigated the effect of annealing treatment on the mechanical properties of aerographite particles. The aerographite particles were annealed in an argon atmosphere at three different temperatures: 800°C, 1600°C, and 2000°C. SEM observations of the annealed particles showed thermal stability with remaining spiky-shell morphologies. A structural change on the nanorod graphitic layers of the aerographite particles was observed using transmission electron microscopy. The crystallinity improved as the annealing temperature increased. Results from the single-particle-level compressive tests indicated that most of the microparticles demonstrated linear elastic behavior with strains of less than 30%. The Young's moduli of individual particles tended to be larger when annealed at higher temperatures. The higher Young's moduli were probably due to the higher crystallinity of the graphitic layers or coalescence of the neighboring nanorods at connected parts. Coalescence of the neighboring nanorods at the connected parts was occasionally observed when particles were annealed at 2000°C. The particles annealed at 2000°C showed the highest Young's modulus values. However, some of these particles reached their critical point faster than the other particles. The microparticles annealed at 1600°C had lower Young's modulus values than those annealed at 2000°C. However, most of these particles showed excellent flexibility and had almost 100% recovery to their original size after compression with a 77% strain. The excellent size recovery may have resulted from the ultra-flexible connected parts of the neighboring nanorods and less defective layers. [1] M. Mecklenburg, et al. Adv. Mater. 24, (2012) 3486. [2] Y. Hirota, et al. Chem. Lett. 43, (2014) 360. [3] K. Hirahara, et al. Carbon 118, (2017) 607. *Acknowledgements:* This work was supported by JSPS KAKENHI Grant Number 19K21920.

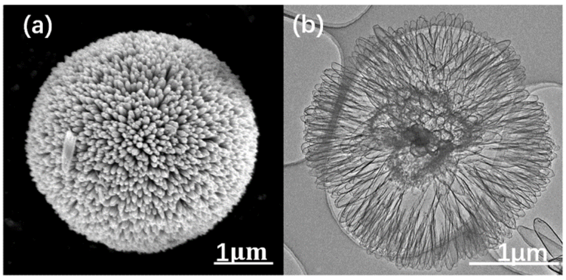

Fig. 1: (a) A SEM image of a ZnO nanorod-microsphere used as the template (b) A TEM image of a typical aerographite particle.

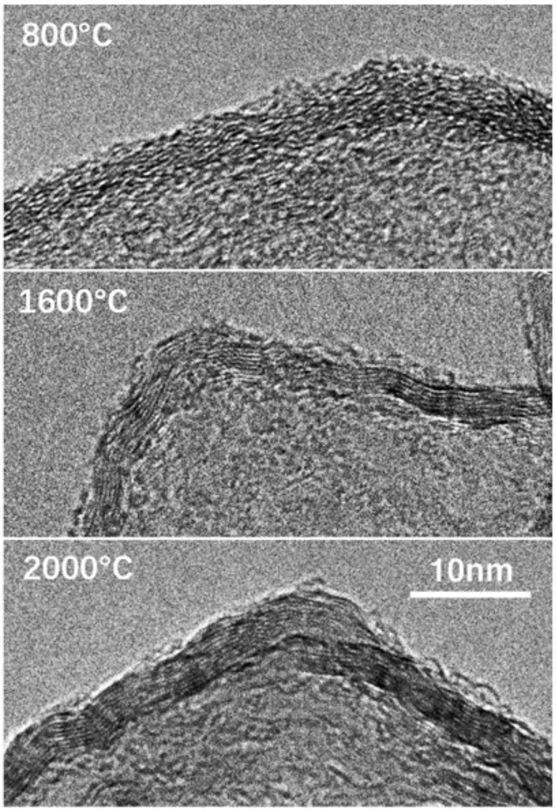

Fig. 2: TEM images of the graphitic layers of the nanorods consisting the aerographite particles annealed at different temperatures.

C114: A light emitter based on polycrystalline graphene patterned directly on silicon substrates from a solid-state carbon source

Kenta Nakagawa*†, Hidenori Takahashi, Yui Shimura, Hideyuki Maki

**Kanagawa Institute of Industrial Science and Technology (KISTEC), Japan*

Graphene light emitters integrated on silicon chips are being developed as an alternative to conventional light sources based on compound semiconductors. Graphene light emitters based on the thermal radiation of graphene by transforming an electrical current into Joule heat are expected due to its (i) broad infrared emission by blackbody radiation, (ii) good compatibility to microfabrication technology, (iii) fabricating inexpensively on a silicon substrate, and (iv) direct modulation with a response speed of less than 100 ps (frequency 10 GHz) [1].In general, graphene sheets are conventionally obtained by (i) mechanical exfoliation method or (ii) CVD. However, both methods require a transferring process, graphene growth methods that allow for direct formation on silicon substrates have been sought after and several attempts have been reported.In this study, we developed a procedure to grow polycrystalline graphene from a solid-state carbon source directly on silicon substrates. To reduce the complexity of the process, the number of steps, and the cost, we have also developed a direct patterning procedure that allows to produce graphene samples with arbitrary position, size, and shape.The optical microscope image of the directly patterned graphene is shown in Fig. 1(a). As shown in Fig. 1(a), graphene samples with various positions, sizes, and shapes were successfully grown. The directly patterned graphene was characterized using Raman spectroscopy (Fig. 1(b) and (c)). It is founded that the graphene is few layers and polycrystalline from the intensity ratio of the G and 2D band and the presence of the D band.In addition, we have demonstrated that our polycrystalline graphene operates in light emitting devices. The optical microscope image of the directly patterned graphene based light emitter is shown in Fig. 2(a). As shown in Fig. 2(b), the emission is highly localized in the graphene region. Fig. 2(c) shows the spectra of the light emitted by the graphene device. The broad spectra in the near IR region can be modelized with Planck's law, and the emission from the directly patterned graphene is considered blackbody radiation generated by Joule heating.Direct patterning graphene based light emitting devices integrated on silicon chips are expected to open new routes to the realization and commercialization of next-gen optical interconnects and silicon photonics.References[1] Y. Miyoshi et al., Nat. Commun., 9 (2018) 1279. [2] K. Nakagawa, et al., RSC Advances, 9 (2019) 37906. *Acknowledgements:* This work was supported by a project of KISTEC, KAKENHI (20H02210 and 20K14783) from JSPS and A-STEP (JPMJTR20R4) from JST.

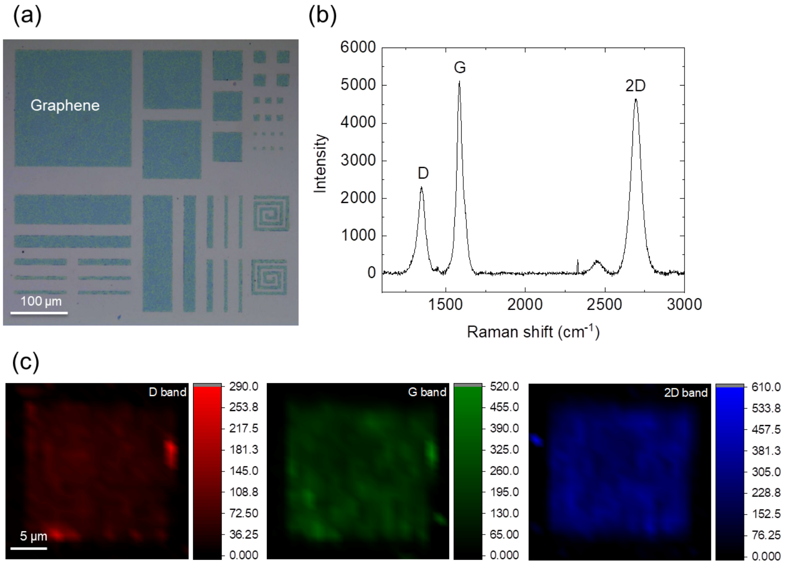

Fig. 1: Optical microscope image (a), Raman spectrum (b) and the D, G, and 2D band Raman mapping images (c) of the direct patterning graphene. Reproduced with permission from RSC.

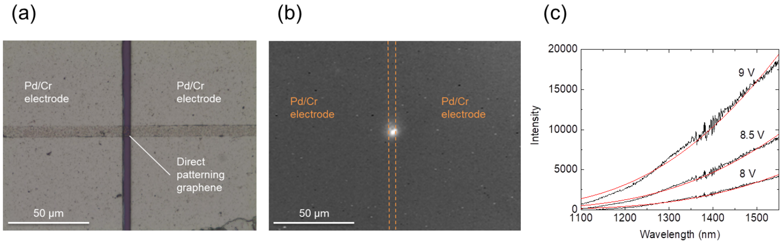

Fig. 2: Optical microscope image (a), IR camera image (b) and emission spectra (c) from the direct patterning graphene light emitter. Reproduced with permission from RSC.

C115: Sonochemical reaction to control the near-infrared photoluminescence properties of single-walled carbon nanotubes

Yui Konno*†, Akane Nishino, Michio Yamada, Yutaka Maeda, Yuhei Miyauchi, Kazunari Matsuda, Jun Matsui, Masaya Mitsuishi, Mitsuaki Suzuki

**Tokyo Gakugei University*

Sidewall functionalization of single-walled carbon nanotubes (SWNTs) has been attended to as an effective method to control their solubility and to add new functionality. Recently it has been revealed that chemical functionalization is effective to emerge new photoluminescence (PL) in the near-infrared region. Therefore, the chemical functionalization of SWNTs is attracted to enhance their usability as bioimaging materials, optical devices, and so on. PL spectra of SWNTs are one of the effective analyses for the assignment of semiconducting SWNTs. For the preparation of the SWNTs PL sample, it is necessary to avoid the interaction between each SWNTs and concentration quenching. Therefore, low concentrated and individually dispersed SWNTs are preferred for the measurements. Typically, the sonication in surfactant D2O solution and subsequent ultracentrifugation is applied to prepare SWNT dispersions. However, it has been reported that sonication induces shortening and damaging of SWNTs. On the other hand, sonication induces radical decomposition of sodium dodecyl sulfate (SDBS), which is known as a typical surfactant for SWNTs dispersion. In this study, we studied the effect of the radical decomposition of SDBS on the PL properties of SWNTs. We compared the difference between SDBS, Sodium dodecyl sulfate (SDS), and Sodium cholate (SC) as a typical surfactant in absorption and PL spectra. The absorption spectra showed typical absorption spectra of SWNTs, which indicates each surfactant is effective as a dispersant reagent for SWNTs. The PL intensity of SWNTs dispersed in SDS solution showed lower than SWNTs dispersed in SC solution, neither emerged new PL peaks. By contrast, new PL peaks emerged at 1043 and 1118 nm in SDBS solution when low concentrated SWNTs were used for the sonication. The new PL peak intensity increased as increase of irradiation time. The treated SWNTs had been further analyzed by Raman and XPS spectra to clarify the factor in the PL characteristic changing. In the presentation, we discuss other factors and the mechanism of PL changing by the sonication. We should notice that sonication affects the PL properties of SWNTs depending on the dispersion condition. *Acknowledgements:* KAKENHI (Grant number JP17H02735 and JP21H01759)

C116: Study of dense colloidal catalyst nanoparticle deposition for super high-density CNT forest

Kento Tabata†, Yuga Kono, Takayuki Nakano, Yoku Inoue*

**Shizuoka University*

High-density CNT forests are expected to be applied to interfacial thermal materials and interlayer wiring materials. In conventional CNT synthesis using Fe thin film formed by sputtering as a catalyst, the size and density of nanoparticle results from the thickness of Fe film for thermodynamic reasons, and a maximum density is limited by the dewetting-limit, which is lower than the close-packed density. In this study, we tried to deposit high density nanoparticles using colloidal particles so that the size and density are independently controlled. We investigated the relationship between the control of loading density of colloidal iron oxide nanoparticles and the CNT forest synthesis mechanism to achieve super high- density synthesis beyond the dewetting-limit. Colloidal iron oxide nanoparticles were prepared by a polyol method. The colloidal particles with varying concentration were spin-coated onto an Al2O3 layer deposited on a thermally oxidized Si substrate. In the CNT forest growth by CVD, acetylene was used as the carbon source, hydrogen as the reducing gas, and argon as the carrier gas. As the colloidal density was increased from 0.5 µg/mL to 10 µg/mL, the mass density of the CNT forest increased linearly from 0.8 mg/cm3 to 50.5 mg/cm3. It was found that the activity of the catalyst in the growth of CNTs was almost the same even when the loading density of nanoparticle was changed significantly. We also controlled the loading density by multiple coatings of colloidal particles. In this study, the mass density of the CNT forest increased as the number of coatings increased. However, beyond a certain number of times, the density decreased due to nanoparticle aggregation. We discuss the relationship between the CNT growth mechanism and forest mass density in several nanoparticle deposition methods.

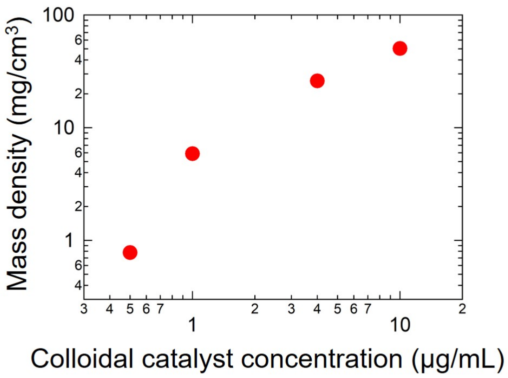

Fig. 1: The relationship between CNT forest mass density and colloidal catalyst concentration.

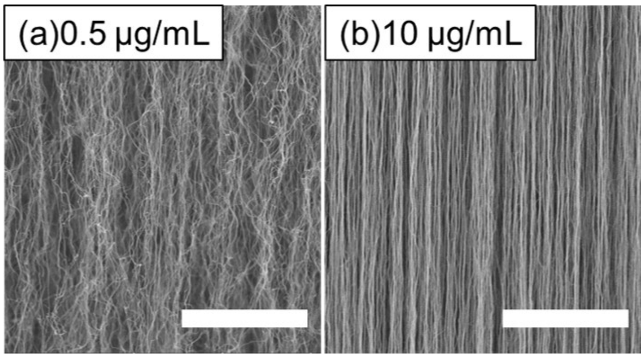

Fig. 2: Comparison of CNT forests grown from nanoparticle density of (a) 1.0 µg/mL and (b) 10 µg/mL. Scale bars show 2 µm.

C117: Device Applications of One-Dimensional van der Waals Heterostructure Nanotubes

Ya Feng*†, Henan Li, Taiki Inoue, Slava V. Rotkin, Rong Xiang, Shigeo Maruyama

**the University of Tokyo*

The synthesis of one-dimensional van der Waals heterostructures was realized recently[1], which offers alternative possibilities for prospective applications in electronics and optoelectronics. The even reduced dimension will enable different properties and further miniaturization beyond the capabilities of their two-dimensional counterparts. The natural doping results in p-type electrical characteristics for semiconducting single-walled carbon nanotubes, while n-type for molybdenum disulfide with conventional noble metal contacts. Therefore, we demonstrate here a one-dimensional van der Waals heterojunction diode from a heterostructure nanotube of 11-nm-wide, with the coaxial assembly of semiconducting single-walled carbon nanotube, insulating boron nitride nanotube, and semiconducting molybdenum disulfide nanotube which induces a radial semiconductor-insulator-semiconductor heterojunction[2]. When opposite potential polarity was applied on semiconducting single-walled carbon nanotube and molybdenum disulfide nanotube, respectively, the rectifying effect was materialized. 1. Xiang, R., et al., One-dimensional van der Waals heterostructures. Science, 2020. 367(6477): p. 537.2. Feng, Y., et al., One-Dimensional van der Waals Heterojunction Diode. ACS Nano, 2021. 15(3): p. 5600-5609.ACKNOWLEDGMENTSPart of this work was supported by JSPS KAKENHI Grant Numbers JP18H05329, JP20H00220, and by JST, CREST Grant Number JPMJCR20B5, Japan. Work of S.V.R. was supported by the National Science Foundation (Grant DMR-2011839).

C118: A Semi-Grand Canonical ddKinetic Monte Carlo study of Single-Walled Carbon Nanotubes growth

Georg Daniel Förster*†, Christophe Bichara

**Aix Marseille University*

Carbon nanotubes are crystals that display a large variety of different allotropes, with given chiralities defined by the Hamada indices (n, m). Control over carbon nanotube chirality is required if one is to exploit their full potential in technological applications. Developing methods of chirality-selective production has been a long-standing challenge.Classically, crystals are formed by nucleation and growth. The former is dominated by the thermodynamic stability of the nucleus, while kinetics is central to the latter. We recently developed a thermodynamic model of the catalyst-tube interface where the fluctuations of the interface structure and the associated entropy were found to be responsible for the stability of the so-called ”chiral” tubes, those which are neither armchair nor zigzag [1]. In this contribution, we explore growth kinetics, using the simplest possible kinetic Monte Carlo (kMC) simulations on a fixed lattice unique to each helicity. Again, we use a simple energetic model that relies on the interface energies of the armchair and zigzag edge atoms as parameters. In our thermodynamic model, the number of armchair (2m) and zigzag (n-m) edge atoms was individually conserved for a (n, m) chirality.We use semi-grand canonical kMC simulations to sample the model in which pairs of atoms are added or removed at the reactives sites, between zigzag and armchair atoms (cosy corners). Barrier states correspond to the incorporation or removal of the first atom of the pair, and a second atom is subsequently placed or removed to complete the hexagon at the interface. Barrier and interfacial energies are parameters of the model. Our goal is to study how such model crystals can grow, and how kinetics may influence selectivity. Series of simulations were carried out, varying parameters (temperature, chemical potential, interface and barrier energies). This allows us to uncover several growth mechanisms and shows the interplay between experimental conditions (temperature, chemical potential), the energetics of the interface and the growth rates, which depend on chiral angles and follow non-monotonic trends. This allows to identify conditions for selective growth. [1] Magnin et al., Science 362, 212 (2018) *Acknowledgements:* The support from the French research funding agency (ANR) under Grant No. 18-CE09-0014-01 (GIANT) is gratefully acknowledged.

C119: Optical properties of two-dimensional transition metal dichalcogenides functionalized with Phenyl-C61-butyric acid derivatives

Ruben Canton Vitoria*†, Ryo Kitaura

**Department of Chemistry, Nagoya University, Nagoya 464-8602, Japan.*

Two-dimensional transition metal dichalcogenides (2DTMDs) have attracted significant interest due to their excellent optical and electronic properties along with air stability at room temperature. Commonly, the composition of representative semiconductor TMDs can be written as MX2, wherein M is Mo or W and X is S, Se, or Te. The excitonic nature of optical responses in TMDs allows them to interact with light strongly, showing characteristic signatures arising from excitons, trions, biexcitons, and B-excitons in optical spectra. Due to the atomically thin structure, surface modification can lead to the tuning of optical responses of TMD, leading to the emergence of new excitonic species.Depending on the relative position of valence and conduction band to molecular orbitals, 2DTMDs can accept or provide electrons when they interact with organic chromophores such as porphyrins[i], Phthalocyanines[ii], and quantum dots. In this presentation, we compare the optical properties of MoX2 and WX2 (X= S, Se, and Te) functionalized by Phenyl-C61-butyric acid linked with Cysteine (C61-Cys). The thiol group in C61-Cys can interact through an organometallic bond with TMDs chalcogen vacancies, allowing an easy purification and abolishing the high-loading of aggregations. [iii] We have successfully distinguished both emissions from TMDs and C61-cys, and we found that new emission peaks were seen in some of those materials. Based on the vacuum energy level of TMDs and the position of HOMO and LUMO of C61-cys (-3.7 and -6.1eV), we will assign the origin of those new emissive bands. [i] Ruben Canton Vitoria, Tobias Scharl, Anastasios Stergiou, Alejandro Cadranel, Raul Arenal, Dirk M. Guldi, Nikos Tagmatarchis ACIE, 2020, 10, 3976-3981. [ii] R. Canton-Vitoria, H. B. Gobeze, V. M. Blas-Ferrando, J. Ortiz, Y. Jang, F. Fernández-Lázaro, Á. Sastre-Santos, Y. Nakanishi, H. Shinohara, F. D'Souza, N.Tagmatarchis. ACIE, 2019, 58, 5712-5717. [iii] L. Vallan, R. Canton-Vitoria, H.B Gobeze, Y. Jang, R. Arenal, A. M. Benito, W. K. Maser, F. D'Souza, N. Tagmatarchis. JACS, 2018, 41, 13488-13496 *Acknowledgements:* This material is also based upon work supported by Japan Society for the Promotion of Science (JSPS) postdoctoral fellowship grant agreement

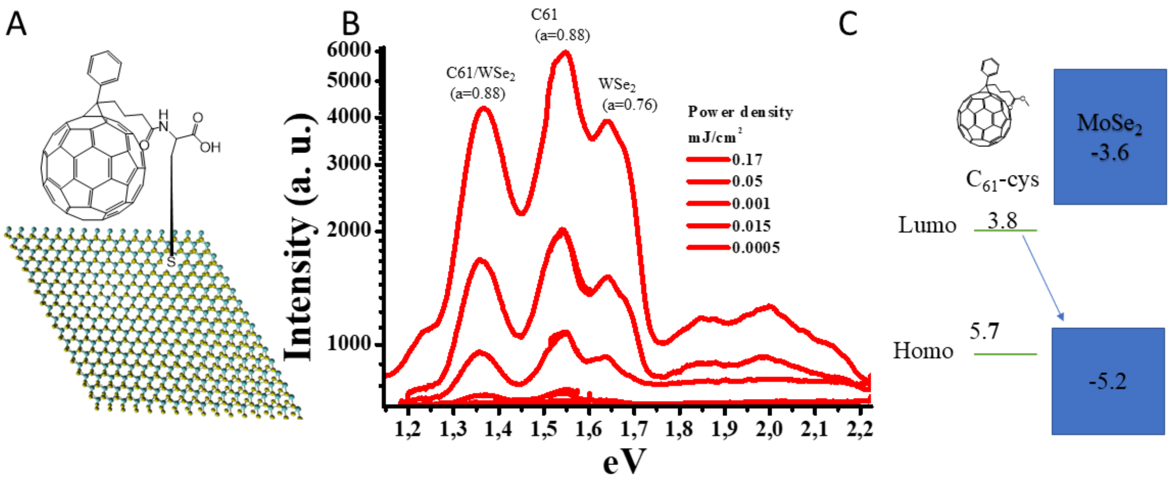

Fig. 1: Figure1. (a) Representative picture of TMDs layer carrying C61-Cys. (B) PL emission at different under 532 laser irradiation at different powers densities of WSe_2-C61 and (C) Orbital diagram.

C120: Limited heat conduction in graphene by isotopic interfaces

Yoshito Hata†, Takayuki Arie*, Kuniharu Takei, Seiji Akita

**Osaka Prefecture University*

Graphene is expected as a candidate for thermal management devices due to its outstanding thermal properties. Since the main heat carrier in graphene is phonon, the heat transport in graphene can be controlled by introducing isotope interfaces that act as a phonon scatterer. In this study, we investigate the effect of the phonon mean free path reduced by isotopic interfaces on the heat conduction in graphene. We synthesized isotopically separated graphene heterostructures with isotopic interfaces by suppling $^{12}CH_4$ and $^{13}CH_4$ alternately during chemical vapor deposition. Figure 1(a) and 1(b) show the optical microscope and Raman mapping images of graphene heterostructures. The grown heterostructure is single-crystalline graphene composed of 12C (12C-graphene) and 13C (13C-graphene) periodically. Typical Raman spectra from the heterostructures (Fig. 1(c)) show that 12C (13C) peaks appear with 13C (12C) subpeaks in the 12C-grapene (13C-graphene) region because of the diffraction limit of the microscope. Heat conduction was measured by measuring the temperature dependence of the Raman peak shift of the suspended heterostructures when the number of the interfaces (N) changes. The thermal resistance of the suspended heterostructures increases linearly as N increases up to N=3, indicating that the heat conduction is considered as in the diffusive regime. However, the thermal resistance significantly increases when N is more than four, where the distance between the interfaces becomes smaller than the phonon mean free path at room temperature (≈600 nm), implying that thermal phonons behave in the quasi-ballistic transport regime. The increased thermal resistance results in the decreased thermal conductivity of graphene with N=5 by almost 85%

relative to the thermal conductivity of graphene (N=0). *Acknowledgements:* This study was partially supported by JSPS KAKENHI Grant Number JP19H02082.

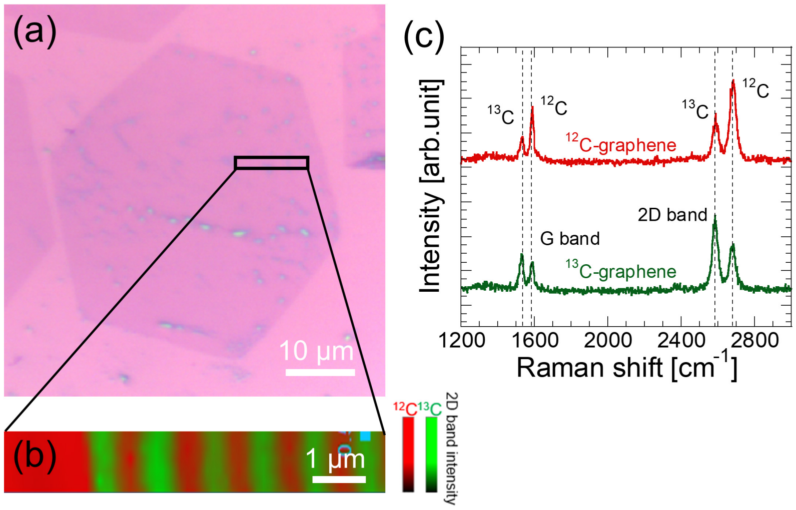

Fig. 1: (a) Optical microscope and (b) Raman 2D mapping images of isotopic heterostructures in a single crystalline graphene. (c) Raman spectra from the graphene heterostructures.

C121: Rayleigh Scattering Spectra from SWCNT@BNNT with Water Adsorption

Koki Kozaki*†, Masanori Bamba, Shu Sato, Satoshi Yotsumoto, Shigeo Maruyama, Shohei Chiashi

**the University of Tokyo*

The synthesis of one-dimensional hetero structure was recently reported[1], and its properties have attracted much attention. Especially, the optical properties of single-walled carbon nanotube wrapped with boron-nitride nanotube (SWCNT@BNNT) are very interesting, Because the properties of SWCNTs are sensitive to the surrounding conditions, it is expected that BNNT works as the protective layer for inner SWCNTs. However, their optical properties are still unclear. In this study, we measured Rayleigh scattering spectra from SWCNT@BNNTs in various conditions and investigated its optical properties. First, we synthesized SWCNTs with ACCVD method on a slit substrate, and then we synthesized boron-nitride layer on SWCNT using BNCVD method. To control the environment around SWCNT@BNNTs, we built up an environmental chamber suited for measuring Rayleigh scattering lights. As shown in Fig. 1, we obtained Rayleigh image of SWCNT@BNNT. Rayleigh scattering spectra was also obtained and some of SWCNT@BNNTs showed clear peaks originating from the van Hove singularity of the inner SWCNT. As the chamber was evacuated, the thermal energy loss due to heat transfer from SWCNT@BNNTs became smaller and SWCNT@BNNTs under the incident laser irradiation were heated up. As the result, the peaks in Rayleigh scattering spectra shifted to lower energy. Next, we introduced water vapor and air in the chamber, respectively, and measured Rayleigh spectra with different pressure. With increasing water vapor pressure, the peak shifted to higher energy, as shown in Fig. 2 (a).The pressure dependance of water vapor and air on the peak energy was shown in Fig. 2 (b). In the low pressure range, there was no difference between water and air cases. On the other hand, in the case of air, the optical transition energy was almost the constant above a pressure, indicating that water molecules adsorbed on the most outer surface of SWCNT@BNNT. [1] R. Xiang, T. Inoue, Y. Zheng, A. Kumamoto, Y. Qian, Y. Sato, M. Liu, D. Gokhale, J. Guo, et al., "One-dimensional van der Waals heterostructures," Science . 542, 537 (2020).

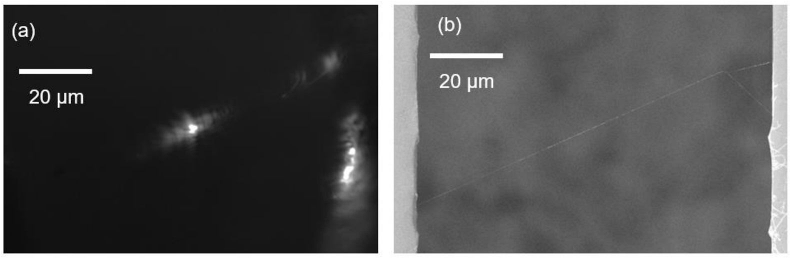

Fig. 1: (a) Rayleigh scattering image and (b) SEM image of suspended SWCNT@BNNT.

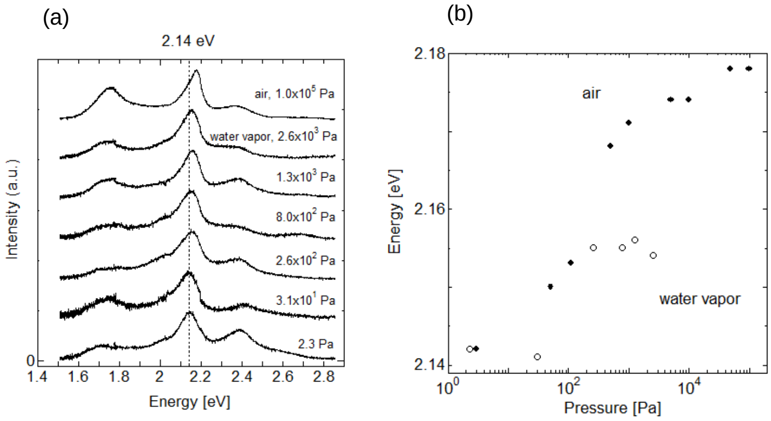

Fig. 2: (a) Rayleigh spectra of SWCNT@BNNT under different water vapor pressure. (b) Pressure dependence of the transition energy of SWCNT@BNNT. Solid circles for air and open circles for water vapor,

C122: Templated Synthesis of MoS_2 Single Crystal Nanotubes Inside Carbon Nanotubes

Jia Guo[†], Yan Li*

**Peking University*

A class of new material has recently attracted much attention, in which carbon nanotubes and other inorganic nanotubes are coaxially stacked through van der Waals (vdW) interactions to form one-dimensional vdW heterostructures[1]. Via a one-step chemical vapour deposition (CVD) method, we realized the controlled growth of molybdenum disulphide (MoS_2) nanotubes encapsulated within carbon nanotubes (CNTs) employing the CNT as a structural template and Fe5C2 as the catalyst. We could further obtain the MoS_2 nanotubes of single crystalline by using plasma to decently remove outer carbon layers. Our findings are expected to give a significant boost to the synthesis of one-dimensional vdW heterostructures and nanotubes of inorganic materials.Reference:[1] Xiang, R.; Inoue, T.; Zheng, Y., et al., Science 367, 537-542 (2020).

C123: Nano Structure Fabrication of 1D and 2D hetero materials using direct and epitaxial growth and transfer method

Shu Sato*[†], Daisuke Ito, Yuta Fujisaki, Kenta Kusakabe, Keigo Otsuka, Shigeo Maruyama, Shohei Chiashi

**the University of Tokyo*

Single-walled carbon nanotube is expected to be used as optoelectronic device elements because of its high charge mobility and special optical properties. However, photoelectronic conversion on substrates is not realized because the optical properties are degraded on substrates. Hexagonal boron nitride (h-BN) is atomically flat and 2-dimensional nonconductor, and it is reported that SWCNT on h-BN substrate exhibits photoluminescence because h-BN has no dangling bonds. In Graphene/h-BN van der Waals heterostructure and SWCNT wrapped by BN nanotube (SWCNT@BNNT), BN acts as protective layer, and graphene and SWCNT hold excellent properties. In order to apply the hetero-structured nanomaterials to device, it is important to develop the nano-structure fabrication techniques both in the synthesis stage and after synthesis. In this study, we performed the nano-structure fabrication, based on chemical vapor deposition (CVD) growth techniques of SWCNTs and graphene/h-BN, and the mechanical transfer methods.Graphene was grown epitaxially on h-BN on sapphire substrate by CVD process using acetylene as the carbon source, as shown in Fig. 1. The synthesized graphene flake was one- or two-layered and the orientation angle was almost uniform within the single BN domain.Aligned SWCNTs on Si substrate were prepared by transferring SWCNTs grown on single-crystal quartz substrate or directly synthesizing using gas-flow oriented CVD process. Mechanically exfoliated h-BN and synthesized SWCNTs were transferred onto silicon substrates with prefabricated metal electrodes by PPC and PDMS polymer. The fabricated structure including SWCNTs were characterized by Raman scattering imaging of the G-band intensity, as shown in Fig. 2. The combination of hetero synthesis and their integration would enable the fabrication of more precise structures than before.

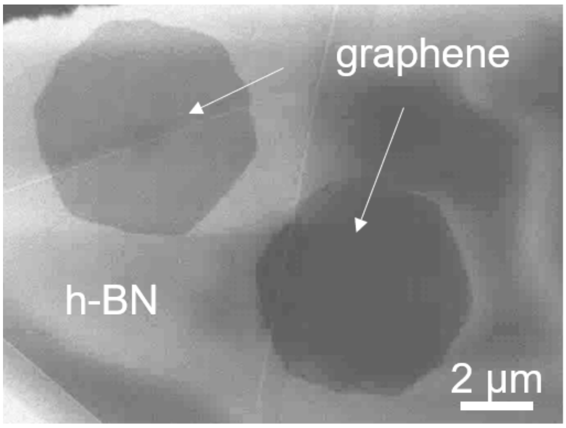

Fig. 1: SEM image of epitaxially grown graphene on h-BN by CVD process

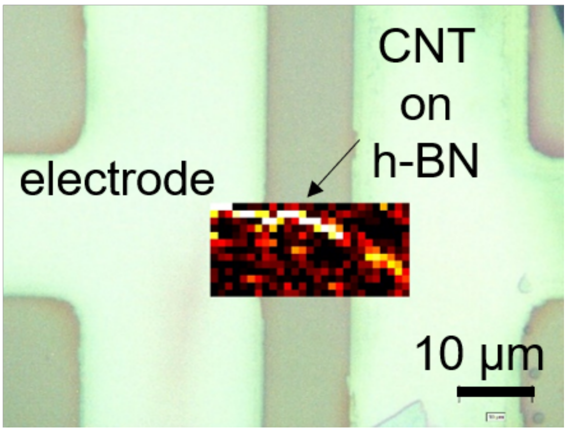

Fig. 2: G-band Raman scattering image of a SWCNT on h-BN transferred on pre-patterned electrode

C124: Hydrogen storage in boron doped carbon nanotubes: Role of dopant concentration

Shrilekha Sawant*†, Seemita Banerjee, Ashwin W Patwardhan, Jyeshtharaj B Joshi, Kinshuk Dasgupta

**Institute of Chemical Technology, Mumbai, India*

Chemical vapor deposition (CVD) is one of the widely used methods for the synthesis of pristine carbon nanotubes (CNTs) and doped carbon nanotubes. Herein, we report a simple and scalable method for synthesizing boron-doped CNTs (B-CNTs) using the floating catalyst chemical vapor deposition (FC-CVD) technique. Ethanol, ferrocene, and boric acid were utilized as carbon source, catalyst, and boron precursor respectively. Effect of boric acid concentration on the properties and extent of incorporation of boron into graphitic lattice were explored. The synthesized B-CNTs were characterized using electron microscope analysis, X-ray photoelectron spectroscopy (XPS), Raman spectroscopy, thermogravimetric analysis (TGA), etc. The boron content in the synthesized product varied from 0 to 8.00 at% which was controlled by inlet boron precursor concentration. Moreover, from Raman spectroscopy, it can be observed that full-width half maxima of D band increase with boron content. The metallic impurities in the synthesized boron-doped carbon nanotubes were less than 8 wt% as confirmed by TGA. In literature, there has been growing evidence showing that doping heteroatoms (like N, B, P, S, etc.) into the CNT framework can remarkable alter the electrochemical and physical properties of carbon materials. However, it lacks the correlation between hydrogen adsorption and the amount of a specific type of dopant. Hence, the main focus of the work is to study the hydrogen adsorption dependence on boron doping in carbon nanotubes. The maximum hydrogen adsorption recorded was 0.497 wt% at 273 K and 16 bar with~3.86 at% B-CNTs. It was observed that hydrogen adsorption values do not vary linearly with boron content in B-CNTs. It can be concluded that crystallinity and defect play a vital role in hydrogen adsorption. Hydrogen adsorption data with time were analyzed for the adsorption model which was found to be well fitted by the pseudo second-order model. In addition to this, hydrogen adsorption repeatability for B-CNTs with maximum hydrogen adsorption was also studied. *Acknowledgements:* Authors would like to acknowledge DAE-ICT for funding this work.

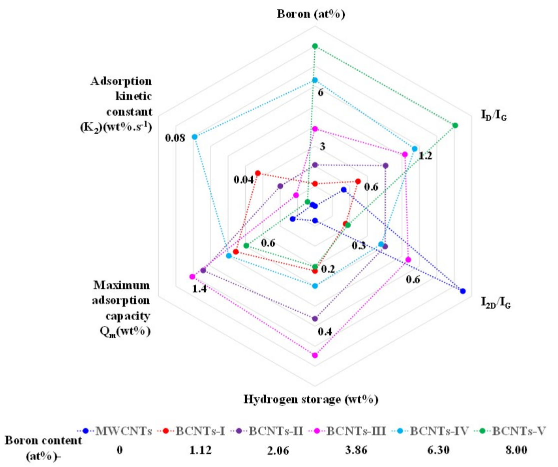

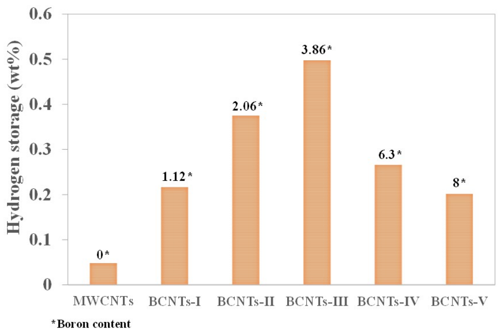

Fig. 1: Hydrogen storage performance comparison spider chart for with varying boron content BCNTs

Fig. 2: Bar chart for different boron content B-CNTs and their hydrogen adsorption values

C125: Supercapacitor Electrode with High Charge Density using Boron-based Covalent Organic Frameworks-derived Porous Carbon

Shigeyuki Umezawa*†, Takashi Douura, Koji Yoshikawa, Daisuke Tanaka, Yasuhiko Hayashi

**Graduate school of Natural Science and Technology, Okayama University, Okayama*

We attempted to synthesize boron (B)-doped porous carbons by a simplistic process (Figure 1). Carbonizing B-based covalent organic frameworks (COF-5) produced non-porous carbon (CCOF-5) with boron oxides (B2O3). The specific surface area SBET of the sample was around 80 m2 g-1. Subsequently, B-doped porous carbons (WCCOF-5) were successfully by readily washing CCOF-5 with gentle water to remove B2O3, resulting in the SBET of around 800 m2 g-1. The process can be considered very facile and safe compared to use of strong acids, such as hydrofluoric (HF) or hydrochloric acid (HCl), which are hazardous. To demonstrate the feasibility of energy storage devices, the electrochemical properties of COF-5 derived carbons were tested for supercapacitor electrode materials. Higher charge density (~15 mF cm-2) was achieved compared to the conventional activated carbons (~7 mF cm-2) due to the pseudocapacitive effect induced by B atoms in the carbon frameworks, when using organic electrolytes (Figure 2). Further, the carbons exhibited the capacitance retention of 72 % after 10000 galvano charge/discharge cycling tests. *Acknowledgements:* We would like to Dr. Y. Takashima, Ms. M. Yoneda, Prof. K. Gotoh, Dr. V. Stolojan and Prof. S. R. P. Silva for experimental support and disc

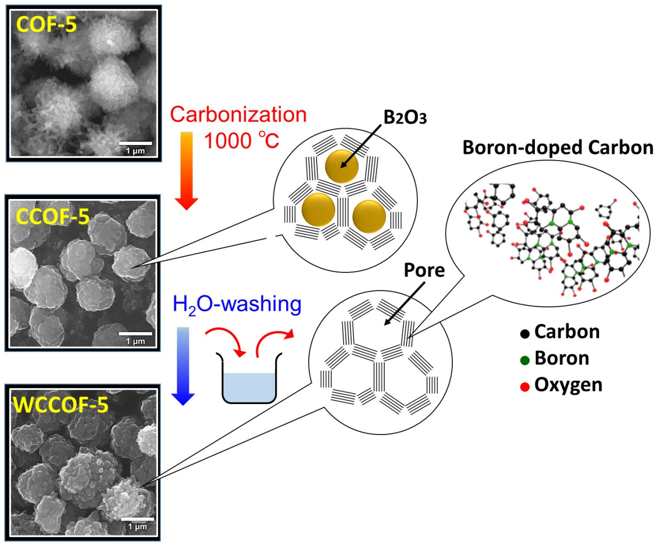

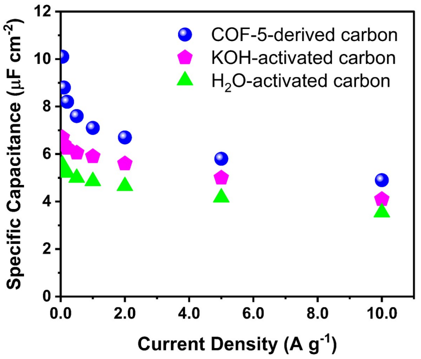

Fig. 1: Schematic of the process to produce COF-5-derived Boron-doped porous carbons.

Fig. 2: Specific capacitance of COF-5 derived carbon, KOH-activated carbon, and H2O-activated carbon recorded at 0.05–10 A g−1.

C126: Photoactivated gas responses of gas sensor based on MoS_2 monolayers to various biogas species

Taishi Goto[†], Ryota Inao, Hiroshi Tabata*, Mitsuhiro Katayama, Osamu Kubo

Osaka University

Thin layers of molybdenum disulfide (MoS_2) have been attracting attention as an excellent gas sensing material, because it has a unique property to exhibit an effective photoactivated gas response under visible light, resulting in excellent sensitivity and a fast response and recovery at room temperature [1]. We have recently shown that the photoactivated gas response of the MoS_2 sensor to NO2 gas is due to the carrier mobility modulation of MoS_2, caused by the dipole scattering of adsorbed NO2 molecules, rather than to changes in the carrier density caused by the charge transfer mechanism [2]. However, the gas response of the MoS_2 sensor under light illumination has yet to be investigated for only a few gas species. In this study, we investigated the effect of light illumination on the response to various biogas species such as NH3, CH4, H2, and ethanol and acetone vapors. Figure 1 shows the dynamic response of the drain current for the monolayer MoS_2 sensor upon the exposure of various NH3 concentrations under light and dark conditions. A blue LED (peak wavelength: 470 nm) was used as the light source, with a typical irradiance of 50 mW/cm2. Since NH3 acts as an electron donor, the drain current increased upon the NH3 exposure. Unlike the case of NO2 exposure, the light illumination did not accelerate the response and recovery rates. On the other hand, sensor response SG defined by SG=ΔI/I0, where ΔI is change in drain current during NH3 exposure, and I0 is the initial drain current just before NH3 exposure, drastically increased under the light condition. Similar trends were observed for the other four gas species. Table 1 summarized the sensor responses SG in the dark and light conditions for each gas species. For all gas species measured, the sensor showed a response of increasing current, which may mean that they are reducing gases. Even for the gas species which can not be detected in dark condition, the gas sensor clearly showed responses to them under the light condition. These results indicate that light illumination increases the sensitivity of the MoS_2 sensor to reducing gas species. [1] T. Pham et al., ACS Nano13, 3196 (2019). [2] H. Tabata et al., ACS Nano 15, 2542 (2021). *Acknowledgements:* This work was financially supported from the Murata Science Foundation.

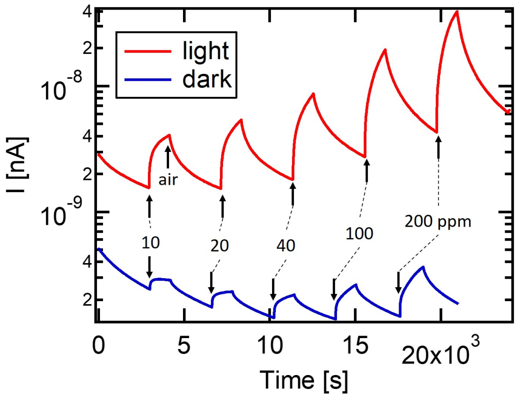

Fig. 1: Dynamic response of the drain current for the MoS_2 FET upon exposure of various NH3 concentrations under light (at irradiance of 50 mW/cm2 from the blue LED) and dark conditions.

	Sensor response (S_G)	
	light	dark
NH_3 (200 ppm)	8.11	1.47
CH_4 (200 ppm)	0.37	n.d.
H_2 (300 ppm)	0.15	n.d.
Ethanol (300 ppm)	0.87	0.12
Acetone (300 ppm)	0.36	n.d.

n.d. : not detected

Fig. 2: Comparison of sensor response (SG) in the dark and light conditions for each gas species

C127: Synthesis and Characterization of 1D Vander Waals heterostructure based on CNT-BNNT-NbS2

Wanyu Dai*[†], Yongjia Zheng, Rong Xiang, Shigeo Maruyama

University of Tokyo

One-dimensional (1D) van der Waals heterostructures is a class of materials where different atomic layers are coaxially stacked, which was proposed by us. Also, the as-synthesized hexagonal boron nitride (BN) and molybdenum disulfide (MoS_2) single crystals on single-walled carbon nanotubes (SWCNTs) was acquired previously. The extended library of 1D Vander Waals heterostructures based on other Transition metal dichalcogenides (TMDCs) was also predicted. Here we demonstrate the experimental synthesis of single-crystal layers of BN and niobium disulfide (NbS2) on SWCNTs. Electron diffraction verifies that all shells in the heterostructures are single crystals. This work suggests that materials in the current 2D TMDCs library other than MoS_2 are highly likely able to be rolled into their 1D counterparts and a plethora of function-designable 1D heterostructures could be realized by controlled CVD synthesis procedure.

C128: FibreCOP: An open access tool for estimation of orientation order in CNT textiles

Adarsh Kaniyoor*†, Thurid Gspann, Jenifer Mizen, James Elliott

**University of Cambridge*

We present an open access image analysis tool, FibreCOP, together with the theoretical background for the estimation of uniaxial orientation in aligned CNT films or similar 2D systems [1]. Alignment is an important metric to understand structure-property relations in macroscopic materials because many of the physical properties of anisotropic systems, such as electrical and thermal conductivities, tensile strengths etc., are usually correlated with the degree of internal orientation.Although anisotropy in material properties such as birefringence, fluorescence and Raman peak intensities along orthogonal axes are often used to estimate the degree of alignment, a more systematic measure is given by the orientation distribution function (ODF); a continuous function describing the orientation of all sub-elements with respect to a principal axis. The Hermans orientation parameter (HOP) is obtained when the ODF, inferred indirectly from diffraction measurements (X-ray or Fourier transform of images), is averaged over the 3D sub-elemental space [2]. However, most CNT films are formed by the assembly of CNT layers via a spin-coating or wind-up process which restrict CNTs to individual layers or planes. We prove mathematically that the use of HOP to describe orientation of 2D CNT films is inappropriate and instead, propose the use of a 2D parameter, which we call the Chebyshev orientation parameter (COP) [3]. We have developed an image analysis method and an open access tool to rapidly estimate orientation parameters – which we demonstrate taking scanning electron micrographs of CNT textiles as examples. Further, we show that the values of both the 2D and 3D orientation parameters depend on the shape, width and number of the distribution peaks – hence, as best practice, orientation values must be compared only when similar fitting functions and parameters are used. We also discuss with examples why the full width at half maximum of ODFs, which is often used as a linear measure of orientation, can give misleading results. Orientation parameters, although non-linear between zero and unity, provide a complete description of the internal orientation.References:[1] J. A. Elliott, A. Kaniyoor, 2021, DOI 10.5281/zenodo.4435029. [2] M. van Gurp, Colloid Polym. Sci. 1995, 273, 607. [3] A. Kaniyoor, T. S. Gspann, J. E. Mizen, J. A. Elliott, J. Appl. Polym. Sci. 2021, Accepted. *Acknowledgements:* We thank the funding support from EPSRC (grant number EP/M015211/1).

C129: The effect of highly polydisperse CNT solutions on the macroscopic electrical and mechanical properties of wet spun CNT fibers.

Michelle Duran-Chaves*†, Ivan Rosa De Siqueira, Glen Irvin, Matteo Pasquali

**Rice University*

Carbon nanotubes have the ability of strongly bundling together via Van Der Waals forces to form lightweight macro materials with high electrical, mechanical, and thermal properties. Consequently, there has been a great interest in developing wet spun CNT fibers, since their promising properties can be used in a wide variety of applications such as cabling, wearable electronics, biomedical applications, and energy applications. CNT fiber technology has improved dramatically over time. However, the spinning process needs to become more efficient to decrease the CNT fibers cost and environmental impact. In this work, we study the effect of CNT length and diameter polydispersity on the macroscopic electrical and mechanical properties of CNT fibers. CNT polydispersity is an approach to decrease the cost of spinning as more efficiently produced, short CNTs can be incorporated into the solution. The effect of high polydispersity in CNT solutions has not been previously reported, and there are no indications on how it can affect the overall macroscopic properties of fibers. Two types of CNTs, high aspect ratio (rod length divided by rod diameter L/D) CNTs produced by Meijo Nano Carbon (L/D ~3000) and relatively low aspect ratio CNTs such as Tuball produced by OCSiAl (L/D ~800) are mixed in different weight fractions. Wet spinning was performed for each CNT solution with optimized parameters to guaranty that the variability across the fibers is primarily due to polydispersity and not fiber morphology. The results show that both electrical conductivity and tensile strength have the tendency to increase with the fraction of high aspect ratio material, which is expected as a higher aspect ratio yields better macroscopic properties. However, the correlation is not linear. When the fraction of high aspect ratio material is half or higher, the properties reach a plateau. These results suggest that we are able to obtain similar properties using only half of the high aspect ratio material. Polydispersity seems to be playing a significant role in the fiber properties. Further studies will help us understand this behavior and gain a fundamental understanding of the effect of highly polydisperse solutions while achieving high-performance properties at a lower cost of fiber production.

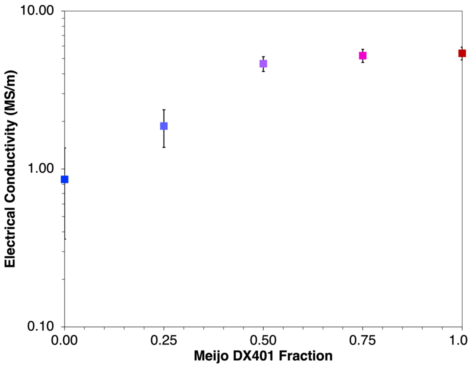

Fig. 1: Electrical conductivity of high polydisperse CNT fibers

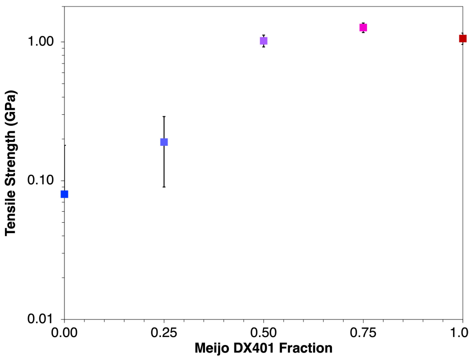

Fig. 2: Tensile strength of high polydisperse CNT fibers

C130: Ultrafast in-situ optical visualization of suspended ultralong carbon nanotubes and carbon nanotube webs

Run Li*†

**Tsinghua University*

The visualization of individual ultralong carbon nanotubes (CNTs) in ambient condition has always been a significant problem for their nanoscale size is far beyond the resolution of naked eye or optical microscopy (OM). The observation of CNTs usually requires electron microscopes under high vacuum, which is adverse for the transfer and manipulation of them. Here, we present an ultrafast and facile approach for optical observation of individual CNTs as well as carbon nanotube webs (CNWs)under conventional OMs with the assistance of tar nanoparticles (NPs). This approach is of huge advantageous. Firstly, the sources of tar NPs are easily available including cigarette, paper, wood, incense, etc. Moreover, we can keep or remove the NPs as we want by laser heating in a controlled manner, which greatly facilitates the location and application of CNTs. Besides, we can observe the growing process of tar NPs on CNTs and CNWs in situ. In addition, we synthesize CNWs composed of ultralong CNT bundles and prove that they can catch crystal particles and powders after optical visualization by this approach. We showed that this approach is ultrafast, facile, controllable, non-destructive, and contamination-free, indicating wide potential applications.

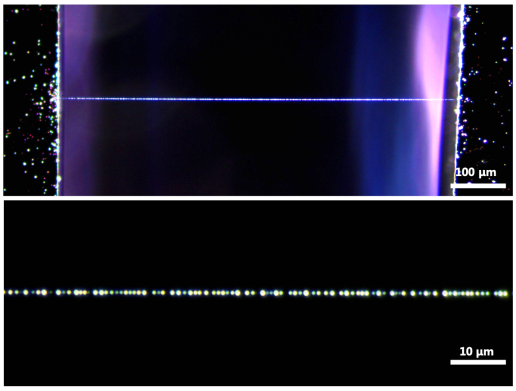

Fig. 1: Schematic illustration of the process of optical visualization of suspended ultralong CNTs assisted by tar particles.

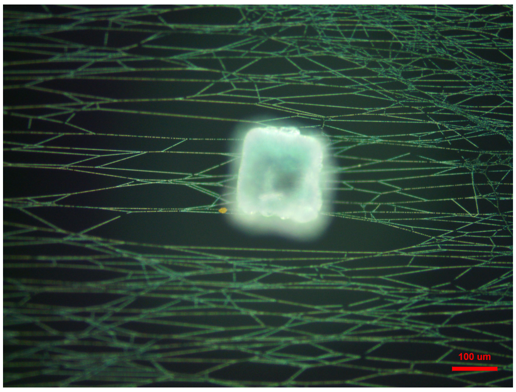

Fig. 2: OM images of CNWs catching a NaCl crystal particle.

C131: Catalyst-Free Synthesis of High-Crystalline Free-Standing Boron Nitride Nanotube Films

Shuhui Wang*†, Ming Liu, Esko Kauppinen, Rong Xiang, Shigeo Maruyama

**the University of Tokyo*

Boron nitride nanotube (BNNT) has attracted considerable attention in various scientific fields due to its outstanding optical, thermal, and electrical properties. BNNT exhibits intriguing properties, including electrically insulating, thermal oxidation resistance, high thermal conductivity, and ultraviolet luminescence. Here, we report an approach of synthesizing high-crystalline free-standing BNNT films by a catalyst-free chemical vapor deposition method. In this method, single-walled carbon nanotube (SWCNT) served as a template for wrapping boron nitride (BN) layers to achieve a heterostructure of SWCNT coaxially coated by BNNT (SWCNT@BNNT). High-quality BNNT films were obtained after removing the inner SWCNT of SWCNT@BNNT heteronanotubes by annealing in the presence of a reduced pressure of oxygen. The crystalline structure of BNNTs was observed by high-resolution TEM. The Raman spectroscopy and Fourier transformed infrared (FTIR) spectroscopy were implemented to examine the quality of BNNT films. This free-standing BNNT film was fully transparent within the visible range of wavelengths, which was confirmed by the Ultraviolet-visible-near-IR (UV-vis-NIR) spectrum. A large optical band gap (5.76 eV) was obtained from the optical absorption spectrum which suggests the potential application of this BNNT film in optoelectronic devices.

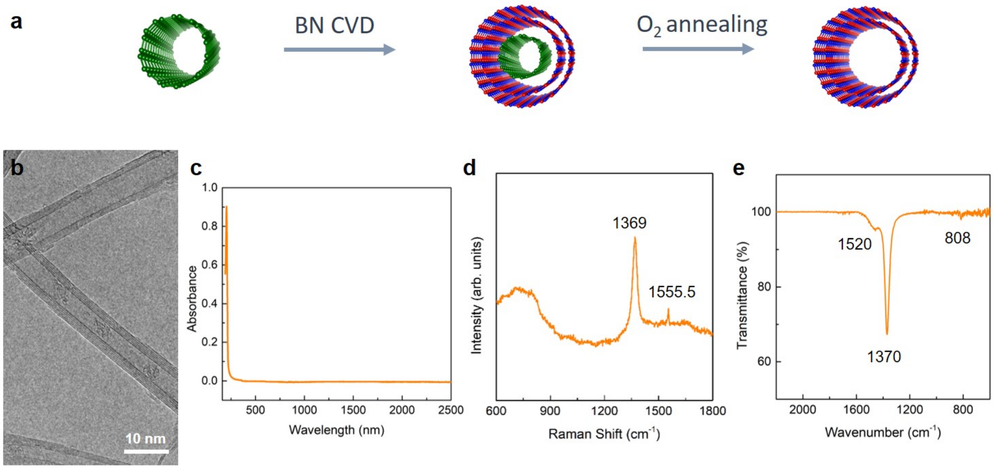

Fig. 1: (a) Schematic illustration of synthesizing BNNT films. (b) HRTEM image of the BNNTs. (c) Optical absorption spectrum, (d) Resonant Raman spectrum, and (e) FTIR spectrum of a BNNT film.

C132: Controlled growth of single-walled carbon nanotubes using carbon monoxide as carbon source

Xue Zhao*†, Yan Li

**Peking University*

Carbon feeding conditions play important roles in the chemical vapor deposition growth of single-walled carbon nanotubes (SWCNTs). Carbon monoxide (CO) has been used as a superior carbon source for the growth of SWCNTs in bulk synthesis. Here, we chose CO as carbon source for the growth of SWCNTs on Si/SiO2 substrates. When using cobalt as catalyst, vertically aligned SWCNTs (VA-SWCNTs) were grown at the temperature range of 600-800 °C. SWCNTs with larger diameter were synthesized at higher growth temperature and present high quality at 750 °C. When using Co7W6 catalyst, we observed the selective growth of (12, 6) tubes.

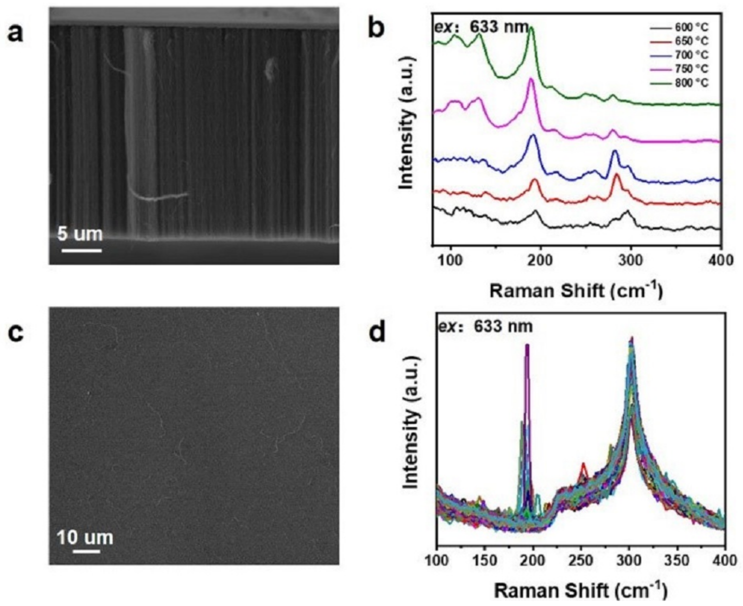

Fig. 1: (a) SEM image and (b) Raman spectra at different temperatures of VA-SWCNTs using Co catalyst. (c) SEM image and (d) Raman spectra at 750 °C of SWCNTs using Co7W6 catalyst.

C133: PVDF-Fe3O4 Nanocomposites: Spectroscopic and Thermal Investigations

Mircea Chipara*†, Dorina Chipara, Karen Martirosyan, Karen Lozano, Bryan Hooke, Alexandro Trevino

**University of Texas Rio Grande Valley*

Nanocomposites of polyvinylidene fluoride - iron oxide (PVDF - Fe3O4) have been obtained by melt mixing of micron-sized powder of PVDF (from Alfa Aesar) with Fe3O4 nanoparticles with an average diameter of 75 nm (from Nanostructured & Amorphous Materials, Inc.), by using a counter-rotating two-screw mixer (POLYLAB). Samples containing 0 to 30 % weight Fe3O4 nanoparticles dispersed within PVDF have been obtained and investigated by Raman spectroscopy using a Renishaw InVia Confocal Raman Microscope system operating at 785 nm. Wide Angle X-Ray Scattering (WAXS) measurements were performed by using a Bruker Advanced Discovery 8 spectrometer, operating at room temperature. Electron Paramagnetic Resonance spectra of the nanocomposites were obtained by using a Bruker Elexsys spectrometer, operating in the X Band, at room temperature. Pristine PVDF does not show any EPR spectrum; all recorded spectra of PVDF - Fe3O4 nanocomposites are originating from magnetic nanoparticles, reflecting the cooperative evolution of coupled electronic spins (magnetization) around the direction of the external magnetic field. The thermal stability of PVDF - Fe3O4 nanocomposites has been investigated by thermogravimetric analysis, using a Q50 spectrometer from TA Instruments. Measurements have been performed in a nitrogen atmosphere at a heating rate of 10 K/min. DSC investigations on the melting and crystallization processes in pristine PVDF and PVDF- Fe3O4 nanocomposite, performed by using a Q100 TA instrument, are reported and analyzed in detail. Isothermal crystallization was also investigated by using an equilibration temperature of 160 oC and isothermal monitoring of the heat transfer in the temperature range 120 to 130 oC, for 60 minutes. The positions and widths of the main Raman and WAXS spectral lines were fitted in OriginPro, assuming Lorentzians lineshapes. The effect of the nanofiller on the crystalline structure of the polymeric matrix was reported. WAXS and Raman spectroscopies were used to calculate the fraction of the beta (ferroelectric) phase of PVDF and the alpha (isotropic) phase of PVDF. *Acknowledgements:* Department of Defense W911NF-15-1-0063

C134: Spectroscopic Titration Shows (n,m)-Dependent Displacement of SDS By ssDNA on Single-Wall Carbon Nanotubes

Kunhua Lei*†, Sergei Bachilo, R. Bruce Weisman

**Rice University*

Single-stranded DNA oligonucleotides (ssDNA) are uniquely customizable polymers that are useful for coating, suspending, and structurally sorting single-wall carbon nanotubes (SWCNTs) in water. However, SWCNT dispersions are instead commonly prepared using inexpensive amphiphilic surfactants such as SDS. By monitoring changes in the nanotube fluorescence wavelengths and intensities, we show that such SDS coatings on dispersed SWCNTs can be controllably displaced by the addition of small amounts of ssDNA. The displacement data can be well represented by kinetic modeling, giving the time scales for equilibration of the coating composition. We measured spectra of SWCNT samples that were dispersed in low concentrations of SDS, then treated with small amounts of ssDNA and allowed to reach equilibrium. Plots of the final spectral shifts as a function of added ssDNA provide (n,m)-specific "titration" curves that show strongly diameter-dependent behavior. Smaller diameter nanotubes undergo SDS displacement at the lowest ssDNA concentrations. The limiting spectral shifts suggest that SWCNT surfaces become coated with adsorbed SDS as well as ssDNA. We will also illustrate how the (n,m)-dependent displacements found here can be used for structural sorting of mixed SWCNT samples. *Acknowledgements:* We would like to thank the support from National Science Foundation and The Welch Foundation.

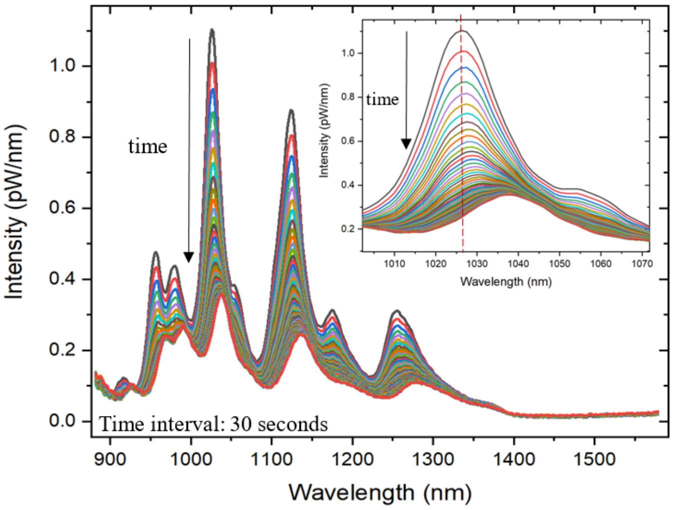

Fig. 1: Spectral changes were recorded using sequential measurements.

C135: Suspended Carbon Nanotube Networks and Their Applications in Photodetection

Qinyuan Jiang*†, Run Li, Rufan Zhang

**Tsinghua University*

Devices based on suspended carbon nanotubes (CNTs) have shown great potential in the fields of mechanics, electronics and optics. However, controlled synthesis and large-scale production of these devices still remain challenges. Suspended carbon nanotube networks (SCNWs) with nanometre-scale thickness and millimeter-square-scale area were successfully synthesized by a floating catalyst CVD process. The formation of SCNWs can be attributed to the self-assembly of ultralong CNTs and short CNTs in gas phase, which delicately avoids the interference of substrates and facilitates the free growth of CNTs. SCNWs exhibit a very low defect concentration and relatively high purity of semiconducting CNTs. Photoconducting devices based on SCNWs were further fabricated for the detection of UV to NIR light, and exhibited great sensitivities and fast responses.

C136: Exciton localization in surfactant-wrapped single-walled carbon nanotubes via surface charge perturbations

Trevor Tumiel*†, Erin Christensen, Todd Krauss

**University of Rochester*

Local topological and electrostatic perturbations have long been known to affect the photophysical properties of single-walled carbon nanotubes (SWCNTs), often with unintended consequences. For example, recent unpublished work in our laboratory has revealed the impact of surfactant buildup on the nanotube (NT) surface, which can lead to localized and unavoidable charge states near the NT. In this presentation, we detail experiments designed to probe the impact of local electrostatic perturbations on the optical properties of SWCNTs. Our study employs a technique that allows for the correlation of single molecule (SM) photoluminescence (PL) spectroscopy and atomic force microscopy (AFM) images, making it possible to directly compare the PL and physical properties of individual SWCNTs and their immediate surroundings. Our results unambiguously show localized excitonic PL along the length of the NT, often at sites of intense surfactant coverage. PL emission energy shifts also appear dependent on the proximity to surfactant buildup. Interestingly, these sites routinely display greater static charge accumulation, which suggests a strong connection between the electrostatic and optical characteristics of SWCNTs. We will also present a detailed comparison of the charge and emissive profiles of individual NTs by relating single molecule spectroscopy images with the location and magnitude of localized charge states imaged using electrostatic force microscopy (EFM). It is important to note that correlated spectroscopy and microscopy techniques also provide the opportunity to directly study the impact that unintentional defects and deformations have on both electrostatic and optical properties of individual SWCNTs. To this end, we will present data that shows variation in SWCNT optical properties that are dependent on topological irregularities which can segment the NT into regions displaying vastly different optical and electrostatic character.

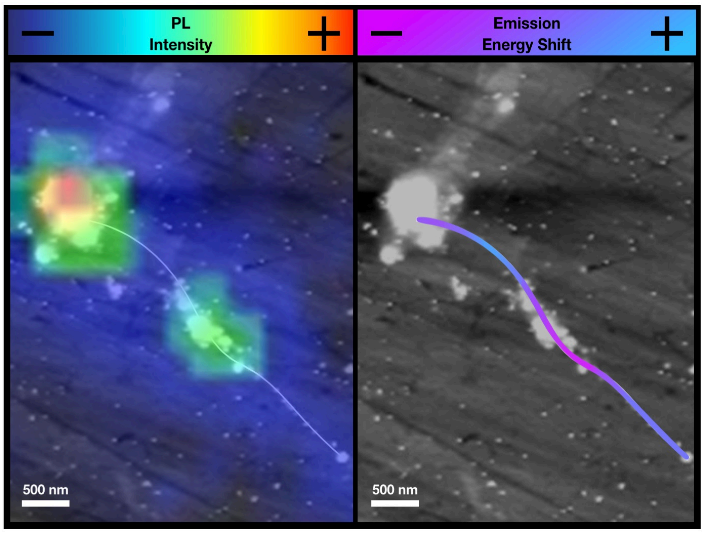

Fig. 1: (Left) PL intensity map overlaying an AFM image, demonstrating localized excitonic activity at sites of surfactant buildup. (Right) Emission energy shifts that are dependent on the location of surfactant buildup.

C137: Stable doping of single-walled carbon nanotubes for flexible transparent conductive films

Wenqing Yan*†, Zeyao Zhang, Yan Li

**Peking University*

Single-walled carbon nanotube (SWCNT) thin films are the primary candidates for the next generation of flexible transparent conductive thin films. The development of stable dopants is critical for this application. We reported that solid acids such as phosphotungstic acid (PTA) can stably dope SWCNT thin films. The sheet resistance of a PTA-doped SWCNT film only increased from 50.1 Ω/sq to 53.6 Ω/sq after 25 days in ambient and to 67.9 Ω/sq after an ultra-long storage of 500 days. Excellent flexibility of the PTA-doped film was demonstrated by a bending test of 1000 cycles, during which its sheet resistance was basically unaffected and the fluctuation (±7%) was within the relative standard deviation (±10%) of the measured sheet resistance of the film. The blueshift of G band in the Raman spectra of an individual SWCNT confirmed the p-type nature of PTA doping. The work function of the SWCNT film was raised by PTA doping for about 440 meV. In addition, we confirmed that the doping effect comes from the acidity rather than the oxidizing ability. The doping mechanism is that the solid acid raises the redox potential of the O2 adsorbed on SWCNTs, and thus brings down the Fermi level of the SWCNTs. Our results may help to promote the practical applications of SWCNT transparent conductive films and expand the dopant library of SWCNTs as well.

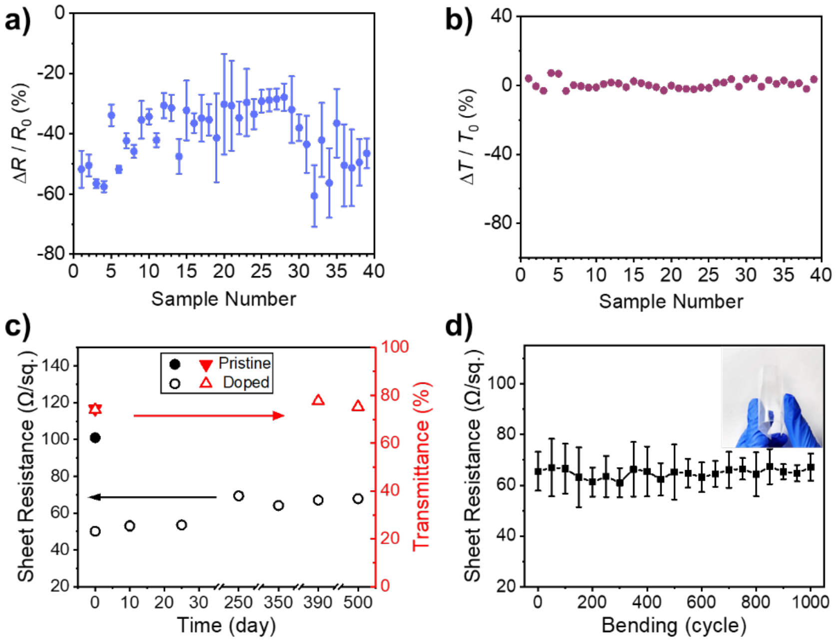

Fig. 1: (a, b) The change of the sheet resistance and transparency after doping. (c) Long-term stability at ambient temperature. (d) The bending test of a PTA-doped SWCNT film.

D138: Fast-Flow-Assisted Floating-Catalyst Chemical Vapor Deposition for Direct Fabrication of Carbon Nanotube Fibers

Toshihiko Fujimori*†, Daiji Yamashita, Yoshiya Kishibe, Takamasa Onoki, Daisuke Tanioka, Takeshi Hikata, Soichiro Okubo, Keishi Akada, Jun-ichi Fujita

**Sumitomo Electric Industries, Ltd.*

Carbon nanotubes (CNTs) are one of the strongest materials in the nanoscale, providing a rich potential for the next-generation light-weight structural materials. We have shown that ultra-long, defect-free, and aligned CNT bundles exhibit the tensile strength over 50 GPa (T. Fujimori et al. Appl. Phys. Lett. 115, 023106 (2019).), opening up a great possibility for high-performance CNTs fibers. Herein we report the one-step fabrication of high-crystallinity and aligned CNTs fibers using a laboratory-designed floating-catalyst chemical vapor deposition (FCCVD) system. A multi-channel honeycomb filter, which has the ability to rectify and accelerate laminar flow of the process gas (hydrogen and ethylene with a catalyst precursor consisting of ferrocene and thiophene), was set inside a horizontal reactor. In a certain synthesis condition, we found that CNT fibers are protruded from the channels of the honeycomb filter (Fig. 1). Polarized Raman spectroscopy and fast Fourier Transformation (FFT) image analysis reveal that highly-crystalline CNTs (G/D ratio~40) are aligned along the fiber axis. Computational fluid dynamics (CFD) simulation shows that gas velocity inside multi-channels becomes twice as high as that inside the reactor tube, indicating that a strong shear stress could be induced by the fast laminar flow inside the channels. We infer from our experimental observation and CFD result that the induced shear force plays an important role for simultaneous assembling and alignment of CNT aerogel into CNT fibers. However the resulting CNT fiber is porous because the CNT fiber consists of loosely-aggregated CNT bundles. To further densify as-grown CNT fiber, we performed a post-processing technique, which includes immersion of an as-grown CNT fiber in chlorosulfonic acid and succeeding stretching process. In this presentation, we will discuss (1) the fundamental effect of multi-channel honeycomb filters and (2) mechanical properties and electric properties of the obtained CNT fibers. *Acknowledgements:* This work was supported by Innovative Science and Technology Initiative for Security, ATLA, Japan (Grant Number JPJ004596).

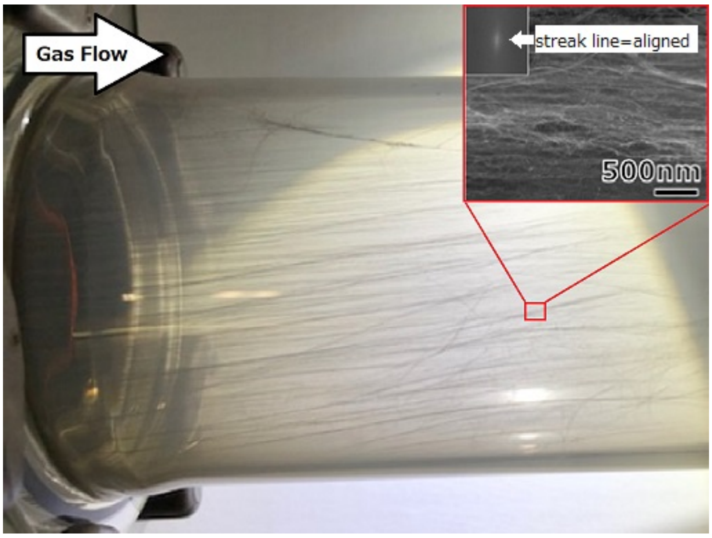

Fig. 1: A photo of as-grown CNT fibers synthesized via our modified FCCVD system using a multi-channel honeycomb filer with a representative SEM image and a corresponding power spectrum (inset).

D139: Rare-Earth Metal Ions Doped Graphene Quantum Dots Utilized for Near-IR In Vitro/In Vivo Imaging Applications

Md Tanvir Hasan*, Roberto Gonzalez-Rodriguez, Ching-Wei Lin, Elizabeth Campbell†, Satvik Vasireddy, Uyanga Tsedev, Angela M. Belcher, Anton Naumov

**National Institute of Standards and Technology*

Biocompatible nanomaterials that emit in the near-infrared (NIR) are desirable for biotechnology applications as they allow for higher penetration depth for fluorescence imaging probes. This work utilizes novel NIR-emissive Nd3+ -doped or Tm3+ -doped biocompatible graphene quantum dots (GQDs) that exhibit NIR fluorescence at approximately 1060/925 nm which is attributed to the intrinsic transitions of Nd3+/Tm3+. They show high biocompatibility with >80% cell viability at 1 mg/mL for Nd-GQDs and 0.25 mg/mL for Tm-GQDs, making them well suited for bioimaging. Both GQD types show efficient internalization in vitro with their intracellular emission maximized at 6 hours. GQDs enable in vivo NIR imaging in live sedated NCr nude mice with IV administration: their NIR emission maximized at 6 hours post-injection is primarily detected in intestine, kidneys, liver, and spleen, however, diminishing to none is detected at 48 hours. This capability of NIR fluorescence imaging in cells, tissues, and real-time detection in live animals makes biocompatible rare-earth metal-doped GQDs an attractive new candidate for in vitro/in vivo/ex vivo theranostics. *Acknowledgements:* The authors would like to acknowledge the TCU RCAF, Marble Center for Cancer Nanomedicine, and the Koch Institute Support (core) Grant.

D140: Toward Largescale Separation of Single-Chirality Single Wall Carbon Nanotubes by Aqueous Two-Phase System

Min Lyu*†, Yan Li

**Peking University Shenzhen Institute*

Previous studies have shown that aqueous two-phase systems are very effective for the sorting of Single Wall Carbon Nanotubes (SWCNTs). By combining the diameter sorting and semiconducting/metallic sorting strategy, we are able to separate (6,5) SWCNTs of high concentration and high purity from a synthetic mixture. The resolution of sorting can be improved by adding cyclodextrin to form supramolecular assembly with one of the surfactant molecules to finely modulate the effective composition of surfactants. Our results may promote the application of single-chirality SWCNTs obtained from aqueous two-phase systems.

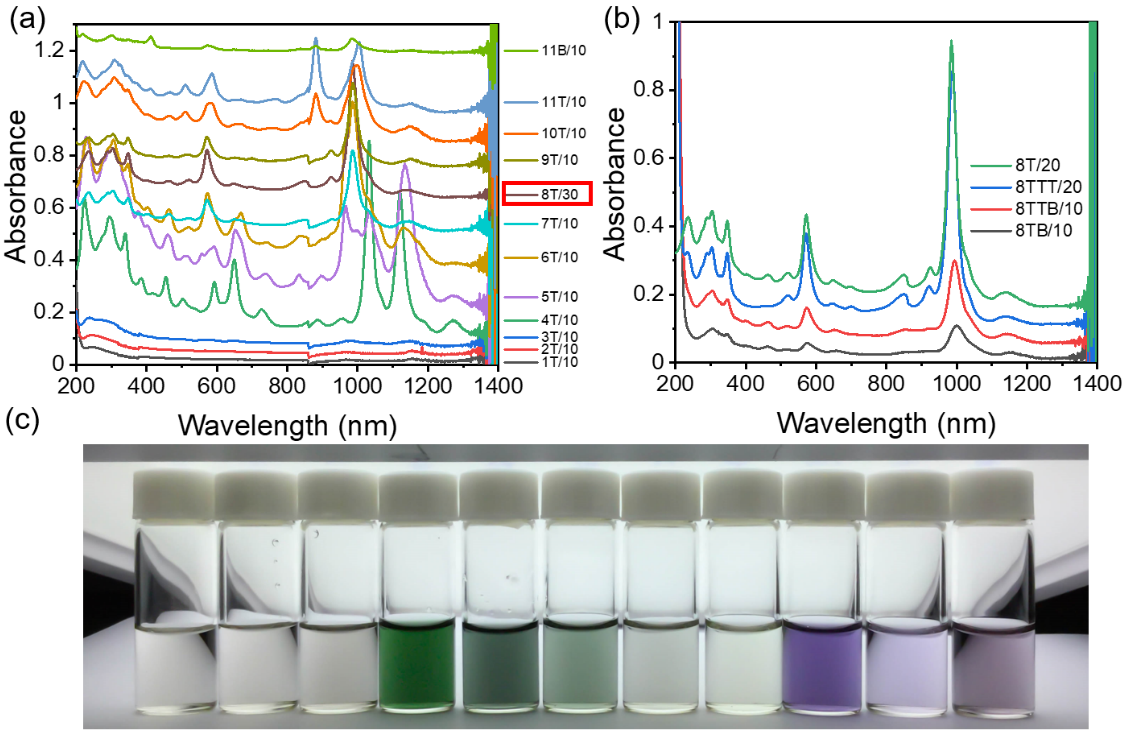

Fig. 1: (a) Diameter sorting of SWCNTs. (b) Semiconducting/Metallic sorting of 8T obtained from part a. (c) Photographs of each fractions obtained during diameter sorting.

D141: Tuning Heat Flow Across Two-dimensional Stacked van der Waals Materials via Interfacial Engineering

Wenyu Yuan*†, Kan Ueji, Takashi Yagi, Takashi Endo, Hong En Lim, Yasumitsu Miyata, Yohei Yomogida, Kazuhiro Yanagi

**Tokyo Metropolitan University*

The understanding of heat flow across solid interfaces and its control are extremely important for the applications of advanced electronics, thermal energy conversion, and thermal management in devices. Two-dimensional (2D) material family with ultrathin thickness as a new rising star makes it possible to tune the thermal property at the atomic scale [Y. Liu et al. Nature, 567, 323(2019)]. For instance, the stacking structure of graphene, MoS$_2$, and WSe$_2$ shows extremely high thermal isolator properties on a sub-2-nm scale [S. Vaziri et al. Sci. Adv., 5, eaax1325 (2019)], and disordered WSe$_2$ exhibits very low thermal conductivity [C. Chiritescu et al. Science, 315, 351 (2007)]. Therefore, experimental understanding on the heat flow across the 2D interfaces is of great importance. Here, we provide a polyethylene glycol (PEG)-assisted TDTR method to evaluate thermal transport properties across four layered (4L)-transition metal dichalcogenides (TMDCs) with improved sensitivity (Fig. 1). A series of 4L van der Waals (vdW)-stacked TMDC materials were prepared via a multi-step transfer process, and their thermal conductances are further systematical investigated. Among all investigated stacked 4L-materials, the stacked MoSe$_2$-MoS$_2$-MoSe$_2$-MoS$_2$ heterostructure demonstrates the lowest thermal conductance (1.5 MW m-2 K-1). A roadmap to tune thermal conductance via homo-interfacial mismatch, interfacial coupling, and hetero-interfacial mismatch, is further demonstrated (Fig. 2). The obtained large-area stacked vdW materials are promising as ultrathin thermal insulators and efficient thermoelectrical materials.

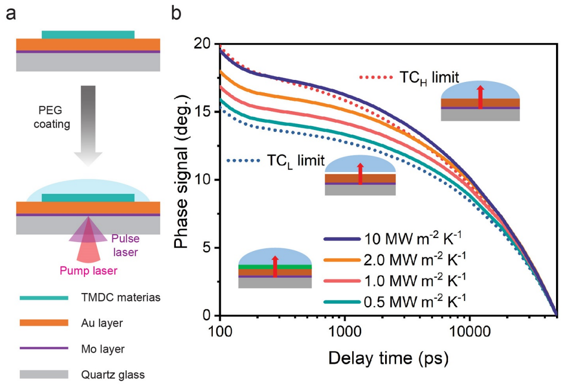

Fig. 1: PEG-assisted TDTR technique to determine the thermal conductance of ultrathin materials. (a) Schematic for the PEG-assisted TDTR method. (b) Thermal conductance-dependent TDTR signal change via simulation.

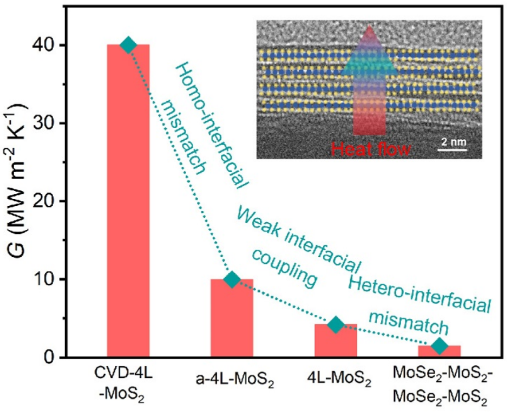

Fig. 2: Roadmap to control the thermal conductance of 4L-stacked vdW materials via interfacial engineering.

D142: Relationship between surface structure and fluorescence properties of carbon quantum dots

Takaki Yoda*†, Hironori Ogata

**Hosei University*

Carbon quantum dots (C-QDs) are one of the nanomaterials that have attracted much attention in recent years. They have many advantages over conventional semiconductor quantum dots and organic dyes, including chemical stability, dispersibility, fluorescence properties, hydrophilicity, and high resistance to photodegradation [1].The main factors contributing to the fluorescence properties of C-QD are the quantum size effect and the type and density of functional groups on the surface of C-QDs. Several groups have been reported on the relationship between functional groups and the fluorescent properties of C-QDs. In particular, it has been previously reported that nitrogen doping of C-QD with ethylenediaminetetraacetic acid (EDTA) improves fluorescence properties [2].In recent years, biomass has been attracting attention as a material for C-QD. C-QD is reported to have been synthesized from organic materials such as soymilk [3] and plant seeds [4]. These studies use a simple process of heating only, and the synthesis can be done at low cost.Our group has succeeded in synthesizing C-QD by using lignin and cellulose nanofiber (CNF) as raw materials. In this study, we will report the characteristics of the local structure, crystallinity and fluorescence characteristics of these C-QDs, and explain the effect of the various kinds of surface functional groups and nitrogen doping on these C-QDs on their fluorescence characteristics. Detailed results will be reported at the meeting.References:[1] Wang,Y. et al., J.Mater.Chem.C. 2,6921(2014). [2] Ma,C. et al., Nanoscale,10,1039(2015)[3] Chengzhou,Z. et al., Chem.C. ,48,9367(2012). [4] Akansha,D. et al., Sci.Rep. ,9,14004(2019).

D143: Quick n-type doping of CNT yarns using N-DMBI for thermoelectric application

Jun Kametaka†, Yuichiro Tanaka, Mitsuaki Maetani, Kyohei Nasu, Takeshi Nishikawa, Hiroo Suzuki, Aung Ko Ko Kyaw, Yasuhiko HAYASHI*

**Okayama University*

The problems with conventional thermoelectric devices are high cost, low productivity, and difficulty in mounting on curved or uneven surfaces due to toxic elements and poor processability. Therefore, it is important to develop new thermoelectric elements that can be flexible, lightweight, and low-cost for the wide application of thermoelectric elements. One of the possible candidates is a material using carbon nanotubes (CNTs) [1]. Many CNT-based membranes have been studied, but we can fabricate CNT spun yarn by dry spinning and investigating its application as a thermoelectric device in our laboratory. CNT yarns originally have p-type thermoelectric properties. If it can be partially n-type doped, a thermoelectric generator can be fabricated from one CNT yarn. Since the performance of simple CNT spun yarns is lower than that of conventional inorganic materials for thermoelectric conversion, it is desirable to improve the Seebeck coefficient, electrical conductivity and decrease the thermal conductivity. Recently, 1,3-dimethyl-2-phenyl-2,3-dihydro-1 H-benzimidazole (N-DMBI) has been attracting attention as a high-performance n-type doping agent[2]. In this study, we doped CNT spun yarn with N-DMBI and investigated its effect on the performance of thermoelectric elements. The thermoelectric properties of CNT yarns with Joule annealing were evaluated by varying the doping concentration, immersion time, and temperature. As a result, N-DMBI showed a faster doping reaction rate and a higher power factor than polyethylenimine (PEI) as the n-type doping agent for CNT yarn, as shown in Figure 1. It was also found that the reaction rate of doping increased with concentration and solution temperature. By optimizing these parameters, a maximum value of 1289 μW/m•K2 was obtained when doping was carried out at a concentration of 8 mM, a solution temperature of 40°C, and an immersion time of 1 min. The Seebeck coefficient and electrical conductivity were 66.4 μV/K and 2925 S/cm. [1] C. Jaeyoo et al., ACS Nano11 (8), 7608-7614 (2017). [2] Q. Hu et al., J. Mater. Chem. A, 8, 13095-13105 (2020). *Acknowledgements:* We would like to Y. Shigeeda, H. Inoue, T. Nakagawa at Okayama University for experimental support.

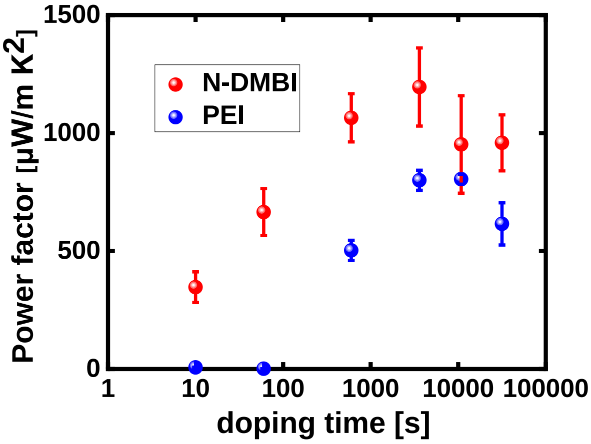

Fig. 1: Power factor as a function of doping time

D144: Hall effect measurement and ionic-liquid gating of single-walled carbon nanotube thin films

Hiroki Date*†, Mika Nagatomo, Akari Kobayashi, Taiki Inoue, Takenori Fujii, Esko Kauppinen, Shigeo Maruyama, Shohei Chiashi

**The University of Tokyo*

Single-walled carbon nanotubes (SWCNTs) are expected to be applied in various industrial fields because of their high mechanical strength and electrical/thermal conductivity. Many studies have been conducted on the electrical conductivity of SWCNTs. While each individual SWCNTs have a very high electrical conductivity [1], macroscale SWCNT materials such as yarns and films, which are composed of bundled SWCNTs, have low electrical conductivity [2]. The doping effects of molecules in the air on the electrical conductivity of macroscale SWCNTs have been also studied [3]. However, the origin of the low electrical conductivity is unknown and the yarn or thin films with high electrical conductivity have not been obtained. Therefore, in this study, in order to clarify and control the carrier properties, the magnetic field and the gate voltage dependences of the conductivity were measured. The electrical conductivity of SWCNT thin films [4] with different densities (i.e. different light transmittance) transferred on or suspended over the substrate was analyzed considering the adsorption effect. The device for Hall measurement is shown in Fig. 1(a). The resistance change was measured in a vacuum in the temperature range from room temperature to 400 K, and then the magnetic field response of the Hall resistance was measured at 300 K. It was found that the resistance increased with increasing temperature, and activation energy obtained from the temperature dependence of the resistance rise rate suggested that water molecule desorption increased the electrical resistance. Furthermore, the magnetic field response of the Hall resistance revealed that the carriers are holes and that the Hall resistance shows a non-linear change with respect to the magnetic field (Fig. 1(b)). The non-linearity is thought to be due to the existence of two types of carriers with different mobilities or the one-dimensionality of SWCNTs [5]. Figure 2 shows the gate voltage dependence of the resistance. It was found that the resistance decreases when gate voltage was applied, and ionic-liquid gated SWCNT thin films exhibited ambipolar characteristics. [1] T.W. Ebbesen et al., Nature, 382, 54 (1996). [2] N. Behabtu et al., Science, 339, 182 (2013). [3] P.G. Collins et al., Science, 287, 1801 (2000). [4] A.G. Nasibulin et al., ACS Nano, 5, 3214 (2011). [5] M.L. Roukes et al., Phys. Rev. Lett., 59, 3011 (1987).

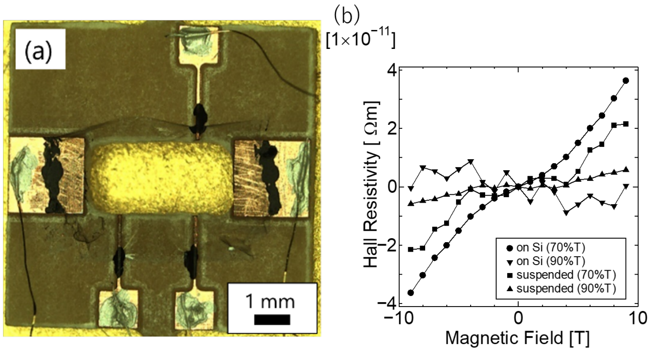

Fig. 1: (a) Optical image of device for Hall effect measurement. (b) Magnetic field dependence of Hall resistivity of SWCNT thin film.

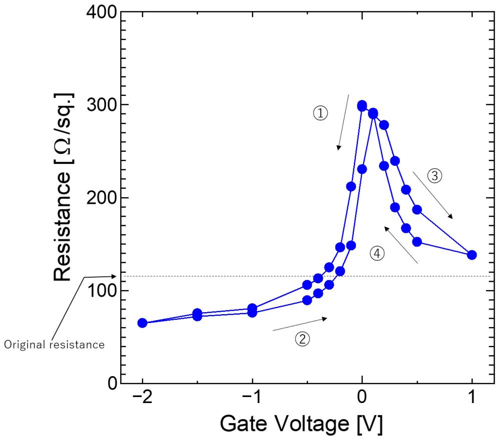

Fig. 2: Gate voltage dependence of resistance of SWCNT thin film.

D145: Study on origin of memristive behavior in hBN-grown CNT assemblies

Misaki Kishibuchi†, Kyohei Nasu, Mitsuaki Maetani, Yuichiro Tanaka, Yasuhiko HAYASHI, Hiroo Suzuki*

**Okayama University*

Van-der-Waals (VdW) heterostructure is getting a lot of attention because of its potential to develop a new electronic device application. In 2020, one-dimensional (1D) VdW heterostructure has been realized by direct growth of two-dimensional (2D) materials such as hexagonal boron nitride (hBN) and transition metal dichalcogenide (TMDC) on carbon nanotube (CNT) [1]. Because of its advantage in terms of higher integration density of heterojunctions than that of conventional 2D VdW hetero junctions owing to its extremely small size, assembling 1D VdW heterostructure is a reliable way for practical applications. In this research, we attempted the integration of 1D VdW heterostructure up to bulk-scale with CNT assemblies and investigated their electrical properties. In our research group, we have developed the fabrication technique of bulk-scale CNT assemblies such as sheet and yarn [2]. The CNT sheet and yarn can be fabricated by a dry process with the drawable CNT forest grown by precisely tuned chemical vapor deposition (CVD) (Fig. 1(a)). In this research, we performed hBN growth directory on the CNT assemblies by conventional powder CVD with a source of NH3BH3. The heterogeneous growth of hBN on the CNT sheet was confirmed by UV-vis-NIR spectroscopy, Fourier transform infrared (FT-IR) spectroscopy, X-ray photoelectron spectroscopy (XPS), and transmittance electron microscopy (TEM). From electrical transport measurements, we found the clear hysteresis in I-V curves, that is memristive behavior, with hBN-grown CNT assemblies (Fig. 1(b)). By the systematic experiments and structural observations, we proposed the possible mechanism of the memristive behavior relating to the presence of the amorphous carbon (a-C) between hBN/CNT heterostructures and disordered structure of hBN layer. TEM measurement clarified the grain boundaries and turbostratic hBN layers. XPS spectra indicated the existence of additional species: BC2O, having a large dipole moment comparing to natural C. This will enhance the motion of a-C because BC2O should be sensitive to an external electric field. The a-C seemingly formed a conductive filament channel (CFC) in the disordered hBN layer under a high electric field, resulting in the memristive behavior. The memristive behavior and its mechanism we proposed will contribute to the application of neuromorphic computing and non-volatile memory, and the understanding of the fundamentals in such abnormal phenomenon. [1] R. Xiang, et al. Science 367, 537–542 (2020). [2] H. Inoue, et al. Carbon 158, 662–671 (2020).

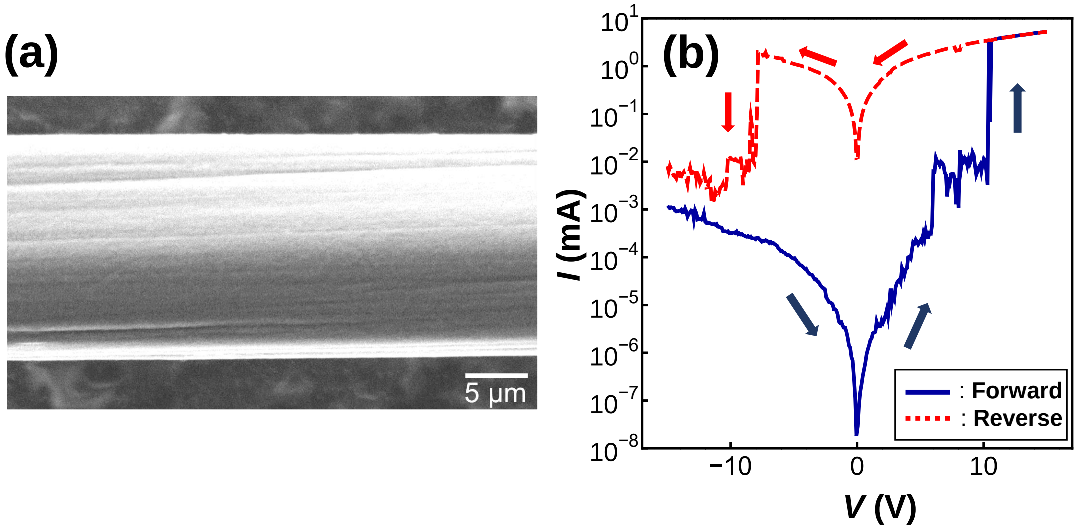

Fig. 1: (a)Scanning electron microscopy (SEM) image of CNT yarn. (b)I-V carve measured in hBN-grown CNT yarn.

D146: One-dimensional WS_2 growth by salt-assisted chemical vapor deposition

Hiroo Suzuki*†, Misaki Kishibuchi, Zheng Liu, Yasumitsu Miyata, Yasuhiko HAYASHI
**Okayama University*

Transition metal dichalcogenides (TMDCs) are potential candidates for the next-generation optoelectronics device such as photodetectors, light-emitting diodes, and solar cells due to their superior optoelectronic properties and flexibility. The optoelectronic properties of TMDCs are sensitive to their crystal structures such as the number of layers, crystal phase, defect density, and presence of edges. Because the dimension of the crystal is also an impactful factor, the dimension control from 3D to 2D (multilayer to monolayer) has been studied well, showing the significant increase of photoluminescence (PL) intensity. In contrast to such studies from 3D to 2D, much less study has been conducted on downscaling from 2D to 1D. The structure control from 2D to 1D is possible to allow us to investigate novel optoelectronic physics and applications derived from quantum confinement effect and presence of edges. The two strategies for the synthesis of 1D-TMDC can be considered. One is a top-down, and the other is a bottom-up process. The top-down approach by the conventional lithography technique is frequently used, but there is a great advantage in the bottom-up process in terms of the cleanness of the surface and edge. In this research, we have investigated the growth of 1D-WS_2 by chemical vapor deposition (CVD) with a metal salt, which is a bottom-up process. The cold-wall CVD system with the infrared gold image furnace was established for TMDC growth. The solution of Na2WO3 was employed as a W source for WS_2 and deposited on SiO2/Si substrates. The vapor of (t-C4H9)2S2 was introduced to a CVD chamber as an S source. From the systematic investigation of CVD growth, we found that the fiber-like materials can be grown with a relatively low (t-C4H9)2S2 supply. The atomic force microscopy (AFM) presented the fibers having around 3-5 nm in thickness, which is relatively thicker than monolayer WS_2, and its bundled structure (Fig. 1(a)). The fibers showed both almost the same Raman and PL peaks as monolayer WS_2 (Fig. 1(b)). The transmission electron microscopy (TEM) observations revealed the presence of WxOy nanowires in the sample. These results suggest that the 1D-WS_2 could be formed on the CVD-grown WxOy nanowire.

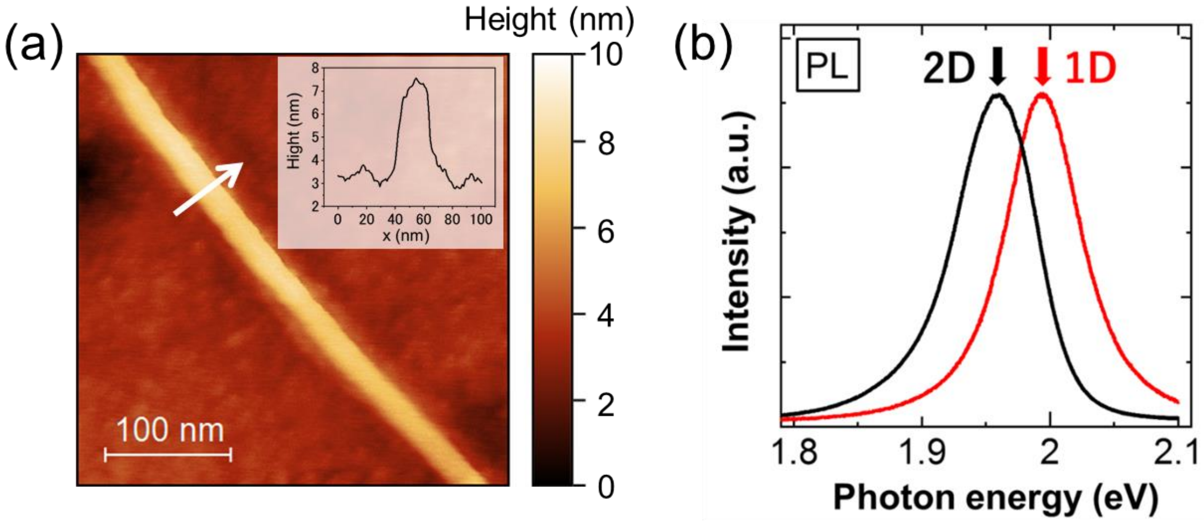

Fig. 1: Fig. 1. (a) AFM image of the fiber showing similar Raman and PL spectra of monolayer WS_2. Inset shows height profile along the white allow. (b) PL spectra of 1D-

D147: Microplasma synthesis of highly crystalline carbon nanotubes

Takashi Tsuji*†, Yoshiki Shimizu, Jaeho Kim, Hajime Sakakita, Guohai Chen, Kenji Hata, Don Futaba, Shunsuke Sakurai

**National Institute of Advanced Industrial Science and Technology (AIST)*

In demonstrating new synthesis techniques, the term ”scale-up” commonly enters the discussion as it is a necessary step for industrial usage. During the scale-up process of the gas-phase synthesis, often the synthesis process becomes more complex as the crucial mechanisms become affected by scale, such as thermal exchange, gas mixing, gas distribution, etc. As an attempted to simplify this situation, we have done the opposite.In this work, we report a compact gas-phase CNT synthesis reactor. This reactor consisted of a microplasma source which replaced the large thermal furnace to dissociate the reactant species, form the catalyst nanoparticles, and nucleate the carbon nanotubes. In thereby doing, we could create a continuous-flow, gas-phase synthesis of high quality CNTs, analogous to conventional gas-phase synthesis, but with a reaction zone 1/1000th the scale. The grown CNTs were highly crystalline small diameter CNTs (G-D band ratio: >100, diameter: ~2 nm) at an exceptionally high growth rate of >1000 µm/s. In addition, being in gas phase and channeled through a 0.8 mm inner diameter ceramic reactor, the grown CNTs could be locally deposited onto a substrate [1]. Furthermore, we also found that addition of H2 was critically important in increasing the yield and purity of the growth CNTs [2]. Optical emission spectroscopy of the plasma showed that without H2, the highly energetic electrons in plasma induced the decomposition of the catalyst and carbon precursors too quickly and simultaneously, which inhibited the formation of catalyst nanoparticles and led to the formation of amorphous carbon particles. In contrast, with the inclusion of H2, we observed that the gas temperature of the microplasma increased due to the electron-induced dissociation and recombination of the H2 molecules. This reaction consumed energetic electrons and created a thermal component to the reaction which slowed the decomposition of the carbon feedstock, thus allowing the formation nanoparticles and the consequent CNT growth. Based on our spectroscopic examination of this phenomenon, a simple reaction pathway model was proposed.

D148: Growth of high-density vertically aligned carbon nanotubes by suppressing Fe migration by the introduction of Fe/MoxOy catalyst

Mitsuaki Maetani†, Haolu Lin, Kyohei Nasu, Takeshi Nishikawa, Hiroo Suzuki, Yasuhiko HAYASHI*

**Okayama University*

Carbon nanotube (CNT) yarn; numerous CNTs are spun and form fiber, is the ideal structure for practical applications owing to its ease of handling. In our research group, we have developed the fabrication technique of CNT yarn by the dry spinning process with a vertically aligned CNT (VACNT) on a substrate. The reasonable strategy to improve the performances such as mechanical strength, electrical conductivity, and thermal conductivity is to increase the crystallinity of individual CNTs. For the drawability of VACNT, precise tuning of height and density are necessary [1]. The difficulty of the coexistence of high crystallinity and density of VACNT is a critical issue for realizing the high-performance CNT yarn. For this, we attempt the high-temperature growth (>700°C) which can suppress the formation of kinks and defects in CNTs. To increase the structural stability of catalyst particles under high temperature, we employed bimetallic catalysts with Iron (Fe) and Molybdenum (Mo) having a high melting point. The use of Mo can suppress the migration, aggregation, and coarsening of the catalyst particle, resulting in the extension of catalyst lifetime even under high temperature [2]. We employed MoxOy having a lower melting point (795°C in case of MoO3) prepared by pre-oxidation process than pure Mo (2623°C) to achieve homogeneous dispersion of catalyst particles on a substrate. The pre-oxidation process was carried out by annealing in air. CNTs were grown by a cold-wall CVD system in H2/N2 atmosphere with C2H2. The surface morphology of the substrate at the start point of CNT growth without C2H2 supply was measured by atomic force microscope (AFM) measurement. AFM analysis revealed that the pre-oxidation of Mo suppressed the coarsening of catalyst particles. This implies that the reduction from MoxOy to pure Mo happened after particle forming and suppress the coarsening of the catalyst particles with its high melting point. The Raman spectra of the CNTs grown with Fe/MoxOy catalyst showed a high G/D band ratio (~15), indicating the high crystalline of the CNTs. [1] H. Inoue, et al. Carbon 158, 662–671 (2020). [2] E. R. Meshot et al., Carbon 159, 236-246 (2020). *Acknowledgements:* We would like to H. Inoue, T. Nakagawa at Okayama University for experimental support.

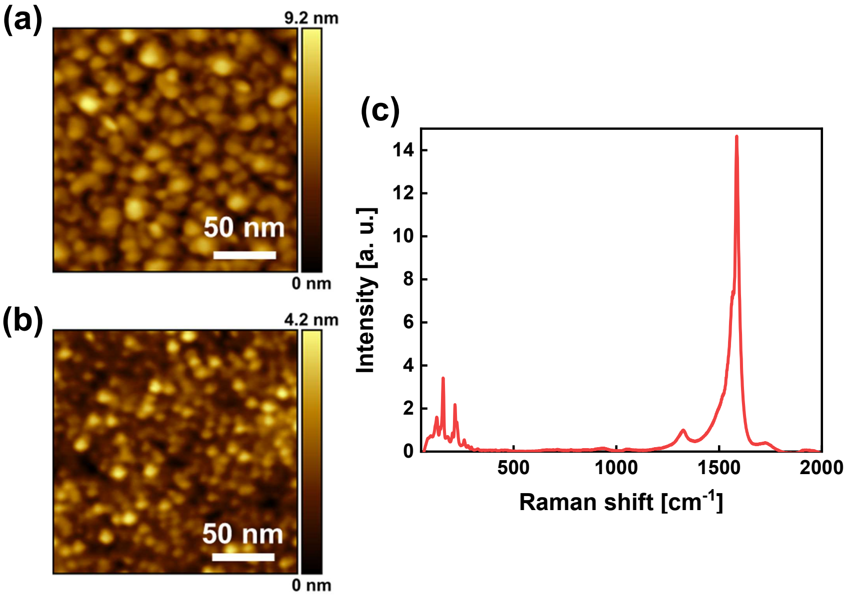

Fig. 1: AFM images of the surface of the substrate after annealing in H2/N2/nitrogen atmosphere (a) without and (b) with pre-oxidation of Mo. (c)The Raman spectra obtained by synthesized CNT.

D149: Synthesis and structural characterizations of zeolite-supported coaxial carbon nanotubes and boron nitride nanotubes van der Waals hetero structures

Ruixi Zhang*†, Ya Feng, Yongjia Zheng, Rong Xiang, Shigeo Maruyama

**The University of Tokyo*

Since the one-dimensional van der Waals heterostructures [1] were first invented, the synthesis of coaxial carbon nanotubes and boron nitride nanotubes structure has attracted great attention. Single-walled carbon nanotubes (SWCNTs) films were successfully used as the template, outside of which boron nitride nanotubes (BNNTs) were coaxially wrapped. Meanwhile, this successful development made it possible that various types of SWCNTs can be selected as the templates as well. Among these candidate templates, zeolite-supported SWCNTs were expected to synthesize the SWCNT-BNNT heterostructure in a high yield due to the porous surface of zeolite powder where catalytic nanoparticles were coated inside. In this study, a transfer-free CVD synthesis process was introduced. Zeolite powder was dissolved in ethanol solvent and transferred onto Mo/SiO2 TEM grid. The in-situ growth process was carried out to synthesize SWCNTs and BNNT in order. The structure of products was observed by Transmission Electron Microscope (TEM) and the results proved the successful growth of zeolite-supported SWCNT-BNNT heterostructure in principle, which was shown in Fig.1. Therefore, zeolite powders were directly used to synthesize

SWCNT-BNNT heterostructure in CVD system in order to achieve its mass production, which might provide great possibility for the practical application of SWCNT-BNNT heterostructure [2]. In this research, SWCNT-BNNT heterostructure on zeolite powder was measured under four kinds of excitation wavelengths by Raman spectroscopy, however there was no clear peak shift after wrapping BNNT outside the SWCNT structure. Zeolite-supported SWCNT-BNNT heterostructure was dispersed in heavy water solution and high-speed ultracentrifuge was used to seperate synthesized SWCNT-BNNT heterostructure out of zeolite powder. Afterwards, dispersed heterostructure solution was examined by optical absorption spectroscopy. The results in Fig.2 showed that there was no clearly specific peak of boron nitride structure compared with the one of carbon nanotubes, which might be caused by the very strong absorbance SWCNTs [3]. In addition, the Sodium deoxycholate surfactant was only effectively used to separate SWCNTs thus BNNTs might remain little in the dispersion solution, which resulted in the weak specific absorbance peak. Meantime, the surfactant was proposed to be removed by air annealing method, which was regarded as the big challenge to successfully characterize the BNNTs outside the SWCNTs.Reference[1] R. Xiang, et.al, Science 367 (6477), 537 (2020). [2] R. Nakanish, et.al, Scientific Reports volume 3, Article number: 1385 (2013)[3] Y. Feng, et.al, Journal of Applied Physics 129, 015101 (2021) *Acknowledgements:* Part of this work was supported by JSPS KAKENHI Grant Numbers JP18H05329, JP20H00220, and by JST, CREST Grant Number JPMJCR20B5, Japan.

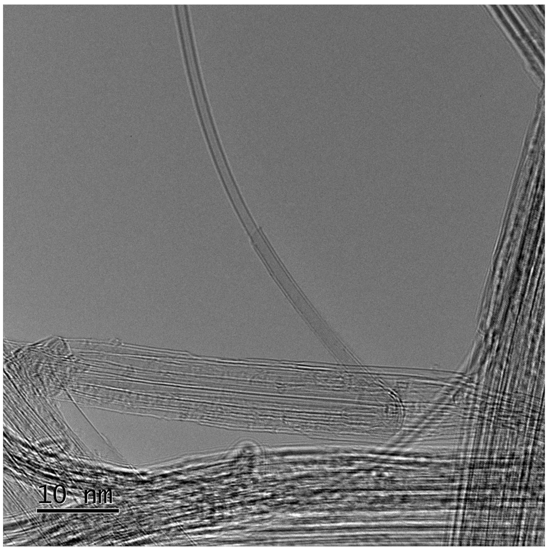

Fig. 1: The TEM images of SWCNT-BNNT heterostructure, the structure of SWCNT and BNNT were clearly observed.

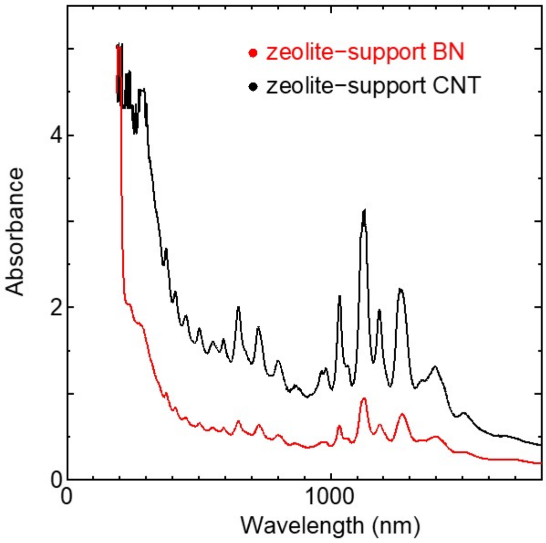

Fig. 2: The absorption spectra of dispersed SWCNT and BNNT structure, the difference of two peaks were not clearly found out.

D150: Large crystal growth of MoS_2 by Vapor-liquid-solid method with stacked growth substrates

Ryoki Hashimoto[†], Yijun Liu, Misaki Kishibuchi, Yasumitsu Miyata, Yasuhiko HAYASHI, Hiroo Suzuki*
**Okayama University*

Transition metal dichalcogenides (TMDCs); one of the semiconducting two-dimensional materials, have been attracting attention for optoelectronic device applications such as a solar cell, photodetector, and light-emitting diode owing to its high flexibility, light absorption and emission coefficient with direct band-gap. The most common issue on the crystal growth of TMDCs for practical applications is grain size control to achieve the smaller number of the grain boundaries in a continuous sheet of TMDCs which can reduce the negative influence from defects and impurities at the grain boundaries. In this research, we investigated the chemical vapor deposition (CVD) growth of single-layer MoS_2 and its size control based on the vaper-liquid-solid (VLS) method with metal salt employing the modified configuration of growth substrates. The CVD growth was conducted by the cold-wall CVD system with the infrared gold image furnace. A metal salt of Na2MoO4 was employed as a Mo source and its solution was spin-coated on a Si/SiO2 substrate. The vapor of (t-C4H9)2S2 was introduced into a CVD chamber as an S source. We employed the modified configuration of the growth substrates; the spin-coated substrate (B) was covered by another clean substrate (A) (Fig. 1a). The MoS_2 growth proceeded at both A and B sides, however, we obtained larger crystal size at A side than that of B. The maximum crystal size obtained at A side was more than 100 µm which is 10 times larger than that of conventional configuration using only one substrate (~10 µm) (Fig. 1b). We investigated the effect of the growth temperature on crystal size and photoluminescence (PL) intensity. Furthermore, we will report the growth of lateral heterostructure of MoS_2/WS_2 based on this method with staked growth substrates.

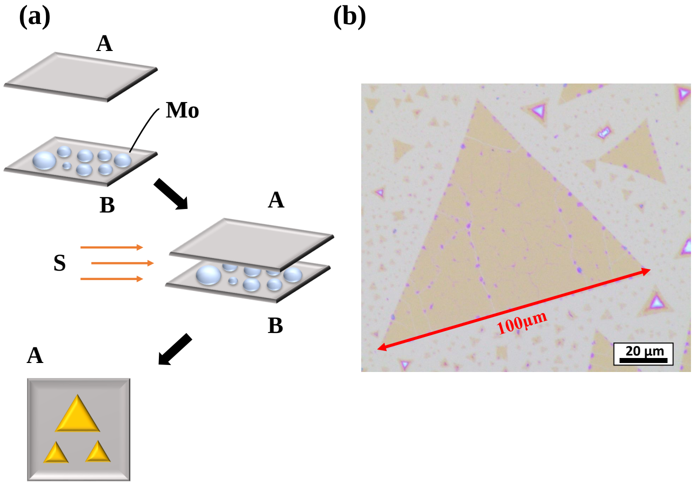

Fig. 1: (a)Growth process of MoS_2 with stacked substrates. (b)Optical microscope image of large size single-layer MoS_2 crystal (~100 µm).

D151: CNT growth manner of sulfur-assisted ethanol CVD with isotope labeling

Yoshiya Kishibe*†, Keishi Akada, Toshihiko Fujimori, Takamasa Onoki, Jun-ichi Fujita

**University of Tsukuba*

Thiophane dissolving in carbon sources for CNT grows to be an essential technique to enlarge the length and minimize the defects. However, the detailed understanding of the growth mechanism regarding the role of the thiophene is still unclear. In this study, we traced the CNT growth manner from the viewpoint of the CNT length and the diameter under the ethanol CVD of high-speed laminar flow combined with the 13C labeling. We conducted two steps of CNT growth process; the first process was the seed growth of the CNT using ferrocene dissolved ethanol mist, following by the body growth with pure ethanol mist. Typically, the ferrocene concentration was 0.01wt%, and 5µL of the mist was sprayed into the furnace at 980°C in 1L/min. of hydrogen carrier gas flow for the first step, and the second step was conducted by 750µL of pure 12C-ethanol for 3min. Thiophene dissolving for the seed growth showed effectively enlarge the CNT length and reduced the CNT diameter, as shown in Fig.1. Thiophene dissolving in the initial growth widens the length spread up to 25µm as shown in Fig.1(a) . In contrast, seed without thiophene showed the shorter length and concentrated around 3µm as shown in Fig.1(b). The Thiophene also reduced the CNT diameter around 1.3nm with the narrow distribution shown in Fig.1(c). In contrast, the wide distribution and wider diameter around 1.8nm as shown in Fig.1(d) of the seed without thiophene. We also estimated the carbon transfer efficiency in the iron catalyst of the CVD growth. We introduce the ferrocene and thiophene dissolved 13C-ethanol for the first stage and 12C-ethanol for the second stage. In Fig.2, Raman map appeared as the blue-colored edge area represented by 1545cm-1 of G-band, and the red-colored of body growth area by 1590cm-1.Here, the carbon atoms supplied by the first step were roughly 1020atoms during 0.1sec. Thus the 1nm diameter of the CNT could grow 5µm if the whole of the carbon source trapped at the iron particle. But the 2µm of observed growth length suggested the carbon source transfer efficiency to CNT growth was about 40%. In contrast, the second step was about 1.5x1022atoms/3minutes, and the 12C-CNT could grow 750µm for the body growth region. However, the observed 8µm length of the red area suggested that carbon transfer for the body growth efficiency was small, below 1%. *Acknowledgements:* This work was supported by Innovative Science and Technology Initiative for Security Grant Number JPJ004596, ATLA, Japan.

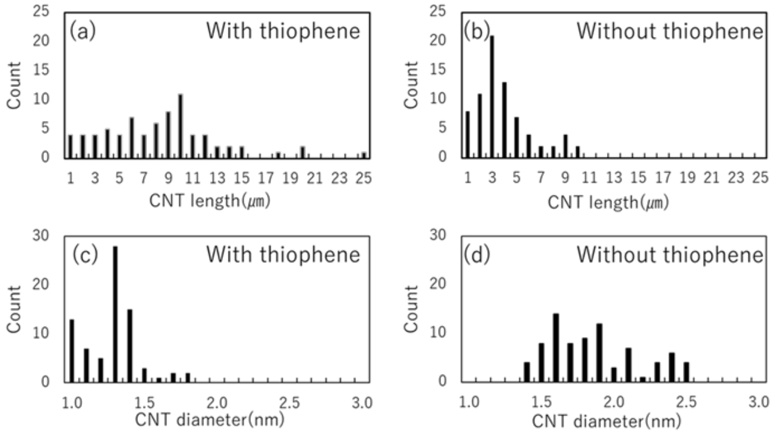

Fig. 1: Histograms of CNT length for with thiophene(a) and without thiophene(b) ,and diameter for with thiophene(c) and without thiophene(d).

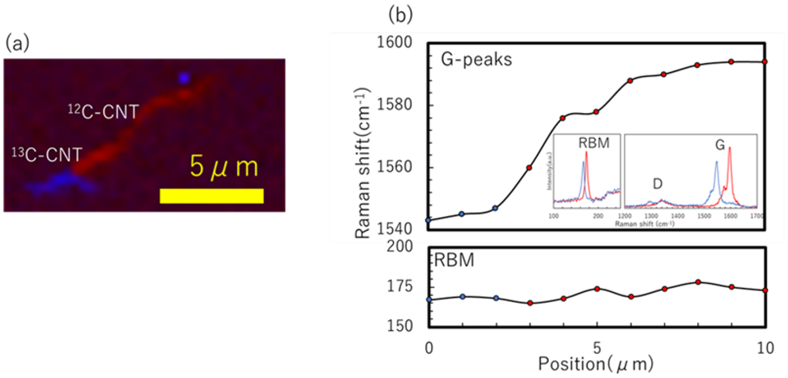

Fig. 2: (a)Raman mapping image of 13C-CNT(blue) to 12C-CNT(red), (b)Frequencies of G-peaks and RBM of the CNT versus distance from the edge.

D152: Comparison of gate-tuned high-harmonic generation between metallic single-walled carbon nanotubes and graphene

Hiroyuki Nishidome*†, Kohei Nagai, Kent Uchida, Kenji Kawahara, Junko Eda, Hitomi Okubo, Yohei Yomogida, Hiroki Ago, Koichiro Tanaka, Kazuhiro Yanagi

**Tokyo Metropolitan University*

High-harmonic generation (HHG), which is the generation of light with multiple optical harmonics, is an unconventional nonlinear optical phenomenon beyond the perturbation regime. HHG has been demonstrated in solid state materials [1] and control of such extreme nonlinear optical phenomena has been a challenging subject. Recently we succeeded to control the HHG of single walled carbon nanotubes (SWCNTs) with various electronic structures, from metallic and semiconducting with different bandgap, using electrolyte gating techniques [2]. We found the enhancement of 3rd order harmonics and the reduction of the other orders by the shift of Fermi-level in (6,5) SWCNTs [2]. It is expected that materials with large anharmonicity in the band dispersions would efficiently emit higher harmonics. Therefore, graphene and metallic single-walled carbon nanotubes (m-SWCNTs) with Dirac points in their band structures will exhibit unique HHG generation. Actually, highly efficient HHG has been demonstrated in Graphene [3], and its control by field effect has also been one of important subjects. In this study, we investigated relationships between HHG and carrier injections in the metallic SWCNTs and the graphene, and compared their behaviors. We prepared aligned-m-SWCNT film, transferred it on sapphire substrate, and employed side-gating device using ionic liquid to tune Fermi-level through the gate voltage VG. For measurements on graphene, we prepared chemical-vaper-growth monolayer graphene on Si/SO2 substrate and fabricated back-gating device. These samples were irradiated by 0.26 eV mid-infrared pulsed laser, and we investigated the relations between HHG and carrier injection. Figure (a) shows the HH intensities and source-drain current, ISD, in m-SWCNTs as a function of VG. The results indicate that carrier injection suppress all HHG: 5th harmonic intensity was drastically suppressed, and 3rd was a little suppressed. Figure (b) shows the HH intensities and ISD in graphene as a function of VG. In the case of graphene, HHG was almost constant through carrier injection. We observed clear difference between the HHG of m-SWCNTs and graphene. We will discuss experimental details and these backgrounds.References;[1] S. Ghimire et al. Nat. Phys., 15, 10 (2019). [2] H. Nishidome et al. Nano Lett., 20, 6215 (2020). [3] N. Yoshikawa et al. Science, 356, 736 (2017). *Acknowledgements:* This work is supported by JSPS KAKENHI through Grant Numbers JP17H01069.

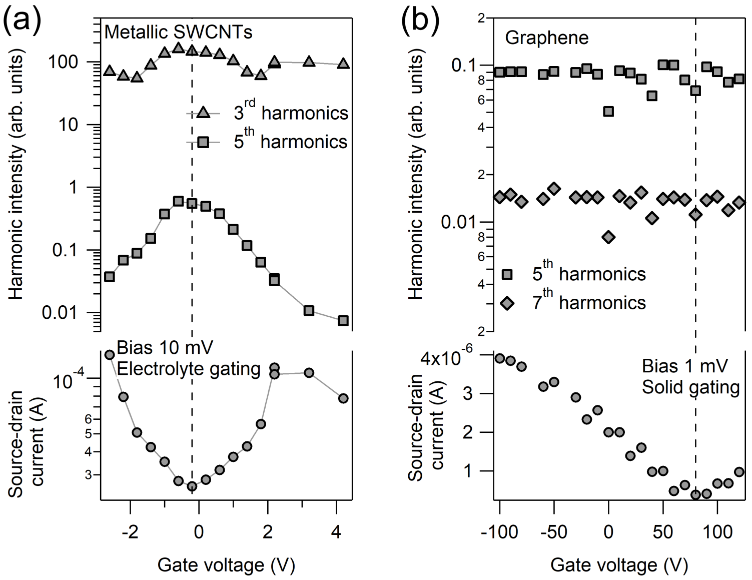

Fig. 1: High-harmonic intensity (top) and source-drain current (bottom) with the shift of the gate voltage in (a) metallic SWCNTs and (b) graphene.

D153: Highly efficient semi-transparent perovskite solar cells by MoO3-doping of carbon nanotube top contact and their four-terminal perovskite-silicon tandem solar cell application

Seungju Seo*, Kosuke Akino, Ahmed Shawky, Rong Xiang, Hiroki Nagaya, Hao-Sheng Lin, Bowen Zhang, Mohamad Almesfer, Esko Kauppinen, Yutaka Matsuo, IL Jeon, Shigeo Maruyama†

**the University of Tokyo*

To supersede the commercially available silicon solar cells (SiSCs), thin-film photovoltaics such as PSCs should extend the application to solar panel windows and tandem solar cells. Micrometer-thinness, light-weight and bandgap tunability of perovskite solar cells (PSCs) enable solar energy-harvesting windows which SiSCs cannot achieve. In addition, by combining PSCs with SiSCs in a tandem structure, the theoretical Shockley-Queisser (SQ) of ~33% can be surpassed thanks to the wider band gap of PSCs compared with that of SiSCs. However, both of those applications require PSCs to be semi-transparent while having high PCE.Recently, single-walled carbon nanotube (CNT) transparent electrode has been reported as the top electrode in semi-transparent PSCs and demonstrated high PCE surpassing even that of the metal electrode-based PSCs. Use of CNT electrodes drastically reduces the fabrication cost as they are made from abundant carbon sources and can easily be laminated onto devices by a simple mechanical transfer. The prospect of such CNT top electrode-based PSCs will be boosted if the efficiency and the transparency of the devices improve even further.Herein, we report multifunctional effects of MoO3 doping on CNT electrode in semi-transparent metal electrode-free PSCs (CNT-PSCs). MoO3 is thermally deposited onto the CNT top electrodes. By optimizing the thickness of MoO3, 8-nm-thick MoO3layer was found to give the highest PCE of 20.25% when deposited on CNT-PSCs, in which 70% transparent CNT electrode at a wavelength of 550nm was used. The devices showed increases in all of the photovoltaic parameters upon MoO3 doping, namely, VOC of 1.162V, JSC of 23.09 mA/cm2, and FF of 0.755. All of which are ascribed to the better aligned energy level, the enhanced electron-blocking ability and the conductivity of the CNT electrodes. The obtained PCE of CNT-PSCs surpasses that of the gold electrode-based control devices by 10.5%. The full potential of the MoO3-doped CNT-PSCs were assessed by stacking them to SiSCs using a computational model and simulating the 4-terminal tandem solar cells. The enhanced transparency in both visible and near-infrared region through the minimum parasitic absorption of MoO3 demonstrated expected higher performance of the MoO3-doped CNT-PSCs compared with ITO-based semi-transparent PSCs.

D154: Quasi 2D bulk Carbon Nanotube Film electrode enable low dopant additives for hole transport layer in perovskite solar cells

Bowen Zhang*†, Seungju Seo, Hao-Sheng Lin, Keigo Otsuka, Esko Kauppinen, Yutaka Matsuo, Shigeo Maruyama
**the University of Tokyo*

Perovskite solar cells (PSCs), since the first report in 2009, have outshined other photovoltaic counterparts with a soaring power conversion efficiency (PCE) from 3.8% to 25.5% in 2021. However, Au top electrodes have undermined the stability because of its diffusive nature into underlying constituent layers in PSCs. What's more, the high cost of Au electrodes also limits large-scale fabrication, thus finding a stable, cheap and highly efficient alternative for metal top electrodes becomes necessary. Among all candidates, carbon nanotubes (CNTs) stand out with superb chemical and mechanical stability as well as high conductivity. CNT synthesis technique has also been dramatically developed which makes CNTs more feasible for large-scale fabrication. Photovoltaic performance of CNT-top-electrode-based PSCs can be further improved by p-doping CNT with dopants including Trifluoromethanesulfonic acid (TFMS) and MoO3 as p-doping of CNTs can tune the work function of CNTs and achieve a better energy band alignment with photoactive perovskite layer. With proper p-doping of CNTs, the PCE of CNT-top-electrode-based PSCs can reach close or surpass that of gold electrode. P-type organic semiconductors such as Spiro-OMeTAD and Poly[bis(4-phenyl)(2,4,6-trimethylphenyl)amine (PTAA) have been employed as hole transport layer (HTL) to achieve high PCE in PSCs but they require dopant additive, Lithium bis(trifluoromethanesulfonyl)imide (Li-TFSI) to enhance their poor conductivity. Li-TFSI improves the conductivity of HTL but it also degrades PSC stability due to its hygroscopic nature. Therefore, minimizing the dopant additive as well as maintaining high enough conductivity for charge transfer in HTL is needed. Herein, we report our new finding that CNT top electrode enables less dopant additive for HTL to that of metal electrodes as charge transfer within HTL can benefit from high conductivity of quasi-two-dimensional CNT network. We fabricated PSCs in a configuration of glass/ITO/SnO2/CH3NH3PbI3/PTAA/CNT or Au to elucidate optimal amount of dopant additive for HTL. CNT-top-electrode-based PSC achieved PCE of 18.9% with dopant concentration of 0.323 mg/ml. whereas Au-top-electrode-based PSC achieved PCE of 17.07% with dopant concentration of 0.646 mg/ml.

D155: Bioinspired Ti3C2Tx MXene Architectures for High Performance Applications

Ken Aldren Usman*†, Ya Yao, Jizhen Zhang, Si Qin, Dylan Hegh, Minoo Naebe, Luke Henderson, Joselito Razal
**Insitute for Frontier Materials, Deakin University, Waurn Ponds, Australia*

Two-dimensional (2D) transition metal carbides and nitrides (MXenes), in particular, Ti3C2Tx received significant interest because of their outstanding conductivity and electrochemical capacitance. However, translating these properties into macroscopic structures and devices remains a challenge (e.g., pure MXene films and fibers possess poor tensile strength of ~34 and ~40 MPa, respectively). In this study, we explore strategies involving the addition of biologically derived bridging additives (e.g., polydopamine, nanocellulose, and silk nanofibrils) organized in between MXene sheets, resembling natural structures such as nacre, to significantly enhance the mechanical properties of free-standing MXene films and fibers, while simultaneously retaining their high conductivity and volumetric capacitance. Through links, via either hydrogen bonding, van der Waals, or ligand-metal interactions between the bridging additives and MXene sheets, composite films with strength, conductivity, and capacitance of up to ~339 MPa, ~4,850 S cm-1 and ~1,125 F cm-3, respectively, can be realized. We also showed that the particular surface chemistry, geometry, and colloidal stability of these bridging additives, are crucial factors in the formation of non-agglomerated and highly aligned sheets during solution processing of MXene architectures. We envisage that the knowledge gained in this study provides critical insights towards the processing of robust and multi-functional MXene-based materials without compromising electrical conductivity and electrochemical performance. *Acknowledgements:* The authors acknowledge the Deakin's Advanced Characterization, Australian Synchrotron and the Australian National Fabrication Facilities.

D156: Chemically activated porous nitrogen-doped carbon for sodium-ion batteries

Yuliya Fedoseeva*†, Elena Shlyakhova, Anna Vorfolomeeva, Svetlana Stolyarova, Mariya Grebenkina, Lyuba Bulusheva, Alexandr Okotrub

**Nikolaev Institute of Inorganic Chemistry SB RAS, Novosibirsk, Russia*

Nitrogen-doped carbon materials with hierarchical highly porous structure facilitate adsorbing/inserting of more sodium ions making them promising anode materials for sodium-ion batteries. Herein, porous nitrogen-doped carbon materials have been synthesis via template-assisted chemical vapour deposition (CVD) technique at 750 °C. The process includes the production of template nanoparticles through thermal decomposition of calcium tartrate or calcium glutarate, followed by CVD growth using acetonitrile and removal of the mineral template with diluted hydrochloric acid. These materials contain template-induced mesopores and micropores from nitrogen-inserting and atomic defects. In the present work, a hydrothermal treatment in ammonia solution, etching with potassium hydroxide and bromination were used for chemical activation of mesoporous nitrogen-doped carbon materials. Morphology, composition, atomic structure and textural characteristics of the original and activated nitrogen-doped carbon materials were studied by transmission electron microscopy, X-ray photoelectron spectroscopy, near-edge X-ray absorption fine structure spectroscopy, Raman scattering, infrared spectroscopy, and nitrogen gas adsorption methods. Electrochemical testing toward sodium-ion storage and electrochemical impedance spectroscopy measurements have been performed. Hydrothermal treatment and activation with KOH increased specific surface area and micropores and small mesopores due to the etching of carbon surface. Such activated samples demonstrate the highest electrochemical capacitance of 250 mAh g-1 at 0.05 A g-1. Bromination of nitrogen-doped porous carbon induced the additional reversible electrochemical reactions at 1.4 and 2.1 V from covalently bonded bromine and intercalated Br2, which result in to increase in total capacity value by 90 mAh g-1.This work was supported by the Russian Science Foundation (project No. 19-73-10068). *Acknowledgements:* This work was supported by the Russian Science Foundation (project No. 19-73-10068).

D157: Molecular Dynamics Simulation of Single-Walled Carbon Nanotube Growth from Metal Carbide Nanoparticles

Ryo Yoshikawa†, Kaoru Hisama, Ikuma Kohata, Shohei Chiashi, Shigeo Maruyama*

**The University of Tokyo*

It has been debated for years whether catalytic metal nanoparticles are solid or liquid and whether they should be pure metal, carbide, or oxides for efficient growth of single-walled carbon nanotubes (SWCNT) [1]. Elaborated environmental TEM studies combined with molecular dynamics (MD) studies nicely suggested the nucleation of SWCNTs from catalytics metal nanoparticles in carbide form, Co2C [2]. However, there are no MD simulations that show SWCNTs continuously grow on carbide nanoparticles. In this study, we show how SWCNTs grow on carbide nanoparticles using MD. By employing the same potential field as in our previous MD works demonstrated the Octopus growth [3] and chirality definable growth [4], we observed two different cobalt carbide structures and one iron carbide structure which can nucleate and grow SWCNTs. We used slightly larger catalysts diameter, say 80-100 metal atoms, with the temperature range similar to our previous works [3,4]. The carbon diffusion, and thus the growth rate of SWCNTs, depended largely on the carbide structure. As shown in Fig. 1, on layered hexagonal Co2C carbide nanoparticles, carbon chains, which act as the precursor of SWCNTs and the "octopus tentacles" to bind the catalysts and the SWCNTs, formed along the carbon layers. This means that there are several fitting intervals between the carbon chains, and thus between the carbon atoms on the growth edge of SWCNTs. Carbon atom intervals on the growth edge closely relate to the chiral angle. Considering that SWCNTs on cobalt nanoparticles grew in the tangential mode [5] (or octopus mode) [3] and the diameters solely depended on the nanoparticle diameters, there could be some suitable chiralities of SWCNTs on the hexagonal cobalt carbide nanoparticles.References:[1] F. Yang, M. Wang, D. Zhang, J. Yang, M. Zheng, Yan Li, Chem. Rev., 120, 2693–2758 (2020). [2] M. Picher, P. A. Lin, J. L. Gomez-Ballesteros, P. B. Balbuena, R. Sharma, Nano Lett., 14, 6104–6108 (2014). [3] K. Hisama, R. Yoshikawa, T. Matsuo, T. Noguchi, T. Kawasuzuki, S. Chiashi, S. Maruyama, J. Phys. Chem. C, 122, 9648-9653 (2018). [4] R. Yoshikawa, K. Hisama, H. Ukai, Y. Takagi, T. Inoue, S. Chiashi, S. Maruyama, ACS Nano, 13, 6506-6512 (2019). [5] M.-F. C. Fiawoo, A.-M. Bonnot, H. Amara, C. Bichara, J. Thibault-Pénisson, A. Loiseau, Phys. Rev. Lett. 108, 195503 (2012). *Acknowledgements:* Part of this work was supported by JSPS KAKENHI Grant Numbers JP18H05329, JP20H00220, and by JST, CREST Grant Number JPMJCR20B5, Japan.

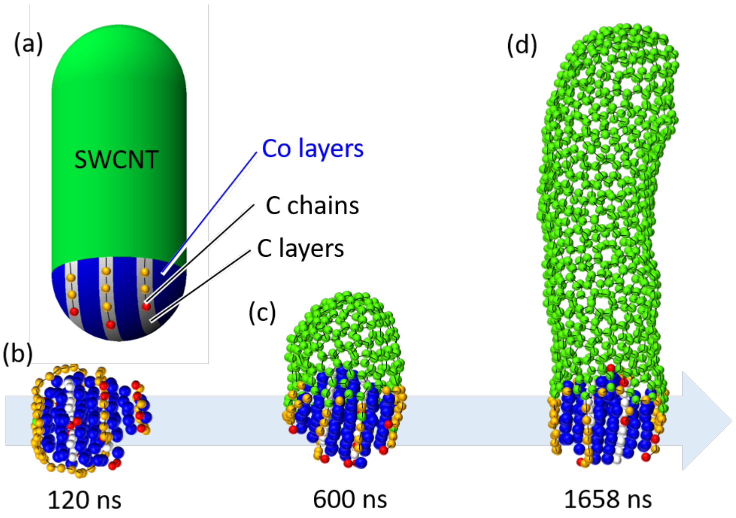

Fig. 1: (a) Schema and (b), (c), (d) Time evolution of SWCNT growth from Co100 carbide catalyst. The SWCNT and the carbon chains on the growth edge grew along the carbon layers.

D158: SWNT/SDS aqueous dispersions as photoluminescent nano-thermometers

Rosa D'Ambrosio*†, Ty Phou, Christophe Blanc, Eric Anglaret

Université de Montpellier

Temperature is one of the basic parameters often required to characterize a system. A great demand has arisen for local measurements, especially in liquids or complex biological environments. Various approaches have been proposed to study the temperature at the nano-scale level. Some of them are based on the spectroscopic properties of carbon nanotubes (CNT) used as sensors. Raman spectroscopy is indeed a powerful technique to identify single-walled carbon nanotubes (SWNT) and to study their structure, defects and electronic properties through the measurement of specific Raman signatures (RBM, D, G and 2D bands). On the other hand, individual SWNT or small bundles emit light in the near infrared and the photoluminescence (PL) spectra is very sensitive to the quality of the dispersion and the dielectric environment of the nanotubes. In particular, when SWNT are dispersed in aqueous solutions, the PL energies are sensitive to the nature of the surfactants or polymers, to their concentration, and to the way they adsorb on/wrap around the nanotubes. In this work we show that the PL/Raman spectra of SWNT dispersed with sodium dodecyl sulfate (SDS) is very sensitive to the temperature (figure 1) in a large range of SDS concentrations. We discuss the influence of the chiral angle of the SWNT on these PL changes, and the origin of the changes in terms of SDS reorganization at the surface of the nanotubes. Similar changes are obtained with increasing laser power (figure 2), showing the local heating of the nanotubes. These results pave the way for the development of SWNT-based nano-thermometers.

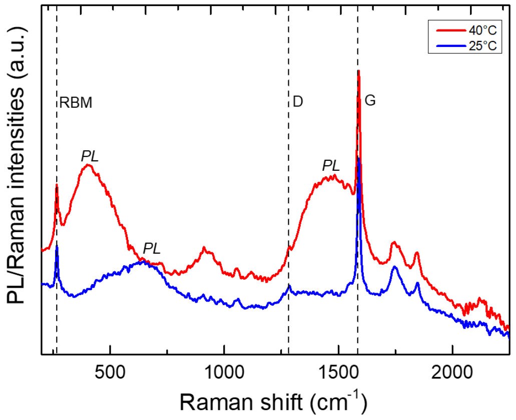

Fig. 1: Coupled micro-Raman/PL spectra of a SWNT:SDS dispersion at 25 °C and 30 °C, excited at λexc = 1064 nm and a laser power P(laser) = 2.1 mW.

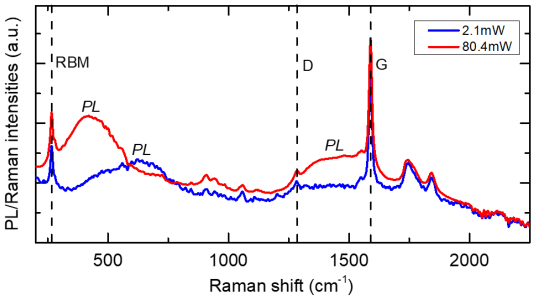

Fig. 2: Coupled micro-Raman/PL spectra of a SWNT/SDS dispersion at room temperature, excited at λexc = 1064 nm with two different laser powers.

D159: Thermodynamic control of quantum defects on functionalized single-walled carbon nanotubes

Yutaka Maeda*†, Yui Konno, Hiyori Murakoshi, Haruto Tambo, Michio Yamada, Pei Zhao, Masahiro Ehara

**Tokyo Gakugei University*

Chemical functionalization of single-walled carbon nanotubes (SWNTs) have attracted attention as a method to control their photoluminescent properties in near-infrared region. It has been reported that the photoluminescence (PL) wavelength of functionalized SWNTs depends on the method of functionalization and the PL quantum yields depend on the functionalization degree of functionalized SWNTs. For example, PL wavelength of oxidized SWNTs depends on the synthetic conditions, specifically the PL peak was observed at 1120 nm in the solution phase reaction and at 1300 nm in the solid phase reaction. This difference has been explained by the explanation that the PL wavelength strongly depends on the addition patterns of addenda based on the results of the theoretical studies using density functional theory (DFT) of model compounds.In this study, we conducted functionalization of SWNTs and subsequent thermal treatment to achieve stepwise control of their PL characteristics. A series of functionalized SWNTs were designed and prepared by the reductive alkylation of SWNTs using alkyldibromide. After the functionalization, new red-shifted PL peaks were observed as dominant peaks at 1215 - 1240 nm. The excitation spectra of these red-shifted PL peaks showed characteristic peaks at approximately 567 and 980 nm, which was in good agreement with the characteristic absorption peaks of (6,5) SWNTs, suggesting that these PL peaks originated from functionalized (6,5) SWNTs. Interestingly, the PL peaks assigned to the functionalized SWNTs were increased by thermal treatment. In addition, the PL peak shifted depending on the structure of addenda. In order to clarify the phenomena, DFT and time-dependent DFT calculations of functionalized SWNTs were conducted.
Acknowledgements: JSPS KAKENHI Grant-in-Aid for Scientific Research (B) (17H02735, 16H06511, 16H04104, 20H02210, 21H01759)

D160: Preparation of Fractal-shaped Graphene Sheets by Electrochemical Exfoliation based on Biasedly Switched Direct Current Method

Sungmook Lim†, Wonoh Lee*

**Chonanm National University*

Graphene, a sp2 bond honeycomb lattice carbon atom sheet, has gathered great interests in various engineering applications owing to its extraordinary property. Among different synthesis methods of graphene sheets, a chemical oxidation has become popular for mass production; however, it can be less desirable in a viewpoint of eco-friendliness because harmful chemical reagents to be cleaned are necessary to oxidate and exfoliate graphite. Recently, electrochemical exfoliation has been regarded as an alternative mass production method, where the exposure to toxic chemicals is less severe and the process time is much shorter; therefore, higher-quality graphene sheets can be produced with a lower degree of oxidation. Unfortunately, conventional electrochemical exfoliation applying constant direct current (cDC) to bulk graphite (BG) has shown the unsatisfactory quality and slow production rate of graphene sheets because the accumulation of intercalating ions is unavoidable owing to one-directional current flow. In this work, we used expanded graphite (EG) instead of BG and applied biasedly switched DC (b-sDC) in order to achieve more efficient intercalation between graphite layers. Since the EG has a larger interspacing distance and the switching current has both positive and negative voltages, the intercalating ions can effectively penetrate into the innermost region of graphite. As shown in Fig. 1, the graphene sheets by the b-sDC method using EG exhibited 400% larger area, 50% thinner thickness, and 15 times higher electrical conductivity than those by the cDC method using BG. In addition, the b-sDC technique with EG produced fractal-shaped graphene sheets having non-Euclidean geometry (Fig. 2), where the dimensional edge-to-area ratios are large enough to be efficiently hybridized with various nanomaterials. *Acknowledgements:* This work was supported by the National Research Foundation (NRF) of Korea grant (2021R1A2C2005751).

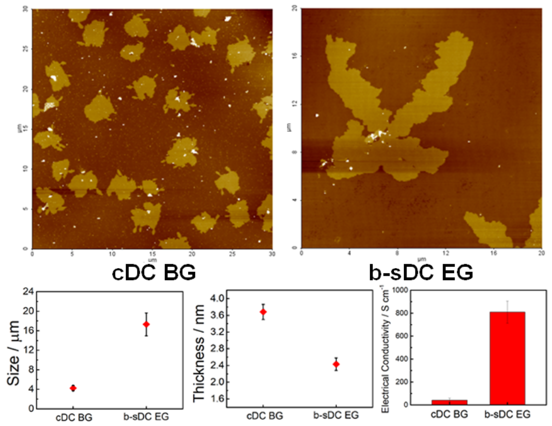

Fig. 1: Atomic force microscopy images, sizes, thicknesses, and electrical conductivities of the graphene sheets by the cDC with BG and the b-sDC with EG.

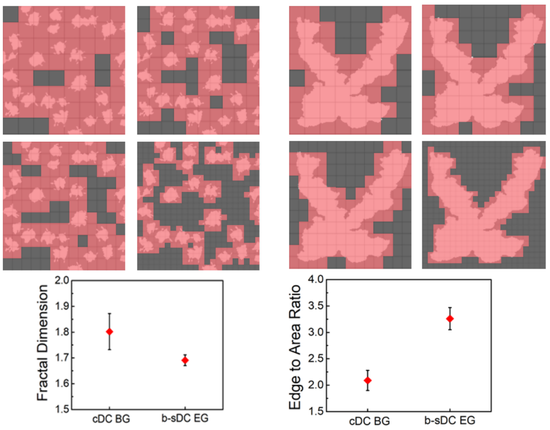

Fig. 2: Fractal dimension analyses and edge-to-area ratio of the graphene sheets by the cDC with BG and the b-sDC with EG.

D161: Catalyst-Mediated Enhancement of Carbon Nanotube Alignment and Crystallinity by Laser Irradiation

Thurid Gspann*†, Adarsh Kaniyoor, Wei Tan, Philipp Kloza, John Bulmer, Jenifer Mizen, James Elliott

**Institute of Nanotechnology, Karlsruhe Institute of Technology, Karlsruhe 76021, Germany*

The photonic post-processing of suspended carbon nanotube (CNT) ribbons made by floating catalyst chemical vapor deposition (FC-CVD) results in selective sorting of the carbon nanotubes present [1]. Defective, thermally non-conductive or unconnected CNTs are burned away, in some cases leaving behind a highly crystalline (as indicated by the Raman G:D ratio), highly conductive network. However, the improvement in crystallinity does not always occur but is dependent on sample composition. Here, we report on fundamental features, which are observed for all samples. Pulse irradiation (not only by laser but also white light camera flashes, as well as thermal processes such as Joule heating) lead to (1) the sweating-out of catalyst nanoparticles resulting in molten catalyst beads of up to several hundreds of nanometres in diameter on the textile surface and (2) a significant improvement in CNT bundle alignment [2]. The behavior of the catalyst beads is material dependent. Here, we show the underlying mechanisms of the photonic post-treatment by modelling the macro- and microstructural changes of the CNT network and show that it is mainly the amount of residual catalyst which determines how much energy these materials can withstand before their complete decomposition. [1] Bulmer et al., Sci. Rep. 2017, 7, 12977[2] Gspann et al., Catalysts 2021, 11, 368

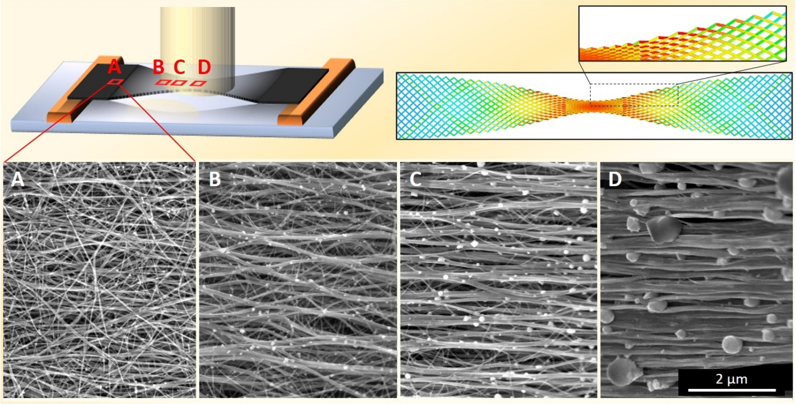

Fig. 1: Measurement positions on an irradiated sample as marked on the sketch: Alignment and bundle diameter increase with temperature, as does the size of the catalyst particles sweating out.

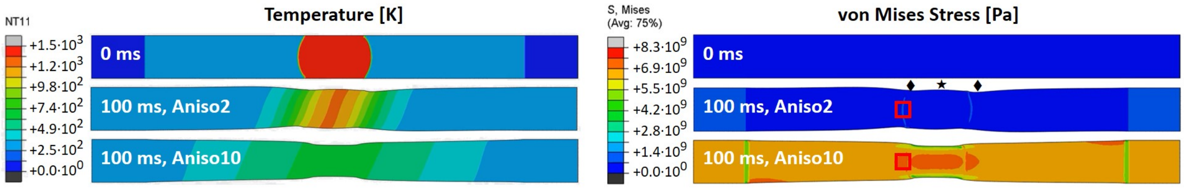

Fig. 2: Temperature profiles and von Mises stress snapshots at the initial state, and temperature and stress distribution after 100 ms, for CNT films with anisotropy factors of 2 and 10.

D162: Advances in Surfactant Aqueous Two-Phase Extraction of Single (n,m) SWCNTs

Jeff Fagan*†

National Institute of Standards and Technology

This poster will present and discuss some of the recent advancements in technology and methodology of aqueous two-phase extraction (ATPE) using surfactants for the isolation of individual (n,m) species of SWCNTs. Examples will be shown across different SWCNT diameter ranges and species type, and will include utilization of information from fluorescence-based characterization of the ATPE system. Method variations to improve yield or to compensate for local variables will also be included.

D163: MD Simulation of a SERS Sensor by Attachment of the Au Cluster to Graphene Nanopore to Define Vibrational Spectra of Nucleotides

Tatiana Zolotoukhina*†, Mohd Aidil Amin Bin Mohd Nasir, Shingo Iwakura

University of Toyama

Sensing and analysis of protein structure and DNA sequences and epigenetic modifications are essential for the understanding of the mechanism of cell functions and the development of diseases. The surface-enhanced Raman scattering (SERS) nanoprobes have opened a way to identify molecular structures in a label-free way and investigate mechanisms of interaction with the environment in biomolecules with the high sensitivity and specificity of their fingerprint-like spectra. As current Raman scanners rely on multiple spectra acquisitions, the use of nanoparticle agglomerates provides sufficient enhancement for the single-molecule measurements [1]. Development of the SERS spectroscopy promotes work on DNA and protein identification at a single oligomer resolution and with respect to interactions [2-3]. The study of the vibrational spectra of the nucleotides in the dynamic interaction with the Au nanoparticles (NP) located close to (grown on) graphene nanopore combines (1) translocation localization by graphene nanopore and (2) nucleotide interaction enhancement by Au NP. The spectral maps of the nucleotides were obtained by molecular dynamics (MD) simulation with LJ interaction between components. The spectra of various bonds were evaluated in reaction coordinates for DNA nucleotides and in Cartesian ones for Au NP. Spectra at the interaction with the Au NP helps to select a transient COM velocity of nucleotide passing along the cluster and at the edge of the graphene pore. The COM velocity of nucleotide has been set at 0.025 m/s after some estimation. We test the nucleotide-graphene-NP system to understand the influence of the LJ interaction with Au NP at the translocation time on the transient spectra calculated by MD. The frequencies that can serve as markers of the corresponding Au – nucleotide interaction are evaluated. The proposed simulation method can create spectral libraries for vibrations of molecules vs. different types of interaction to specify the interaction's type and strength in SERS measurements. Vibrational spectra of the tip atoms of Au20 nanoparticle and Cytosine C-C ring bond marked on the right panel. [1] L. M. Almehmadi, S. M. Curley, N. A. Tokranova, S. A. Tenenbaum & I. K. Lednev, Sci. Reports, 9, 12356 (2019). [2] T. Zolotoukhina, M. Yamada and S. Iwakura., Biosensors, 11, 37 (2021)[3] D. Macdonald, E. Smith, K. Faulds, D. Graham, Analyst, 145, 1871-1877 (2020). *Acknowledgements:* T.Z. gratefully acknowledges the assistance in calculations and preparation of the results of [2] done by M. Yamada that were extended here.

D164: Antifouling Graphene Oxide Membranes

Aaron Morelos-Gomez*†, Souya Terashima, Rodolfo Cruz-Silva, Josue Ortiz-Medina, Roque Sánchez Salas, Juan Fajardo, Emilio Muñoz-Sandoval, Florentino López-Urías, Kenji Takeuchi, Mauricio Terrones, Morinobu Endo

**Shinshu university*

Membrane technology is used to provide potable water and for food processing. Unfortunately, typical polymeric membranes are prone to fouling during operation due to the presence of organic material in natural water sources and food. Hence, antifouling membranes are highly desired. Graphene oxide (GO) membranes have been studied for molecular separation, however, little attention has been given to their antifouling properties. In this work, we studied the fouling properties of bovine serum albumin (BSA), lysozyme and milk. Protein fouling experiments, demonstrate high antifouling of negatively charged BSA and minimum adsorption of positively charged lysozyme. Hence, molecular charge is influential for antifouling. Furthermore, we studied fouling when using GO membranes for milk filtration by alternating water and milk filtration stages to analyze the permeate flux. Here, we observed that GO membranes, commercial nanofiltration (NF) and ultrafiltration (UF) membranes exhibit fouling with the same composition as milk (lactose, proteins and fat). Surprisingly, GO membranes exhibit a porous foulant layer that allow a higher permeate flux recovery than commercial NF and UF membranes. The obtained results demonstrate that GO membranes are promising for real-world applications that include organic matter such as food industry, medicine, pharmaceuticals, and other related applications. *Acknowledgements:* A.M.G., R.C.S., K.T., and M.E acknowledge that this work was supported by the Center of Innovation Program, Global Aqua Innovation

D165: Influence of crystallinity on the electrical conductivity of individual carbon nanotubes

Mattias Flygare*†, Krister Svensson

**Karlstad University*

The material properties of graphene and carbon nanotubes are highly sensitive to defects. Future exploitation of these materials will thereby rely on both a detailed understanding and classification schemes for material quality [1,2]. For graphene there have been suggestions of scaling laws, that could link the electrical conductance to the average grain size in polycrystalline graphene [3]. Similar studies on carbon nanotubes are also highly desirable in order to develop classification schemes and quality measures of these materials.Here we have used electron diffraction to measure the mean effective crystallite size of individual multi-walled carbon nanotubes, while simultaneously probing their electrical resistance. By keeping the bias voltage low and avoiding end contact with the tubes we limit conduction to only the outermost layer. We find a significant link between crystallite size and electrical conductivity. For larger crystallite sizes (diameter above 10nm) we find that the conduction can be described by highly conductive grains, separated by lower conductivity grain-boundaries that dominate the overall conductivity. For smaller grain sizes (diameter below 10nm) we find that both the conductivity within each grain and the conductivity of the grain-boundary is strongly reduced. We infer that this behaviour is due to quantum confinement and edge effects, similar to those that arise in graphene nanoribbons [4]. We suggest a scaling model for the electrical conductivity within a single layer of a CNT which connects its electrical conductivity with the effective crystallite size and tube diameter. This may provide an important but previously missing piece of the puzzle of trying to distinguish and classify different types of carbon nanotubes and their properties. [1] A. P. Kauling, A. T. Seefeldt, D. P. Pisoni, R. C. Pradeep, R. Bentini, R. V. B. Oliveira, K. S. Novoselov, and A. H. C. Neto, Adv. Mater. 30, 1803784 (2018). [2] M. Flygare and K. Svensson, Mater. Today Commun. 18, 39 (2019). [3] A. Isacsson, A. W. Cummings, L. Colombo, L. Colombo, J. M. Kinaret, and S. Roche, 2D Mater. 4, 012002 (2016). [4] Son, Y. W., Cohen, M. L., & Louie, S. G. (2006). Energy gaps in graphene nanoribbons. Physical Review Letters, 97(21), 1–4.

D166: Sustainable Solvents for Graphene Production: Yield and Structural Defect Analysis

Kai Ling Ng*†, Barbara Maciejewska, Ling Qin, Zhicheng Xu, Dillon McGurty, Dmitry Eskin, Iakovos Tzanakis, Kyriakos Porfyrakis, Jiawei Mi, Nicole Grobert

**Department of Materials, University of Oxford, Oxford OX1 3PH, UK*

Efficient liquid phase exfoliation of graphite to produce graphene is still relying on harmful solvents to the environment, e.g., 1-Methyl-2-pyrrolidinone (NMP), because green solvents with low boiling points are inefficient and produce only low graphene yields due to the limited dispersibility of graphene in these solvents. However, both the dispersibility of graphite and the solvent exfoliation efficiency are key parameters and contribute independently to the final graphene yield. By studying shear-mixing processes and understanding the actual exfoliation efficiency of the solvents, it is possible to increase the dispersibility of graphene by over 40 times. We studied the solvent exfoliation efficiency of graphite flakes and powders in a series of green solvents. The highest exfoliation efficiency which was comparable to that of NMP for both types of graphite was found to be for isopropanol (IPA), despite the poor dispersibility of graphene in IPA. By redispersing the products in NMP after exfoliation in green solvents, we could show that the dispersibility and graphene concentration in IPA can be further improved by a simple 2 min-sonication post-exfoliation step. The graphene produced by this method typically exhibited ca. 10 layers and an ID/IG ratio of 0.25. Our studies prove that the graphene yield in green solvents is not limited by the exfoliation efficiency as such but is due to the poor dispersibility. Our findings pave the way for other post-exfoliation methods and the use sustainable solvents for industrial-scale graphene production. *Acknowledgements:* We thank the Physical Sciences Research Council (Grant No. EP/L019965/1, EP/L019884/1, EP/L019825/1 and EP/R031975/1) and the Royal Society.

D167: Dual-targeted o-MWCNT to enhanced cancer therapy

Mahsa Saramiforoshani*†, Lorena García-Hevia, Mónica L Fanarraga

**Instituto de Investigacion Marques de Valdecilla (IDIVAL)*

Today chemotherapy (chemical agents) and targeted therapy (monoclonal antibodies and anti-angiogenesis drugs) are used to treat cancers. Chemotherapy is a broad therapy, killing both normal and cancer cells1. Also, in targeted therapy, patients have limited responses to monoclonal antibody therapy due to the development of resistance2. Consequently, these methods are not efficient enough. In many cancers, Human epidermal growth factor receptors (HER2) signaling increases through overexpression3. Escalating signaling cascade of HER2 with the help of vascular endothelial growth factor receptors (VEGFR) that trigger angiogenesis, develop and progress aggressive types of Cancers4,5. We designed recombinant proteins engineered to target cancer cells expressing HER2 and new blood vessel cells expressing VEGFR. In the next step, we coupled these recombinant chimera targeting proteins with oxidized multi-walled nanotubes (o-MWCNTs) that are biodegradable. When this system attaches to the receptors (HER2 and VEGFR), o-MWCNTs inter cancer and vascular cells. As a result, our system not only can block the receptors on the surface of cancer and vascular cells but also can kill cancer and vascular cells through o-MWCNTs intrinsic antitumoral effects (our group researches) 6. We can apply a laser beam to increase the cells' temperature and kill them since carbon nanotubes can absorb near-infrared and convert to heat7. With this double targeted strategy towards HER2 and VEGFR, we will be able to inhibit cancer cell proliferation and neovascular formation more efficiently and prevent metastasis.Majidi J, Barar J, Baradaran B, Abdolalizadeh. Target therapy of cancer: Implementation of monoclonal antibodies and nanobodies. Hum Antibodies. 2009;18. Aldeghaither DS, Zahavi DJ, Murray JC, et al. A Mechanism of Resistance to Antibody-Targeted Immune Attack. Cancer Immunol Res. 2019;7(2):230. Meric-Bernstam F, Johnson AM, Dumbrava EEI, et al. Advances in HER2-Targeted Therapy: Novel Agents and Opportunities Beyond Breast and Gastric Cancer. Clin Cancer Res. 2019;25(7).Yang J, Wang Q, Qiao C, et al. Potent anti-angiogenesis and anti-tumor activity of a novel human anti-VEGF antibody, MIL60. Cell Mol Immunol. 2014;11(3):285-293.Oh DY, Bang YJ. HER2-targeted therapies - a role beyond breast cancer. Nat Rev Clin Oncol. 2020 Jan;17(1):33-48.García-Hevia, L.; Villegas, J. C.; Fernández, F.; Casafont, Í.; González, J.; Valiente, R.; Fanarraga, M. L. Multiwalled Carbon Nanotubes Inhibit Tumor Progression in a Mouse Model. Adv. Healthc. Mater. 2016, 5 (9), 1–21.Singh, R., & Torti, S. V. (2013). Carbon nanotubes in hyperthermia therapy. Advanced drug delivery reviews, 65(15), 2045–2060. *Acknowledgements:* This work has been supported by the Spanish MINECO, Instituto de Salud Carlos III, European Union (European Regional Development Fund-ERDF)

D168: Water adsorption phenomena of vertically-aligned SWCNT forests measured by Raman scattering spectroscopy

Shohei Chiashi*†, Masanori Bamba, Shu Sato, Taiki Inoue, Shigeo Maruyama

The University of Tokyo

Vertically-aligned SWCNTs (VA-SWCNTs) have structural advantages, such as highly-alignment, high density, and large surface area. Due to these features, VA-SWCNTs are expected to be excellent gas molecule adsorber. Especially, the adsorbed water molecule on an isolated and suspended SWCNT are interesting and they have been spectroscopically investigated [1,2]. However, the water adsorption properties of VA-SWCNTs are not clear. In this study, we investigated the water adsorption phenomena on VA-SWCNT forests by using Raman scattering spectroscopy.VA-SWCNTs were synthesized on SiO2/Si substrates by CVD method using Co/Mo catalyst and ethanol as the carbon source. The VA-SWCNT thickness was approximately 5 um, as shown in Fig. 1. Raman scattering spectra were measured from the forest top side in an environmental chamber with different water vapor pressure and temperature. The excitation laser wavelength was 488 nm. Radial breathing mode (RBM) peaks are shown in Fig. 2. They were measured at different water vapor pressure at room temperature. RBM peaks showed changes in Raman shift and intensity due to water adsorption, and water adsorbed on the larger diameter SWCNTs at lower vapor pressure. The temperature and vapor pressure dependence suggested that VA-SWCNT samples contained both partially-isolated SWCNTs and bundled SWCNTs. The partially-isolated SWCNTs exhibited adsorption and desorption phenomena as the RBM peak changes, while bundled SWCNTs did not show any changes. Additionally, it was found that bundled SWCNTs affected the water adsorption on partially-isolated SWCNTs. The adsorption rapidly occurred with increasing water vapor pressure in VA-SWCNT with lower density. On the other hand, the adsorption showed a delay in higher density cases. [1] Y. Homma, et al., Phys. Rev. Lett., 110, 157402 (2013). [2] S. Chiashi et al. Phys. Rev. B, 91, 155415 (2015).

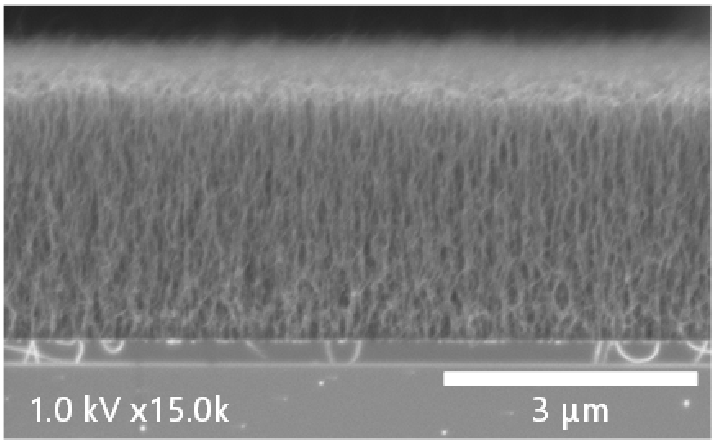

Fig. 1: SEM image of VA-SWCNTs.

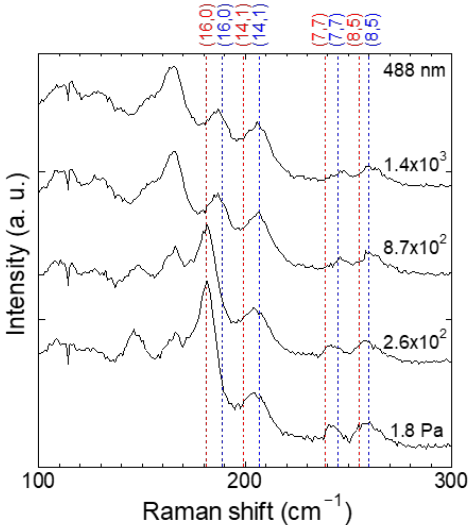

Fig. 2: RBM peaks at different vapor pressures. The red and blue lines indicate Raman shift in vacuum, and ambient air, respectively.

D169: Fingerprints of Moiré Interference between Carriers in Graphene Superlattices and Analogies to Twisted Graphene Bilayers at Magic Angles

Saúl Herrera*†, Gerardo G. Naumis

Universidad Nacional Autónoma de México

Motivated by recent experimental findings on the low-energy spectrum of Kekulé-patterned graphene, the optoelectronic signatures of graphene superlattices with a spatial modulation that triples the size of the unit cell and folds the valleys to the center of the Brillouin zone are studied. For superlattices like those visualized in recent experiments, the optoelectronic response reveals multiple species of carriers distinguished by their effective masses or Fermi velocities. Their signatures are similar to those of multifold fermions in which different frequency intervals are dominated by different types of quasiparticles.Remarkably, the response of these systems exhibits a characteristic peak in the optical conductivity suggesting a kind of moiré interference between the different species of carriers. We also show a relation between these systems and moiré superlattices obtaining a minimal model for a graphene superlattice that exhibits flat bands like those found in twisted graphene bilayers.

D170: HiPCO SWCNT Based Strain Sensor for VR Gloves

Anto Godwin*†, Sreekanth S, Aparna Allannavar, Sneha Sreedhar Rao, Kartik Shrivastava, Gadhadar Reddy, Robert Kelley Bradley

**NoPo Nanotechnologies India Private Limited*

Single Walled Carbon Nanotubes (SWCNT) have gained a immense interests in the field of piezo-resistive sensors due to is exceptional electrochemical properties. For a liner increase in the strain, the stretchable SWCNT network provides a linear change in the electrical resistivity. In this work, we have showcased the development of the horizontally aligned HiPCO® SWCNT film, the fabrication of the strain sensor and the smart glove developed using the strain sensor. The sensors were tested for more than 60,000 cycles which showcases a stable and repetitive resistance change with respect to the applied strain with less than 5msec response time. This performance makes it suitable for the use in real time tracking of finger movements which can be used in the various VR and AR industries. *Acknowledgements:* NoPo Nanotechnologies

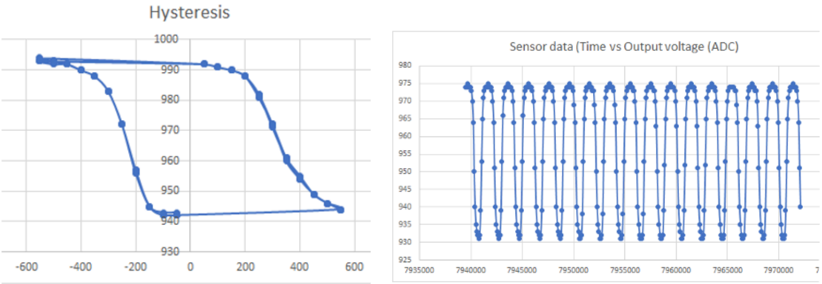

Fig. 1: The sensor response with respect to strain (left), with respect to time (Right)

Fig. 2: Hand movement in close and open position

D171: Latest developments in HiPCO® process

Anto Godwin*†, Varun Shenoy G, Selvamani S, Gadhadar Reddy, Robert Kelley Bradley, Andrew Barron

**NoPo Nanotechnologies India Private Limited*

High pressure carbon monoxide (HiPCO®) synthesized single-walled carbon nanotubes (SWCNTs) have been a widely studied carbon nanomaterial for nearly two decades. It has been the de facto standard for SWCNT research-be it functionalization, separation and purification, or composites- as a result of the consistent, high quality material that was made available at an affordable price to researchers worldwide. The recent shutdown of the HiPCO reactor at Rice University has resulted in a scarcity of HiPCO material to the research community, and a new source of similar SWCNTs was desperately in need. Continued research and development on the design, materials used, and the overall process have led to a new HiPCO reactor, referred as NoPo HiPCO, as an alternative to the erstwhile Rice HiPCO SWCNTs. In this work, we have compared the two HiPCO materials, and also discuss how the newer NoPo HiPCO can provide for a better starting material as well. *Acknowledgements:* NoPo Nanotechnologies

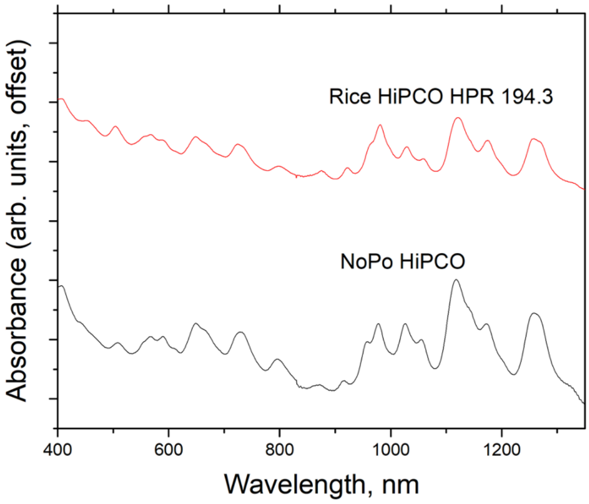

Fig. 1: UV-vis-NIR spectroscopy comparing an example Rice HiPCO batch to NoPo HiPCO. The spectra show a similar distribution of metallic- and semiconducting-SWCNTs in both ensembles.

D172: SWCNT Enhanced Thin film composite Desalination Membrane

Anto Godwin*†, Sreekanth S, Arpan Sahoo, Risshabh Balasubramanian, Sneha Sreedhar Rao, Gadhadar Reddy, Robert Kelley Bradley

**NoPo Nanotechnologies India Private Limited*

Development of energy efficient desalination technologies have always actively been pursued by scientists. While developing such technology the energy consumption, cost, market viability is becoming a major challenge. Recently carbon nanotubes are studied for various type desalination membranes among them thin film composite (TFC) based reverse osmosis membranes have been largely studied. In this work, we have demonstrated the construction of the carbon nanotubes based TFC membrane and its performance over different ppm of saline water. The TFC were constructed in such a way that the majority of the carbon nanotubes have their end open across the composite layer providing a path for the water molecule to pass through with high flux rate. The membranes were tested on the crossflow filtration setup. The membranes were able to reject the salt up to 95% while having the flux rate of 38 LMH.

D173: Bioapplications of NIR-Emissive Graphene Quantum Dots

Anton Naumov*†

**Texas Christian University*

Recently carbon nanomaterials have gained a significant attention in the field of biotechnology acting as drug delivery vehicles, theragnostic moieties or nanoscale biosensors. Near-infrared (NIR) emissive nanostructures pose additional advantage having the capability of therapeutic imaging in the NIR water window where biological tissue is more transparent. Here we develop and explore the most prominent applications of such near-infrared active graphene quantum dots (GQDs) in biotechnology.Graphene quantum dots synthesized top-down from graphitic carbon precursors or in bottom-up from simple sugars and biomolecules can be designed to perform a number of functions desired from the nanomaterials in biomedicine. Although there are very few reports of the GQDs fluorescing in the NIR due to the scarcity of NIR detection capabilities, a number of synthetic procedures developed in this work yield NIR-emissive structures. This emission in GQDs is related in or work to defect states and can be modified or enhanced via chemical functionalization/passivation of those.GQDs developed in our work are highly biocompatible (up to several mg/mL) and biodegradable in cell culture at 36h for a number of structures. They can be doped or pre-designed to exhibit bright (with up to 60% quantum yield) fluorescence in the visible and in near-infrared (with up to 7% quantum yield). Several GQD bioapplications are explored in this work. 1. Serving as a platform for targeting and drug delivery: GQDs successfully internalize in vitro and, as targeting agents are attached to their platform, show preferential accumulation in cancer cells and successful delivery of a variety of cancer therapeutics. 2. Imaging: GQDs enable visible and NIR fluorescence imaging in the healthy and cancer cell cultures. Injected intravenously, GQDs are used for in vivo imaging, as their near-infrared fluorescence is detected from the organs of live sedated mice. 4. Sensing: GQDs allow for optical radiometric pH sensing enabling detection of cancerous environments as well as optical temperature detection in the biological range with linear response in the visible and near-infrared. 5. MRI capabilities: GQDs functionalized with Gd and Mn show the potential to serve as T1 and T2 MRI contrast agents with biocompatibility and relaxation parameters enhanced over the conventional corresponding metal chelate contrast agents.

D174: Phase behavior and effective aspect ratio of bimodal carbon nanotube solutions in chlorosulfonic acid

Ivan Siqueira*†, Michelle Duran-Chaves, Oliver Dewey, Glen Irvin, Matteo Pasquali

**Rice University*

Carbon nanotubes (CNTs) are well known for their remarkable material properties, being attractive building blocks for multifunctional materials like fibers and thin films. The performance of these CNT materials is a strong function of CNT aspect ratio, which directly impacts the phase behavior of CNTs in solution. Most works to date focused on producing and characterizing CNT materials made from solutions with a single CNT species. Previous work demonstrated that CNTs usually follow a log-normal length distribution that is narrowly disperse in comparison to standard polymeric samples. In addition, the phase behavior of these CNT samples is well described by CNT aspect ratio, such that the isotropic-to-nematic phase transition behaves accordingly to Onsager's classical theory for rigid rods. Highly polydisperse samples in which long and short CNTs coexist in solution might be a feasible alternative to produce high-performance CNT materials at lower cost and higher efficiency. Nevertheless, the phase behavior of strongly length-polydisperse CNT solutions as well as a measure of their effective aspect ratio have not been addressed in the literature and are not yet fully understood. In this work, we present an experimental study of highly polydisperse CNT solutions. We use two different CNT batches with distinct aspect ratios and prepare dilute and semidilute solutions in chlorosulfonic acid at different proportions of each batch. We use transmission electron microscopy, cross-polarized optical microscopy, and extensional rheometry to characterize the phase behavior and viscosity-averaged effective aspect ratio of these bimodal CNT solutions. The results show how the fraction of long-to-short tubes in solution affect the isotropic-to-nematic phase transition and the solution effective aspect ratio as determined by capillary thinning extensional viscosity measurements. These predictions are key to better understand and optimize the properties of macroscopic CNT materials made from polydisperse solutions at high concentrations.

D175: Methodologies for Quality-Assessment of Boron Nitride Nanotube Materials

Michael Jakubinek*†, Yadienka Martinez-Rubi, Keun Su Kim, Zygmunt Jakubek, Maohui Chen, Shan Zou, Benoit Simard, Christopher Kingston

**National Research Council Canada*

Boron nitride nanotubes (BNNTs) are emerging nanomaterials with similarly impressive mechanical properties to carbon nanotubes (CNTs) but unique chemistry and complimentary multifunctional properties. While first reported in the mid-1990s, it is only relatively recently that this type of nanotube became more available through improved, larger-scale synthesis methods and the emergence of several commercial suppliers. The corresponding increase in research and use of BNNTs necessitates a set of repeatable and accessible methods to assess BNNT materials, but methods now commonly accepted and routinely employed in the CNT community (e.g., thermogravimetric analysis, Raman spectroscopy and VIS-NIR absorption spectroscopy) are less useful in assessing BNNT samples. Several new methods for BNNT assessment have been proposed and described in the literature. Here we summarize a range of characterization of BNNT materials produced at NRC by the hydrogen-assisted BNNT synthesis process [1], which is used in the production of commercial BNNT materials from Tekna Advanced Materials, and

describe two assessment methods: one based on X-ray photoelectron spectroscopy [2] and one based on absorption spectroscopy of regiorandom poly(3-hexyl-thiophene) aggregates on the surface of BNNTs dispersed in solution [3], which are used by our team in assessing the quality of as-synthesized, purified, and modified BNNT materials. [1] Kim et al, ACS Nano 8, 6211-6220 (2014). [2] Jakubinek et al, Can J Chem 97, 457 (2019) [3] Martinez-Rubi et al, ACS Appl Nano Mater 2, 2054-2063 (2019). *Acknowledgements:* This work was supported through the Security Materials Technology Program of the National Research Council Canada

D176: Individual Carbon Nanotube Nanofluidics

Matthias Kuehne*†, Samuel Faucher, Michael Strano

**Massachusetts Institute of Technology*

Single digit nanopore (SDN) fluidics is at the frontier of current science and has important applications in fields such as energy harvesting, water filtration, and gas separation. Experiments that can resolve changes in fluid behavior with angstrom-scale changes in pore size are urgently needed to advance our understanding in this space. To this end we explore carbon nanotubes (CNTs) as a unique nanofluidic testbed. Using standard patterning techniques, we generate arrays of identical diameter CNT devices allowing us to interrogate fluid behavior in these at the individual tube level all while generating reliable statistics. We probe characteristic CNT vibrational modes using Raman spectroscopy to reveal fluid filling as a stochastic process-SDN clogging being the norm rather than the exception. We report non-monotonic diameter dependence of filling dynamics as well as radial breathing mode (RBM) shifts characteristic of molecular packing effects. A systematically observed RBM softening upon heating further reveals a reversible adsorption process that can explain a long-standing controversy in the field regarding environmental effects on the RBM.

D177: Localized Charge on Individual Single-Walled Carbon Nanotubes Arising from Surfactant

Erin Christensen*†, Mitesh Amin, Todd Krauss

**University of Rochester*

As-synthesized, single-walled carbon nanotubes (SWCNTs) are nominally charge neutral. However, ionic surfactants that are commonly used to disperse SWCNTs in solution have been hypothesized to cause a heterogeneous surface charge buildup along the NT. Such electrostatic perturbations will significantly affect the photophysical properties of SWCNTs and therefore a study of the electrostatic interactions between a single NT and its local environment is crucial. In this presentation, we report the spatial distribution and magnitude of spatial charge distributions along individual NTs and its environment as measured by electrostatic force microscopy (EFM). EFM is a modification of atomic force microscopy which allows for a quantitative determination of localized charges and dielectric constants at the nanometer scale. For dozens of long NTs (> 1.5 microns) solubilized in aqueous suspension using standard ionic surfactants (e.g. sodium cholate) we found charge variations all along the NT with magnitudes on the order of 1 eto a few e, with both positive and negative signs. EFM data of NTs before and after photoexcitation suggests surfactant aggregates create local perturbations in the band structure by acting as electrostatic potential barriers for exciton transport, which leads to distinct localized regions of charge (Figure 1). Additionally, we report that topological defects such as kinks, bends, and curves can also prevent diffusive exciton transport. For example, the region between the bend and curve (Figure 1) remains relatively unchanged after photoexcitation, while all other regions show pronounced changes in charge. Altogether, our EFM data provides a compelling explanation for the source of the potential energy fluctuations along the NT that have the potential to localize excitons.

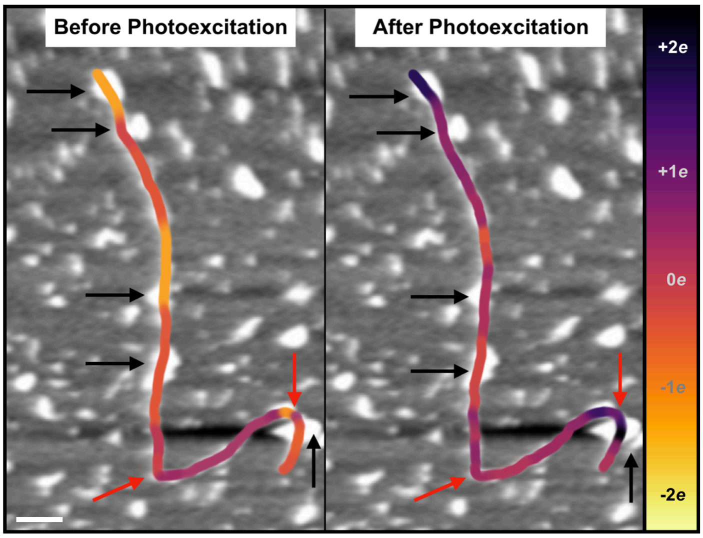

Fig. 1: Charge profile before and after photoexcitation. Black (red) arrows indicate surfactant aggregates (topological defects) that may act as potential barriers. Scale bar is 200 nm.

D178: Mechanism of Alignment Enhancement of CNT Fibres by AC Electric Fields

Philipp Kloza†, James Elliott*

**University of Cambridge*

Experiments on the electric field alignment of CNTs during FCCVD synthesis show that CNTs can only be aligned by AC fields in the MHz regime, whereas very little alignment can be observed in the case of DC fields. Recent theoretical work [1] on DC electric field alignment of CNTs estimated that the field strengths necessary for measurable CNT alignment would exceed the dielectric breakdown voltage of the hydrogen process gas. However, this does not explain why AC fields do lead to alignment. Here, we propose a ”z-pinch” mechanism which leads to the stiffening of CNTs in the presence of AC electric fields. In turn, the stiffened CNTs facilitate easier alignment by the applied electric field. The main difference between CNTs in a DC and AC field is the continuous presence of an axial electric current in a CNT for the AC case. Hence, this current is likely responsible for any improvement in the alignment compared to the DC case. Physically, the mechanism we propose is that the compressive Lorentz force, due to the z-pinch arises from interaction of induced magnetic field on the axial current, acts as a restoring force when the CNT is curved, effectively straightening and thus stiffening the CNT. While CNTs in a DC electric field undergo a rigid-to-elastic transition above a threshold length, which limits the strength of the field coupling, stiffened CNTs may still be treated as rigid. The strength of z-pinch stiffening is limited by current saturation. As the saturation current increases with the number of graphitic layers, we predict that the effect becomes significant in individual MWCNTs and bundles of SWCNTs. Furthermore, we demonstrate that z-pinch stiffening allows for measurable alignment of these CNT structures with field strengths which lie below the dielectric breakdown voltage of hydrogen. Thus, z-pinch stiffening provides an explanation for the successful AC electric field alignment of CNTs during FCCVD synthesis. [1] Kloza & Elliott, Macromol. Theory Simul., 29 (2020) 2000049.

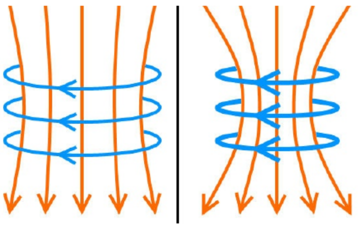

Fig. 1: Schematic of ”z-pinch” effect - a compressive Lorentz force arises from circumferential magnetic field (blue) induced by axial current (orange) from AC field.

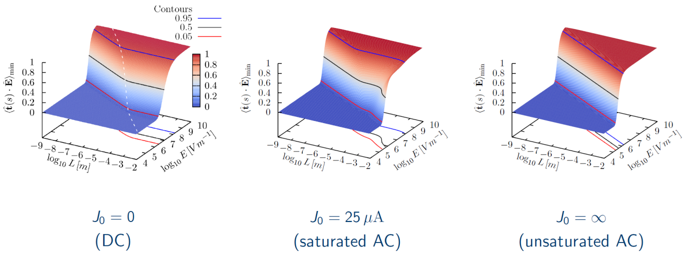

$J_0 = 0$ (DC)

$J_0 = 25\,\mu$A (saturated AC)

$J_0 = \infty$ (unsaturated AC)

Fig. 2: Effect of saturation current on threshold E-field required to achieve alignment as function of CNT length. Zero saturation current corresponds to DC, wherea realistic saturation current is 25 microamps.

D179: Mechanistic Study of Oxygen Doping of Single-Wall Carbon Nanotubes using Hypochlorite

Vanessa Espinoza*†, Yu Zheng, Sergei Bachilo, R. Bruce Weisman

Rice University

Chemically induced defects along the sidewalls of single-wall carbon nanotubes (SWCNTs) are a topic of great current interest. These chemical modifications have the potential to affect optical transitions in a way that can shift semiconducting fluorescence emission further into the near-infrared region. These shifts can be valuable in bio-imaging applications. Here we present further studies on the use of photoexcited hypochlorite ions as a reactant to produce oxygen-doped SWCNTs. Our studies focus on the effects of excluding dissolved oxygen during the reaction. We find greatly increased reaction rates and the appearance of additional shifted emission bands. These results, combined with kinetic data and quantum computations, provide insight into the doping mechanism. This work will enable more efficient and controlled production of carbon nanotubes with tailored optical properties. *Acknowledgements:* The NSF Foundation and Welch Foundation for funding.

D180: Computational study of selective interactions between ssDNA and SWCNTs

Ali A. Alizadehmojarad*†, Sergei Bachilo, Anatoly B. Kolomeisky, R. Bruce Weisman

Rice University

Structure-specific interactions between single-stranded DNA oligos and SWCNTs form the basis of important selective sorting methods yet remain poorly understood. Among these interactions is the differential affinity of (ATT)4 for one of the two (7,5) enantiomers. To understand the nature of the affinity difference, we have performed molecular dynamics (MD) simulations followed by free energy (replica exchange) calculations over the temperature range of 290 to 727 K. Comparisons between conformational free energy landscape of (ATT)4 structure on right-handed and left-handed (7,5) SWCNTs (respectively known as M and P in stereochemical convention) suggest that (ATT)4 has more contact area with M than P enantiomer. However, the corresponding end-to-end distances of (ATT)4 fall nearly in the same region on the landscape. Our standard MD simulations for (ATTT)3 interactions with SWCNTs also suggest that this DNA sequence covers (8,4) SWCNT more effectively than (7,6) and (8,3) SWCNTs, which is consistent with dye-quenching of SWCNTs in our experiments. The use of molecular dynamics simulation is a useful tool for gaining new insights into atomic-level interactions between SWCNTs and their biopolymer coatings. *Acknowledgements:* National Science Foundation and the Welch Foundation

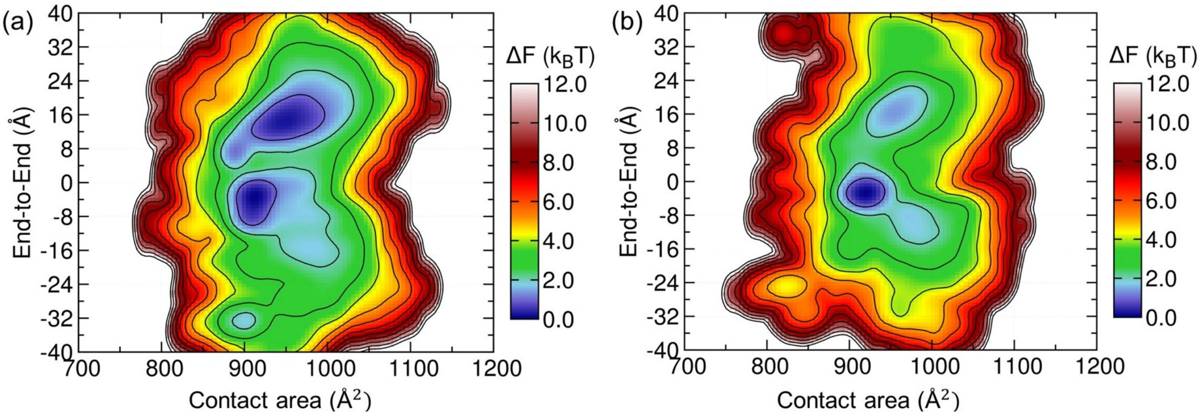

Fig. 1: Figure 1. (a) Free energy landscape of (ATT)4 at right-handed (7,5) enantiomers. (b) Free energy landscape of (ATT)4 at left-handed (7,5) enantiomers.

D181: Two-Step Aerosol Assisted Synthesis of Structurally Uniform BXCYNZ Nanotubes: Tuning Nanotube Properties via Co-Doping

Dillon McGurty*†, Eoin O'Sullivan, John Ballentine, Kai Ling Ng, Philip Holdway, Barbara Maciejewska, Nicole Grobert

**University of Oxford*

Borocarbonitride nanotubes (BCN-NTs) are considered for application in catalysis, electronics, and energy storage.1-3 Through the modification of their chemical composition, electronic and physical properties such as oxidation behaviour and chemical reactivity can be tuned. Previous synthesis techniques for BCN-NTs, which include arc-discharge, polymeric-based pyrolysis and chemical vapour deposition face drawbacks, such as high-energy requirements non-uniform reaction products and the use of the use of toxic, corrosive and pyrophoric gases respectively.2, 4, 5Herein, we report an ammonia-free synthesis route that overcomes these bottlenecks and that allows the successful incorporation of boron and nitrogen dopants within the nanotubes. The novel combination of aerosol-assisted chemical vapour deposition (AACVD) techniques in conjunction with a substitutional reaction leads to high yields (ca. 600 mg/day) of bundles of structurally and chemically uniform BCN-NTs. Scanning electron microscopy revealed uniform flakes of vertically aligned nitrogen doped multi-wall carbon nanotubes (N-MWCNTs); these were utilised as a precursor for the BCN-NTs. Transmission electron microscopy revealed that the substitutional doping was non-destructive and X-ray photoelectron spectroscopy showed that the combined nitrogen and boron doping levels were ranging between 2.8 and 8.9 at.% depending on the reaction temperature. The highest boron doping levels obtained here (4.2 at.%) were higher than previously reported for AACVD alone.6, 7 Our results suggest that the boron doping occurs preferentially at pyridinic nitrogen sites within the nanotube. Raman spectroscopy showed that the co-doping procedure improved the graphitisation of the BCN-NTs in comparison to the precursor material. Optical band gaps were determined and found to be 2.7 eV for N-MWCNTS and 2.3 eV for BCN-NTs. Thermogravimetric analysis showed that the oxidation resistance of the co-doped nanotubes could be increased by ca. 100 oC compared to the starting material.The two-step co-doping procedure reported here, paves the way to a finer control of the doping levels and hence the overall properties of the nanotubes. The high yields now allow the testing of these materials in applications.NT21 Abstract References and Acknowledgements Dillon McGurty.docx *Acknowledgements:* EPSRC/Royal Society/David Cockayne Centre for Electron Microscopy/Oxford Materials Characterisation Service

D182: Quenching of SWCNT Fluorescence by Rose Bengal Provides Insight about Coating Coverage

Nima Soltani*†, R. Bruce Weisman, Sergei Bachilo

**Rice University*

Single-walled carbon nanotubes (SWCNTs) have attracted a great deal of attention during the past two decades because of their unique optoelectronic properties and their potential applications in biomedical theranostics as well as nanoelectronics. One important goal is a deeper understanding of the specific interactions between nanotubes and the coatings that are widely used to suspend and individualize them.1,2 We report a spectroscopic study of charge transfer complex formation between nanotubes and the dye Rose Bengal. The complexation causes quenching of SWCNT fluorescence and the appearance of a charge transfer absorption feature near 600 nm. These effects are interpreted as resulting from p-doping of the nanotubes from dye adsorption. Interestingly, the extent of SWCNT fluorescence quenching by Rose Bengal is found to vary significantly with (n,m) structure. This effect therefore provides a simple approach to monitor structure-specific interactions between SWCNTs and coatings, including ssDNA and conventional ionic surfactants.References(1) Yang, F.; Wang, M.; Zhang, D.; Yang, J.; Zheng, M.; Li, Y. Chirality Pure Carbon Nanotubes: Growth, Sorting, and Characterization. Chem. Rev. 2020, 120 (5), 2693–2758. https://doi.org/10.1021/acs.chemrev.9b00835.(2) Zeng, X.; Yang, D.; Liu, H.; Zhou, N.; Wang, Y.; Zhou, W.; Xie, S.; Kataura, H. Detecting and Tuning the Interactions between Surfactants and Carbon Nanotubes for Their High-Efficiency Structure Separation. Adv. Mater. Interfaces 2018, 5 (2), 1–11. https://doi.org/10.1002/admi.201700727.

D183: Spin-resolved quantum point contact in p-type trilayer tungsten diselenide van der Waals heterostructure

Kohei Sakanashi*†, Peter Krueger, Jonathan Bird, David Ferry, Kenji Watanabe, Takashi Taniguchi, Gil-Ho Kim, Nobuyuki Aoki

**Chiba University*

Quantum device such as quantum dot or quantum point contact (QPC) in transitional metal dichalcogeniodes (TMD) has been receiving large attention as promising device structure for future application of spin-valley qubit or spin-valley filter due to their non-trivial valley degeneracy and strong intrinsic spin-orbit coupling. To date, the number of study related the electrostatically induced quantum confined structure in TMD was very limited due to their low crystal quality and low contact properties. In this study, we have realized first p-type electrostatically induced QPC device in trilayer tungsten diselenide (WSe_2) by using modified 2D/2D contact with degenerately doped MoS_2 crystals and hBN encapsulation as shown in Figure.1, and shows high mobility at 2 K. The conductance as a function of split gate voltage shows clear conductance quantization and pinch-off state (Figure.2). The unit of quantized conductance is related to the degeneracy of conducting carrier, and holes in trilayer WSe_2 should have the level degeneracy of 2e2/h by spin degeneracy, however the transport measurement indicates the spin-resolved degeneracy of e2/h even at zero magnetic field. This lifted spin degeneracy indicates the strong intrinsic spin-orbit coupling in the valence band of trilayer WSe_2. *Acknowledgements:* This study was supported by JSPS KAKENHI Grant No. 18H01812 and 20J20052.

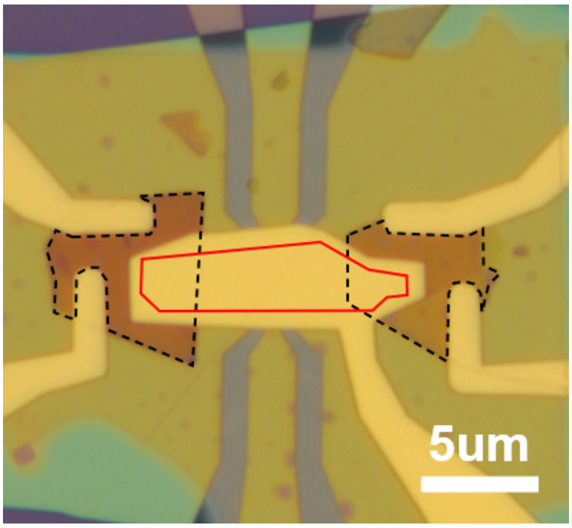

Fig. 1: Optical microscope image of WSe_2-QPC device. Red solid line and black dashed line indicates the tilayer WSe_2 and degenerately doped MoS_2 crystals, respectively.

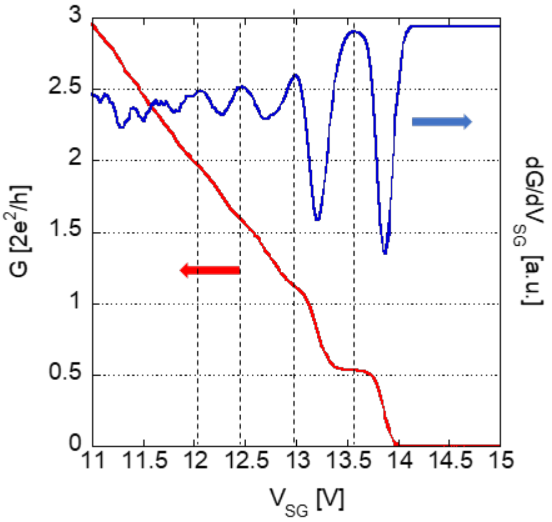

Fig. 2: Conductance and differential conductance curves as a function of split-gate voltage at constant top gate voltage of -12 volts under 2 K.

E185: Ultra-long carbon nanotube forest via in situ supplements of iron and aluminum vapor sources

Hisashi Sugime*†, Toshihiro Sato, Rei Nakagawa, Tatsuhiro Hayashi, Yoku Inoue, Suguru Noda

**Kindai University*

A carbon nanotube forest with a length of 14 cm grew with an average growth rate of 1.5 µm s−1 and a growth lifetime of 26 h. Several key factors to realize this unprecedented long growth such as catalyst conditions, growth conditions in chemical vapor deposition, and reactor system were clarified. It was found that the combination of the catalyst system of iron/gadolinium/aluminum oxide (Fe/Gd/Al2Ox) and the in situ supplements of Fe and Al vapor sources at very low concentration was crucially important. A cold-gas system, where only the substrate is heated while keeping the gas at room temperature, was employed to suppress unnecessary reactions and depositions. The long carbon nanotube forest enabled macroscopic measurements of the tensile and electrical properties of the carbon nanotube wires, and it gave several important insights for industrial applications of the carbon nanotubes in the future. *Acknowledgements:* This work was supported by JSPS KAKENHI Grant Number 19K22090.

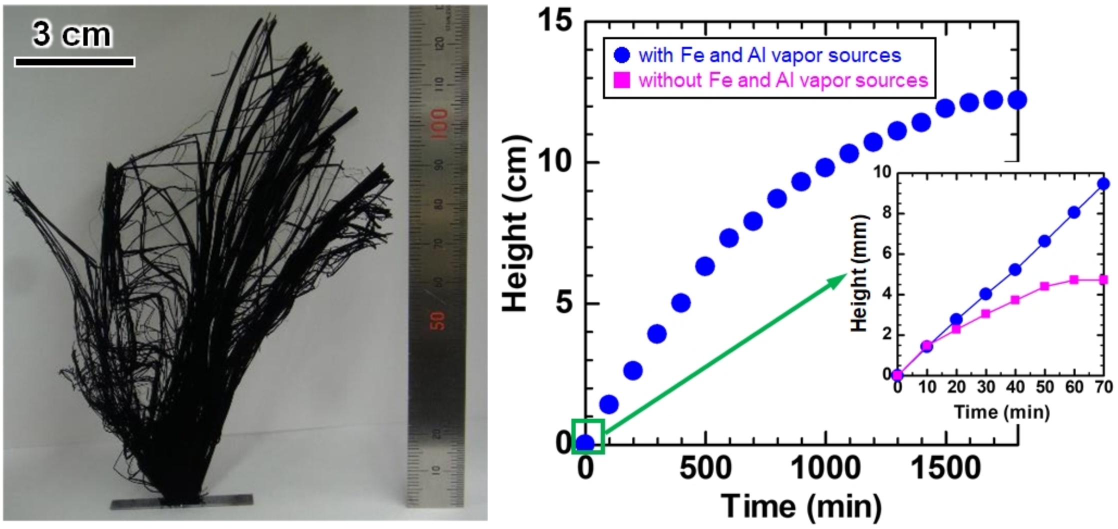

Fig. 1: Picture of 14-cm-long carbon nanotube forest and growth curve with and without Fe/Al vapor sources.

E186: Gradient-index electron optics in graphene p-n junction

Emmanuel Paredes-Rocha*†, Yonatan Betancur-Ocampo, Nikodem Szpak, Thomas Stegmann

**Instituto de Ciencias Físicas, Universidad Nacional Autónoma de México*

We investigate the electron transport in smooth graphene p-n junctions, generated by gradually varying electrostatic potentials. The numerically calculated coherent current flow patterns can be understood largely in terms of semiclassical trajectories, equivalent to the ones obtained for light beams in a medium with a gradually changing refractive index. In smooth junctions, energetically forbidden regions emerge, which increase reflections and can generate pronounced interference patterns, for example, whispering gallery modes. The investigated devices do not only demonstrate the feasibility of the gradient-index electron optics in graphene p-n junctions, such as Luneburg and Maxwell lenses, but may have also technological applications, for example, as electron beam splitters, focusers, and waveguides. The semiclassical trajectories offer an efficient tool to estimate the current flow paths in such nanoelectronic devices. For more details see Paredes-Rocha et al., Phys. Rev. B 103: 045404 (2021) DOI: 10.1103/PhysRevB.103.045404 *Acknowledgements:* EPR thanks CONACYT for a graduate scholarship. We acknowledge financial support from project CONACYT A1-S-13469 and UNAM-PAPIIT IA103020.

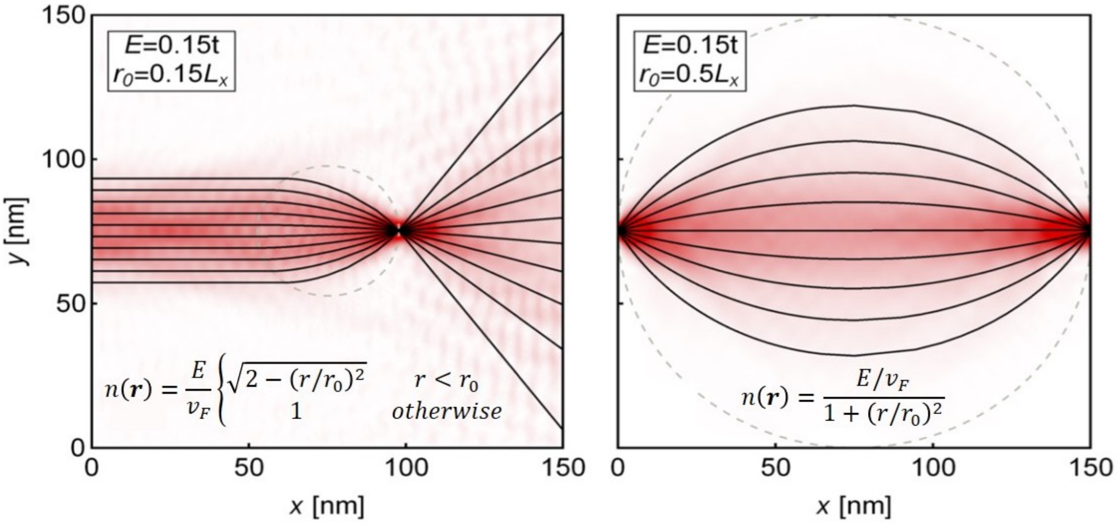

Fig. 1: Current flow in a Luneburg lens (left) and a Maxwell's fish-eye lens (right) in graphene. The corresponding gradient-index and its trajectories are shown for each lens

E187: Piezoimpedance Response of Carbon Nanotube Yarns

Mohammad Alsubhani*†

The Catholic University of America

ABSTRACT Alsubhani, Mohammad, PiezoImpedance Response of CNT Yarn. PhD in Mechanical Engineering Department, Jan 24th, The Catholic University of America, Washington, D.C. As a result of research in the field of integrated sensors, there is an increased demand for electronic devices. Multifunctional sensors give the same quantity of data using less sensors. Our study shows that the carbon nanotube (CNT) yarns exhibit a piezoresistive behavior that can be tapped for sensing purposes including strain, temperature, damage, and chemicals detection, as well as non-selectively sensitivity to strain, gas, and temperature. Therefore, CNT yarns are ideal candidates for designing multifunctional sensors. This project is going to emphasize on two factors: humidity and temperature. At this point, we have three specific aims: Determining the complete impedance versus frequency response of CNT yarns up to 3 GHz; exploring a design of multifunctional sensors using the concept of source-invariant frequencies observed in CNTs; and determining the source invariant frequency for the CNT yarn, independent of the temperature and independent of the humidity. Results from previous studies indicate that the CNT yarns could be influenced by the tunneling effects, thermal activation, and capacitive and inductive reactance. The experiments are being designed and first results are being collected. This project will help the research to identify the parameters that affect the frequency. KEY WORDS: Carbon nanotube yarns; Sensors; Impedance; Frequency; temperature sensor; humidity sensor; sensing mechanism

E189: Atomically precise fabrication of one-dimensional transition metal chalcogenides inside nanotubes

Yusuke Nakanishi*†, Naoyuki Kanda, Masataka Nagata, Zheng Liu, Hisanori Shinohara

Tokyo Metropolitan University

Since the discovery of buckminsterfullerene in 1985, nanocarbon materials have played a crucial role in modern materials science. Recently, significant efforts have been redirected towards exploring ‘post-nanocarbons’. Over the past decade, 2D layers of transition metal dichalcogenides (TMDs) have been widely recognized as ‘beyond graphene’ owing to their versatile chemistry and physics. On the other hand, their 1D counterparts such as transition metal monochalcogenide (TMM) nanowires could exhibit the unique electrical and optical properties, significantly distinct from 2D TMDs as well as 1D nanocarbons [1]. However, exploring the potential of TMM nanowires has been hampered by their limited availability. Although these materials have been prepared by using chemical and lithographic methods [2], the reliable production of well-defined TMM nanowires remains a significant challenge. Here we report atomically precise fabrication of TMM nanowires inside carbon nanotubes (CNTs). Chemical reactions confined within CNTs promote and stabilize the bottom-up growth of isolated MoTe and WTe nanowires to prevent oxidation, allowing their easy handling and characterization [3, 4]. We revealed that the choice of suitable metal oxides as a precursor provides feasible yields for their characterization. Atomic-level transmission electron microscopy revealed their unusual torsional waves not seen in the bulk (Figure 1).These TMM nanowires exhibit a significant optical absorption in the visible-light region. More important, electronic properties of CNTs can be tuned by encapsulating different TMM nanowires. Our findings suggest that TMM nanowires could provide new building blocks for future flexible nanoelectronics. [1] I. Popov et al. Phys. Rev. Lett. 99, 085503 (2007); I. Popov et al. Nano Lett. 8, 4093 (2008) [2] J. Kibsgaard et al. Nano Lett. 8, 3928 (2008); J. Lin et al. Nat. Nanotechnol. 9, 436 (2014) [3] M. Nagata et al. Nano Lett. 19, 4845 (2019) (Front cover of this issue) [4] N. Kanda et al. Nanoscale 12, 17185 (2021) (Front cover of this issue) *Acknowledgements:* This work was financially supported by KAKENHI (18K14088 and 20H02572).

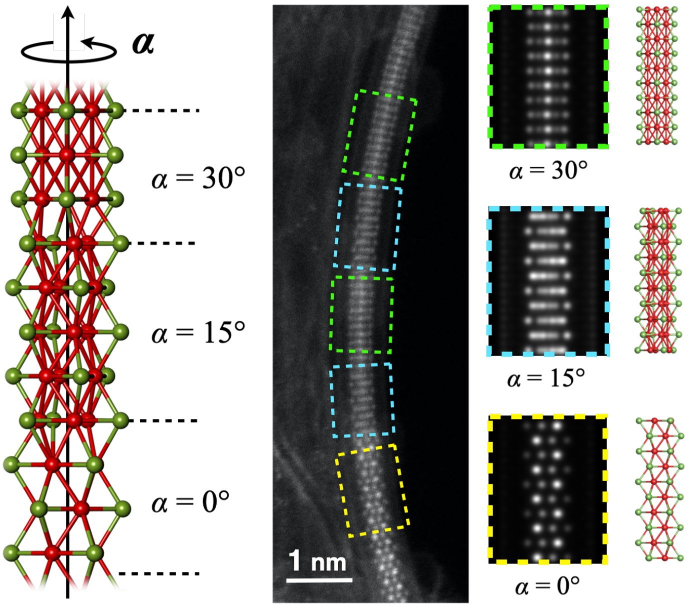

Fig. 1: Torsional behaviors of an individual MoTe nanowire inside a single-walled CNT.

E190: Ultrasonication-induced extraction of inner tubes and energy transfer from inner to outer double-wall carbon nanotubes

Maksiem Erkens*†, Emmanuel Flahaut, Frédéric Fossard, Annick Loiseau, Wim Wenseleers, Sofie Cambré

Nanostructured and Organic Optical and Electronic Materials, Department of Physics, University of Antwerp, Antwerp, Belgium

The electronic and optical properties of double-wall carbon nanotubes (DWCNT), consisting of two coaxial single-wall CNTs (SWCNTs), are modulated by the inter-wall van der Waals interactions and the relative chiral angles of the individual CNTs [1]. Even though experiments on individual DWCNTs show a drastic quenching of the fluorescence (PL) of the inner DWCNT [2], it remains a highly debatable topic whether inner DWCNTs fluoresce or not. Typically, DWCNTs are solubilized using ultrasonication prior to their PL characterization. Here we demonstrate that even very brief ultrasonication will extract inner tubes from DWCNTs, resulting in fluorescing SWCNTs that can be easily mistaken for PL of the inner DWCNT. Additionally, detailed photoluminescence-excitation (PLE) and wavelength-dependent resonant Raman spectroscopy (RRS) characterizations reveal an energy transfer from the inner to the outer DWCNT, possibly explaining the mechanism behind the drastic PL-quenching of the inner DWCNTs. DWCNTs were first purified from SWCNTs and bundles by density gradient ultracentrifugation (DGU) [3]. To select the ultrapure DWCNTs in the ultracentrifuge tube, in situ characterization with PLE and RRS was performed [4]. Next, ultrasonication was applied in accumulating time steps while intermittently measuring PL and RRS. This revealed a rapidly growing yet saturating increase in SWCNTs, see Figure 1, that originates from the extraction of inner tubes from the DWCNTs, as confirmed by transmission electron microscopy (TEM). Using DGU again, these extracted inner DWCNTs were separated from the remaining DWCNTs. The ultrapure DWCNTs were characterized together with reference SWCNTs, with diameter distributions matching those of the inner and outer DWCNTs. Two-dimensional fits of the RRS and PLE maps established a relation between the radial breathing modes of the SWCNTs and inner DWCNTs. Moreover, from these fits the shifted optical transitions of the inner and outer DWCNTs are determined with respect to the reference SWCNTs. From these results, the exact locations on the PLE map of the possible energy transfer for each inner and outer DWCNT combination were determined. By integrating the PLE map of the DWCNTs (red) and the reference SWCNTs (black) over these ranges, the energy transfer peaks were revealed, see Figure 2. [1] A. Ghedjatti et al. Nano Lett. 11, 4840 (2017) ; [2] D. Levshov et al. Phys. Rev. B 96, 195410 (2017) ; [3] E. Flahaut et al. Chem. Commun. 12, 1442 (2003) ; [4] S. Cambré et al. Nanoscale 7, 20015 (2015)

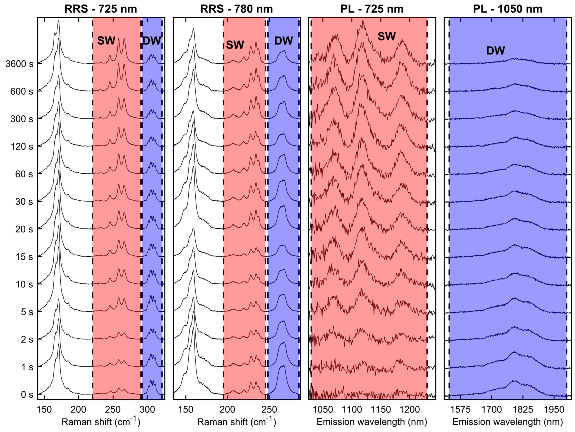

Fig. 1: RRS and PL spectroscopy measurements as a function of ultrasonication time showing an increase of SWCNTs (red) compared to inner DWCNTs in RRS (blue) and outer DWCNTs in PL (blue).

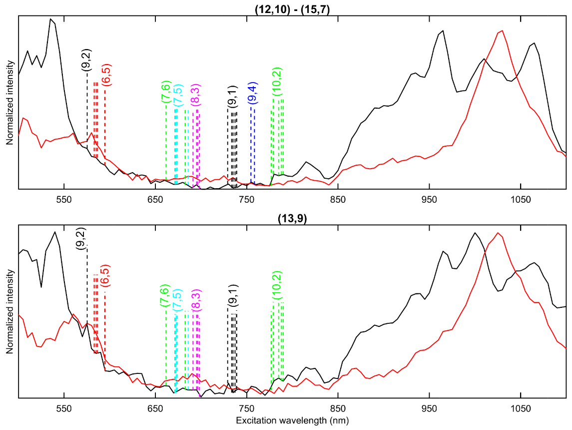

Fig. 2: PLE-Excitation slices of DWCNTs (red) and SWCNTs (black), centered around an outer DWCNT-chirality, revealing energy transfer peaks at the optical transitions of the allowed inner DWCNTs.

E191: Fluidized bed production of 99.9 wt%-pure and 0.3 mm-long single-wall carbon nanotubes at 28% carbon yield using ethylene and carbon dioxide

Mochen LI*†, Soichiro Hachiya, Zhongming Chen, Toshio Osawa, Hisashi Sugime, Suguru Noda

**Waseda University*

For practical production of carbon nanotubes (CNTs), it is essential to realize high carbon source concentration and high carbon yield. In this research, the uniform Fe/AlOx catalyst were deposited on the spherical ZrO2 beads by sputtering using a rotating octagonal drum. By feeding moderately active ethylene at 10–20 vol% with mildly oxidative carbon dioxide at 1 vol%, submillimeter-long single-wall CNT (SWCNT) arrays were synthesized by fluidized bed chemical vapor deposition. SWCNTs with high purity (99.9 wt%), small average diameter (2.9 nm), long length (0.3 mm), and high specific surface area of 1178 m2/g were obtained at a high carbon yield of 28 %. This study thus introduce a promising route for more efficient and cleaner production of long and pure SWCNTs.

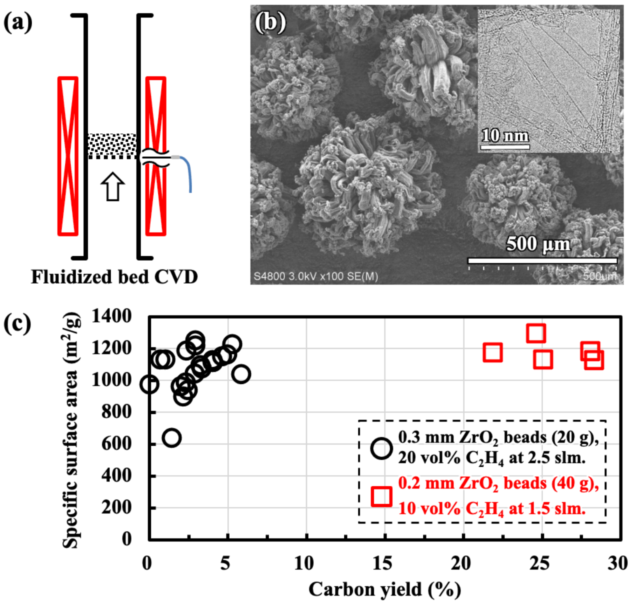

Fig. 1: (a) The vertical reactor used to synthesize SWCNTs via FBCVD. (b) SEM image and inset TEM image of SWCNTs. (c) Specific surface area and carbon yield of synthesized SWCNTs.

E192: Deterministic dry transfer of carbon nanotubes into photonic devices using single-crystalline anthracene

Keigo Otsuka*†, Nan Fang, Daiki Yamashita, Takashi Taniguchi, Kenji Watanabe, Yuichiro Kato

**the University of Tokyo*

When continued device scaling reaches the ultimate limit imposed by atoms, technology based on atomically precise structures is expected to emerge. Device fabrication will then require building blocks with identified atomic arrangements and assembly of the components without contamination. Carbon nanotubes offers unique position among various candidates as their atomic arrangements can be accurately specified by chiral indices. To harness the full functionality and performance of carbon nanotubes, methods for manipulating chirality-identified tubes with negligible contamination are desired. Here we report on a versatile dry transfer technique for deterministic placement of optical-quality carbon nanotubes [1]. Figure 1 shows the procedure for nanotube transfer assisted by single-crystalline anthracene as a medium. The anthracene crystal readily sublimes by mild heating, leaving behind clean nanotubes. When aligned nanotubes grown on a quartz substrate are transferred onto a trenched substrate, air-suspended region over a 5-µm-wide trench exhibits as bright photoluminescence as as-grown ones (Figure 2(a)). As we are able to position nanotubes of a desired chirality with a sub-micron accuracy under in-situ optical monitoring on single nanotubes, deterministic coupling of single nanotube emission to a photonic crystal nanobeam cavity is demonstrated. Figure 2(b) shows a photoluminescence spectrum of an individual (13,5) nanotube, which is coupled to the cavity through a hexagonal boron nitride thin layer (inset). A cross junction structure is also designed and constructed by repeating the nanotube transfer, where intertube exciton transfer is observed. Our results represent an important step towards development of devices consisting of atomically precise components and interfaces. [1] K. Otsuka et al., arXiv:2012.01741. *Acknowledgements:* Parts of this study are supported by JSPS, MEXT, and JST. K.O. and D.Y. are supported by JSPS (Research Fellowship for Young Scientists).

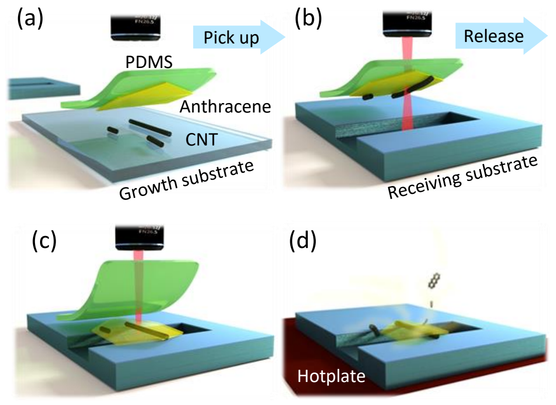

Fig. 1: (a) CNTs are picked up with the anthracene stamp, (b) followed by nanotube spectroscopy. (c) Anthracene/nanotubes are released on a receiving substrate. (d) Heating of the substrate removes the anthracene.

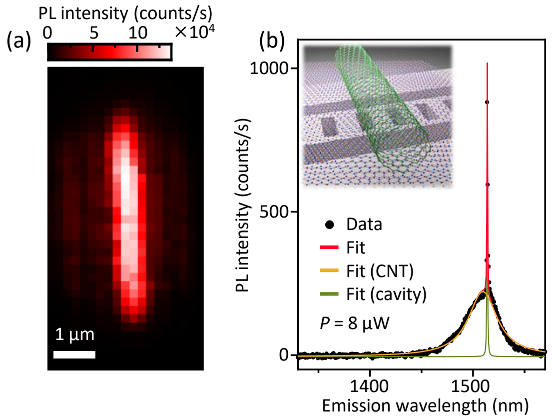

Fig. 2: (a) PL image of an air-suspended CNT transferred from a quartz substrate at emission wavelength of 1379 nm. (b) PL spectrum of the cavity-coupled CNT.

E193: Mechanical and electrical properties of 14-cm-long continuous CNT and connected spun CNT yarns

Yoku Inoue*†, Tatsuhiro Hayashi, Takayuki Nakano, Hirotaka Inoue, Yasuhiko HAYASHI, Hisashi Sugime, Suguru Noda

**Shizuoka University*

The mechanical and electrical properties of long fibers with different crystal continuity, including 14 cm ultra-long CNTs and dry-spun CNT yarns, were investigated. The 14 cm long CNTs have a few walled structure and were grown by a thermal chemical vapor deposition (CVD) on a Si substrate. To maintain the catalyst activity for a long time growth duration, Gd was predeposited on the alumina support layer, and Fe and Al vapor sources were supplied during the CVD process. The dry-spun yarns were fabricated using CNTs having various diameters of 5.5 nm, 11 nm, and 28 nm. 14-cm CNT bundles and dry-spun CNT webs were formed into long fibers with a circular cross-section through pinholes, and tensile tests and electrical measurements were performed. In tensile tests of continuous crystalline fibers, the tensile strength and Young's modulus were lower than those of the previously reported individual CNTs because the load was concentrated on the fatal crystalline defects. On the contrary, the tensile properties of the spun yarn were higher than those of the continuous crystals because the load was dispersed from CNT to CNT. The charge transport was found to be significantly affected by the scattering by crystal defects in the as-grown CNTs rather than the CNT interfaces. Therefore, the conductivity was greatly improved by the graphitization treatment. However, the current capacity was found to be dominated by the heat dissipation characteristics of the measured samples rather than the individual CNT properties and was higher for bundles with lower CNT cohesive density.

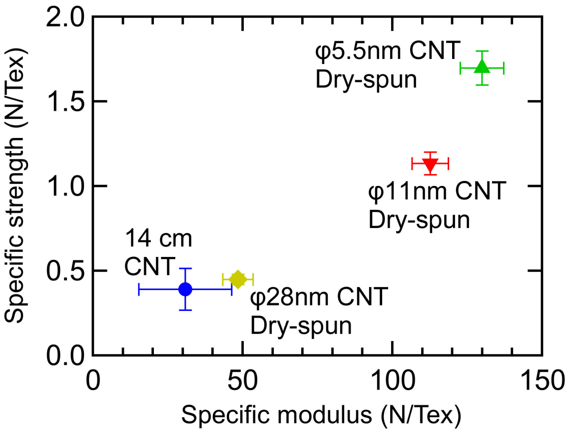

Fig. 1: Specific strength and modulus of 14 cm long CNT, and dry-spun yarns using CNTs with variable diameters

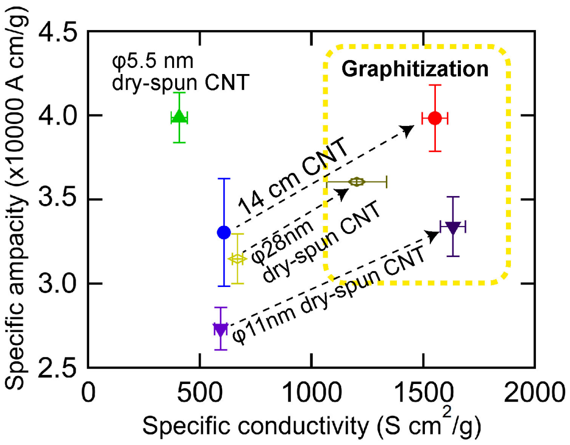

Fig. 2: Specific ampacity and electrical conductivity of 14 cm long CNT, and dry-spun yarns using CNTs with variable diameters

E194: Mechanical Properties of Carbon Nanotubes - Deep Learning Approach

Marko Canadija*†

**University of Rijeka, Faculty of Engineering*

The research at hand presents a thorough investigation into mechanical properties of single-walled carbon nanotubes (SWCNT). The Young's modulus, ultimate tensile stress and strain at fracture were computed by the molecular dynamics (MD) from a comprehensive set of tensile tests. AIREBO potential was used, while the elongation of SWCNT was performed in the constant strain regime. Length/diameter ratio of all SWCNT was kept at L/D=5. To the best knowledge of authors, for the first time, all possible SWCNT configurations – armchair, zigzag and chiral within the diameter range 0.36-4.00 nm and chiral angles 0-30 were considered. Results show that chiral nanotubes that are structurally the closest to zigzag SWCNT exhibit the highest Young's modules, while the lowest modules were obtained in armchair SWCNT, the smallest one in particular. On the other side, armchair and structurally closest chiral SWCNTs have the highest ultimate tensile stress and strain at fracture. In general, nanotubes of smaller radius have somewhat lower ultimate tensile stress, while the fracture strain is rather uniformly distributed for a chosen chirality. Instead of the usual representation in terms of diameter as the variable, the results herein are provided in terms of chiral indices. Although the described method provided a clear illustration of SWCNT mechanical properties, the question of how to provide a sound, but approximate model of the described properties remains open. To this end, deep learning methodology is employed to provide an artificial neural network that approximate the Young's modulus. A feedforward neural network composed of the following layers was used: 128 neurons, linear activation function; dropout layer with the rate 0.4; 64/ReLU; 64/ ReLU; 32/ReLU; 32/ ReLU; 32/ ReLU; 16/ ReLU; 16/ ReLU; 8/ ReLU; 8/ReLU; 4/ReLU; 1 linear. Momentum optimizer with learning rate 0.1 was exploited, while the number of epochs was 30000. L2 regulation was used in hidden layers. The final value of R2 for the approximation of Young's modulus was 0.92. This indicates a good fit to data obtained by MD and justifies the approach. *Acknowledgements:* This work has been supported in by Croatian Science Foundation under the project IP-2019-04-4703. This support is gratefully acknowledged.

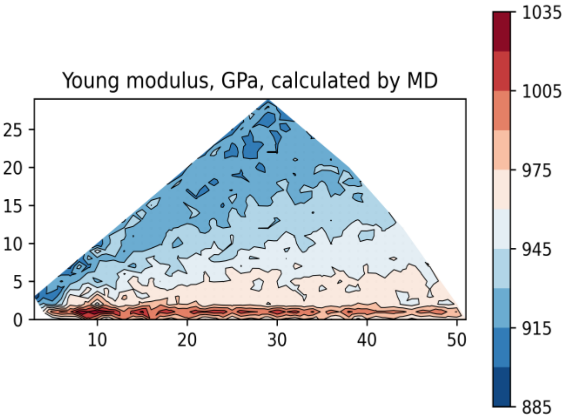

Fig. 1: Young's modulus for SWCNT 0.36-4.00 nm as calculated by MD

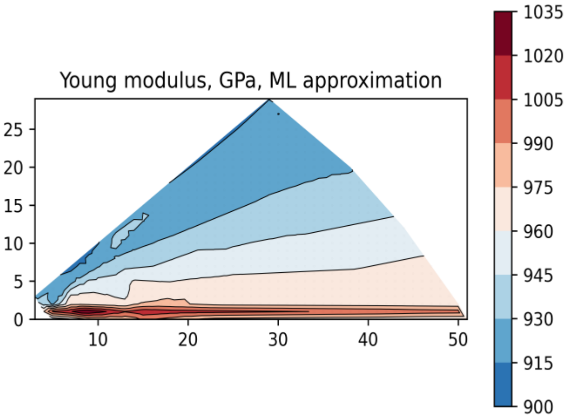

Fig. 2: Machine learning approximation of the Young's modulus of SWCNT

E195: Influence of strong uniform electrostatic field on optical transitions in CdS/HgS/CdS core/shell/shell cylindrical nanoststructure

Volodya Harutyunyan*†

**Russian-Armenian University*

The single-particle states of charge carriers in a cylindrical layered CdS/HgS/CdS core/shell/shell nanoheterostructure in the presence of a strong lateral uniform electrostatic field are considered in this report. The consideration is carried out for the case when the regime of strong size quantization is realized for charge carriers in the HgS layer of the structure under consideration. Using the variational method, the envelope wave functions and the energy spectrum of charge carriers in the HgS layer in the presence of a strong lateral electrostatic field are determined in an explicit form. The states of charge carriers along the symmetry axis of the system (axis z) are considered both in the free motion regime (nanotube) and in the size-quantization regime (cylindrical quantum dot - nanoshim). Comparison of the results of analytical and numerical calculations of the carrier energy shows the physical adequacy of the variational approach proposed in this work for the analytical solution of the problem. It is shown that with an increase of the external field strength (F), the energy of the ground state of the radial motion of charge carriers also increases (according to the $F^{2/3}$). A strong external field radically changes the character of the movement of charge carriers along the angular variable in the HgS layer. The rotational motion of carriers disappears and under the influence of a strong external field the carriers begin to oscillate in a narrow angular segment in the plane of the cross section of structure - around the direction of the field. The value of the segment of the particles' localization along the angular variable decreases with an increase of the external field. Accordingly, as the field increases, the oscillation frequency increases also. The results of the description of single-particle states are used to consider interband and intersubband optical transitions in the HgS layer of the structure under consideration. In the case of a nano-washer, the transitions are strictly resonant. In the case of a nanotube, the frequency dependence of transitions is described by a function $\sim (1-x)^{-1/2}$. For both interband and intraband transitions, the external field leads to a significant shift of the threshold absorption-emission frequencies to the short-wavelength region. A similar modulating effect of an external field can be used to controllably change the frequency intervals of optical transitions in the structure under consideration.

E196: Charge Transport in Light-Emitting Field-Effect Transistors with sp3-Functionalized Single-Walled Carbon Nanotube Networks

Nicolas Frederic Zorn*†, Felix Berger, Jana Zaumseil

**Heidelberg University*

The controlled introduction of luminescent sp3 defects into semiconducting single-walled carbon nanotubes (SWCNTs) leads to narrowband, tunable emission in the near-infrared and increases their photoluminescence (PL) quantum yield for potential optoelectronic applications [ACS Nano 2019, 13, 9259]. While the spectroscopic properties of sp3-functionalized SWCNTs are already well-established, a detailed understanding of the impact of functionalization on their electrical performance especially in a network is still lacking. Here, we investigate charge transport in ambipolar, light-emitting field-effect transistors based on networks of pristine and sp3-functionalized (6,5) SWCNTs. While both hole and electron mobilities decrease with increasing degree of functionalization, the transistors remain fully operational, showing electroluminescence from the defect states. Charge-modulated PL spectroscopy, which exclusively probes the mobile charge carriers in SWCNT networks [ACS Nano 2020, 14, 2412], confirms that the defects are efficiently sampled by mobile carriers and consequently, sp3-functionalized SWCNTs actively participate in the charge transport. Temperature-dependent transport measurements provide further insights into the impact of sp3-functionalization on charge transport within the networks.

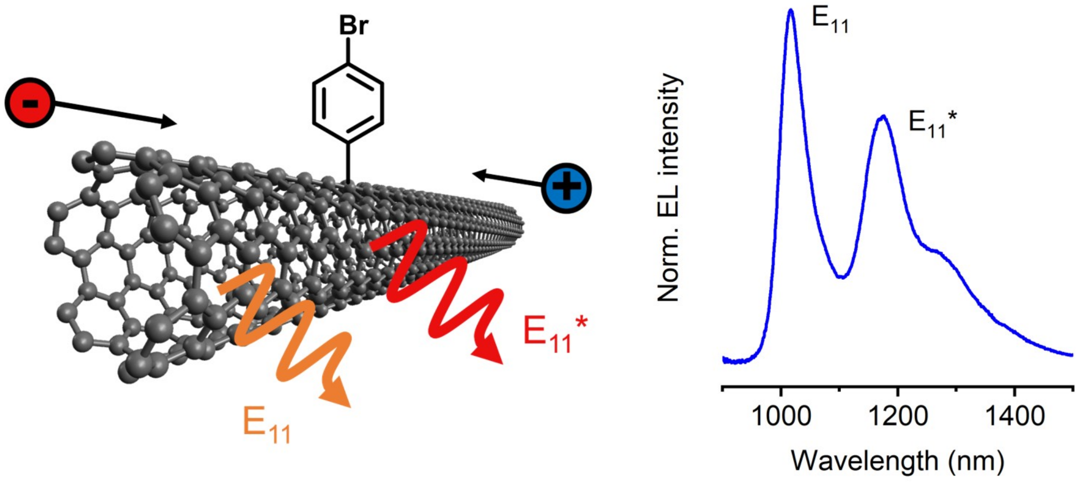

Fig. 1: Electrically generated emission from sp3 defects: When FETs with sp3-functionalized (6,5) SWCNT networks are biased in the ambipolar regime, electroluminescence from mobile (E11) and trapped excitons (E11*) is observed.

E197: Confined Carbyne: Strongest Raman Scatterer and Nanoscale Temperature Sensor

Cla Duri Tschannen*†, Martin Frimmer, Georgy Gordeev, Lei Shi, Thomas Pichler, Stephanie Reich, Sebastian Heeg, Lukas Novotny

**Photonics Laboratory, ETH Zürich, 8093 Zürich, Switzerland*

Carbyne is the paradigmatic sp-hybridized and truly one-dimensional allotrope of carbon. Finite realizations of carbyne with chain lengths up to 6000 atoms have been synthesized inside carbon nanotubes, which act as nanoreactors and protective nanocontainers [1]. As for other carbon nanostructures, Raman spectroscopy is a powerful tool to study the properties of carbyne, owing to its sensitivity to vibrational, optical, and electronic information. On top, the Raman response of carbyne is so strong that even short individual chains comprising a mere few hundred atoms can be readily detected. Here, we use a combination of tip-enhanced and wavelength-dependent Raman spectroscopy to experimentally quantify the Raman scattering from individual carbyne chains confined inside double-walled carbon nanotubes (DWCNTs) [2]. We find that the resonant differential Raman scattering cross section of confined carbyne is on the order of 10–22 cm2 sr–1 per atom, exceeding that of any other known material or molecule by two orders of magnitude or more. Moreover, we demonstrate that carbyne's record-high Raman scattering cross section enables Raman sideband thermometry at the single chain level [3]. Using laser irradiation as a heating source, we investigate the temperature dependence of the anti-Stokes/Stokes ratio and demonstrate the applicability of carbyne as a robust nanoscale thermometer. Our results establish confined carbyne as the strongest Raman scatterer ever reported and as optically interrogated temperature probe of molecular dimension. Its unrivaled Raman cross section renders carbyne a promising platform for experiments that rely on strong interaction between light and vibrational modes as well as for a wide range of applications. In particular, Raman sideband thermometry offers a promising perspective for thermal management in carbyne-based devices, which is a key requirement for their functioning and control. [1] Shi et al., Nat. Mater. 15(6), 634–639 (2016) [2] Tschannen et al., Nano Lett. 20(9), 6750–6755 (2020) [3] Tschannen et al., in preparation

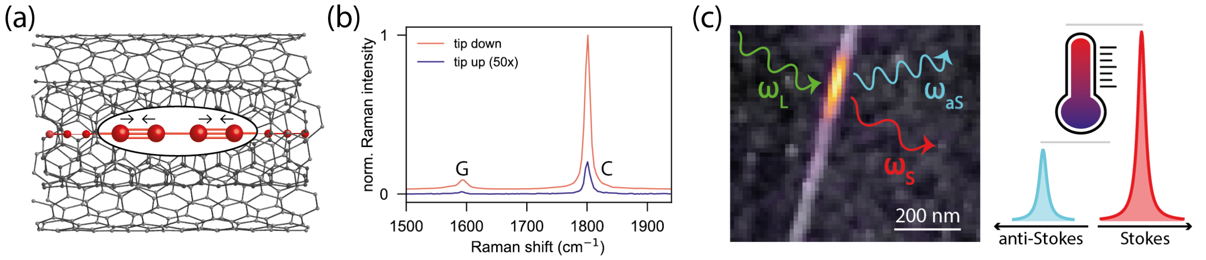

Fig. 1: (a) Carbyne chain encapsulated inside a DWCNT. (b) Near-field and far-field Raman spectrum of confined carbyne. (c) Illustration of Raman sideband thermometry of a single confined carbyne chain.

E198: Speed and Linearity of Asymmetric High Frequency CNT Transistors

Martin Hartmann*†, Sascha Hermann, Michael Schröter

**Chemnitz University of Technology*

The high intrinsic speed and prospected linearity of carbon nanotube-based field effect transistors (CNTFETs) make them highly interesting for future efficient transceiver electronics in communication systems. This is underlined by recent breakthroughs showing CNTFETs with a transit frequency (fT) as well as maximum frequency of oscillation (fmax) of around 100 GHz [1] challenging incumbent technologies such as GaAs pHEMTs and RF-CMOS [2]. We report on the impact of device architecture variations of high frequency (HF) CNTFETs onto their operating speed as well as linearity and contact resistance. Therefore, the spacers between the gate and the source electrode (S-spacer) and gate to drain electrode (D-spacer) were varied and the S-parameters of the HF CNTFETs were measured. By manipulating the spacer region, the device electrostatics can be balanced in the CNT-metal contact area, which influences the charge carrier injection and reflection at the Schottky-like barriers (SBs) that form between the metal covered CNT ends and the uncovered CNT channel region. Moreover, the size of the spacer influence the parasitic device capacitances and thereby the transit frequency. Until now, the dependence of the S-spacer and D-spacer on the HF CNTFET speed and linearity has only been shown by simulations [3]. Mothes et al. point out, especially within the S-spacer the fringing fields are needed to modulate the SBs, which is essential to gain highest speed and linearity. We report on single gate HFCNTFETs with a buried bottom gate, in contrast to a top gate approach, for lowest possible parasitic capacitance. Thereby we followed scalable device fabrication procedures based on a wafer-level prototyping platform allowing to fabricate sufficiently large device counts for systematic and conclusive studies. The studies exposed a speed increase, measured by the external fT and fmax, of up to 20% for a specific asymmetrical gate electrode position in the channel. The fabricated devices show transit frequencies up to 16 GHz for 280 nm long channels with randomly oriented CNTs and a tube density of up to 30 CNTs/µm [4]. Additionally, we will present the impact of the S- and D-spacer onto the device contact resistance as well as linearity. [1] Rutherglen et al., Nat. Electron. 2 (11) 2019 [2] Hartmann et al., IEEE Journ. of Microwaves 1 (1) 2021 [3] Mothes et al., SISPAD 2015 [4] Hartmann et al., ACS Mat. & Interf. 12 (24) 2020

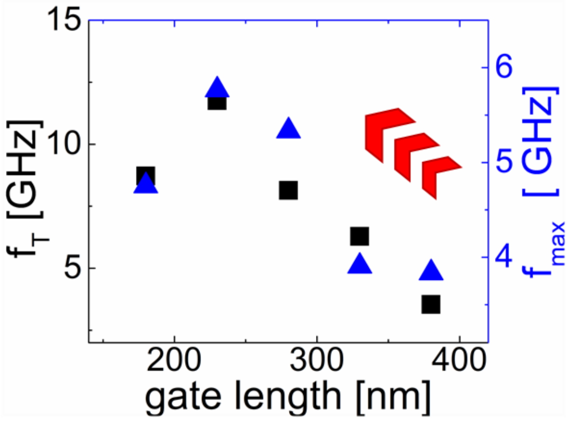

Fig. 1: Gate-length dependent speed of bottom gate HF-CNTFET

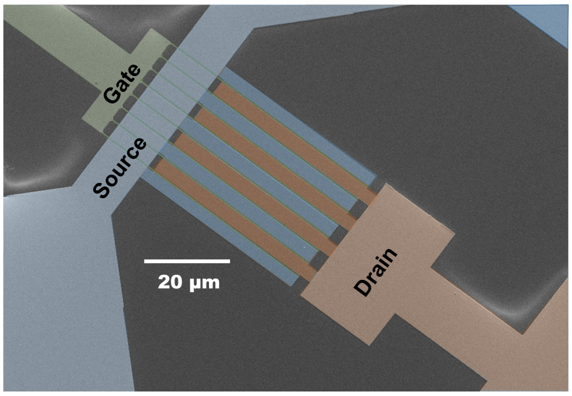

Fig. 2: Scanning electron microscopy false coulure picture of a HF CNTFET

E199: Out of equilibrium dynamics in carbon nanotubes: from THz emission to transient absorption spectum

Marco Battiato*†

Nanyang Technological University

Accurate description of out of equilibrium dynamics is becoming essential as a number of ultrafast phenomena arise due to the complex interplay of scattering with different quasiparticles, transport while out of equilibrium and, in general, far from equilibrium quasiparticle distributions. Moving away from equilibrium requires handling increasing theoretical and numerical complexity. The numerical costs spike critically when abandoning perturbative approaches. In this case the costs become extremely prohibitive in realistic systems, unless new numerical approaches are developed. By a fully non perturbative Boltzmann approach applied to realist band structures [1-2], a variety of quasiparticles in the presence of several channels of scattering and transport, we can describe to high precision the ultrafast dynamics of electrons, excitons and phonons in carbon nanotubes. Single-wall carbon nanotubes (SWCNTs) have been shown to produce bright THz emission when used as active component of photoconductive antennas. These emitters have a number of attractive properties like high thermal and chemical stability, biocompatibility, brightness, as well as strong geometrical control of the induced currents. However a straightforward application of concepts developed for standard photoconductive antennas fail, as the SWCNT THz emitters display a number of unexpected behaviours. They are brightest when resonantly pumped at excitonic transition, but even more puzzling is the difference between the THz-bias dependence and the photocurrent-bias dependence (which is never observed in semiconducting photoconductive antennas). In this joined experimental-theoretical collaboration, [3] we have to describe the full process of THz emission by a detailed description of electronic, excitonic, and phonon degrees of freedom, as well as transport in external electric field (Fig. 1). The approach above is however more general than that. In a more recent collaboration, [4] we are able to reproduce both static and transient absorption spectra. In particular we highlight the origin of the high energy shoulder of the phonon side bands (Fig. 2). [1] M. Wais, K. Held, M. Battiato, Numerical solver for the time-dependent far-from-equilibrium Boltzmann equation, accepted in Comput. Phys. Commun. [2] Indrajit Wadgaonkar, Rishabh Jain, Marco Battiato, Numerical scheme for the far-out-of-equilibrium time-dependent Boltzmann collision operator: 1D second-degree momentum discretisation and adaptive time stepping, Comput. Phys. Commun 263 (2021) [3] F. R. Bagsican, et al. Terahertz Excitonics in Carbon Nanotubes: Exciton Autoionization and Multiplication, Nano Letters 20, 3098 (2020) [4] S. Dal Forno et al, work in progress *Acknowledgements:* The presenting author acknowledges the contribution of several other authors who could not fit in the author list.

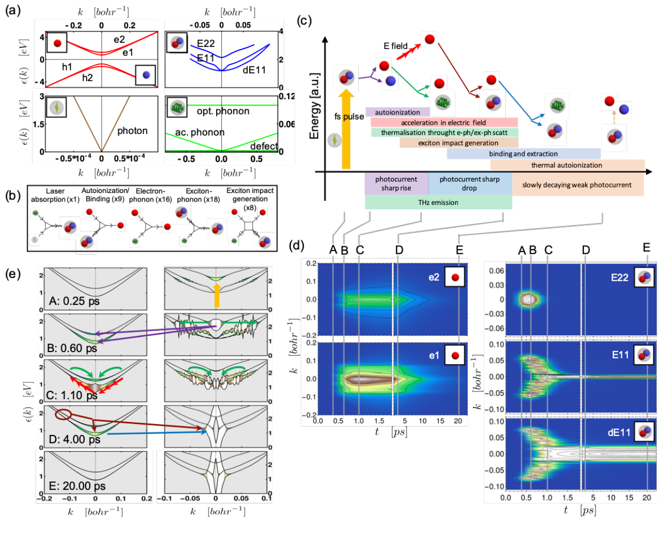

Fig. 1: (a) Quasiparticles, bands included. (b) Included scattering channels (c) Sketch of the dynamics (d) Density plot of the population for selected quasiparticle/bands (d) Snapshots of the population over band dispersion.

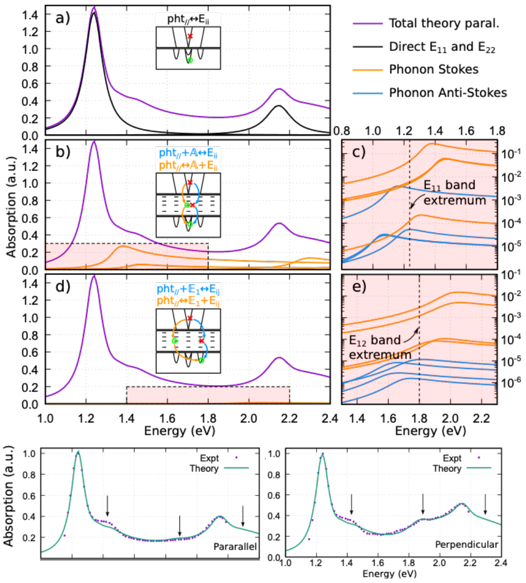

Fig. 2: Boltzmann absorption spectrum with comparison with experimental results. (a,b,d) Contribution from different transitions (zoomed in (c,e)). Bottom: Comparison with experiments

E200: Progress in developing lightweight robust Cu/Carbon nanotube composite electric conductors

Rajyashree Sundaram*†, Guohai Chen, Takeo Yamada, Don Futaba, Ken Kokubo, Kenji Hata, Atsuko Sekiguchi
**National Institute of Advanced Industrial Science and Technology*

We will report our progress with developing copper-matrix/carbon nanotube composites (Cu/CNT) lighter than copper with competing electrical performances and robustness. Such materials are promising copper substitutes for aircraft/automobile wire harnesses for improved weight-reduction and fuel-efficiencies as well as in micro-interconnects for smaller more powerful electronics [1]. We have fabricated our composites as cm-scale wires for harness applications and as via-like structures for interconnect applications [2-6]. Our composites show densities < 5.2 g/cm3 (at least 2/3rd as light as copper) irrespective of the structure due to a high nanotube vol% (>40%) mixed uniformly with copper. Our Cu/CNT room temperature electrical conductivities are in the range of ~1-4 × 105 S/cm, competitive to that of pure copper (5.9 × 105 S/cm). Our composites show superior current and temperature stability, with current carrying capacities (CCC) > Cu and temperature coefficients of resistivity (TCR) as low as 10% that of copper. The lower TCR of Cu/CNT (vs. copper) implies more temperature-stable electric conductivity, vital for applications needing stable high-temperature operation, e.g., motor windings and cables near aircraft/automobile engines. Further, both Cu/CNT wire and via-structures show better thermal expansion stability with coefficients of thermal expansion (CTE) ~4-7 ppm/K, closer to Si-CTE (~3 ppm/K) than Cu-CTE (~17 ppm/K). Besides demonstrating Cu/CNT's promise as a robust lightweight electrical conductor, we will discuss the effect of key factors such as Cu and nanotube spatial distribution, nanotube attributes, metal/nanotube interface, etc. on composite performances. References [1] R. Sundaram, A. Sekiguchi, M. Sekiya, T. Yamada, K. Hata, Royal Society Open Science, 5(11) (2018) 1-21. [2] R. Sundaram, T. Yamada, K. Hata, A. Sekiguchi, Scientific Reports, 7(1) (2017) 1-11. [3] R. Sundaram, T. Yamada, K. Hata, A. Sekiguchi, Materials Today Communications, 13 (2017) 119-125. [4] R. Sundaram, T. Yamada, K. Hata, A. Sekiguchi, Japanese Journal of Applied Physics, 57(4) (2018) 04FP08 (1-7). [5] R. Sundaram, T. Yamada, K. Hata, A. Sekiguchi, Journal of Materials Research and Technology, 9(3) (2020) 6944-6949. [6] G. Chen, R. Sundaram, A. Sekiguchi, K. Hata, D. Futaba, ACS Appl. Nano Materials, 4(1) (2021) 869-876.

E201: Quantitative 2D fitting of fluorescence-excitation maps: Excitation line shape of single-wall carbon nanotubes

Miguel De Clercq*†, Sofie Cambré, Wouter Van Werveke, Miles Martinati, Maksiem Erkens, Wim Wenseleers
**University of Antwerp*

Each single-walled carbon nanotube's (SWCNT) chiral structure possesses a unique set of optical transitions. Due to this one-to-one correspondence, two-dimensional (2D) fluorescence-excitation (PLE) spectroscopy is a powerful tool for analyzing SWCNT samples. PLE is therefore often employed to determine the chirality distribution present in a particular sample, e.g. as a measure of the sample's purity after chiral sorting. Interestingly, the optical properties of SWCNTs are also extremely sensitive to both the inner and outer environment of the SWCNTs, resulting in shifts of the peak positions, peak broadening, amplitude changes, etc [1,2,3]. Consistent quantification of this physically relevant information requires the fitting of an accurate model to the data. To date such a model did not exist for the excitation line shape of SWCNTs. Here we propose a highly accurate excitation line shape model and combine it with one for the emission lineshape in a 2D fitting model. This model is implemented within a graphical user interface (GUI) which allows for the flexible and accurate fitting of any SWCNT sample and the extraction of meaningful quantitative information about the line shape and intensity of every chirality present in the sample. The GUI greatly aides the usage of this model through various features e.g. a comparison of integrated ranges (slices) between data and fit can be monitored throughout the fitting process, difference plots can be made and fitted features can be extracted and saved in multiple different graphical forms. 1.Cambré, S. & Wenseleers, W. Angew. Chemie - Int. Ed. 50, 2764–2768 (2011). 2.Cambré, S. et al. ACS Nano 6, 2649–2655 (2012). 3.Cambré, S. et al. Nat. Nanotechnol. 10, 248–252 (2015).

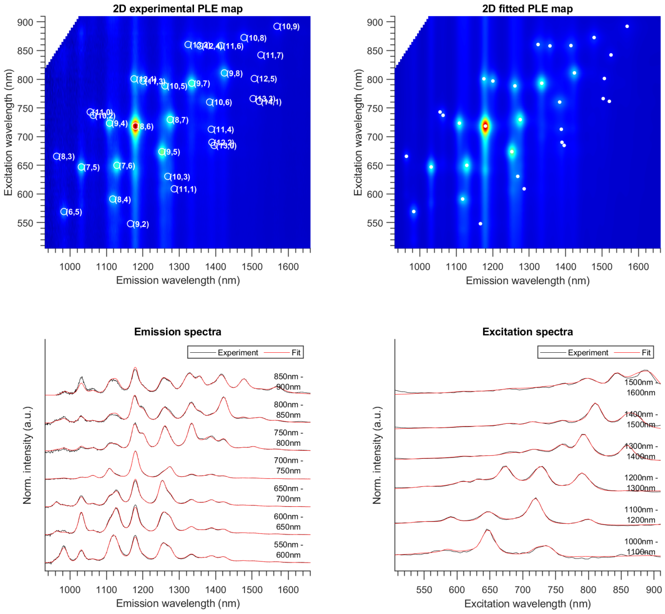

Fig. 1: Converged fit of a PLE map of HiPco SWCNT in DOC/D2O saved together in one panel and showing 7 and 6 slices in excitation and emission respectively.

E202: ZnPc/graphene nanoflake near membrane cell: theoretical behavior

Philippe Sonnet†, Fabien Picaud*, Eric Duverger, Louise Stauffer

**Université de Franche-Comté*

The development of carbon-based nanovectors present great interest due to their diverse forms. Most of them present a very large surface area as the graphene nanoflake. Indeed, its tailored size allows anchoring large molecules as the phthalocyanines on its surface. This strategy helps restrict the molecular self-aggregation and to develop functionalized nanoplatforms. The zinc phthalocyanine molecules noted ZnPc have received significant attention in the design of photosensitizers for photodynamic therapy (PDT) applications. This family of molecules presents interesting properties: strong light absorption between 650 and 850 nm, high yield of singlet oxygen production, stability and biocompatibility, low dark toxicity and strong phototoxicity, and ease of chemical modifications. We perform calculations within different technics (ab-initio methods and classical molecular dynamics) to study the ZnPc molecule on a graphene nanoflake in a vacuum, in a presence of water and in the biological environment. In previous work, we proposed an approach by carrying the ZnPc molecule via π–π interactions with a graphene nanoflake to enhance its targeting [1]. In this present study, the molecules ended by a –NH2 group allow a covalent bond between the molecule and the graphene nanoflake to increase the stability of the systems [2]. In order to increase the ZnPc molecule/graphene nanoflake solubility in the bodily fluids and avoid molecule aggregation, hydrophilic groups in ZnPc have been introduced. The long groups allow enhancing the solubility and avoiding molecule aggregation, but make the membrane approach harder. By shortening the ligand lengths one favors the membrane approach while decreasing the solubility and certainly increasing the molecule aggregation. Finally, a balance between the diffusion of the ZnPc/graphene nanoflake system toward the membrane cell and the solubility, both related to the ligand length, should be found to optimize the PDT efficiency. [1] Duverger, Picaud, Stauffer, Sonnet, ACS Applied Materials and Interfaces 9 (2017) 37554 [2] Picaud, Duverger, Stauffer, Sonnet, Structural Chemistry 31 (2020) 1935–1943

E203: Role of Carbon nanotubes in environmental gas sensor

Shivani Dhall*†

**DAV Colllege, Jalandhar*

The development of gas sensors for the detection of toxic gases like NH3, CO and H2 existing in the atmosphere. Among these gases, H2 is odorless, colorless and flammable at concentrations greater than 4%. However, H2 is explosive over the range of 15% at standard atmospheric temperature. H2 gas is predictable to be extensively used as an energy source for fuel cells and it has wide applications in civil transportation. Therefore, H2 gas sensor is necessary to ensure safe operation of hydrogen based energy storage systems and facilities such as H2 gas stations, fuel cell based vehicles, semiconductor manufacturing and in rockets for space vehicles, since H2 leakage leads to explosive accidents. To shun this accidents, H2 gas sensors have been developed using carbon nanotubes (CNTs) and their nanostructures with metal/metal oxides nano-particles. A wide range of semiconducting metal oxides have been used as H2 gas sensor because of their structural simplicity and low cost. But these sensors detect the gases at particular temperature (nearly 200 °C). But nowadays, researcher's goal is to develop the sensors, which can operate at room temperature and consume low power. CNTs based sensors have been studied due to their exceptional electrical, mechanical and sensing properties. Due to the high surface area, CNTs can adsorb large amount of gases, which make them a probable contender for gas sensor with very high sensitivity and low response time. In the present work, we have fabricated H_2 gas sensors at room temperature (25 °C) using only 2% by wt. multiwalled carbon nanotubes (MWCNTs) as a base material. The fabricated sensor with area (100μm × 120μm) was used to detect the low concentrations (0.05-1%) of H2 gas with excellent resistance recovery, low recovery time, good repeatability and baseline stability in N2 atmosphere. In addition, a simple approach has been used to synthesize hybrid nanostructures with nanotubes, which enhanced structural, and sensing properties of nanotubes.

Acknowledgements: The author S. Dhall acknowledges to SERB (DST, Govt. of India) for providing TARE funding (letter no. TAR/2019/000113)

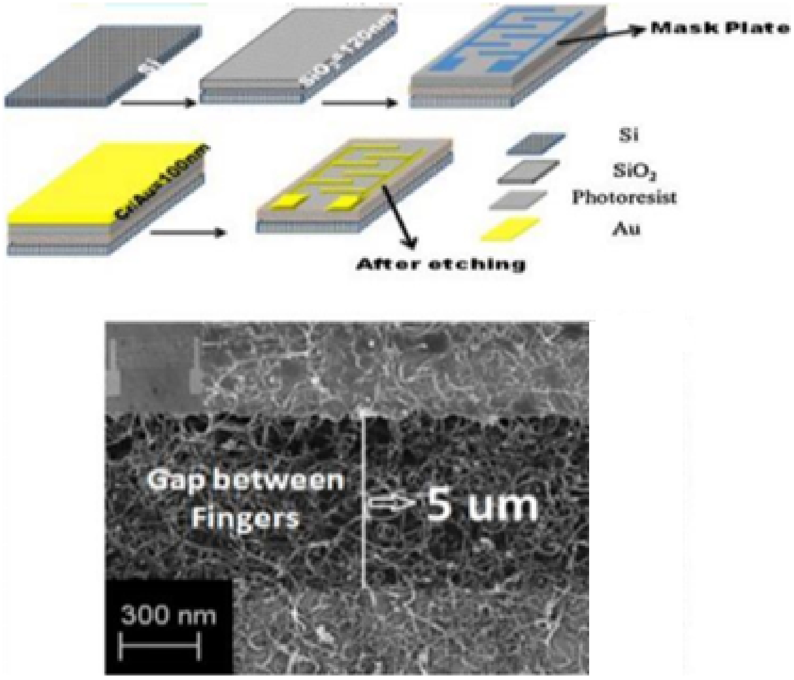

Fig. 1: Fabrication of gas sensor

E204: An Oligonucleotide Sensor with Parallel Electrical Pathways

Benjamin Barnes*†, YuHuang Wang

**University of Maryland*

Point-of-care sensors can combat the spread of infectious diseases and inform timely treatments. But in order to be used in this capacity, point-of-care sensors need to combine rapid detection speed with high sensitivity. Detection speed has traditionally been reduced by increasing the sensing surface area of the device, but this can increase noise and reduce sensitivity. In this work we align multiple tube-in-a-tube ($Tube^2$) nanostructures across a trench between two electrodes. Each $Tube^2$ consists of a semiconducting carbon nanotube nested within an outer nanotube densely functionalized with oligonucleotide probes. This device design provides a high surface area, while forcing the electrical current through distinct electrical pathways, allowing the binding events to be sensitively detected. Using this device architecture, we demonstrate the selective detection of Lyme disease oligonucleotide biomarkers in physiological ionic strength conditions on the order of seconds.

E205: Synthetic Control over the Binding Configuration of Luminescent sp3-Defects in Single-walled Carbon Nanotubes

Simon Settele*†, Felix Berger, Sebastian Lindenthal, Shen Zhao, Abdurrahman Ali El Yumin, Nicolas Frederic Zorn, Alexander Högele, Jana Zaumseil

**Heidelberg University*

The controlled functionalization of single-walled carbon nanotubes (SWNTs) with luminescent sp3-defects has emerged as a powerful tool to enhance their usually low photoluminescence (PL) quantum yields and has created the potential to employ them as quantum-light sources in the near-infrared (NIR). For that, it is crucial to control their spectral diversity and generate sp3-defects with deeper optical trap depths. The emission wavelength is determined by the binding configuration of the defects rather than the molecular structure of the attached groups. However, current functionalization methods produce a variety of binding configurations with strongly red-shifted emission features usually being a minority. Here, we introduce a simple base-promoted functionalization protocol for polymer-sorted (6,5) SWNTs in organic solvents for the selective creation for sp3-defects with strongly red-shifted E11*– emission (~1250 nm). These defects exhibit longer photoluminescence lifetimes and single-photon emission with high purity at room temperature. The selectivity of this method is maintained when expanding the functionalization to other polymer-sorted nanotubes (e.g., (7,5) and (10,5)) and enables better matching with telecom bands. Mechanistic studies reveal that the selectivity of the reaction depends on the presence and strength of an organic base. Thus, in contrast to commonly found aryl radical and reductive alkylation reactions we propose nucleophilic addition as the reaction mechanism. This novel functionalization method expands the available chemistry for controlled introduction of luminescent sp3-defects with a broad variety of functional groups. *Acknowledgements:* ERC-2018-COG, TRIFECTs: Trions and sp3 Defects in Single-Walled Carbon Nanotubes for Optoelectronics GrantNo.: 817494

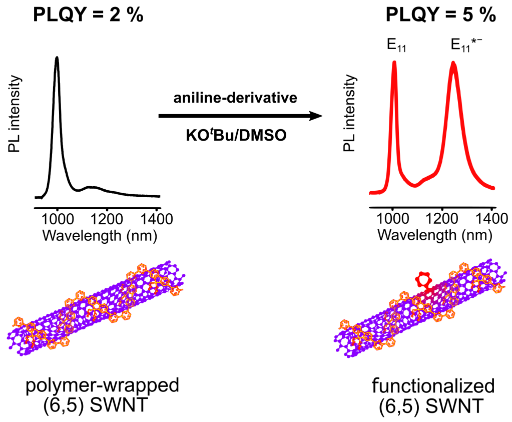

Fig. 1: Synthetic control over the binding configuration by functionalization of PFO-BPy-wrapped (6,5) SWNTs with aniline derivatives and base KOtBu.

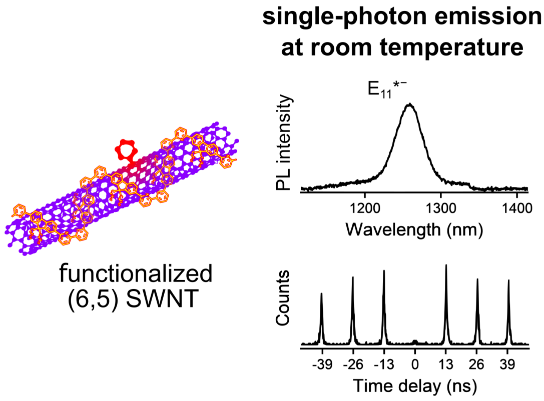

Fig. 2: Red-shifted E11*– defects exhibiting single-photon emission with high purity at room temperature.

E206: Radio frequency heating of carbon nanomaterial-based structures: Universal patterns and application to printed film characterization

Muhammad Anas*†, Mazin Mustafa, Victoria Hicks, Lee Moores, Micah Green

**Texas A&M University*

Our group has recently demonstrated low frequency (1-200 MHz) and low power (< 100 W) radio frequency (RF) heating of carbon nanomaterial-loaded structures such as thin films and polymer nanocomposites using an array of contact and non-contact applicators. These heating techniques opened up routes for faster and efficient composite manufacturing, 3D printing, and fiber processing. It is known that electrical conductivity is required for RF heating of carbon-based nanomaterials. However, it is not well understood how RF heating rates vary with conductivity and if the pattern is generalizable for all types of RF susceptor-loaded structures. In this work, we use experiments and simulations to explore the universal patterns observed between RF heating rates and in-plane electrical conductivity for thin films made of carbon nanotubes, laser-induced graphene, and carbon nanofiber-polyamide composites. We also investigate existence of similar patterns in chirality-sorted single-walled carbon nanotube films. Finally, we show a novel RF heating-based high-throughput quality screening technique for printed carbon nanotube circuits.

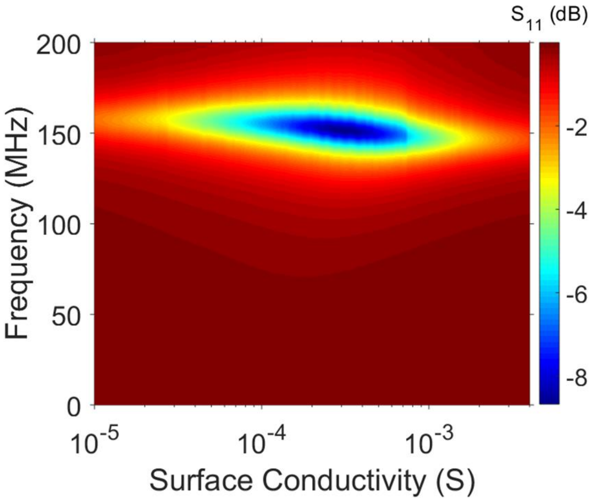

Fig. 1: Simulated reflection coefficient as a function of frequency and surface conductivity for thin films.

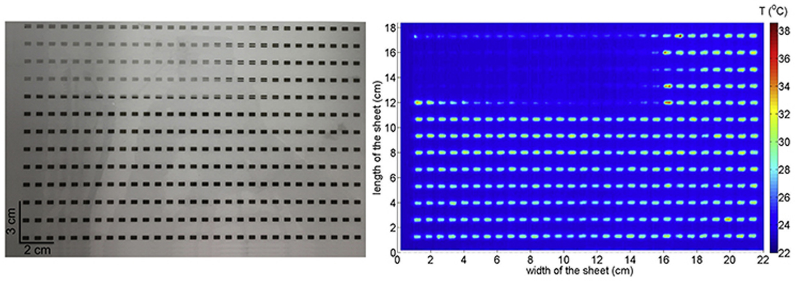

Printed CNT circuits

RF heating response

Fig. 2: Printed CNT films and the corresponding RF heating response. Faulty ones can be quickly determined using the thermal response.

E207: Charged Fermion and Boson Exciton Complexes in quasi-2D Semiconductors

Igor Bondarev*†

North Carolina Central University

We present the results of the binding energy calculations to demonstrate the stability and robustness for few-particle electron-hole (e-h) complexes in quasi-monolayer Transition Metal Dichalcogenide (TMD) heterostructures [1,2]. Van der Waals (vdW) bound planar semiconducting TMD heterostructures have recently been a subject of intense theoretical and experimental research due to their unique physical properties originating from the vertical quantum confinement and peculiar electronic structure [1-8]. For ultrathin materials of controlled thickness, the vertical confinement leads to the effective dimensionality reduction from 3D to 2D while still retaining the thickness as a parameter to represent the vertical size [9,10]. Quite generally, this is the transdimensional regime - neither 3D nor 2D but something in-between - turning into 2D as thickness tends to zero, challenging to study what the 3D-to-2D continuous transition has to offer to improve material functionalities [10]. As an example, vdW bound TMD bilayers (interlayer distance ~0.6 nm) are recently shown both theoretically and experimentally to not only form the long-lived and so very stable states of Interlayer Excitons (IE) and biexcitons (two- and four-particle neutral boson e-h complexes, respectively [4-7]) but also to form the single-Charge Interlayer Excitons (CIE, or the interlayer trion, a three-particle fermion complex) [6,8]. With non-zero charge, spin and permanent dipole moment, the CIEs in TMD bilayers can be controlled by both external electrostatic and magnetostatic fields, and so are good for future spinoptronics applications. Adding a metallic substrate to this system further increases its functionality by making possible the formation of robust (long-lived) quaternion e-h complexes – four-particle double-charge bosons [2]. This is possible since the like-charge repulsion is now reduced due to the image-charge attraction. A

Bose-Einstein condensate of such quaternions opens the door to a new kind of unconventional high-T superconductivity. [1] I.V.Bondarev, et al., arXiv2002.09988 (2021). [2] Z.Sun, et al., arXiv2003.05850 (2021). [3] A.Arora, et al., Nanoscale 7, 10421 (2015). [4] Z.Wang, et al., Nano Lett. 18, 137 (2018). [5] Z.Sun, et al., ACS Photonics 7, 1622 (2020). [6] L.A.Jauregui, et al., Science 366, 870 (2019). [7] M.Kremser, et al., npj 2D Mater. Appl. 4, 8 (2020). [8] I.V.Bondarev and M.R.Vladimirova, Phys. Rev. B 97, 165419 (2018). [9] I.V.Bondarev, H.Mousavi, and V.M.Shalaev, Phys. Rev. Research 2, 013070 (2020). [10] A.Boltasseva and V.M.Shalaev, ACS Photonics 6, 1 (2019). *Acknowledgements:* Supported by the U.S. DOE office of BES under award DE-SC0007117 (I.B.) and by the U.S. ARO under MURI award W911NF-17-1-0312 (D.S.)

E208: Influence of the Dielectric Environment on Trion Emission in Networks of (6,5) Carbon Nanotubes

Sonja Wieland*†, Jana Zaumseil

**Heidelberg University*

The optical properties of semiconducting single-walled carbon nanotubes (SWCNTs) are governed by excitons with large binding energies and narrow emission in the near-infrared. In the presence of excess charge carriers, trions (i.e., positively or negatively charged excitons) are formed. Their emission is red-shifted by 100-200 meV compared to the corresponding excitons depending on the nanotube diameter. Theoretical calculations have shown that the medium surrounding the SWCNT not only affects the band gap and exciton binding energy, but also reduces the trion binding energy through dielectric screening, however this has not yet been shown experimentally. Strong variations of the ratio of trion to exciton population (i.e., emission) depending on the type of device have been observed, but remain largely unexplained (see Adv. Electron. Mater. 2020, 6, 2000717). Due to the charged nature of trions as opposed to the neutral excitons, a stabilization effect by polar environments can be expected. Here, we investigate the influence of the dielectric environment on trion energetics and population in electrostatically doped networks of semiconducting (6,5) SWCNTs. For this purpose, we employ nanotube networks as the semiconducting layer in top gate/bottom contact field-effect transistors and vary the dielectric constant (ε) of the gate dielectric from Teflon AF2400 (ε = 1.9) to HfOx (ε = 14.3). We discuss the role of charge carrier density and static dielectric constant vs. refractive index as critical parameters. We aim to gain a more systematic understanding of trions in SWCNTs as low-energy, charged quasi-particles and their impact on optoelectronic devices.

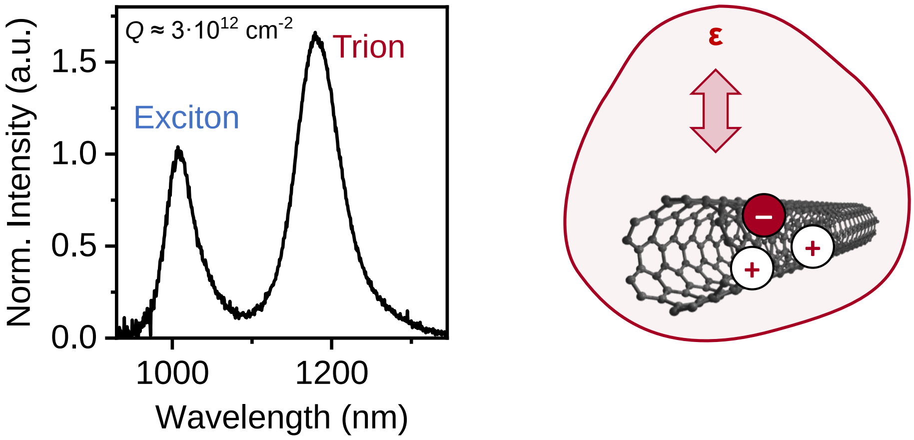

Fig. 1: Photoluminescence spectrum of a (6,5) SWCNT network in a field-effect transistor in hole accumulation and schematic illustration of positively charged trions in carbon nanotubes interacting with the dielectric environment.

E209: Guiding Charge Transport in Semiconducting Carbon Nanotube Networks by Local Optical Switching

Sonja Wieland†, Maximilian Brohmann*, Simon Angstenberger, Niklas J. Herrmann, Jan Lüttgens, Daniele Fazzi, Jana Zaumseil

**Heidelberg University*

Field-effect transistors (FETs) are conventionally used as switches and amplifiers. However, additional properties such as optical memory, photoswitching etc. can be integrated to obtain multifunctional optoelectronic devices.

Here, we use a photochromic spiropyran derivative embedded in the polymer gate dielectrics of (6,5) single-walled carbon nanotube (SWCNT) network FETs. Spiropyran can be converted to its isomer merocyanine, which has a much higher dipole moment, by UV illumination. This process is reversible by thermal annealing. The presence of merocyanine strongly reduces the mobilities of both holes and electrons and hence also the on-currents of the irradiated SWCNT FETs. Thus, they can act as optical memory devices. The reproducible and reversible nature of the spiropyran/merocyanine photoisomerization furthermore allows us to create defined areas of high and low carrier mobility in a transistor channel with good spatial resolution by local UV illumination through a photomask. The resulting distribution of current density can be visualized directly by recording the near-infrared electroluminescence from the FET channel in the ambipolar regime. Composite electroluminescence images (see Fig. 1) show that the mobility differences between UV-exposed and not-exposed areas force charge carriers to deviate from their straight trajectory along the lateral electric field between source and drain electrode. We can thus create and visualize charge transport pathways in operating SWCNT FETs on the micrometer scale (ACS Appl. Mater. Interfaces 2020, 12, 25, 28392–28403).

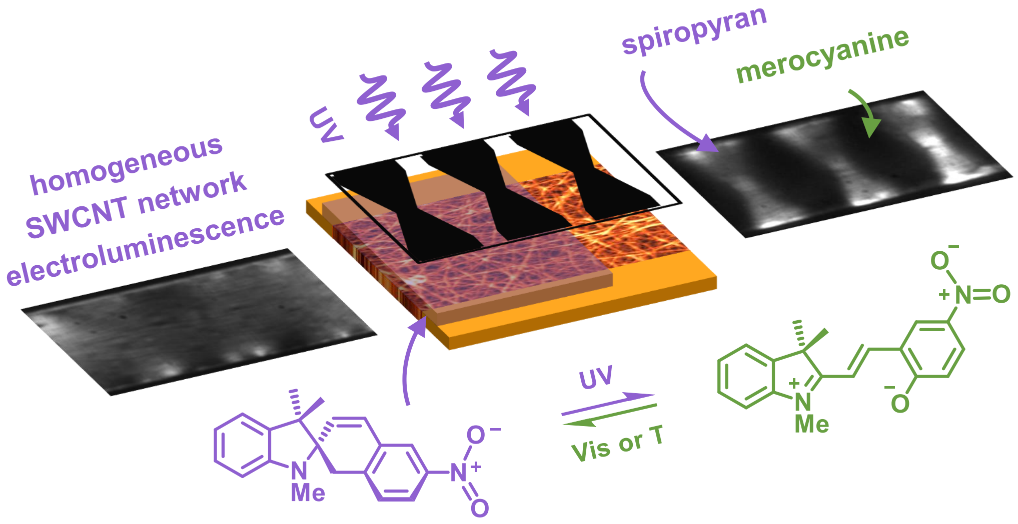

Fig. 1: Local reduction of charge carrier mobilities and thus electroluminescence from SWCNT FETs by UV-induced photoisomerization of spiropyran embedded in the gate dielectric.

E210: High Aspect Ratio Carbon Nanotube Arrays and their Application as Neural Probes and Through-Silicon-Via Interposer

Guohai Chen*†, Rajyashree Sundaram, Atsuko Sekiguchi, Robert Davis, Kenji Hata, Don Futaba

**National Institute of Advanced Industrial Science and Technology*

The processing of materials into arbitrary architectures represents an important process in utilizing their properties in any applications. In this presentation, we demonstrate the synthesis of high aspect ratio (60:1) and free-standing vertically aligned carbon nanotubes (VACNT) posts using an approach akin to sacrificial layers to overcome the synthetic limitation due to mechanical requirements for VACNTs synthesis [1-3]. To maintain perfectly vertical growth of each pillar within the array of millimeter-tall, high aspect ratio, free-standing VACNT posts, a "hedge" structure was grown connected to the posts for support and was later removed. As a result, individual posts of 1.2 mm-height and 20 um-diameter were achieved. With this structure used the mechanically compliant posts of CNTs as neural probes. Examination of the electrochemical detection to methyl viologen and dopamine using an individual CNT microelectrode showed fast-electrochemical response. In another direction, CNT posts were utilized to demonstrate the feasibility of a CNT-Cu composite as a via material for through-silicon-via (TSV) interposers which can potentially possess both the high electrical conductivity of Cu and the low coefficient of thermal expansion (CTE) of CNTs [4, 5]. The CNT-Cu TSV showed both Cu-level electrical conductivity (~2.5×105 S/cm) and Si-level CTE (~7×10-6 /K). The greatly reduced CTE mismatch between CNT-Cu and Si was achieved and its functionality was demonstrated for several configurations. References: 1. G. Chen, D.N. Futaba, H. Kimura, S. Sakurai, M. Yumura, K. Hata, ACS Nano, 7 (2013) 10218-10224. 2. G. Chen, R.C. Davis, D.N. Futaba, S. Sakurai, K. Kobashi, M. Yumura, K. Hata, Nanoscale, 8 (2016) 162-171. 3. G. Chen, B. Dodson, D.M. Hedges, et al, ACS Biomater. Sci. Eng., 4 (2018) 1900-1907. 4. R. Sundaram, T. Yamada, K. Hata, A. Sekiguchi, J Mater Res Technol, 9

(2020) 6944-6949. 5. G. Chen, R. Sundaram, A. Sekiguchi, K. Hata, D.N. Futaba, ACS Appl. Nano Mater., 4 (2021) 869-876.

E211: PEGylated polymer-wrapped semiconducting carbon nanotubes for electrochemical transistors with high transconductance

Daniel Heimfarth*[†], Merve Balci Leinen, Patrick Klein, Ullrich Scherf, Jana Zaumseil

Ruprecht Karl University of Heidelberg

Selective polymer-wrapping with conjugated polymers yields purely semiconducting single-walled carbon nanotubes (SWCNT) that show remarkable performance in a variety of electrolyte-gated (electrochemical) transistors. However, the employed wrapping polymers (e.g., polyfluorene-bypyridine copolymer with octyl side-chains, PFO-BPy) are usually hydrophobic. While this is no problem for electrolyte-gating with ionic liquids or iongels (e.g., Carbon 2017, 118, 26) it becomes a limiting factor for water-gated transistors that are used for biosensing (Sens. Actuators, B 2018, 255, 1507). A common route for improving ion transport and biocompatibility in organic electrochemical transistors (OECTs) is PEGylation (i.e., introduction of oligo(ethylene glycol) chains). Here, we apply a polymer-exchange protocol (J. Phys. Chem. C 2019, 123, 22680) to replace the original wrapping polymer PFO-BPy of sorted (6,5) SWCNTs with a conjugated polymer having the same backbone but hydrophilic tetraethylene glycol instead of alkyl side-chains (TEG-PFO-BPy). Thick, aerosol-jet printed films of these SWCNT-polymer hybrids show increased water uptake and much stronger photoluminescence (PL) quenching and trion emission when gated with water, thus indicating more thorough doping of the entire film. Consequently, the effective volumetric capacitance and transconductance of PEGylated SWCNT networks are significantly higher than reference samples of PFO-BPy wrapped SWCNTs. Their performance makes them viable alternatives for polymer semiconductors in OECTs while also providing better chemical stability, mechanical stretchability, and a wide variety of options for further functionalization for sensing.

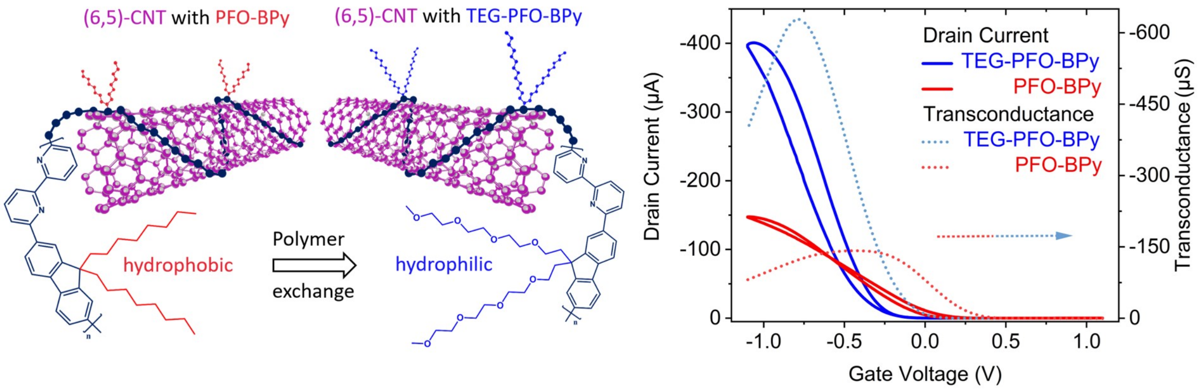

Fig. 1: Polymer-wrapped (6,5) SWCNTs with hydrophilic TEG side-chains show steeper transfer characteristics at -100 mV drain voltage and a fourfold increase in peak transconductance compared to the hydrophobic reference.

E212: C60 adsorption on germanene/Al(111) : experimental and theoretical studies

Natalia MASSARA*, Adil MARJAOUI, Régis STEPHAN[†], Marie-Christine HANF, Mickael DERIVAZ, Didier DENTEL, Samar HAJJAR-GARREAU, Ahmed MEHDAOUI, Mustapha Diani, Philippe Sonnet, Carmelo Pirri

Université de Haute Alsace, CNRS, IS2M UMR7361, 68100 Mulhouse, France

The first observation by scanning tunneling microscopy (STM) of a continuous layer of germanene on Al(111) substrate has been carried out in 2015 [1]. Density function theory (DFT) calculations have shown that the structure of the germanene layer was buckled with a unit cell composed of eight Ge atoms, seven Ge atoms lying within the basal plane and one uplifted Ge atom. The protrusion associated with the uplifted Ge atom gives the topographic hexagonal contrast observed in STM [2]. Since no covalent bond exists between the germanene layer and the Al substrate, the formation of a van der Waals heterostructure composed of the 2D material and an organic molecules layer is worth investigating. In the present work, we have studied the adsorption of C60 molecules on germanene/Al(111) with experimental and theoretical tools. This is one of the first experimental study investigating the interaction of organic molecules with a germanene/Al(111) substrate [3]. The STM observations show the possibility, at room temperature, to reach experimentally a single C60 monolayer on germanene, but without long range order. For a deeper understanding of the C60/germanene/Al(111) system, density functional theory calculations have been performed. These show that the C60 layer and the germanene interact by means of van der Waals and electrostatic interactions without formation of covalent bond. The interface between germanene and the Al(111) substrate is not modified upon C60 adsorption, whether it concerns the crystallographic structure or the electric charges. Bader charges calculations show that the charges gained by the C60 molecules are very low, and are mainly provided by the germanene layer, whose behavior corresponds to that of an electronic reservoir. The germanene layer plays the role of a barrier for electron transfer from Al substrate to C60 molecules and protects electronically the Al crystal thanks to the presence of specific interactions, As a result, the electron attractor properties of the C60 molecules are not modified for the growth of further layers on it. Finally, a novel property of a 2D crystal interacting with a metal substrate has been evidenced, since the germanene layer acts as an electronic buffer. [1] M. Derivaz et al, Nanolett. 15 (2015) 2510-2516[2] R. Stephan et al J. Phys. Chem. Lett. 8 (2017) 4587-4593[3] N. Massara et al, 2D Mater. 6 (2019) 035016 *Acknowledgements:* The calculations have been performed with a financial support French National Research Agency ANR-17-CE09-0021-03 and the CPER Alsacalcul

E213: Spiropyran-Functionalized Polymer--Carbon Nanotube Hybrids for Dynamic Optical Memory Devices and UV Sensors

Merve Balci Leinen*†, Patrick Klein, Finn L. Sebastian, Nicolas Frederic Zorn, Sylwia Adamczyk, Sybille Allard, Ullrich Scherf, Jana Zaumseil

**Heidelberg University*

Single-walled carbon nanotubes (SWNTs) possess outstanding optoelectronic properties and are highly sensitive to chemical and physical changes in their environment (see J. Phys. Chem. C 2019, 123, 22680). They are also great platforms to create hybrid structures that can react to certain analytes or stimuli. Light is such a stimulus for the properties of photochromic compounds. Among the variety of photoswitchable molecules, spiropyran has attracted much attention due to its large change in dipole and color when photoisomerized to merocyanine. Here, we use sorted, monochiral (6,5) SWNTs that are wrapped with polyfluorene polymers whose sidechains were decorated with different amounts of spiropyran moieties. We find that stepwise UV illumination of networks of these spiropyran-polymer-SWNT hybrids leads to PL quenching, p-doping as indicated by the increasing trion emission and enhanced electrical conductivity by up to three orders of magnitude, which further increases with exposure time. All these changes are reversible by heating the sample briefly. The cycle of UV illumination and heating can be repeated many times and thus enables application of the hybrid networks as optical memory devices (Adv. Electron. Mater. 2020, 6, 2000717).

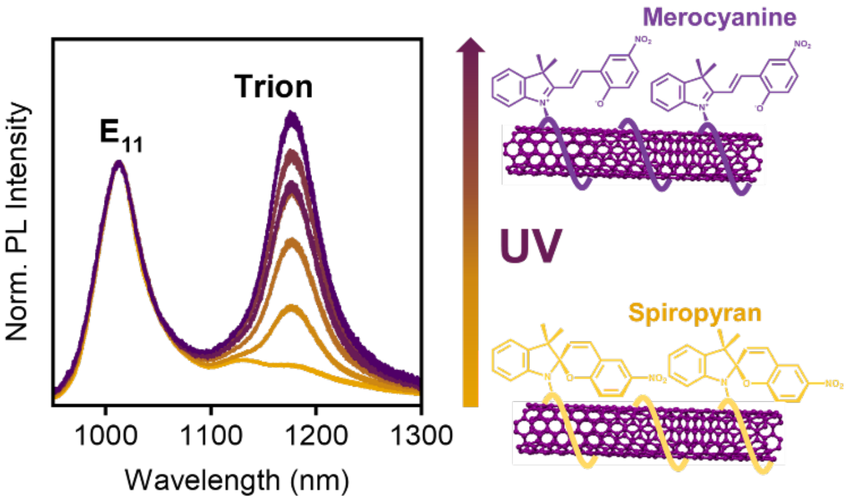

Fig. 1: Normalized photoluminescence spectra of (6,5) SWNTs wrapped with spiropyran-functionalized polyfluorene after UV illumination in air indicating increasing p-doping.

E214: Ultrawide gap moire diamanes: theoretical investigation

Victor Demin*†, Dmitry Kvashnin, Leonid Chernozatonskii

**IBCP RAS*

Diamane is the fully sp3 hybridized carbon structure based on bilayer graphene (BG) [1]. The adsorption of atoms on the BG surface leads to the formation of interlayer covalent bonds. In this work new type of hydrogenated and fluorinated diamanes (Dnθ) based on twisted bilayer graphene with a layer rotation angle θ of about 30° are considered by DFT method [2,3]. Structural features of Dnθ lead to increasing of the bandgaps in comparison with the bandgaps of ordinary diamanes with AA- or AB-stacking [4]. The maximum value of the bandgap Eg=4.5 eV corresponds to fluorinated Dn27.4. Mechanical properties of proposed structure were estimated by means of nanoindentaton technique simulations. Possible applications of these two-dimensional dielectrics were also discussed.Chernozatonskii L.A., Demin V.A., Kvashnin D.G. Fully Hydrogenated and Fluorinated Bigraphenes–Diamanes: Theoretical and Experimental Studies // J. Carbon Res. C., 2021. Vol. 7, № 1. P. 17.Chernozatonskii L.A., Demin V.A., Kvashnin D.G. Ultrawide-bandgap Moiré diamanes based on bigraphenes with the twist angles Θ ~ 30° // Appl. Phys. Lett. American Institute of Physics, 2020. Vol. 117, № 25. P. 253104Chernozatonskii L.A. et al. Moiré diamanes based on the hydrogenated or fluorinated twisted bigraphene: The features of atomic and electronic structures, Raman and infrared spectra // Applied Surface Science. 2021. Vol. 537. P. 148011.Chernozatonskii L. A. et al. Diamond-like C2H nanolayer, diamane: Simulation of the structure and properties // JETP Lett. 2009. Vol. 90. №2. P. 134. *Acknowledgements:* RFBR, project No.20-02-0055

E215: Diamanes -- Fully Hydrogenated and Fluorinated Bigraphenes: Theory, Experiments and Application Perspectives

Leonid Chernozatonskii*†, Victor Demin, Dmitry Kvashnin

**IBCP RAS*

Diamanes are diamond-like films obtained in the process of fully hydrogenation or fluorination of bilayer graphenes (BG). Structure of diamanes depends on bilayer graphene stacking. In the case of AB-stacked BGs half of the C atoms are functionalized by H(or F) and second half forms interlayer bonds that corresponds to C2H(F) stoichiometry [1-3]. In the case of twisted BGs with twisted angles near 30°pairs of adatoms form H(F)-C-C-H(F) complexes that increases relative amounts of hydrogens (fluorines) in comparison with the AB diamanes. So twisted diamanes have C2H(F)1+x stoichiometry [4,5]. Structures of diamanes based on AA-, AB-stacked BGs and commensurate BGs with 21.8°, 27.8° and 29.4° twisted angles are described in detail. All diamanes have unique properties as high thermal conductivity, wide bandgap and high hardness. Last experimental and theoretical researches and potential diamane applications also will be considered. Chernozatonskii L.A., Demin V.A., Kvashnin D.G. Fully Hydrogenated and Fluorinated Bigraphenes–Diamanes: Theoretical and Experimental Studies // J. Carbon Res. C., 2021. Vol. 7, № 1. P. 17.Piazza F. et al. Progress on Diamane and Diamanoid Thin Film Pressureless Synthesis // J. Carbon Res. C., 2021. Vol. 7, № 1. P. 9.Bakharev P.V. et al. Chemically induced transformation of chemical vapour deposition grown bilayer graphene into fluorinated single-layer diamond // Nature Nanotechnology. 2020. Vol. 15, № 1. P. 59–66Chernozatonskii L.A., Demin V.A., Kvashnin D.G. Ultrawide-bandgap Moiré diamanes based on bigraphenes with the twist angles Θ ~ 30° // Appl. Phys. Lett. American Institute of Physics, 2020. Vol. 117, № 25. P. 253104Chernozatonskii L.A. et al. Moiré diamanes based on the hydrogenated or fluorinated twisted bigraphene: The features of atomic and electronic structures, Raman and infrared spectra // Applied Surface Science. 2021. Vol. 537. P. 148011. *Acknowledgements:* RFBR, project No.20-02-0055

E216: Giant Terahertz Polarization Rotation in Ultrathin Films of Aligned Carbon Nanotubes

Andrey Baydin*†, Natsumi Komatsu, Fuyang Tay, Saunab Ghosh, Takuma Makihara, G. Timothy Noe, Junichiro Kono

**Rice University*

For facile manipulation of polarization states of light for applications in communications, imaging, and information processing, an efficient mechanism is desired for rotating light polarization with a minimum interaction length.

Here, we report giant polarization rotations for terahertz (THz) electromagnetic waves in ultrathin (~45 nm), high-density films of aligned carbon nanotubes. We observed polarization rotations of up to ~20° and ~110° for transmitted and reflected THz pulses, respectively. The amount of polarization rotation was a sensitive function of the angle between the incident THz polarization and the nanotube alignment direction, exhibiting a ”magic” angle at which the total rotation through transmission and reflection becomes exactly 90°. Our model quantitatively explains these giant rotations as a result of extremely anisotropic optical constants, demonstrating that aligned carbon nanotubes promise ultrathin, broadband, and tunable THz polarization devices.

E217: Understanding the separation mechanisms of carbon nanotubes using aqueous two-phase extraction and density gradient ultracentrifugation

Marina Avramenko*†, Miguel Angel Lopez Carrillo, Joeri Defillet, Miles Martinati, Wim Wenseleers, Sofie Cambré
**University of Antwerp*

Aqueous two-phase extraction (ATPE) and density gradient ultracentrifugation (DGU) are among the mainstream techniques for carbon nanotubes sorting [1]. Both of these techniques allow for sorting of carbon nanotubes by diameter, chirality, metallicity, and even enantiomer separation is possible [2-5]. In ATPE, two water-soluble, yet immiscible polymers are mixed together at sufficiently high concentration after which they spontaneously form two phases with different hydrophilicity. In a typical separation protocol, SWCNTs are added to this two-polymer mixture with a combination of different surfactants, resulting in separation of different chiral species among both phases. In DGU, this method, carbon nanotubes can be separated based on the difference in their density in a gradient medium using ultracentrifugation. Furthermore, in situ DGU experiments are of particular interest: they allow one to understand the mechanisms driving the separations and the role of different surfactants used [5]. Despite the major progress of both methods in the past decade, the separation mechanisms are not yet well understood, and various parameters are not yet optimised, which makes it difficult to fully predict and control the separations. Therefore we have aimed at finding a way to attain more control over the separation processes. In this paper, we present (i) a series of ATPE separations, in which surfactant combinations and concentrations are systematically varied and (ii) the results of several in situ DGU experiments with different concentrations of the surfactants used. Absorption spectroscopy, multi-wavelength resonant Raman scattering and wavelength-dependent photoluminescence-excitation spectroscopy, combined with detailed two-dimensional spectral analysis, are applied to characterize our samples and to investigate the underlying separation mechanisms in both methods. [1] B. Podlesny et al., Sci. Rep. 2020, 10, 9250 [2] C.Y. Khripin et al., J. Am. Chem. Soc. 2013, 135, 6822 [3] N.K. Subbaiyan et al., ACS Nano 2014, 8, 1619 [4] H. Li et al., ACS Nano 2020, 14, 948 [5] S. Cambré et al., Nanoscale 2015, 7, 20015 *Acknowledgements:* The authors acknowledge funding by the European Research Council under starting Grant ORDERin1D 679841.

E218: First realization of isotope labelled carbyne@CNT using liquid precursors

Weili Cui*†, Lei Shi, Kecheng Cao, Ute Kaiser, Takeshi Saito, Paola Ayala, Thomas Pichler
**University of Vienna, Faculty of Physics, 1090 Wien, Austria*

Carbyne, as a novel sp1 hybridized carbon allotrope is one of the most interesting existing one-dimensional materials because of its predicted outstanding mechanical, thermal and electronic properties. But synthesizing it has remained challenging for more than 125 years due to its instability and reactivity. In our previous studies, we showed a versatile pathway to overcome this issue by confining very long carbon chains, i.e. carbyne, inside the hollow core of double walled carbon nanotubes by high temperature and high vacuum annealing. [1] Combined with the fact that carbine is the strongest Raman scatterer so far (see abstract of ClaDuri Tschannen) [2] which paves the way of confined carbyne applied as tracers or contact free temperature sensor. However, gaining control on the tailored growth and functionality of confined carbyne remained as an open question. Our most recent study showed a novel pathway by stepwise growth of confined carbyne with single walled carbon nanotubes transformed to double walled carbon nanotubes first. [3] Here, based on this study we report a breakthrough in the controlled growth of confined carbyne with greatly enhanced yield using nanotubes filled with liquid precursors as starting material. [4] (see Figure 1) This method also enabled us to realize isotope labelling of this confined carbyne for the first time. This uniquely facilitates to tailor the functionality of confined carbyne. As shown in the sketch, we used isotopic labelled liquid precursors and encapsulated them inside carbon nanotubes as carbon source for further synthesis of confined carbyne. This allowed us to achieve pioneering results on isotope engineered carbyne with around 11.9% of 13C-labelling using 13C-methanol as precursor (see Figure 2). The isotope engineering of carbyne brings unprecedented capability to tune the properties of these confined linear carbon chains since currently only the interaction with nanotubes that host and protect them from the environment has been found to offer a possibility to control carbyne´s properties rather than designing the structure itself. And this opens a new opportunity for the design of advanced heterostructured nanomaterials and paves the way to applications in quantum spin transport, nanoelectronics, nuclear magnetic resonance. [1] Shi, Lei, et al. Nature Mater. 2016, 15, 634-639. [2] Tschannen, Cla Duri, et al. Nano Lett. 2020, 20, 6750-6755. [3] Shi, Lei, et al. Nano Lett. 2021, 21, 1096-1101. [4] Cui, Weili, et al. "Isotopic labelling of confined carbyne." Angew. Chem. Int. Ed. 2021, DOI: 10.1002/anie.202017356. *Acknowledgements:* The work was supported by FWF and the National Natural Science Foundation of China.

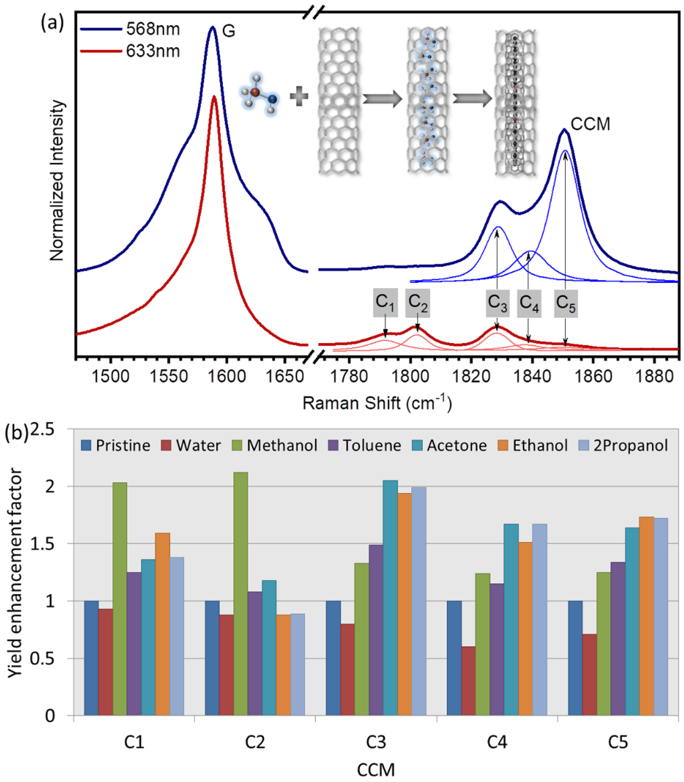

Fig. 1: (a) Raman Spectra and line-shape analysis of the methanol-filled sample. (b) Yield enhancement factors for CCM components (C1-C5).

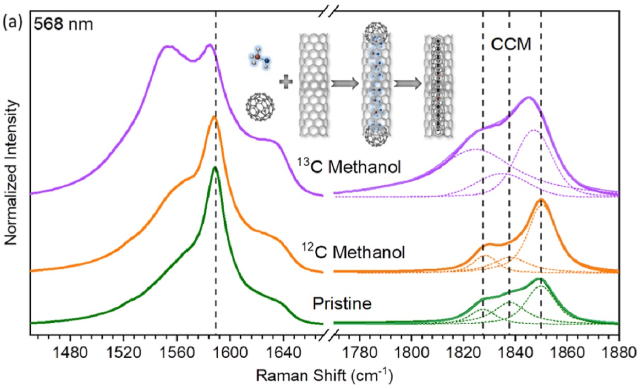

(b)

CCM		C_1	C_2	C_3	C_4	C_5
Relative Shifts	^{12}C Methanol	-0.4	+0.6	+0.9	+0.2	+0.5
	^{13}C Methanol	-8.0	-4.0	-2.8	-3.0	-2.7
^{13}C-incorporation ratio		11.9%	6.4%	4.7%	5.0%	4.6%

Fig. 2: Raman spectra and peak analysis of annealed pristine, 12C methanol, and 13C-labelled (99%) methanol filled SWCNTs excited by a 568 laser.

E220: Excitonic vs Mott insulator in carbon nanotubes: A proposed experimental test

Giacomo Sesti*†, Daniele Varsano, Elisa Molinari, Massimo Rontani
**UNIMORE*

Ultraclean, undoped carbon nanotubes are always insulating, even when the gap predicted by band theory is zero. The residual, intrinsic gap is thought to have a many-body origin, associated with either a Mott or an excitonic phase. Whereas the two scenarios are fundamentally different, as they are driven by the short- and long-range part of Coulomb interaction, respectively, a conclusive experiment has been missing so far. Here we propose as a unique fingerprint of the excitonic insulator the presence of a cusp in the evolution of the gap with the axial magnetic field, close to the gap mimimum. On the contrary, the Mott phase exhibits a featureless, rounded profile. The non-analytic spike originates from the extreme sensitivity of electron-electron interactions to the Aharonov-Bohm gap modulation, as we demonstrate by combining a first-principles analysis of screening with extensive model calculations for tubes of different size and chirality. *Acknowledgements:* MIUR PRIN2017 No. 2017BZPKSZ; EU grant No. 824143.

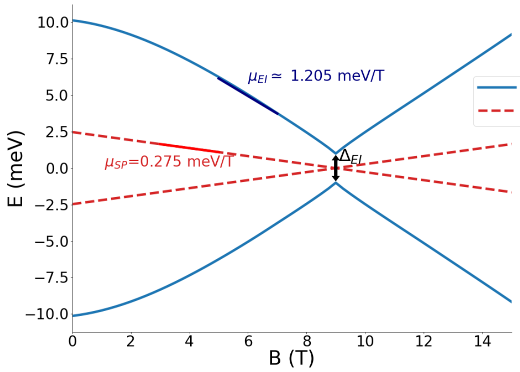

Fig. 1: Dispersion of the gap with the magnetic field in the Excitonic Insulator phase of a carbon nanotube. We plot with a dashed line the single-particle energies for guidance.

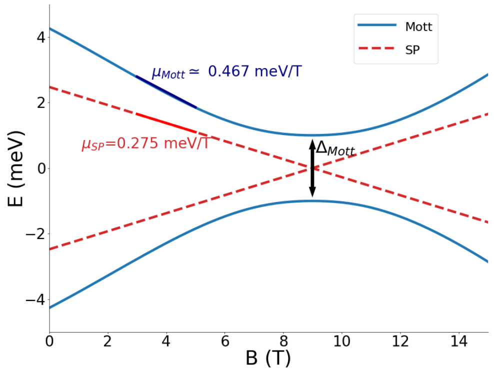

Fig. 2: Dispersion of the gap with the magnetic field in the Mott-Hubbard phase of a carbon nanotube. We plot with a dashed line the single-particle energies for guidance.

E221: Triplet excitons in sorted (6,5) and (7,5) SWCNTs: a study by optically-detected magnetic resonance spectroscopy

Sofie Cambré*†, Ivan Sudakov, Jeff Blackburn, Juan G. Duque, Wim Wenseleers, Etienne Goovaerts
**Nanostructured and Organical Optical and Electronic Materials, Department of Physics, University of Antwerp, Antwerp, Belgium*

Single-wall carbon nanotubes (SWCNTs) possess unique electronic and optical properties, all depending on their exact chiral structure. Their quasi one-dimensional character results in the formation of strongly bound electron-hole pairs (excitons) that can even be observed at room temperature (i.e. binding energies of the order of several hundred meV). [1] The exciton fine structure of SWCNTs is quite complex, with multiple singlet and triplet excitonic states, of which only one is optically allowed, thereby resulting in extremely low fluorescence (PL) quantum yields. While the singlet excitons have already been investigated thoroughly, little is known about the longer-living triplet excitons. In this work, we report the characterization of triplet excitons in chirality-purified samples of (7,5) and (6,5) SWCNTs by means of spin-sensitive optically detected magnetic resonance spectroscopy. In both chiralities the nanotubes are shown to sustain two types of triplet exciton states, both with axial symmetry but a different localization as shown by the magnitude of their zero-field splitting parameter in the spin Hamiltonian. This symmetry and magnitude of the zero-field splitting of both types of triplet excitons are determined by careful simulation of magnetic-field orientation-dependent ODMR spectra of in-plane aligned SWCNTs. While the parameters only weakly depend on the nanotube environment, an increase in zero-field splitting is found for (6,5) with respect to (7,5) nanotubes, in good agreement with the tighter confinement expected in the narrower-diameter nanotubes. [1] M.S. Dresselhaus et al, Ann. Rev. Phys. Chem. 2007, 58, 719 [2] D. Stich et al, Nature Photon. 2014, 8, 139; J. Palotás et al, ACS Nano 2020, 14, 11254 *Acknowledgements:* European Research Council - Starting Grant ORDERin1D (679841) and Flemisch Fund for Scientific Research - FWO (PhD fellowhip of I.S.)

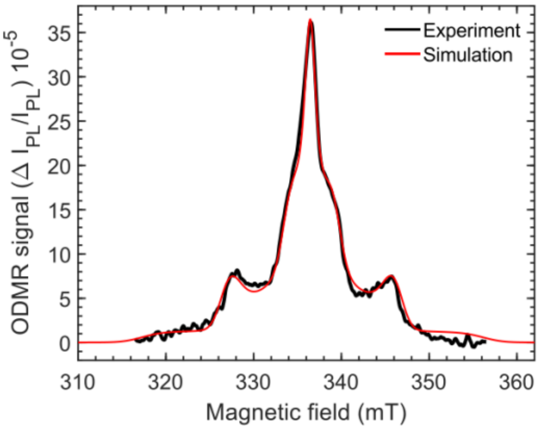

Fig. 1: The ODMR signal and the EPR simulation of the triplet excitons in (6,5) SWCNTs.

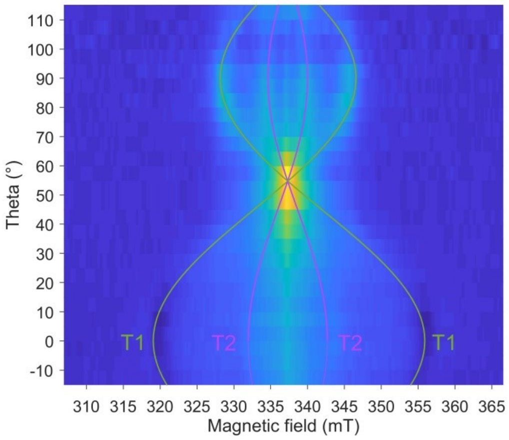

Fig. 2: Angular variation of the B-field with respect to the SWCNTs alinged inside the film plane.

E222: Band Gap and Full Electronic Spectrum of Carbyne inside Carbon Nanotubes from Laser-Wavelength-Dependent Raman Spectroscopy

Wim Wenseleers*†, Miles Martinati, Sofie Cambré, Philip Rohringer, Lei Shi, Paola Ayala, Thomas Pichler, Marius Wanko, Angel Rubio, Sören Waßerroth, Stephanie Reich

**University of Antwerp*

The hollow core and well-defined diameters of carbon nanotubes (CNTs) make them the ideal template for ordering one-dimensional (1D) arrays of molecules and for the controlled synthesis of 1D carbon nanostructures from suitable precursor molecules. For instance, we previously demonstrated that in this way dipolar dye molecules can be naturally aligned in an ideal head-to-tail arrangement to create assemblies with a giant total nonlinear optical response,[1] and that the optical properties of dye molecules encapsulated in SWCNTs can be strongly modulated by the SWCNT diameter, indicating very specific diameter-dependent stacking and interactions of the molecules. [2] By thermal conversion also well-defined carbon structures such as long 1D carbon chains and graphene nanoribbons[3] can be synthesized inside the hollow core of CNTs. Here we show that the structure and properties of such 1D carbon chains (with very long length such that they have converged to the properties of infinite chains, i.e. carbyne) are strongly modulated by the interaction with the host tube, which greatly modifies the chains' bond-length alternation. [4] We also show how the band-gap and electronic spectrum of the encapsulated carbyne can be measured in detail, through extensive wavelength dependent resonance Raman (excitation) spectroscopy, disentangling the vibrational and electronic spectra of the different structures. Thanks to the fact that the carbyne in different diameter nanotubes also shows different vibrational frequencies, the Raman excitation spectroscopy allows for eliminating the inhomogeneous broadening of the electronic spectra due to the different CNT environments, and thus for resolving the complete electronic and vibronic fine structure of the spectra. [1] S. Cambré, J. Campo et al., Nature Nanotechnol. 10, 248 (2015). [2] S. van Bezouw, D. H. Arias et al., ACS Nano 12, 6881 (2018). [3] H. Kuzmany et al., Carbon 171, 221 (2021). [4] L. Shi et al., Phys. Rev. Mater. 1, 075601 (2017).

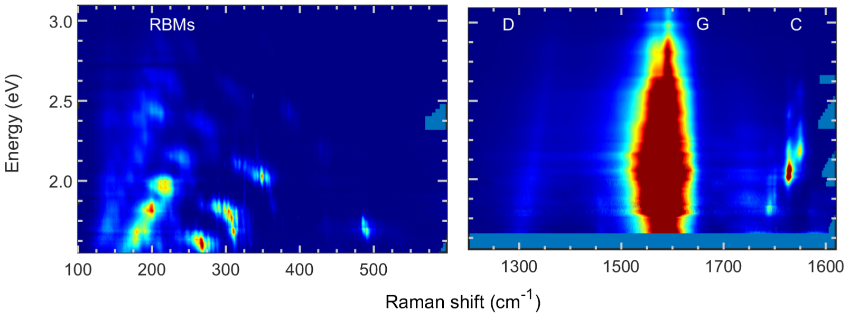

Fig. 1: 2D resonant Raman spectroscopy of carbyne inside DWCNTs. The high frequency vibration range shows, beside the nanotubes' D and G bands, the carbyne signal (C) around 1790-1850cm-1.

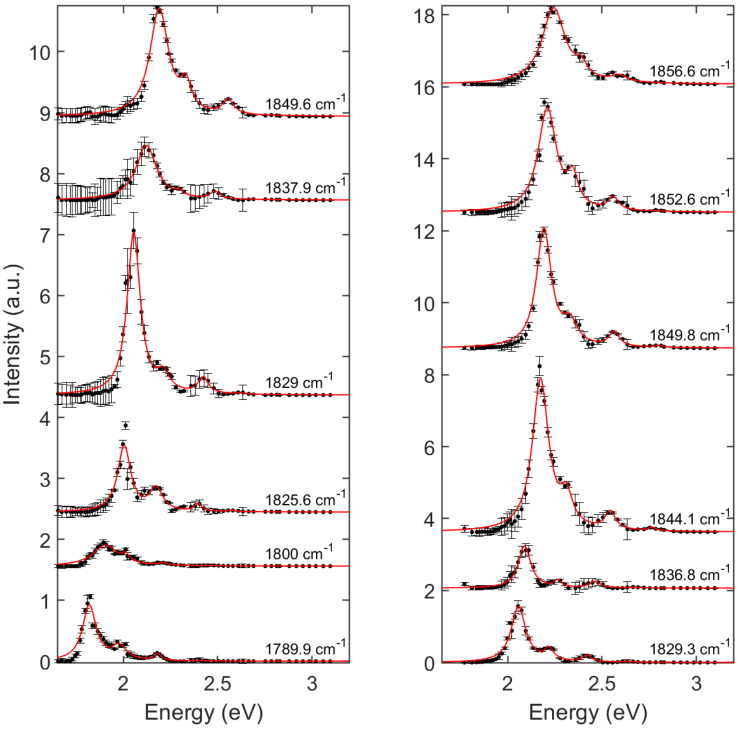

Fig. 2: Raman excitation spectra of the different carbyne Raman signals corresponding to carbyne inside different diameter nanotubes.

E223: Universal strength scaling in carbon nanotube bundles with frictional load transfer

Evgeni Penev*†, Nitant Gupta, Boris Yakobson

**Rice University*

Carbon nanotubes (CNTs) individually display exceptional mechanical properties, but the strength of their mesoscale assemblies such as bundles has a fundamental disconnect, with limited understanding of its scaling. The talk will outline an expedient coarse-grained (CG) model [1] including effective friction, f, that allows us to hierarchically explore the load transfer starting from an individual CNT–CNT interface to that in a representative bundle volume element and ultimately for a micrometer-long finite-width bundle composed of tubes with an aspect ratio as large as L/d ~1500. The model allows us to quantitatively demonstrate that in the regime where strength is governed by frictional load transfer the ratio s/fL is invariant with respect to the tube length or interface friction, Fig. 1. Furthermore, all geometrical perturbations caused by length distribution and bundle dimensions result in a net stress concentration effect, without influencing the scaling behavior. This suggests that general strategies to enhance tube length during growth, by enhancing either growth rate or growth duration, can improve the strength of the bundles significantly. On the other hand, an increase in cross-link density should have a similar effect. Furthermore, if progress can be made in novel strategies to induce stronger chemical cross-links, it could lead to a big boost in s. Thus, from an experimental perspective, depending on whether the conditions favor control over f or L or both, multiple pathways of enhancing bundle strength exist. The proposed model, implemented in LAMMPS [2], builds on a basic bead-and-spring CG representation of an individual CNT and can be directly, or with minimal modification, applied to a variety of other low-density CNT-based assemblies, such as branched nanotube networks, buckypaper, or CNT–polymer composites. [1] N. Gupta, J. M. Alred, E. S. Penev, B. I. Yakobson, ACS Nano 15, 1342–1350 (2021) [2] S. Plimpton, Comput. Phys. 117, 1– 19 (1995); https://lammps.sandia.gov/ *Acknowledgements:* This work was supported by the U.S. Department of Defense: Air Force Office of Scientific Research (AFOSR), Grant FA9550-17-1-0262.

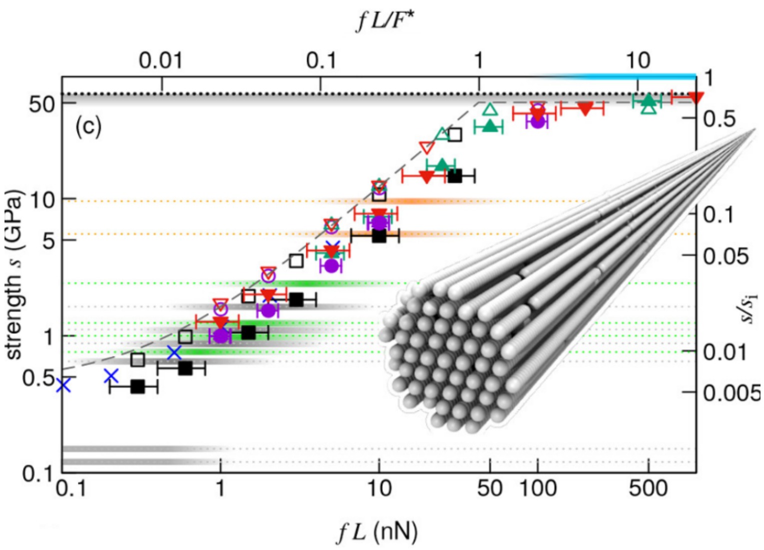

Fig. 1: Strength scaling for finite-diameter bundles composed of CNTs with identical length (open symbols) or normally distributed length (filled symbols) with standard deviation shown as horizontal error bars [1].

E225: Carbon Nanotube Mask Filters Demonstrate Hydrophobic Barrier and Hyperthermic Antiviral Effects on SARS-CoV-2

IL Jeon, Sangsu Lee[*†], Esko Kauppinen

Pusan National University

Carbon nanotube face mask filters with strong and uniform hydrophobicity, high durability, and high thermal conductivity exhibit excellent barrier and antiviral effects against saliva containing SARS-CoV-2. The nanocarbon filter functions as a superior barrier compared with conventional masks owing to the stronger, more uniform, and more durable hydrophobic nature of the carbon nanotubes. A tightly knit carbon nanotube network reveals that its pore size is smaller than an average coronavirus, yet the breathability is equal to that of the conventional polypropylene filter. Exceptional thermal conductivity of carbon nanotubes transpires hyperthermic antiviral effects which allude to stronger protection against the virus as well as reusability of the filter, contributing to environmental sustainability. The facile processability, low-cost, and light-weight of the aerosol-synthesized carbon nanotube filter warrants viability of the carbon nanotube filter reinforcing the fight against the COVID-19 pandemic.

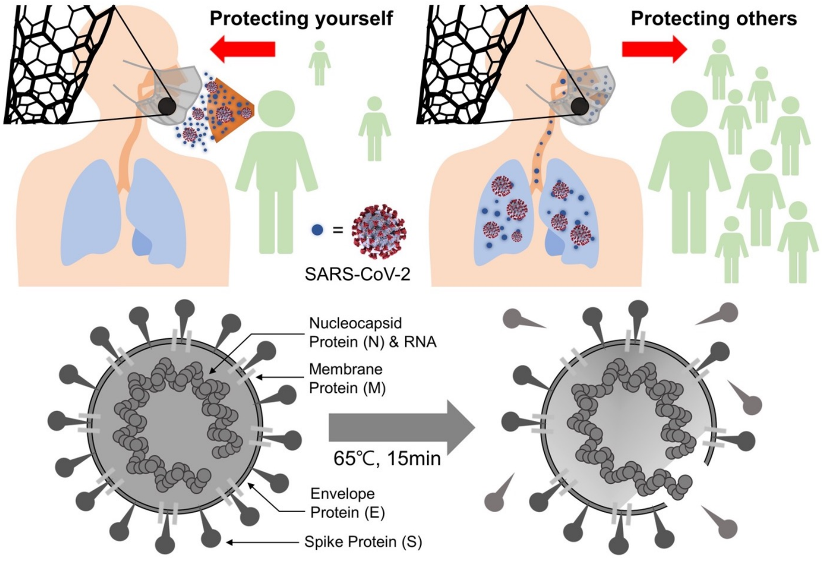

Fig. 1: Illustration of the carbon nanotube filter-based face mask demonstrating hypothermal anti-viral effect

E226: Selective heating and curing of thermosetting resins using localized radio-frequency heating

Anubhav Sarmah[†], Suchi Desai, Micah Green*

**Texas A&M University*

Our research demonstrates a new method for curing thermosetting resins using localized Radio-Frequency heating in a thermosetting resin reservoir. Multi-walled carbon nanotubes are used as fillers in the resin to make it responsive to an RF field, thus allowing for heating and curing of the resin. The RF power can be modulated to maintain a target epoxy curing temperature. An RF applicator generates a fringing electric field, which heats and cures the nano-filled resin exposed to the field and allows for localized curing of the resin. The RF applicator was moved relative to the resin bath at a calculated scan speed to print simple 1D and 2D structures. Thermal and mechanical properties of these RF printed samples were compared against: (i) RF-printed samples followed by post-curing in an oven, and (ii) samples conventionally cured in an oven. Characterization of cured samples showed comparable Glass Transition Temperatures and Storage Moduli for the samples cured using the mentioned three methods. This method of curing thermosetting resins using RF heating allows for rapid, free-form processing of such resins without a mold, in contrast to conventional oven curing.

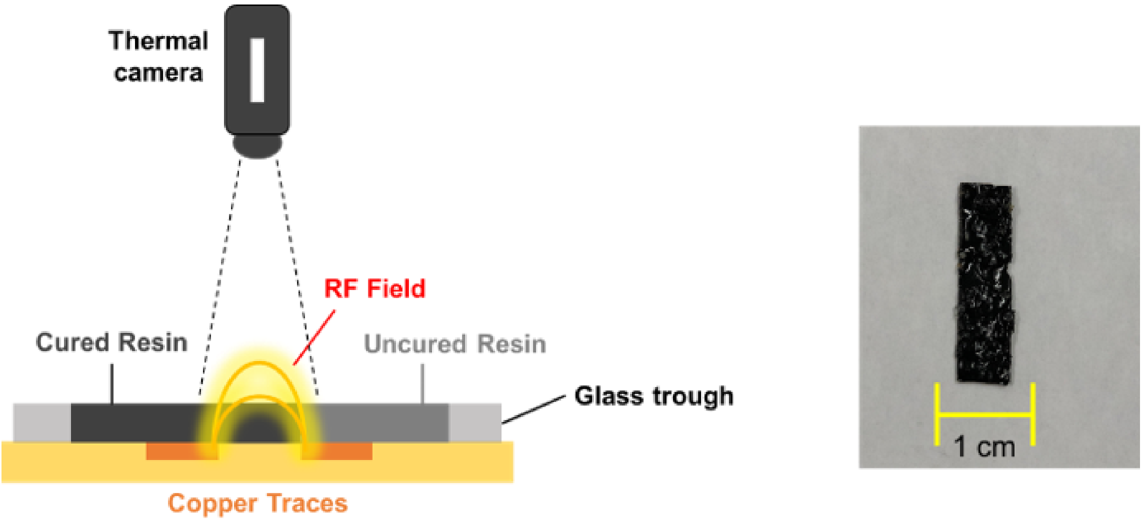

Fig. 1: Curing and printing of thermosetting resins using localized RF heating

Author Index

Conference Schedule

Time Zones			Daily Schedule					
Houston (UTC-5)	Paris (UTC+2)	Tokyo (UTC+9)	**Sunday, June 6**	**Monday, June 7**	**Tuesday, June 8**	**Wednesday, June 9**	**Thursday, June 10**	**Friday, June 11**
6:30	**13:30**	**20:30**		**Opening Session:** remarks by Prof. Robert Curl, Nobel Laureate, and David Leebron, President of Rice University				
7:00	**14:00**	**21:00**	**Parallel Symposia** See detailed program below	**Zhiping Xu** “Morphogenesis of Assembled Carbon Nanostructures Towards High-performance Materials”	**Yuan Chen** “Carbon Nanomaterial Enabled Oxygen Electrocatalysts”	**Fei Wei** “Directed Evolution of Carbon Nanotube Growth and its Unique Properties”	**Yoshihiro Iwasa** “Symmetry Engineering in Nanotubes and Heterostructures of Transition Metal Dichalcogenides”	**Masako Yudasaka** “Imaging of Brown Adipose Tissues by Using Carbon Nanotubes as NIR Fluorescent Probes”
7:30	**14:30**	**21:30**		**Jong-Hyun Ahn** “Skin-attachable Sensor Based on Graphene”	**Sarah Haigh** “Developing Twisted, Stacked 2D Heterostructures with Atomic Resolution In Situ Imaging and Vice-versa”	**Seung-Min Kim** “The Effects of Gas Flow Patterns and Configurations of Injection Part of Reactor on the Synthesis of Carbon Nanotube/Carbon Nanotube Fiber”	**Alain Penicaud** “Raman D Band Appears upon Folding: The Case of Flattened Carbon Nanotubes”	**Ralph Krupke** “Electroluminescence from Graphene-Contacted (7,5) Carbon Nanotubes with Defects”
8:00	**15:00**	**22:00**		**Hiromichi Kataura** “Separation of Metallic Single-chirality Carbon Nanotubes Using Gel-column Chromatography”	**Vincent Jourdain** “Dynamic Instability of Individual Carbon Nanotube Growth Revealed by In Situ Optical Imaging”	**Yuichiro K. Kato** “Near-unity Radiative Quantum Efficiency of Excitons in Carbon Nanotubes”	**Wim Wenseleers** “Well-defined Armchair Graphene Nanoribbons Synthesized inside Carbon Nanotubes”	**Rufan Zhang** “Synthesis and Applications of Ultralong Carbon Nanotubes”
8:15	**15:15**	**22:15**		**Break**	**Break**	**Break**	**Break**	**NT22 Announcement**
8:30	**15:30**	**22:30**		**Pulickel Ajayan** “Carbon Nanotechnology: A Timeline”	**Ute Kaiser** “Understanding Electron-beam-stimulated Reactions within Functionalized Low-dimensional Materials”	**Kaili Jiang** “Synthesis and Applications of Carbon Nanotubes”	**Riichiro Saito** “Optical Properties of Nanotubes and 2D Materials”	**Jana Zaumseil** “Purified and Functionalized CNTs for Optical and Electronic Applications”
9:15	**16:15**	**23:15**		**Adam Boies** “Pushing the Bounds of CNT Floating Catalyst Synthesis Quality Versus Quantity”	**James Tour** “Flash Graphene. Trash to Treasure”	**Jing Kong** “Synthesis and Electrical Contact to Two Dimensional Materials”	**Jeffrey Blackburn** “SWCNT Heterojunctions with Low-dimensional Perovskites for Novel Optoelectronic Functionality and Devices”	**Markita Landry** “Carbon Nanotubes Enable Delivery of Biomolecules to Plants Without Transgene Integration”
9:45	**16:45**	**23:45**		**Break**	**Poster I** Sessions A–E	**Poster II** Sessions A–E	**Poster III** Sessions A–E	**Break**
10:00	**17:00**	**0:00 +1**		**Chongwu Zhou** “High-performance Radio-frequency and Nano Electronics Based on Assembled High-density and High-semiconducting-purity Carbon Nanotube Films”				**Vasili Perebeinos** “Electrical Conductance Mechanisms in Carbon Nanotube Films”
10:15	**17:15**	**0:15 +1**	**Welcome reception** on gather.town	**Alice Castan** “Determining SWCNT Chiralities from High Resolution Electron Microscopy Images using Deep Learning”				**Todd Krauss** “The Light, the Dark, and the Role of Charges and Defects in Carbon Nanotubes”
10:30	**17:30**	**0:30 +1**		**Mijin Kim** “In Vivo Nanosensors using Organic Color Centers for Pharmacodynamic Monitoring”				**Ethan Minot** “Extremely Efficient Photocurrent Generation in Individual Carbon Nanotube Photodiodes”
10:45	**17:45**	**0:45 +1**		**Katherine Jinkins** “Wafer-scale Alignment of 2D Carbon Nanotube Liquid Crystals for Electronics”				**Awards & Closing**

Symposium Schedule

Time Zones			Symposium Schedule – Sunday, June 6						
Houston (UTC-5)	Paris (UTC+2)	Tokyo (UTC+9)	**2nd Symposium on Synthesis, Purification, Functionalization, and Manufacturing of Carbon Nanotubes and Low-Dimensional Materials**	**3rd Symposium on Nanocarbon Materials for Energy and Sustainability**	**8th Symposium on Carbon Nanotube Macromaterials and Their Electronic, Thermal, and Structural Properties**	**11th Symposium on Carbon Nanomaterials Biology, Medicine and Toxicology**	**11th Graphene and 2D Materials Symposium**	**14th Symposium on Nanotube Spectroscopy, Photonics, and Applications in Metrology**	**15th Symposium on Computational Challenges in Nanotubes, 2-D Materials, and Their Macroscopic Assemblies**
6:45	**13:45**	**20:45**	Opening	Opening	Opening	Opening	Opening	Opening	Opening
7:00	**14:00**	**21:00**	**Renu Sharma** “Revealing the nucleation, growth mechanisms and role of catalyst of single walled carbon nanotube growth”	**Michael De Volder** “3D CNT Current Collectors for Li-Ion Batteries”	**Andrey Khlobystov** “Chemistry in the World’s Tiniest Test Tube”	**Rachel Meidl** “Accelerating the Energy Transition with Carbon Nanotubes Requires Closing Critical Policy Gaps and an Understanding of Nano-related Environment, Health and Safety Information”	**Dmitri Efetov** "Competing phases of correlated Chern insulators in Superconducting Twisted Bilayer Graphene”	**Shohei Chiashi** “Synthesis of single-walled carbon nanotube @ boron nitride nanotubes and their optical properties”	**Feng Ding** “Contact-Induced Phase Separation of Alloy Catalyst to Promote Carbon Nanotube Growth”
7:30	**14:30**	**21:30**	**Suguru Noda** “Enhancing Carbon Nanotube Production via Careful Control over Catalyst”	**Dawid Janas** “Is Nanocarbon Black, Green, or Both? Towards Sustainable Energy with Carbon Nanotubes”	**Chris Ewels** “1D-nanomaterial confinement: Red-phosphorus encapsulated within single-walled carbon nanotubes”	**Ardemis Boghossian** “Bioengineering DNA-based Optical Nanotube Sensors Using Directed Evolution and Xenonucleic Acids (XNAs)”	**Guillaume Cassabois** “Deep-ultraviolet spectroscopy in hexagonal boron nitride: from bulk to monolayer”	**Salomé Forel** “Calibrating Raman Cross-sections of Sorted SWCNT Samples”	**Boris Yakobson** “New Theory Insights in 1D-Nanotubes and 2D-Layers Growth and Properties”
8:00	**15:00**	**22:00**	**Arthur Sloan** “Rapid Feedback Experimentation for Continuous Carbon Nanotube Growth”	**IL Jeon** “Foldable Perovskite Solar Cells Using Carbon Nanotube-Embedded Ultrathin Polyimide Conductor”	**Filchito Renee Bagsican** “Carrier-Exciton Dynamics in Aligned and Random Semiconducting Carbon Nanotubes Probed by Terahertz Emission and Photocurrent Spectroscopy”	**Robert Nißler** “Detection of Plant Polyphenols via Near Infrared Fluorescent SWCNT Nanosensors”	**Kai Liu** “Laser Direct Writing of 2D Transition Metal Chalcogenides/Oxides Heterostructures”	**Laurent Cognet** “Tailoring Carbon Nanotubes to Propel Super-resolution Microscopy Applications at Near-Infrared Wavelengths”	**Zhao Wang** “Aligned Carbon Nanotubes and Twisted Bilayer Graphene as Linear Nanoactuators”
8:15	**15:15**	**22:15**	**Jiangtao Wang** “Selectively Twisting Carbon Nanotubes into Semiconducting Chiralities by Low-Work-Function Contact”	**Gideon Oyibo** “Harnessing the Photovoltaic Properties of Carbon Nanotube Networks”	**Alexander Tonkikh** “Tunable Doping and Characterization of Single-Wall Carbon Nanotube Macrosystems in Air”	**Lorena García-Hevia** “The CNT Biocorona: A Challenge in Nanobiotechnology”	**Sunny Gupta** “What Dictates Rashba Splitting in 2D van der Waals Heterobilayers?”		**Umedjon Khalilov** “Catalyst-Feedstock Tandem in the Structure Synthesis inside a Carbon Nanotube”
8:30	**15:30**	**22:30**	Break	Break	Break	Break	Break	Break	Break
8:45	**15:45**	**22:45**	**Benjamin Flavel** “The Effect of Endohedral Filling on Separation”	**Juan José Vilatela** “High-Performance Materials Based on Nanoscopic Building Blocks: From Composites to Electrodes”	**Thomas Pichler** “Unravelling the Properties of Carbyne Confined inside Carbon Nanotubes”	**Dan Roxbury** “Multispectral Fingerprinting Resolves Dynamics of Nanomaterial Trafficking in Primary Endothelial Cells”	**Ajit Srivastava** “Interacting Excitons in van der Waals Heterostructures of TMDs”	**Paul Finnie** “Full Spectrum Raman Excitation Mapping of Carbon Nanotubes and Making Raman Spectroscopy More Metrological”	**Nicola Marzari** “Computational Exfoliation of All Inorganic Materials, and What One Can Find There”
9:15	**16:15**	**23:15**	**Wei Sun** “DNA-directed precise pitch-scaling for high-performance CNT FETs”	**Andrew Ferguson** “Harvesting Radio-frequency Signals with Carbon Nanotube Electronic Ratchets”	**Esko Kauppinen** “SW, DW and FW CNTs and Graphene-CNT Hybrids for Flexible Electronics Applications”	**Matteo Palma** “Protein Site-Specific Coupling to Carbon Nanotubes: From Single-Molecule Nanohybrids to Nanoscale Biosensors with Tuned Electrostatic Gating”	**Aditya Mohite** “Semiconductor Physics of 2D Organic-Inorganic Perovskites”	**Edward Egelman** “Application of Cryo-EM to DNA-CNTs”	**Tony Low** “2D materials plasmons: physics and applications”
9:45	**16:45**	**23:45**	**Christopher Sims** “Determining SWCNT Extraction Conditions in Aqueous Two-Polymer Phase Extraction with Near-Infrared Fluorescence”		**Qiang Zhang** “Transparent and Freestanding Single-Walled Carbon Nanotube Films Synthesised Continuously via Floating Catalyst Chemical Vapor Deposition”	**Zvi Yaari** “Machine Learning Enabled Nanosensor Array Platform for Cancer Diagnosis”	**Ksenia Bets** “Lateral Epitaxy: the Entropic Source of Ordered Monocrystalline Growth of 2D Materials”	**Achim Hartschuh** “Time-resolved Optical Microscopy of Single Semiconducting Carbon Nanotubes”	**Igor Bondarev** “Collective Excitations and Optical Response of Ultrathin Carbon Nanotube Films”
10:00	**17:00**	**0:00 +1**	**Jan Gotthardt** “Molecular n-Doping of Large- and Small-Bandgap Carbon Nanotube Field-Effect Transistors with ttmgb”		**Cedric Ginestra** “Liquid Crystals of Neat Boron Nitride Nanotubes and their Assembly into Ordered Macroscopic Materials”	**Nicole Iverson** “In Vivo Detection and Tissue Extraction of Single Walled Carbon Nanotube Sensors from a Large Animal Model”	**Chongwu Zhou** “Gold-Vapor-Assisted Chemical Vapor Deposition of Aligned Monolayer WSe_2 with Large Domain Size and Fast Growth Rate”	**Klaus Eckstein** “Comparison of Infrared and Raman Spectra of Doped (6,5) Single-Wall Carbon Nanotubes”	**Grigorii Drozdov** “Densification of Single-Walled Carbon Nanotube Films: Mesoscopic Distinct Element Method (mDEM) Simulations and Experimental Validation”
10:15	**17:15**	**0:15 +1**	**Welcome Reception**